Carbon cycling in (sub-) Antarctic marine anoxic sediments

Lea Charlotte Wunder

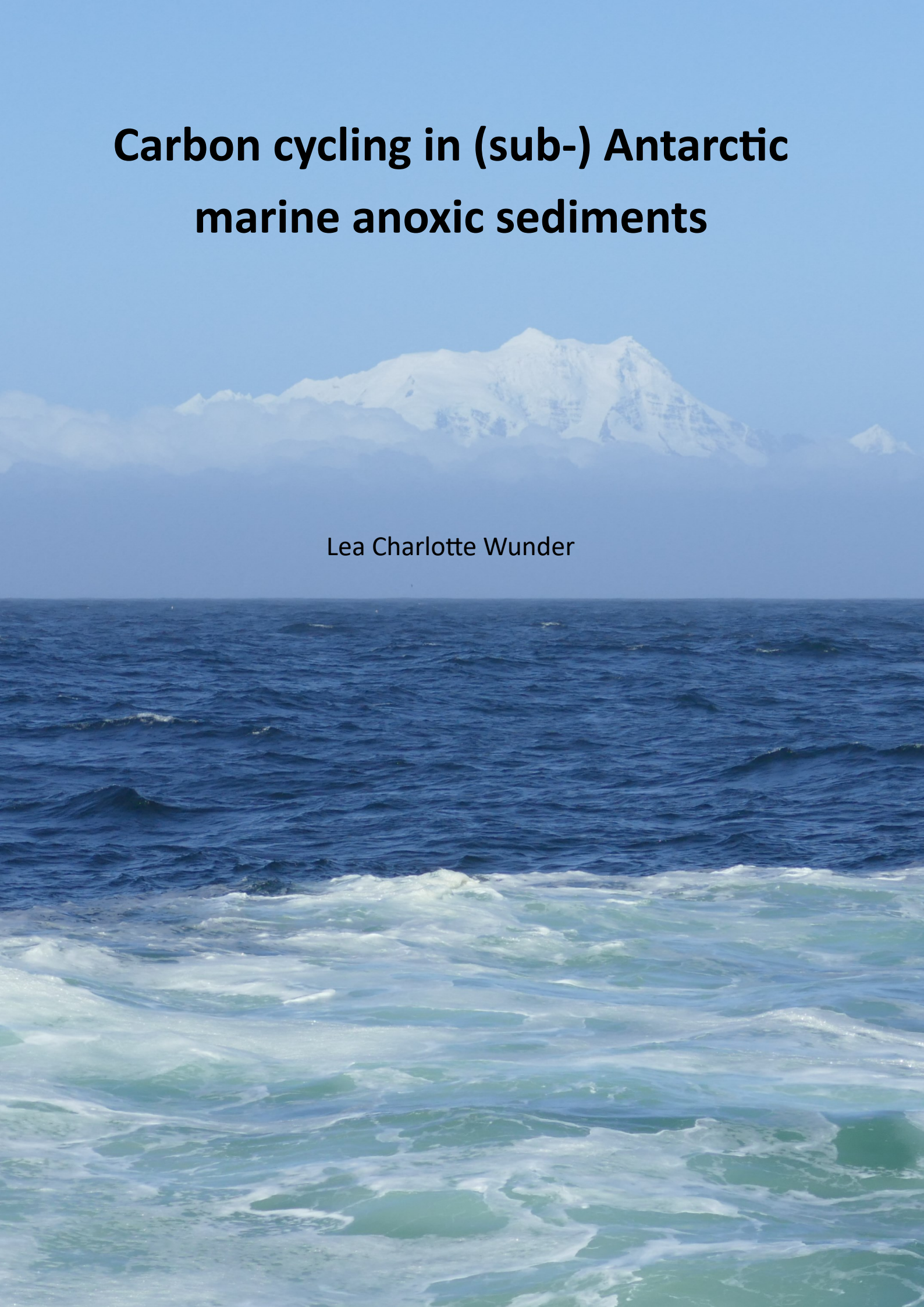

Carbon cycling in (sub-) Antarctic marine anoxic sediments

DISSERTATION

zur

Erlangung des Grades eines

Doktors der Naturwissenschaften

– Dr. rer. nat. –

dem Fachbereich Biologie/Chemie der

Universität Bremen vorgelegt von

Lea Charlotte Wunder

Bremen

December 2024

This PhD thesis was conducted in the frame work of
the International Max-Planck Research School of
Marine Microbiology (MarMic)
and partially financed by DFG the project
“Environmental control of iron reducing
microorganisms in Antarctic marine sediments
(ECIMAS)” as part of the DFG priority program
“Antarctic Research with Comparative Investigations
in Arctic Ice Areas” (SPP 1158)

1. Gutachter: Prof. Dr. Michael W. Friedrich (Universität Bremen)

2. Gutachter: Prof. Dr. Ian P.G. Marshall (Aarhus University, Dänemark)

Promotionskolloquim: 13.02.2025

In loving memory of my grandfather

Prof. Dr. Ruprecht Düll

Table of content

Summary

Anaerobic degradation of organic carbon by microbial communities in marine sediments is an important part of the global carbon cycle. In polar environments, marine sediments already experience the consequences of global warming to a high extent. The temperature rises and melting of glaciers accelerates, resulting in increased amounts of nutrients such as metal oxides supplied to the sediments by glacial meltwater. These changes are proposed to influence the anaerobic degradation of organic carbon and the associated microorganisms, as glacial supplied metal oxides can serve as terminal electron acceptors for these processes. However, changes can only be predicted if the current state of the system is known but especially Antarctic marine sediments are understudied.

The sediments of Antarctic and sub-Antarctic study sites investigated in this thesis, i.e., Potter Cove, at King George Island/Isla 25 de Mayo, West Antarctic Peninsula, and South Georgia in the South Atlantic, are heavily influenced by glacial melting. I studied the *in situ* microbial communities and geochemistry, focusing on final organic carbon mineralization. Additionally, I identified the acetate degrading microbial community by simple incubations or RNA stable isotope probing (SIP) incubation experiments, testing iron oxides, manganese oxides and sulfate as terminal electron acceptors. Mainly iron, but when supplied also manganese oxides, served as electron acceptors for acetate oxidation. The uncultured group Sva1033 (Desulfuromonadales) was identified as the main responsible iron reducer in all studied sediments. This is the first experimental evidence about the metabolic capabilities of this understudied group. I could identify Sva1033 as keystone species for acetate oxidation in the studied environments, as it was the dominant iron reducing microorganisms both, *in situ* and in RNA-SIP incubations, even at higher temperatures.

Further, acetate degradation in SIP experiments showed a microbial community that was able to thrive over a wide temperature range, such as Sva1033 and *Desulfuromonas*. In contrast, some specialist microorganisms were only active at few temperatures, such as *Arcobacteraceae* at low temperatures and *Desulfuromusa* at high temperatures. In addition, *Desulfuromusa* was the dominant manganese reducing microorganism oxidizing acetate at low *in situ* temperature.

In all these experiments, sulfate reducing microorganisms did not seem to contribute to acetate oxidation, despite their abundance in *in situ* sediments and in the background of multiple SIP incubations. An autotrophic lifestyle of sulfate reducers could not be shown by SIP experiments, despite a stimulation of sulfate reduction by the addition of acetate and hydrogen.

The electron donors used by sulfate reducers remained elusive and require further investigation. Instead, in SIP experiments with highest sulfate reduction rate, a potential novel *Sulfurimonas* strain performed an anaerobic, psychrophilic lifestyle and assimilated acetate and CO_2. I suggest sulfide as utilized electron donor in syntrophy with another microorganism as electron accepting partner, however further experiments are needed to support these hypotheses and elucidate the conducted metabolism by this microorganism.

The findings of this thesis contribute to the knowledge about anaerobically respiring microorganisms by supplying one of the few descriptions of the microbial community in glacial influenced marine sediments from Antarctica and propose the conducted metabolisms. I propose that the microbial community responsible for organic carbon degradation is highly influenced by glacial meltwater supplied nutrients and therefore sensitive to future changes in this global warming affected environment.

Zusammenfassung

Im marinen Sediment stellt die anaerobe Zersetzung organischen Kohlenstoffs durch eine mikrobielle Gemeinschaft einen wichtigen Teil des globalen Kohlenstoffzyklus dar. Die Folgen der globalen Erwärmung sind in den marinen Sedimenten der polaren Regionen bereits jetzt deutlich wahrnehmbar. Die Temperatur steigt und beschleunigtes Abschmelzen der Gletscher führt durch Gletscherschmelzwasser zu einem erhöhten Eintrag von Nährstoffen wie Metalloxiden in die Sedimente. Da diese Metalloxide als terminale Elektronenakzeptoren für anaeroben organischen Kohlenstoffabbau dienen können, wird ein Einfluss der beschriebenen Änderungen auf jene Prozesse und die assoziierten Mikroorganismen vorausgesagt. Änderungen können allerdings nur sinnvoll vorausgesagt werden, wenn der aktuelle Status des untersuchten Systems verstanden wurde und insbesondere marine Sedimente in der Antarktis sind bisher kaum untersucht worden.

Die Sedimente der in dieser Dissertation untersuchten Gebiete, Potter Cove auf der König-Georg-Insel/Isla 25 de Mayo an der Westantarktischen Halbinsel und Südgeorgien im Südatlantik, werden stark durch schmelzende Gletscher beeinflusst. Ich habe die mikrobielle Gemeinschaft und Geochemie *in situ* untersucht, fokussiert auf den finalen Kohlenstoffabbau. Zusätzlich habe ich in simplen Inkubationsexperimenten und Inkubationen mit stabiler Isotopenbeprobung (stable isotope probing: SIP) auf RNA-Level die acetatabbauenden Mikroorganismen untersucht und Eisenoxide, Manganoxide und Sulfat als terminale Elektronenakzeptoren getestet. Eisenoxide und, wenn zugesetzt, auch Manganoxide, dienten als Elektronenakzeptoren für die Acetatoxidierung. Der hauptsächlich verantwortliche Mikroorganismus für die Eisenreduktion in allen untersuchten Sedimenten war der unkultivierte Sva1033 (Desulfuromonadales). Dies ist der erste experimentelle Nachweis für eine Stoffwechselfähigkeit dieser kaum untersuchten Gruppe. Da Sva1033 der dominante eisenreduzierende Mikroorganismus *in situ* und in RNA-SIP Inkubationen, sogar bei höheren Temperaturen, war, konnte ich ihn als Schlüsselart für Acetatoxidation in den untersuchten Umgebungen identifizieren.

Des Weiteren konnte durch acetatabbauende SIP Experimente eine mikrobielle Gemeinschaft gezeigt werden, die über einen weiten Temperaturgradienten aktiv war, zum Beispiel die Mikroorganismen Sva1033 und *Desulfuromonas*. Andere Mikroorganismen waren nur bei bestimmten Temperaturen aktiv, zum Beispiel *Arcobacteraceae* bei niedrigen und *Desulfuromusa* bei hohen Temperaturen. *Desulfuromusa* war zusätzlich der dominierende

Mikroorganismus, der bei niedriger *in situ* Temperatur Manganoxide reduziert und Acetat oxidiert hat.

Trotz ihrer hohen Abundanz in den *in situ* Sedimenten, schienen sulfatreduzierende Mikroorganismen in all den durchgeführten Experimenten nicht zur Acetatoxidation beizutragen, waren allerdings in mehreren SIP Experimenten im Hintergrund vorhanden. Des Weiteren konnten SIP Experimente keinen autotrophischen Lebensstil der Sulfatreduzierer zeigen, obwohl Sulfatreduktion durch Acetat- und Wasserstoffzugabe stimuliert werden konnte. Auch die durch Sulfatreduzierer verwendeten Elektronendonoren bleiben schwer zu fassen und weitere Untersuchungen sind notwendig. Stattdessen wurde ein potentiell neuer Bakterienstamm von *Sulfurimonas* in SIP Experimenten mit den höchsten Sulfatreduktionsraten identifiziert, welcher einen anaeroben, psychrophilen Lebensstil vollführt und Acetat und CO_2 assimiliert hat. Ich schlage Sulfid als genutzten Elektronendonor und Syntrophie mit einem anderen Mikroorganismus als elektronenakzeptierenden Partner vor, allerdings werden weitere Experimente benötigt um diese Hypothesen zu bestätigen und weiteres Licht auf den durch den Mikroorganismus durchgeführten Metabolismus zu werfen.

Durch Beschreibungen und vorausgesagte Stoffwechselaktivitäten der mikrobiellen Gemeinschaft in gletscherbeeinflussten, marinen Sedimenten der Antarktis tragen die Untersuchungsergebnisse dieser Dissertation zum Forschungsfeld der anaeroben Mikroorganismen in marinen Sedimenten bei. Aufgrund meiner Forschungsergebnisse halte ich es für wahrscheinlich, dass die organische Materialien zersetzende mikrobielle Gemeinschaft stark durch vom Gletscherschmelzwasser eingetragene Nährstoffe beeinflusst wird und dadurch höchst sensibel auf zukünftige Änderungen in dieser durch globale Erwärmung beeinflussten Umwelt reagieren könnte.

Chapter 1

Introduction

1.1 Effects of global warming on coastal polar environments

Our planet currently experiences rapid climate change by global warming. The global surface temperature reached 1.1°C higher values in the last decade compared to pre-industrial times (1850-1900) (IPCC 2023). Responsible for this extraordinary rapid global warming is an increasing amount of greenhouse gases such as carbon dioxide (CO_2), methane (CH_4), and nitrous oxide (N_2O) in the atmosphere (Hegerl et al. 1996). Part of these greenhouse gases are released by natural sources such as volcanic activities and the biological carbon pump in general (Ciais et al. 2013). However, greenhouse gas emissions have substantially increased since the beginning of the Industrial Era and are mainly responsible for global warming (Ciais et al. 2013). There are many consequences of global warming, which are often tightly connected; here, I will mainly focus on coastal areas and marine environments.

Effects on the ocean

The ocean plays a very important role in the global carbon cycle and as a buffer for global warming, already visible by an increased sea surface temperature of 0.6°C since 1980 (Fox-Kemper et al. 2021). Until now, it absorbed more than a quarter of all anthropogenic CO_2 emissions (Gruber et al. 2019) and stored 90% of all heat associated with anthropogenic greenhouse gas emissions (Rhein et al. 2013), half of it only in recent decades (Gleckler et al. 2016). The consequences of this are already visible, e.g., by lower oxygen content in the water (Schmidtko et al. 2017, Gulev et al. 2021), which has a negative impact on oxygen dependent marine ecosystems (Diaz and Rosenberg 2008, Vaquer-Sunyer and Duarte 2008). Furthermore, increased CO_2 concentrations cause ocean acidification (Doney et al. 2009) with varying effects on different ecosystems (Gao et al. 2019). Moreover, the elevated temperatures cause glaciers and sea ice to melt more rapidly, which results in rising sea levels and changes in salinity (Rignot et al. 2019, Gulev et al. 2021).

Warming of polar environments

The earth does not warm uniformly but certain areas are more affected than others, in particular the poles. The warming of the Arctic and Antarctic region is above the global average, a phenomenon called ‘polar amplification’ (Manabe and Wetherald 1975, Casado et al. 2023). In the Arctic, the surface air temperature has already increased more than twice as much

(+ 1.7°C 2019 vs. 1981-2010) compared to the global average (+ 0.6°C) (Overland et al. 2020), some models even suggesting four times faster warming (Rantanen et al. 2022). The sea ice cover declined substantially across the seasonal cycle, e.g., in September 2019 by nearly 50% compared to 1980, and multiyear sea ice disappeared almost completely (Gulev et al. 2021).
The other polar environment, the Antarctic, behaves differently and does not warm and melt uniformly. While the surface water of the subpolar Southern Ocean warms up more slowly than the global average with even some slight cooling since 1980 and some individual ice sheets have a mass balance of zero, the subsurface water warms up rapidly and the total mass of the Antarctic Ice Sheet decreases, with contributions from West and East Antarctica and the Antarctic Peninsula (Kennedy et al. 2019, Rignot et al. 2019, Haumann et al. 2020). The Antarctic sea ice cover fluctuates between increase and decrease, trending towards decrease since 2016, though (Parkinson 2019, Gulev et al. 2021). The West Antarctic Peninsula is one of the fastest warming places on earth (Jones et al. 2019) and experienced extreme warming events especially in the last years such as in 2020 and 2022 (Francelino et al. 2021, Gorodetskaya et al. 2023).
The melting of glaciers and sea ice also influences their environment in other ways than just increasing the sea level; on a global scale, the addition of very cold fresh water is highly important for crucial ocean circulation and has therefore the potential to change it (Li et al. 2023). Furthermore, sea ice can serve as a source of nutrients such as iron by releasing trapped sediment when the ice melts, fertilizing the ocean (Raiswell et al. 2016).

Effects of global warming and glacial melting in fjord systems

Coastal systems such as fjords are good systems to study local effects. In these environments, global warming induced effects are already visible in the short timeframe of the past 20 years. Two main changing factors are accelerated glacial melting and increased temperature. Locally observed increased surface air and water temperatures, especially extreme heatwave events, can have a negative effect on the local phytoplankton, i.e., some of the primary producers in this environment (Schloss et al. 2012, Latorre et al. 2023), and accelerate glacial melting (Cook et al. 2016). Glacial melting can have many effects on the environment. These can be direct physical effects, for example, calving of icebergs, which then travel out of the fjords potentially scraping off benthic organisms and mixing the sediment on their way, so called ice scouring (Wölfl et al. 2016, Deregibus et al. 2017). The retreat of a glacier also reveals new, hard substrate underneath, which can be colonized by larger organisms such as macroalgae or benthic fauna (Quartino et al. 2013, Torre et al. 2021).

Furthermore, many effects, especially on the carbon cycle, are due to the supply of glacial meltwater. During the process of glacial retreat, most glaciers will go through different glacier types, transitioning from grounded to floating tidewater glacier to land-terminating glacier (Figure 1). The type of glacier influences where in the water column the fresh meltwater enters the fjord, e.g., for tidewater glaciers subglacial discharge is most important where the meltwater enters the fjord below the glacier (e.g., Meire et al. 2017). This results in upwelling of deep, nutrient rich water in front of tidewater glaciers, which enhances primary productivity (Meire et al. 2017, Hoshiba et al. 2024); when the glacier retreats to land, the upwelling stops and primary productivity declines (Meire et al. 2017, Torsvik et al. 2019).

Suspended particulate matter supplied by glacial meltwater

Glacial meltwater transports lithogenic material from subglacial erosion and surface outwash, often in form of suspended particulate matter (SPM), into the surrounding environment in close and further proximity to the glacier (Hawkings et al. 2014). On the one hand, these particles cause a higher turbidity in the water column, which limits light penetration and therefore primary productivity in the water column and on the ground, e.g., by macroalgae (Schloss et al. 2012, Campana et al. 2018, Hoshiba et al. 2024). On the other hand, SPM contains nutrients such as bioavailable iron or trace elements (Monien et al. 2017, Herbert et al. 2020), which can enhance primary productivity, especially in the iron-limited Southern Ocean (Martin et al. 1990, Hodson et al. 2017). Additionally, the supply of SPM has an impact on the next step of the carbon cycle, the organic matter mineralization in the underlying sediment, which is discussed in further detail below.

In general, increased glacial discharge correlates with increased supply of SPM (Braeckman et al. 2021). However, the characteristics of the underlying bedrock determine the composition, and the type of glacier the bioavailability and quantity of supplied SPM (Figure 1; Wehrmann et al. 2014, Henkel et al. 2018, Herbert et al. 2020). Higher sedimentation rates, for example, are rather found at tidewater glaciers than at land-terminating glaciers (Herbert et al. 2020). With further glacial retreat, a lower supply of SPM was proposed due to a smaller area of bedrock the glacier scrapes on and due to sedimentation of particles already during over-land transport in glacial-derived rivers (Milner et al. 2017, Herbert et al. 2020, Herbert et al. 2021, Neder et al. 2022). The characteristics and bioavailability of glacial supplied nutrients especially affect the organic matter mineralization processes in the sediments (e.g., Herbert et al. 2020, Michaud et al. 2020, Herbert et al. 2021).

Glacial derived iron oxides

Iron oxides are an important part of glacial meltwater supplied nutrients (Monien et al. 2017). Their composition and bioavailability depend on their sources: more 'easily reducible' iron oxides and pyrite (FeS_2) were found close to marine-terminating glaciers, originating from subglacial meltwater, while the total amount of 'reactive' iron oxides was higher close to surficial, oxic meltwater discharge (Henkel et al. 2018, Herbert et al. 2020). Note that 'reactive' iron oxides include, but are not limited to 'easily reducible' iron oxides (as term used by Henkel et al. 2018). Those 'easily reducible' iron oxides were defined as leachable with hydroxylamine-HCl and were mostly ferrihydrite and lepidocrocite (Poulton and Canfield 2005). They were assumed as easily accessible for iron reducing microorganisms (Bonneville et al. 2004), however, recent studies showed that the 'Poulton and Canfield extraction protocol' led to an overestimation of iron which was accessible for microbial iron reduction (Laufer et al. 2020).

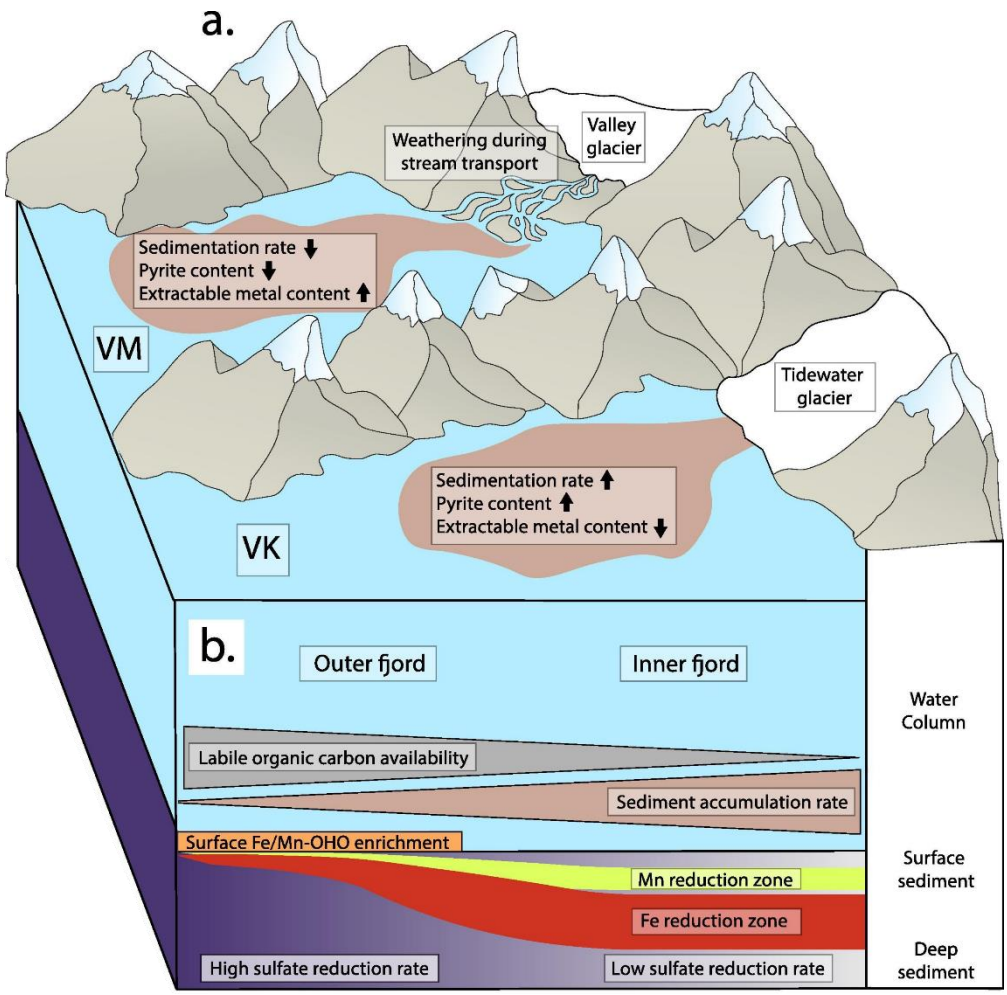

Figure 1: A schematic diagram illustrating (a) differences in source sediment between two fjords related to glacial input via surficial meltwater streams from a land-terminating glacier (VM) and a tidewater glacier (VK). (b) The head-to-mouth gradients in fjord sediment Fe, Mn, and sulfur cycling as controlled by organic carbon (i.e. the concentration of labile organic carbon per unit volume of sediment) and sediment accumulation rate. Reprint from Herbert et al. (2020), Figure 13 a, b, Copyright (2024) with permission from Elsevier.

Altogether, global warming has various effects on the coastal polar environments, many interact and some even counteract each other. In a glacial influenced bay in Antarctica, for example Potter Cove at King George Island/Isla 25 de Mayo, increased amount of SPM in the water column led to decreased primary productivity rates of macroalgae. The colonization of the newly exposed area by macroalgae, however, led to higher biomass counteracting the lower productivity and to a positive carbon fixation rate (Deregibus et al. 2023). This is one example showing the complexity of these systems and the necessity to understand the different, interacting puzzle pieces in order to put the whole image together. It is important to understand the present and past states and dynamics of these ecosystems to predict future changes. One of these puzzle pieces investigated in this thesis is the mineralization of organic matter in glacial influenced sediments, as an important part of the carbon cycle.

1.2 Organic matter degradation and geochemical cycling in anoxic sediments

The global carbon cycle

As simplified overview, the global carbon cycle consists of carbon fluxes between carbon reservoirs with different turnover times. The "slow" reservoirs have turnover times on a geological timescale and are mainly connected by geological process, such as volcanic activities or rock formation (Sundquist 1986). In this introduction and in the thesis, I will focus on biological processes responsible for carbon fluxes between the "more rapid" reservoirs, such as CO_2 in atmosphere and ocean, and organic carbon in form of biomass in ocean, marine surface sediment, and on land (Ciais et al. 2013). Part of the global carbon cycle consists of CO_2 fixation by primary producers, which convert it to organic carbon that organisms of higher trophic levels feed on, releasing CO_2 back to the environment by respiration (Ciais et al. 2013). Primary producers are plants on land, and algae and phytoplankton in the water, all utilizing light as energy source (Beer et al. 2010, Ciais et al. 2013). In the dark of the ocean and in sediments, chemoautotrophic microorganisms use inorganic compounds as energy source for carbon fixation (Middelburg 2011). However, they only minorly contribute to CO_2 fixation and most of the fixed carbon is recycled back to CO_2 by heterotrophic organism (Middelburg 2011). Only < 0.3-1% of marine fixed carbon is buried in most sediments, while in very shallow marine sediments it can be up to 30% (Burdige 2007, LaRowe et al. 2020).

The rate and efficiency of primary productivity removing CO_2 from the atmosphere on the one hand, and the organic carbon degradation adding CO_2 back to the atmosphere on the other hand, largely influence the future development of greenhouse gases and therefore global warming (Arndt et al. 2013). In addition, the effects of global warming described above substantially

influence this cycle. Therefore, it is important to understand the different processes themselves and in context to each other.

Organic matter mineralization in marine sediments

The process investigated in this thesis was terminal organic matter mineralization by microorganisms in polar sediments. Part of the organic matter, produced by photosynthetic primary producers in the light penetrated surface layer, sinks down to the bottom of the ocean, where it fuels heterotrophic and partially autotrophic life (Middelburg 2011, Arndt et al. 2013, LaRowe et al. 2020). The organic matter arrives in form of complex organic molecules and polymers, which are, as a first degradation step, hydrolyzed to monomers and smaller compounds by a cocktail of extracellular enzymes released by microorganisms (Arnosti 2011). Oxygen, the prime electron acceptor, is depleted rapidly in the top mm to cm in coastal sediments with high organic carbon supply, thus deeper in the sediments the mineralization processes are anoxic (Arndt et al. 2013). The next step is the fermentation to short-chain fatty acids, dicarboxylic acids, lactate, alcohols, hydrogen and CO_2 (Schink 1997, LaRowe et al. 2020). The responsible organisms are not well defined yet, as many potentially involved microorganisms are facultative anaerobes, e.g., they can switch between fermentation and other metabolisms; however, members of Bathyarchaeota, Hadesarchaea, Atribacter and even some eukaryotes were suggested to contribute to this process (LaRowe et al. 2020). Intermediates produced by this first step of fermentation are usually maintained at a low concentration by close coupling to their degrading processes, further fermentation or oxidation coupled to terminal electron acceptors (Finke and Jørgensen 2008, Glombitza et al. 2019).

Key intermediate acetate

One of these products, acetate, is the main electron donor for terminal electron-accepting processes, accounting for up to 40% of anaerobic respiration in marine sediments (Finke et al. 2007, Jørgensen et al. 2019). It is mostly produced by the above mentioned degradation processes, and additionally by acetogenesis, especially at deeper sediment depths (Ijiri et al. 2012). It is further oxidized to CO_2, coupled to a terminal electron acceptor, or used by methanogens to produce methane (Sansone and Martens 1982, Finke et al. 2007, Jørgensen and Parkes 2010). The overall rate of organic matter mineralization is controlled by organic matter flux, and hydrolysis and fermentation of the larger molecules, and not by the final step of mineralization (Kristensen and Holmer 2001, Arnosti 2004, Beulig et al. 2018, Jørgensen et al. 2020). However, this final step does control the concentration of the intermediates (Jørgensen 1982, Røy et al. 2012, Glombitza et al. 2015, Glombitza et al. 2019). Most of the degradation occurs close to the sediment surface and degradation rates decrease with depth

(Wellsbury and Parkes 1995, Dyksma et al. 2018). Acetate can be degraded and assimilated by a large diversity of microorganisms, such as Desulfobacterales, Desulfobulbales, Desulfuromonadales, Gammaproteobacteria and *Arcobacter* (Vandieken and Thamdrup 2013, Na et al. 2015, Dyksma et al. 2018, Cho et al. 2020).

Terminal electron-accepting processes

The used electron acceptor depends on the availability and structures the associated microbial community (Petro et al. 2017). In the classical view, the utilization of electron acceptors follows a redox cascade in which one is used after the energetically better one is depleted (Froelich et al. 1979, Lovley and Goodwin 1988). Oxygen and nitrate are the energetically most favorable electron acceptors and therefore deplete very rapidly, especially in sediments with high organic matter input (Froelich et al. 1979, Canfield and Thamdrup 2009). For acetate mineralization in the surface sediments above the methanic zone, the main electron acceptors used are sulfate and iron oxides and, in some locations, manganese oxides (Vandieken et al. 2006a, Finke et al. 2007, Vandieken et al. 2014, Glombitza et al. 2015). As sulfate is present in the sea water, it is the most abundant electron acceptor in the surface sediments, where it can be replenished from overlaying water and only depletes in deeper layers, thus representing a major electron acceptor for organic matter degradation (Jørgensen 1982, Jørgensen et al. 2019).

However, metal oxides such as iron and manganese oxides are energetically more favorable (Froelich et al. 1979). They play a more important role especially in polar areas (Jørgensen et al. 2020), where glaciers or sea ice fuel the environment with nutrients such as metal oxides (e.g., Wehrmann et al. 2014, Monien et al. 2017).

Dissimilatory iron and sulfate reducers can both utilize the inorganic fermentation product hydrogen as electron donor, thereby coupling the processes indirectly to organic matter degradation (Weber et al. 2006, Jørgensen et al. 2019). Many iron, manganese and sulfate reducing microorganisms are phylogenetically located within the phylum Desulfobacterota, i.e., Desulfuromonadales for metal reduction and Desulfobulbales and Desulfobacterales for sulfate reduction, but are also found in other taxa such as Firmicutes, Chloroflexi, Gammaproteobacteria or Campylobacterales (Vandieken et al. 2006b, Weber et al. 2006, Jørgensen et al. 2019, Cho et al. 2020). Sulfate-reducing microorganisms present an important part of the microbial community in many sediments, influencing the microbial community assembly (Liang et al. 2023).

Interactions of sulfur, manganese and iron cycling in marine sediments

Even though the classical view of redox zonation implies exclusiveness of different electron-accepting processes (Froelich et al. 1979, Lovley and Goodwin 1988), overlapping zonation, especially for iron and sulfate reduction, were found in many marine sediments (Canfield et al. 1993a, Canfield et al. 1993b, Vandieken et al. 2006a, Jørgensen et al. 2019, Bourceau et al. 2023). Often, the overlap is not even visible in the geochemical profiles due to interactions and recycling of produced and consumed compounds, such as ferrous iron, sulfide and sulfate, leading to cryptic cycling (Jørgensen and Nelson 2004, Canfield et al. 2010). Iron, manganese, sulfur, and to a lesser extent, nitrogen cycles are tightly linked in the sediment environment (Wasmund et al. 2017).

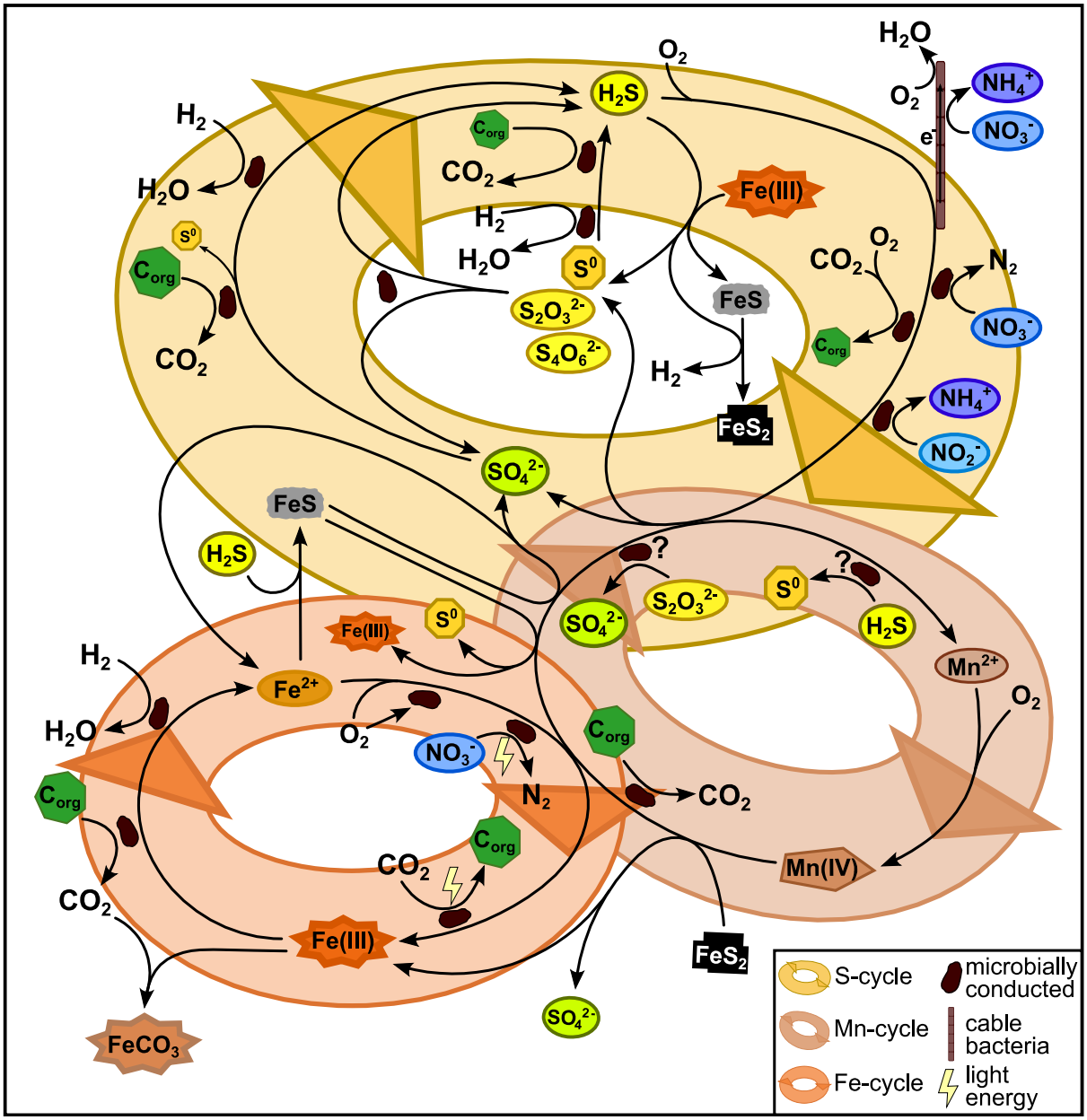

Figure 2: Complex interactions between sulfur, manganese and iron cycle in marine sediments. Biotic (shown by microbial cell, see legend) and abiotic reactions (direct connection of arrows) were displayed. The actual occurrence of the displayed processes likely varies between different environments.

Firstly, ferrous iron (Fe^{2+}) and sulfide react rapidly with each other, forming FeS and after an additional reaction pyrite (Figure 2) (Glasby 2006). Ferrous and ferric (Fe^{3+}) iron absorbs on mineral and iron oxide surfaces and precipitates with carbonates and phosphates (Glasby 2006). Ferrous iron is re-oxidized back to ferric iron, either microbially, i.e., phototrophically, aerobically or anaerobically with nitrate; or abiotically with oxygen, nitrite, nitric oxide or manganese oxides (Figure 2; Weber et al. 2006, Laufer et al. 2016). These re-oxidation processes replenish Fe(III) oxides, called rejuvenation, and occur mainly close to the oxic sediment surface (Beam et al. 2018). Rejuvenation stimulates iron reduction rates and enhances iron cycling, as the produced iron oxides are very bioavailable and microbial iron reduction rates are not only controlled by the crystallinity but especially by the bioavailability of present iron oxides (Jensen et al. 2003, Laufer et al. 2020). This process is proposed to occur in fjord systems with further distance to the glacier where more organic matter is available (Figure 1), and bioturbation further stimulates it by bringing oxygen into deeper layers (Michaud et al. 2020, Laufer-Meiser et al. 2021). Additionally, ferrous iron, often in form of FeS or pyrite, is abiotically oxidized by manganese oxides (Jørgensen and Nelson 2004).

Especially manganese, but also iron oxides rapidly oxidize sulfide, which is kinetically and thermodynamically more favorable than direct sulfide oxidation by oxygen; however biotic sulfide oxidation rates exceed the abiotic rates due to thermodynamic and kinetic constraints in the actual environment (Luther et al. 2011). There are multiple biotic sulfide oxidation processes, e.g., coupled to nitrate or oxygen, which produce sulfate (Jørgensen and Nelson 2004, Meysman 2018). However, abiotic sulfide oxidation usually ends with sulfur intermediates such as elemental sulfur, which are then further oxidized or disproportionated by microorganisms, demonstrating the important microbial role in this complex cycling (Schippers and Jørgensen 2001). FeS and elemental sulfur are more rapidly turned over than pyrite, which presents the main stable sulfur pool in sediments (Jørgensen and Nelson 2004). Elemental sulfur was also shown as side product of dissimilatory sulfate reduction, but sulfide still presented the main product (Wang et al. 2023). Next to elemental sulfur, also thiosulfate is an important sulfur intermediate, which is usually oxidized, reduced, but mainly disproportionated along the whole sediment depth gradient (Jørgensen 1990, Jørgensen and Bak 1991).

Quantification of geochemical processes

The contribution and quantification of all these different processes is a very difficult task due to the many possible reactions and interactions (Figure 2). The quantitative measurement of sulfate reduction rates with radioactive ^{35}S-sulfate is one of the few, well-established methods

(Røy et al. 2014). However, quantifying the different intermediate and oxidation reactions in the sulfur cycle represents a major challenge due to natural isotope exchange between reduced sulfur compounds (Fossing and Jørgensen 1990, Fossing et al. 1992). Recently, a new approach for measuring sulfide oxidation rates with radioactive ^{35}S-sulfide was tested, but still had a lot of limitations as it only measured complete oxidation to sulfate and not to more reduced sulfur compounds such as elemental sulfur (Findlay et al. 2020).

For the delineating contribution of different electron acceptors to organic matter degradation often a certain metabolism was inhibited, e.g., sulfate reduction by molybdate addition, and the accumulation of substrates was measured, assuming these would normally be utilized by the inhibited process (Sørensen et al. 1981). Another approach was to measure depletion and accumulation of associated compounds, often with the help of radiotracers, and calculate the different contributions based on assumptions which processes were involved in the first place (Vandieken et al. 2006a, Finke et al. 2007). However, these calculations themselves often already showed their limitations, e.g., when a lack of electron donor became noticeable (Finke et al. 2007, Michaud et al. 2020), indicating that an important part of the process could not be identified and was therefore not taken into consideration.

Identification of responsible microorganisms

Next to these questions about geochemical and biogeochemical rates, there is the contribution and identity of the associated microorganisms, which were often neglected in these studies (e.g., Finke et al. 2007, Michaud et al. 2020, Herbert et al. 2021). Nowadays, next generation sequencing enables large scale studies, exploring microbial diversity and function globally in the marine environment (Louca et al. 2016). Furthermore, high sensitive methods, such as RNA stable isotope probing (SIP), enables to identify microorganisms associated with more or less known metabolic pathways without the need of pure cultures (Dumont and Murrell 2005). Substrates, labeled with stable isotopes, e.g., ^{13}C-carbon or ^{18}O-water, are supplied and active organisms incorporate them into their RNA and, over longer time, DNA; nucleic acids are extracted, density separated and sequenced, identifying microorganisms in heavy, i.e., labeled, fractions as the ones which utilized the substrates (Dumont and Murrell 2005, Schwartz 2007).

In summary, organic matter mineralization to CO_2 in marine sediments is an important part of the global carbon cycle. Acetate is a major intermediate of the degradation process and its oxidation can be coupled to different terminal electron acceptors such as metal oxides or sulfate. These degradation processes can be masked by complex interactions of compounds in

the sediments. Quantification of the contribution of different terminal electron-accepting processes is a difficult task and the associated microbial community is often unknown.

1.3 Study sites

The sites investigated in this thesis were both located in the high latitudes of the Southern Hemisphere (Figure 2b); (1) fjords and troughs around the sub-Antarctic island South Georgia (Figure 2a) and (2) Potter Cove at the Antarctic King George Island/Isla 25 de Mayo, at the tip of the West Antarctic Peninsula (Figure 2d). South Georgia, isolated in the Southern Atlantic, serves as a hotspot of iron supply, fueling large phytoplankton blooms south of the island (Atkinson et al. 2001, Schlosser et al. 2018). Thus, the shelf areas were also characterized by high organic matter content (0.65 wt.%) and active methane seepage was found around the island and within the fjords (Geprägs et al. 2016). Especially, sediments in the fjords were characterized by high iron content (~ 0.6 mol/kg), fueled by many glaciers running off the island (Hodgson et al. 2014, Schlosser et al. 2018, Schnakenberg et al. 2021). One main fjord investigated in this thesis was Cumberland Bay (South Georgia), which is highly influenced by the large tidewater Nordenskjöld glacier terminating into the investigated arm of the fjord (Figure 3c; Hodgson et al. 2014)). As most glaciers on the globe, also this glacier shows accelerating retreat due to global warming (Berg et al. 2021). Furthermore, Cumberland Bay was affected by intense whaling in the last century, which supplied more organic matter as found in deeper sediment layers and potentially more iron originating from the blood of whales (Majewski et al. 2024). Before the project of this thesis, only the microbial community of deeper sediments was investigated for few locations around South Georgia (Schnakenberg et al. 2021), but the microbial community associated with organic matter degradation processes in surface sediments was unknown.

The second sampling site Potter Cove is a wide, at the head relatively shallow bay influenced by the Fourcade Glacier (Figure 2e), which retreats rapidly and recently transformed from marine- to land-terminating (Rückamp et al. 2011, Meredith et al. 2018). Subglacial and surficial meltwater supplies large amount of iron oxides into the sediments of the bay, fueling iron reduction especially in sediments close to the glacier (Monien et al. 2014, Monien et al. 2017, Henkel et al. 2018). Similarly to South Georgia, King George Island fertilizes the surrounding ocean with iron (Hopkinson et al. 2007, Ardelan et al. 2010). The bay is mixed vertically by wind and horizontally by a cyclonic current that brings in water from outside the bay, flows along the glacier front to the southern coast and transports material out of the bay again (Meredith et al. 2018, Torre et al. 2021). Pelagic and benthic fauna, flora and

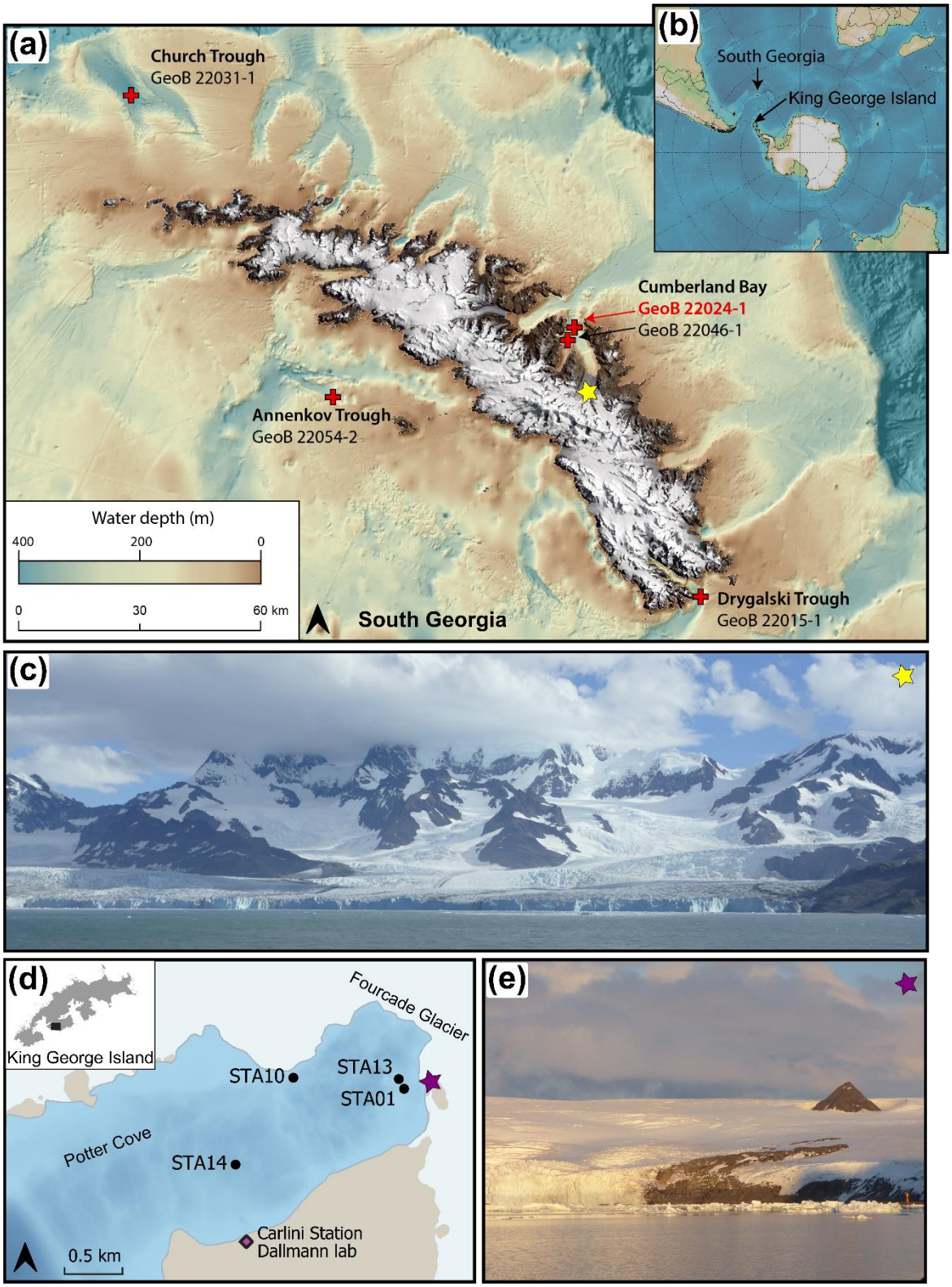

Figure 3: Overview of glacial influenced sampling locations. (**a**) Map of South Georgia with indicated sampling locations, star represents location of picture **c**, map modified from chapter 2. (**b**) Overview map. (**c**) Tidewater Nordenskjöld Glacier at head of Cumberland Bay, provided by L.C. Wunder. (**d**) Map of Potter Cove with indicated sampling sites, star represents location of picture **e**. (**e**) Land-terminating Fourcade Glacier at head of Potter Cove, provided by G. Willis-Poratti. Note that the height of the glacier terminus in picture **c** (Cumberland Bay) is ~ 30-40 m and that in picture **e** (Potter Cove) is ~ 15 m.

microorganisms were investigated over the years (Hernández et al. 2015, Pasotti et al. 2015a, Abele et al. 2017). Multiple food-web models were constructed showing macroalgae as the main primary producers in this environment (Quartino and Boraso de Zaixso 2008, Pasotti et al. 2015b, Braeckman et al. 2024), but all these studies did not take the microbial community into account, which were responsible for degrading organic matter in the anoxic sediments. During the duration of this thesis, the influence of macroalgae addition on the anoxic microbial community was shown, which stimulated iron reduction and showed a new family of iron reducing bacteria (Aromokeye et al. 2021). Still, the identity of the microbial community in the anoxic surface sediments was so far unknown.

1.4 Aims of the thesis

The aim of this thesis was to identify terminal electron-accepting processes and associated microbial communities, which were relevant for acetate degradation in glacial influenced sediments. Furthermore, I investigated the effect of climate change based environmental factors such as changing nutrient supply and temperature on biogeochemical processes and microorganisms involved. For this, two sites with permanently cold sediments were selected, Cumberland Bay at South Georgia, and Potter Cove at King George Island/Isla 25 de Mayo, West Antarctic Peninsula. Glacial supplied metal oxides (iron, manganese) were tested in comparison to sulfate as typical electron acceptor in anoxic surface sediments. A combination of simple slurry incubations and incubations with ^{13}C-labeled acetate or dissolved inorganic carbon for RNA-stable isotope probing were conducted. Resulting processes were monitored by qualitative geochemical measurements of compounds in the supernatant and quantitative sulfate reduction rate measurements using ^{35}S-sulfate. The active community was investigated by 16S rRNA and 16S rRNA gene amplicon sequencing on fractionated and not-fractionated samples. I raised the following hypotheses to be answered in this thesis:

(1) In glacial influenced sediments, the microbial community is adapted to fresh supply of metal oxides as electron acceptors.
(2) Similar communities are shaped by the same electron-accepting process at different sampling sites with similar geochemical settings, even compared to Arctic locations.
(3) All electron acceptors tested in this study, iron oxides, manganese oxides and sulfate, are utilized for the oxidation of acetate by microorganisms.
(4) Nutrient supply and temperature impact the dominating terminal electron-accepting process and the activated microbial community.

1.5 References

Abele, D., S. Vazquez, A. G. J. Buma, E. Hernandez, C. Quiroga, C. Held, S. Frickenhaus, L. Harms, J. L. Lopez, E. Helmke, and W. P. Mac Cormack. (2017). Pelagic and benthic communities of the Antarctic ecosystem of Potter Cove: Genomics and ecological implications. Mar. Genomics **33**:1-11. doi:10.1016/j.margen.2017.05.001.

Ardelan, M. V., O. Holm-Hansen, C. D. Hewes, C. S. Reiss, N. S. Silva, H. Dulaiova, E. Steinnes, and E. Sakshaug. (2010). Natural iron enrichment around the Antarctic Peninsula in the Southern Ocean. Biogeosciences **7**:11-25. doi:10.5194/bg-7-11-2010.

Arndt, S., B. B. Jørgensen, D. E. LaRowe, J. Middelburg, R. Pancost, and P. Regnier. (2013). Quantifying the degradation of organic matter in marine sediments: A review and synthesis. Earth-Sci. Rev. **123**:53-86. doi:10.1016/j.earscirev.2013.02.008.

Arnosti, C. (2004). Speed bumps and barricades in the carbon cycle: Substrate structural effects on carbon cycling. Mar. Chem. **92**:263-273. doi:10.1016/j.marchem.2004.06.030.

Arnosti, C. (2011). Microbial extracellular enzymes and the marine carbon cycle. Annu. Rev. Mar. Sci. **3**:401-425. doi:10.1146/annurev-marine-120709-142731.

Aromokeye, D. A., G. Willis-Poratti, L. C. Wunder, X. Yin, J. Wendt, T. Richter-Heitmann, S. Henkel, S. Vázquez, M. Elvert, W. Mac Cormack, and M. W. Friedrich. (2021). Macroalgae degradation promotes microbial iron reduction via electron shuttling in coastal Antarctic sediments. Environ. Int. **156**:106602. doi:10.1016/j.envint.2021.106602.

Atkinson, A., M. J. Whitehouse, J. Priddle, G. C. Cripps, P. Ward, and M. A. Brandon. (2001). South Georgia, Antarctica: A productive, cold water, pelagic ecosystem. Mar. Ecol. Prog. Ser. **216**:279-308. doi:10.3354/meps216279.

Beam, J. P., J. J. Scott, S. M. McAllister, C. S. Chan, J. McManus, F. J. R. Meysman, and D. Emerson. (2018). Biological rejuvenation of iron oxides in bioturbated marine sediments. ISME J. **12**:1389-1394. doi:10.1038/s41396-017-0032-6.

Beer, C., M. Reichstein, E. Tomelleri, P. Ciais, M. Jung, N. Carvalhais, C. Rödenbeck, M. A. Arain, D. Baldocchi, G. B. Bonan, A. Bondeau, A. Cescatti, G. Lasslop, A. Lindroth, M. Lomas, S. Luyssaert, H. Margolis, K. W. Oleson, O. Roupsard, E. Veenendaal, N. Viovy, C. Williams, F. I. Woodward, and D. Papale. (2010). Terrestrial gross carbon dioxide uptake: Global distribution and covariation with climate. Science **329**:834-838. doi:10.1126/science.1184984.

Berg, S., S. Jivcov, S. Kusch, G. Kuhn, D. White, G. Bohrmann, M. Melles, and J. Rethemeyer. (2021). Increased petrogenic and biospheric organic carbon burial in sub-Antarctic fjord sediments in response to recent glacier retreat. Limnol. Oceanogr. **66**:4347-4362. doi:10.1002/lno.11965.

Beulig, F., H. Røy, C. Glombitza, and B. B. Jørgensen. (2018). Control on rate and pathway of anaerobic organic carbon degradation in the seabed. Proc. Natl. Acad. Sci. USA **115**:367-372. doi:10.1073/pnas.1715789115.

Bonneville, S., P. Van Cappellen, and T. Behrends. (2004). Microbial reduction of iron(III) oxyhydroxides: Effects of mineral solubility and availability. Chem. Geol. **212**:255-268. doi:10.1016/j.chemgeo.2004.08.015.

Bourceau, O. M., T. Ferdelman, G. Lavik, M. Mussmann, M. M. M. Kuypers, and H. K. Marchant. (2023). Simultaneous sulfate and nitrate reduction in coastal sediments. ISME commun. **3**:17. doi:10.1038/s43705-023-00222-y.

Braeckman, U., F. Pasotti, R. Hoffmann, S. Vázquez, A. Wulff, I. R. Schloss, U. Falk, D. Deregibus, N. Lefaible, A. Torstensson, A. Al-Handal, F. Wenzhöfer, and A. Vanreusel. (2021). Glacial melt disturbance shifts community metabolism of an Antarctic seafloor ecosystem from net autotrophy to heterotrophy. Commun. Biol. **4**:148. doi:10.1038/s42003-021-01673-6.

Braeckman, U., K. Soetaert, F. Pasotti, M. L. Quartino, A. Vanreusel, L. A. Saravia, I. R. Schloss, and D. van Oevelen. (2024). Glacial melt impacts carbon flows in an Antarctic benthic food web. Front. Mar. Sci. **11**. doi:10.3389/fmars.2024.1359597.

Burdige, D. J. (2007). Preservation of organic matter in marine sediments: Controls, mechanisms, and an imbalance in sediment organic carbon budgets? Chem. Rev. **107**:467-485. doi:10.1021/cr050347q.

Campana, G. L., K. Zacher, D. Deregibus, F. R. Momo, C. Wiencke, and M. L. Quartino. (2018). Succession of Antarctic benthic algae (Potter Cove, South Shetland Islands): Structural patterns and glacial impact over a four-year period. Polar Biol. **41**:377-396. doi:10.1007/s00300-017-2197-x.

Canfield, D. E., B. B. Jørgensen, H. Fossing, R. Glud, J. Gundersen, N. B. Ramsing, B. Thamdrup, J. W. Hansen, L. P. Nielsen, and P. O. J. Hall. (1993a). Pathways of organic carbon oxidation in three continental margin sediments. Mar. Geol. **113**:27-40. doi:10.1016/0025-3227(93)90147-N.

Canfield, D. E., F. J. Stewart, B. Thamdrup, L. De Brabandere, T. Dalsgaard, E. F. Delong, N. P. Revsbech, and O. Ulloa. (2010). A cryptic sulfur cycle in oxygen-minimum-zone waters off the Chilean coast. Science **330**:1375-1378. doi:10.1126/science.1196889.

Canfield, D. E. and B. Thamdrup. (2009). Towards a consistent classification scheme for geochemical environments, or, why we wish the term 'suboxic' would go away. Geobiology **7**:385-392. doi:10.1111/j.1472-4669.2009.00214.x.

Canfield, D. E., B. Thamdrup, and J. W. Hansen. (1993b). The anaerobic degradation of organic matter in Danish coastal sediments: Iron reduction, manganese reduction, and sulfate reduction. Geochim. Cosmochim. Acta **57**:3867-3883. doi:10.1016/0016-7037(93)90340-3.

Casado, M., R. Hébert, D. Faranda, and A. Landais. (2023). The quandary of detecting the signature of climate change in Antarctica. Nat. Clim. Chang. **13**:1082-1088. doi:10.1038/s41558-023-01791-5.

Cho, H., B. Kim, J. S. Mok, A. Choi, B. Thamdrup, and J. H. Hyun. (2020). Acetate-utilizing microbial communities revealed by stable-isotope probing in sediment underlying the upwelling system of the Ulleung Basin, East Sea. Mar. Ecol. Prog. Ser. **634**:45-61. doi:10.3354/meps13182.

Ciais, P., C. Sabine, G. Bala, L. Bopp, V. Brovkin, J. Canadell, A. Chhabra, R. DeFries, J. Galloway, M. Heimann, C. Jones, C. Le Quéré, R. B. Myneni, P. S., and T. P. (2013). Carbon and Other Biogeochemical Cycles. *in* T. F. Stocker, D. Qin, G.-K. Plattner, M. Tignor, S. K. Allen, J. Boschung, A. Nauels, Y. Xia, V. Bex, and P. M. Midgley, editors. Climate Change 2013: The Physical Science Basis. Working Group I Contribution to the Fifth Assessment Report of the Intergovernmental Panel on Climate Change. Cambridge University Press, Cambridge, United Kingdom and New York, NY, USA. p. 465-570. doi:10.1017/CBO9781107415324.015.

Cook, A. J., P. R. Holland, M. P. Meredith, T. Murray, A. Luckman, and D. G. Vaughan. (2016). Ocean forcing of glacier retreat in the western Antarctic Peninsula. Science **353**:283-286. doi:10.1126/science.aae0017.

Deregibus, D., G. L. Campana, C. Neder, D. K. A. Barnes, K. Zacher, J. M. Piscicelli, K. Jerosch, and M. L. Quartino. (2023). Potential macroalgal expansion and blue carbon gains with northern Antarctic Peninsula glacial retreat. Mar. Environ. Res. **189**:106056. doi:10.1016/j.marenvres.2023.106056.

Deregibus, D., M. L. Quartino, K. Zacher, G. L. Campana, and D. K. A. Barnes. (2017). Understanding the link between sea ice, ice scour and Antarctic benthic biodiversity – The need for cross-station and international collaboration. Polar Rec. **53**:143-152. doi:10.1017/S0032247416000875.

Diaz, R. J. and R. Rosenberg. (2008). Spreading dead zones and consequences for marine ecosystems. Science **321**:926-929. doi:10.1126/science.1156401.

Doney, S. C., V. J. Fabry, R. A. Feely, and J. A. Kleypas. (2009). Ocean acidification: The other CO_2 problem. Annu. Rev. Mar. Sci. **1**:169-192. doi:10.1146/annurev.marine.010908.163834.

Dumont, M. G. and J. C. Murrell. (2005). Stable isotope probing – Linking microbial identity to function. Nat. Rev. Microbiol. **3**:499-504. doi:10.1038/nrmicro1162.

Dyksma, S., S. Lenk, J. E. Sawicka, and M. Mußmann. (2018). Uncultured *Gammaproteobacteria* and *Desulfobacteraceae* account for major acetate assimilation in a coastal marine sediment. Front. Microbiol. **9**. doi:10.3389/fmicb.2018.03124.

Findlay, A. J., A. Pellerin, K. Laufer, and B. B. Jørgensen. (2020). Quantification of sulphide oxidation rates in marine sediment. Geochim. Cosmochim. Acta **280**:441-452. doi:10.1016/j.gca.2020.04.007.

Finke, N. and B. B. Jørgensen. (2008). Response of fermentation and sulfate reduction to experimental temperature changes in temperate and Arctic marine sediments. ISME J. **2**:815-829. doi:10.1038/ismej.2008.20.

Finke, N., V. Vandieken, and B. B. Jørgensen. (2007). Acetate, lactate, propionate, and isobutyrate as electron donors for iron and sulfate reduction in Arctic marine sediments, Svalbard. FEMS Microbiol. Ecol. **59**:10-22. doi:10.1111/j.1574-6941.2006.00214.x.

Fossing, H. and B. B. Jørgensen. (1990). Isotope exchange reactions with radiolabeled sulfur compounds in anoxic seawater. Biogeochemistry **9**:223-245. doi:10.1007/BF00000600.

Fossing, H., S. Thode-Andersen, and B. B. Jørgensen. (1992). Sulfur isotope exchange between ^{35}S-labeled inorganic sulfur compounds in anoxic marine sediments. Mar. Chem. **38**:117-132. doi:10.1016/0304-4203(92)90071-H.

Fox-Kemper, B., H. T. Hewitt, C. Xiao, G. Aðalgeirsdóttir, S. S. Drijfhout, T. L. Edwards, N. R. Golledge, M. Hemer, R. E. Kopp, G. Krinner, A. Mix, D. Notz, S. Nowicki, I. S. Nurhati, L. Ruiz, J.-B. Sallée, A. B. A. Slangen, and Y. Yu. (2021). Ocean, Cryosphere and Sea Level Change. *in* V. Masson-Delmotte, P. Zhai, A. Pirani, S. L. Connors, C. Péan, S. Berger, N. Caud, Y. Chen, L. Goldfarb, M. I. Gomis, M. Huang, K. Leitzell, E. Lonnoy, J. B. R. Matthews, T. K. Maykock, T. Waterfield, O. Yelekçi, R. Yu, and B. Zhou, editors. Climate Change 2021: The Physical Science Basis. Contribution of Working Group I to the Sixth Assessment Report of the Intergovernmental Panel on Climate Change. Cambridge University Press, Cambridge, United Kingdom and New York, NY, USA. p. 1211-1362. doi:10.1017/9781009157896.011.

Francelino, M. R., C. Schaefer, M. d. L. M. Skansi, S. Colwell, D. H. Bromwich, P. Jones, J. C. King, M. A. Lazzara, J. Renwick, S. Solomon, M. Brunet, and R. S. Cerveny. (2021). WMO evaluation of two extreme high temperatures occurring in February 2020 for the Antarctic Peninsula Region. BAMS **102**:E2053-E2061. doi:10.1175/BAMS-D-21-0040.1.

Froelich, P. N., G. P. Klinkhammer, M. L. Bender, N. A. Luedtke, G. R. Heath, D. Cullen, P. Dauphin, D. Hammond, B. Hartman, and V. Maynard. (1979). Early oxidation of organic matter in pelagic sediments of the eastern equatorial Atlantic: Suboxic diagenesis. Geochim. Cosmochim. Acta **43**:1075-1090. doi:10.1016/0016-7037(79)90095-4.

Gao, K., J. Beardall, D.-P. Häder, J. M. Hall-Spencer, G. Gao, and D. A. Hutchins. (2019). Effects of ocean acidification on marine photosynthetic organisms under the concurrent influences of warming, UV radiation, and deoxygenation. Front. Mar. Sci. **6**. doi:10.3389/fmars.2019.00322.

Geprägs, P., M. E. Torres, S. Mau, S. Kasten, M. Römer, and G. Bohrmann. (2016). Carbon cycling fed by methane seepage at the shallow Cumberland Bay, South Georgia, sub-Antarctic. Geochemistry, Geophys. Geosystems **17**:1401-1418. doi:10.1002/2016gc006276.

Glasby, G. P. (2006). Manganese: Predominant Role of Nodules and Crusts. *in* H. D. Schulz and M. Zabel, editors. Marine Geochemistry. Springer-Verlag Berlin Heidelberg, Berlin Heidelberg, Germany. p. 371-427. doi:10.1007/3-540-32144-6_11.

Gleckler, P. J., P. J. Durack, R. J. Stouffer, G. C. Johnson, and C. E. Forest. (2016). Industrial-era global ocean heat uptake doubles in recent decades. Nat. Clim. Chang. **6**:394-398. doi:10.1038/nclimate2915.

Glombitza, C., M. Egger, H. Røy, and B. B. Jørgensen. (2019). Controls on volatile fatty acid concentrations in marine sediments (Baltic Sea). Geochim. Cosmochim. Acta **258**:226-241. doi:10.1016/j.gca.2019.05.038.

Glombitza, C., M. Jaussi, H. Røy, M.-S. Seidenkrantz, B. Lomstein, and B. Jørgensen. (2015). Formate, acetate, and propionate as substrates for sulfate reduction in sub-Arctic sediments of Southwest Greenland. Front. Microbiol. **6**. doi:10.3389/fmicb.2015.00846.

Gorodetskaya, I. V., C. Durán-Alarcón, S. González-Herrero, K. R. Clem, X. Zou, P. Rowe, P. Rodriguez Imazio, D. Campos, C. Leroy-Dos Santos, N. Dutrievoz, J. D. Wille, A. Chyhareva, V. Favier, J. Blanchet, B. Pohl, R. R. Cordero, S.-J. Park, S. Colwell, M. A. Lazzara, J. Carrasco, A. M. Gulisano, S. Krakovska, F. M. Ralph, T. Dethinne, and G. Picard. (2023). Record-high Antarctic Peninsula temperatures and surface melt in February 2022: A compound event with an intense atmospheric river. npj Clim. Atmos. Sci. **6**:202. doi:10.1038/s41612-023-00529-6.

Gruber, N., D. Clement, B. R. Carter, R. A. Feely, S. van Heuven, M. Hoppema, M. Ishii, R. M. Key, A. Kozyr, S. K. Lauvset, C. Lo Monaco, J. T. Mathis, A. Murata, A. Olsen, F. F. Perez, C. L. Sabine, T. Tanhua, and R. Wanninkhof. (2019). The oceanic sink for anthropogenic CO_2 from 1994 to 2007. Science **363**:1193-1199. doi:10.1126/science.aau5153.

Gulev, S. K., P. W. Thorne, J. Ahn, F. J. Dentener, C. M. Domingues, S. Gerland, D. Gong, D. S. Kaufman, H. C. Nnamchi, J. Quaas, J. A. Rivera, S. Sathyendranath, S. L. Smith, B. Trewin, K. von Schuckmann, and R. S. Vose. (2021). Changing State of the Climate System. *in* V. Masson-Delmotte, P. Zhai, A. Pirani, S. L. Connors, C. Péan, S. Berger, N. Caud, Y. Chen, L. Goldfarb, M. I. Gomis, M. Huang, K. Leitzell, E. Lonnoy, J. B. R. Matthews, T. K. Maykock, T. Waterfield, O. Yelekçi, R. Yu, and B. Zhou, editors. Climate Change 2021: The Physical Science Basis. Contribution of Working Group I to the Sixth Assessment Report of the Intergovernmental Panel on Climate Change. Cambridge University Press, Cambridge, United Kingdom and New York, NY, USA. p. 287-422. doi:10.1017/9781009157896.004.

Haumann, F. A., N. Gruber, and M. Münnich. (2020). Sea-ice induced Southern Ocean subsurface warming and surface cooling in a warming climate. AGU adv. **1**:e2019AV000132. doi:10.1029/2019AV000132.

Hawkings, J. R., J. L. Wadham, M. Tranter, R. Raiswell, L. G. Benning, P. J. Statham, A. Tedstone, P. Nienow, K. Lee, and J. Telling. (2014). Ice sheets as a significant source of highly reactive nanoparticulate iron to the oceans. Nat. Commun. **5**:3929. doi:10.1038/ncomms4929.

Hegerl, G. C., H. von Storch, K. Hasselmann, B. D. Santer, U. Cubasch, and P. D. Jones. (1996). Detecting greenhouse-gas-induced climate change with an optimal fingerprint method. J. Clim. **9**:2281-2306. doi:10.1175/1520-0442(1996)009<2281:DGGICC>2.0.CO;2.

Henkel, S., S. Kasten, J. F. Hartmann, A. Silva-Busso, and M. Staubwasser. (2018). Iron cycling and stable Fe isotope fractionation in Antarctic shelf sediments, King George Island. Geochim. Cosmochim. Acta **237**:320-338. doi:10.1016/j.gca.2018.06.042.

Herbert, L. C., N. Riedinger, A. B. Michaud, K. Laufer, H. Røy, B. B. Jørgensen, C. Heilbrun, R. C. Aller, J. K. Cochran, and L. M. Wehrmann. (2020). Glacial controls on redox-sensitive trace element cycling in Arctic fjord sediments (Spitsbergen, Svalbard). Geochim. Cosmochim. Acta **271**:33-60. doi:10.1016/j.gca.2019.12.005.

Herbert, L. C., Q. Zhu, A. B. Michaud, K. Laufer-Meiser, C. K. Jones, N. Riedinger, Z. S. Stooksbury, R. C. Aller, B. B. Jørgensen, and L. M. Wehrmann. (2021). Benthic iron flux influenced by climate-sensitive interplay between organic carbon availability and sedimentation rate in Arctic fjords. Limnol. Oceanogr. **66**:3374-3392. doi:10.1002/lno.11885.

Hernández, E. A., A. M. T. Piquet, J. L. Lopez, A. G. J. Buma, and W. P. Mac Cormack. (2015). Marine archaeal community structure from Potter Cove, Antarctica: High temporal and spatial dominance of the phylum Thaumarchaeota. Polar Biol. **38**:117-130. doi:10.1007/s00300-014-1569-8.

Hodgson, D. A., A. G. C. Graham, H. J. Griffiths, S. J. Roberts, C. Ó. Cofaigh, M. J. Bentley, and D. J. A. Evans. (2014). Glacial history of sub-Antarctic South Georgia based on the submarine geomorphology of its fjords. Quat. Sci. Rev. **89**:129-147. doi:10.1016/j.quascirev.2013.12.005.

Hodson, A., A. Nowak, M. Sabacka, A. Jungblut, F. Navarro, D. Pearce, M. L. Ávila-Jiménez, P. Convey, and G. Vieira. (2017). Climatically sensitive transfer of iron to maritime Antarctic ecosystems by surface runoff. Nat. Commun. **8**:14499. doi:10.1038/ncomms14499.

Hopkinson, B. M., B. G. Mitchell, R. A. Reynolds, H. Wang, K. E. Selph, C. I. Measures, C. D. Hewes, O. Holm-Hansen, and K. A. Barbeau. (2007). Iron limitation across chlorophyll gradients in the southern Drake Passage: Phytoplankton responses to iron addition and photosynthetic indicators of iron stress. Limnol. Oceanogr. **52**:2540-2554. doi:10.4319/lo.2007.52.6.2540.

Hoshiba, Y., Y. Matsumura, N. Kanna, Y. Ohashi, and S. Sugiyama. (2024). Impacts of glacial discharge on the primary production in a Greenlandic fjord. Sci. Rep. **14**:15530. doi:10.1038/s41598-024-64529-z.

Ijiri, A., N. Harada, A. Hirota, U. Tsunogai, N. O. Ogawa, T. Itaki, B.-K. Khim, and M. Uchida. (2012). Biogeochemical processes involving acetate in sub-seafloor sediments from the Bering Sea shelf break. Org. Geochem. **48**:47-55. doi:10.1016/j.orggeochem.2012.04.004.

IPCC. (2023). Climate Change 2023: Synthesis Report. Contribution of Working Groups I, II and III to the Sixth Assessment Report of the Intergovernmental Panel on Climate Change. Geneva, Switzerland.

Jensen, M. M., B. Thamdrup, S. Rysgaard, M. Holmer, and H. Fossing. (2003). Rates and regulation of microbial iron reduction in sediments of the Baltic-North Sea transition. Biogeochemistry **65**:295-317. doi:10.1023/A:1026261303494.

Jones, M. E., D. H. Bromwich, J. P. Nicolas, J. Carrasco, E. Plavcová, X. Zou, and S.-H. Wang. (2019). Sixty years of widespread warming in the southern middle and high latitudes (1957–2016). J. Clim. **32**:6875-6898. doi:10.1175/JCLI-D-18-0565.1.

Jørgensen, B. B. (1982). Mineralization of organic matter in the sea bed – The role of sulphate reduction. Nature **296**:643-645. doi:10.1038/296643a0.

Jørgensen, B. B. (1990). A thiosulfate shunt in the sulfur cycle of marine sediments. Science **249**:152-154. doi:10.1126/science.249.4965.152.

Jørgensen, B. B. and F. Bak. (1991). Pathways and microbiology of thiosulfate transformations and sulfate reduction in a marine sediment (Kattegat, Denmark). Appl. Environ. Microbiol. **57**:847-856. doi:10.1128/aem.57.3.847-856.1991.

Jørgensen, B. B., A. J. Findlay, and A. Pellerin. (2019). The biogeochemical sulfur cycle of marine sediments. Front. Microbiol. **10**:849. doi:10.3389/fmicb.2019.00849.

Jørgensen, B. B., K. Laufer, A. B. Michaud, and L. M. Wehrmann. (2020). Biogeochemistry and microbiology of high Arctic marine sediment ecosystems – Case study of Svalbard fjords. Limnol. Oceanogr. **66**:S273-S292. doi:10.1002/lno.11551.

Jørgensen, B. B. and D. C. Nelson. (2004). Sulfide Oxidation in Marine Sediments: Geochemistry Meets Microbiology. *in* J. P. Amend, K. J. Edwards, and T. W. Lyons, editors. Sulfur Biogeochemistry - Past and Present. Geological Society of America. p. 63-81. doi:10.1130/0-8137-2379-5.63.

Jørgensen, B. B. and R. J. Parkes. (2010). Role of sulfate reduction and methane production by organic carbon degradation in eutrophic fjord sediments (Limfjorden, Denmark). Limnol. Oceanogr. **55**:1338-1352. doi:10.4319/lo.2010.55.3.1338.

Kennedy, J. J., N. A. Rayner, C. P. Atkinson, and R. E. Killick. (2019). An ensemble data set of sea surface temperature change from 1850: The Met Office Hadley Centre HadSST.4.0.0.0 data set. J. Geophys. Res. (D Atmos.) **124**:7719-7763. doi:10.1029/2018JD029867.

Kristensen, E. and M. Holmer. (2001). Decomposition of plant materials in marine sediment exposed to different electron acceptors (O_2, NO_3^-, and SO_4^{2-}), with emphasis on substrate origin, degradation kinetics, and the role of bioturbation. Geochim. Cosmochim. Acta **65**:419-433. doi:10.1016/S0016-7037(00)00532-9.

LaRowe, D. E., S. Arndt, J. A. Bradley, E. R. Estes, A. Hoarfrost, S. Q. Lang, K. G. Lloyd, N. Mahmoudi, W. D. Orsi, S. R. Shah Walter, A. D. Steen, and R. Zhao. (2020). The fate of organic carbon in marine sediments – New insights from recent data and analysis. Earth-Sci. Rev. **204**:103146. doi:10.1016/j.earscirev.2020.103146.

Latorre, M. P., C. M. Iachetti, I. R. Schloss, J. Antoni, A. Malits, F. de la Rosa, M. De Troch, M. D. Garcia, X. Flores-Melo, S. I. Romero, M. N. Gil, and M. Hernando. (2023). Summer heatwaves affect coastal Antarctic plankton metabolism and community structure. J. Exp. Mar. Biol. Ecol. **567**:151926. doi:10.1016/j.jembe.2023.151926.

Laufer-Meiser, K., A. B. Michaud, M. Maisch, J. M. Byrne, A. Kappler, M. O. Patterson, H. Røy, and B. B. Jørgensen. (2021). Potentially bioavailable iron produced through benthic cycling in glaciated Arctic fjords of Svalbard. Nat. Commun. **12**:1349. doi:10.1038/s41467-021-21558-w.

Laufer, K., J. M. Byrne, C. Glombitza, C. Schmidt, B. B. Jørgensen, and A. Kappler. (2016). Anaerobic microbial Fe(II) oxidation and Fe(III) reduction in coastal marine sediments controlled by organic carbon content. Environ. Microbiol. **18**:3159-3174. doi:10.1111/1462-2920.13387.

Laufer, K., A. B. Michaud, H. Røy, and B. B. Jørgensen. (2020). Reactivity of iron minerals in the seabed toward microbial reduction – A comparison of different extraction techniques. Geomicrobiol. J. **37**:170-189. doi:10.1080/01490451.2019.1679291.

Li, Q., J. Marshall, C. D. Rye, A. Romanou, D. Rind, and M. Kelley. (2023). Global climate impacts of Greenland and Antarctic meltwater: A comparative study. J. Clim. **36**:3571-3590. doi:10.1175/JCLI-D-22-0433.1.

Liang, Q.-Y., J.-Y. Zhang, D. Ning, W.-X. Yu, G.-J. Chen, X. Tao, J. Zhou, Z.-J. Du, and D.-S. Mu. (2023). Niche modification by sulfate-reducing bacteria drives microbial community assembly in anoxic marine sediments. Mbio **14**:e03535-03522. doi:10.1128/mbio.03535-22.

Louca, S., L. W. Parfrey, and M. Doebeli. (2016). Decoupling function and taxonomy in the global ocean microbiome. Science **353**:1272-1277. doi:10.1126/science.aaf4507.

Lovley, D. R. and S. Goodwin. (1988). Hydrogen concentrations as an indicator of the predominant terminal electron-accepting reactions in aquatic sediments. Geochim. Cosmochim. Acta **52**:2993-3003. doi:10.1016/0016-7037(88)90163-9.

Luther, G. W., A. J. Findlay, D. J. MacDonald, S. M. Owings, T. E. Hanson, R. A. Beinart, and P. R. Girguis. (2011). Thermodynamics and kinetics of sulfide oxidation by oxygen: A look at inorganically controlled reactions and biologically mediated processes in the environment. Front. Microbiol. **2**. doi:10.3389/fmicb.2011.00062.

Majewski, W., W. Szczuciński, J. Pawłowska, M. Szymczak-Żyła, L. Lubecki, and P. Niedzielski. (2024). Environmental degradation and recovery after termination of whaling in sub-Antarctic fjord, South Georgia. Sci. Total Environ. **957**:177536. doi:10.1016/j.scitotenv.2024.177536.

Manabe, S. and R. T. Wetherald. (1975). The effects of doubling the CO_2 concentration on the climate of a general circulation model. J. Atmos. Sci. **32**:3-15. doi:10.1175/1520-0469(1975)032<0003:TEODTC>2.0.CO;2.

Martin, J. H., S. E. Fitzwater, and R. M. Gordon. (1990). Iron deficiency limits phytoplankton growth in Antarctic waters. Global Biogeochem. Cycles **4**:5-12. doi:10.1029/GB004i001p00005.

Meire, L., J. Mortensen, P. Meire, T. Juul-Pedersen, M. K. Sejr, S. Rysgaard, R. Nygaard, P. Huybrechts, and F. J. R. Meysman. (2017). Marine-terminating glaciers sustain high productivity in Greenland fjords. Global Change Biol. **23**:5344-5357. doi:10.1111/gcb.13801.

Meredith, M. P., U. Falk, A. V. Bers, A. Mackensen, I. R. Schloss, E. Ruiz Barlett, K. Jerosch, A. Silva Busso, and D. Abele. (2018). Anatomy of a glacial meltwater discharge event in an Antarctic cove. Philos. Trans. Royal Soc. A **376**:20170163. doi:10.1098/rsta.2017.0163.

Meysman, F. J. R. (2018). Cable bacteria take a new breath using long-distance electricity. Trends Microbiol. **26**:411-422. doi:10.1016/j.tim.2017.10.011.

Michaud, A. B., K. Laufer, A. Findlay, A. Pellerin, G. Antler, A. V. Turchyn, H. Røy, L. M. Wehrmann, and B. B. Jørgensen. (2020). Glacial influence on the iron and sulfur cycles in Arctic fjord sediments (Svalbard). Geochim. Cosmochim. Acta **280**:423-440. doi:10.1016/j.gca.2019.12.033.

Middelburg, J. J. (2011). Chemoautotrophy in the ocean. Geophys. Res. Lett. **38**. doi:10.1029/2011GL049725.

Milner, A. M., K. Khamis, T. J. Battin, J. E. Brittain, N. E. Barrand, L. Füreder, S. Cauvy-Fraunié, G. M. Gíslason, D. Jacobsen, D. M. Hannah, A. J. Hodson, E. Hood, V. Lencioni, J. S. Ólafsson, C. T. Robinson, M. Tranter, and L. E. Brown. (2017). Glacier shrinkage driving global changes in downstream systems. Proc. Natl. Acad. Sci. USA **114**:9770-9778. doi:10.1073/pnas.1619807114.

Monien, D., P. Monien, R. Brünjes, T. Widmer, A. Kappenberg, A. A. Silva Busso, B. Schnetger, and H.-J. Brumsack. (2017). Meltwater as a source of potentially bioavailable iron to Antarctica waters. Antarct. Sci. **29**:277-291. doi:10.1017/S095410201600064X.

Monien, P., K. A. Lettmann, D. Monien, S. Asendorf, A.-C. Wölfl, C. H. Lim, J. Thal, B. Schnetger, and H.-J. Brumsack. (2014). Redox conditions and trace metal cycling in coastal sediments from the maritime Antarctic. Geochim. Cosmochim. Acta **141**:26-44. doi:10.1016/j.gca.2014.06.003.

Na, H., M. A. Lever, K. U. Kjeldsen, F. Schulz, and B. B. Jørgensen. (2015). Uncultured *Desulfobacteraceae* and Crenarchaeotal group C3 incorporate ^{13}C-acetate in coastal marine sediment. Environ. Microbiol. Rep. **7**:614-622. doi:10.1111/1758-2229.12296.

Neder, C., V. Fofonova, A. Androsov, I. Kuznetsov, D. Abele, U. Falk, I. R. Schloss, R. Sahade, and K. Jerosch. (2022). Modelling suspended particulate matter dynamics at an Antarctic fjord impacted by glacier melt. J. Mar. Syst. **231**:103734. doi:10.1016/j.jmarsys.2022.103734.

Overland, J. E., T. J. Ballinger, E. Hanna, I. Hanssen-Bauer, S.-J. Kim, J. E. Walsh, M. Wang, U. S. Bhatt, and R. L. Thoman. (2020). Surface Air Temperature. *in* J. Richter-Menge and M. L. Druckenmiller, editors. State of the Climate in 2019. Bull. Amer. Meteor. Soc. p. S246-S249. doi:10.1175/BAMS-D-20-0086.1.

Parkinson, C. L. (2019). A 40-y record reveals gradual Antarctic sea ice increases followed by decreases at rates far exceeding the rates seen in the Arctic. Proc. Natl. Acad. Sci. USA **116**:14414-14423. doi:doi:10.1073/pnas.1906556116.

Pasotti, F., E. Manini, D. Giovannelli, A.-C. Wölfl, D. Monien, E. Verleyen, U. Braeckman, D. Abele, and A. Vanreusel. (2015a). Antarctic shallow water benthos in an area of recent rapid glacier retreat. Mar. Ecol. **36**:716-733. doi:10.1111/maec.12179.

Pasotti, F., L. A. Saravia, M. De Troch, M. S. Tarantelli, R. Sahade, and A. Vanreusel. (2015b). Benthic trophic interactions in an Antarctic shallow water ecosystem affected by recent glacier retreat. PLoS One **10**:e0141742. doi:10.1371/journal.pone.0141742.

Petro, C., P. Starnawski, A. Schramm, and K. U. Kjeldsen. (2017). Microbial community assembly in marine sediments. Aquat. Microb. Ecol. **79**:177-195. doi:10.3354/ame01826.

Poulton, S. W. and D. E. Canfield. (2005). Development of a sequential extraction procedure for iron: Implications for iron partitioning in continentally derived particulates. Chem. Geol. **214**:209-221. doi:10.1016/j.chemgeo.2004.09.003.

Quartino, M. L. and A. L. Boraso de Zaixso. (2008). Summer macroalgal biomass in Potter Cove, South Shetland Islands, Antarctica: Its production and flux to the ecosystem. Polar Biol. **31**:281-294. doi:10.1007/s00300-007-0356-1.

Quartino, M. L., D. Deregibus, G. L. Campana, G. E. J. Latorre, and F. R. Momo. (2013). Evidence of macroalgal colonization on newly ice-free areas following glacial retreat in Potter Cove (South Shetland Islands), Antarctica. PLoS One **8**:e58223. doi:10.1371/journal.pone.0058223.

Raiswell, R., J. R. Hawkings, L. G. Benning, A. R. Baker, R. Death, S. Albani, N. Mahowald, M. D. Krom, S. W. Poulton, J. Wadham, and M. Tranter. (2016). Potentially bioavailable iron delivery by iceberg-hosted sediments and atmospheric dust to the polar oceans. Biogeosciences **13**:3887-3900. doi:10.5194/bg-13-3887-2016.

Rantanen, M., A. Y. Karpechko, A. Lipponen, K. Nordling, O. Hyvärinen, K. Ruosteenoja, T. Vihma, and A. Laaksonen. (2022). The Arctic has warmed nearly four times faster than the globe since 1979. Commun. Earth Environ. **3**:168. doi:10.1038/s43247-022-00498-3.

Rhein, M., S. R. Rintoul, S. Aoki, E. Campos, D. Chambers, R. A. Feely, S. Gulev, G. C. Johnson, S. A. Josey, A. Kostianoy, C. Mauritzen, D. Roemmich, L. D. Talley, and F. Wang. (2013). Observations: Ocean. *in* T. F. Stocker, D. Qin, G.-K. Plattner, M. Tignor, S. K. Allen, J. Boschung, A. Nauels, Y. Xia, V. Bex, and P. M. Midgley, editors. Climate Change 2013: The Physical Science Basis. Working Group I Contribution to the Fifth Assessment Report of the Intergovernmental Panel on Climate Change. Cambridge University Press, Cambridge, United Kingdom and New York, NY, USA. p. 255-316. doi:10.1017/CBO9781107415324.010.

Rignot, E., J. Mouginot, B. Scheuchl, M. van den Broeke, M. J. van Wessem, and M. Morlighem. (2019). Four decades of Antarctic Ice Sheet mass balance from 1979–2017. Proc. Natl. Acad. Sci. USA **116**:1095-1103. doi:10.1073/pnas.1812883116.

Røy, H., J. Kallmeyer, R. R. Adhikari, R. Pockalny, B. B. Jørgensen, and S. D'Hondt. (2012). Aerobic microbial respiration in 86-million-year-old deep-sea red clay. Science **336**:922-925. doi:10.1126/science.1219424.

Røy, H., H. S. Weber, I. H. Tarpgaard, T. G. Ferdelman, and B. B. Jørgensen. (2014). Determination of dissimilatory sulfate reduction rates in marine sediment via radioactive ^{35}S tracer. Limnol. Oceanogr. Methods **12**:196-211. doi:10.4319/lom.2014.12.196.

Rückamp, M., M. Braun, S. Suckro, and N. Blindow. (2011). Observed glacial changes on the King George Island ice cap, Antarctica, in the last decade. Global Planet. Change **79**:99-109. doi:10.1016/j.gloplacha.2011.06.009.

Sansone, F. J. and C. S. Martens. (1982). Volatile fatty acid cycling in organic-rich marine sediments. Geochim. Cosmochim. Acta **46**:1575-1589. doi:10.1016/0016-7037(82)90315-5.

Schink, B. (1997). Energetics of syntrophic cooperation in methanogenic degradation. Microbiol. Mol. Biol. Rev. **61**:262-280. doi:10.1128/mmbr.61.2.262-280.1997.

Schippers, A. and B. B. Jørgensen. (2001). Oxidation of pyrite and iron sulfide by manganese dioxide in marine sediments. Geochim. Cosmochim. Acta **65**:915-922. doi:10.1016/S0016-7037(00)00589-5.

Schloss, I. R., D. Abele, S. Moreau, S. Demers, A. V. Bers, O. González, and G. A. Ferreyra. (2012). Response of phytoplankton dynamics to 19-year (1991–2009) climate trends in Potter Cove (Antarctica). J. Mar. Syst. **92**:53-66. doi:10.1016/j.jmarsys.2011.10.006.

Schlosser, C., K. Schmidt, A. Aquilina, W. B. Homoky, M. Castrillejo, R. A. Mills, M. D. Patey, S. Fielding, A. Atkinson, and E. P. Achterberg. (2018). Mechanisms of dissolved and labile particulate iron supply to shelf waters and phytoplankton blooms off South Georgia, Southern Ocean. Biogeosciences **15**:4973-4993. doi:10.5194/bg-15-4973-2018.

Schmidtko, S., L. Stramma, and M. Visbeck. (2017). Decline in global oceanic oxygen content during the past five decades. Nature **542**:335-339. doi:10.1038/nature21399.

Schnakenberg, A., D. A. Aromokeye, A. Kulkarni, L. Maier, L. C. Wunder, T. Richter-Heitmann, T. Pape, P. P. Ristova, S. I. Bühring, I. Dohrmann, G. Bohrmann, S. Kasten, and M. W. Friedrich. (2021). Electron acceptor availability shapes Anaerobically Methane Oxidizing Archaea (ANME) communities in South Georgia sediments. Front. Microbiol. **12**:726. doi:10.3389/fmicb.2021.617280.

Schwartz, E. (2007). Characterization of growing microorganisms in soil by stable isotope probing with $H_2{}^{18}O$. Appl. Environ. Microbiol. **73**:2541-2546. doi:10.1128/aem.02021-06.

Sørensen, J., D. Christensen, and B. B. Jørgensen. (1981). Volatile fatty acids and hydrogen as substrates for sulfate-reducing bacteria in anaerobic marine sediment. Appl. Environ. Microbiol. **42**:5-11. doi:10.1128/aem.42.1.5-11.1981.

Sundquist, E. T. (1986). Geologic Analogs: Their Value and Limitations in Carbon Dioxide Research. *in* J. R. Trabalka and D. E. Reichle, editors. The Changing Carbon Cycle: A Global Analysis. Springer New York, New York, NY. p. 371-402. doi:10.1007/978-1-4757-1915-4_19.

Torre, L., G. Alurralde, C. Lagger, D. Abele, I. R. Schloss, and R. Sahade. (2021). Antarctic ascidians under increasing sedimentation: Physiological thresholds and ecosystem hysteresis. Mar. Environ. Res. **167**:105284. doi:10.1016/j.marenvres.2021.105284.

Torsvik, T., J. Albretsen, A. Sundfjord, J. Kohler, A. D. Sandvik, J. Skarðhamar, K. Lindbäck, and A. Everett. (2019). Impact of tidewater glacier retreat on the fjord system: Modeling present and future circulation in Kongsfjorden, Svalbard. Estuar. Coast. Shelf Sci. **220**:152-165. doi:10.1016/j.ecss.2019.02.005.

Vandieken, V., N. Finke, and B. B. Jørgensen. (2006a). Pathways of carbon oxidation in an Arctic fjord sediment (Svalbard) and isolation of psychrophilic and psychrotolerant Fe(III)-reducing bacteria. Mar. Ecol. Prog. Ser. **322**:29-41. doi:10.3354/meps322029.

Vandieken, V., N. Finke, and B. Thamdrup. (2014). Hydrogen, acetate, and lactate as electron donors for microbial manganese reduction in a manganese-rich coastal marine sediment. FEMS Microbiol. Ecol. **87**:733-745. doi:10.1111/1574-6941.12259.

Vandieken, V., M. Nickel, and B. B. Jørgensen. (2006b). Carbon mineralization in Arctic sediments northeast of Svalbard: Mn(IV) and Fe(III) reduction as principal anaerobic respiratory pathways. Mar. Ecol. Prog. Ser. **322**:15-27. doi:10.3354/meps322015.

Vandieken, V. and B. Thamdrup. (2013). Identification of acetate-oxidizing bacteria in a coastal marine surface sediment by RNA-stable isotope probing in anoxic slurries and intact cores. FEMS Microbiol. Ecol. **84**:373-386. doi:10.1111/1574-6941.12069.

Vaquer-Sunyer, R. and C. M. Duarte. (2008). Thresholds of hypoxia for marine biodiversity. Proc. Natl. Acad. Sci. USA **105**:15452-15457. doi:10.1073/pnas.0803833105.

Wang, S., Q. Lu, Z. Liang, X. Yu, M. Lin, B. Mai, R. Qiu, W. Shu, Z. He, and J. D. Wall. (2023). Generation of zero-valent sulfur from dissimilatory sulfate reduction in sulfate-reducing microorganisms. Proc. Natl. Acad. Sci. USA **120**:e2220725120. doi:doi:10.1073/pnas.2220725120.

Wasmund, K., M. Mußmann, and A. Loy. (2017). The life sulfuric: Microbial ecology of sulfur cycling in marine sediments. Environ. Microbiol. Rep. **9**:323-344. doi:10.1111/1758-2229.12538.

Weber, K. A., L. A. Achenbach, and J. D. Coates. (2006). Microorganisms pumping iron: Anaerobic microbial iron oxidation and reduction. Nat. Rev. Microbiol. **4**:752-764. doi:10.1038/nrmicro1490.

Wehrmann, L. M., M. J. Formolo, J. D. Owens, R. Raiswell, T. G. Ferdelman, N. Riedinger, and T. W. Lyons. (2014). Iron and manganese speciation and cycling in glacially influenced high-latitude fjord sediments (West Spitsbergen, Svalbard): Evidence for a benthic recycling-transport mechanism. Geochim. Cosmochim. Acta **141**:628-655. doi:10.1016/j.gca.2014.06.007.

Wellsbury, P. and R. J. Parkes. (1995). Acetate bioavailability and turnover in an estuarine sediment. FEMS Microbiol. Ecol. **17**:85-94. doi:10.1111/j.1574-6941.1995.tb00133.x.

Wölfl, A.-C., N. Wittenberg, P. Feldens, H. C. Hass, C. Betzler, and G. Kuhn. (2016). Submarine landforms related to glacier retreat in a shallow Antarctic fjord. Antarct. Sci. **28**:475-486. doi:10.1017/S0954102016000262.

Chapter 2

Iron and sulfate reduction structure microbial communities in (sub-)Antarctic sediments

Lea C. Wunder, David A. Aromokeye, Xiuran Yin, Tim Richter-Heitmann, Graciana Willis-Poratti, Annika Schnakenberg, Carolin Otersen, Ingrid Dohrmann, Miriam Römer, Gerhard Bohrmann, Sabine Kasten, Michael W. Friedrich

Manuscript published in The ISME Journal

Volume 15, Issue 12, December 2021

https://doi.org/10.1038/s41396-021-01014-9

Running title:
Iron and sulfate reduction in South Georgia sediments

Contribution of the candidate to the total work

Experimental concept and design	50%
Experimental work/acquisition of experimental data	60%
Data analysis and interpretation	70%
Preparation of figures and tables	100%
Drafting of the manuscript	50%

The ISME Journal
https://doi.org/10.1038/s41396-021-01014-9

ARTICLE

Iron and sulfate reduction structure microbial communities in (sub-) Antarctic sediments

Lea C. Wunder[1,2] · David A. Aromokeye[1,3] · Xiuran Yin[1,3] · Tim Richter-Heitmann[1] · Graciana Willis-Poratti[1,4,5] · Annika Schnakenberg[1,2] · Carolin Otersen[1] · Ingrid Dohrmann[6] · Miriam Römer[3,7] · Gerhard Bohrmann[3,7] · Sabine Kasten[3,6,7] · Michael W. Friedrich[1,3]

Received: 11 November 2020 / Revised: 4 May 2021 / Accepted: 12 May 2021

Abstract

Permanently cold marine sediments are heavily influenced by increased input of iron as a result of accelerated glacial melt, weathering, and erosion. The impact of such environmental changes on microbial communities in coastal sediments is poorly understood. We investigated geochemical parameters that shape microbial community compositions in anoxic surface sediments of four geochemically differing sites (Annenkov Trough, Church Trough, Cumberland Bay, Drygalski Trough) around South Georgia, Southern Ocean. Sulfate reduction prevails in Church Trough and iron reduction at the other sites, correlating with differing local microbial communities. Within the order *Desulfuromonadales*, the family Sva1033, not previously recognized for being capable of dissimilatory iron reduction, was detected at rather high relative abundances (up to 5%) while other members of *Desulfuromonadales* were less abundant (<0.6%). We propose that Sva1033 is capable of performing dissimilatory iron reduction in sediment incubations based on RNA stable isotope probing. Sulfate reducers, who maintain a high relative abundance of up to 30% of bacterial 16S rRNA genes at the iron reduction sites, were also active during iron reduction in the incubations. Thus, concurrent sulfate reduction is possibly masked by cryptic sulfur cycling, i.e., reoxidation or precipitation of produced sulfide at a small or undetectable pool size. Our results show the importance of iron and sulfate reduction, indicated by ferrous iron and sulfide, as processes that shape microbial communities and provide evidence for one of Sva1033's metabolic capabilities in permanently cold marine sediments.

Introduction

Organic matter degradation is the main source of electron donors and carbon for microbial metabolism in marine sediments [1, 2]. The estimated 5.39×10^{29} microbial cells in marine sediments [3] form a microbial food chain. Below the oxic zone, the anaerobic portion of this food chain starts with specialists, which perform hydrolytic and fermentative processes [4], and ends with anaerobically respiring microorganisms, which oxidize fermentation products with available terminal electron acceptors such as nitrate, Mn(IV), Fe(III), sulfate, and CO_2. Because nitrate and Mn(IV) are rapidly depleted in the uppermost centimeters of most coastal and upper slope surface sediments [2, 5], sulfate and Fe(III) are the most abundant terminal electron

These authors contributed equally: Lea C. Wunder, David A. Aromokeye

Supplementary information The online version contains supplementary material available at https://doi.org/10.1038/s41396-021-01014-9.

✉ David A. Aromokeye
david.aromokeye@uni-bremen.de

✉ Michael W. Friedrich
michael.friedrich@uni-bremen.de

[1] Microbial Ecophysiology Group, Faculty of Biology/Chemistry, University of Bremen, Bremen, Germany

[2] Max Planck Institute for Marine Microbiology, Bremen, Germany

[3] MARUM – Center for Marine Environmental Sciences, University of Bremen, Bremen, Germany

[4] Instituto Antártico Argentino, Buenos Aires, Argentina

[5] Facultad de Ciencias Exactas, Universidad Nacional de La Plata, Buenos Aires, Argentina

[6] Alfred Wegener Institute Helmholtz Centre for Polar and Marine Research, Bremerhaven, Germany

[7] Faculty of Geosciences, University of Bremen, Bremen, Germany

Published online: 21 June 2021

acceptors utilized by microorganisms for mineralization of fermentation products in these depositional environments [6–8].

Iron enters the ocean from various sources including terrigenous origins via weathering and erosion and subsequent transport by rivers and windblown dust; hydrothermal vents [9]; melting sea ice and icebergs [10]; and glacial associated erosion, weathering, and meltwater [11–14]. Due to global warming, glacial associated input of iron is predicted to increase in the future, resulting in enhanced amounts of iron reaching coastal sediments and adjacent ocean areas especially in higher latitudes [13, 15, 16]. Sulfate, which is generally present in high concentrations in the water column (~28 mM), is supplied to the sediment by downward diffusion, accelerated by bio-irrigation and other advective processes [7, 8, 17]. In addition, it is the final product of reoxidation of sulfide [18, 19], which itself is produced by sulfate reduction [20], potentially resulting in a cryptic sulfur cycle [18, 19, 21]. Iron reduction is constrained by the reactivity and lower availability of ferric iron compared to sulfate [5, 22]. Therefore, while iron reduction is favored in certain marine settings [23, 24], organic matter oxidation by sulfate reduction is often more important than iron reduction in marine sediments [7, 8], a competition shown to be also regulated by the availability and reactivity of organic matter and ferric iron [22, 25].

Geochemical and biogeochemical factors have been previously shown to be key parameters shaping the microbial communities in marine sediments [1, 26, 27]. Besides the availability of terminal electron acceptors [1], i.e., Fe(III) and sulfate, these factors include quantity, composition, and reactivity of organic matter [26, 28, 29], sediment geochemistry [27, 30, 31], salinity [32], temperature [33], ocean currents [34], primary productivity in the overlying water column [35], and sedimentation rate [24].

The permanently cold surface sediments around the island of South Georgia in the South Atlantic Ocean, which we have investigated in this study, are influenced by high organic matter content around the shelf areas (0.65 wt% Cumberland Bay [36]), and high iron content within or close to the fjords (ref. [37], Cumberland Bay: total Fe solid phase 47 g/kg [38]; 0.7 wt% ferrihydrite and lepidocrocite [39]). In addition, the studied sediments were found to be characterized by widespread active methane seepage within the fjords and on the shelf, mostly associated with cross-shelf glacial troughs [36, 40, 41]. So far, we studied the microbial communities inhabiting deeper sediments (down to 10 m below seafloor) at three sites around South Georgia [42] and in the present study, a detailed analysis of the surface sediments at very fine scales is provided.

The sediments of the second study site Potter Cove, a small fjord located at the southwest of King George Island/Isla 25 de Mayo (South Shetland Islands) on the northern tip of the West Antarctic Peninsula, are characterized by a high input of iron from glacial meltwater and bedrock erosion [13, 14, 43]. Especially, sediments close to the glacier termination show a deeper ferruginous zone compared with sediments not directly influenced by glaciers [14] similarly to Cumberland Bay, South Georgia [41].

We hypothesize that differing geochemical characteristics in the surface sediments (top 20–30 cm) at various sites around South Georgia shape the local microbial communities. To test this hypothesis, four sites, located on the outer shelf (Annenkov Trough, Church Trough) or within or close to one of the fjords (Cumberland Bay, Drygalski Trough), were selected around the island of South Georgia. These sites were characterized by either high ferrous iron or hydrogen sulfide concentrations. The microbial communities of these sediments were investigated by 16S rRNA gene sequencing, quantitative PCR and RNA stable isotope probing (SIP) incubations. Correlation and multivariate regression analyses were performed to identify which geochemical parameters primarily shape the microbial community composition. The active iron-reducing microbial community of South Georgia sediments was compared to those in geochemically similar sediments of Potter Cove (Antarctic Peninsula) using RNA-SIP experiments.

Materials and methods

Study area and sampling

Samples from South Georgia sediments were collected during the RV METEOR M134 expedition in January to February 2017 [41]. To study microbial communities in the surface sediments (Fig. 1), four sites were selected: two sites on the outer shelf (Church Trough, Annenkov Trough) and two sites within or close to one of the fjords (Cumberland Bay and Drygalski Trough, respectively). All sites are located close to (<500 m) areas where active methane seepage has been observed from the sediments during the M134 cruise [41]. Surface sediments were retrieved using a multicorer (MUC, length 50 cm). The exact coordinates and sampling information are provided in Table S1.

For each station, two replicate MUC cores were retrieved, one for pore water geochemistry and one for microbiology. Sampling for both geochemistry and microbiology was done on board of the ship in a cold room at 4 °C. Microbiology samples were frozen in liquid nitrogen and transported to Bremen for molecular biology analyses. In addition, a gravity core (10 m length) was retrieved from the site in Cumberland Bay (detailed information Table S1) and kept at 4 °C until and during transport back to Bremen where it was sectioned and stored anoxically until use.

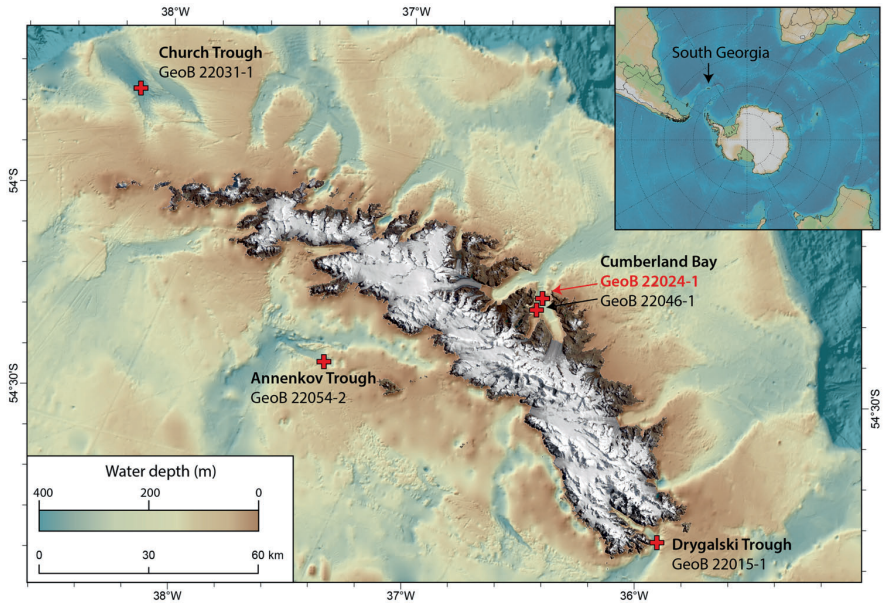

Fig. 1 Sampling locations around South Georgia. Core identifications are displayed, the red marked core was used for SIP incubations.

Antarctic surface sediments from Potter Cove (King George Island/Isla 25 de Mayo), Station 13, were retrieved during a field campaign with a push core in January 2019 (detailed information Table S1). The sampling site (Fig. S1) and geochemistry were previously described in Henkel et al. [14].

Pore water geochemistry

Pore water was retrieved from the MUC and gravity cores using rhizon samplers according to the procedure described by Seeberg-Elverfeldt et al. [44]. Dissolved iron(II) (Fe^{2+}), phosphate (PO_4^{3-}), ammonium (NH_4^+), dissolved inorganic carbon (DIC) and silicate (SiO_2) were measured on-board as described in Bohrmann et al. [41], while samples for sulfate (SO_4^{2-}, diluted 1:50 with Milli-Q water) and hydrogen sulfide (H_2S, fixation in 2.5% zinc-acetate solution) measurements were stored for later analysis. H_2S and SO_4^{2-} measurements were performed following Oni et al. [45].

DNA extraction and 16S rRNA gene sequencing

To explore the microbial communities in the South Georgia surface sediments, 1.5 g of frozen sediment was taken from 10 depths per site, selected according to the geochemical profiles, for DNA extraction. DNA extraction (by a phenol-chloroform protocol), PCR, and amplicon sequencing on a HiSeq 4000 System (Illumina, San Diego, CA; 2x 150 bp, only forward reads analyzed) at GATC GmbH (Konstanz, Germany) of bacterial and archaeal 16S rRNA genes were done following Aromokeye et al. [46]. The primer pair Bac515F (5′-GTGYCAGCMGCCGCGGTAA-3′; ref. [47]) and Bac805R (5′-GACTACHVGGGTATCTAATCC-3′; ref. [48]) targeted bacteria and the primer pair Arc519F (5′-CAGCMGCCGCGGTAA-3′; ref. [49]) and Arc806R (5′-GGACTACVSGGGTATCTAAT-3′; ref. [50]) targeted archaea. Unassigned reads or those assigned to chloroplasts, mitochondria, and archaea (in the bacterial dataset) or bacteria (in the archaeal dataset) were removed from the OTU tables. Normalization of sequencing data was done by calculating relative abundances, which were summed up for each taxon on all available ranks (for more details see supplementary methods, Table S2 and Fig. S2).

SIP experiments using (sub-)Antarctic sediments

RNA-SIP incubations were set up in order to identify active iron reducers using the top sediments of a gravity core from Cumberland Bay, South Georgia (GeoB22024-1; 0–14 cm, stored at 4 °C). The setup is described in more detail in the supplementary methods. Briefly, 40 ml anoxic slurries were prepared at a ratio of 1:4 of sediment and sulfate-free artificial seawater (per liter 26.4 g NaCl, 11.2 g $MgCl_2{\cdot}6\ H_2O$, 1.5 g $CaCl_2{\cdot}2\ H_2O$, 0.7 g KCl, prepared with purified water (Milli-Q)). Before addition of substrates, slurries were pre-incubated at 5 °C in the dark for 4–6 days to allow for system equilibration and pre-reduce small amounts of alternative electron acceptors (e.g., nitrate) potentially present in the starting sediments. Four different treatments were set up in triplicates (Table S3), containing 0.5 mM ^{13}C-labeled acetate as electron donor and carbon source and as electron acceptor either 5 mM lepidocrocite, 5 mM sulfate, or none. Lepidocrocite was chosen as easily reducible

iron oxide typically found in surface sediments, including the study site [39]. One treatment contained 10 mM sodium molybdate in addition to lepidocrocite in order to inhibit sulfate reduction. For each treatment, a control with unlabeled (^{12}C) acetate was set up. An unamended incubation with only sediment and artificial sea water was used as control. Aqueous Fe^{2+} formation was monitored during the course of the incubation for each bottle individually using a ferrozine assay [51], modified by fixing the samples in 0.5 M HCl in order to prevent further oxidation. Aqueous sulfate was measured at day 0 and day 15 (end point) of the incubation using a Metrohm 930 Compact IC Flex ion chromatograph. After 15 days, RNA was extracted from pooled triplicates in order to retrieve sufficient biomass for fractionation.

To support the observations from Cumberland Bay, a second SIP experiment was performed using Antarctic sediments from Potter Cove (push core 0–29 cm) with similar geochemistry as Cumberland Bay [14, 36]. For Potter Cove sediment incubations, the procedure for experimental setup and Fe^{2+} measurement was similar as described above with the modifications of using only 30 ml slurry (ratio 1:6) in 60- ml serum bottles, an incubation temperature of 2 °C and a pre-incubation time of 7 days. The single treatment contained 0.5 mM ^{13}C-labeled or unlabeled acetate and 5 mM lepidocrocite as substrate. The incubation was carried out for 10 days.

RNA-SIP

The steps of nucleic acid extraction, removal of DNA, quantification, density separation, and preparation of 16S rRNA sequencing were performed following a previously described protocol [52] with the following modifications. Briefly, nucleic acids were extracted from 15 ml slurry per treatment, using a phenol-chloroform extraction protocol, followed by DNase treatment and an additional phenol-chloroform purification and RNA precipitation step with isopropanol and sodium acetate. RNA was quantified with Quanti-iT RiboGreen and 1 µg was used for density separation by ultracentrifugation. This resulted in 14 fractions of which fraction 1 had the highest density (= heaviest) and fraction 14 the lowest. The RNA content of each fraction was quantified and fractions were defined and pooled by their RNA concentration-density profile as ultra-heavy = fraction 3 + 4 (1.814–1.826 g/ml); heavy = fraction 5 + 6 (1.799–1.810 g/ml); midpoint = fraction 7 + 8 (1.783–1.799 g/ml); light = fraction 9 + 10 (1.768–1.783 g/ml); ultra-light = fraction 11 + 12 (1.753–1.768 g/ml). The pooled fractions were used for cDNA synthesis. The bacterial 16S rRNA amplicon library was prepared as previously described [46] and paired-end sequenced at Novogene Co. Ltd. (Cambridge, UK) using Novaseq6000 platform (2x 250 bp). Sequencing analysis was done following Aromokeye et al. [46] with modifications described in the supplementary material (sequencing details Table S4 and Fig. S3) and in the 16S rRNA gene sequencing paragraph above.

Quantitative PCR

Bacterial and archaeal 16S rRNA gene copy numbers of South Georgia surface sediments were determined by quantitative real-time PCR (qPCR). The qPCR assay followed Aromokeye et al. [53] with 1 ng DNA template and a cycling program of 95 °C: 5 min; 40 cycles at 95 °C: 15 or 30 s, 58 °C: 30 s, 72 °C: 40 s (Table S5); with efficiencies >80% and $R^2 > 0.99$. For bacteria quantification, the primers Bac8Fmod (5′-AGAGTTTGATYMTGGCTCAG-3′; modified from ref. [54]) and Bac338Rmod (5′-GCWGCCWCCCGTAGGWGT-3′; modified from ref. [55]) were used. For archaea quantification Ar806F (5′-ATTAGATACCCSBGTAGTCC-3′; alternative name Arc787F in ref. [55]) and Ar912rt (5′-GTGCTCCCCCGCCAATTCCTTTA-3′; ref. [56]) were used. The gene copy number calculation was based on standard curves of 16S rRNA gene fragments of *Escherichia coli* (strain SB1) and *Methanosarcina barkeri* (strain DSM800), amplified with 27F (5′-AGAGTTTGATCCTGGCTCAG-3′; ref. [57]) and Ba1492 (5′-GGTTACCTTGTTACGACTT-3′; ref. [57]), and 109F (5′-ACKGCTCAGTAACACGT-3′; ref. [58]) and A1492 (5′-GGCTACCTTGTTACGACTT-3′; ref. [57]) primer pairs, respectively (Table S5), prepared and analyzed according to Reyes et al. [59].

In surface sediment samples and Cumberland Bay SIP fractions, the functional gene for sulfate reduction, alpha-subunit of the dissimilatory sulfite reductase (*dsrA*), was used for the quantification of sulfate reducers following the qPCR protocol of Reyes et al. [59]. For the qPCR reaction, the primer pair DSR1-F+ (5′-ACSCACTGGAAGCAC GGCGG-3′; ref. [60]) and DSR-R (5′-GTGGMRCCG TGCAKRTTGG-3′; ref. [60]) was used. As standard, the *dsrAB* gene of *Desulfovibrio burkinensis* (strain DSM 6830) was amplified with a mix of modified DSR1F/DSR4R primers (for details see Reyes et al. [59]).

Statistical analysis

Selected pairwise Pearson correlations were calculated between OTU abundances, gene copy numbers, and environmental variables. A distance-based redundancy analysis (dbRDA) was performed on a Bray-Curtis dissimilarity distance matrix between geochemical parameters and bacterial relative abundances from sequencing and tested for predictor variable collinearity, statistical significance (at $p < 0.05$) for the full model, and constrains for each variable. *P* values were adjusted for multiple testing according to the false discovery method [61], if necessary.

All statistical analysis and figures were made within the R environment version 3.6.1 [62] using the vegan package [63].

Closest sequences of the most abundant OTUs assigned as Sva1033 were exported from 16S rRNA gene ARB tree of Silva release 138 (SILVA_138_SSURef_NR99_05_01_20, ref. [64]; >1300 bp, randomly selected) as well as closest named neighboring clusters. A maximum-likelihood tree was inferred with RAxML (version 8.2.11, ref. [65]) using the GTRGAMMA model with 1000 times rapid bootstrapping. The tree file was visualized using iTOL software (v4, ref. [66]) and edited in Inkscape (version 1.0.1, ref. [67]).

Results

Pore water geochemistry

Seven different geochemical pore water parameters were analyzed in the context of their correlation to the microbial community in the sediment. Notable differences across the sites were observed in the pore water concentrations and profiles of Fe^{2+}, SO_4^{2-}, and H_2S (Fig. 2). Of all parameters, Fe^{2+} concentrations showed the strongest variability among the study sites.

At the sampling site in Church Trough, Fe^{2+} became rapidly depleted with depth and undetectable below 3 cm core depth. Below this depth, downward increasing H_2S concentrations (up to 20 mM at 30 cm) coincided with decreasing SO_4^{2-} concentrations (28 mM at 0 cm to 5 mM at 30 cm). This defines the sampling site in Church Trough as being sulfide-rich (Fig. 2). At the other sampling sites, Fe^{2+} predominated in the sampled sediment interval. The maximum Fe^{2+} concentration was measured in the sediments sampled in Annenkov Trough (440 µM). Therein, Fe^{2+} concentrations became completely depleted down-core followed by detection of low H_2S concentrations below 30 cm (500 µM). In the investigated sediments of both Cumberland Bay and Drygalski Trough, Fe^{2+} was detected throughout the sampled sediment depth with maximum concentrations of 204 and 256 µM, respectively, while H_2S was below detection limit. The predominance of Fe^{2+} over H_2S in the sediments of these sites thus defines them as iron-rich sites (Fig. 2). In the sediments at the iron-rich sites, SO_4^{2-} concentrations stayed stable with depth (~28 mM) with only minor decreases observed in the surface sediments collected in Cumberland Bay (below 18 cm from 27 to 23 mM).

Profiles of NH_4^+ and DIC showed similar distribution and shapes with increasing values over depth at all sites (Fig. 2). DIC concentrations in Church Trough sediments reached double the concentrations observed in the sediments of the other sites toward the bottom of the core. Close

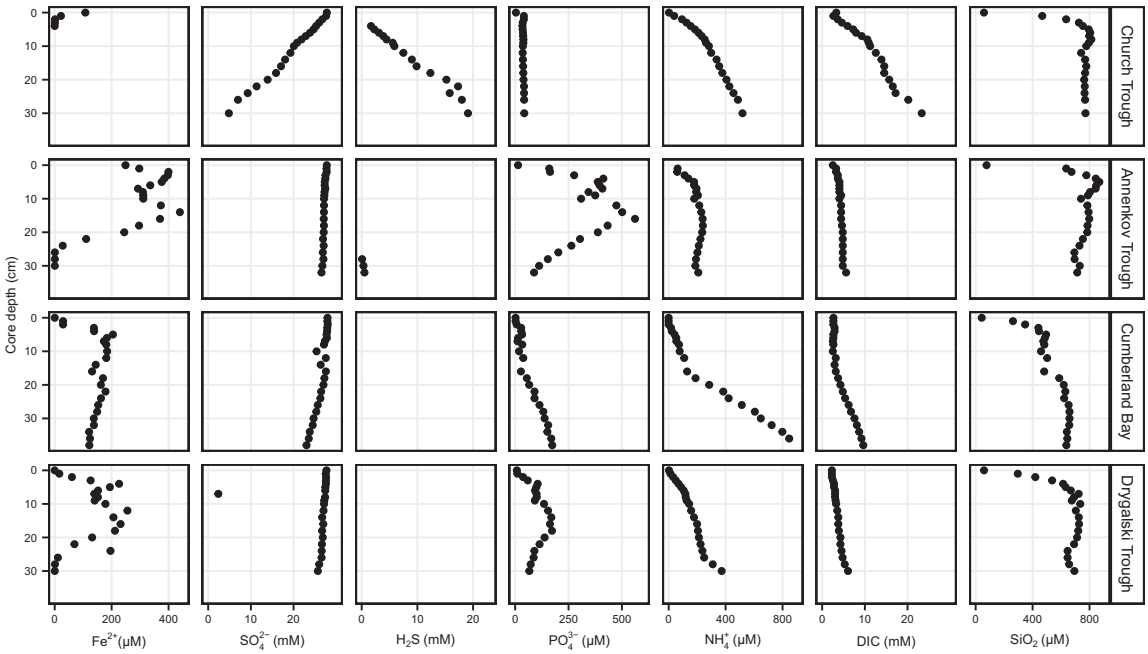

Fig. 2 Pore water concentrations of iron(II) (Fe^{2+}), sulfate (SO_4^{2-}), sulfide (H_2S), phosphate (PO_4^{3-}), ammonium (NH_4^+), dissolved inorganic carbon (DIC), and silicate (SiO_2) in surface sediments, South Georgia. All missing values in Fe^{2+} and H_2S profiles were for data points below detection limit.

to the surface, SiO_2 concentrations increased downward rapidly to a maximum value differing between sites and stayed stable through the rest of the core.

Microbial community composition and abundance estimation

The bacterial community composition of South Georgia surface sediments was investigated by 16S rRNA gene sequencing. Distinct similarities were observed in the distribution of core communities across all sites (Fig. 3A). Relative abundance of sequences falling into *Flavobacteriales*, the *Alphaproteobacteria Rhodobacterales* (mostly *Rhodobacteraceae*); the *Gammaproteobacteria Cellvibrionales* (mostly *Halieaceae*); *Planctomycetacia* (mostly *Pirellulaceae*); and *Verrucomicrobiales* (mostly *Rubritaleaceae*) decreased with sediment depth, while the relative abundance of sequences associated with *Anaerolineae*

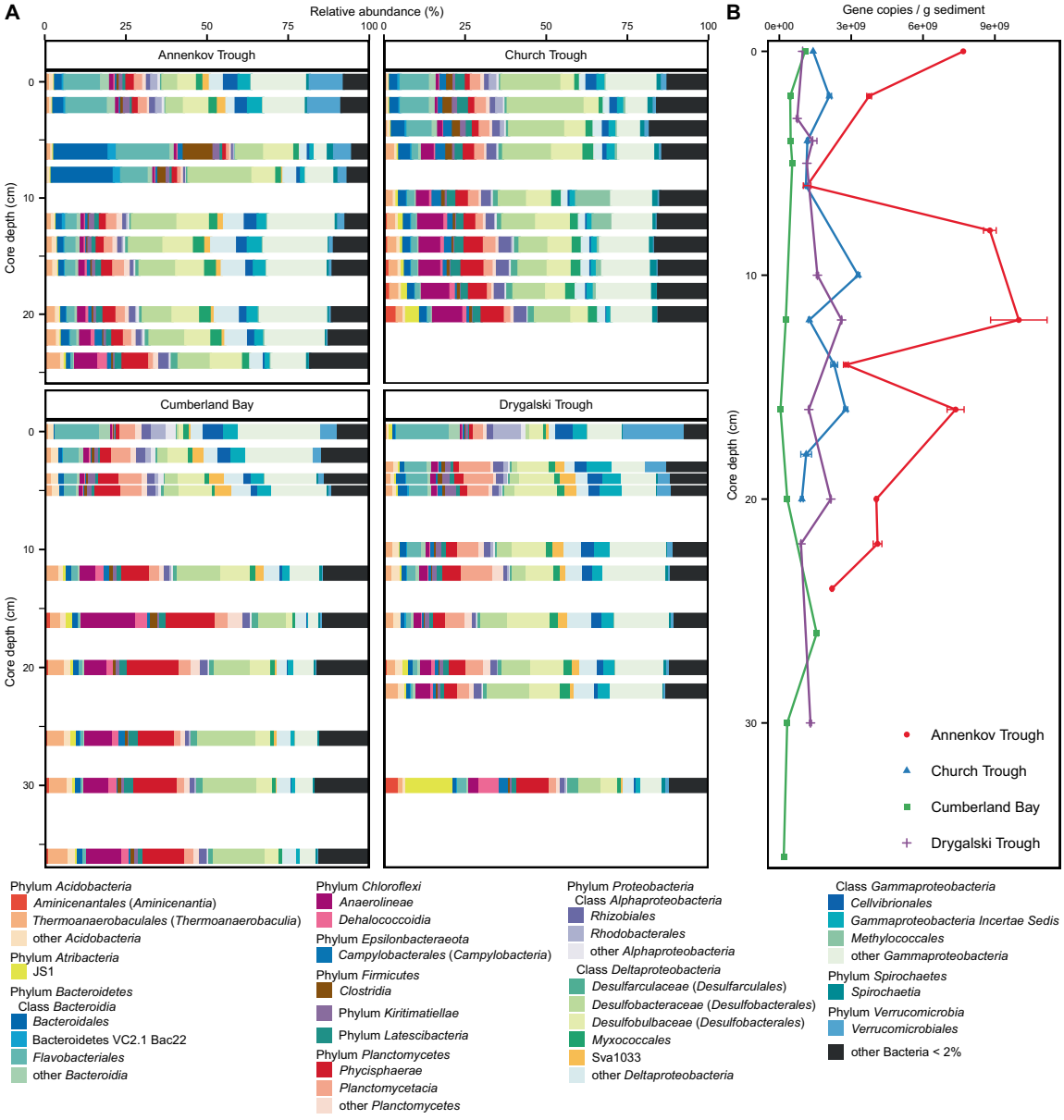

Fig. 3 Bacterial community composition and gene copy numbers in South Georgia surface sediments. A Relative abundance of bacterial 16S rRNA genes in 10 depths of Annenkov Trough, Church Trough, Cumberland Bay and Drygalski Trough. **B** Bacterial 16S rRNA gene copies per gram wet sediment of samples displayed in (**A**) with error bars displaying SD of technical qPCR replicates.

(phylum *Chloroflexi*), *Phycisphaerae* (mostly clade MSBL9), and the *Atribacteria* JS1 increased.

Certain differences between sites were also evident: the relative abundance of *Desulfobacteraceae* was low (<5%) in the top sediments of the iron-rich sites in Annenkov Trough, Cumberland Bay, and Drygalski Trough and only increased down-core, but was very high (18%) in the top sediments of the sulfide-rich site Church Trough. One major difference between all sites was the presence of *Methylococcales* throughout the Church Trough core (up to 11%), whereas it was present in very low relative abundance at the other sites (<0.5%). Conversely, the *Desulfuromonadales* family Sva1033 was present in all sites but with very low abundance in the Church Trough core (5% vs. 0.6%).

Bacterial 16S rRNA genes were quantified by qPCR with gene copy numbers ranging between 5×10^7 and 1×10^{10} copies per gram sediment and differed significantly between sites (Fig. 3B). Specifically, highest gene copy number estimates were obtained from the sediments sampled in Annenkov Trough (up to 1×10^{10} at 12 cm) and lowest in Cumberland Bay (5×10^7–1.6×10^9).

Archaeal sequences recovered after quality filtering were much less compared to bacterial sequences (Table S2). A complete depth profile of the archaeal community was only possible for samples derived from Church Trough and Cumberland Bay (Fig. S4A), because the archaeal read numbers and sequencing depth from the majority of the sampled depths in Drygalski Trough and Annenkov Trough were too low (<900 reads, Table S2). The most abundant archaea in all sites were *Bathyarchaeota* (up to 31% in Cumberland Bay) and the genus *Candidatus* "Nitrosopumilus" (up to 70% in Cumberland Bay) with their relative abundance decreasing with depth (Fig. S4A). In Church Trough sediments, anaerobic methane oxidizing archaea groups ANME-2a-2b and -2c were found in high relative abundances below 5 cm core depth (ANME-2a-2b up to 15%, ANME-2c up to 31%). Archaeal 16S rRNA gene copy numbers from qPCR were in general a magnitude lower than the bacterial gene copies (Fig. S4B). In contrast to bacterial copy numbers, archaeal copy numbers were highest in Church Trough sediments ranging from 8.6×10^7 to 4.6×10^8 copies per gram sediment. Again, the lowest gene copy numbers of archaea were detected in samples from Cumberland Bay with only 1.6×10^7 to 1.1×10^8 copies.

Statistical correlations between geochemical parameters and bacterial communities

In order to identify potential geochemical filters that shape the microbial communities across all sites, a dbRDA was performed (Fig. 4, $F = 4.99$, $p < 0.01$, Df: 5, 34). Fe^{2+}, PO_4^{3-}, NH_4^+, SiO_2, and H_2S were included as explanatory variables

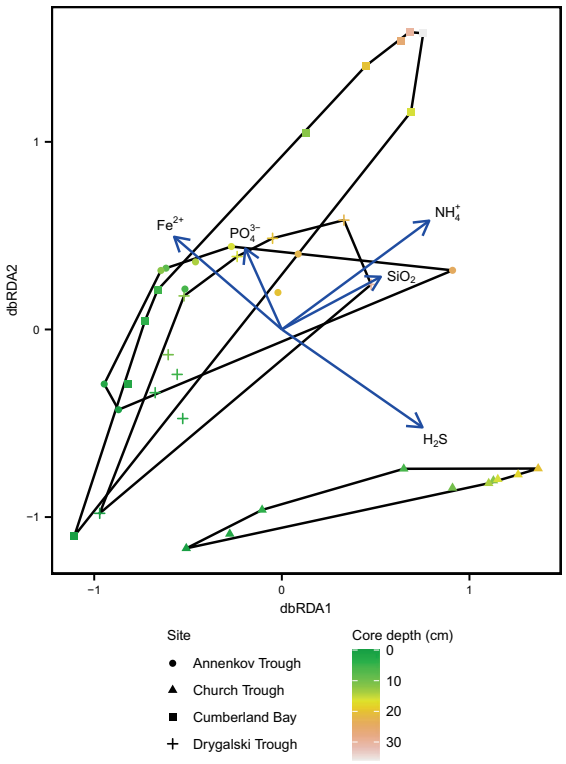

Fig. 4 Distance-based redundancy analysis (dbRDA) ordination plot of bacterial communities in surface sediments of South Georgia. Sample points are distinguished by site and core depth by shape and color, respectively. dbRDA1 (variation 47%) and dbRDA2 (variation 22%) axes are displayed, which constrain the Bray-Curtis distance matrix with geochemical parameters Fe^{2+}, PO_4^{3-}, NH_4^+, SiO_2, and H_2S. The total model ($F = 4.99$, $p < 0.01$, Df: 5, 34) and each individual parameter ($p < 0.05$) was significant.

in the model and together explained 42% of the total variation in the bacterial community. DIC and SO_4^{2-} were removed due to collinearity to other factors (NH_4^+ and H_2S, respectively). Increasing NH_4^+ concentrations with sediment depth explained most of the variation of the bacterial community ($F = 5.85$, $p < 0.01$), followed by H_2S ($F = 3.61$, $p < 0.01$), SiO_2 ($F = 2.90$, $p < 0.01$), Fe^{2+} ($F = 2.25$, $p = 0.012$), and PO_4^{3-} ($F = 2.12$, $p = 0.015$). The clustering in the site ordination space showed a clear distinction between Church Trough and the other three sites (Fig. 4). The model strongly attributed this distinction to Fe^{2+} and H_2S concentration differences between sites. Accordingly, removing these two variables from the model caused the clustering by sampling site in the ordination to disappear (Fig. S5).

Since H_2S and Fe^{2+} concentrations, as indicators for sulfate and iron reduction, were identified as the key environmental factors for the microbial community composition in the sediments (Fig. 4), correlations between these geochemical parameters and taxa known to possess the capability of sulfate and iron reduction were performed.

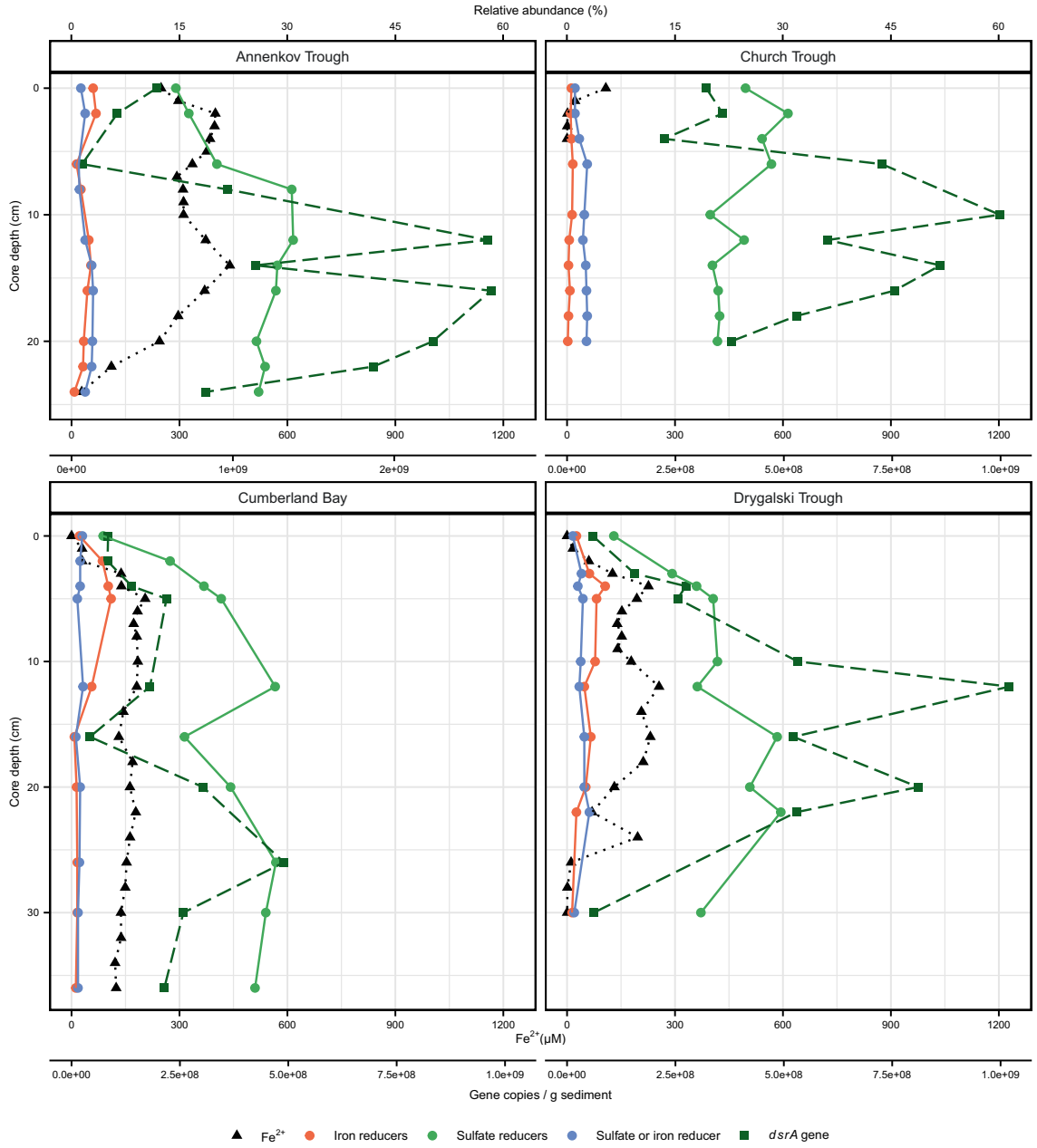

Fig. 5 Depth profile of contribution of sulfate and iron reducing microorganisms in *Deltaproteobacteria* to bacterial community and quantification of sulfate reducers (*dsr*A gene) in South Georgia surface sediments. Relative abundance of 16S rRNA gene of taxa known for iron and/or sulfate reducing capabilities within *Deltaproteobacteria* (details in the text) was summed up per sediment depth. Fe^{2+} profile from Fig. 2 and *dsrA* gene copies per gram wet sediment are displayed. Note the different scale for gene copies/g sediment for Annenkov Trough. Sequences of taxa known for iron reducing capabilities consisted of >78% Sva1033 in all depths of Annenkov Trough, Cumberland Bay, and Drygalski Trough.

Therefore, relative abundance of known sulfate reducers within the *Deltaproteobacteria* was summed up for each sample (Fig. 5). This included the taxa *Desulfarculales* [68], *Desulfobacterales* [69], *Desulfohalobiaceae* [70], clade NB1-j [71], clade SAR324 [72], clade Sva0485 [71], and *Syntrophobacterales* [73]. Among the known iron reducers from marine sediments (e.g., [74–79]), members of *Desulfuromonadales* were the most abundant clade in this study.

Summed up individual families included *Desulfuromonadaceae* [75, 80], *Geobacteraceae* [74] and *Deferrisoma* [81], and the family Sva1033 for which iron reducing capabilities were recently suggested [82]. The taxa *Desulfovibrionaceae* [83, 84] and *Myxococcales* [85] were separated as taxa known for both sulfate and iron reduction.

The relative abundance of sulfate reducers was high across all sites (8–30%; Fig. 5), despite the absence of indication for sulfate reduction, i.e., sulfide accumulation, in the pore water of Cumberland Bay, Drygalski Trough, and Annenkov Trough (Fig. 2). The presence of organisms capable of sulfate reduction was confirmed by qPCR of the *dsrA* gene as a functional marker gene for sulfate reduction: across all sites, the *dsrA* gene copies varied between 4.2×10^7 (Cumberland Bay) and 2.6×10^9 copies per gram sediment (Annenkov Trough; Fig. 5) and were positively correlated to the bacterial gene copies ($r = 0.74$, $p < 0.001$). Compared to sulfate reducers, the relative abundance of known iron reducers was lower across the iron-rich sites (1–5%; Fig. 5). In Church Trough sediments, where sulfate reduction was apparent, relative abundance of iron reducers was lower compared to the other sites (<0.6%). A significant correlation between relative abundance of iron reducers and Fe^{2+} concentrations was found for Drygalski Trough ($r = 0.77$, $p < 0.01$). Correlations were also calculated for the most dominant members of the order *Desulfuromonadales*, the family Sva1033 (Figs. 3 and S6). Sva1033 showed significant correlations with Fe^{2+} for Annenkov Trough ($r = 0.63$, $p = 0.049$) and Drygalski Trough ($r = 0.77$, $p < 0.01$), but not Cumberland Bay. Although the highest relative abundance of known (or proposed) bacteria capable of iron reduction was found in Cumberland Bay sediments, depth-wise relative distribution of iron reducers did not correlate with Fe^{2+} concentrations. Instead, a correlation was found between Fe^{2+} concentration and relative abundance of known sulfate reducers ($r = 0.78$, $p < 0.01$).

SIP experiments with (sub-)Antarctic sediments

The abundance and distribution of known iron and sulfate reducers in the sediment communities raised questions about their metabolic activities in this environment. Sva1033 was the dominant member of *Desulfuromonadales* (Fig. S6), an order known for its iron reducing capabilities (e.g., [74–79]). It was found across all iron-rich sites, but this clade is only so far predicted—but not proven—to perform iron reduction due to phylogenetic affiliation to *Desulfuromonadales* (ref. [82], Fig. S7). Counterintuitively, sulfate reducers were significantly more abundant compared to iron reducers in the sites where iron reduction prevailed (Fig. 5). To further investigate these observations, we set up RNA-SIP incubations using acetate as ^{13}C-labeled substrate with Cumberland Bay surface sediments in order to label active acetate oxidizers with the prediction that iron-reducing microorganisms capable of utilizing acetate as electron donor will be labeled in the heavy fractions [78, 86]. Given that obtaining a pure culture for Sva1033 was outside the scope of this study, we aimed with this strategy to obtain an indirect indication for iron reduction capability in the Sva1033 clade. In these incubations, increasing Fe^{2+} concentrations were detected in all treatments without significant differences between them, except in the treatment with acetate, lepidocrocite, and molybdate (Fig. S8A). In the molybdate-amended treatment, only moderate increase in Fe^{2+} concentrations was observed over time. No further increase of Fe^{2+} concentrations was detected by day 15 of the incubation experiment in all treatments. Sulfate was measured over time (Fig. S8B). A general trend of changing sulfate concentrations could only be observed in the acetate only treatment (decrease by up to 0.4 mM). Meanwhile, the range of sulfate concentration was different in the treatment amended with 5 mM sulfate (3.8–5.7 mM).

Deltaproteobacteria dominated the general bacterial community in the five defined gradient fractions per treatment (ultra-light, light, midpoint, heavy, ultra-heavy) after isopycnic separation. Their relative abundance ranged from at least 50% up to over 80% in some ^{13}C ultra-heavy fractions. Clear differences were observed between the communities in the light and heavy fractions, thus confirming that the SIP separation was successful (Fig. 6A, B). The mostly enriched taxon in the ^{13}C heavy and ultra-heavy fractions of all treatments was *Desulfuromonadales* within the *Deltaproteobacteria* (yellow-orange-brown in Fig. 6B), including the family Sva1033 (10–23%), *Desulfuromonas* (8–21%), *Geopsychrobacter* (8–10%), and *Geothermobacter* (8–13%). In total, the order *Desulfuromonadales* was more abundant in the ^{13}C incubations, reaching up to 70% in the ultra-heavy fractions, compared to the ^{12}C control incubations where their relative abundance was below 25% and mostly in the lighter fractions. Their relative abundance was slightly lower in the ultra-heavy fractions of the sulfate amended treatments (55%) compared to the other treatments (64–69%).

Within the class *Deltaproteobacteria*, the other abundant taxa were members of *Desulfobacterales*: *Desulfobacteraceae*, especially clade Sva0081, and *Desulfobulbaceae*, which together reached abundances of up to 50%. These groups of known sulfate reducers were more abundant in the ^{13}C acetate and sulfate amended ultra-heavy fraction (23%) compared to the other ^{13}C acetate amended treatments (6–18%). The lowest relative proportion of sulfate reducers in the ultra-heavy fraction (6%) was observed in the molybdate amended treatment. Quantification of the *dsrA* transcripts (Fig. 6C) showed very low copy numbers in the control treatment with molybdate (0–6700 transcript

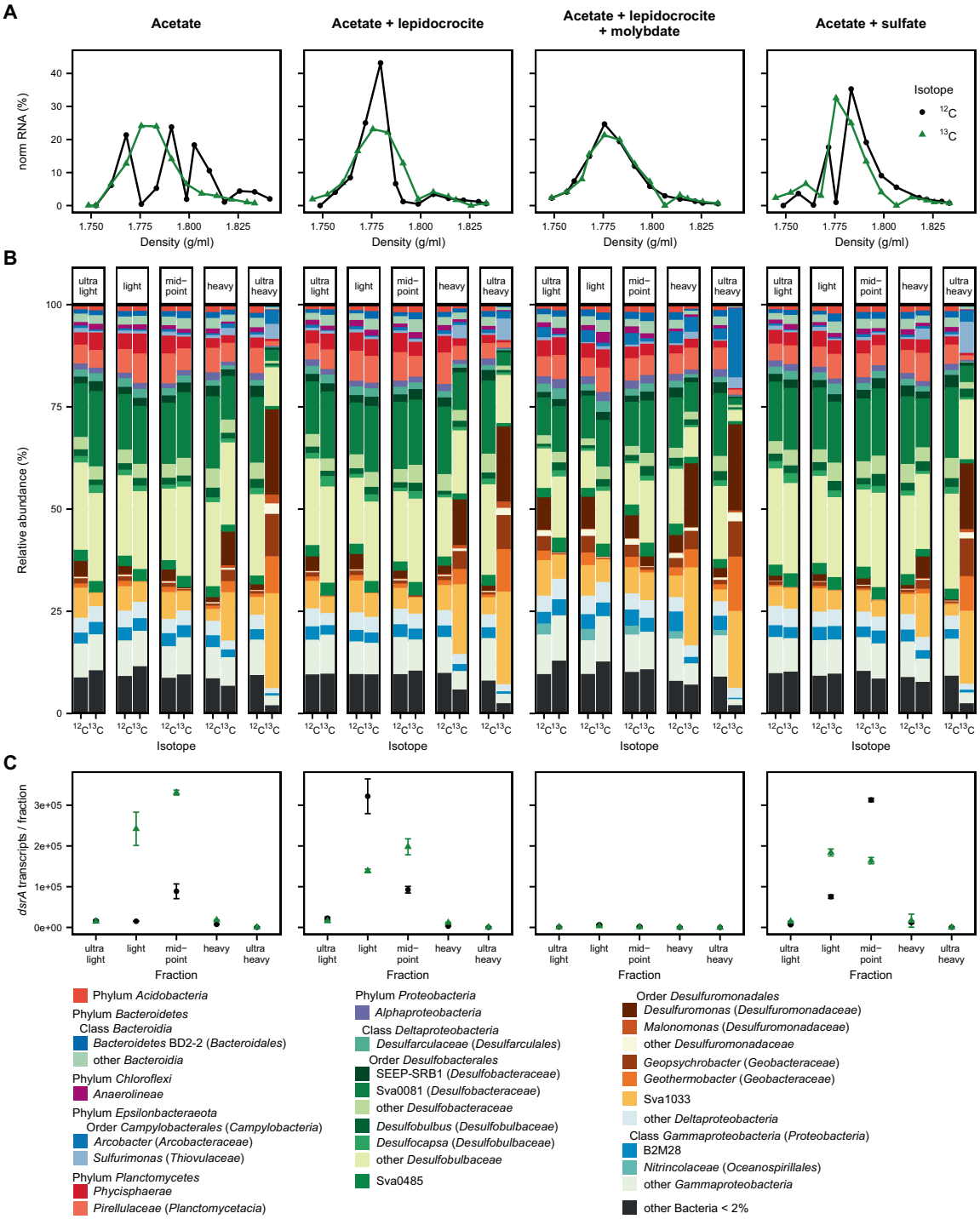

Fig. 6 Results of SIP incubation with Cumberland Bay sediment. **A** Visualization of RNA density separation with normalized RNA amount (ng RNA in fraction per total recovered ng RNA of sample). **B** Density separated 16S rRNA community composition. **C** *dsrA* transcript copies per ng cDNA from recovered RNA per fraction with SD of technical qPCR replicates as error bars. In the molybdate-amended treatment, the transcript copies were below detection limit (<100 copies) for the ultra-heavy fraction and highest in the light fraction with 3000 (^{13}C) to 6700 (^{12}C) copies per ng cDNA from recovered RNA. Legend of **A** corresponds to **C**.

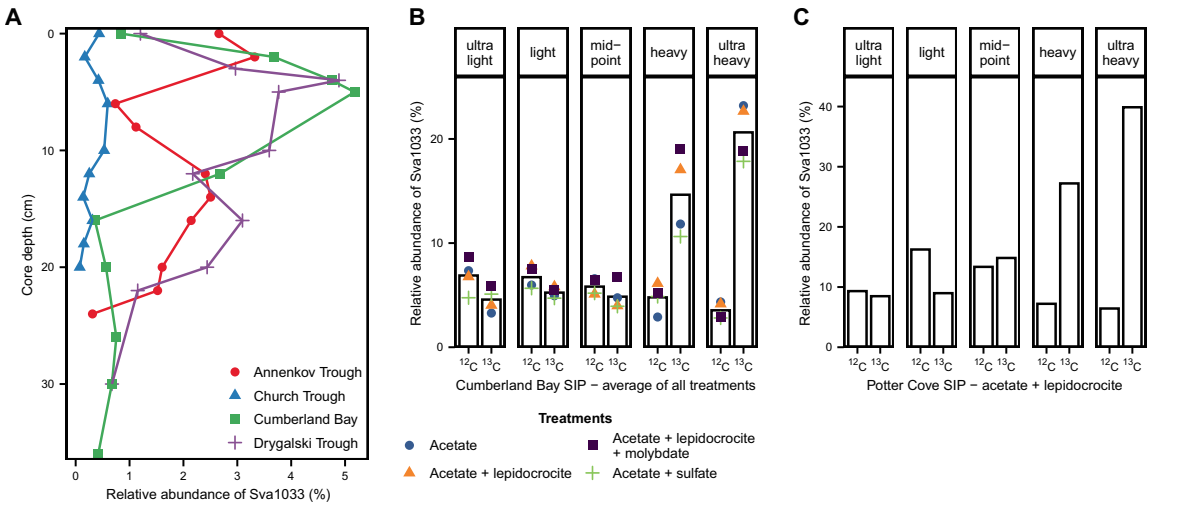

Fig. 7 Abundance and activity of Sva1033. Relative abundance of Sva1033 in South Georgia surface sediments (**A**) and in SIP incubations with Cumberland Bay (**B**) and Potter Cove sediment (**C**). **A** Separation between sites by color and shape. **B** Averaged relative abundance of Sva1033 across all SIP treatments displayed by bars while relative abundance of each treatment is individually displayed by data points distinguishable by shape and color.

copies/ng cDNA from recovered RNA per fraction) compared to the other treatments (up to 300 000 transcript copies/ng cDNA per fraction). Sulfur oxidizing bacteria, *Arcobacter* and *Sulfurimonas* [87, 88] were the other enriched taxa in the ultra-heavy fractions. *Arcobacter* was mainly enriched in the ^{13}C acetate, lepidocrocite, and molybdate treatment (17%) while *Sulfurimonas* was enriched in the treatments with acetate and lepidocrocite or sulfate (5–8%).

In addition to SIP incubations with surface sediments from Cumberland Bay, a SIP treatment amended with acetate and lepidocrocite was set up with sediments from Potter Cove, Antarctica, as a geochemically similar site in order to compare iron reducing communities from different locations. SIP was performed after running the incubation for 10 days from which iron reduction was observed (Fig. S8C). The most dominant enriched taxon in the ^{13}C ultra-heavy fraction was the family Sva1033 (40% of bacterial 16S rRNA genes; Figs. 7C and S9), a similar observation to the SIP incubations with sediments from Cumberland Bay.

In order to investigate the phylogenetic relations of the most-enriched taxon Sva1033 (Fig. 7), a phylogenetic tree was constructed with the closest neighbors to the most abundant OTUs assigned as Sva1033 in South Georgia in situ sediments and Cumberland Bay SIP incubations and the closest neighboring clades from the Silva ARB tree (release 138). OTUs detected in situ were closely related to OTUs detected in the SIP experiment (Fig. S7). The clade closest related to the family Sva1033 was “Desulfuromonas 2” (as assigned by Silva 138).

Discussion

Permanently cold coastal sediments from sub-Antarctic and Antarctic regions are subject to increased input of iron and other terrigenous compounds as a consequence of intensified weathering, erosion, and glacial melt due to observed global warming [10–15, 89, 90]. The impact of these altered element and material flux on the microbial communities in such sediments is currently understudied. Likewise, the bacterial communities present in surface sediments around the sub-Antarctic island South Georgia were not previously studied in detail. This study investigated the impact of environmental change on microbial communities in permanently cold (sub-)Antarctic sediments. Our findings show how geochemical characteristics such as the predominant electron accepting process and quality of organic matter potentially shape sediment communities in various sites around South Georgia. Importantly, in the iron reduction sites, we obtained evidence for dissimilatory iron reduction as one of Sva1033 clade’s ecological roles in permanently cold sediments using RNA-SIP. Finally, indications for concurrent sulfate reduction were obtained, despite the dominance of iron reduction in incubation experiments.

Geochemical footprints shape microbial community composition

Selective survival of taxa buried below the upper 10 cm bioturbation zone has been identified as the significant process relevant for microbial community assembly in

marine sediments [91–94]. Using the geochemical parameters as environmental factors for selection of the microbial community composition in the dbRDA (Figs. 4 and S5), various trends were observed. For example, depth-wise variation in community composition across all sites was strongly explained by the ammonium concentrations (Fig. 4), whose presence—along with DIC—is an indicator for organic matter degradation [95]. This was reflected in the core microbial community; the taxa *Flavobacteriales*, *Rhodobacterales*, *Cellvibrionales*, and *Verrucomicrobiales*, known for degradation of labile organic matter such as proteins, amino acids, polysaccharides, and simple sugars [96–99], were more abundant in the surface and decreased with depth across all sites (Fig. 3A). A similar trend was previously observed for some of these taxa in sediments of the Antarctic shelf [100]. In contrast, known "persister" microorganisms [91–93] such as *Anaerolineae*, *Phycisphaerae*, and the *Atribacteria* clade JS1 [101–104], showed a consistent increase in relative abundance along increasing depth across all sites (Fig. 3A). Differing supply of fresh organic matter on the outer shelf sites (Church Trough and Annenkov Trough) compared to sites located closer to the island was a possible explanation for likely higher microbial activity at these sites, as corroborating data from the geochemical profiles and gene copy numbers of microorganisms in the sediments (Figs. 2, 3B, 5, and S4B) indicated. This idea was supported by known large phytoplankton blooms and high primary production on the outer shelves around South Georgia [37, 40, 105].

Beyond ammonium shaping the communities along the sediment depth gradient, the dbRDA similarly showed a distinct selection of microbial communities in the study sites based on ferrous iron and sulfide concentrations. Thus, the likely dominant TEAP, i.e., iron and sulfate reduction, served as a factor for identifying the sites as either a group of iron reduction sites (Annenkov Trough, Cumberland Bay, Drygalski Trough) or sulfate reduction site (Church Trough; Fig. 4). A strong dependency of microbial community composition on TEAP was previously demonstrated in deeper sediments (down to 10 m below seafloor) from South Georgia [42] and from the Baffin Bay in the Arctic [27], in which iron and sulfate or iron and manganese reduction dominated, respectively.

Since ferrous iron and sulfide as products of microbial iron and sulfate reduction, respectively, were recognized by dbRDA as the environmental factors in our sediments to shape local communities, we hypothesize that the microorganisms contributing to these processes are important members of the microbial community. Thus identification of potential sulfate and iron reducers in the sediments will reveal which microorganisms are likely involved in the terminal respiratory processes. Amongst the sulfate reducers (Fig. 5), *Desulfobacteraceae*, *Desulfobulbaceae*, and *Desulfarculaceae* were most dominant, even down to the deeper layers of Cumberland Bay and Church Trough sediments [42]. The order *Desulfuromonadales* harbors many species with the metabolic capability to perform dissimilatory iron reduction [74, 75, 77], but also sulfur reduction [106–110] and even a few microorganisms are capable of sulfate reduction [111]. Members of *Desulfuromonadales* are typically found in ferruginous sediments (e.g., [45, 112, 113]). This order was the most abundant potential dissimilatory iron reducing clade in this study. Here, the main representative identified was the family Sva1033 (Figs. 3A, 7A, and S6), which was recently suggested to be capable of iron reduction in a Terrestrial Mud Volcano site [82] and Arctic sediments [112]. Based on the calculated phylogenetic tree (Fig. S7), this family is closely related to the clade "Desulfuromonas 2" (as assigned by Silva release 138 [64]). Until now, there are no cultivated members of this clade and its metabolic capabilities are yet to be confirmed. The significant correlation between depth-wise Fe^{2+} concentrations with relative abundance of Sva1033 in Annenkov Trough and Drygalski Trough (Fig. S6) strengthens the hypothesis that Sva1033 is involved in microbial iron reduction in surface sediments of South Georgia.

The Sva1033 clade is capable of dissimilatory iron reduction

As the Sva1033 clade was first identified in Arctic sediments [114], we tested the hypothesis that this clade is ecologically adapted to perform iron reduction as one of its metabolic capabilities in permanently cold sediments. This was done by setting up RNA-SIP incubations using acetate as labeled substrate with Cumberland Bay and Antarctic Potter Cove sediments, especially as both Potter Cove and Cumberland Bay are characterized by a broad ferruginous zone [14]. Due to thermodynamic constraints in dissimilatory utilization, acetate has been frequently used successfully for specifically tracing anaerobically respiring microorganisms such as iron reducers (e.g., [78, 86]). Within Cumberland Bay sediments, iron reduction is very likely the dominant TEAP occurring in all SIP incubations as indicated by the increasing Fe^{2+} concentrations in the treatments, including controls (Fig. S8A). The slurry likely retained endogenous iron oxides and organic matter from the original sediment. In surface sediments from Cumberland Bay (same sampling site but previous expedition), total Fe content of the solid phase of 46.8 g/kg was reported [38], of which ferrihydrite and lepidocrocite contributed 0.65–0.7 wt% Fe [39]. Therefore, iron reduction could be stimulated without the amendment of additional electron acceptors or donors (see unamended control treatment, Fig. S8A). Given the similarity in the microbial community

composition and proportion of enriched taxa in the heavy fractions (Fig. 6B), we conclude that dissimilatory iron reduction is the most likely dominant process conducted by the labeled taxa enriched in the heavy fractions of all treatments, i.e., members of *Desulfuromonadales* with Sva1033 as the most abundant taxon. This conclusion was supported by the observed similar geochemistry in the treatments (Fig. S8). The possibility that other processes such as sulfate and sulfur reduction, which could occur in these incubations, stimulated the enrichment of *Desulfuromonadales* is not supported by the formation of Fe^{2+} in the incubation experiment over time (Fig. S8A). The likelihood that Sva1033 performs iron reduction in situ as in the RNA-SIP incubations is supported by the close relation of OTU sequences from the in situ sediment and the SIP experiment (Fig. S7). Likewise, in Potter Cove sediment incubations, Sva1033 was also identified as the most dominant organism taking up the acetate label (40% relative abundance in ultra-heavy fraction, Figs. 7C and S9). Our study thus provides evidence for the capability for microbial iron reduction in the uncultured Sva1033 clade from permanently cold (sub-)Antarctic sediments with acetate as electron donor and carbon substrate (Fig. 7). Other taxa enriched in the heavy fractions of the SIP experiments included *Desulfuromonas*, *Geopsychrobacter*, and *Geothermobacter*, species with known iron reducing capabilities [75, 80, 115, 116].

Activity of sulfate reducers in the iron reduction sites

Sulfate reducers are metabolically flexible. Their primary metabolic capabilities are essential for the global sulfur cycle as utilizers of the most oxidized form of sulfur [117] and they are capable of syntrophic growth, e.g., with methanogens [118, 119]. In addition, sulfate reducers are capable of growth with TEAPs such as nitrate [84, 120] and Fe(III) under sulfate limitation [83, 121]. In similar permanently cold marine sediments from the Arctic, sulfate reducers were relatively less abundant compared to iron reducers when iron reduction predominated [27, 112], which is in contrast to this study (Fig. 5). Despite the high abundance of sulfate reducers in the sediments of the iron-rich sites (Figs. 3 and 5), evidence for sulfate reduction was not directly obtained from the pore water profiles (Fig. 2). Hence, an open question emerges regarding the metabolism that keeps sulfate reducers persistent across these sites such that their relative abundances outnumber the iron reducers who likely perform the clearly more dominant TEAP in situ (Fig. 2). We hypothesize for our study that sulfate reduction, masked by the reoxidation of the produced sulfide back to sulfate, fuels the persistence of sulfate reducers [19, 21] in the iron reduction sites.

The results from SIP incubations showed that sulfate reducers were present and active in all treatments. However, they were present in higher abundance in the light compared to the heavy fractions (Fig. 6B). This can be explained by their high abundance in the starting sediment material (42%, Fig. S10). Sulfate reducers responded to the addition of electron acceptor as evidenced by their increased relative abundance in the heavy fractions of the sulfate-amended treatment compared to the other treatments (25% vs. 7–18% ultra-heavy labeled fraction). In general, the lower enrichment of sulfate reducers in the heavy fractions compared to the potential iron reducers is likely because (I) iron reducers were more efficient in the uptake of electron donors such as the provided acetate [122]; (II) iron reduction was the dominant biogeochemical process observed (as discussed above, Fig. 6B and S8A); or/and (III) sulfate reducers were thriving on different, sediment endogenous electron donors [123]. Nevertheless, the detection of *dsrA* transcripts in the SIP fractions (Fig. 6C) supported the hypothesis of co-occurring sulfate reduction in the treatments. Following the observations of the SIP experiment, we suggest that minor concurrent sulfate reduction, in the background of the dominant TEAP i.e. iron reduction, likely fuels the persistence of sulfate reducers in situ in the iron reduction sites Annenkov Trough, Cumberland Bay, and Drygalski Trough (Figs. 3A and 5). The non-detection of sulfide in the incubations could be explained by precipitation with Fe^{2+} forming mackinawite (FeS) and/or pyrite (FeS_2) [124, 125], or reoxidation microbially or abiotically by reactive Fe(III) oxides [21]. Recently, this type of cryptic sulfur cycling, indicated by high sulfide oxidation rates in surface sediments, was shown in multiple studies [21, 126, 127]. In addition, concurrent sulfate and iron reduction in the same zone was reported multiple times [17, 20, 77, 124], but detailed information about the associated microbial community is lacking. These studies [21, 126–129] assign the majority of ferrous iron production to the abiotic process of iron reduction by sulfide oxidation. Although this process likely also occurs in the sediments investigated in this study, sulfide concentrations below detection limit (Fig. 2) and the high activity of mainly iron reducing microorganisms (Fig. 6B) indicate that these abiotic processes provide a minor contribution to observed high Fe^{2+} concentrations (Figs. 2 and S8A).

A limitation of our study is the unexpected lack of dissolved Fe^{2+} over time in the acetate, lepidocrocite and molybdate treatment from the SIP incubation (Fig. S8A). While this result suggested that iron reduction did not occur in this treatment, the enrichment of *Desulfuromonadales* members in similar proportion as in the other treatments shows that iron reduction certainly occurred (Fig. 6B). Besides, inhibition of iron reduction by molybdate has not been shown previously. In comparable studies, molybdate concentrations of 10 mM [83] or even 20 mM

[124] did not inhibit microbial iron reduction. Instead, in our study, the produced dissolved Fe^{2+} reacted abiotically with the added molybdate, preventing the detection of Fe^{2+} (see supplementary material, Figs. S11 and S12, for details).

Conclusion

This study has shown how the microbial communities in sub-Antarctic South Georgia surface sediments are shaped by the dominant TEAP; sulfate reduction in Church Trough and iron reduction in Cumberland Bay, Drygalski Trough, and Annenkov Trough. We provide evidence for microbial iron reduction as one of the metabolic capabilities of the family Sva1033 using RNA-SIP with Cumberland Bay surface sediments. Coincidentally, in all iron reduction sites, Sva1033 was the dominant member of *Desulfuromonadales* found in situ, while other known marine iron reducers were scarce. We also identified iron-reducing capabilities of Sva1033 members in similar surface sediments from Potter Cove in the Antarctic Peninsula. Therefore, this clade might be very important for iron reduction in permanently cold marine sediments given the input of iron from enhanced glacial erosion, weathering, and glacial melt as a result of global warming. Furthermore, our data show high relative abundance of persistent sulfate reducers and suggest their activity in the iron reduction zone of marine sediments potentially participating in cryptic sulfur cycling, with the produced sulfide precipitating as metal sulfide mineral or being reoxidized.

Data availability

The raw sequence data of this study were submitted to GenBank Short Reads Archive (SRA) under the BioProject numbers PRJNA658241 and PRJNA668691 (BioSample numbers SAMN16419039–SAMN16419043 and SAMN16419024–SAMN16419028). The environmental geochemical data were submitted to PANGAEA data publisher for Earth & Environmental Science database under the following doi: 10.1594/PANGAEA.927101.

Acknowledgements The authors thank the captain and entire shipboard crew of the RV METEOR M134 research expedition to South Georgia in January to February 2017. The authors also thank the Alfred Wegener Institute Helmholtz Centre for Polar and Marine Research and the Instituto Antártico Argentino (IAA) for logistical support during the Antarctic summer sampling campaign (January to March 2019) to the King George Island/Isla 25 de Mayo in the Antarctic Peninsula. The authors also thank the crew at the Argentinian Research Station Base Carlini and the Argentinian Army (Ejército Argentino) divers of the CAV (January to March 2019) for logistics support during the campaign.

Funding This project was funded by the Deutsche Forschungsgemeinschaft (DFG) Research Center/Cluster of Excellence EXC 309 (project-ID 49926684) "The Ocean in the Earth System," and within the DFG infrastructure priority program 1158 "Antarctic Research with Comparative Investigations in Arctic Ice Areas" (project-ID 404648014), and the University of Bremen. The expedition under the title "Emissions of free gas around South Georgia: distribution, quantification, and sources for methane ebullition sites in sub-Antarctic waters" was carried out with the support of MARUM — Center for Marine Environmental Sciences, Research Faculty University of Bremen. We also acknowledge additional funding from the Helmholtz Association (Alfred Wegener Institute Helmholtz Centre for Polar and Marine Research, Bremerhaven). The cruise was sponsored by the German Research Foundation (DFG) and by the Federal Ministry of Education and Research (BMBF). Open Access funding enabled and organized by Projekt DEAL.

Compliance with ethical standards

Conflict of interest The authors declare no competing interests.

Publisher's note Springer Nature remains neutral with regard to jurisdictional claims in published maps and institutional affiliations.

References

1. D'Hondt S, Jørgensen BB, Miller DJ, Batzke A, Blake R, Cragg BA, et al. Distributions of microbial activities in deep subseafloor sediments. Science. 2004;306:2216–21.
2. Froelich PN, Klinkhammer GP, Bender ML, Luedtke NA, Heath GR, Cullen D, et al. Early oxidation of organic matter in pelagic sediments of the eastern equatorial Atlantic: suboxic diagenesis. Geochim Cosmochim Acta. 1979;43:1075–90.
3. Parkes RJ, Cragg B, Roussel E, Webster G, Weightman A, Sass H. A review of prokaryotic populations and processes in subseafloor sediments, including biosphere: geosphere interactions. Mar Geol. 2014;352:409–25.
4. Arnosti C. Microbial extracellular enzymes and the marine carbon cycle. Annu Rev Mar Sci. 2011;3:401–25.
5. Thamdrup B, Rosselló-Mora R, Amann R. Microbial manganese and sulfate reduction in Black Sea shelf sediments. Appl Environ Microbiol. 2000;66:2888–97.
6. Thamdrup B. Bacterial manganese and iron reduction in aquatic sediments. In: Schink B, editor. Advances in microbial ecology. Boston, MA, US: Springer; 2000. p. 41–84.
7. Jørgensen BB, Kasten S. Sulfur cycling and methane oxidation. In: Schulz HD, Zabel M, editors. Marine geochemistry. 2nd ed. Berlin, Heidelberg, Germany: Springer-Verlag; 2006. p. 271–309.
8. Bowles MW, Mogollón JM, Kasten S, Zabel M, Hinrichs K-U. Global rates of marine sulfate reduction and implications for sub–sea-floor metabolic activities. Science. 2014;344:889–91.

9. Jickells TD, An ZS, Andersen KK, Baker AR, Bergametti G, Brooks N, et al. Global iron connections between desert dust, ocean biogeochemistry, and climate. Science. 2005;308:67–71.
10. Raiswell R, Hawkings JR, Benning LG, Baker AR, Death R, Albani S, et al. Potentially bioavailable iron delivery by iceberg-hosted sediments and atmospheric dust to the polar oceans. Biogeosciences. 2016;13:3887–900.
11. Hawkings JR, Wadham JL, Tranter M, Raiswell R, Benning LG, Statham PJ, et al. Ice sheets as a significant source of highly reactive nanoparticulate iron to the oceans. Nat Commun. 2014;5:3929.
12. Death R, Wadham JL, Monteiro F, Le Brocq AM, Tranter M, Ridgwell A, et al. Antarctic ice sheet fertilises the Southern Ocean. Biogeosciences. 2014;11:2635–43.
13. Monien D, Monien P, Brünjes R, Widmer T, Kappenberg A, Silva Busso AA, et al. Meltwater as a source of potentially bioavailable iron to Antarctica waters. Antarct Sci. 2017;29:277–91.
14. Henkel S, Kasten S, Hartmann JF, Silva-Busso A, Staubwasser M. Iron cycling and stable Fe isotope fractionation in Antarctic shelf sediments, King George Island. Geochim Cosmochim Acta. 2018;237:320–38.
15. Hodson A, Nowak A, Sabacka M, Jungblut A, Navarro F, Pearce D, et al. Climatically sensitive transfer of iron to maritime Antarctic ecosystems by surface runoff. Nat Commun. 2017;8:14499.
16. Wang S, Bailey D, Lindsay K, Moore JK, Holland M. Impact of sea ice on the marine iron cycle and phytoplankton productivity. Biogeosciences. 2014;11:4713–31.
17. Jørgensen BB, Findlay AJ, Pellerin A. The biogeochemical sulfur cycle of marine sediments. Front Microbiol. 2019;10:849.
18. Findlay AJ, Kamyshny A. Turnover rates of intermediate sulfur species (S_x^{2-}, S^0, $S_2O_3^{2-}$, $S_4O_6^{2-}$, SO_3^{2-}) in anoxic freshwater and sediments. Front Microbiol. 2017;8:2551.
19. Findlay AJ, Pellerin A, Laufer K, Jørgensen BB. Quantification of sulphide oxidation rates in marine sediment. Geochim Cosmochim Acta. 2020;280:441–52.
20. Canfield DE, Jørgensen BB, Fossing H, Glud R, Gundersen J, Ramsing NB, et al. Pathways of organic carbon oxidation in three continental margin sediments. Mar Geol. 1993;113:27–40.
21. Michaud AB, Laufer K, Findlay A, Pellerin A, Antler G, Turchyn AV, et al. Glacial influence on the iron and sulfur cycles in Arctic fjord sediments (Svalbard). Geochim Cosmochim Acta. 2020;280:423–40.
22. Jensen MM, Thamdrup B, Rysgaard S, Holmer M, Fossing H. Rates and regulation of microbial iron reduction in sediments of the Baltic-North Sea transition. Biogeochemistry. 2003;65:295–317.
23. Beckler JS, Kiriazis N, Rabouille C, Stewart FJ, Taillefert M. Importance of microbial iron reduction in deep sediments of river-dominated continental-margins. Mar Chem. 2016;178:22–34.
24. Riedinger N, Brunner B, Krastel S, Arnold GL, Wehrmann LM, Formolo MJ, et al. Sulfur cycling in an iron oxide-dominated, dynamic marine depositional system: the Argentine Continental Margin. Front Earth Sci. 2017;5:33.
25. Thamdrup B, Fossing H, Jørgensen BB. Manganese, iron and sulfur cycling in a coastal marine sediment, Aarhus Bay, Denmark. Geochim Cosmochim Acta. 1994;58:5115–29.
26. Arndt S, Jørgensen BB, LaRowe DE, Middelburg J, Pancost R, Regnier P. Quantifying the degradation of organic matter in marine sediments: a review and synthesis. Earth-Sci Rev. 2013;123:53–86.
27. Algora C, Vasileiadis S, Wasmund K, Trevisan M, Krüger M, Puglisi E, et al. Manganese and iron as structuring parameters of microbial communities in Arctic marine sediments from the Baffin Bay. FEMS Microbiol Ecol. 2015;91:fiv056.
28. Franco M, De Mesel I, Diallo MD, Van Der Gucht K, Van Gansbeke D, Van, et al. Effect of phytoplankton bloom deposition on benthic bacterial communities in two contrasting sediments in the southern North Sea. Aquat Micro Ecol. 2007;48:241–54.
29. Zonneveld KAF, Versteegh GJM, Kasten S, Eglinton TI, Emeis K-C, Huguet C, et al. Selective preservation of organic matter in marine environments; processes and impact on the sedimentary record. Biogeosciences. 2010;7:483–511.
30. Jorgensen SL, Hannisdal B, Lanzén A, Baumberger T, Flesland K, Fonseca R, et al. Correlating microbial community profiles with geochemical data in highly stratified sediments from the Arctic Mid-Ocean Ridge. Proc Natl Acad Sci U S A. 2012;109:E2846–55.
31. Zinke LA, Glombitza C, Bird JT, Røy H, Jørgensen BB, Lloyd KG, et al. Microbial organic matter degradation potential in Baltic Sea sediments is influenced by depositional conditions and in situ geochemistry. Appl Environ Microbiol. 2019;85:e02164-18.
32. Yang J, Jiang H, Wu G, Dong H. Salinity shapes microbial diversity and community structure in surface sediments of the Qinghai-Tibetan Lakes. Sci Rep. 2016;6:25078.
33. Hicks N, Liu X, Gregory R, Kenny J, Lucaci A, Lenzi L, et al. Temperature driven changes in benthic bacterial diversity influences biogeochemical cycling in coastal sediments. Front Microbiol. 2018;9:1730.
34. Hamdan LJ, Coffin RB, Sikaroodi M, Greinert J, Treude T, Gillevet PM. Ocean currents shape the microbiome of Arctic marine sediments. ISME J. 2013;7:685–96.
35. Schulz HD, Zabel M, editors. Marine geochemistry. 2nd ed. Berlin, Heidelberg, Germany: Springer-Verlag; 2006.
36. Geprägs P, Torres ME, Mau S, Kasten S, Römer M, Bohrmann G. Carbon cycling fed by methane seepage at the shallow Cumberland Bay, South Georgia, sub-Antarctic. Geochem, Geophys Geosystems. 2016;17:1401–18.
37. Atkinson A, Whitehouse MJ, Priddle J, Cripps GC, Ward P, Brandon MA. South Georgia, Antarctica: a productive, cold water, pelagic ecosystem. Mar Ecol Prog Ser. 2001;216:279–308.
38. Löffler B. Geochemische Prozesse und Stoffkreisläufe in Sedimenten innerhalb und außerhalb des Cumberland-Bay Fjordes, Süd Georgien. Bachelor Thesis. Bremen, Germany: University of Bremen; 2013.
39. Köster M. (Bio-)geochemische Prozesse in den eisenreichen Seep-Sedimenten der Cumberland-Bucht Südgeorgiens, Subantarktis. Bachelor Thesis. Bremen, Germany: University of Bremen; 2014.
40. Römer M, Torres M, Kasten S, Kuhn G, Graham AG, Mau S, et al. First evidence of widespread active methane seepage in the Southern Ocean, off the sub-Antarctic island of South Georgia. Earth Planet Sci Lett. 2014;403:166–77.
41. Bohrmann G, Aromokeye AD, Bihler V, Dehning K, Dohrmann I, Gentz T, et al. R/V METEOR Cruise Report M134, emissions of free gas from cross-shelf troughs of South Georgia: distribution, quantification, and sources for methane ebullition sites in sub-Antarctic waters, Port Stanley (Falkland Islands)—Punta Arenas (Chile), 16 January–18 February 2017. 2017.
42. Schnakenberg A, Aromokeye DA, Kulkarni A, Maier L, Wunder LC, Richter-Heitmann T, et al. Electron acceptor availability shapes Anaerobically Methane Oxidizing Archaea (ANME) communities in South Georgia sediments. Front Microbiol. 2021;12:726.
43. Rückamp M, Braun M, Suckro S, Blindow N. Observed glacial changes on the King George Island ice cap, Antarctica, in the last decade. Global Planet Change. 2011;79:99–109.

44. Seeberg-Elverfeldt J, Schlüter M, Feseker T, Kölling M. Rhizon sampling of porewaters near the sediment-water interface of aquatic systems. Limnol Oceanogr Methods. 2005;3:361–71.
45. Oni OE, Miyatake T, Kasten S, Richter-Heitmann T, Fischer D, Wagenknecht L, et al. Distinct microbial populations are tightly linked to the profile of dissolved iron in the methanic sediments of the Helgoland mud area, North Sea. Front Microbiol. 2015;6:365.
46. Aromokeye DA, Richter-Heitmann T, Oni OE, Kulkarni A, Yin X, Kasten S, et al. Temperature controls crystalline iron oxide utilization by microbial communities in methanic ferruginous marine sediment incubations. Front Microbiol. 2018;9:2574.
47. Parada AE, Needham DM, Fuhrman JA. Every base matters: assessing small subunit rRNA primers for marine microbiomes with mock communities, time series and global field samples. Environ Microbiol. 2016;18:1403–14.
48. Herlemann DPR, Labrenz M, Jürgens K, Bertilsson S, Waniek JJ, Andersson AF. Transitions in bacterial communities along the 2000 km salinity gradient of the Baltic Sea. ISME J. 2011;5:1571–9.
49. Ovreås L, Forney L, Daae FL, Torsvik V. Distribution of bacterioplankton in meromictic Lake Saelenvannet, as determined by denaturing gradient gel electrophoresis of PCR-amplified gene fragments coding for 16S rRNA. Appl Environ Microbiol. 1997;63:3367–73.
50. Takai K, Horikoshi K. Rapid detection and quantification of members of the archaeal community by quantitative PCR using fluorogenic probes. Appl Environ Microbiol. 2000;66:5066–72.
51. Viollier E, Inglett P, Hunter K, Roychoudhury A, Van Cappellen P. The ferrozine method revisited: Fe(II)/Fe(III) determination in natural waters. Appl Geochem. 2000;15:785–90.
52. Yin X, Kulkarni AC, Friedrich MW. DNA and RNA stable isotope probing of methylotrophic methanogenic Archaea. In: Dumont MG, Hernández García M, editors. Stable isotope probing: methods and protocols. New York, NY: Springer; 2019. p. 189–206.
53. Aromokeye DA, Kulkarni AC, Elvert M, Wegener G, Henkel S, Coffinet S, et al. Rates and microbial players of iron-driven anaerobic oxidation of methane in methanic marine sediments. Front Microbiol. 2020;10:3041.
54. Eden PA, Schmidt TM, Blakemore RP, Pace NR. Phylogenetic analysis of *Aquaspirillum magnetotacticum* using polymerase chain reaction-amplified 16S rRNA-specific DNA. Int J Syst Evol Microbiol. 1991;41:324–5.
55. Yu Y, Lee C, Kim J, Hwang S. Group-specific primer and probe sets to detect methanogenic communities using quantitative real-time polymerase chain reaction. Biotechnol Bioeng. 2005;89:670–9.
56. Lueders T, Friedrich MW. Effects of amendment with ferrihydrite and gypsum on the structure and activity of methanogenic populations in rice field soil. Appl Environ Microbiol. 2002;68:2484–94.
57. Lane DJ. 16S/23S rRNA sequencing. In: Stackebrandt E, Goodfellow M, editors. Nucleic acid techniques in bacterial systematics. New York: John Wiley and Sons; 1991. p. 115–75.
58. Großkopf R, Janssen PH, Liesack W. Diversity and structure of the methanogenic community in anoxic rice paddy soil microcosms as examined by cultivation and direct 16S rRNA gene sequence retrieval. Appl Environ Microbiol. 1998;64:960–9.
59. Reyes C, Schneider D, Thürmer A, Kulkarni A, Lipka M, Sztejrenszus SY, et al. Potentially active iron, sulfur, and sulfate reducing bacteria in Skagerrak and Bothnian Bay sediments. Geomicrobiol J. 2017;34:840–50.
60. Kondo R, Nedwell DB, Purdy KJ, Silva SQ. Detection and enumeration of sulphate-reducing Bacteria in estuarine sediments by competitive PCR. Geomicrobiol J. 2004;21:145–57.
61. Benjamini Y, Yekutieli D. The control of the false discovery rate in multiple testing under dependency. Ann Stat. 2001;29:1165–88.
62. R Core Team. R: a language and environment for statistical computing, 3.6.1. Vienna, Austria: R Foundation for Statistical Computing; 2019. Available from: https://www.R-project.org.
63. Oksanen J, Blanchet FG, Friendly M, Kindt R, Legendre P, McGlinn D, et al. vegan: Community Ecology Package, 2.5-6. 2019. Available from: https://CRAN.R-project.org/package=vegan.
64. Quast C, Pruesse E, Yilmaz P, Gerken J, Schweer T, Yarza P, et al. The SILVA ribosomal RNA gene database project: improved data processing and web-based tools. Nucleic Acids Res. 2012;41:D590–6.
65. Stamatakis A. RAxML version 8: a tool for phylogenetic analysis and post-analysis of large phylogenies. Bioinformatics. 2014;30:1312–3.
66. Letunic I, Bork P. Interactive Tree Of Life (iTOL) v4: recent updates and new developments. Nucleic Acids Res. 2019;47:W256–9.
67. Inkscape Team. Inkscape, 1.0.1. 2020. Available from: https://inkscape.org.
68. Sun H, Spring S, Lapidus A, Davenport K, Glavina Del Rio T, Tice H, et al. Complete genome sequence of *Desulfarculus baarsii* type strain (2st14T). Stand Genom Sci. 2010;3:276–84.
69. Kümmel S, Herbst F-A, Bahr A, Duarte M, Pieper DH, Jehmlich N, et al. Anaerobic naphthalene degradation by sulfate-reducing *Desulfobacteraceae* from various anoxic aquifers. FEMS Microbiol Ecol. 2015;91:fiv006.
70. Belyakova EV, Rozanova EP, Borzenkov IA, Tourova TP, Pusheva MA, Lysenko AM, et al. The new facultatively chemolithoautotrophic, moderately halophilic, sulfate-reducing bacterium *Desulfovermiculus halophilus* gen. nov., sp. nov., isolated from an oil field. Microbiology. 2006;75:161–71.
71. Rezadehbashi M, Baldwin SA. Core sulphate-reducing microorganisms in metal-removing semi-passive biochemical reactors and the co-occurrence of methanogens. Microorganisms. 2018;6:16.
72. Sheik CS, Jain S, Dick GJ. Metabolic flexibility of enigmatic SAR324 revealed through metagenomics and metatranscriptomics. Environ Microbiol. 2014;16:304–17.
73. Sorokin DY, Chernyh NA. '*Candidatus* Desulfonatronobulbus propionicus': a first haloalkaliphilic member of the order *Syntrophobacterales* from soda lakes. Extremophiles. 2016;20:895–901.
74. Lovley DR, Giovannoni SJ, White DC, Champine JE, Phillips E, Gorby YA, et al. *Geobacter metallireducens* gen. nov. sp. nov., a microorganism capable of coupling the complete oxidation of organic compounds to the reduction of iron and other metals. Arch Microbiol. 1993;159:336–44.
75. Roden EE, Lovley DR. Dissimilatory Fe(III) reduction by the marine microorganism *Desulfuromonas acetoxidans*. Appl Environ Microbiol. 1993;59:734–42.
76. Lovley DR, Coates JD, Saffarini DA, Lonergan DJ. Dissimilatory iron reduction. In: Winkelmann G, Carrano CJ, editors. Transition metals in microbial metabolism. Amsterdam: Harwood Academic Publishers; 1997. p. 187–215.
77. Vandieken V, Finke N, Jørgensen BB. Pathways of carbon oxidation in an Arctic fjord sediment (Svalbard) and isolation of psychrophilic and psychrotolerant Fe(III)-reducing bacteria. Mar Ecol Prog Ser. 2006;322:29–41.
78. Vandieken V, Thamdrup B. Identification of acetate-oxidizing bacteria in a coastal marine surface sediment by RNA-stable isotope probing in anoxic slurries and intact cores. FEMS Microbiol Ecol. 2013;84:373–86.

79. Hori T, Aoyagi T, Itoh H, Narihiro T, Oikawa A, Suzuki K, et al. Isolation of microorganisms involved in reduction of crystalline iron(III) oxides in natural environments. Front Microbiol. 2015;6:386.
80. Vandieken V, Mußmann M, Niemann H, Jørgensen BB. *Desulfuromonas svalbardensis* sp. nov. and *Desulfuromusa ferrireducens* sp. nov., psychrophilic, Fe(III)-reducing bacteria isolated from Arctic sediments, Svalbard. Int J Syst Evol Microbiol. 2006;56:1133–9.
81. Slobodkina GB, Reysenbach A-L, Panteleeva AN, Kostrikina NA, Wagner ID, Bonch-Osmolovskaya EA, et al. *Deferrisoma camini* gen. nov., sp. nov., a moderately thermophilic, dissimilatory iron(III)-reducing bacterium from a deep-sea hydrothermal vent that forms a distinct phylogenetic branch in the Deltaproteobacteria. Int J Syst Evol Microbiol. 2012;62:2463–8.
82. Tu T-H, Wu L-W, Lin Y-S, Imachi H, Lin L-H, Wang P-L. Microbial community composition and functional capacity in a terrestrial ferruginous, sulfate-depleted mud volcano. Front Microbiol. 2017;8:2137.
83. Lovley DR, Roden EE, Phillips EJP, Woodward JC. Enzymatic iron and uranium reduction by sulfate-reducing bacteria. Mar Geol. 1993;113:41–53.
84. Bale SJ, Goodman K, Rochelle PA, Marchesi JR, Fry JC, Weightman AJ, et al. *Desulfovibrio profundus* sp. nov., a novel barophilic sulfate-reducing Bacterium from deep sediment layers in the Japan Sea. Int J Syst Evol Microbiol. 1997;47:515–21.
85. Treude N, Rosencrantz D, Liesack W, Schnell S. Strain FAc12, a dissimilatory iron-reducing member of the *Anaeromyxobacter* subgroup of Myxococcales. FEMS Microbiol Ecol. 2003;44:261–9.
86. Hori T, Müller A, Igarashi Y, Conrad R, Friedrich MW. Identification of iron-reducing microorganisms in anoxic rice paddy soil by ^{13}C-acetate probing. ISME J. 2010;4:267–78.
87. Han Y, Perner M. The globally widespread genus Sulfurimonas: versatile energy metabolisms and adaptations to redox clines. Front Microbiol. 2015;6:989.
88. Roalkvam I, Drønen K, Stokke R, Daae FL, Dahle H, Steen IH. Physiological and genomic characterization of Arcobacter anaerophilus IR-1 reveals new metabolic features in Epsilonproteobacteria. Front Microbiol. 2015;6:987.
89. Schlosser C, Schmidt K, Aquilina A, Homoky WB, Castrillejo M, Mills RA, et al. Mechanisms of dissolved and labile particulate iron supply to shelf waters and phytoplankton blooms off South Georgia, Southern Ocean. Biogeosciences. 2018;15:4973–93.
90. Sahade R, Lagger C, Torre L, Momo F, Monien P, Schloss I, et al. Climate change and glacier retreat drive shifts in an Antarctic benthic ecosystem. Sci Adv. 2015;1:e1500050.
91. Petro C, Starnawski P, Schramm A, Kjeldsen KU. Microbial community assembly in marine sediments. Aquat Micro Ecol. 2017;79:177–95.
92. Petro C, Zäncker B, Starnawski P, Jochum LM, Ferdelman TG, Jørgensen BB, et al. Marine deep biosphere microbial communities assemble in near-surface sediments in Aarhus Bay. Front Microbiol. 2019;10:758.
93. Starnawski P, Bataillon T, Ettema TJ, Jochum LM, Schreiber L, Chen X, et al. Microbial community assembly and evolution in subseafloor sediment. Proc Natl Acad Sci USA. 2017;114:2940–5.
94. Marshall IPG, Ren G, Jaussi M, Lomstein BA, Jørgensen BB, Røy H, et al. Environmental filtering determines family-level structure of sulfate-reducing microbial communities in subsurface marine sediments. ISME J. 2019;13:1920–32.
95. Berner RA. Early diagenesis: a theoretical approach. Princeton, New Jersey: Princeton University Press; 1980.
96. Cottrell MT, Kirchman DL. Natural assemblages of marine Proteobacteria and members of the *Cytophaga-Flavobacter* cluster consuming low- and high-molecular-weight dissolved organic matter. Appl Environ Microbiol. 2000;66:1692–7.
97. Bissett A, Bowman JP, Burke CM. Flavobacterial response to organic pollution. Aquat Micro Ecol. 2008;51:31–43.
98. Martinez-Garcia M, Brazel DM, Swan BK, Arnosti C, Chain PSG, Reitenga KG, et al. Capturing single cell genomes of active polysaccharide degraders: an unexpected contribution of Verrucomicrobia. PLoS ONE. 2012;7:e35314.
99. Sabree ZL, Kambhampati S, Moran NA. Nitrogen recycling and nutritional provisioning by *Blattabacterium*, the cockroach endosymbiont. Proc Natl Acad Sci U S A. 2009;106:19521–6.
100. Bowman JP, McCuaig RD. Biodiversity, community structural shifts, and biogeography of Prokaryotes within Antarctic continental shelf sediment. Appl Environ Microbiol. 2003;69:2463–83.
101. Blazejak A, Schippers A. High abundance of JS-1- and Chloroflexi-related Bacteria in deeply buried marine sediments revealed by quantitative, real-time PCR. FEMS Microbiol Ecol. 2010;72:198–207.
102. Yamada T, Sekiguchi Y, Hanada S, Imachi H, Ohashi A, Harada H, et al. *Anaerolinea thermolimosa* sp. nov., *Levilinea saccharolytica* gen. nov., sp. nov. and *Leptolinea tardivitalis* gen. nov., sp. nov., novel filamentous anaerobes, and description of the new classes Anaerolineae classis nov. and Caldilineae classis nov. in the bacterial phylum Chloroflexi. Int J Syst Evol Microbiol. 2006;56:1331–40.
103. Storesund JE, Øvreås L. Diversity of Planctomycetes in iron-hydroxide deposits from the Arctic Mid Ocean Ridge (AMOR) and description of *Bythopirellula goksoyri* gen. nov., sp. nov., a novel *Planctomycete* from deep sea iron-hydroxide deposits. Antonie Van Leeuwenhoek. 2013;104:569–84.
104. Kovaleva OL, Merkel AY, Novikov AA, Baslerov RV, Toshchakov SV, Bonch-Osmolovskaya EA. *Tepidisphaera mucosa* gen. nov., sp. nov., a moderately thermophilic member of the class Phycisphaerae in the phylum Planctomycetes, and proposal of a new family, *Tepidisphaeraceae* fam. nov., and a new order, Tepidisphaerales ord. nov. Int J Syst Evol Microbiol. 2015;65:549–55.
105. Borrione I, Schlitzer R. Distribution and recurrence of phytoplankton blooms around South Georgia, Southern Ocean. Biogeosciences. 2013;10:217–31.
106. Pfennig N, Biebl H. *Desulfuromonas acetoxidans* gen. nov. and sp. nov., a new anaerobic, sulfur-reducing, acetate-oxidizing bacterium. Arch Microbiol. 1976;110:3–12.
107. Finster K, Bak F, Pfennig N. *Desulfuromonas acetexigens* sp. nov., a dissimilatory sulfur-reducing eubacterium from anoxic freshwater sediments. Arch Microbiol. 1994;161:328–32.
108. Lovley DR, Phillips EJP, Lonergan DJ, Widman PK. Fe(III) and S^0 reduction by *Pelobacter carbinolicus*. Appl Environ Microbiol. 1995;61:2132–8.
109. An TT, Picardal FW. *Desulfuromonas carbonis* sp. nov., an Fe(III)-, S^0- and Mn(IV)-reducing bacterium isolated from an active coalbed methane gas well. Int J Syst Evol Microbiol. 2015;65:1686–93.
110. Pjevac P, Kamyshny A Jr, Dyksma S, Mußmann M. Microbial consumption of zero-valence sulfur in marine benthic habitats. Environ Microbiol. 2014;16:3416–30.
111. Miao Z-Y, He H, Tan T, Zhang T, Tang J-L, Yang Y-C, et al. Biotreatment of Mn^{2+} and Pb^{2+} with sulfate-reducing bacterium *Desulfuromonas alkenivorans* S-7. J Environ Eng. 2018;144:04017116.
112. Buongiorno J, Herbert L, Wehrmann L, Michaud A, Laufer K, Røy H, et al. Complex microbial communities drive iron and

sulfur cycling in Arctic fjord sediments. Appl Environ Microbiol. 2019;85:e00949-19.
113. Zhang H, Liu F, Zheng S, Chen L, Zhang X, Gong J. The differentiation of iron-reducing bacterial community and iron-reduction activity between riverine and marine sediments in the Yellow River estuary. Mar Life Sci Technol. 2020;2:87–96.
114. Ravenschlag K, Sahm K, Pernthaler J, Amann R. High bacterial diversity in permanently cold marine sediments. Appl Environ Microbiol. 1999;65:3982–9.
115. Kashefi K, Holmes DE, Baross JA, Lovley DR. Thermophily in the *Geobacteraceae: Geothermobacter ehrlichii* gen. nov., sp. nov., a novel thermophilic member of the *Geobacteraceae* from the "Bag City" hydrothermal vent. Appl Environ Microbiol. 2003;69:2985–93.
116. Holmes DE, Nicoll JS, Bond DR, Lovley DR. Potential role of a novel psychrotolerant member of the family *Geobacteraceae, Geopsychrobacter electrodiphilus* gen. nov., sp. nov., in electricity production by a marine sediment fuel cell. Appl Environ Microbiol. 2004;70:6023–30.
117. Jørgensen BB. Mineralization of organic matter in the sea bed—the role of sulphate reduction. Nature. 1982;296:643–5.
118. Bryant M, Campbell LL, Reddy C, Crabill M. Growth of *Desulfovibrio* in lactate or ethanol media low in sulfate in association with H_2-utilizing methanogenic bacteria. Appl Environ Microbiol. 1977;33:1162–9.
119. Muyzer G, Stams AJ. The ecology and biotechnology of sulphate-reducing bacteria. Nat Rev Microbiol. 2008;6:441–54.
120. Dalsgaard T, Bak F. Nitrate reduction in a sulfate-reducing bacterium, *Desulfovibrio desulfuricans*, isolated from rice paddy soil: sulfide inhibition, kinetics, and regulation. Appl Environ Microbiol. 1994;60:291–7.
121. Holmes DE, Bond DR, Lovley DR. Electron transfer by *Desulfobulbus propionicus* to Fe (III) and graphite electrodes. Appl Environ Microbiol. 2004;70:1234–7.
122. Lovley DR, Phillips EJP. Competitive mechanisms for inhibition of sulfate reduction and methane production in the zone of ferric iron reduction in sediments. Appl Environ Microbiol. 1987;53:2636–41.
123. Finke N, Vandieken V, Jørgensen BB. Acetate, lactate, propionate, and isobutyrate as electron donors for iron and sulfate reduction in Arctic marine sediments, Svalbard. FEMS Microbiol Ecol. 2007;59:10–22.
124. Canfield DE, Thamdrup B, Hansen JW. The anaerobic degradation of organic matter in Danish coastal sediments: iron reduction, manganese reduction, and sulfate reduction. Geochim Cosmochim Acta. 1993;57:3867–83.
125. Jørgensen BB. The sulfur cycle of a coastal marine sediment (Limfjorden, Denmark). Limnol Oceanogr. 1977;22:814–32.
126. Jørgensen BB, Laufer K, Michaud AB, Wehrmann LM. Biogeochemistry and microbiology of high Arctic marine sediment ecosystems—case study of Svalbard fjords. Limnol Oceanogr. 2021;66:S273–92.
127. Laufer K, Michaud AB, Røy H, Jørgensen BB. Reactivity of iron minerals in the seabed toward microbial reduction—a comparison of different extraction techniques. Geomicrobiol J. 2020;37:170–89.
128. Holmkvist L, Ferdelman TG, Jørgensen BB. A cryptic sulfur cycle driven by iron in the methane zone of marine sediment (Aarhus Bay, Denmark). Geochim Cosmochim Acta. 2011;75:3581–99.
129. Riedinger N, Brunner B, Formolo MJ, Solomon E, Kasten S, Strasser M, et al. Oxidative sulfur cycling in the deep biosphere of the Nankai Trough, Japan. Geology. 2010;38:851–4.

2.2 Supplementary

2.2.1 Supplementary figures

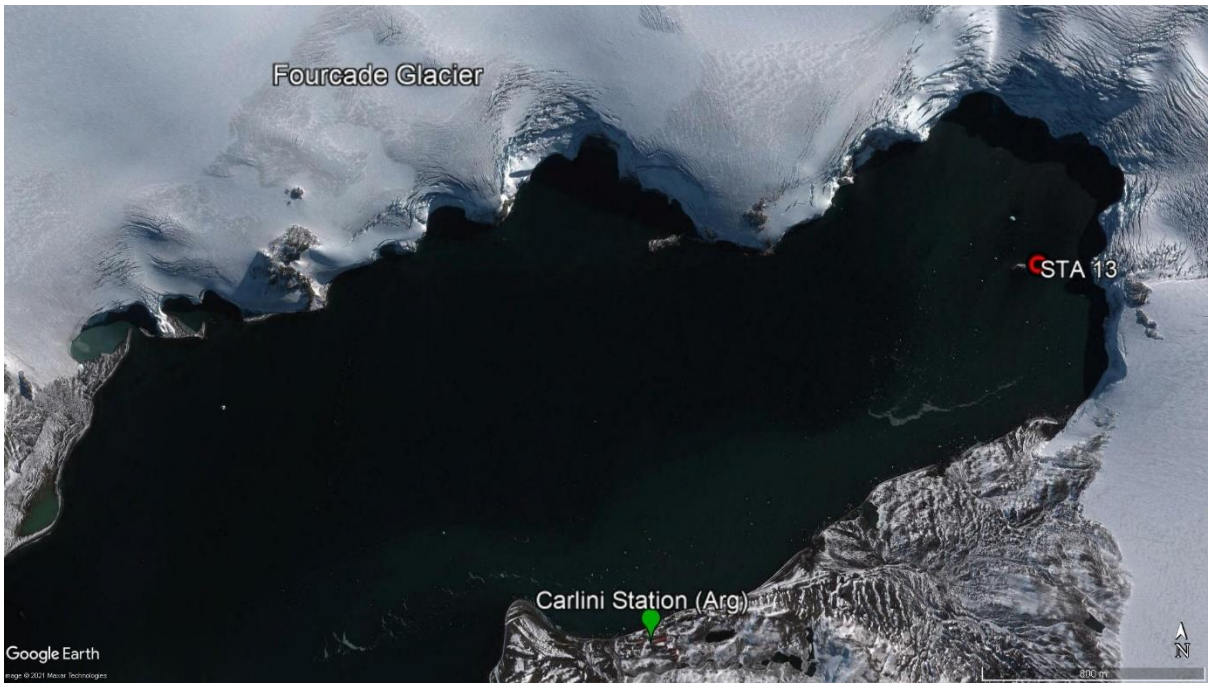

Fig. S1: Sampling location of Station 13 in Potter Cove (King George Island/Isla 25 de Mayo, Antarctic Peninsula). Produced with Google Earth.

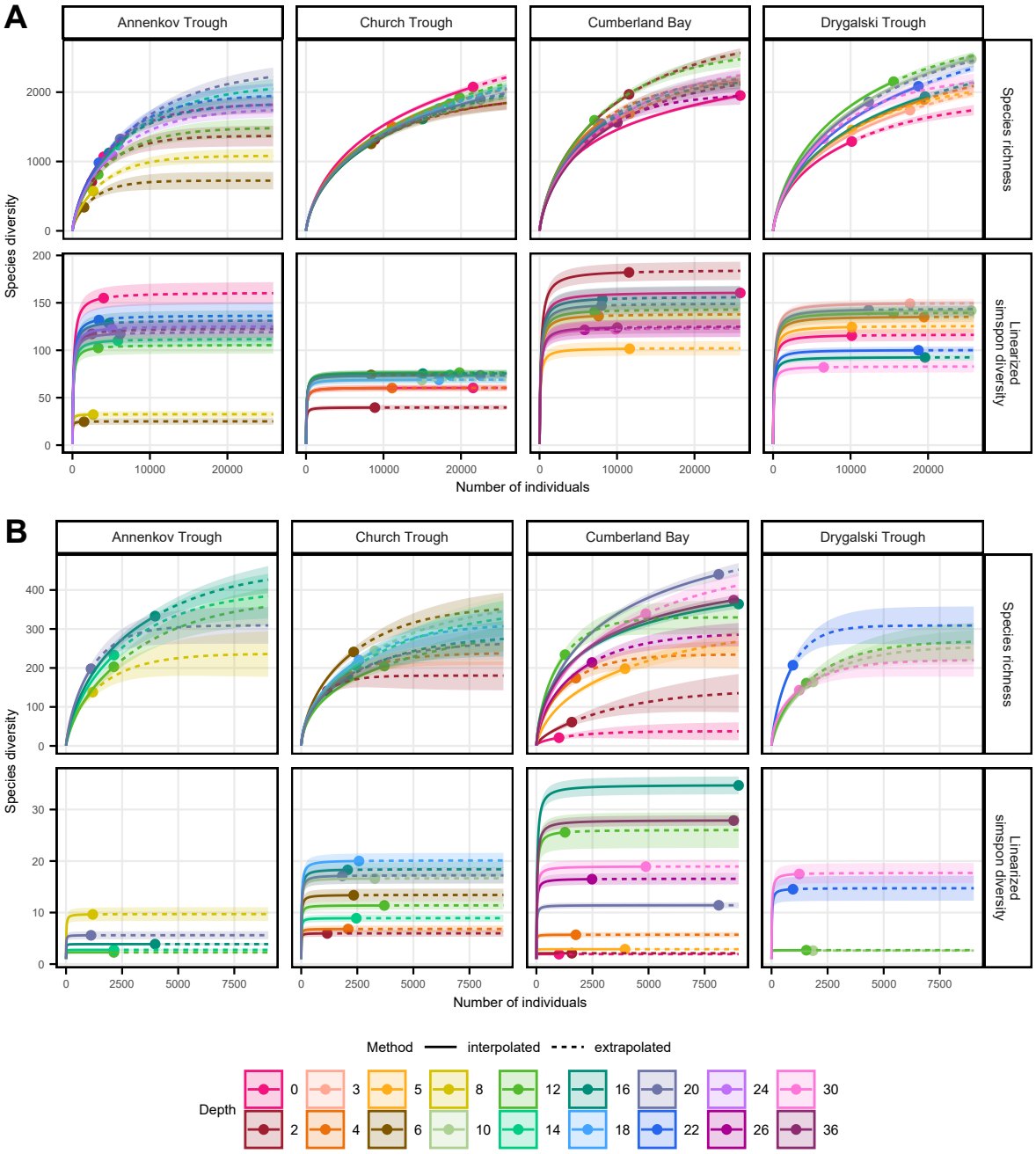

Fig. S2: Rarefaction curves of 16S rRNA sequencing of South Georgia surface sediment for bacteria (**a**) and archaea (**b**). Depth in cm below seafloor. **b** Samples after removing low read samples (see Table S2) leaving Annenkov Trough n = 5, Church Trough n = 9, Cumberland Bay n = 10, Drygalski Trough n = 4.

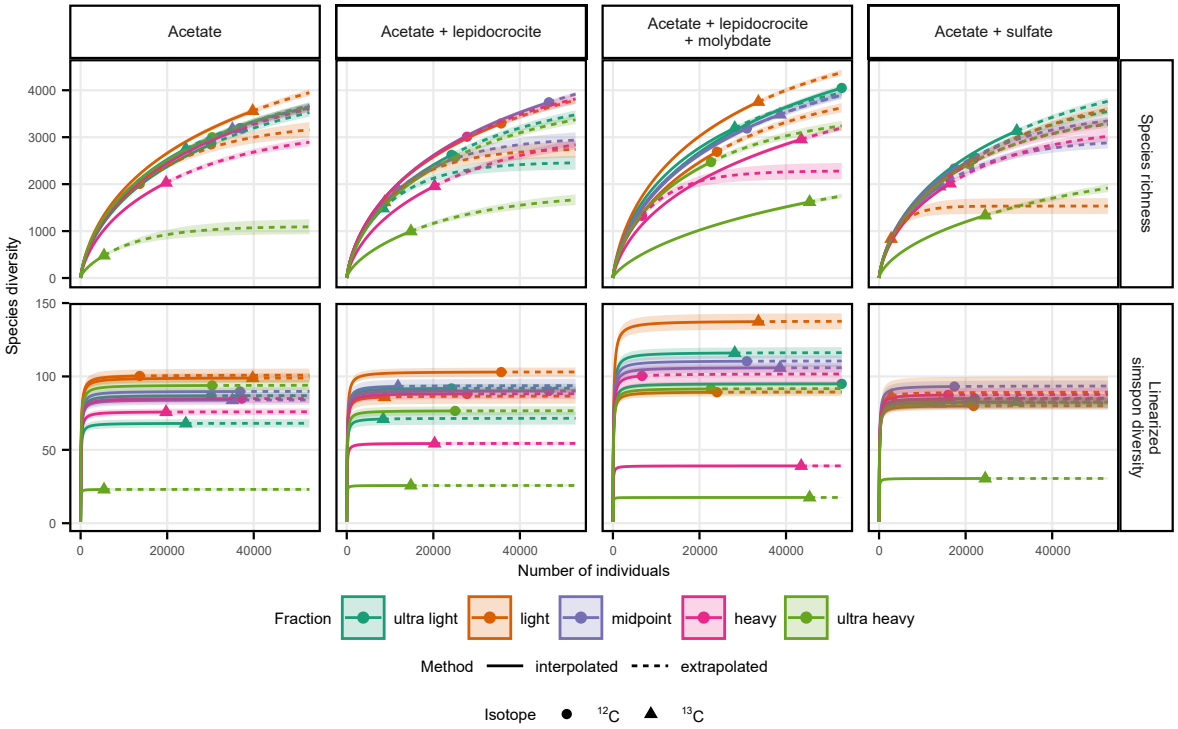

Fig. S3: Rarefaction curve of bacterial 16S rRNA sequencing of SIP incubations with Cumberland Bay sediments.

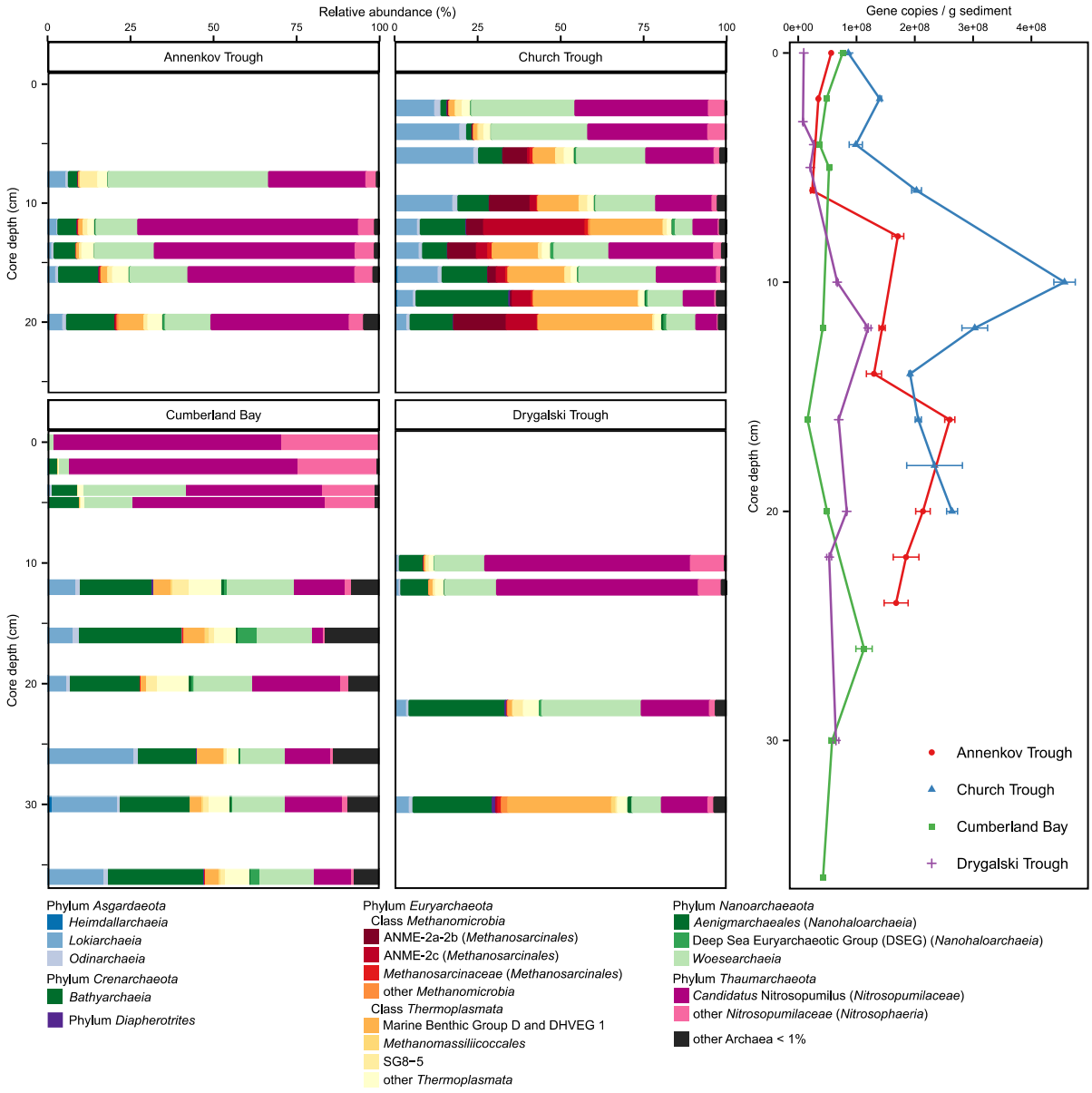

Fig. S4: Archaeal community composition and gene copy numbers in South Georgia surface sediments. **a** Relative abundance of bacterial 16S rRNA genes in Annenkov Trough, Church Trough, Cumberland Bay and Drygalski Trough. From the originally sequenced 10 samples per site, some were removed due to insufficient coverage (see Table S2). **b** Archaeal 16S rRNA gene copies per gram wet sediment of 10 samples per site with error bars displaying SD of technical qPCR replicates (n = 3).

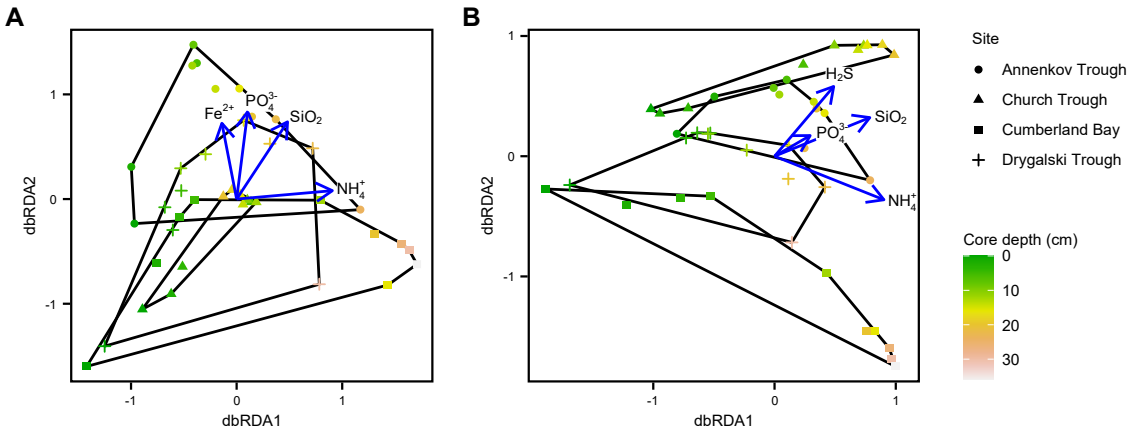

Fig. S5: Partial distance-based redundancy analysis (dbRDA) ordination plot of bacterial communities in surface sediments of South Georgia. Variation explained by (**a**) H_2S or (**b**) Fe^{2+} were removed from the model. Sample points are distinguished by site and core depth by shape and color respectively. dbRDA1 and dbRDA2 axes are displayed which constrain the Bray Curtis distance matrix with geochemical parameters PO_4^{3-}, NH_4^+, SiO_2 and Fe^{2+} or H_2S. The total model (**a** F = 4.13, $p < .01$, Df 4, 34; **b** F = 4.57, $p < .01$, Df 4, 34) and each individual parameter ($p < 0.05$) was significant.

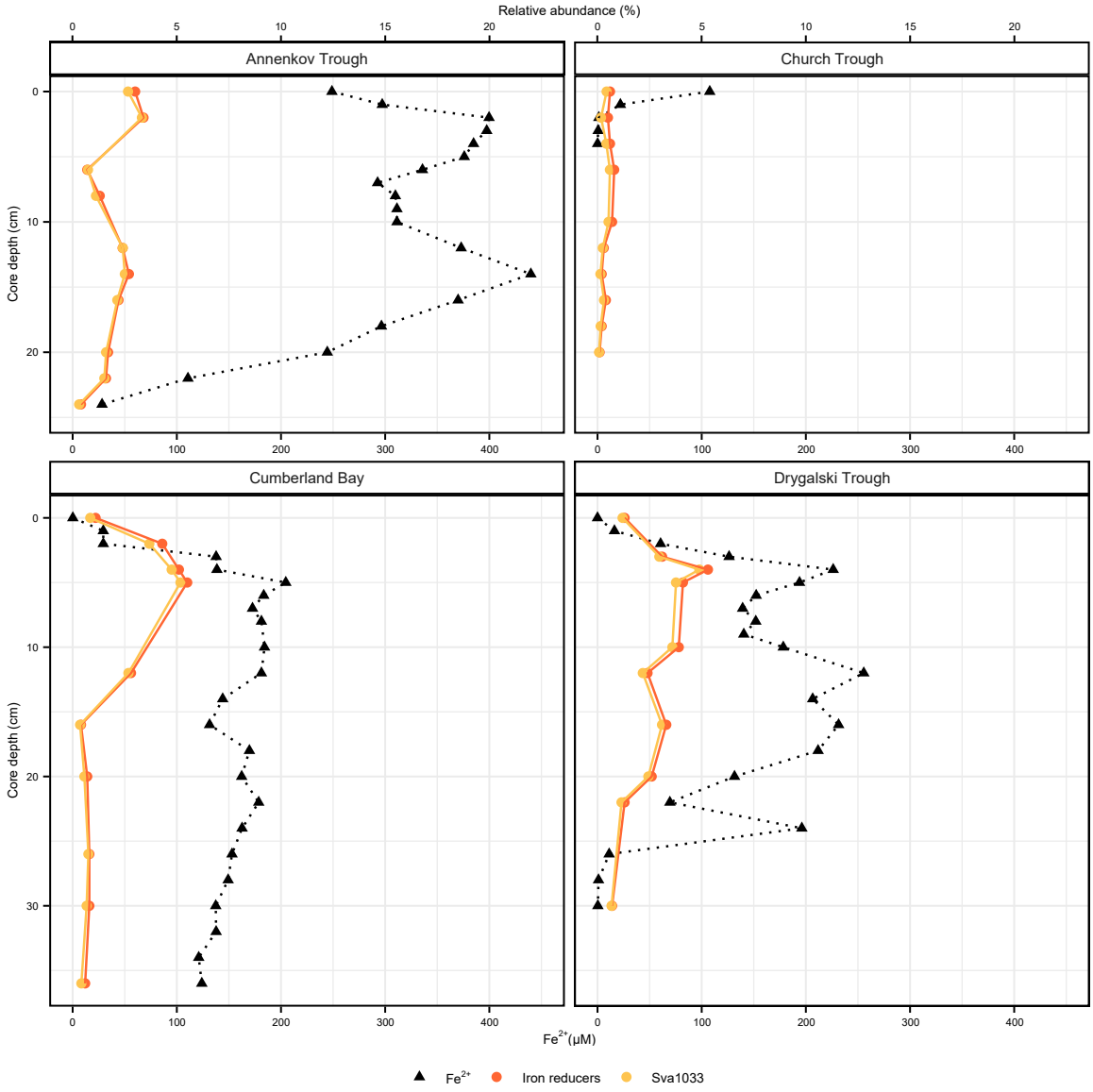

Fig. S6: Depth profile of contribution of iron reducing microorganisms in *Deltaproteobacteria* and family Sva1033 to bacterial 16S rRNA gene community in South Georgia surface sediments. Fe^{2+} profile from Fig. 2 was displayed.

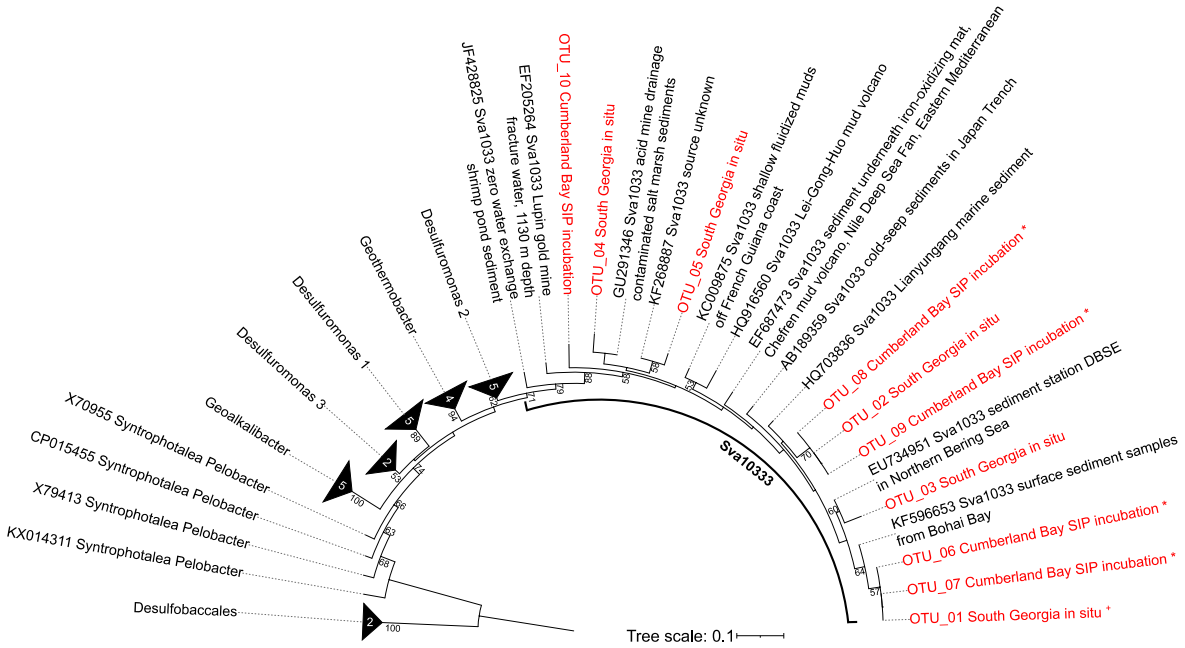

Fig. S7: Phylogenetic tree of family Sva1033 and closest sister clusters including the most abundant OTUs of this study (in red). Bootstrap values > 50% are shown in the tree. The reference sequences were exported from the ARB tree of SILVA release 138, Quast *et al.* (1). Accession numbers of sequences in collapsed nodes: Desulfobaccales FJ437876, AF002671; Geoalkalibacter CP010311, KJ817771, KT699114, DQ309326, MG602814; Desulfuromonas 3 JQ801020, JF727697; Desulfuromonas 1 JX223285, MF806540, JX224539, JX222942, HM141856; Geothermobacter KF741402, AY155599, GQ433952; Desulfuromonas 2 EU052234, KC470887, JX391250, KC471166, KM203496.

* : most abundant OTUs from SIP incubations representing together 96% of all Sva1033 sequences

+ : most abundant OTU from *in situ* sediments representing 90% of all Sva1033 sequences

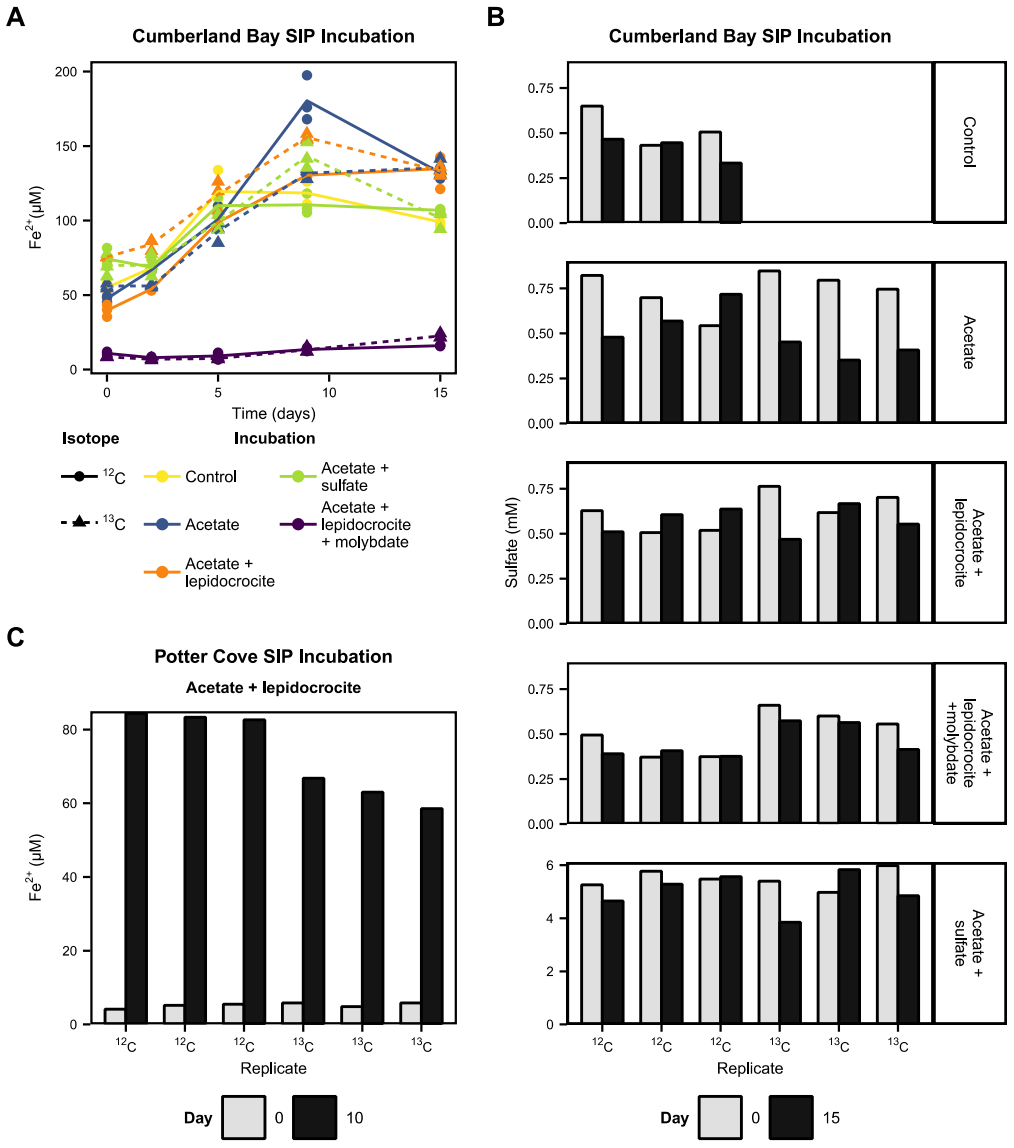

Fig. S8: Time course of Fe^{2+} and sulfate concentrations in SIP incubations of Cumberland Bay and Potter Cove sediments. **a** Fe^{2+} concentration of Cumberland Bay SIP incubations over time separated by treatment. Lines connect mean of triplicates of each treatment, separate for ^{12}C and ^{13}C acetate. **b** Sulfate concentration of Cumberland Bay SIP incubations of each replicate at start and end time point (day 0 – 15). The technical measurement error for sulfate measurements was 2%. **c** Fe^{2+} concentration of single Potter Cove SIP incubation treatment at start and end time point (day 0 – 10).

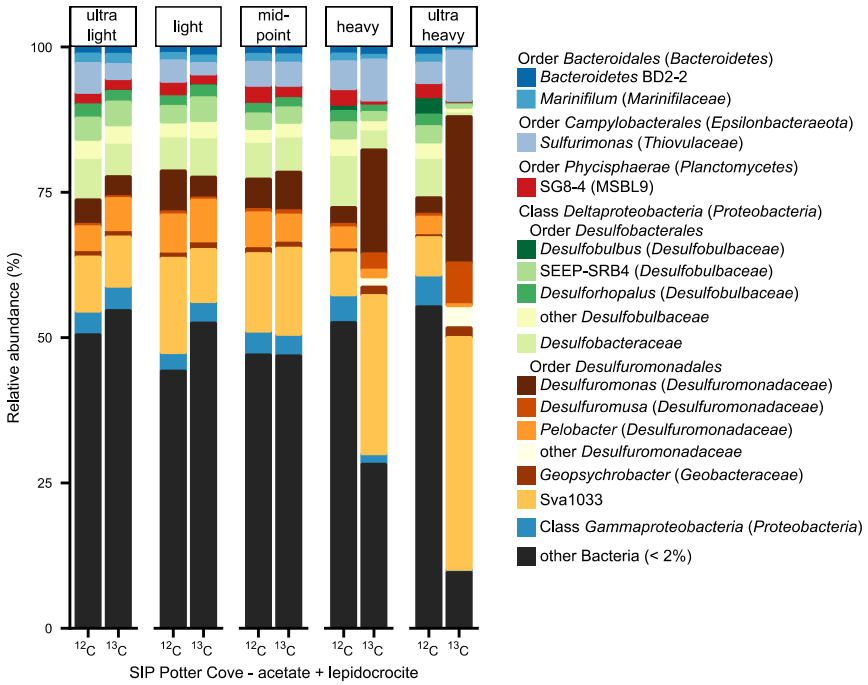

Fig. S9: SIP incubation of Potter Cove sediments. Density separated bacterial 16S rRNA community composition of taxa with > 2% relative abundance.

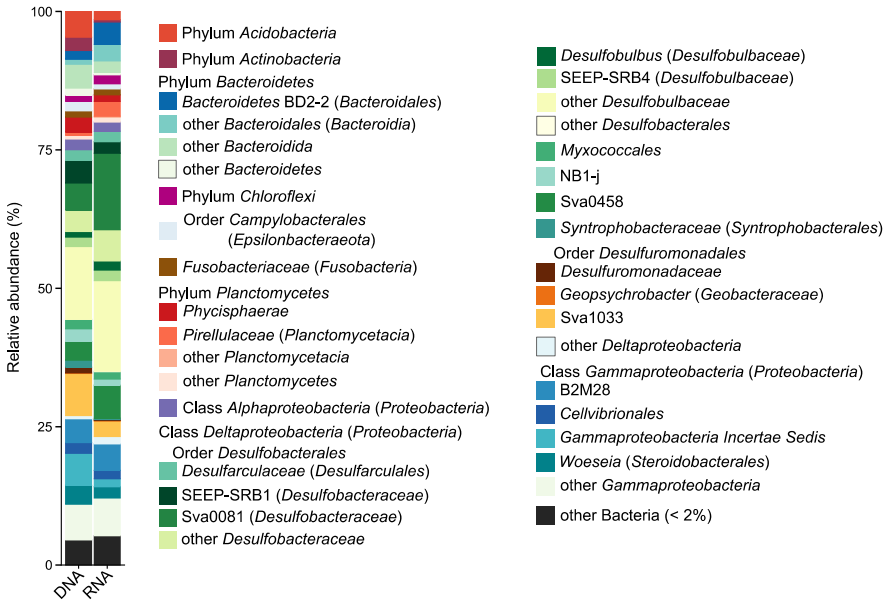

Fig. S10: SIP incubation of Cumberland Bay sediments bacterial 16S rRNA starting community on RNA and DNA level.

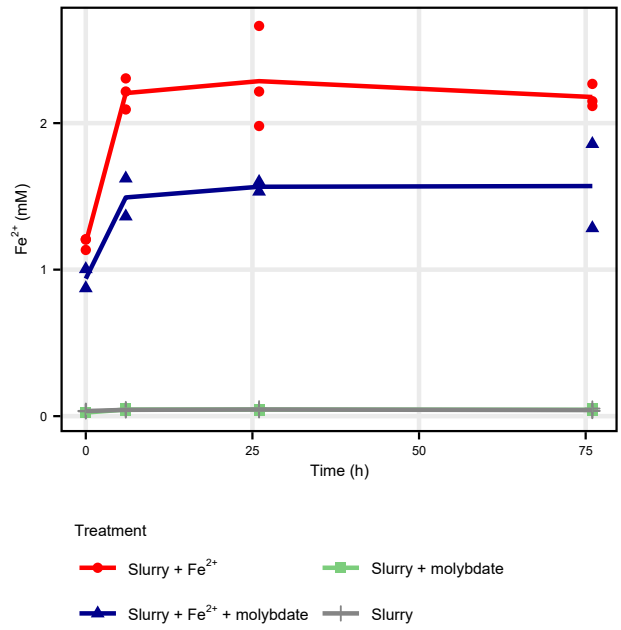

Fig. S11: Measured Fe^{2+} of abiotic ferrous iron. The line connects the mean for replicates of each treatment with n = 3 for all except Slurry + Fe^{2+} + molybdate with n = 2. For details see text below.

Fig. S12: Serum bottles of abiotic control experiment. One replicate of each treatment, from left to right: slurry + molybdate, slurry + Fe^{2+}, slurry + Fe^{2+} + molybdate, slurry only.

2.2.2 Supplementary tables

Table S1: Sampling location and sample details

Sampling objective	Site Core ID	Core depth (cm)*	Coordinates	
			Latitude	Longitude
Archaeal and bacterial community composition analysis and quantification, *dsrA* gene quantification	Annenkov Trough GeoB22054-2 (MUC-12)	0 – 1 2 – 3 6 – 7 8 – 9 12 – 14 14 – 16 16 – 18 20 – 22 22 – 24 24 – 26	54°26.169 S	37°21.094 W
Geochemical measurements on pore water		0 – 10 every 1 cm 10 – 34 every 2 cm		
Archaeal and bacterial community composition analysis and quantification, *dsrA* gene quantification	Church Trough GeoB22031-1 (MUC-5)	0 – 1 2 – 3 4 – 5 6 – 7 10 – 12 12 – 14 14 – 16 16 – 18 18 – 20 20 – 22	53°46.209 S	38°08.413 W
Geochemical measurements on pore water		0 – 10 every 1 cm 10 – 30 every 2 cm		
Archaeal and bacterial community composition analysis and quantification, *dsrA* gene quantification	Cumberland Bay GeoB22046-1 (MUC-8)	0 – 1 2 – 3 4 – 5 5 – 6 12 – 14 16 – 18 20 – 22 26 – 28 30 – 32 36 – 38	54°17.270 S	36°27.710 W
Geochemical measurements on pore water		0 – 10 every 1 cm 10 – 40 every 2 cm		
Archaeal and bacterial community composition analysis and quantification, *dsrA* gene quantification	Drygalski Trough GeoB22015-1 (MUC-4)	0 – 1 3 – 4 4 – 5 5 – 6 10 – 12 12 – 14 16 – 18 20 – 22 22 – 24 30 – 32	54°51.269 S	35°54.667 W
Geochemical measurements on pore water		0 – 10 every 1 cm 10 – 32 every 2 cm		
SIP incubation	Cumberland Bay GeoB22024-1 (GC-6)	0 – 14	54°15.885 S	36°26.225 W
SIP incubation	Potter Cove Station 13-04	0 – 29 (whole core)	62°13.523 S	58°38.470 W

* In the text, other tables and figures only start depth is displayed

Table S2: Sequencing details surface sediments, South Georgia
Red labelled archaea samples were removed from the analyses due to insufficient sequencing depth

Site Core ID	Core depth (cm)	Total reads		Total OTUs	
		Bacteria	Archaea	Bacteria	Archaea
Annenkov Trough GeoB22054-2	0	4025	423	1067	74
	2	2497	334	707	80
	6	1494	670	340	133
	8	2680	1192	573	140
	12	3326	2132	814	204
	14	5870	2138	1236	235
	16	4712	3973	1123	336
	20	6165	1113	1325	199
	22	3420	502	982	121
	24	5129	618	1093	133
Church Trough GeoB22031-1	0	21567	761	2074	111
	2	8887	1167	1316	146
	4	11103	2093	1504	182
	6	8405	2342	1255	243
	10	14952	3284	1607	246
	12	19810	3706	1923	206
	14	18582	2456	1833	207
	16	15080	2071	1616	177
	18	17165	2579	1764	222
	20	22506	1829	1898	170
Cumberland Bay GeoB22046-1	0	25910	1009	1951	21
	2	11546	1581	1968	61
	4	7618	1761	1548	174
	5	11630	3952	1693	198
	12	7098	1280	1594	235
	16	8106	9021	1516	367
	20	7996	8132	1546	442
	26	5828	2481	1263	214
	30	9828	4883	1616	341
	36	10034	8799	1562	375
Drygalski Trough GeoB22015-1	0	10154	122	1288	37
	3	17665	142	1740	41
	4	19482	568	1892	90
	5	10165	805	1455	103
	10	25580	1853	2476	166
	12	15554	1551	2151	161
	16	19605	732	1936	129
	20	12337	451	1859	137
	22	18759	955	2084	207
	30	6532	1239	1328	144

Table S3: SIP incubation set-up Cumberland Bay

Treatment (n = 3)	Acetate (500 µM)	Lepidocrocite (5 mM)	Sulfate (5 mM)	Molybdate (10 mM)	Days pre-incubation
Control					4
Acetate	^{12}C				6
Acetate	^{13}C				6
Acetate + lepidocrocite	^{12}C	x			6
Acetate + lepidocrocite	^{13}C	x			6
Acetate + sulfate	^{12}C		x		6
Acetate + sulfate	^{13}C		x		6
Acetate + lepidocrocite + molybdate	^{12}C	x		x	4
Acetate + lepidocrocite + molybdate	^{13}C	x		x	6

Table S4.1: Sequencing details SIP incubation samples

Treatment	Isotope	Fraction	Total reads	Total OTUs	Density (g/ml)
Cumberland Bay Acetate	^{12}C	3+4	30386	3000	1.818 – 1.826
		5+6	37248	3184	1.803 – 1.810
		7+8	36816	3194	1.791 – 1.799
		9+10	13656	2006	1.776 – 1.783
		11+12	30136	2849	1.760 – 1.768
	^{13}C	3+4	5410	479	1.814 – 1.822
		5+6	19743	2030	1.799 – 1.806
		7+8	35068	3172	1.783 – 1.791
		9+10	39751	3557	1.768 – 1.776
		11+12	24305	2753	1.753 – 1.760
Cumberland Bay Acetate + lepidocrocite	^{12}C	3+4	25033	2575	1.814 – 1.822
		5+6	27784	3010	1.799 – 1.806
		7+8	46695	3743	1.787 – 1.791
		9+10	35683	3293	1.772 – 1.779
		11+12	24208	2623	1.756 – 1.764
	^{13}C	3+4	14822	995	1.814 – 1.818
		5+6	20291	1958	1.799 – 1.806
		7+8	11846	1886	1.783 – 1.791
		9+10	8732	1616	1.768 – 1.776
		11+12	8416	1483	1.753 – 1.760
Cumberland Bay Acetate + sulfate	^{12}C	3+4	20815	2427	1.818 – 1.822
		5+6	15954	2151	1.799 – 1.806
		7+8	17408	2333	1.783 – 1.791
		9+10	21839	2534	1.772 – 1.776
		11+12	22078	2570	1.756 – 1.764
	^{13}C	3+4	24520	1333	1.814 – 1.822
		5+6	16403	2014	1.799 – 1.806
		7+8	14038	1950	1.783 – 1.791
		9+10	2782	834	1.768 – 1.776
		11+12	31827	3133	1.753 – 1.760

Table S4.2: Sequencing details SIP incubation samples

Treatment	Isotope	Fraction	Total reads	Total OTUs	Density (g/ml)
Cumberland Bay Acetate + lepidocrocite + molybdate	^{12}C	3+4	22646	2470	1.814 – 1.820
		5+6	6721	1324	1.799 – 1.806
		7+8	30945	3186	1.783 – 1.791
		9+10	24045	2689	1.768 – 1.776
		11+12	52866	4049	1.756 – 1.760
	^{13}C	3+4	45440	1620	1.814 – 1.818
		5+6	43504	2954	1.799 – 1.806
		7+8	38599	3482	1.783 – 1.791
		9+10	33612	3752	1.768 – 1.776
		11+12	28149	3196	1.756 – 1.764
Potter Cove Acetate + lepidocrocite	^{12}C	3+4	45543	3806	1.815 – 1.817
		5+6	44232	3689	1.803 – 1.806
		7+8	53991	3738	1.792 – 1.794
		9+10	54971	3609	1.780 – 1.783
		11+12	26062	2756	1.769 – 1.774
	^{13}C	3+4	10703	629	1.820 – 1.826
		5+6	2123	476	1.809 – 1.815
		7+8	31702	3045	1.797 – 1.803
		9+10	15678	2245	1.789 – 1.794
		11+12	20690	2647	1.783 – 1.777

Table S5: Primer details 16S rRNA gene qPCR

Primer	Sequence (5'-3')	Target	Denaturation time	Reference
Bac8Fmod	AGAGTTTGATYMTGGCTCAG	bacteria	15 s	modified from (2)
Bac338Rmod	GCWGCCWCCCGTAGGWGT	bacteria	15 s	modified from (3)
27F	AGAGTTTGATCCTGGCTCAG	bacteria		(4)
Ba1492	GGTTACCTTGTTACGACTT	bacteria		(4)
Ar806F*	ATTAGATACCCSBGTAGTCC	archaea	30 s	(3)
Ar912rt	GTGCTCCCCCGCCAATTCCTTTA	archaea	30 s	(5)
Ar109F	ACKGCTCAGTAACACGT	archaea		(6)
A1492	GGCTACCTTGTTACGACTT	archaea		(4)

* alternative name Arc787F

2.2.3 Supplementary material and methods

2.2.3.1 Experimental set up for stable isotope probing incubations

Anoxic slurries were prepared by homogenizing sediment with sulfate-free artificial sea water (per liter 26.4 g NaCl, 11.2 g $MgCl_2 \cdot 6\ H_2O$, 1.5 g $CaCl_2 \cdot 2\ H_2O$, 0.7 g KCl, prepared with purified water (Milli-Q)) at a ratio of 1:4 under a stream of nitrogen gas (N_2 5.0). 40 ml slurry was transferred into 120 ml serum bottles sealed with butyl rubber stoppers. The headspace gas was exchanged with N_2. The detailed set up is shown in Table S3. Both C-atoms in acetate

were ^{13}C-labelled. Incubation was conducted at 5°C in the dark for a total of 15 days after substrate addition.

When samples for Fe^{2+} measurements were taken anoxically, 1 ml slurry was frozen for later analyses. These samples were subsequently used to determine aqueous sulfate concentrations by fixing 200 µl slurry supernatant in 800 µl 1% zinc acetate. The measurement was performed with a Metrohm 930 Compact IC Flex ion chromatograph (sulfate detection limit 50 µM).

For RNA extraction the slurry of treatment triplicates were pooled and 15 ml were used in order to retrieve sufficient biomass for fractionation.

2.2.3.2 Sequencing analysis

The sequence read analysis of surface sediment samples was performed as previously described (7) with updated software, using the QIIME 1.9.0 and USEARCH 11.0. For sequencing data of the *in situ* surface sediment samples (2x 150 bp), only the forward reads were used for further analysis and truncated to a minimum sequence length of 143 bp.

For sequences of SIP incubation samples (2x 250 bp), the pipeline was modified in its first steps before de-replication: forward and reverse reads were joined with minimum overlap of 10 bases followed by de-multiplexing and quality filtering to minimum sequence length of 242 bp and expected error of < 0.5 using QIIME 1.9.0 and USEARCH 11.0. The taxonomic assignment was based on the 16S rRNA database Silva release 132 (1).

Unassigned reads or assigned as archaea, chloroplast or mitochondria were removed from the bacterial OTU tables and respectively bacterial and unassigned reads were removed from the archaeal OTU table prior to further analyses. Sequencing details are provided in Table S2 and S4. Rarefaction curves were generated (vegan package (8)) and all samples not reaching the inflection point of the rarefaction curve were removed from the dataset, as their community coverage was considered insufficient (Fig. S2, S3). Differing sample sizes were normalized by scaling OTU abundance to the observation totals in each sample ("relative data"). Separately, the relative abundance of each taxon on all available ranks was summed up, i.e. for all phyla, classes, orders and so on.

2.2.4 Fe^{2+} measurement in molybdate treated incubations – abiotic controls

During the course of the stable isotope probing (SIP) incubations with Cumberland Bay sediments, measured Fe^{2+} concentrations in the treatment containing acetate + lepidocrocite + molybdate was much lower compared to the other incubations, including the control (Fig. S8). However, the microbial community from the sequencing results indicated on-going iron reduction: the same known iron reducing microorganisms as in the other incubations were

present and active (Fig. 6). One hypothesis for the lower concentrations of detectable Fe^{2+} concentrations was abiotic reaction of Fe^{2+} from iron reduction with molybdate. To address this hypothesis, supplementary incubations were set up and the findings are discussed below.

Material and methods

Experiments investigating the abiotic reaction of Fe^{2+} and molybdate were set up in 120 ml serum bottles with 40 ml 1:4 slurry containing 10 g Cumberland Bay sediment (gravity core, 0 – 14 cm, same as used for main SIP experiments) and 30 ml artificial sea water (ASW, see supplementary methods above and main text). The slurry was autoclaved and all oxygen removed by flushing with N_2 gas before the substrate was added. Four treatments were set-up containing 10 mM molybdate (n = 3), 1 mM Fe^{2+} (n = 3, added as $FeCl_2$), both together (n = 2) or only sediment (n = 3).

Fe^{2+} measurements were performed following the ferrozine assay from Viollier *et al.* (9). Fe^{2+} was measured the first time directly after the substrate was added to all treatments, followed by measurements after 6, 26 and 76 h (Fig. S11). During that time, the treatments were incubated at 5°C in the dark.

Results and discussion

The Fe^{2+} concentrations showed clear differences between the treatments (Fig. S11). Lower Fe^{2+} concentrations were measured in the treatment slurry + Fe^{2+} + molybdate (7 – 13 mM) compared to the treatment slurry + Fe^{2+} (11 – 19 mM). Fe^{2+} concentrations in the other treatments slurry only and slurry + molybdate stayed very low between 0.025 – 0.038 mM and 0 – 0.006 mM respectively. An immediate color change was observed in the slurry + Fe^{2+} + molybdate treatment after adding the substrates, but not in any of the other control treatments (Fig. S12). Higher Fe^{2+} concentrations were observed than initial Fe^{2+} was added in according incubations. The addition of Fe^{2+} in the form of $FeCl_2$ lowered the pH in these treatments probably resulting in the elution of Fe^{2+} from the sediment particles.

The observations from these abiotic sediment incubations give clear indication for an abiotic reaction between the added Fe^{2+} and the molybdate, therefore limiting the possibility to measure the exact levels of iron reduction in the acetate, lepidocrocite and molybdate treatments of the initial experiments (Fig. S8A). In summary, based on the results from these abiotic sediment incubations, we argue that in the acetate, lepidocrocite and molybdate treatments (Fig. 6 main text, Fig. S8A), iron reduction was on-going but most of the Fe^{2+} formed reacted abiotically with molybdate.

2.2.5 References

1. Quast C, Pruesse E, Yilmaz P, Gerken J, Schweer T, Yarza P, *et al.* The SILVA ribosomal RNA gene database project: improved data processing and web-based tools. *Nucleic Acids Res* 2012; **41**: D590-D596.

2. Eden PA, Schmidt TM, Blakemore RP, Pace NR. Phylogenetic analysis of *Aquaspirillum magnetotacticum* using Polymerase Chain Reaction-amplified 16S rRNA-specific DNA. *Int J Syst Evol Microbiol* 1991; **41**: 324-325.

3. Yu Y, Lee C, Kim J, Hwang S. Group-specific primer and probe sets to detect methanogenic communities using quantitative real-time polymerase chain reaction. *Biotechnol Bioeng* 2005; **89**: 670-679.

4. Lane DJ. 16S/23S rRNA sequencing. In: Stackebrandt E, Goodfellow M (eds). *Nucleic acid techniques in bacterial systematics*. John Wiley and Sons: New York, 1991, pp 115-175.

5. Lueders T, Friedrich MW. Effects of amendment with ferrihydrite and gypsum on the structure and activity of methanogenic populations in rice field soil. *Appl Environ Microbiol* 2002; **68**: 2484-2494.

6. Großkopf R, Janssen PH, Liesack W. Diversity and structure of the methanogenic community in anoxic rice paddy soil microcosms as examined by cultivation and direct 16S rRNA gene sequence retrieval. *Appl Environ Microbiol* 1998; **64**: 960-969.

7. Aromokeye DA, Richter-Heitmann T, Oni OE, Kulkarni A, Yin X, Kasten S, *et al.* Temperature controls crystalline iron oxide utilization by microbial communities in methanic ferruginous marine sediment incubations. *Front Microbiol* 2018; **9**: 2574.

8. Oksanen J, Blanchet FG, Friendly M, Kindt R, Legendre P, McGlinn D, *et al.* vegan: Community Ecology Package, 2.5-6. 2019. Available from: https://CRAN.R-project.org/package=vegan

9. Viollier E, Inglett P, Hunter K, Roychoudhury A, Van Cappellen P. The ferrozine method revisited: Fe(II)/Fe(III) determination in natural waters. *Appl Geochem* 2000; **15**: 785-790.

Chapter 3

Manganese reduction and associated microbial communities in Antarctic surface sediments

Lea C. Wunder, Inga Breuer, Graciana Willis-Poratti, David A. Aromokeye, Susann Henkel, Tim Richter-Heitmann, Xiuran Yin, Michael W. Friedrich

Manuscript published in Frontiers in Microbiology

Volume 15, July 2024

https://doi.org/10.3389/fmicb.2024.1398021

Running title:

Manganese reduction in Antarctic sediments

Contribution of the candidate to the total work

Experimental concept and design	80%
Experimental work/acquisition of experimental data	40%
Data analysis and interpretation	80%
Preparation of figures and tables	100%
Drafting of the manuscript	100%

frontiers | Frontiers in Microbiology

TYPE Original Research
PUBLISHED 03 July 2024
DOI 10.3389/fmicb.2024.1398021

OPEN ACCESS

EDITED BY
Andreas Teske,
University of North Carolina at Chapel Hill,
United States

REVIEWED BY
Mark Alexander Lever,
The University of Texas at Austin,
United States
Paraskevi Mara,
Woods Hole Oceanographic Institution,
United States

*CORRESPONDENCE
Michael W. Friedrich
✉ michael.friedrich@uni-bremen.de

RECEIVED 08 March 2024
ACCEPTED 17 June 2024
PUBLISHED 03 July 2024

CITATION
Wunder LC, Breuer I, Willis-Poratti G, Aromokeye DA, Henkel S, Richter-Heitmann T, Yin X and Friedrich MW (2024) Manganese reduction and associated microbial communities in Antarctic surface sediments. *Front. Microbiol.* 15:1398021. doi: 10.3389/fmicb.2024.1398021

Manganese reduction and associated microbial communities in Antarctic surface sediments

Lea C. Wunder[1], Inga Breuer[1], Graciana Willis-Poratti[1,2,3], David A. Aromokeye[1], Susann Henkel[4], Tim Richter-Heitmann[1], Xiuran Yin[1,5] and Michael W. Friedrich[1,6]*

[1]Microbial Ecophysiology Group, Faculty of Biology/Chemistry, University of Bremen, Bremen, Germany, [2]Instituto Antártico Argentino, San Martín, Buenos Aires, Argentina, [3]Consejo Nacional de Investigaciones Científicas y Técnicas (CONICET), Buenos Aires, Argentina, [4]Alfred Wegener Institute Helmholtz Centre for Polar and Marine Research, Bremerhaven, Germany, [5]State Key Laboratory of Marine Resource Utilization in South China Sea, Hainan University, Haikou, China, [6]MARUM – Center for Marine Environmental Sciences, University of Bremen, Bremen, Germany

The polar regions are the fastest warming places on earth. Accelerated glacial melting causes increased supply of nutrients such as metal oxides (i.e., iron and manganese oxides) into the surrounding environment, such as the marine sediments of Potter Cove, King George Island/Isla 25 de Mayo (West Antarctic Peninsula). Microbial manganese oxide reduction and the associated microbial communities are poorly understood in Antarctic sediments. Here, we investigated this process by geochemical measurements of *in situ* sediment pore water and by slurry incubation experiments which were accompanied by 16S rRNA sequencing. Members of the genus *Desulfuromusa* were the main responder to manganese oxide and acetate amendment in the incubations. Other organisms identified in relation to manganese and/or acetate utilization included *Desulfuromonas*, Sva1033 (family of *Desulfuromonadales*) and unclassified *Arcobacteraceae*. Our data show that distinct members of *Desulfuromonadales* are most active in organotrophic manganese reduction, thus providing strong evidence of their relevance in manganese reduction in permanently cold Antarctic sediments.

KEYWORDS

manganese reduction, Potter Cove, marine surface sediment, *Desulfuromusa*, Sva1033, *Arcobacteraceae*, Antarctic, organic carbon degradation

1 Introduction

Organic matter degradation in marine sediments is an important part of the global carbon cycle. The flux of carbon in marine sediments is regulated by microbial mineralization of organic matter to CO_2 (LaRowe et al., 2020 and references therein) which contributes as potent greenhouse gas to global warming and drives the climate change (Mitchell, 1989). In anoxic sediments, the degradation of organic matter is performed by microorganisms in multiple steps. Briefly, polymeric carbon compounds are first hydrolyzed, then monomers are fermented and finally fermentation intermediates are oxidized coupled to the reduction of terminal electron acceptors such as nitrate, metal oxides and sulfate (Jørgensen, 2006).

10.3389/fmicb.2024.1398021

Polar regions such as the Arctic and Antarctic are especially affected by climate change and are therefore warming-up multiple times faster than other areas of earth (Rantanen et al., 2022; Casado et al., 2023). Elevated temperatures result in accelerated melting of sea ice and glaciers and consequently increased meltwater input into the surrounding environment. Meltwater of sea ice and glaciers deliver nutrients, including different metals, into the ocean and underlying sediments (Death et al., 2014; Herbert et al., 2020; Forsch et al., 2021). There, the metal (iron and manganese) oxides can be used as terminal electron acceptors for microbial organic matter oxidation (Canfield et al., 1993b).

Microorganisms can couple manganese reduction to the oxidation of organic and inorganic electron donors (e.g., lactate, acetate, formate, hydrogen) (Burdige, 1993; Thamdrup, 2000). Reduced sulfur compounds such as elemental sulfur, thiosulfate or sulfide can also be used by microorganisms as electron donors for manganese reduction (Burdige, 1993; Thamdrup, 2000) and potentially contribute to a cryptic sulfur cycle (Aller and Rude, 1988). Bacteria associated with manganese reduction belong to different taxa such as *Pelobacter*, *Colwelliaceae, Arcobacteraceae, Shewanellaceae*, and *Oceanospirillaceae* (Thamdrup et al., 2000; Vandieken et al., 2012; Cho et al., 2020) and many iron reducing bacteria are also capable of reducing manganese oxides (Lovley, 1991; Vandieken et al., 2006a).

Microbial manganese reduction contributes up to 45% to carbon mineralization in manganese oxide rich sediments (Canfield et al., 1993a; Hyun et al., 2017). This process can also play a role in extreme environments such as the polar regions. It has been studied in different Arctic, manganese oxide rich sediments of the Barents Sea (Vandieken et al., 2006c), Beaufort Sea (Magen et al., 2011) and Svalbard fjords (Vandieken et al., 2006a; Wehrmann et al., 2014). There are only few studies that investigated specific organic matter degradation processes, e.g., iron reduction, and the related microbial communities in Antarctic subsurface sediments (Monien et al., 2014a; Aromokeye et al., 2021; Wunder et al., 2021; Baloza et al., 2022, 2023; Burdige and Christensen, 2022). The occurrence of manganese reduction and the respective microbial players have not been studied in any Antarctic sediments yet.

Our study site Potter Cove (King George Island/Isla 25 de Mayo, West Antarctic Peninsula) is heavily influenced by a glacier, which retreats rapidly turning from sea- to mostly land-terminating in the last decades (>1 km between 1956 and 2008; Rückamp et al., 2011; Neder et al., 2022). In the fjord sediments, iron oxides have been shown to be prominent terminal electron acceptors of organic matter degradation based on pore water iron concentrations (Monien et al., 2014a; Henkel et al., 2018) and incubation experiments (Aromokeye et al., 2021). The microbial processes using other possible electron acceptors for anaerobic organic matter degradation processes have not been studied yet at this site, but are potentially occurring due to the presence of dissolved manganese in the pore water, sufficient manganese oxide content (over 0.15 wt.%; Monien et al., 2014b) in the sediment and an abundance of sulfate (in average 20 mM across the cove; Monien et al., 2014a; Henkel et al., 2018).

Here, we explore manganese oxide as electron acceptor for organic matter degradation in Potter Cove sediments, Antarctica. We use geochemical profiles to indicate the likelihood of ongoing *in situ* manganese reduction, and further investigate the prerequisites of the process in terms of electron donor with sediment slurry incubations at an environmentally relevant temperature of 2°C. Finally, we identified *Desulfuromusa* as the active microbial player for manganese reduction by amplicon sequencing.

2 Materials and methods

2.1 Sampling site and *in situ* data

Sediment samples were collected in Potter Cove during austral summer 2018/2019. Sampling sites were selected based on previous geochemical measurements (Monien et al., 2014a; Henkel et al., 2018). For this study, sediments from Station 01 (STA 01) were used for further slurry preparation. STA 01 is located in close proximity of the glacial front (Figure 1, S62°13′34.16″/W58°38′25.1″). Five sediment replicate cores (25–35 cm length, diameter 60 mm) were retrieved with a hand-held gravity corer (USC 06000, UWITEC, Austria) and carefully transported in a vertical position to the Dallmann Laboratory at the Argentine Research Carlini Station. Two replicate cores were used for pore water collection with Rhizons (Rhizosphere Research Products, Netherlands) (Seeberg-Elverfeldt et al., 2005) in 1-cm intervals for the top 10 cm, followed by 2-cm intervals for the rest of the core. An aliquot of pore water samples (400 µL) was fixed with 100 µL of 0.5 M HCl for dissolved Fe^{2+} measurements, which was immediately determined in the Dallmann Laboratory. Another aliquot of the pore water was fixed with 50 µL 35% ultra-pure HCl and used for dissolved manganese and other cations determination at the Alfred Wegener Institute Helmholtz Centre for Polar and Marine Research (AWI). Pore water samples for sulfate measurement were not fixed with Zn-acetate as no sulfide smell was detected during sampling.

The other three replicate cores were used for solid phase sampling, and sediment samples were collected in the same depth resolution as

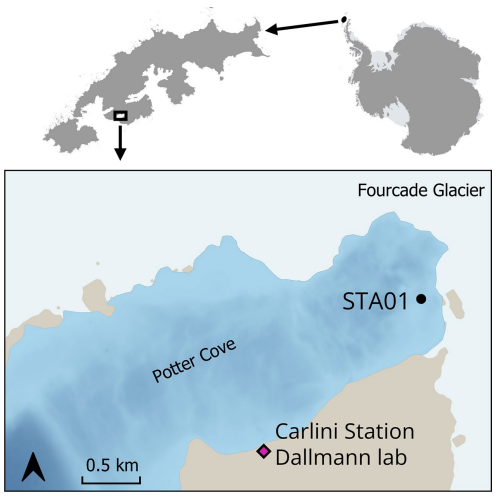

FIGURE 1
Sediment cores were taken at STA 01 in Potter Cove, King George Island/Isla 25 de Mayo, in close proximity to the Fourcade glacier. Map created with QGIS 3.34.3, bathymetry data (Neder et al., 2022) updated from Jerosch et al. (2015), basemap data from SCAR Antarctic Digital Database 2023, rock outcrop from Gerrish (2020) manually smoothed.

10.3389/fmicb.2024.1398021

for pore water. At each depth, part of the sediment was frozen at −20°C for analyzing the *in situ* microbial community by Illumina 16S rRNA gene amplicon sequencing. The rest of the sediment core was pooled in 5-cm depth-sections and stored at 2°C in 250-ml Schott-bottles sealed with rubber stoppers under N_2 headspace (99.999% purity, Linde, Germany). The sediments were kept at 2°C in the dark for 2 years until the start of incubation experiments in the home laboratory.

2.2 Slurry incubations

In order to investigate the potential for manganese reduction in the Antarctic sediments collected and the microorganisms involved, slurry incubation experiments were conducted. Stored sediment from core STA01-02 was used for slurry incubations, pooling the whole length of the core (25 cm). The slurry was prepared in 1:5 ratio with sulfate-free artificial sea-water [26.4 g NaCl, 11.2 g $MgCl_2 \cdot 6\ H_2O$, 1.5 g $CaCl_2 \cdot 2\ H_2O$, 0.7 g KCl per liter; prepared with purified water (Milli-Q)] under flushing with N_2 (99.999% purity, Linde, Germany). Slurry (30 mL) was distributed into 60-ml serum bottles and sealed with butyl rubber stoppers under N_2 headspace. After a pre-incubation of 5 days at 2°C in the dark, substrates were added. Six different treatments were prepared in triplicates; four treatments contained a final concentration of 10 mM of the manganese oxide birnessite (MnO_2, synthesized after McKenzie, 1971) as electron acceptor and (1) elemental sulfur (solid, crystalline orthorhombic sulfur S_8, 1 mmol per liter added), (2) thiosulfate ($S_2O_3^{2-}$, 1 mM, sodium salt), (3) acetate (1 mM, sodium salt), or (4) nothing as electron donor. All treatments without acetate contained 20 mM dissolved inorganic carbon (DIC, $NaHCO_3$) as carbon source. Two control treatments with (5) 1 mM acetate or (6) 20 mM DIC were prepared. A treatment containing only birnessite and DIC and an additional DIC-only control treatment were set up in spring 2023. All the other incubations were performed in summer 2021, but were otherwise conducted the same way (see Supplementary material for more details).

The incubations ran for 20 days and were sampled over time for geochemical measurements and nucleic acid extraction. At each sampling time point, 2 mL of slurry was taken anoxically using a nitrogen-flushed syringe, centrifuged (20817 *g*, 4°C, 10 min) in a nitrogen pre-flushed 2-ml tube and the supernatant was fixed according to the parameter of interest. For dissolved manganese measurements, 0.5 mL supernatant was fixed with 50 µL 35% ultra-pure HCl and stored in the dark at 4°C until the measurement. For dissolved Fe^{2+} measurements, 100 µL of the supernatant was directly injected into the ferrozine reagent (see next section). For sulfide measurements, the supernatant was fixed as ZnS with a final concentration of 1.5% Zn-acetate and measured at the same day. For treatments containing thiosulfate, the ZnS pellet was washed with Milli-Q water and resuspend in the same volume of Milli-Q water to prevent interference of thiosulfate with the measurement reagents. For sulfate measurements, supernatant samples were fixed with a final concentration of 0.5% Zn-acetate to prevent the oxidation of free sulfide and samples were stored in the dark at 4°C until measurement. Samples for nucleic acid extraction were frozen at −80°C until further processing.

2.3 Geochemical methods

Dissolved manganese was measured by inductively coupled plasma optical emission spectrometry (ICP-OES) analysis (iCAP7400, Thermo Fisher Scientific Inc.) using an internal yttrium standard to correct for differences in the ionic strength of samples. The limit of quantification of the method was 1.35 µM Mn. No distinction between redox states of manganese is possible with this method. In all samples dissolved Fe^{2+} was measured following the ferrozine method (Viollier et al., 2000). In incubation samples sulfide (H_2S, HS^-, S^{2-}) was measured following the methylene-blue method by Cline (1969). Absorbance measurements for Fe^{2+} and sulfide determination were performed on a spectrophotometer (Libra S12, Biochrom, Berlin, Germany). Sulfate was measured by ion chromatography equipped with a conductivity detector (incubation samples Metrohm 930 Compact IC Flex; *in situ* samples Metrohm Compact IC 761, Metrohm, Filderstadt, Germany).

2.4 Nucleic acid extraction and sequencing

In order to explore the bacterial community *in situ* and during the incubation, nucleic acids were extracted from 0.5 g frozen *in situ* sediment in depth intervals described above, and of 4 mL slurry of the incubation experiment samples. Combined extraction of RNA and DNA was performed using a phenol-chloroform protocol modified from Lueders et al. (2004) as follows: during precipitation with polyethylene glycol 6000, the samples were incubated at 4°C for 30 min and centrifuged at 20817 *g* at 4°C for 45 min. Nucleic acid pellets were washed twice with ice-cold 70% ethanol and eluted in 50 µL diethyl pyrocarbonate (DEPC) treated water (detailed protocol in Supplementary material). Nucleic acid extract quality was evaluated spectrophotometrically with a NanoDrop 1000 (Peqlab Biotechnologie, Erlangen, Germany) using A260/A230 and A260/A280 ratios (Olson and Morrow, 2012). For slurry nucleic acid extracts, DNase treatment was performed on subsamples (DNA-*free*™ Kit, Thermo Fisher Scientific) and cDNA was synthesized (GoScript™ Reverse Transcriptase Kit, Promega) for 16S rRNA sequencing following manufacturers' instructions. DNA and cDNA concentrations were quantified with PicoGreen (Quant-iT PicoGreen™ dsDNA Assay Kit, Invitrogen™, Thermo Fisher Scientific) measured on a Fluoroskan Ascent FL fluorometer (Thermo Fisher Scientific).

PCR reactions for DNA of *in situ* samples and DNA and cDNA of slurry samples were performed targeting the bacterial 16S rRNA gene V4 region with the primer pair Bac515F (5′-GTGYCAGCMGCC GCGGTAA-3′) (Parada et al., 2016) and Bac805R (5′-GACTACHVGG GTATCTAATCC-3′) (Herlemann et al., 2011) in preparation of Illumina sequencing. Each primer had a unique 8-bp barcode at the 5′-end attached (Hamady et al., 2008), which allowed multiplexing of several samples in the same sequencing library. The PCR reaction (50 µL) contained 1x KAPA HiFi buffer, 0.3 mM dNTP mix, 0.02 U KAPA HiFi DNA polymerase (KAPA Biosystems), 0.2 mg/mL bovine serum albumin (BSA), 1 mM $MgCl_2$, 1.5 µM each of forward and reverse primer and 2 ng template. The thermal cycling program was initial denaturation at 95°C for 5 min, 28 cycles of denaturation 98°C: 13 s, annealing 60°C: 20 s, elongation 72°C: 20 s followed by final elongation at 72°C for 1 min. PCR products were checked by agarose gel electrophoresis. If unspecific bands were visible, the PCR for the sample was repeated with reduced template amount. PCR products were

purified (Monarch PCR and DNA Cleanup Kit, New England Biolabs, Germany) and quantified with PicoGreen™. PCR products were pooled in equimolar amounts per sequencing library. Further PCR-free sequencing preparations, including ligation of sequencing adapters, and paired-end 2× 250 bp Illumina sequencing (Novaseq6000 platform) was performed by Novogene Co. Ltd. (Cambridge, UK).

2.5 Sequence analysis

Sequencing data were analyzed following Hassenrueck (2022) based on the sequencing pipeline as described in Callahan et al. (2016). Demultiplexing and primer clipping was done with cutadapt (version 3.1, Martin, 2011). All following steps were performed in the R software (version 4.3.1, R Core Team, 2023) using the dada2 R package (version 1.28.0, Callahan et al., 2016). Forward (R1) and reverse reads (R2) were filtered to a maximum number of 2 expected errors. They were truncated to a summed length of 290 bp (R1 and R2) according to their quality profiles individually per sequence lane (Supplementary Table S1 for details). Error learning and correction was performed using a modified version of the loessErrfun function (Salazar, 2021) until convergence was reached. Reads were dereplicated and denoised into amplicon sequence variants (ASVs) and paired forward and reverse reads were merged. Reverse-complement sequences were turned around and chimeras were removed. Sequences outside of a range of 249–254 bp were discarded with the exception of 276 and 300 bp long sequences (details for sequence length selection see Supplementary material). These long ASVs were recovered from previously unmerged reads and mapped against the SILVA database (SSU Ref NR 99 release 138.1, Quast et al., 2012) using bbmap (version 38.86, Bushnell, 2014) and were merged accordingly. Taxonomic assignment was done with the SILVA database (SSU Ref NR 99 release 138.1, Quast et al., 2012) using a bootstrap value of 80.

For subsequent steps, the R packages taxa (version 0.4.2, Foster et al., 2018), metacoder (version 0.3.6, Foster et al., 2017), phyloseq (version 1.42.0, McMurdie and Holmes, 2013) and tidyverse (version 2.0.0, Wickham et al., 2019) were used. ASVs associated outside bacteria or to mitochondria or chloroplasts were removed and subsequently singletons and doubletons were removed. Reads per sample were normalized by relative abundance calculation and sufficient sequencing depth was checked with rarefaction curves (iNEXT package version 3.0.0, Chao et al., 2014; Supplementary Figures S1, S2).

For the taxa *Arcobacteraceae*, *Desulfuromusa*, *Desulfuromonas* and Sva1033 the most abundant ASVs in the incubation experiment were selected and the blastn tool was used to find the most similar sequences in the NCBI database (blastn version 2.14.1+, Altschul et al., 1997, Supplementary Tables S2–S5; for detailed settings see Supplementary material). A dissimilarity matrix was calculated for ASV sequences of *Desulfuromusa* from this study and a previous study of Potter Cove (Aromokeye et al., 2021) and 16S rRNA gene sequences of *Desulfuromusa* type strains using megablast (Zhang et al., 2000; Supplementary Table S6, for more details and accession no. see Supplementary material).

2.6 Statistical analysis of geochemical data

The general linear hypothesis test (Herberich et al., 2010) was used to distinguish at which time points the dissolved manganese concentrations differed significantly ($p < 0.05$) between treatments. For each individual time point, a linear model was created using the "lm" function with default settings and multiple comparisons between treatments were done using the function "glht" with the "Tukey" setting in the R package multcomp (version 1.4.25, Hothorn et al., 2008). Note, that this procedure does not require any assumption regarding the distribution of data points, sample sizes or variance homogeneity.

3 Results

3.1 Geochemistry of *in situ* sediments reveals potential for manganese reduction

Different geochemical parameters (dissolved manganese, ferrous iron and sulfate) were measured in pore water of duplicate sediment cores of STA 01 to identify the dominant terminal electron accepting processes (Figure 2). Dissolved manganese concentrations increased linearly with depth up to 20 or 50 µM at the end of the core, while ferrous iron concentrations peaked with 55–85 µM at around 10 cm core depth. The presence of dissolved manganese and ferrous iron along the depth indicates ongoing manganese and iron reduction in the studied sediments. Sulfate concentrations decreased with core depth from 27 mM down to 23 mM. Hydrogen sulfide as proxy for sulfate reduction was undetected throughout both cores.

3.2 Manganese reduction observed in incubation experiments

To investigate the potential for manganese reduction in the sediments, anoxic slurry incubations were conducted using the manganese oxide birnessite as electron acceptor and acetate, elemental sulfur or thiosulfate as electron donors at 2°C (*in situ* temperature) for 20 days. An increase of dissolved manganese (Mn) up to 300–600 µM was detected in all treatments containing birnessite, while in control treatments without manganese oxide, the dissolved Mn remained below 10 µM (Figure 3). The effect of amended electron donors on the dissolved Mn concentration was only significant ($p < 0.05$) when acetate and birnessite were added (Supplementary Figure S3), resulting in the highest dissolved Mn concentration of 600 µM after 20 days. The addition of elemental sulfur or thiosulfate and birnessite resulted in similar dissolved Mn concentrations of up to 350 µM compared to the control treatment with only birnessite + DIC.

Sulfide, sulfate and dissolved ferrous iron were also monitored during incubation time. Ferrous iron remained <8 µM and sulfide <45 µM during the incubation time (Supplementary Figure S4). No additional sulfate was provided, so it ranged from 0.5–2 mM, decreasing between day 10 and 20 in treatments birnessite + acetate, acetate-only and DIC-only (Supplementary Figure S4).

3.3 Identification of microbial manganese reducers

The active bacterial community was identified by 16S rRNA sequencing (RNA), supplemented with the complete bacterial community by 16S rRNA gene sequencing (DNA). Presumably,

10.3389/fmicb.2024.1398021

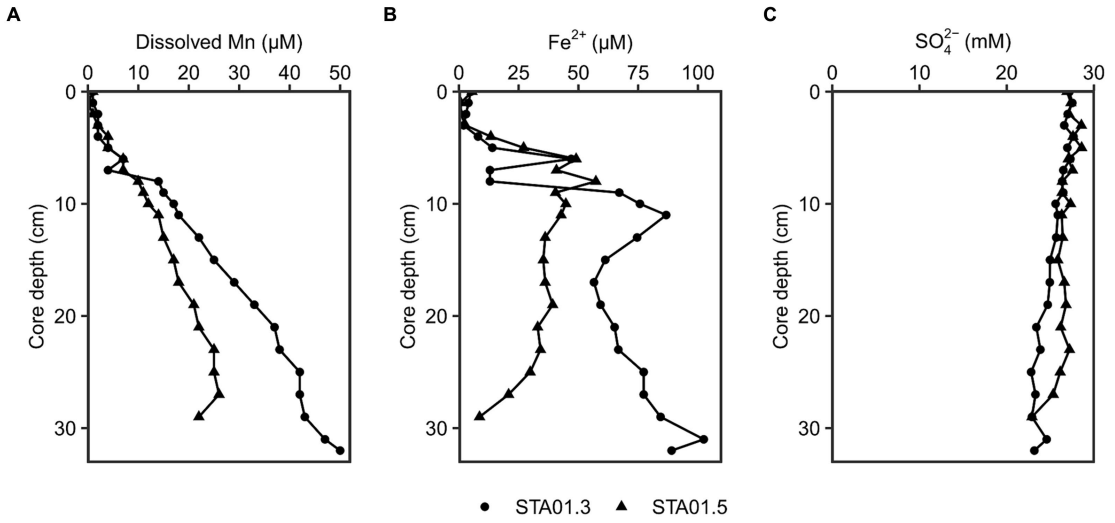

FIGURE 2
Geochemical parameters in the pore water of duplicate cores from STA 01 over sediment depths. **(A)** Dissolved manganese. **(B)** Dissolved Fe^{2+}. **(C)** Sulfate. Duplicate cores STA01-3 (●) and STA01-5 (▲) of the same station are distinguished as indicated.

tracking 16S rRNA enables detecting potentially active microorganisms, whereas an increase in 16S rRNA gene abundance might enable following microbial growth (Blazewicz et al., 2013; Foesel et al., 2014). Only communities of the treatments birnessite + acetate and the associated controls, i.e., acetate-only, birnessite + DIC, DIC-only, were sequenced, as only here the electron donor coupled to manganese reduction could be identified (Figure 3). The stimulated microorganisms detected were unclassified members of the *Arcobacteraceae* family (class *Campylobacteria*) and members of the *Desulfuromonadales* order (class *Desulfuromonadia*), i.e., *Desulfuromusa*, *Desulfuromonas* and Sva1033 (uncultured family) (Figure 4). Other microorganisms that were not clearly stimulated by substrate addition, i.e., detected by 16S rRNA and 16S rRNA gene sequencing, but not increasing up to day 20, were members of *Desulfobacterales*, *Desulfobulbales*, *Gammaproteobacteria* and other less abundant groups <10% relative abundance (Supplementary Figures S5, S6).

Desulfuromusa was the only taxon stimulated by the addition of both, acetate and birnessite and not by addition of acetate or birnessite alone (Figures 4A,E). In the birnessite + acetate treatment it reached relative abundances of up to 15 and 7% for 16S rRNA and 16S rRNA gene, respectively, after 20 days, while in all controls the relative abundance remained <0.5% (<3% for birnessite + DIC) for both 16S rRNA and 16S rRNA gene. The peak in relative abundance of *Desulfuromusa* concurred with the maximum concentration of dissolved manganese after 20 days (Figure 3). The *Desulfuromusa* ASV had the closest BLAST hit with the uncultured *Desulfuromusa* sp. Fe30-7C-S previously identified in Black Smoker Chimneys (Caldera Vent Field, Takai et al., 2009; 100% 16S rRNA gene sequence identity, Supplementary Table S4). The closest cultured relative was *Desulfuromusa bakii* (99.6% 16S rRNA gene sequence identity, Supplementary Tables S4, S6).

The taxon Sva1033 was already present with 6% relative 16S rRNA gene abundance (DNA level) at the start of the incubation and only increased slightly (max. 9% at day 20 in birnessite + acetate, Figure 4B) in all sequenced treatments over time. However, Sva1033 16S rRNA (RNA level) increased from 3% to over 10% relative abundance in treatments birnessite + acetate and the associated acetate-only control in 20 days with a more rapid reaction in the acetate-only treatment (Figure 4F).

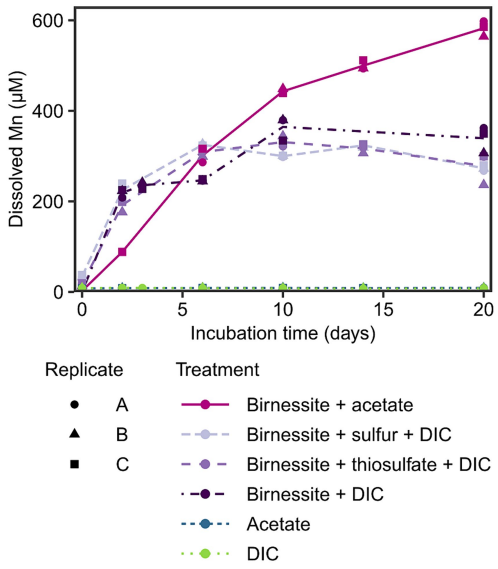

FIGURE 3
Dissolved manganese concentration in the incubation experiment over time. Different treatments are displayed by color and line type, and incubation triplicates by shape. The lines connect calculated means per treatment. Note, acetate and DIC treatment data points overlap.

Wunder et al.

10.3389/fmicb.2024.1398021

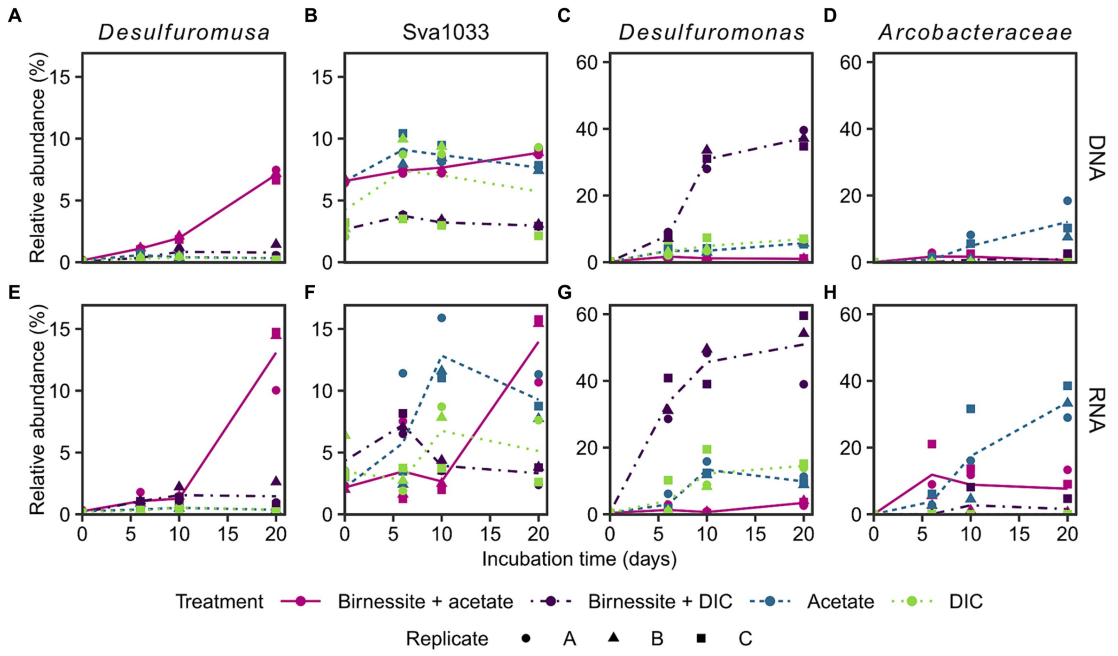

FIGURE 4
Relative abundance of 16S rRNA gene (**A–D**: DNA) and 16S rRNA (**E–H**: RNA) of most stimulated bacterial taxa (see text) in incubation experiment. Different treatments are displayed by color and line type, and incubation triplicates by shape. The lines connect calculated means per treatment. Sva1033 is a family of *Desulfuromonadales*. Plotted *Arcobacteraceae* were unclassified on genus level. Treatment birnessite + DIC was conducted separately and DIC replicate C is the associated control (see Supplementary material). For time point day 0, the associated slurry sample is plotted for all treatments (Supplementary Figures S5, S6). Note the different y-scales.

Arcobacteraceae was only stimulated by the addition of acetate with 16S rRNA gene (DNA level) abundance increasing from <0.2% up to 18% at day 20 (Figure 4D) and more rapid increase of 16S rRNA (RNA level) abundance to already 10% at day 6, all the way to >40% at day 20 (Figure 4H). In the control treatments without acetate addition, the 16S rRNA abundance remained <1%, except for one higher birnessite + DIC replicate C (Figures 4D,H). *Desulfuromonas*, as the only microbial player, showed a clear response in the birnessite + DIC treatment increasing rapidly in 16S rRNA and 16S rRNA gene abundance from 0.5% at day 0 to up to 60 and 40%, respectively, on day 20 (Figures 4C,G). The response in the other control treatments with DIC-only and acetate-only was much lower (max. 15% 16S rRNA day 10, Figure 4G) and reached only 4% in the birnessite + acetate treatment at day 20 with an even lower response on 16S rRNA gene level (2–7% day 20, Figure 4C).

In control treatments containing DIC, *Sulfurimonas* (class *Campylobacteria*) increased in 16S rRNA and 16S rRNA gene abundance up to 33 and 15%, respectively by day 20, but were < 3% at earlier timepoints (Supplementary Figures S5, S6). Some members of *Desulfocapsaceae* peaked on relative 16S rRNA abundance at day 10, but then decreased again at day 20, corroborated by no detectable increase of relative 16S rRNA gene abundance (Supplementary Figure S7).

The taxa enriched in the incubation experiment were also present in the *in situ* sediments (Supplementary Figure S8). However, only Sva1033 (class *Desulfuromonadia*) was present with high relative abundances of 16S rRNA genes up to 10%, while *Desulfuromusa* (class *Desulfuromonadia*) reached only 0.2% relative abundance and *Desulfuromonas* (class *Desulfuromonadia*) and *Arcobacteraceae* (class *Campylobacteria*) were < 0.1% relative abundance.

4 Discussion

Anaerobic organic carbon mineralization to CO_2 can be coupled to different electron acceptors such as manganese oxides, iron oxides or sulfate (Jørgensen, 2006). The contribution of manganese reduction is often overlooked and thought to be confined to very shallow sediment depths where manganese oxides deplete in the top 2 cm (Thamdrup, 2000) or extremely manganese oxide rich sediments (e.g., Ulleung Basin 200 μmol/cm^3, Hyun et al., 2017). Thamdrup (2000) proposed microbial manganese reduction only as important process if the manganese oxide concentration in the sediment is >20 μmol/cm^3 and penetrates deeper than 2 cm below the surface. At the study site Potter Cove, solid phase manganese oxides reach 20 μmol/cm^3 at the bottom of the 20 cm long core (recalculated from wt.%, Monien et al., 2014b; Supplementary material; Supplementary Figure S9). However, the availability of the electron acceptor alone does not warrant its reduction. For this, dissolved Mn in the pore water serves as indicator (Canfield et al., 1993a). At the sampling station STA 01, dissolved Mn accumulated with depth up to 50 μM (Figure 2). Pore water profiles of sediments taken 7 years earlier (2011) even showed accumulations up to 200 μM closer to the glacier front (station P04 in Monien et al., 2014a) and up to 100 μM in close proximity to STA 01 of this study

(station P01 in Monien et al., 2014a, data replotted Supplementary Figure S9 from Monien et al., 2014b). The concentration differences might be due to local variability in the sediment or due to change of the environment, e.g., glacier retreat. Between austral summer 2013 and 2019, the glacier completely retreated from the shore closest to STA 01 (personal communication G. Willis-Poratti, M. sierra, Supplementary Figure S10) which might have had a direct influence on the sediment environment. Until now, there are no studies investigating manganese reduction in the Antarctic in detail. However, the process has been proposed to be relevant in a variety of Arctic sites, where dissolved Mn concentrations of a similar range were detected. For example, in sediments of Kongsfjorden and Van Keulenfjorden of Svalbard dissolved Mn reached 30–200 µM, and fluxes of 80 µmol m^{-2} d^{-1} Mn were calculated at stations with highest Mn concentrations (Wehrmann et al., 2014). In the Barents Sea and Baffin Bay, dissolved Mn accumulated up to 75–150 µM and 50 µM in the top 20 cm, respectively, and dissimilatory iron and manganese reduction were identified as important processes (Vandieken et al., 2006c; Algora et al., 2013, 2015). For Potter Cove, Monien et al. (2014a) suggested ongoing microbial manganese reduction based on the pore water profiles in the sediment, but the associated microbial community remained unknown. In this study, we aim to close this knowledge gap and provide first data for the Antarctic environment.

4.1 Manganese reduction also contributes to organic matter mineralization in Potter Cove sediments

After detecting manganese reduction in sediments of Potter Cove based on pore water profiles, the potential for active organotrophic manganese reduction was further confirmed by incubation experiments; dissolved Mn accumulation (up to 600 µM in 20 days) was observed when fresh manganese oxide (birnessite) was fed to slurry incubations with acetate as electron donor (Figure 3). These concentrations were similar to other manganese reducing incubation experiments with coastal or shelf sediments from Sweden, Ulleung Basin, Barents Sea or Beaufort Sea, with accumulation of 400–800 µM dissolved manganese within 10–20 days (Vandieken et al., 2006c, 2012, 2014; Magen et al., 2011; Hyun et al., 2017). However, in contrast to these previous studies, we added birnessite to selectively stimulate manganese reduction against other competing processes such as iron or sulfate reduction. The addition of the electron donor (i.e., acetate) alone was not sufficient to stimulate this process, however an accumulation of dissolved Mn was observed in the control incubation birnessite + DIC (Figure 3). This might have been caused by biotic or abiotic manganese reduction with internally produced or residual electron donors in the sediment. For example, manganese oxides can be reduced abiotically by the oxidation of residual FeS or pyrite (Schippers and Jørgensen, 2001), which is one scenario how the iron, manganese and sulfur cycle interplay with each other. However, no concurrent increase of the oxidation product sulfate was observed during the incubation period (Supplementary Figure S4). The addition of reduced sulfur compounds (elemental sulfur or thiosulfate) to the incubated sediments, as electron donors for probing lithotrophic manganese reduction, did not result in a statistically relevant distinction of dissolved Mn formation compared to the control incubations (Figure 3; Supplementary Figure S3). Therefore, we conclude that the tested reduced sulfur compounds could not serve as electron donors for microbial manganese reduction in these sediments. Other inorganic electron acceptors such as hydrogen or sulfide would need to be tested to exclude lithotrophic manganese reduction in general. Most likely, endogenous organic matter had served as electron donor for manganese reduction in control incubations.

It must be noted that dissolved Mn accumulation does not represent the rate of manganese reduction, as Mn^{2+} can rapidly adsorb to manganese and iron oxide surfaces and organic compounds or precipitate as $MnCO_3$ or MnS (Suess, 1979; Burdige, 1993; Thamdrup, 2000). We exclude a large contribution of abiotic reduction of manganese oxide by ferrous iron produced by iron reduction (Thamdrup, 2000) as no additional fresh iron oxides were added. Yet, residual iron oxides in the incubated sediments were not sufficient to stimulate iron reduction activities beyond the 5 µM of ferrous iron detected, including in incubations supplemented with acetate (Supplementary Figure S4). We conclude that manganese reduction occurs mainly organotrophically and is not coupled to oxidation of tested reduced sulfur compounds in these sediments.

4.2 Active microbial players in organotrophic manganese reduction in Potter Cove sediments

The responsible microorganisms for organotrophic manganese reduction were investigated by 16S rRNA and 16S rRNA gene sequencing in treatments with acetate amendment and compared to control treatments. Four distinct taxa of microorganisms (*Desulfuromusa*, *Desulfuromonas*, *Arcobacteraceae* and Sva1033) were stimulated in the incubation experiment; *Desulfuromusa* was only active and grew when both, acetate and birnessite were supplied. Sva1033 (family of *Desulfuromonadales*) and *Arcobacteraceae* were also stimulated in the control treatments by the addition of acetate in the absence of birnessite, while *Desulfuromonas* was mainly stimulated in the birnessite + DIC control (Figure 4).

In the treatment with acetate and birnessite, the signature of manganese reduction (Figure 3) correlated with the stimulation of *Desulfuromusa* (Figures 4A,E). This taxon was found previously in RNA stable isotope probing experiments with Potter Cove sediment (100% identical ASVs, Supplementary Table S6), and it could use acetate with the addition of iron oxides and an electron shuttle in form of anthraquinone-2,6-disulfonic acid (AQDS) (Aromokeye et al., 2021). However, in these experiments, other microorganisms such as Sva1033 were more successful, i.e., more abundant, in thriving with iron oxides. Furthermore, *Desulfuromusa* was not detected in iron reducing incubation experiments by 16S rRNA gene sequencing only (Aromokeye et al., 2021), because apparently it prefers manganese oxide as electron acceptor at near *in situ* temperature conditions. Possibly, the same explanation applies for the lack of activity of *Desulfuromusa* in our incubations with only acetate. Furthermore, *Desulfuromusa* relied on supply of fresh organic compounds, i.e., acetate, as further confirmed by its lack of activity in the birnessite + DIC treatment (Figure 4E). In these control treatments, the other active microorganisms probably competed more successfully for remaining compounds in the sediment. In contrast, when both

manganese oxide and acetate were added to our incubations, *Desulfuromusa* increased 50x in 20 days, even on 16S rRNA gene level (Figure 4A).

Members of the *Desulfuromusa* genus are known for utilizing acetate as electron donor (Finster and Bak, 1993; Liesack and Finster, 1994; Vandieken et al., 2006b). However, the use of manganese oxide as electron acceptor was only demonstrated in *Desulfuromusa ferrireducens* (Vandieken et al., 2006b), while all other isolated strains are able to use iron but were not tested for manganese reduction (Finster and Bak, 1993; Lonergan et al., 1996). The closest cultured relative of the *Desulfuromusa* strain found in our study is *Desulfuromusa bakii* (99.6% sequence identity, Supplementary Tables S4, S6). *Desulfuromusa* species were previously also detected in Arctic (Vandieken et al., 2006a,c; Buongiorno et al., 2019; Magnuson et al., 2023) and Antarctic environments (Bowman et al., 2000; Taboada et al., 2020). However, their presence was only linked to a potential activity of iron reduction in few cases (Vandieken et al., 2006a). The *Desulfuromusa* strain found in our study apparently does not compete for iron reduction or other residual electron acceptors at environmentally relevant temperature, which is in contrast to previous studies at different locations (Vandieken et al., 2006a; An et al., 2020; Hamdan and Salam, 2020). Possibly, the low, close-to-*in situ* temperature of 2°C used in our study promoted the manganese reducing activity of this microorganism, avoiding competition with the other present acetate utilizers. We propose that *Desulfuromusa* occupied a niche of organotrophic manganese reduction in glacially influenced sediments, providing strong evidence for its relevance in microbial manganese reduction in Antarctic sediments.

While *Desulfuromusa* was the only microbe which clearly performed manganese reduction in our incubation experiments, other microbes were stimulated in the various other control treatments not optimized for manganese reduction. For example, *Arcobacteraceae* increased in relative 16S rRNA and 16S rRNA gene abundance, but strongly only in the presence of acetate, less with birnessite and acetate and was nearly absent without it (Figures 4D,H). This agrees with reports of anaerobic acetate oxidation by this taxon (Vandieken and Thamdrup, 2013); still it was previously shown that they can also use manganese as electron acceptor (Vandieken et al., 2012).

Next, *Desulfuromonas* showed a strong positive response to the amendment of birnessite alone, but surprisingly not in the birnessite + acetate treatment, while increasing in the DIC-only and acetate-only controls (Figures 4C,G). The ASV mainly stimulated in the treatments (sq1) was most closely related to *Desulfuromonas svalbardensis* (100% sequence identity, Supplementary Table S3), which is known to couple iron or manganese reduction to oxidation of fermentation products such as acetate (Vandieken et al., 2006b). In our study, *Desulfuromonas* was likely outcompeted by other microorganisms utilizing the amended acetate when birnessite was provided. However, when only birnessite (and DIC) were provided to the sediment background, *Desulfuromonas* possibly competed more successfully for a different residual electron donor.

In contrast to the other described stimulated taxa which showed low abundances at the start of the experiment, the largely unexplored family Sva1033 (*Desulfuromonadales*) was already present at day 0 and still increased during the incubation in 16S rRNA abundance in acetate amended and associated DIC-only control treatments (5x increase, Figure 4F). At the study site, this taxon likely plays an important role as indicated by its high relative abundance in the *in situ* sediments (Supplementary Figure S8) and its high presence already at the start and throughout the experiment. This is in agreement with previous studies investigating Antarctic sediments (Aromokeye et al., 2021; Baloza et al., 2023) and sub-Antarctic sediments around South Georgia (Wunder et al., 2021). Sva1033 was shown before to oxidize acetate and reduce iron oxides in sediments of Potter Cove (Aromokeye et al., 2021; Wunder et al., 2021), and also here it showed higher relative 16S rRNA abundance in acetate amended treatments. The late 7-fold relative abundance increase in 16S rRNA in the birnessite + acetate treatment at day 20 (Figure 4F) even hints at a potential to switch to manganese oxides as electron acceptor after a period of adaptation, e.g., from iron reduction (Wunder et al., 2021).

Species of *Desulforhopalus* and *Desulfocapsaceae* also responded in the birnessite + acetate treatment within 6–10 days (Supplementary Figure S7). However, as these responses were only transient and did not increase further despite ongoing manganese reduction after day 10 (Figure 3), it was unclear whether these bacteria reacted to the substrate addition.

The microbial community linked to manganese reduction in other marine environments was so far mostly associated with *Pelobacter*, *Colwelliaceae, Arcobacteraceae, Shewanellaceae*, *Oceanospirillaceae*, or *Burkholderiales* (Thamdrup et al., 2000; Vandieken et al., 2012; Algora et al., 2015; Cho et al., 2020). Except for *Arcobacteraceae*, none of these other taxa were present or were only extremely low abundant in the incubations and in the *in situ* sediments (<0.05%, *Colwellia* 0.2% at 2 cm *in situ*, *Burkholderiales* < 1% in incubation). However, most of the previously studied sites for manganese reduction and the associated microbial community are extremely manganese-rich, e.g., Ulleung Basin and Skagerrak with 200–600 μmol/cm^3 (Vandieken et al., 2012) versus 20 μmol/cm^3 for Potter Cove (Supplementary Figure S9). Another parameter differing at these sites is temperature: most of the previous study sites are in temperate environments. In Arctic sediments from the deep basin of Baffin Bay, one of the locations where Mn reduction was investigated in a cold environment (Algora et al., 2013), the dissolved manganese concentrations were in a comparable range to Potter Cove with of 20–60 μM. Here, manganese reduction was proposed to be an important part of anaerobic organic matter degradation (Algora et al., 2013), but the associated microbial community was different again, suggesting *Betaproteobacteria* as potential manganese and iron reducers (Algora et al., 2015). Both, the availability of manganese oxides and the colder temperature might be responsible factors for a different manganese reducing community in our Antarctic sediment samples with the above discussed *Desulfuromusa* as key microorganism. Further investigations are needed to unravel influencing factors on the manganese reducing community on a larger, global scale.

4.3 Relevance of manganese reduction in rapidly warming Antarctic sediments

At the study site Potter Cove, the *in situ* geochemistry and the incubation experiments with manganese oxides clearly demonstrated the potential for the contribution of manganese reduction to organic matter degradation in the sediments. At other sampling locations in Potter Cove, elevated dissolved manganese concentrations up to even 200 μM indicate that this process might contribute to organic

matter degradation there as well (e.g., stations P05, K48, Figure 3 in Monien et al., 2014a). The high dissolved ferrous iron concentrations of 100–800 µM detected in the pore water in our study (Figure 2) and multiple previous studies (Monien et al., 2014a; Henkel et al., 2018) indicate contribution of microbial iron reduction to organic matter degradation (Aromokeye et al., 2021). Iron was also shown as important electron acceptor in glacially or sea ice influenced sediments in the Arctic, such as Svalbard (Vandieken et al., 2006a,c) or Greenland (Glud et al., 2000), and also at the Antarctic shelf (Baloza et al., 2022). Rate measurements of carbon oxidation as conducted for some Arctic sediment (Vandieken et al., 2006c) would be necessary to investigate the contribution of the different processes, i.e., iron, manganese and sulfate reduction, in Potter Cove sediments.

An open question remains how glacial input influences manganese reduction in the marine sediment. For Potter Cove, it has been clearly shown that suspended particulate matter transported by surficial glacial meltwater supplies iron and manganese into the cove (Monien et al., 2017). There are many studies showing high amounts of iron supplied to the ocean and underlying sediments by subglacial or surficial meltwater (Wehrmann et al., 2014; Monien et al., 2017; Raiswell et al., 2018; Forsch et al., 2021). The bioavailability of this iron varies depending on the source, and subsequent biogeochemical cycling plays an important role to make this supplied iron bioavailable to, e.g., fuel primary production (Henkel et al., 2018; Herbert et al., 2021; Laufer-Meiser et al., 2021). Perhaps, the same applies to manganese and this study has demonstrated that the manganese supply from glacial input will likely increase the likelihood for manganese reduction to contribute to organic matter degradation in Antarctic sediments.

5 Conclusion

We show that organotrophic manganese reduction has the potential to contribute to organic matter mineralization in the Antarctic sediments of Potter Cove (King George Island/Isla 25 de Mayo). We identified *Desulfuromusa* as a key organism for organotrophic manganese reduction and propose that it occupies a niche of manganese reduction at a low, environmentally relevant temperature. *Arcobacteraceae* also contributed to organic carbon mineralization (i.e., acetate oxidation); however, this group likely did not reduce manganese but thrived on unidentified residual electron acceptors. *Desulfuromonas* was stimulated, but the underlying processes are not clear yet. The largely uncharacterized group Sva1033 (family of *Desulfuromonadales*) also contributed to acetate oxidation with the potential to link it to manganese oxide reduction which would extend the known utilized electron acceptors for this microorganism. The manganese reducing bacterial community identified in Potter Cove differed from other previously studied locations. This raises the question whether the observed diversity is caused by geographical location effects, i.e., whether Antarctica hosts a different microbial community than, e.g., the Arctic, or by other factors such as temperature, glacial influence, or sediment composition. In the context of a rapidly changing environment due to global warming, it is of interest to gain a better understanding of the ecology in the current environment to be able to predict future changes. This study brings us one step further by showing manganese reduction might become more relevant for organic matter degradation in permanently cold marine environments.

Data availability statement

The datasets presented in this study can be found in online repositories. The names of the repository/repositories and accession number(s) can be found at: https://www.ebi.ac.uk/ena, PRJEB72873; https://www.ebi.ac.uk/ena, PRJEB72882; https://www.pangaea.de/; https://doi.pangaea.de/10.1594/PANGAEA.941109; https://github.com/Microbial-Ecophysiology/Mn-red-PotterCove.

Author contributions

LW: Conceptualization, Formal analysis, Investigation, Visualization, Writing – original draft. IB: Conceptualization, Formal analysis, Investigation, Writing – review & editing. GW-P: Conceptualization, Funding acquisition, Investigation, Writing – review & editing. DA: Conceptualization, Investigation, Writing – review & editing. SH: Investigation, Writing – review & editing. TR-H: Writing – review & editing. XY: Conceptualization, Writing – review & editing. MF: Funding acquisition, Project administration, Writing – review & editing.

Funding

The author(s) declare that financial support was received for the research, authorship, and/or publication of this article. This work was supported by the Deutsche Forschungsgemeinschaft (DFG) in the framework of the priority program "Antarctic Research with Comparative Investigation in Arctic Ice Areas" SPP 1158 in the project "Environmental Control on Iron-Reducing Microorganisms in Antarctic sediment (ECIMAS)" (project number 404648014) and the University of Bremen. GW-P was funded by individual fellowships supported by the Deutscher Akademischer Austauschdienst [German Academic Exchange Service (DAAD)]: Research Stays for University Academics and Scientists, 2019 (grant number 57440915), Research Grants - Short-Term Grants, 2020 (grant number 57507442) and Research Stays for University Academics and Scientists, 2023 (grant number 57681226).

Acknowledgments

The authors thank the Instituto Antártico Argentino (IAA) – Dirección Nacional del Antártico (DNA), the crew at Carlini Station and the Alfred Wegener Institute Helmholtz Centre for Polar and Marine Research (AWI) for the logistics support during the field campaign to the King George Island/Isla 25 de Mayo in the Antarctic Peninsula. The authors acknowledge Principal Corporal Javier Alvarez from the crew at Carlini Station and Argentinian Navy (Armada Argentina) and the Argentinian Army (Ejército Argentino) divers of CAV 2018-2019 for their support during the sampling at Potter Cove.

The authors thank Ingrid Dohrmann of the Alfred Wegener Institute (AWI, Bremerhaven, Germany) for support with the geochemical measurements. The authors thank Annika Schnakenberg for providing the birnessite and sulfur substrates.

Conflict of interest

The authors declare that the research was conducted in the absence of any commercial or financial relationships that could be construed as a potential conflict of interest.

The author(s) declared that they were an editorial board member of Frontiers, at the time of submission. This had no impact on the peer review process and the final decision.

Publisher's note

Supplementary material

The Supplementary material for this article can be found online at: https://www.frontiersin.org/articles/10.3389/fmicb.2024.1398021/full#supplementary-material

References

Algora, C., Gründger, F., Adrian, L., Damm, V., Richnow, H.-H., and Krüger, M. (2013). Geochemistry and microbial populations in sediments of the northern Baffin Bay, Arctic. *Geomicrobiol J.* 30, 690–705. doi: 10.1080/01490451.2012.758195

Algora, C., Vasileiadis, S., Wasmund, K., Trevisan, M., Krüger, M., Puglisi, E., et al. (2015). Manganese and iron as structuring parameters of microbial communities in Arctic marine sediments from the Baffin Bay. *FEMS Microbiol. Ecol.* 91:fiv056. doi: 10.1093/femsec/fiv056

Aller, R. C., and Rude, P. D. (1988). Complete oxidation of solid phase sulfides by manganese and bacteria in anoxic marine sediments. *Geochim. Cosmochim. Acta* 52, 751–765. doi: 10.1016/0016-7037(88)90335-3

Altschul, S. F., Madden, T. L., Schäffer, A. A., Zhang, J., Zhang, Z., Miller, W., et al. (1997). Gapped BLAST and PSI-BLAST: a new generation of protein database search programs. *Nucleic Acids Res.* 25, 3389–3402. doi: 10.1093/nar/25.17.3389

An, S.-U., Cho, H., Jung, U.-J., Kim, B., Lee, H., and Hyun, J.-H. (2020). Invasive *Spartina anglica* greatly alters the rates and pathways of organic carbon oxidation and associated microbial communities in an intertidal wetland of the Han River estuary, Yellow Sea. *Front. Mar. Sci.* 7:59. doi: 10.3389/fmars.2020.00059

Aromokeye, D. A., Willis-Poratti, G., Wunder, L. C., Yin, X., Wendt, J., Richter-Heitmann, T., et al. (2021). Macroalgae degradation promotes microbial iron reduction via electron shuttling in coastal Antarctic sediments. *Environ. Int.* 156:106602. doi: 10.1016/j.envint.2021.106602

Baloza, M., Henkel, S., Geibert, W., Kasten, S., and Holtappels, M. (2022). Benthic carbon remineralization and Iron cycling in relation to sea ice cover along the eastern continental shelf of the Antarctic Peninsula. *J. Geophys. Res. (C Oceans)* 127:e2021JC018401. doi: 10.1029/2021JC018401

Baloza, M., Henkel, S., Kasten, S., Holtappels, M., and Molari, M. (2023). The impact of sea ice cover on microbial communities in Antarctic shelf sediments. *Microorganisms* 11:1572. doi: 10.3390/microorganisms11061572

Blazewicz, S. J., Barnard, R. L., Daly, R. A., and Firestone, M. K. (2013). Evaluating rRNA as an indicator of microbial activity in environmental communities: limitations and uses. *ISME J.* 7, 2061–2068. doi: 10.1038/ismej.2013.102

Bowman, J. P., Rea, S. M., McCammon, S. A., and McMeekin, T. A. (2000). Diversity and community structure within anoxic sediment from marine salinity meromictic lakes and a coastal meromictic marine basin, Vestfold Hills, eastern Antarctica. *Environ. Microbiol.* 2, 227–237. doi: 10.1046/j.1462-2920.2000.00097.x

Buongiorno, J., Herbert, L., Wehrmann, L., Michaud, A., Laufer, K., Røy, H., et al. (2019). Complex microbial communities drive iron and sulfur cycling in Arctic fjord sediments. *Appl. Environ. Microbiol.* 85, e00949–e00919. doi: 10.1128/AEM.00949-19

Burdige, D. J. (1993). The biogeochemistry of manganese and iron reduction in marine sediments. *Earth-Sci. Rev.* 35, 249–284. doi: 10.1016/0012-8252(93)90040-E

Burdige, D. J., and Christensen, J. P. (2022). Iron biogeochemistry in sediments on the western continental shelf of the Antarctic Peninsula. *Geochim. Cosmochim. Acta* 326, 288–312. doi: 10.1016/j.gca.2022.03.013

Bushnell, B. (2014). BBMap: a fast, accurate, splice-aware aligner. Version 38.86. Lawrence Berkeley National Laboratory. LBNL report: LBNL-7065E. Available at: https://escholarship.org/uc/item/1h3515gn.

Callahan, B. J., McMurdie, P. J., Rosen, M. J., Han, A. W., Johnson, A. J. A., and Holmes, S. P. (2016). DADA2: high-resolution sample inference from Illumina amplicon data. *Nat. Methods* 13, 581–583. doi: 10.1038/nmeth.3869

Canfield, D. E., Jørgensen, B. B., Fossing, H., Glud, R., Gundersen, J., Ramsing, N. B., et al. (1993a). Pathways of organic carbon oxidation in three continental margin sediments. *Mar. Geol.* 113, 27–40. doi: 10.1016/0025-3227(93)90147-N

Canfield, D. E., Thamdrup, B., and Hansen, J. W. (1993b). The anaerobic degradation of organic matter in Danish coastal sediments: iron reduction, manganese reduction, and sulfate reduction. *Geochim. Cosmochim. Acta* 57, 3867–3883. doi: 10.1016/0016-7037(93)90340-3

Casado, M., Hébert, R., Faranda, D., and Landais, A. (2023). The quandary of detecting the signature of climate change in Antarctica. *Nat. Clim. Chang.* 13, 1082–1088. doi: 10.1038/s41558-023-01791-5

Chao, A., Gotelli, N. J., Hsieh, T. C., Sander, E. L., Ma, K. H., Colwell, R. K., et al. (2014). Rarefaction and extrapolation with Hill numbers: a framework for sampling and estimation in species diversity studies. *Ecol. Monogr.* 84, 45–67. doi: 10.1890/13-0133.1

Cho, H., Kim, B., Mok, J. S., Choi, A., Thamdrup, B., and Hyun, J. H. (2020). Acetate-utilizing microbial communities revealed by stable-isotope probing in sediment underlying the upwelling system of the Ulleung Basin, East Sea. *Mar. Ecol. Prog. Ser.* 634, 45–61. doi: 10.3354/meps13182

Cline, J. D. (1969). Spectrophotometric determination of hydrogen sulfide in natrual waters. *Limnol. Oceanogr.* 14, 454–458. doi: 10.4319/lo.1969.14.3.0454

Death, R., Wadham, J. L., Monteiro, F., Le Brocq, A. M., Tranter, M., Ridgwell, A., et al. (2014). Antarctic ice sheet fertilises the Southern Ocean. *Biogeosciences* 11, 2635–2643. doi: 10.5194/bg-11-2635-2014

Finster, K., and Bak, F. (1993). Complete oxidation of propionate, valerate, succinate, and other organic compounds by newly isolated types of marine, anaerobic, mesophilic, gram-negative, sulfur-reducing eubacteria. *Appl. Environ. Microbiol.* 59, 1452–1460. doi: 10.1128/aem.59.5.1452-1460.1993

Foesel, B. U., Nägele, V., Naether, A., Wüst, P. K., Weinert, J., Bonkowski, M., et al. (2014). Determinants of Acidobacteria activity inferred from the relative abundances of 16S rRNA transcripts in German grassland and forest soils. *Environ. Microbiol.* 16, 658–675. doi: 10.1111/1462-2920.12162

Forsch, K. O., Hahn-Woernle, L., Sherrell, R. M., Roccanova, V. J., Bu, K., Burdige, D., et al. (2021). Seasonal dispersal of fjord meltwaters as an important source of iron and manganese to coastal Antarctic phytoplankton. *Biogeosciences* 18, 6349–6375. doi: 10.5194/bg-18-6349-2021

Foster, Z. S. L., Chamberlain, S., and Grünwald, N. J. (2018). Taxa: An R package implementing data standards and methods for taxonomic data. *F1000research* 7:272. doi: 10.12688/f1000research.14013.2

Foster, Z. S. L., Sharpton, T. J., and Grünwald, N. J. (2017). Metacoder: An R package for visualization and manipulation of community taxonomic diversity data. *PLoS Comput. Biol.* 13:e1005404. doi: 10.1371/journal.pcbi.1005404

Gerrish, L. (2020). Data from: automatically extracted rock outcrop dataset for Antarctica (7.3). UK Polar Data Centre, Natural Environment Research Council, UK Research & Innovation. doi: 10.5285/178ec50d-1ffb-42a4-a4a3-1145419da2bb

Glud, R. N., Risgaard-Petersen, N., Thamdrup, B., Fossing, H., and Rysgaard, S. (2000). Benthic carbon mineralization in a high-Arctic sound (Young Sound, NE Greenland). *Mar. Ecol. Prog. Ser.* 206, 59–71. doi: 10.3354/meps206059

Hamady, M., Walker, J. J., Harris, J. K., Gold, N. J., and Knight, R. (2008). Error-correcting barcoded primers for pyrosequencing hundreds of samples in multiplex. *Nat. Methods* 5, 235–237. doi: 10.1038/nmeth.1184

Hamdan, H. Z., and Salam, D. A. (2020). Response of sediment microbial communities to crude oil contamination in marine sediment microbial fuel cells under ferric iron stimulation. *Environ. Pollut.* 263:114658. doi: 10.1016/j.envpol.2020.114658

Hassenrueck, C. (2022). Paired-end amplicon sequence processing workflow configurable for mixed-orientation libraries and highly variable insert size. Version 1.2.0.

work-flow. Available at: https://git.io-warnemuende.de/bio_inf/workflow_templates/src/branch/master/Amplicon_dada2_MiSeq.

Henkel, S., Kasten, S., Hartmann, J. F., Silva-Busso, A., and Staubwasser, M. (2018). Iron cycling and stable Fe isotope fractionation in Antarctic shelf sediments, King George Island. *Geochim. Cosmochim. Acta* 237, 320–338. doi: 10.1016/j.gca.2018.06.042

Herberich, E., Sikorski, J., and Hothorn, T. (2010). A robust procedure for comparing multiple means under heteroscedasticity in unbalanced designs. *PLoS One* 5:e9788. doi: 10.1371/journal.pone.0009788

Herbert, L. C., Riedinger, N., Michaud, A. B., Laufer, K., Røy, H., Jørgensen, B. B., et al. (2020). Glacial controls on redox-sensitive trace element cycling in Arctic fjord sediments (Spitsbergen, Svalbard). *Geochim. Cosmochim. Acta* 271, 33–60. doi: 10.1016/j.gca.2019.12.005

Herbert, L. C., Zhu, Q., Michaud, A. B., Laufer-Meiser, K., Jones, C. K., Riedinger, N., et al. (2021). Benthic iron flux influenced by climate-sensitive interplay between organic carbon availability and sedimentation rate in Arctic fjords. *Limnol. Oceanogr.* 66, 3374–3392. doi: 10.1002/lno.11885

Herlemann, D. P. R., Labrenz, M., Jürgens, K., Bertilsson, S., Waniek, J. J., and Andersson, A. F. (2011). Transitions in bacterial communities along the 2000 km salinity gradient of the Baltic Sea. *ISME J.* 5, 1571–1579. doi: 10.1038/ismej.2011.41

Hothorn, T., Bretz, F., and Westfall, P. (2008). Simultaneous Inference in General Parametric Models. *Biom. J.* 50, 346–363. doi: 10.1002/bimj.200810425

Hyun, J. H., Kim, S. H., Mok, J. S., Cho, H., Lee, T., Vandieken, V., et al. (2017). Manganese and iron reduction dominate organic carbon oxidation in surface sediments of the deep Ulleung Basin, East Sea. *Biogeosciences* 14, 941–958. doi: 10.5194/bg-14-941-2017

Jerosch, K., Scharf, F. K., Deregibus, D., Campana, G. L., Zacher-Aued, K., Pehlke, H., et al. (2015). Data from: high resolution bathymetric compilation for Potter Cove, WAP, Antarctica, with links to data in ArcGIS format. *PANGAEA*. doi: 10.1594/PANGAEA.853593

Jørgensen, B. B. (2006). "Bacteria and marine biogeochemistry" in Marine Geochemistry. eds. H. D. Schulz and M. Zabel (Berlin, Heidelberg: Springer Berlin Heidelberg), 169–206.

LaRowe, D. E., Arndt, S., Bradley, J. A., Estes, E. R., Hoarfrost, A., Lang, S. Q., et al. (2020). The fate of organic carbon in marine sediments - new insights from recent data and analysis. *Earth-Sci. Rev.* 204:103146. doi: 10.1016/j.earscirev.2020.103146

Laufer-Meiser, K., Michaud, A. B., Maisch, M., Byrne, J. M., Kappler, A., Patterson, M. O., et al. (2021). Potentially bioavailable iron produced through benthic cycling in glaciated Arctic fjords of Svalbard. *Nat. Commun.* 12:1349. doi: 10.1038/s41467-021-21558-w

Liesack, W., and Finster, K. (1994). Phylogenetic analysis of five strains of gram-negative, obligately anaerobic, sulfur-reducing bacteria and description of *Desulfuromusa* gen. nov., including *Desulfuromusa kysingii* sp. nov., *Desulfuromusa bakii* sp. nov., and *Desulfuromusa succinoxidans* sp. nov. *Int. J. Syst. Evol. Microbiol.* 44, 753–758. doi: 10.1099/00207713-44-4-753

Lonergan, D. J., Jenter, H. L., Coates, J. D., Phillips, E. J., Schmidt, T. M., and Lovley, D. R. (1996). Phylogenetic analysis of dissimilatory Fe(III)-reducing bacteria. *J. Bacteriol.* 178, 2402–2408. doi: 10.1128/jb.178.8.2402-2408.1996

Lovley, D. R. (1991). Dissimilatory Fe(III) and Mn(IV) reduction. *Microbiol. Mol. Biol. Rev.* 55, 259–287. doi: 10.1128/mr.55.2.259-287.1991

Lueders, T., Manefield, M., and Friedrich, M. W. (2004). Enhanced sensitivity of DNA- and rRNA-based stable isotope probing by fractionation and quantitative analysis of isopycnic centrifugation gradients. *Environ. Microbiol.* 6, 73–78. doi: 10.1046/j.1462-2920.2003.00536.x

Magen, C., Mucci, A., and Sundby, B. (2011). Reduction rates of sedimentary Mn and Fe oxides: An incubation experiment with Arctic Ocean sediments. *Aquat. Geochem.* 17, 629–643. doi: 10.1007/s10498-010-9117-9

Magnuson, E., Altshuler, I., Freyria, N. J., Leveille, R. J., and Whyte, L. G. (2023). Sulfur-cycling chemolithoautotrophic microbial community dominates a cold, anoxic, hypersaline Arctic spring. *Microbiome* 11:203. doi: 10.1186/s40168-023-01628-5

Martin, M. (2011). Cutadapt removes adapter sequences from high-throughput sequencing reads. *EMBnet J.* 17, 10–12. doi: 10.14806/ej.17.1.200

McKenzie, R. M. (1971). The synthesis of birnessite, cryptomelane, and some other oxides and hydroxides of manganese. *Mineral. Mag.* 38, 493–502. doi: 10.1180/minmag.1971.038.296.12

McMurdie, P. J., and Holmes, S. (2013). Phyloseq: An R package for reproducible interactive analysis and graphics of microbiome census data. *PLoS One* 8:e61217. doi: 10.1371/journal.pone.0061217

Mitchell, J. F. B. (1989). The "greenhouse" effect and climate change. *Rev. Geophys.* 27, 115–139. doi: 10.1029/RG027i001p00115

Monien, P., Lettmann, K. A., Monien, D., Asendorf, S., Wölfl, A.-C., Lim, C. H., et al. (2014a). Redox conditions and trace metal cycling in coastal sediments from the maritime Antarctic. *Geochim. Cosmochim. Acta* 141, 26–44. doi: 10.1016/j.gca.2014.06.003

Monien, D., Monien, P., Brünjes, R., Widmer, T., Kappenberg, A., Silva Busso, A. A., et al. (2017). Meltwater as a source of potentially bioavailable iron to Antarctica waters. *Antarct. Sci.* 29, 277–291. doi: 10.1017/S095410201600064X

Monien, P., Schnetger, B., and Brumsack, H.-J. (2014b). Data from: geochemistry of sediment core PC-P01b, Potter Cove, King George Island. *PANGAEA*. doi: 10.1594/PANGAEA.805935

Neder, C., Fofonova, V., Androsov, A., Kuznetsov, I., Abele, D., Falk, U., et al. (2022). Modelling suspended particulate matter dynamics at an Antarctic fjord impacted by glacier melt. *J. Mar. Syst.* 231:103734. doi: 10.1016/j.jmarsys.2022.103734

Olson, N. D., and Morrow, J. B. (2012). DNA extract characterization process for microbial detection methods development and validation. *BMC. Res. Notes* 5:668. doi: 10.1186/1756-0500-5-668

Parada, A. E., Needham, D. M., and Fuhrman, J. A. (2016). Every base matters: assessing small subunit rRNA primers for marine microbiomes with mock communities, time series and global field samples. *Environ. Microbiol.* 18, 1403–1414. doi: 10.1111/1462-2920.13023

Quast, C., Pruesse, E., Yilmaz, P., Gerken, J., Schweer, T., Yarza, P., et al. (2012). The SILVA ribosomal RNA gene database project: improved data processing and web-based tools. *Nucleic Acids Res.* 41, D590–D596. doi: 10.1093/nar/gks1219

R Core Team (2023). R: A language and environment for statistical computing. Version 4.3.1: R Foundation for Statistical Computing Available at: https://www.R-project.org.

Raiswell, R., Hawkings, J., Elsenousy, A., Death, R., Tranter, M., and Wadham, J. (2018). Iron in glacial systems: speciation, reactivity, freezing behavior, and alteration during transport. *Front. Earth Sci.* 6:222. doi: 10.3389/feart.2018.00222

Rantanen, M., Karpechko, A. Y., Lipponen, A., Nordling, K., Hyvärinen, O., Ruosteenoja, K., et al. (2022). The Arctic has warmed nearly four times faster than the globe since 1979. *Commun. Earth Environ.* 3:168. doi: 10.1038/s43247-022-00498-3

Rückamp, M., Braun, M., Suckro, S., and Blindow, N. (2011). Observed glacial changes on the King George Island ice cap, Antarctica, in the last decade. *Glob. Planet. Chang.* 79, 99–109. doi: 10.1016/j.gloplacha.2011.06.009

Salazar, G. (2021). Modified loessErrfun function in dada2 Github issue #938 Mixed Orientations and Large Data Processing [Online]. Available at: https://github.com/benjjneb/dada2/issues/938#issuecomment-774051061 (Accessed February 18, 2023).

Schippers, A., and Jørgensen, B. B. (2001). Oxidation of pyrite and iron sulfide by manganese dioxide in marine sediments. *Geochim. Cosmochim. Acta* 65, 915–922. doi: 10.1016/S0016-7037(00)00589-5

Seeberg-Elverfeldt, J., Schlüter, M., Feseker, T., and Kölling, M. (2005). Rhizon sampling of porewaters near the sediment-water interface of aquatic systems. *Limnol. Oceanogr. Methods* 3, 361–371. doi: 10.4319/lom.2005.3.361

Suess, E. (1979). Mineral phases formed in anoxic sediments by microbial decomposition of organic matter. *Geochim. Cosmochim. Acta* 43, 339–352. doi: 10.1016/0016-7037(79)90199-6

Taboada, S., Bas, M., Avila, C., and Riesgo, A. (2020). Phylogenetic characterization of marine microbial biofilms associated with mammal bones in temperate and polar areas. *Mar. Biodivers.* 50:60. doi: 10.1007/s12526-020-01082-8

Takai, K., Nunoura, T., Horikoshi, K., Shibuya, T., Nakamura, K., Suzuki, Y., et al. (2009). Variability in microbial communities in black smoker chimneys at the NW Caldera Vent Field, Brothers Volcano, Kermadec Arc. *Geomicrobiol J.* 26, 552–569. doi: 10.1080/01490450903304949

Thamdrup, B. (2000). "Bacterial manganese and iron reduction in aquatic sediments" in Advances in Microbial Ecology. ed. B. Schink (Boston, MA: Springer US), 41–84.

Thamdrup, B., Rosselló-Mora, R., and Amann, R. (2000). Microbial manganese and sulfate reduction in Black Sea shelf sediments. *Appl. Environ. Microbiol.* 66, 2888–2897. doi: 10.1128/aem.66.7.2888-2897.2000

Vandieken, V., Finke, N., and Jørgensen, B. B. (2006a). Pathways of carbon oxidation in an Arctic fjord sediment (Svalbard) and isolation of psychrophilic and psychrotolerant Fe(III)-reducing bacteria. *Mar. Ecol. Prog. Ser.* 322, 29–41. doi: 10.3354/meps322029

Vandieken, V., Finke, N., and Thamdrup, B. (2014). Hydrogen, acetate, and lactate as electron donors for microbial manganese reduction in a manganese-rich coastal marine sediment. *FEMS Microbiol. Ecol.* 87, 733–745. doi: 10.1111/1574-6941.12259

Vandieken, V., Mußmann, M., Niemann, H., and Jørgensen, B. B. (2006b). *Desulfuromonas svalbardensis* sp. nov. and *Desulfuromusa ferrireducens* sp. nov., psychrophilic, Fe(III)-reducing bacteria isolated from Arctic sediments, Svalbard. *Int. J. Syst. Evol. Microbiol.* 56, 1133–1139. doi: 10.1099/ijs.0.63639-0

Vandieken, V., Nickel, M., and Jørgensen, B. B. (2006c). Carbon mineralization in Arctic sediments northeast of Svalbard: Mn(IV) and Fe(III) reduction as principal anaerobic respiratory pathways. *Mar. Ecol. Prog. Ser.* 322, 15–27. doi: 10.3354/meps322015

Vandieken, V., Pester, M., Finke, N., Hyun, J.-H., Friedrich, M. W., Loy, A., et al. (2012). Three manganese oxide-rich marine sediments harbor similar communities of acetate-oxidizing manganese-reducing bacteria. *ISME J.* 6, 2078–2090. doi: 10.1038/ismej.2012.41

Vandieken, V., and Thamdrup, B. (2013). Identification of acetate-oxidizing bacteria in a coastal marine surface sediment by RNA-stable isotope probing in anoxic slurries and intact cores. *FEMS Microbiol. Ecol.* 84, 373–386. doi: 10.1111/1574-6941.12069

Viollier, E., Inglett, P., Hunter, K., Roychoudhury, A., and Van Cappellen, P. (2000). The ferrozine method revisited: Fe(II)/Fe(III) determination in natural waters. *Appl. Geochem.* 15, 785–790. doi: 10.1016/S0883-2927(99)00097-9

Wehrmann, L. M., Formolo, M. J., Owens, J. D., Raiswell, R., Ferdelman, T. G., Riedinger, N., et al. (2014). Iron and manganese speciation and cycling in glacially influenced high-latitude fjord sediments (West Spitsbergen, Svalbard): evidence for a benthic recycling-transport mechanism. *Geochim. Cosmochim. Acta* 141, 628–655. doi: 10.1016/j.gca.2014.06.007

Wickham, H., Averick, M., Bryan, J., Chang, W., McGowan, L. D. A., François, R., et al. (2019). Welcome to the Tidyverse. *J. Open Source Softw.* 4:1686. doi: 10.21105/joss.01686

Wunder, L. C., Aromokeye, D. A., Yin, X., Richter-Heitmann, T., Willis-Poratti, G., Schnakenberg, A., et al. (2021). Iron and sulfate reduction structure microbial communities in (sub-)Antarctic sediments. *ISME J.* 15, 3587–3604. doi: 10.1038/s41396-021-01014-9

Zhang, Z., Schartz, S., Wagner, L., and Miller, W. (2000). A greedy algorithm for aligning DNA sequences. *J. Comput. Biol.* 7, 203–214. doi: 10.1089/10665270050081478

3.2 Supplementary

3.2.1 Supplementary data

3.2.1.1 Incubation set-up

Slurry incubations were prepared as described in the main manuscript. In total six treatments differing in their substrate addition were set up as shown in Table 1.

The substrate birnessite (MnO_2) was synthesized following McKenzie (1971). Briefly, 2 mol of concentrated HCl was added dropwise to a boiling solution of 1 mol $KMnO_4$ (SigmaAldrich, Taufkirchen, Germany) in 2.5 ml of sterile deionized water, under vigorous stirring. The mixture was boiled for 10- 15 min. During cooling of the mixture brownish precipitates settled which were washed 5 times with de-ionized water to remove impurities before transfer into centrifuge tubes. Wet precipitates were centrifuged 3 times at 3,834 *g* for 10 min at room temperature with a Sorvall Evolution RC Centrifuge (Thermo Scientific, Germany). After each centrifugation step, the supernatant was decanted and pellet was rinsed with de-ionized water. MnO_2 was then dispersed in anoxic, de-ionized water and sterilized. The suspension was stored in 120 ml serum flask under N_2 atmosphere (N_2, 99.999%).

The substrate elemental sulfur was prepared as crystalline orthorhombic sulfur (S_8) by dissolving 10 g commercially available sulfur (Applichem, Darmstadt, Germany) in 30 ml carbon disulfide (CS_2). Traces of CS_2 were removed by vigorous stirring of the solution sulfur at 60°C overnight. The S_8 was then ground and dispersed in anoxic, sterile and de-ionized water by long and vigorous shaking. The suspension was stored in 120-ml serum flask under N_2 atmosphere (N_2, 99.999%).

The control treatment birnessite + DIC was performed in 2023 while the rest of the experiment was performed in 2021. The sediment for slurry preparation in 2021 and 2023 originated from the same Schott-bottles used for storage. Control treatments only containing slurry and DIC were done in 2021 and in 2023 in order to check background activities. During the course of incubation, subsamples were taken for geochemical measurements as described in the main manuscript. Treatments containing only DIC set up in 2021 and 2023 behaved similarly for ferrous iron, sulfide and manganese (Figure S 4). However, in both treatments set up in 2023 (DIC_2023, Birnessite + DIC) the sulfate concentration was consistently 1 mM lower compared to treatments set up in 2021. We hypothesize that during the additional 2 years of storage of the sediment used for setting up the slurry, additional remaining sulfate was used up in the sediment by sulfate reduction. This hypothesis was supported by high relative abundance

on RNA level of microorganisms known for sulfate reduction such as members of *Desulfocapsaceae* and *Desulfobacteraceae* (Jørgensen et al., 2019) in the incubation already at day 0 (Figure S 7). However, these taxa showed no further relative abundance **increase** of 16S rRNA or 16S rRNA gene up to day 20 when the dissolved Mn concentrations was highest (Figure S 7). Thus, they were likely not involved in the stimulated process of manganese reduction in the incubations but might have thrived on concurrent sulfate reduction or their RNA was still present from the activity during sediment storage. This hypothesis is further supported by an increase of *Desulforhopalus* (*Desulfocapsaceae*) in the initial slurry from 2023 compared to 2021 (Figure S5, S6). A possible explanation for the lack of development of free sulfide is abiotic reactions with the slurry environment. Sulfide rapidly reacts with ferrous iron, iron or manganese mineral surfaces or could also be re-oxidized (Jørgensen, 1977; Canfield et al., 1993; Michaud et al., 2020).

We did not see a similar effect in 2021 vs. 2023 treatments in dissolved manganese and ferrous iron concentration, likely because any fresh, easily microbially available manganese or iron oxides were already used up by summer 2021. Manganese reducing activity could only be stimulated by the addition of fresh manganese oxide in the form of birnessite (Figure S 3). Here, treatments from 2021 and 2023 behaved similarly if birnessite was added (every treatment with birnessite but without acetate) or not (DIC-only treatments) (Figure S 4). Therefore, we concluded that sediments still behaved similarly in terms of the investigated process of manganese reduction in 2023 compared to 2021. The lower sulfate concentration did not influence the experiment in a way that would alter the conclusion about manganese reduction being influenced by acetate as electron donor, but not thiosulfate or elemental sulfur.

Table 1: Detailed set-up of substrate addition of slurry incubation experiment. Final concentrations of substrates are given in brackets.

Substrate/ Treatment	δ-MnO_2 (10 mM)	S^0 (1 mM)	$S_2O_3^{2-}$ (1 mM)	Acetate (1 mM)	DIC (20 mM)	Date set-up	Replicates
Birnessite + acetate	x			x		03.06.21	A, B, C
Birnessite + sulfur + DIC	x	x			x	03.06.21	A, B, C
Birnessite + thiosulfate + DIC	x		x		x	03.06.21	A, B, C
Acetate	x			x		03.06.21	A, B, C
DIC					x	03.06.21	A, B
Birnessite + DIC	x				x	02.02.23	A, B, C
DIC_2023					x	02.02.23	C

3.2.1.2 Nucleic acid extraction protocol for combined DNA and RNA extraction

Combined nucleic acid extraction of DNA and RNA was performed following a modified protocol from Lueders et al. (2004). Zirconium beads (heat sterilized at 180°C for 4 h, ~0.7 g) for bead beating were filled in a sterile screw cap tube. Maximum 0.5 g beads for extraction were added. 750 µl sodium phosphate buffer (120 mM, pH 8, 112.87 mM Na_2HPO_4 and 7.12 mM NaH_2PO_4 in RNase-free water, autoclaved) and 250 µl TNS solution (500 mM Tris-HCl pH 8.0, 100 mM NaCl, 10 % SDS (w/v), adjust pH with HCl, in RNase free water, autoclaved) were added. Bead beating was performed twice for 45 s at 6.5 m/s. Samples were kept on ice between bead-beating steps and during all steps afterwards. Samples were centrifuged for 20 min at 20817 *g* at 4°C. All following centrifugation steps were performed under the same conditions with varying times. The supernatant was transferred into a new, sterile 2-ml tube and 1 volume Phenol/Chloroform/Isoamyl alcohol (25:24:1, pH 4.5) was added, gently mixed and centrifuged for 5 min. The supernatant was transferred into a new, sterile 2-ml tube and 1 volume Chloroform/Isoamyl alcohol (24:1) was added, gently mixed and centrifuged for 5 min. The supernatant was transferred into a new, sterile 2-ml tube. Roughly 2 volumes PEG (30% (w/v) polyethylene glycol 6000 in 1.6 M NaCl, in RNAse free water, autoclaved) were added up to a volume of 2 ml. Samples were incubated at 4°C for 30 min followed by centrifugation for 45 min. Liquid was carefully removed with a pipet and the remaining nucleic acid pellet was washed twice by adding 500 µl ice-cold 70% ethanol, centrifugation for 5 min and the careful removal of liquid. Nucleic acid pellets were briefly dried by placing the tubes on a normal rack with open lids for a maximum of 5 min under a fume hood. 50 µl DEPC-treated water were used for elution. Samples were checked on NanoDrop.

3.2.1.3 Sequence data analysis – ASV length distribution and rescuing fragments which exceed maximum insert size

The pipeline used to analyze the amplicon sequence data has been described in the main text; here details for retrieving long ASVs were provided.

During merging of forward and reverse reads, the paired reads are required to overlap by at least 10 bp with 0 mismatches. Merging of forward and reverse reads typically expects an overlap of 30 bp to account for variable lengths of 16S rRNA genes in the sequenced region of different microorganisms. Unmerged sequences were mapped against a reference data base and if aligning properly, were merged with their corresponding paired read and potential gaps were filled with ‘N’s. After chimera removal, the ASV length distribution was inspected manually, checking for number of ASVs and reads of different lengths. Usually, a normal distribution of ASV counts and read counts over ASV lengths is expected, with a clear peak around the expected insert size. For the datasets here, 99% of the reads and ASVs were found between 249 and 254 bp ASV length. However, there was a substantial amount of reads and ASVs at 276 or 300 bp (see Table 1). As a quality control, ASV sequences, which were outside of the ASV length range determined by the normal distribution (here 249-254 bp), were exported as

fastq file. The ~ 20 ASVs with the most read counts were compared to a public database using BLAST (see below). Most of the ASVs outside the range only had a very low percent identity hits (< 80%) and were considered to be most likely sequence artifacts, so that they were discarded. However, ASVs belonging to the peak at 276 or 300 bp length were often associated to typical sulfur oxidizing bacteria such as *Sulfurimonas* or *Arcobacter* (Han and Perner, 2015; Jurado et al., 2021). Therefore, in this sequencing pipeline it was decided to keep these long ASVs.

3.2.1.4 BLAST and dissimilatory matrix of ASVs

For taxa enriched in the incubation experiment, the ASV abundance tables were checked for the top 1-4 most abundant ASVs for the taxa *Arcobacteraceae*, *Desulfuromonas*, *Desulfuromusa* and Sva1033. The sequences were uploaded to the online NCBI BLAST tool (https://blast.ncbi.nlm.nih.gov/Blast.cgi?PROGRAM=blastn&PAGE_TYPE=BlastSearch&LINK_LOC=blasthome). The standard database "Nucleotide collection (nr/nt)" was selected, the search was optimized for somewhat similar sequences selecting the search algorithm blastn (Altschul et al., 1997) version 2.14.1+. The search was performed on the 27.11.2023. For Sva1033 ASVs, uncultured and environmental samples were excluded, for the other taxa nothing was excluded. The received results were combined manually in a table (Table S 2 - Table S 5) by selecting the best two results in terms of coverage and identity, and every isolated organism within the top 100 hits.

A dissimilarity matrix was calculated in order to compare the similarity of the *Desulfuromusa* ASV found in the incubations of this study with *in situ* sequences of Potter Cove, previous experiments from Potter Cove (Aromokeye et al., 2021) and *Desulfuromusa* type strains (Table S 6). A fasta file was created containing all sequences for the dissimilatory matrix. The file was uploaded to the NCBI BLAST tool both as query and subject sequence. The megablast algorithm was selected for alignment (Zhang et al., 2000).

ASV sequences used for BLAST and dissimilatory matrix

> sq10;size=126178;Mn-incubations;Arcobacteraceae;

TACGGAGGGTGCAAGCGTTACTCGGAATCACTGGGCGTAAAGAGAATGTAGGCG
GGTTAATAAGTCAGAAGTGAAATCCAATAGCTCAACTATTGAACTGCTTTTGAAA
CTGTTAGCCTAGAATATGGGAGAGGTAGATGGAATTTCTGGTGTAGGGGTAAAA
TCCGTAGAGATCAGAAGGAATACCGATTGCGAAGGCGATCTACTGGAACATTAT
TGACGCTGAGATTCGAAAGCGTGGGGAGCAAACA

> sq23;size=56069;Mn-incubations;Arcobacteraceae;
TACGGAGGGTGCAAGCGTTACTCGGAATCACTGGGCGTAAAGAGAATGTAGGCG
GGTTAATAAGTCAGAAGTGAAATCCAATAGCTCAACTATTGAACTGCTTTTGAAA
CTGTTAGCCTAGAATATGGGAGAGGTAGATGGAATTTCTGGTGTAGGGGTAAAA
TCCGTAGATATCAGAAGGAATACCGATTGCGAAGGCGATCTACTGGAACATTAT
TGACGCTGAGATTCGAAAGCGTGGGGAGCAAACA
> sq60;size=17637;Mn-incubations;Arcobacteraceae;
TACGGAGGGTGCAAGCGTTACTCGGAATCACTGGGCGTAAAGAGAATGTAGGCG
GGTAGATAAGTCAGAAGTGAAATCCAATAGCTCAACTATTGAACTGCTTTTGAAA
CTGTTTACCTAGAATATGGGAGAGGTAGATGGAATTTCTGGTGTAGGGGTAAAAT
CCGTAGAGATCAGAAGGAATACCGATTGCGAAGGCGATCTACTGGAACATTATT
GACGCTGAGATTCGAAAGCGTGGGGAGCAAACA
> sq4;size=337342;Mn-incubations;Desulfuromonas;
TACGGAGGGTGCAAGCGTTGTTCGGAATTATTGGGCGTAAAGCGCGTGTAGGCG
GTTTGTTAAGTCTGATGTGAAAGCCCCGGGCTCAACCTGGGAAGTGCATTGGAA
ACTGGCAAACTTGAGTACGGGAGAGGGAAGTGGAATTTCGAGTGTAGGGGTGAA
ATCCGTAGATATTCGAAGGAACACCAGTGGCGAAGGCGGCTTCCTGGACCGATA
CTGACGCTGAGACGCGAAAGCGTGGGGAGCAAACA
> sq1;size=856795;Mn-incubations;Desulfuromonas;
TACGGAGGGTGCAAGCGTTGTTCGGAATTATTGGGCGTAAAGCGCGTGTAGGCG
GTTAGTTAAGTCTGATGTGAAAGCCCCGGGCTCAACCTGGGAAGTGCATTGGAT
ACTGGCAAACTTGAGTACGGGAGAGGGAAGTGGAATTTCGAGTGTAGGGGTGAA
ATCCGTAGATATTCGAAGGAACACCAGTGGCGAAGGCGGCTTCCTGGACCGATA
CTGACGCTGAGACGCGAAAGCGTGGGGAGCAAACA
> sq18;size=80773;Mn-incubations;Desulfuromonas;
TACGGAGGGTGCAAGCGTTGTTCGGAATTATTGGGCGTAAAGCGCGTGTAGGCG
GTTAGTTAAGTCTGATGTGAAAGCCCCGGGCTCAACCTGGGAAGTGCATTGGAA
ACTGGCAAACTTGAGTACGGGAGAGGGAAGTGGAATTTCGAGTGTAGGGGTGAA
ATCCGTAGATATTCGAAGGAACACCAGTGGCGAAGGCGGCTTCCTGGACCGATA
CTGACGCTGAGACGCGAAAGCGTGGGGAGCAAACA

> sq19;size=80707;Mn-incubations;Desulfuromonas;
TACGGAGGGTGCAAGCGTTGTTCGGAATTATTGGGCGTAAAGCGCGTGTAGGCG
GTTCGTTAAGTCTGATGTGAAAGCCCCGGGCTCAACCTGGGAAGTGCATTGGATA
CTGGCAAACTTGAGTACGGGAGAGGGAAGTGGAATTTCGAGTGTAGGGGTGAAA
TCCGTAGATATTCGAAGGAACACCAGTGGCGAAGGCGGCTTCCTGGACCGATAC
TGACGCTGAGACGCGAAAGCGTGGGGAGCAAACA
> sq22;size=60363;Mn-incubations;Desulfuromusa;
TACGGAGGGTGCAAGCGTTGTTCGGAATTATTGGGCGTAAAGAGCATGTAGGCG
GACTATTAAGTCTGGTGTGAAAGCCCGGGGCTCAACCCCGGAAGTGCATTGGAT
ACTGGTAGTCTTGAGTATGGGAGAGGAAAGTGGAATTCCGAGTGTAGGAGTGAA
ATCCGTAGATATTCGGAGGAACACCAGTGGCGAAGGCGGCTTTCTGGACCAATA
CTGACGCTGAGATGCGAAAGCGTGGGGAGCGAACA
>sq402;size=15546;in-situ-PotterCove;Desulfuromusa;
TACGGAGGGTGCAAGCGTTGTTCGGAATTATTGGGCGTAAAGAGCATGTAGGCG
GTCTGTTAAGTCTGGTGTGAAAGCCCGGGGCTCAACCCCGGAAGTGCATTGGAT
ACTGGCAGACTTGAGTATGGGAGAGGAAAGCGGAATTCCGAGTGTAGGAGTGAA
ATCCGTAGATATTCGGAGGAACACCAGTGGCGAAGGCGGCTTTCTGGACCAATA
CTGACGCTGAGATGCGAAAGCGTGGGGAGCGAACA
>sq875;size=6918;in-situ-PotterCove;Desulfuromusa;
TACGGAGGGTGCAAGCGTTGTTCGGAATTATTGGGCGTAAAGAGCATGTAGGCG
GACTATTAAGTCTGGTGTGAAAGCCCGGGGCTCAACCCCGGAAGTGCATTGGAT
ACTGGTAGTCTTGAGTATGGGAGAGGAAAGTGGAATTCCGAGTGTAGGAGTGAA
ATCCGTAGATATTCGGAGGAACACCAGTGGCGAAGGCGGCTTTCTGGACCAATA
CTGACGCTGAGATGCGAAAGCGTGGGGAGCGAACA
>OTU33687944532408;Macroalgae-PotterCove;Desulfuromusa;
CAGCAGCCGCGGTAATACGGAGGGTGCAAGCGTTGTTCGGAATTATTGGGCGTA
AAGAGCATGTAGGCGGACTATTAAGTCTGGTGTGAAAGCCCGGGGCTCAACCCC
GGAAGTGCATTGGATACTGGTAGTCTTGAGTATGGGAGAGGAAAGTGGAATTCC
GAGTGTAGGAGTGAAATCCGTAGATATTCGGAGGAACACCAGTGGCGAAGGCGG
CTTTCTGGACCAATACTGACGCTG

>OTU76210975478505;Macroalgae-PotterCove;Desulfuromusa;
GGACTACGGGGGTATCTAATCCTGTTCGCTCCCCACGCTTTCGCATCTCAGCGTC
AGTATTGGTCCAGAAAGCCGCCTTCGCCACTGGTGTTCCTCCGAATATCTACGGA
TTTCACTCCTACACTCGGAATTCCACTTTCCTCTCCCATACTCAAGACTACCAGTA
TCCAATGCACTTCCGGGGTTGAGCCCCGGGCTTTCACACCAGACTTAATAGTCCG
CCTACATGCTCTTTACGCC
> sq5;size=306854;Mn-incubations;Sva1033;
TACGGAGGGTGCAAACGTTGTTCGGAATTATTGGGCGTAAAGAGCATGTAGGCG
GTCTGTCAAGTCTGATGTGAAAGCCCGGGGCTCAACCCCGGAAGTGCATTGGAA
ACTGGCAGACTTGAGTACGGGAGAGGAAAGTGGAATTTCGAGTGTAGGGGTGAA
ATCCGTAGATATTCGAAGGAACACCAGTGGCGAAGGCGGCTTTCTGGACCGATA
CTGACGCTGAGATGCGAAAGCGTGGGGAGCAAACA
> sq28;size=45573;Mn-incubations;Sva1033;
TACGGAGGGTGCAAGCGTTGTTCGGAATTATTGGGCGTAAAGAGCATGTAGGCG
GCTCGCCAAGTCTGATGTGAAAGCCCTGGGCTCAACCCAGGAAGTGCATTGGAA
ACTGGCGAACTTGAGTACGGGAGAGGAAAGTGGAATTTCGAGTGTAGGGGTGAA
ATCCGTAGATATTCGAAGGAACACCAGTGGCGAAGGCGGCTTTCTGGACCGATA
CTGACGCTGAGATGCGAAAGCGTGGGGAGCAAACA
> sq33;size=37894;Mn-incubations;Sva1033;
TACGGAGGGTGCAAGCGTTGTTCGGAATTATTGGGCGTAAAGAGCGTGTAGGCG
GCTCGCCAAGTCTGATGTGAAAGCCCTGGGCTCAACCCAGGAAGTGCATTGGAA
ACTGGCGAACTTGAGTACGGGAGAGGAAAGTGGAATTTCGAGTGTAGGGGTGAA
ATCCGTAGATATTCGAAGGAACACCAGTGGCGAAGGCGGCTTTCTGGACCGATA
CTGACGCTGAGACGCGAAAGCGTGGGGAGCAAACA

3.2.1.5 Calculation of solid phase manganese data

Solid phase manganese was extracted and quantified by Monien et al. (2014a) and the data published under doi.pangaea.de/10.1594/PANGAEA.805935 (Monien et al., 2014b). The station P01 sampled by Monien et al. (2014a) was in close proximity to STA01 sampled in this study (Figure S 9A). However, the data was published as wt.%. In order to compare the manganese content to other studies, we converted MnO (salt corrected wt.%) into MnO (µmol/cm³) by the calculations below. The used water content values were also published in Monien et al. (2014b). The density of dry sediment was assumed as 2.6 g/cm³ and the density of water as 1 g/cm³.

[1] $$MnO\ \left[\frac{mg}{g}\right] = MnO\ [wt.\%] \times 10$$

[2] $$MnO\left[\frac{\mu mol}{g\ dry\ sediment}\right] = \frac{MnO\ [\frac{mg}{g}]}{M(MnO)\ [\frac{mg}{mmol}]} \times 1000$$

[3] $$V_{dry\ sediment}\ \left[\frac{cm^3}{1\ g\ wet\ sediment}\right] = \frac{0.01 \times (100 - water\ content\ [\%])}{density_{dry\ sediment}\ \left[\frac{g}{cm^3}\right]}$$

[4] $$V_{water}\ \left[\frac{cm^3}{1\ g\ wet\ sediment}\right] = \frac{0.01 \times water\ content\ [\%]}{density_{water}\ \left[\frac{g}{cm^3}\right]}$$

[5] $$V_{dry\ sediment}\ \left[\frac{cm^3}{1\ cm^3\ wet\ sediment}\right] = \frac{V_{dry\ sediment}\left[\frac{cm^3}{1\ g\ wet\ sediment}\right] \times 1\ [cm^3\ wet\ sediment]}{V_{dry\ sediment}\left[\frac{cm^3}{1\ g\ wet\ sediment}\right] + V_{water}\left[\frac{cm^3}{1\ g\ wet\ sediment}\right]}$$

[6] $$m_{dry\ sediment}\ \left[\frac{g}{1\ cm^3\ wet\ sediment}\right] = V_{dry\ sediment}\ \left[\frac{cm^3}{1\ cm^3\ wet\ sediment}\right] \times density_{dry\ sediment}\ \left[\frac{g}{cm^3}\right]$$

[7] $$Mn\ \left[\frac{\mu mol}{cm^3}\right] = MnO\left[\frac{\mu mol}{g\ dry\ sediment}\right] \times m_{dry\ sediment}\ \left[\frac{g}{1\ cm^3\ wet\ sediment}\right]$$

The R code used for the calculations is also published in the Github repository https://github.com/Microbial-Ecophysiology/Mn-red-PotterCove.

3.2.2 Supplementary figures and tables

3.2.2.1 Supplementary figures

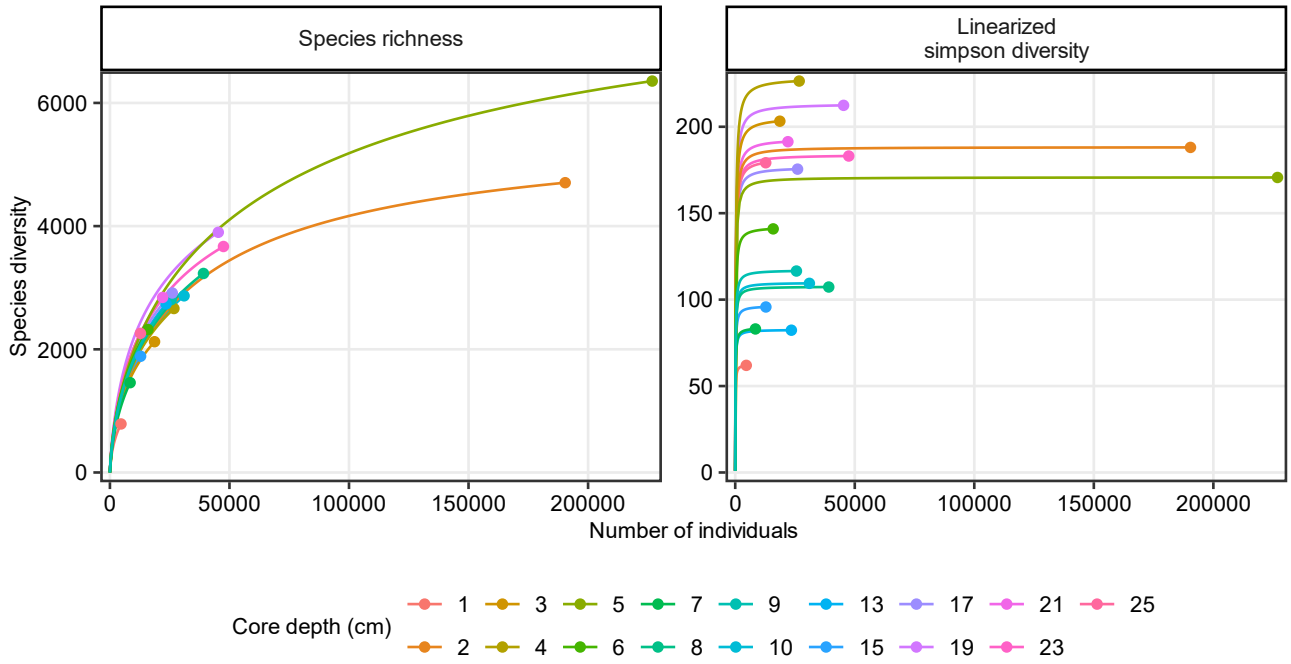

Figure S1: Rarefaction curves of 16S rRNA gene amplicon sequencing of *in situ* sediment core STA01.02.

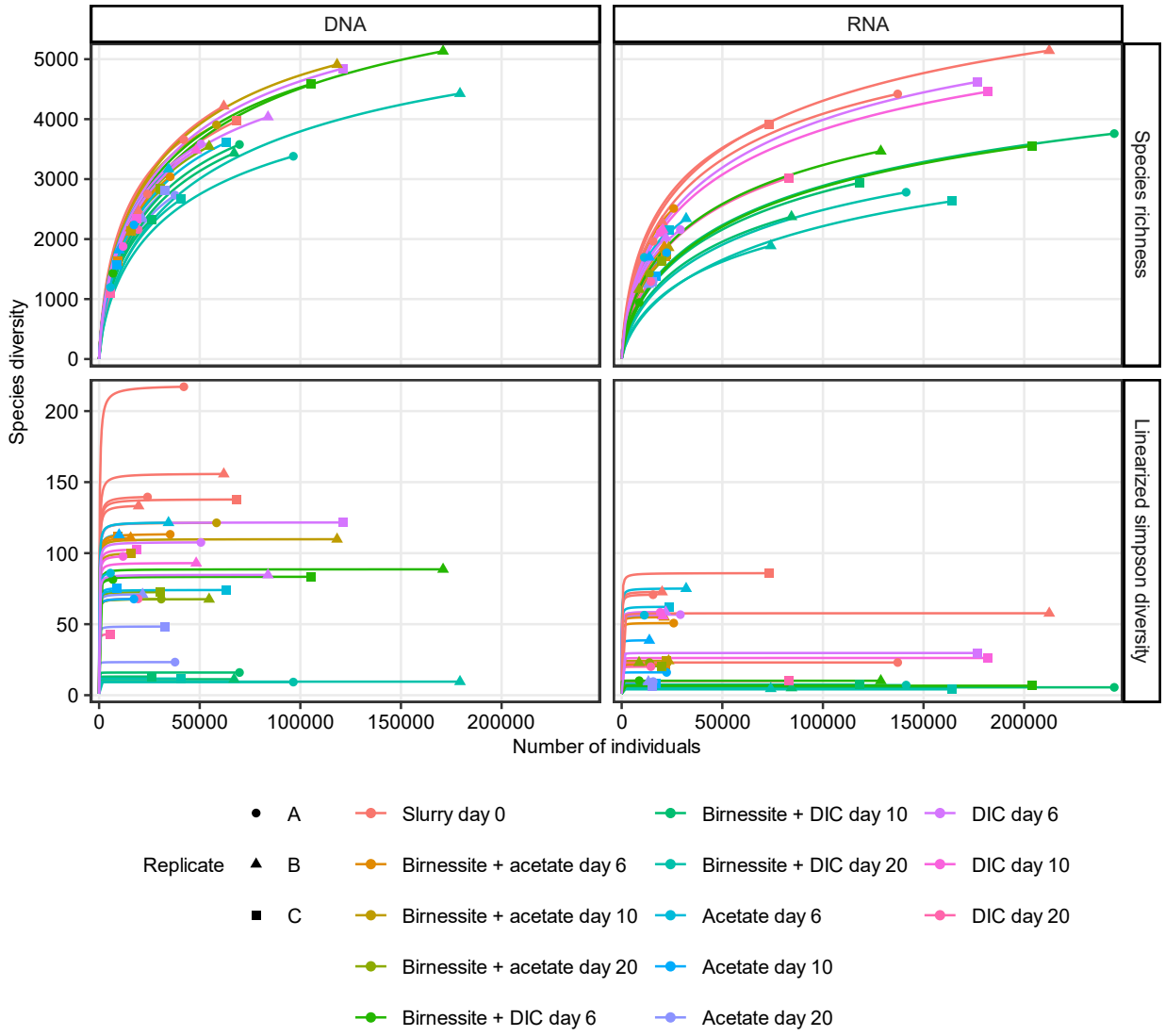

Figure S2: Rarefaction curves of 16S rRNA gene (DNA) and 16S rRNA (RNA) amplicon sequencing of incubation experiment.

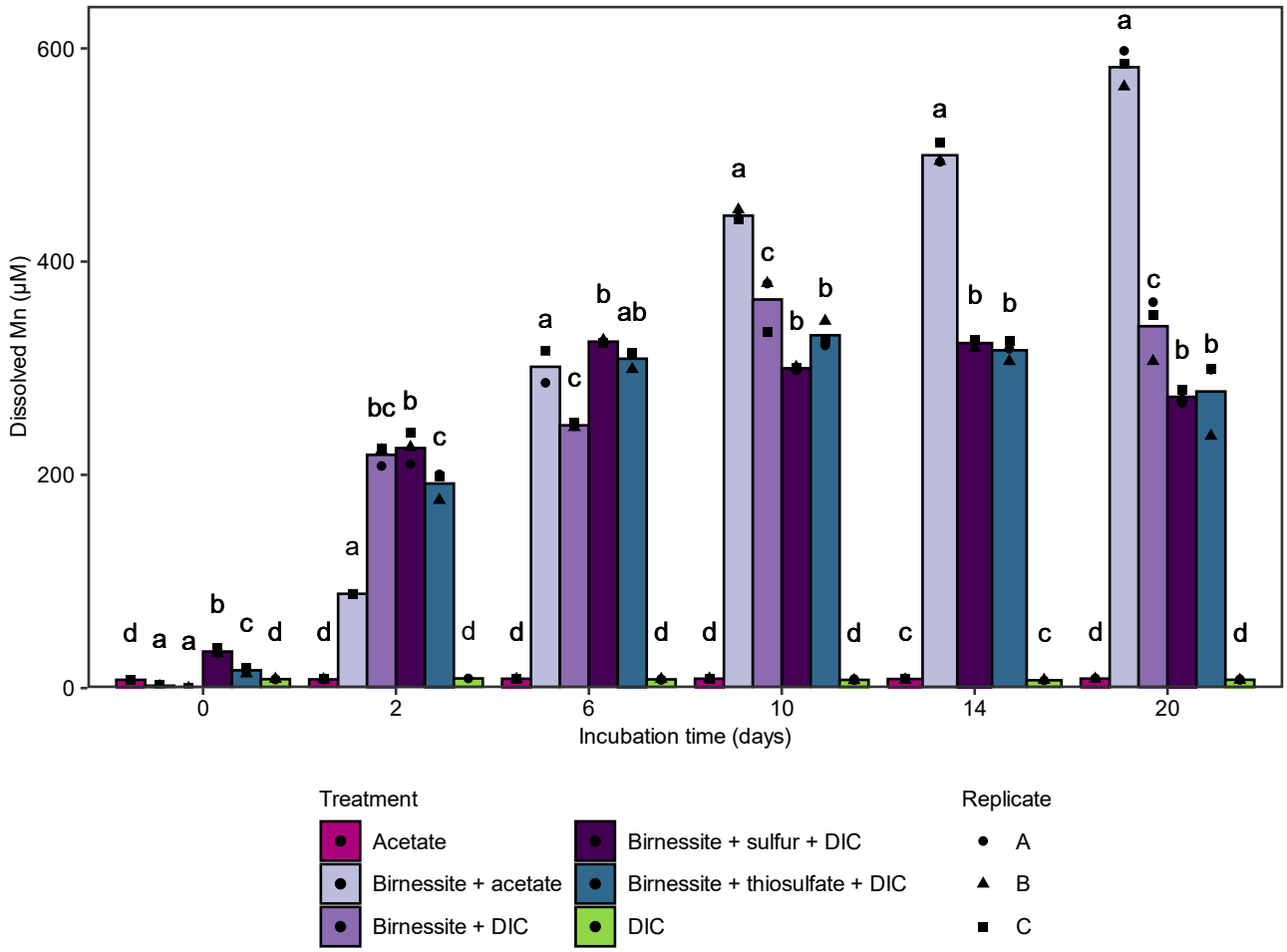

Figure S3: Concentration of dissolved Mn in slurry incubations over the incubation time. The bars represent calculated means per treatment distinguished by color, individual points are displayed on top distinguished by shape. General linear hypothesis for multiple comparisons were performed within each time point and different letters represent statistically significant differences ($p < 0.05$) between treatments.

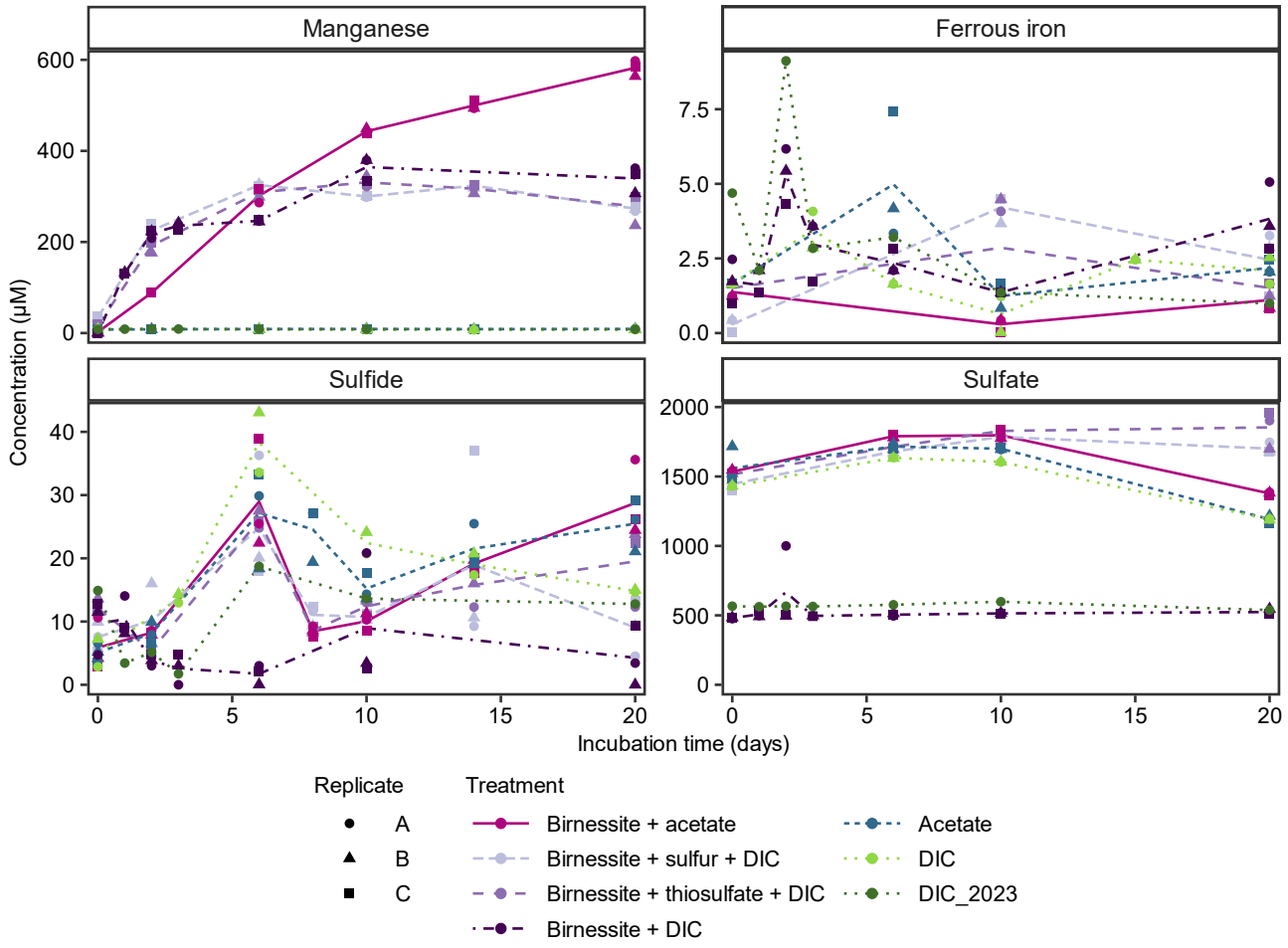

Figure S4: Geochemistry in aqueous slurry phase over time. Incubations Birnessite + DIC and DIC_2023 were run in spring 2023 while all other treatments were run in summer 2021. Likely due to longer storage, the sulfate concentration in the 2023 run treatments were lower (see text for more details).

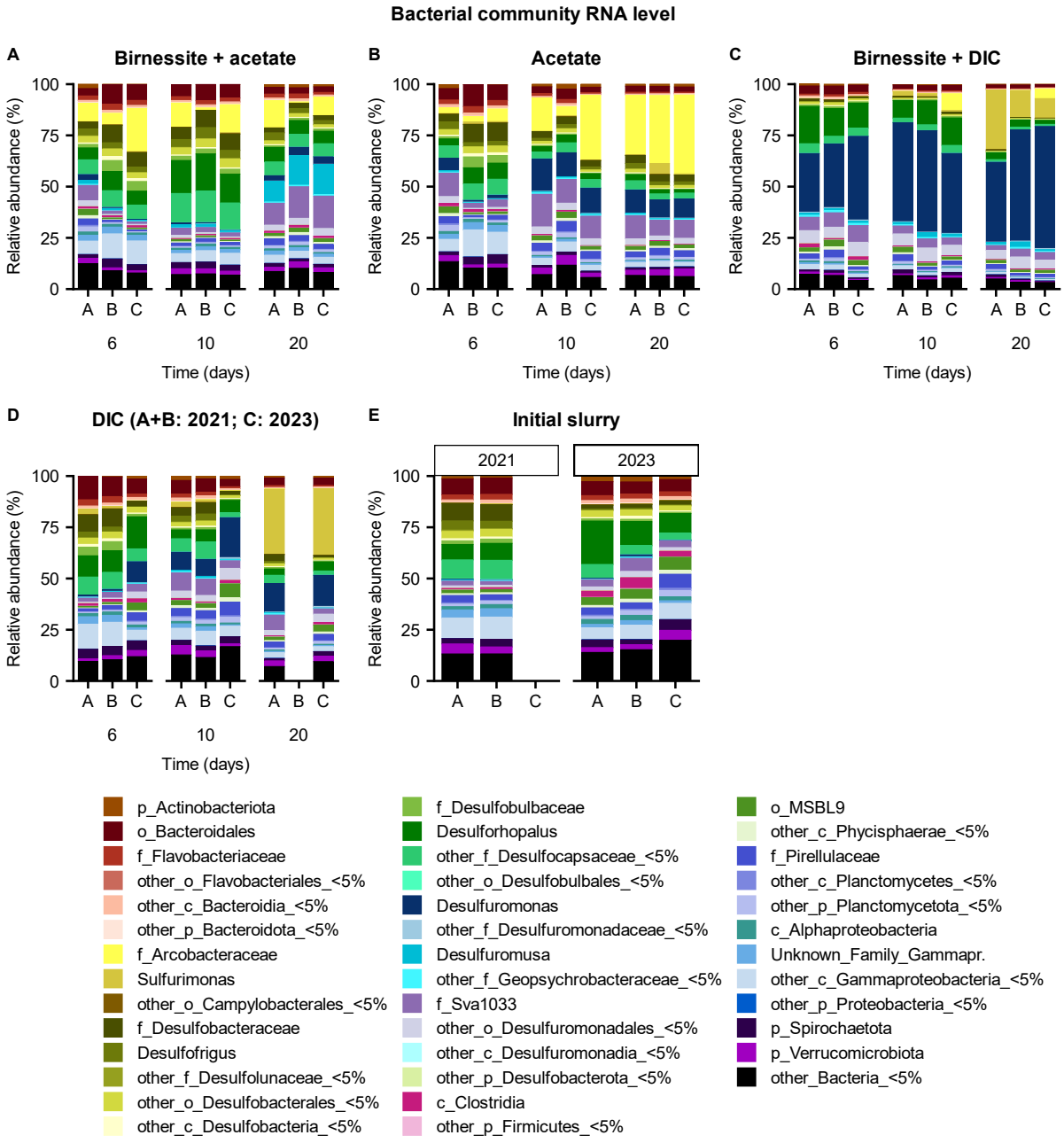

Figure S5: Bacterial 16S rRNA community of incubation experiment. Incubations (A) Birnessite + acetate and (B) Acetate were performed in 2021, incubation (C) Birnessite + DIC was performed in 2023. For both set-ups a control incubation (D) with only DIC was performed, in duplicates for 2021 (replicate A, B) and in single set-up for 2023 (replicate C). For both set-ups the initial slurry of day 0 was sequenced (E) in duplicates for 2021, in triplicates for 2023. All other treatments were performed in triplicate incubation bottles (A, B, C). Plotted is the whole community with genera above 5% relative abundance in at least one sample. If a genus was not above the threshold or not classified on this level, the next higher rank was plotted if it was above the threshold and so on.

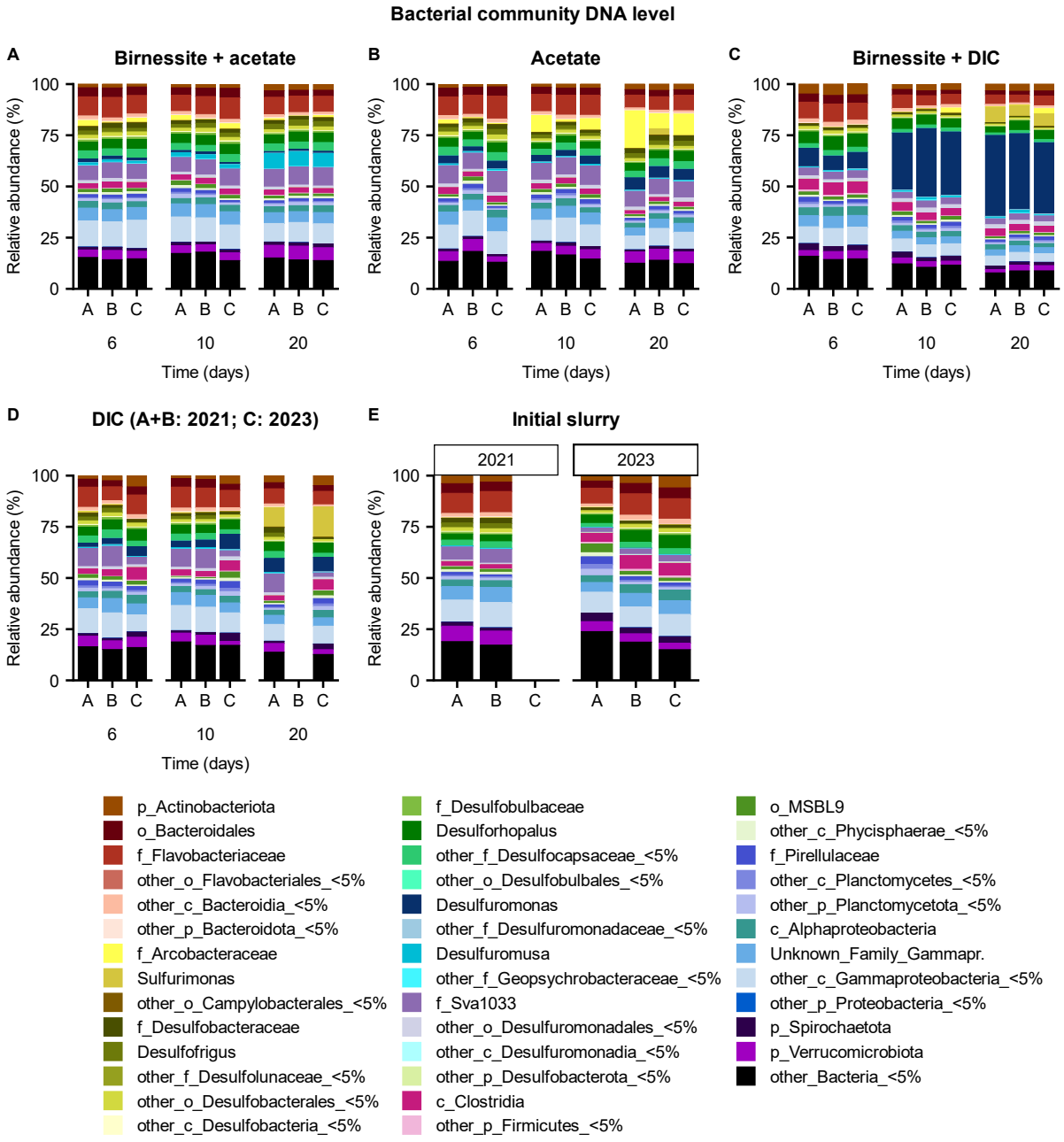

Figure S6: Bacterial 16S rRNA gene community of incubation experiment. Incubations (A) Birnessite + acetate and (B) Acetate were performed in 2021, incubation (C) Birnessite + DIC was performed in 2023. For both set-ups a control incubation (D) with only DIC was performed, in duplicates for 2021 (replicate A, B) and in single set-up for 2023 (replicate C). For both set-ups the initial slurry of day 0 was sequenced (E) in duplicates for 2021, in triplicates for 2023. All other treatments were performed in triplicate incubation bottles (A, B, C). Plotted is the whole community with genera above 5% relative abundance in at least one sample. If a genus was not above the threshold or not classified on this level, the next higher rank was plotted if it was above the threshold and so on.

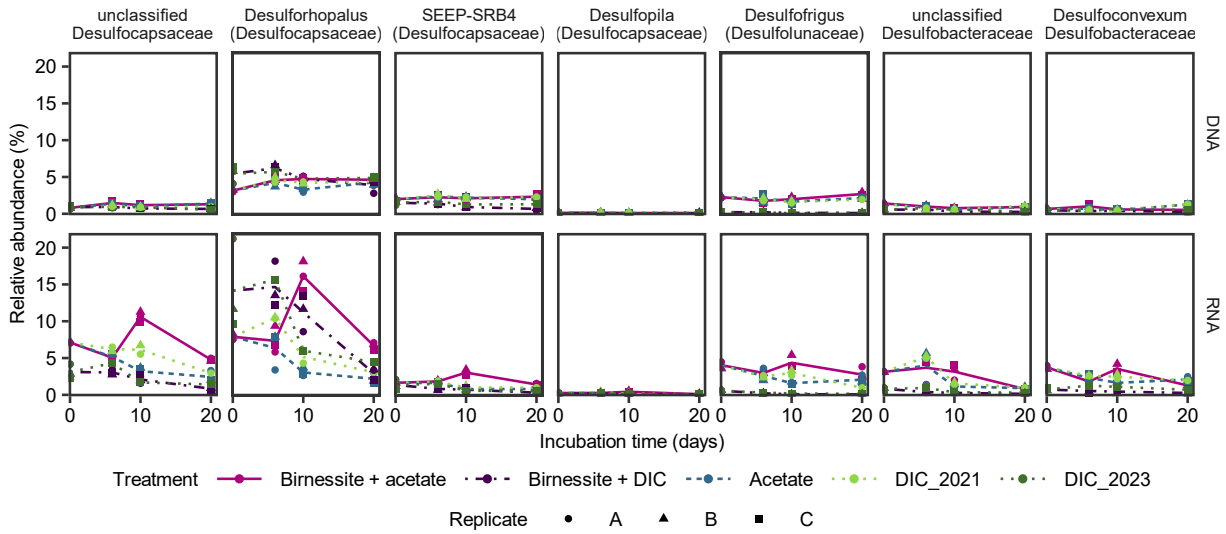

Figure S7: Relative abundance of 16S rRNA gene (top row DNA) and 16S rRNA (bottom row RNA) of selected taxa. Displayed are the same taxonomic groups plotted in Figure S 5 and Figure S 6 in a higher taxonomic resolution. Sample of day 0 was sequenced from duplicate incubation bottles for 2021 incubations while all other time points were sequenced from triplicate incubation bottles separately for each treatment. Different treatments are displayed by color and line type, and incubation triplicates by shape. The lines connect calculated means per treatment. DIC control treatments for 2021 and 2023 are plotted separately.

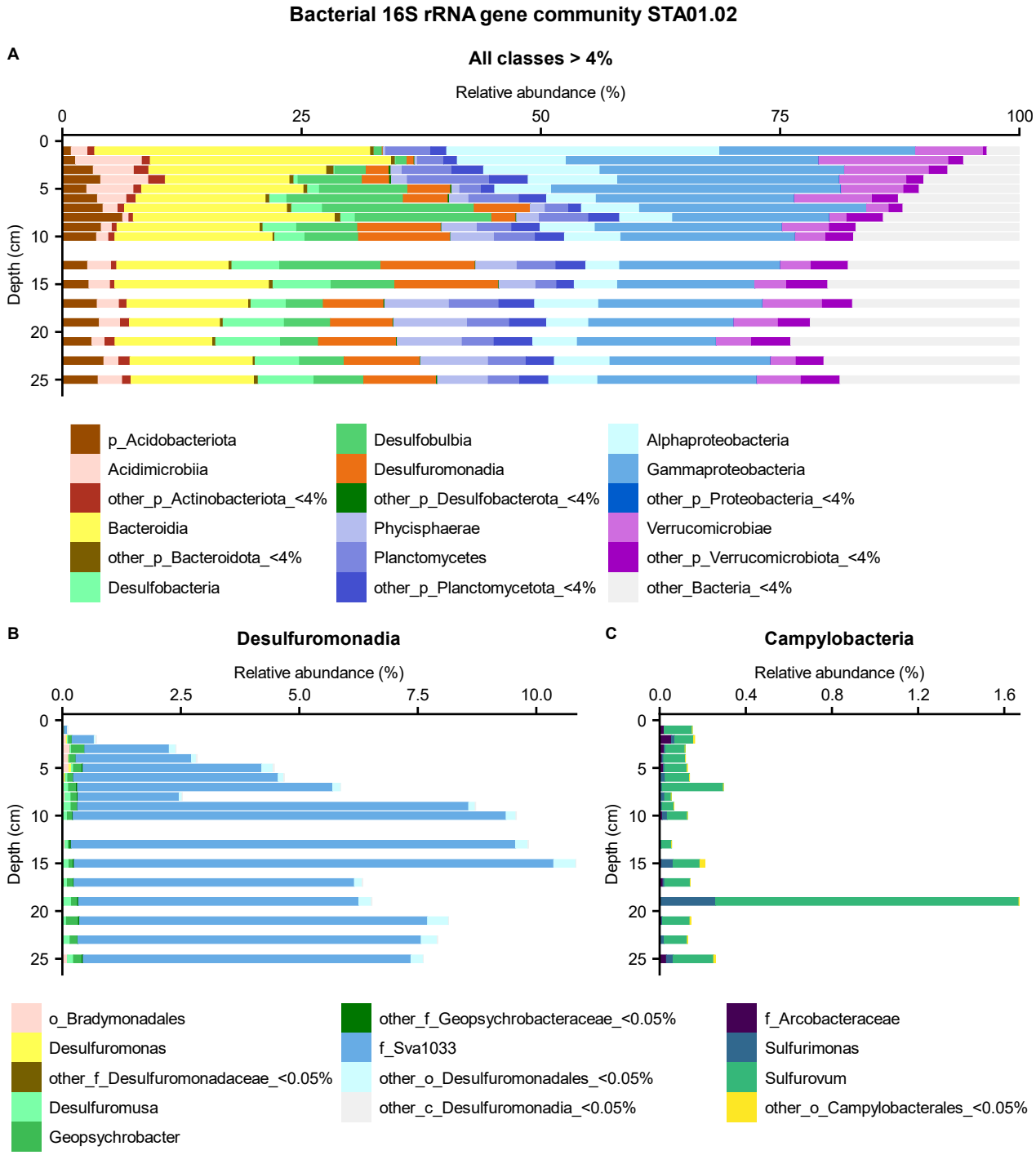

Figure S8: *In situ* bacterial community based on 16S rRNA gene sequencing of core STA01.02 used for incubation set-up. Plotted are (A) the whole community with classes above 4% relative abundance in at least one sample, (B) genera of *Desulfuromonadia* and (C) *Campylobacteria*. Note the different x-scales.

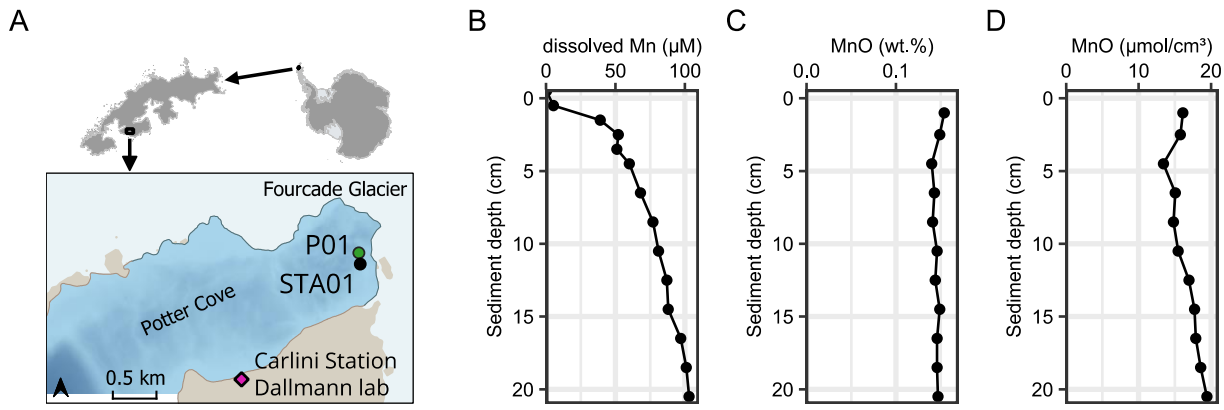

Figure S9: Manganese oxides and dissolved manganese in sediments at site PC-P01 (Monien et al., 2014a), which is near STA01 of this study (A). Data replotted from Monien et al. (2014b) dissolved Mn in pore water (B), solid phase MnO in wt.%, salt corrected (C) and recalculated into µmol/cm³, using provided water content and literature values for sediment density, for comparison with other datasets (D), see text for details. Map created with QGIS 3.34.3, bathymetry data Neder et al. (2022) updated from Jerosch et al. (2015), basemap data SCAR Antarctic Digital Database 2023, rock outcrop from Gerrish (2020) manually smoothed.

Figure S10: Photo Potter Cove Fourcade glacier 2011 with permission by M. Sierra. Location STA 01 indicated by arrow.

3.2.2.2 Supplementary tables

Table S1: Trimming parameters used during sequence analysis for samples sequenced in different libraries. Some samples were sequenced in multiple libraries and flowcells in order to retrieve sufficient reads.

Samples	Lib ID	Flowcell lane ID	Trimming		Sequence lengths kept (bp)
			R1 length (bp)	R2 length (bp)	
Incubation experiment	Lib22	HKMLNDRXY_L1	120	170	249-254, 300
	Lib23	HKMLNDRXY_L1	120	170	249-254, 300
	Lib87	H7H5VDRX5_L1	110	180	249-254, 300
	Lib87	H7JJGDRX5_L1	110	180	249-254, 300
in situ	Lib5	HHMW5DRXX_L1	90	200	249-254, 276
	Lib5	HJ72JDRXX_L2	90	200	249-254, 276
	Lib45	H7W7NDRX2_L2	120	170	249-254, 276
	Lib45	H7WKNDRX2_L2	110	180	249-254, 276

Table S2: BLAST results for most abundant ASVs of *Arcobacteraceae* in incubation experiment

Query ASV	Description	Scientific Name	Max Score	Total Score	Query Cover	E value	Per. ident	Acc. Len	Accession no.	Origin	Potential Linked Publication
sq10	Uncultured bacterium clone EB1_3cmSIP-B50 16S ribosomal RNA gene	uncultured bacterium	453	453	100%	6.E-123	100	897	MK108086.1	Ulleung Basin, East Sea	(Cho et al., 2020)
	Uncultured bacterium clone SS1_B_02_37 16S ribosomal RNA gene	uncultured bacterium	449	449	100%	3.E-121	99.6	1389	EU050947.1	Kings Bay Svalbard	
	Arcobacteraceae bacterium strain IMCC39198 16S ribosomal RNA gene	Arcobacteraceae bacterium	435	435	100%	2.E-117	98.41	1318	OQ807895.1	tidal flat sediment, South Korea Ganghwa island	
	Arcobacter sp. HL735A partial 16S rRNA gene	Arcobacter sp. HL735A	426	426	100%	9.E-115	97.61	1378	LR722870.1	coastal marine surface water, where?	
	Poseidonibacter ostreae strain SJOD-M-33 16S ribosomal RNA gene	Poseidonibacter ostreae	426	426	100%	9.E-115	97.61	1517	MN549520.1	gut of Ostrea, Seomjin River	(Baek et al., 2023)
	Arcobacter sp. strain s4j51-2 16S ribosomal RNA gene	Arcobacter sp.	426	426	100%	9.E-115	97.61	1478	MK140991.1	no info	
	Arcobacter sp. strain s4j41-3 16S ribosomal RNA gene	Arcobacter sp.	426	426	100%	9.E-115	97.61	1478	MK140989.1	no info	
	Poseidonibacter antarcticus strain SM1702 16S ribosomal RNA gene	Poseidonibacter antarcticus	426	426	100%	9.E-115	97.61	1478	MH473590.1	Antarctic intertidal sediment off Ardely Island, West Antarctica	(Guo et al., 2019)
	Halarcobacter bivalviorum strain D-5 16S ribosomal RNA gene	Halarcobacter bivalviorum	417	417	100%	5.E-112	96.81	808	MT254910.1	mussels Ebro Delta	(Miller et al., 2018)
	Arcobacter arenosus strain CAU 1517 16S ribosomal RNA gene	Arcobacter arenosus	417	417	100%	5.E-112	96.81	1482	MK280766.1	marine sediment Busan Korea	

Query ASV	Description	Scientific Name	Max Score	Total Score	Query Cover	E value	Per. ident	Acc. Len	Accession no.	Origin	Potential Linked Publication
sq23	Uncultured bacterium clone SS1_B_02_37 16S ribosomal RNA gene	uncultured bacterium	453	453	100%	7.E-123	100	1389	EU050947.1	Kings Bay Svalbard	
	Uncultured bacterium clone EB1_3cmSIP-B50 16S ribosomal RNA gene	uncultured bacterium	449	449	100%	3.E-121	99.6	897	MK108086.1	Ulleung Basin, East Sea	
	Arcobacteraceae bacterium strain IMCC39198 16S ribosomal RNA gene	Arcobacteraceae bacterium	431	431	100%	8.E-116	98.01	1318	OQ807895.1	tidal flat sediment, South Korea Ganghwa island	
	Arcobacter sp. HL735A partial 16S rRNA gene	Arcobacter sp. HL735A	422	422	100%	4.E-113	97.21	1378	LR722870.1	coastal marine surface water, where?	
	Poseidonibacter ostreae strain SJOD-M-33 16S ribosomal RNA gene	Poseidonibacter ostreae	422	422	100%	4.E-113	97.21	1517	MN549520.1	gut of Ostrea, Seomjin River	(Baek et al., 2023)
	Arcobacter sp. strain s4j51-2 16S ribosomal RNA gene	Arcobacter sp.	422	422	100%	4.E-113	97.21	1478	MK140991.1	no info	
	Arcobacter sp. strain s4j41-3 16S ribosomal RNA gene	Arcobacter sp.	422	422	100%	4.E-113	97.21	1478	MK140989.1	no info	
	Poseidonibacter antarcticus strain SM1702 16S ribosomal RNA gene	Poseidonibacter antarcticus	422	422	100%	4.E-113	97.21	1478	MH473590.1	Antarctic intertidal sediment off Ardely Island, West Antarctica	(Guo et al., 2019)
	Halarcobacter bivalviorum strain D-5 16S ribosomal RNA gene	Halarcobacter bivalviorum	413	413	100%	2.E-110	96.41	808	MT254910.1	mussels Ebro Delta	(Miller et al., 2018)
	Arcobacter arenosus strain CAU 1517 16S ribosomal RNA gene	Arcobacter arenosus	413	413	100%	2.E-110	96.41	1482	MK280766.1	marine sediment Busan Korea	

Query ASV	Description	Scientific Name	Max Score	Total Score	Query Cover	E value	Per. ident	Acc. Len	Accession no.	Origin	Potential Linked Publication
sq60	Arcobacteraceae bacterium strain IMCC39198 16S ribosomal RNA gene	Arcobacteraceae bacterium	453	453	100%	7.E-123	100	1318	OQ807895.1	tidal flat sediment, South Korea Ganghwa island	
	Uncultured Arcobacter sp. clone OTU_A7_SP1_98 16S ribosomal RNA gene	uncultured Arcobacter sp.	449	449	100%	3.E-121	99.6	696	JF928644.1	microplastic surface, coastal marine sediment	(Harrison et al., 2014)
	Arcobacter sp. HL735A partial 16S rRNA gene	Arcobacter sp. HL735A	444	444	100%	3.E-120	99.2	1378	LR722870.1	coastal marine surface water, where?	
	Poseidonibacter ostreae strain SJOD-M-33 16S ribosomal RNA gene	Poseidonibacter ostreae	444	444	100%	3.E-120	99.2	1517	MN549520.1	gut of Ostrea, Seomjin River	(Baek et al., 2023)
	Uncultured bacterium clone EB1_3cmSIP-B50 16S ribosomal RNA gene	uncultured bacterium	435	435	100%	2.E-117	98.41	897	MK108086.1	Ulleung Basin, East Sea	
	Arcobacter sp. strain s4j51-2 16S ribosomal RNA gene	Arcobacter sp.	431	431	100%	8.E-116	98.01	1478	MK140991.1	no info	
	Arcobacter sp. strain s4j41-3 16S ribosomal RNA gene	Arcobacter sp.	431	431	100%	8.E-116	98.01	1478	MK140989.1	no info	
	Poseidonibacter antarcticus strain SM1702 16S ribosomal RNA gene	Poseidonibacter antarcticus	431	431	100%	8.E-116	98.01	1478	MH473590.1	Antarctic intertidal sediment off Ardely Island, West Antarctica	(Guo et al., 2019)

Table S3: BLAST results for most abundant ASVs of *Desulfuromonas* in incubation experiment

Query ASV	Description	Scientific Name	Max Score	Total Score	Query Cover	E value	Per. ident	Acc. Len	Accession no.	Origin	Potential Linked Publication
sq4	Uncultured bacterium clone GAE_41 16S ribosomal RNA gene	uncultured bacterium	453	453	100%	7.E-123	100	799	KF623796.1	sulfur-precipitating mat, Cathedral Hill hydrothermal venting site, Guaymas Basin	(Pjevac et al., 2014)
	Desulfuromonas svalbardensis strain 112 16S ribosomal RNA	Desulfuromonas svalbardensis	453	453	100%	7.E-123	100	1516	NR_043213.1	Arctic marine sediment	(Vandieken et al., 2006)
	Desulfuromonas svalbardensis strain 60 16S ribosomal RNA gene	Desulfuromonas svalbardensis	449	449	100%	3.E-121	99.6	1516	AY835390.1	Arctic marine sediment	(Vandieken et al., 2006)
	Desulfuromonas acetoxidans strain DSM 684 16S ribosomal RNA	Desulfuromonas acetoxidans	444	444	100%	3.E-120	99.2	1558	NR_121678.1	Antarctic sediment South Orkney Islands	(Pfennig and Biebl, 1976)
	Desulfuromonas svalbardensis strain 103 16S ribosomal RNA gene	Desulfuromonas svalbardensis	444	444	100%	3.E-120	99.2	1513	AY835391.1	Arctic marine sediment	(Vandieken et al., 2006)
	Desulfuromonas svalbardensis strain 49 16S ribosomal RNA gene	Desulfuromonas svalbardensis	444	444	100%	3.E-120	99.2	1514	AY835389.1	Arctic marine sediment	(Vandieken et al., 2006)
sq1	Desulfuromonas svalbardensis strain 103 16S ribosomal RNA gene	Desulfuromonas svalbardensis	453	453	100%	7.E-123	100	1513	AY835391.1	Arctic marine sediment	(Vandieken et al., 2006)
	Desulfuromonas svalbardensis strain 49 16S ribosomal RNA gene	Desulfuromonas svalbardensis	453	453	100%	7.E-123	100	1514	AY835389.1	Arctic marine sediment	(Vandieken et al., 2006)
	Desulfuromonas svalbardensis strain 60 16S ribosomal RNA gene	Desulfuromonas svalbardensis	449	449	100%	3.E-121	99.6	1516	AY835390.1	Arctic marine sediment	(Vandieken et al., 2006)
	Uncultured bacterium clone GAE_41 16S ribosomal RNA gene	uncultured bacterium	444	444	100%	3.E-120	99.2	799	KF623796.1	sulfur-precipitating mat, Cathedral Hill hydrothermal venting site, Guaymas Basin	(Pjevac et al., 2014)
	Desulfuromonas svalbardensis strain 112 16S ribosomal RNA	Desulfuromonas svalbardensis	444	444	100%	3.E-120	99.2	1516	NR_043213.1	Arctic marine sediment	(Vandieken et al., 2006)

Query ASV	Description	Scientific Name	Max Score	Total Score	Query Cover	E value	Per. ident	Acc. Len	Accession no.	Origin	Potential Linked Publication
sq18	Desulfuromonas svalbardensis strain 60 16S ribosomal RNA gene	Desulfuromonas svalbardensis	453	453	100%	7.E-123	100	1516	AY835390.1	Arctic marine sediment	(Vandieken et al., 2006)
	Uncultured bacterium clone GAE_41 16S ribosomal RNA gene	uncultured bacterium	449	449	100%	3.E-121	99.6	799	KF623796.1	sulfur-precipitating mat, Cathedral Hill hydrothermal venting site, Guaymas Basin	(Pjevac et al., 2014)
	Desulfuromonas svalbardensis strain 112 16S ribosomal RNA	Desulfuromonas svalbardensis	449	449	100%	3.E-121	99.6	1516	NR_043213.1	Arctic marine sediment	(Vandieken et al., 2006)
	Desulfuromonas svalbardensis strain 103 16S ribosomal RNA gene	Desulfuromonas svalbardensis	449	449	100%	3.E-121	99.6	1513	AY835391.1	Arctic marine sediment	(Vandieken et al., 2006)
	Desulfuromonas svalbardensis strain 49 16S ribosomal RNA gene	Desulfuromonas svalbardensis	449	449	100%	3.E-121	99.6	1514	AY835389.1	Arctic marine sediment	(Vandieken et al., 2006)
sq19	Desulfuromonas svalbardensis strain 103 16S ribosomal RNA gene	Desulfuromonas svalbardensis	449	449	100%	3.E-121	99.6	1513	AY835391.1	Arctic marine sediment	(Vandieken et al., 2006)
	Desulfuromonas svalbardensis strain 49 16S ribosomal RNA gene	Desulfuromonas svalbardensis	449	449	100%	3.E-121	99.6	1514	AY835389.1	Arctic marine sediment	(Vandieken et al., 2006)
	Uncultured bacterium clone GAE_41 16S ribosomal RNA gene	uncultured bacterium	444	444	100%	3.E-12	99.2	799	KF623796.1	sulfur-precipitating mat, Cathedral Hill hydrothermal venting site, Guaymas Basin	(Pjevac et al., 2014)
	Desulfuromonas svalbardensis strain 112 16S ribosomal RNA	Desulfuromonas svalbardensis	444	444	100%	3.E-12	99.2	1516	NR_043213.1	Arctic marine sediment	(Vandieken et al., 2006)
	Desulfuromonas svalbardensis strain 60 16S ribosomal RNA gene	Desulfuromonas svalbardensis	444	444	100%	3.E-12	99.2	1516	AY835390.1	Arctic marine sediment	(Vandieken et al., 2006)

Table S4: BLAST results for most abundant ASVs of *Desulfuromusa* in incubation experiment

Query ASV	Description	Scientific Name	Max Score	Total Score	Query Cover	E value	Per. ident	Acc. Len	Accession no.	Origin	Potential Linked Publication
sq22	Desulfuromusa sp. Fe30-7C-S gene for 16S rRNA	Desulfuromusa sp. Fe30-7C-S	453	453	100%	7.E-123	100	1150	AB304907.1	black smoker chimney North Slope field Brothers Caldera Kermadec Arc	(Takai et al., 2009)
	Desulfuromusa bakii strain Gyprop 16S ribosomal RNA	Desulfuromusa bakii	449	449	100%	3.E-121	99.6	1473	NR_026175.1	Guayamas Basin	(Liesack and Finster, 1994)
	Bacterium N05X partial 16S rRNA gene	bacterium N05X	440	440	100%	1.E-118	98.8	692	AJ786071.1	tidal flat surface sediment, North Sea	(Köpke et al., 2005)
	Malonomonas rubra strain GraMal1 16S ribosomal RNA	Malonomonas rubra	440	440	100%	1.E-118	98.8	1525	NR_026479.1	mud Canal Grande Venice	(Dehning and Schink, 1989)

Table S5: BLAST results for most abundant ASVs of Sva1033 in incubation experiment

Query ASV	Description	Scientific Name	Max Score	Total Score	Query Cover	E value	Per. ident	Acc. Len	Accession no.	Origin	Potential Linked Publication
sq5	Deltaproteobacteria bacterium strain IMCC39542 16S ribosomal RNA gene	Deltaproteobacteria bacterium	453	453	100%	7.E-123	100	1372	OQ808218.1	tidal flat sediment, South Korea Ganghwa island	
	Deltaproteobacteria bacterium strain IMCC39489 16S ribosomal RNA gene	Deltaproteobacteria bacterium	453	453	100%	7.E-123	100	1478	OQ808176.1	tidal flat sediment, South Korea Ganghwa island	
	Pelobacter sp. 16S rRNA gene	Pelobacter sp. A3b3	453	453	100%	7.E-123	100	1551	AJ271656.1	Black Sea shelf sediments	(Thamdrup et al., 2000)
	Deltaproteobacteria bacterium strain IMCC39461 16S ribosomal RNA gene	Deltaproteobacteria bacterium	413	413	100%	2.E-110	96.41	1374	OQ808150.1	tidal flat sediment, South Korea Ganghwa island	
	Deltaproteobacteria bacterium strain IMCC39484 16S ribosomal RNA gene	Deltaproteobacteria bacterium	413	413	100%	2.E-110	96.41	1428	OQ808171.1	tidal flat sediment, South Korea Ganghwa island	
	Desulfuromonas acetoxidans strain DSM 684 16S ribosomal RNA	Desulfuromonas acetoxidans	408	408	100%	3.E-109	96.02	1558	NR_121678.1	Antarctic sediment South Orkney Islands	(Pfennig and Biebl, 1976)
	Delta proteobacterium S1 16S ribosomal RNA gene	Desulfuromusa sp. S1	408	408	100%	3.E-109	96.02	1436	AY187309.1	current-harvesting electrode in marine fuel cell	(Holmes et al., 2004)
	Delta Proteobacterium G50VI partial 16S rRNA gene	delta proteobacterium G50VI	404	404	100%	1.E-107	95.62	705	AJ786070.1	subsurface sediment tidal flat; North Sea	(Köpke et al., 2005)
	Deltaproteobacteria bacterium strain IMCC39547 16S ribosomal RNA gene	Deltaproteobacteria bacterium	399	399	100%	1.E-106	95.22	1411	OQ808222.1	tidal flat sediment, South Korea Ganghwa island	

Query ASV	Description	Scientific Name	Max Score	Total Score	Query Cover	E value	Per. ident	Acc. Len	Accession no.	Origin	Potential Linked Publication
sq28	Deltaproteobacteria bacterium strain IMCC39461 16S ribosomal RNA gene	Deltaproteobacteria bacterium	453	453	100%	7.E-123	100	1374	OQ808150.1	tidal flat sediment, South Korea Ganghwa island	
	Deltaproteobacteria bacterium strain IMCC39547 16S ribosomal RNA gene	Deltaproteobacteria bacterium	440	440	100%	1.E-118	98.8	1411	OQ808222.1	tidal flat sediment, South Korea Ganghwa island	
	Deltaproteobacteria bacterium strain IMCC39484 16S ribosomal RNA gene	Deltaproteobacteria bacterium	426	426	100%	9.E-115	97.61	1428	OQ808171.1	tidal flat sediment, South Korea Ganghwa island	
	Deltaproteobacteria bacterium strain IMCC39542 16S ribosomal RNA gene	Deltaproteobacteria bacterium	413	413	100%	2.E-110	96.41	1372	OQ808218.1	tidal flat sediment, South Korea Ganghwa island	
	Deltaproteobacteria bacterium strain IMCC39489 16S ribosomal RNA gene	Deltaproteobacteria bacterium	413	413	100%	2.E-110	96.41	1478	OQ808176.1	tidal flat sediment, South Korea Ganghwa island	
	Pelobacter sp. 16S rRNA gene	Pelobacter sp. A3b3	413	413	100%	2.E-110	96.41	1551	AJ271656.1	Black Sea shelf sediments	(Thamdrup et al., 2000)
	Delta Proteobacterium G50VI partial 16S rRNA gene	delta proteobacterium G50VI	408	408	100%	3.E-109	96.02	705	AJ786070.1	subsurface sediment tidal flat; North Sea	(Köpke et al., 2005)
	Desulfuromonas acetoxidans strain DSM 684 16S ribosomal RNA	Desulfuromonas acetoxidans	404	404	100%	1.E-107	95.62	1558	NR_121678.1	Antarctic sediment South Orkney Islands	(Pfennig and Biebl, 1976)
	Delta proteobacterium S1 16S ribosomal RNA gene	Desulfuromusa sp. S1	377	377	100%	1.E-99	93.23	1436	AY187309.1	current-harvesting electrode in marine fuel cell	(Holmes et al., 2004)

Query ASV	Description	Scientific Name	Max Score	Total Score	Query Cover	E value	Per. ident	Acc. Len	Accession no.	Origin	Potential Linked Publication
sq33	Deltaproteobacteria bacterium strain IMCC39547 16S ribosomal RNA gene	Deltaproteobacteria bacterium	449	449	100%	3.E-121	99.6	1411	OQ808222.1	tidal flat sediment, South Korea Ganghwa island	
	Deltaproteobacteria bacterium strain IMCC39461 16S ribosomal RNA gene	Deltaproteobacteria bacterium	444	444	100%	3.E-120	99.2	1374	OQ808150.1	tidal flat sediment, South Korea Ganghwa island	
	Deltaproteobacteria bacterium strain IMCC39484 16S ribosomal RNA gene	Deltaproteobacteria bacterium	435	435	100%	2.E-117	98.41	1428	OQ808171.1	tidal flat sediment, South Korea Ganghwa island	
	Delta Proteobacterium G50VI partial 16S rRNA gene	delta proteobacterium G50VI	417	417	100%	5.E-112	96.81	705	AJ786070.1	subsurface sediment tidal flat; North Sea	(Köpke et al., 2005)
	Desulfuromonas acetoxidans strain DSM 684 16S ribosomal RNA	Desulfuromonas acetoxidans	413	413	100%	2.E-110	96.41	1558	NR_121678.1	Antarctic sediment South Orkney Islands	(Pfennig and Biebl, 1976)
	Deltaproteobacteria bacterium strain IMCC39542 16S ribosomal RNA gene	Deltaproteobacteria bacterium	404	404	100%	1.E-107	95.62	1372	OQ808218.1	tidal flat sediment, South Korea Ganghwa island	
	Deltaproteobacteria bacterium strain IMCC39489 16S ribosomal RNA gene	Deltaproteobacteria bacterium	404	404	100%	1.E-107	95.62	1478	OQ808176.1	tidal flat sediment, South Korea Ganghwa island	
	Pelobacter sp. 16S rRNA gene	Pelobacter sp. A3b3	404	404	100%	1.E-107	95.62	1551	AJ271656.1	Black Sea shelf sediments	(Thamdrup et al., 2000)
	Delta proteobacterium S1 16S ribosomal RNA gene	Desulfuromusa sp. S1	368	368	100%	8.E-97	92.43	1436	AY187309.1	current-harvesting electrode in marine fuel cell	(Holmes et al., 2004)

Table S6: Sequence similarities of *Desulfuromusa* ASV from this study compared to *Desulfuromusa* type strains and ASVs and OTUs from other studies from Potter Cove. In the bottom left corner percent identity is displayed, in the top right corner the coverage in percent of the query to the sequence. The ASV sq30 from this study is outlined by thicker border lines. See text section 1.3.1 for ASV sequences of Potter Cove *in situ* (PC in situ) and OTU sequences of the SIP experiment with Potter Cove sediment (PC macroalgae (Aromokeye et al., 2021)). Accession numbers for used type strain sequences: *D.bakii* ENA X79412.1; *D.kysingii* ENA X79414.1; *D.succinoxidans* ENA X79415.1; *D.ferrireducens* ENA AY835392.1

percent identity\coverage	**D.bakii**	**D.kysingii**	**D.succinoxidans**	**D.ferrireducens**	**Mn inc sq30**	**PC in situ sq402**	**PC in situ sq875**	**PC macroalgae OTU33687944532408**	**PC macroalgae OTU76210975478505**
D.bakii	/	100	100	100	100	100	100	100	100
D.kysingii	98.89	/	100	100	100	100	100	100	100
D.succinoxidans	98.19	98.19	/	100	100	100	100	100	100
D.ferrireducens	95.45	95.55	95.9	/	100	100	100	100	100
Mn inc sq30	99.6	98.01	98.01	97.21	/	100	100	93	90
PC in situ sq402	98.01	98.41	99.2	98.41	98.01	/	100	93	90
PC in situ sq875	99.6	98.01	98.01	97.21	100	98.01	/	93	90
PC macroalgae OTU33687944532408	99.58	97.92	97.92	97.08	100	97.78	100	/	80
PC macroalgae OTU76210975478505	98.75	97.08	97.08	96.25	100	97.71	100	100	/

3.2.3 References

Altschul, S.F., Madden, T.L., Schäffer, A.A., Zhang, J., Zhang, Z., Miller, W., et al. (1997). Gapped BLAST and PSI-BLAST: a new generation of protein database search programs. Nucleic Acids Res. 25:17, 3389-3402. doi: 10.1093/nar/25.17.3389

Aromokeye, D.A., Willis-Poratti, G., Wunder, L.C., Yin, X., Wendt, J., Richter-Heitmann, T., et al. (2021). Macroalgae degradation promotes microbial iron reduction via electron shuttling in coastal Antarctic sediments. Environ. Int. 156, 106602. doi: 10.1016/j.envint.2021.106602

Baek, K., Jang, S., Chung, E.J., Ryu, S.H., and Choi, A. (2023). Poseidonibacter ostreae sp. nov., Isolated from the Gut of Ostrea from the Seomjin River. Diversity 15:8, 920.

Canfield, D.E., Thamdrup, B., and Hansen, J.W. (1993). The anaerobic degradation of organic matter in Danish coastal sediments: iron reduction, manganese reduction, and sulfate reduction. Geochim. Cosmochim. Acta 57:16, 3867-3883. doi: 10.1016/0016-7037(93)90340-3

Cho, H., Kim, B., Mok, J.S., Choi, A., Thamdrup, B., and Hyun, J.H. (2020). Acetate-utilizing microbial communities revealed by stable-isotope probing in sediment underlying the upwelling system of the Ulleung Basin, East Sea. Mar. Ecol. Prog. Ser. 634, 45-61. doi: 10.3354/meps13182

Dehning, I., and Schink, B. (1989). Malonomonas rubra gen. nov. sp. nov., a microaerotolerant anaerobic bacterium growing by decarboxylation of malonate. Arch. Microbiol. 151:5, 427-433. doi: 10.1007/BF00416602

Gerrish, L. Data from: Automatically extracted rock outcrop dataset for Antarctica (7.3). UK Polar Data Centre, Natural Environment Research Council, UK Research & Innovation. (2020) doi: 10.5285/178ec50d-1ffb-42a4-a4a3-1145419da2bb

Guo, X.-H., Wang, N., Yuan, X.-X., Zhang, X.-Y., Chen, X.-L., Zhang, Y.-Z., et al. (2019). Poseidonibacter antarcticus sp. nov., isolated from Antarctic intertidal sediment. Int. J. Syst. Evol. Microbiol. 69:9, 2717-2722. doi: 10.1099/ijsem.0.003539

Han, Y., and Perner, M. (2015). The globally widespread genus Sulfurimonas: versatile energy metabolisms and adaptations to redox clines. Front. Microbiol. 6. doi: 10.3389/fmicb.2015.00989

Harrison, J.P., Schratzberger, M., Sapp, M., and Osborn, A.M. (2014). Rapid bacterial colonization of low-density polyethylene microplastics in coastal sediment microcosms. BMC Microbiol. 14:1, 232. doi: 10.1186/s12866-014-0232-4

Holmes, D., Bond, D., O'neil, R., Reimers, C., Tender, L., and Lovley, D. (2004). Microbial communities associated with electrodes harvesting electricity from a variety of aquatic sediments. Microb. Ecol. 48:2, 178-190. doi: 10.1007/s00248-003-0004-4

Jerosch, K., Scharf, F.K., Deregibus, D., Campana, G.L., Zacher-Aued, K., Pehlke, H., et al. Data from: High resolution bathymetric compilation for Potter Cove, WAP, Antarctica, with links to data in ArcGIS format. PANGAEA. (2015) doi: 10.1594/PANGAEA.853593

Jørgensen, B.B. (1977). The sulfur cycle of a coastal marine sediment (Limfjorden, Denmark). Limnol. Oceanogr. 22:5, 814-832. doi: 10.4319/lo.1977.22.5.0814

Jørgensen, B.B., Findlay, A.J., and Pellerin, A. (2019). The biogeochemical sulfur cycle of marine sediments. Front. Microbiol. 10:849, 849. doi: 10.3389/fmicb.2019.00849

Jurado, V., D'Angeli, I., Martin-Pozas, T., Cappelletti, M., Ghezzi, D., Gonzalez-Pimentel, J.L., et al. (2021). Dominance of Arcobacter in the white filaments from the thermal sulfidic spring of Fetida Cave (Apulia, southern Italy). Sci. Total Environ. 800, 149465. doi: 10.1016/j.scitotenv.2021.149465

Köpke, B., Wilms, R., Engelen, B., Cypionka, H., and Sass, H. (2005). Microbial Diversity in Coastal Subsurface Sediments: a Cultivation Approach Using Various Electron Acceptors and Substrate Gradients. Appl. Environ. Microbiol. 71:12, 7819-7830. doi: 10.1128/AEM.71.12.7819-7830.2005

Liesack, W., and Finster, K. (1994). Phylogenetic analysis of five strains of gram-negative, obligately anaerobic, sulfur-reducing bacteria and description of *Desulfuromusa* gen. nov., including *Desulfuromusa kysingii* sp. nov., *Desulfuromusa bakii* sp. nov., and *Desulfuromusa succinoxidans* sp. nov. Int. J. Syst. Evol. Microbiol. 44:4, 753-758. doi: 10.1099/00207713-44-4-753

Lueders, T., Manefield, M., and Friedrich, M.W. (2004). Enhanced sensitivity of DNA- and rRNA-based stable isotope probing by fractionation and quantitative analysis of isopycnic centrifugation gradients. Environ. Microbiol. 6:1, 73-78. doi: 10.1046/j.1462-2920.2003.00536.x

McKenzie, R.M. (1971). The synthesis of birnessite, cryptomelane, and some other oxides and hydroxides of manganese. Mineral. Mag. 38:296, 493-502. doi: 10.1180/minmag.1971.038.296.12

Michaud, A.B., Laufer, K., Findlay, A., Pellerin, A., Antler, G., Turchyn, A.V., et al. (2020). Glacial influence on the iron and sulfur cycles in Arctic fjord sediments (Svalbard). Geochim. Cosmochim. Acta 280, 423-440. doi: 10.1016/j.gca.2019.12.033

Miller, W.G., Yee, E., and Bono, J.L. (2018). Complete Genome Sequence of the Arcobacter bivalviorum Type Strain LMG 26154. Microbiology Resource Announcements 7:12, 10.1128/mra.01076-01018. doi: 10.1128/mra.01076-18

Monien, P., Lettmann, K.A., Monien, D., Asendorf, S., Wölfl, A.-C., Lim, C.H., et al. (2014a). Redox conditions and trace metal cycling in coastal sediments from the maritime Antarctic. Geochim. Cosmochim. Acta 141, 26-44. doi: 10.1016/j.gca.2014.06.003

Monien, P., Schnetger, B., and Brumsack, H.-J. Data from: Geochemistry of sediment core PC-P01b, Potter Cove, King George Island. PANGAEA. (2014b) doi: 10.1594/PANGAEA.805935

Neder, C., Fofonova, V., Androsov, A., Kuznetsov, I., Abele, D., Falk, U., et al. (2022). Modelling suspended particulate matter dynamics at an Antarctic fjord impacted by glacier melt. J. Mar. Syst. 231, 103734. doi: 10.1016/j.jmarsys.2022.103734

Pfennig, N., and Biebl, H. (1976). *Desulfuromonas acetoxidans* gen. nov. and sp. nov., a new anaerobic, sulfur-reducing, acetate-oxidizing bacterium. Arch. Microbiol. 110:1, 3-12. doi: 10.1007/BF00416962

Pjevac, P., Kamyshny Jr, A., Dyksma, S., and Mußmann, M. (2014). Microbial consumption of zero-valence sulfur in marine benthic habitats. Environ. Microbiol. 16:11, 3416-3430. doi: 10.1111/1462-2920.12410

Takai, K., Nunoura, T., Horikoshi, K., Shibuya, T., Nakamura, K., Suzuki, Y., et al. (2009). Variability in Microbial Communities in Black Smoker Chimneys at the NW Caldera Vent Field, Brothers Volcano, Kermadec Arc. Geomicrobiol. J. 26:8, 552-569. doi: 10.1080/01490450903304949

Thamdrup, B., Rosselló-Mora, R., and Amann, R. (2000). Microbial manganese and sulfate reduction in Black Sea shelf sediments. Appl. Environ. Microbiol. 66:7, 2888-2897. doi: 10.1128/aem.66.7.2888-2897.2000

Vandieken, V., Mußmann, M., Niemann, H., and Jørgensen, B.B. (2006). *Desulfuromonas svalbardensis* sp. nov. and *Desulfuromusa ferrireducens* sp. nov., psychrophilic, Fe(III)-reducing bacteria isolated from Arctic sediments, Svalbard. Int. J. Syst. Evol. Microbiol. 56:5, 1133-1139. doi: 10.1099/ijs.0.63639-0

Zhang, Z., Schartz, S., Wagner, L., and Miller, W. (2000). A Greedy Algorithm for Aligning DNA Sequences. J. Comput. Biol. 7:1-2, 203-214. doi: 10.1089/10665270050081478

Chapter 4

Global warming facilitated environmental change effects on CO_2 releasing microbes in Antarctic sediments

David A. Aromokeye, Graciana Willis-Poratti, Lea C. Wunder, Xiuran Yin, Tim Richter-Heitmann, Carolin Otersen, Mara D. Maeke, Susann Henkel, Camila Neder, Susana Vázquez, Marcus Elvert, Walter Mac Cormack and Michael W. Friedrich

Manuscript in review at Nature Communications

Pre-print at Research Square: https://doi.org/10.21203/rs.3.rs-5441636/v1

Running title:

Acetate degradation over temperature

Contribution of the candidate to the total work

Experimental concept and design	20%
Experimental work/acquisition of experimental data	20%
Data analysis and interpretation	60%
Preparation of figures and tables	95%
Drafting of the manuscript	40%

Global warming facilitated environmental change effects on CO_2 releasing microbes in Antarctic sediments

David A. Aromokeye[1,2*], Graciana Willis-Poratti[2,3,4], Lea C. Wunder[2], Xiuran Yin[2,5], Tim Richter-Heitmann[2], Carolin Otersen[2], Mara D. Maeke[2], Susann Henkel[6], Camila Neder[7,8], Susana Vázquez[4,9], Marcus Elvert[10,11], Walter Mac Cormack[3,9] and Michael W. Friedrich[2,10*]

[1]Environment Department, The World Bank. Washington DC, United States

[2]Microbial Ecophysiology Group, Faculty of Biology/Chemistry, University of Bremen, Bremen, Germany

[3]Instituto Antártico Argentino, Buenos Aires, Argentina

[4]Consejo Nacional de Investigaciones Científicas y Técnicas (CONICET), Buenos Aires, Argentina

[5]State Key Laboratory of Marine Resource Utilization in South China Sea, Hainan University, Haikou, China

[6]Alfred Wegener Institute Helmholtz Centre for Polar and Marine Research, Bremerhaven, Germany

[7]Instituto de Diversidad y Ecología Animal (IDEA, CONICET-UNC), Argentina

[8]Ecologia Marina, Facultad de Ciencias Exactas, Físicas y Naturales, Universidad Nacional de Córdoba (UNC), Córdoba, Argentina

[9]Instituto de Nanobiotecnología UBA-CONICET, Facultad de Farmacia y Bioquímica, Universidad de Buenos Aires, CABA, Argentina

[10]MARUM – Center for Marine Environmental Sciences, University of Bremen, Bremen, Germany

[11]Faculty of Geosciences, University of Bremen, Bremen, Germany

* Corresponding author

Correspondence:

David A. Aromokeye,
Environment Department, The World Bank. 1818 H Street, NW, Washington DC, 20433, United States
Email: daromokeye@worldbank.org
Michael W. Friedrich,
Microbial Ecophysiology Group, Faculty of Biology/Chemistry, University of Bremen,
PO Box 33 04 40, D-28334 Bremen, Germany
Email: michael.friedrich@uni-bremen.de

4.1.1 Abstract

Rapid melting of the Western Antarctic Peninsula (WAP) glaciers is a compelling piece of evidence of how climate change affects our planet. This study investigated the impact of global warming-facilitated environmental change on microbial community structure and function by subjecting sediments sampled near the Fourcade Glacier in Potter Cove, WAP, to a temperature gradient and supply of metabolic nutrients relevant for the fate of carbon in marine ecosystems. We found that (i) temperature as a key environmental change driver will significantly impact microbial community structure, but ecological functions supported by fresh supply of nutrients from glacial meltwater will prevail; (ii) keystone species responsible for specialized functions are metabolically flexible, persisting from 2 °C to 25 °C; and (iii) in addition to keystone species, global warming will activate certain hitherto inactive but endogenous microorganisms in response to either changes in temperature or nutrient flux to sustain ecosystem functions. Our study presents evidence of sediment microbiome resilience in response to strong temperature or nutrient flux shifts, thereby adding another layer of evidence of nature's adaptability to global warming.

4.1.2 Introduction

The marine biosphere contributes about 45 percent (global net primary productivity = ~49 Pg C $year^{-1}$) to the amount of organic matter (OM) degraded or preserved in the earth system[1]. The terminal steps in the degradation of organic matter in marine sediments involve coupling fermentation intermediate (H_2/acetate) oxidation to manganese, Fe(III), sulfate, and CO_2 reduction. Therefore, microbes that respire sulfate and metal oxides as terminal electron acceptors are important for the final step of OM mineralization to CO_2 [2]. A previous study[3] showed that these specialists microbes represent keystone species shaping the microbial community composition and function in permanently cold sediments, irrespective of their abundance[4]. Environmental change, such as increased temperature due to global warming, might affect the rates and pathways of OM degradation, and possibly causes a shift in compositions of communities involved in determining the final fate of OM in the environment. It is therefore important to study the effects of environmental change on abundance and activity of sulfate and metal-reducing microbes to enhance knowledge of the terminal fate of organic matter. Understanding the mechanistic control of organic matter degradation and preservation during transport and burial is essential for assessing the impacts of past, present, and future climate and, thus, environmental change on the marine carbon cycle[2].

The Western Antarctic Peninsula (WAP) is one of the fastest-warming places on earth[5]. As a result, terrestrial and marine-terminating glaciers in the area have melted at unprecedented

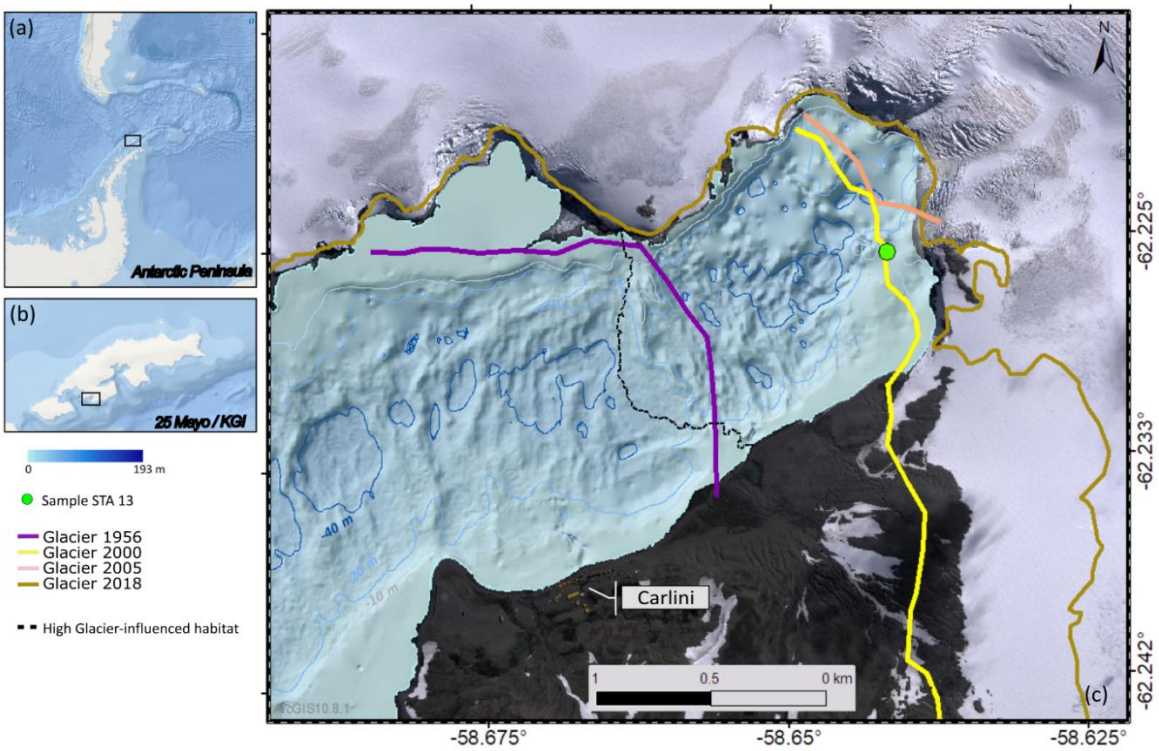

Figure 1: Spatial image showing the extent of the Fourcade Glacier retreat between 1956 - 2018. (a) West Antarctic Peninsula (b) King George Island/Isla 25 de Mayo (c) Potter Cove coastal marine ecosystem surrounded by the Fourcade Glacier. The green dot represents the exact spot the sediment samples for this study were taken. The dashed black line shows the inner cove area highly-influenced by meltwater and sediment run-off input[18,19]. Retreat lines: 1956-2005 Rückamp, et al.[7]; 2018 Deregibus, et al.[6]. Background imagery © 2014 Maxar[65].

rates. For example, the Fourcade Glacier (Fig. 1), a polythermal glacier draining into Potter Cove, King George Island/Isla 25 de Mayo, WAP, has receded by at least 1.5 km^2 between 1956 and 2018 [6], creating several newly ice-free areas and transforming from an initial tidewater glacier to land-terminating glacier[7,8]. Consequently, glacial meltwater transports easily reducible Fe (oxyhydr)oxides either directly, via subglacial groundwater discharge, or via icebergs that are known to contain reactive Fe nanoparticles, into the sediments[9]. The implications that this environmental change brought about by global warming for sediment microbial communities, especially regarding how they respond to and mineralize OM in Antarctica, is barely explored.

It is difficult to detect extreme temperature effects *in situ* on organisms and their biology within realistic climate relevant experimental timeframes (about 20-25 years[10]). Therefore, previous studies evaluating climate change effects on responses of (Ant)arctic biotic communities have either used laboratory cultures to simulate long-term climate change effects[11,12] or network analysis of clustering similarities of metagenomic data[13]. The slow growth rates of marine sediment microbes present another constraint for designing such studies[14]. This constraint has been mitigated by the development of stable isotope probing of DNA and RNA. RNA-stable isotope probing (RNA-SIP) confers the advantage that microbial physiological activity can be

studied within a relatively short incubation period under conditions that closely resemble those of the natural environment, thereby avoiding the enrichment of artificial communities that do not reflect those relevant conditions[15].

Here, we combine stable isotope and molecular biology techniques to investigate the survival strategies of microorganisms that influence the fate of organic matter in marine sediments under current global warming scenarios. We also discuss the implications of microbial adaptation to global warming for the release of CO_2 from marine sediments.

4.1.3 Results and Discussion

Sediment samples were collected from the closest possible distance to the Fourcade Glacier, and used for an analysis of how keystone microbes for the terminal mineralization of organic matter in sediments adapt to changes in temperature (5 °C, 10 °C, 15 °C, 20 °C, 25 °C and 30 °C) versus the baseline *in situ* temperature of 2 °C [16]. While some of the temperatures the sediments were subjected to for the study are experimental, the WAP remains one of the fastest warming places on earth, and continues to experience unprecedented and extreme warming events with certain areas recording up to 17.1 °C to 18.3 °C recently[17]. To avoid the enrichment of target microbes and promote the possibility of mimicking environmental conditions, sediment incubations were supplied with traceable acetate in low concentrations (500 µM ^{13}C) as carbon source. The incubations were also amended with or without fresh electron acceptors to optimize conditions for anaerobic respiration (iron and sulfate reduction). A similar set-up was used with unlabeled acetate (^{12}C) as control. The sediments were incubated in total for 17 days or less depending on rates of CO_2 release in the incubations (suppl. Fig. S1) as indicator for microbial activity, and then subjected to RNA-SIP. The results show that (i) ecological functions in the sediments prevail over the applied temperature range albeit at different rates, despite the change in active microorganisms performing those ecological functions; (ii) keystone microorganisms are more metabolically flexible than expected; certain species persisted from psychrophilic (2 °C) to mesophilic (25 °C) conditions; and (iii) as warming and glacier retreat continues to affect the nutrient balance of Antarctic sediments, microbial communities will develop adaptation strategies that may reactivate hitherto inactive or low activity microbial populations.

Temperature and nutrients have a significant effect on microbial community structure

Recession of the Fourcade Glacier results in increased glacial meltwater discharge, supplying more suspended particulate matter including iron oxides to coastal waters and underlying sediments[18], thereby changing the dynamics of carbon mineralization. Therefore, the experimental design aimed to mimic the prevailing environmental conditions in the sediments

using acetate and lepidocrocite (a low crystallinity, bioavailable γ-FeO(OH)) to stimulate iron reduction as a consequence of a fresh supply of iron oxides as nutrients to the sediments[9]. Subglacial meltwater can supply more labile iron, which is more bioavailable to microorganisms performing iron reduction with OM degradation intermediates such as acetate[9]. However, the glacier has recently started to recede to land[8], which may change the supply and characteristics of iron oxide with predicted possible decrease in suspended particulate matter[19]. This scenario potentially favors other processes such as sulfate reduction over iron reduction[20], since the sediment is replete with up to 28 mM sulfate[21]. Therefore, a separate set of experiments was set up with acetate and sulfate to mimic this scenario of reduced iron supply to the sediments. These conditions are optimal for sulfate reduction or sulfur cycling, which likely becomes more important in an emerging environmental change scenario of very low iron input due to receding glaciers to land[20]. As a baseline control for both scenarios, "acetate only" treatments were also set up. Acetate was selected as a representative volatile fatty acid intermediate of fermentation[22], which is obligatorily used by anaerobically respiring microorganisms as a terminal electron donor and is also suitable for anabolic respiration by organotrophic organisms. In all treatments across all temperatures, we obtained indicators for $^{13}CO_2$ release from microbial catabolic consumption of ^{13}C-acetate (suppl. Fig. S1) and incorporation of ^{13}C-carbon from acetate into the biomass of active organisms (suppl. Fig. S2). The experiments were stopped at different days, based on the pace of build-up of $^{13}CO_2$ in the incubations i.e., after 10 days at 2 °C and 5 °C, 11 days at 10 °C and 15 °C, 15 days at 30 °C and 17 days at 20 °C and 25 °C. Sulfide was not detected in the incubations and a minor net sulfate concentration decrease was detected, mainly between 10 °C and 20 °C (suppl. Fig. S3a). A qualitative measurement of Fe^{2+} build up in the relevant iron amended treatments was used as proxy for iron reduction rates. Iron reduction rates were optimal at 5 °C and 10 °C but decreased consistently as the temperature gradient became more mesophilic (suppl. Fig. S3b).

After sequencing 16S rRNA in the labeled and unlabeled fractions obtained from RNA-SIP experiments, distance-based redundancy analyses (dbRDA), which combines a distance matrix calculation and principal coordinate analysis, were performed on the sequence data to evaluate community composition. The results show significant influence of temperature and nutrient (sulfate and iron as electron acceptors) on microbial communities (Fig. 2; suppl. Table S1, Fig. S4). Temperature had a significant effect ($F(1,205) = 53.4$; $p < 0.001$) on the microbial community composition across all treatments (Fig. 2a). The further the experimental temperature differed from the *in-situ* temperature, the more significant was the shift in

microbial community composition across all treatments (suppl. Table S1). The addition of electron acceptors had a similar, but less pronounced significant effect (F(2,205) = 3.9; $p < 0.001$) on the microbial community compositions (Fig. 2; suppl. Table S1). The influence of electron acceptors was, however, more pronounced than temperature when comparing the communities at 2 °C and 5 °C across all treatments and within the ^{13}C-labelled treatment fractions reflecting active use of ^{13}C-acetate for anabolic function (heavy + ultra-heavy fractions; suppl. Table S1, treatment F(1,8) = 3.27; $p = 0.012$; temperature $p > 0.05$). This finding demonstrates a probable scenario *in situ*. The Northern and Northwestern Antarctic Peninsula have experienced a warming trend of 0.46 °C ± 0.96 °C per decade between 1951 and 2018 or of 3.12 °C ± 1.02 °C in total over the same period[5]. These warming rates are alarming as they represent a 2.5 times increase when compared to the rest of the world's warming rate at currently 0.18 °C to 0.19 °C per decade over the last 50-year period[23,24]. Given the current scenarios, a 3 °C warming over the next 50 – 100 years might occur in the WAP[25,26]. Our study predicts that in the likelihood of increased warming, microbial community structures

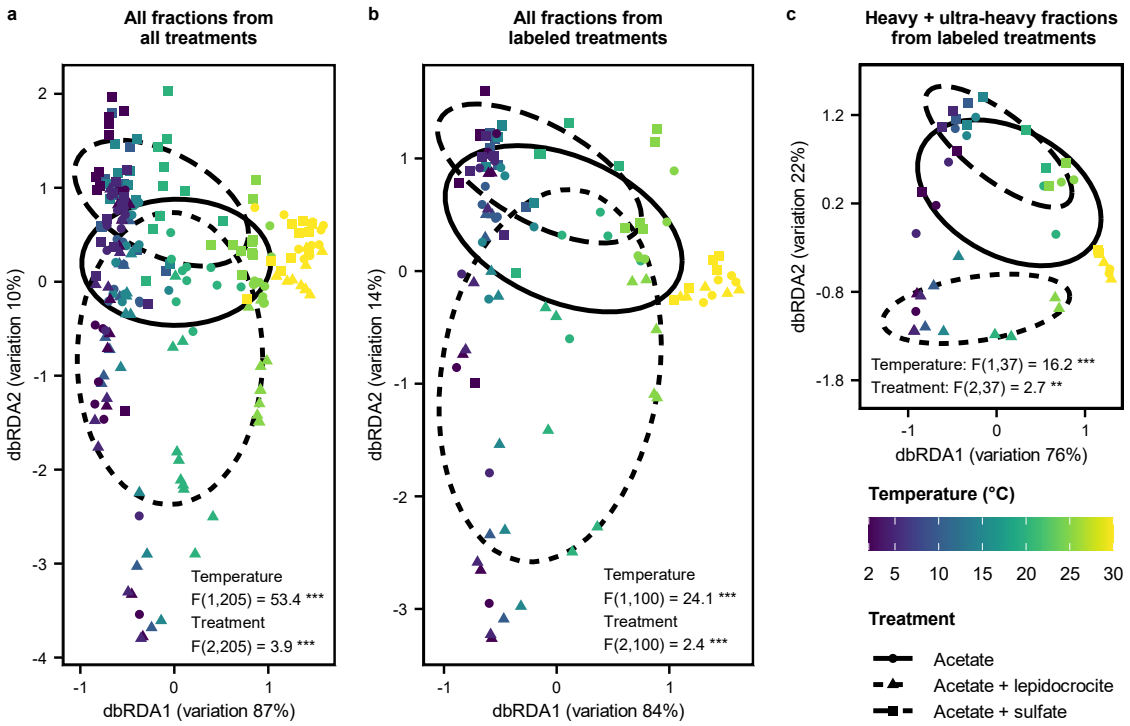

Figure 2: Temperature as the most important factor shaping the microbial community structure and function in the experiments as revealed by distance-based redundancy analyses (dbRDA) (see suppl. Table S1). dbRDA ordination plots show sample clustering for (a) all samples, (b) only samples of ^{13}C (= labeled) treatments, or (c) only ^{13}C samples of the heavy and ultra-heavy fractions in separate models. The variation contribution of dbRDA1 and dbRDA2 constraining the Bray Curtis distance matrix with the explanatory variables temperature and treatment are displayed. Sample points are distinguished by color for temperature and shape for treatment. The ellipses are drawn around the centroids of each treatment and are distinguished by line type. The model of each individual analysis was globally significant (a: F(3,205) = 20.4, $p < 0.001$; b: F(3,100) = 9.6, $p < 0.001$; c: F(3,37) = 7.2, $p < 0.001$) and each model statistics for temperature and treatment are shown. Significance levels are displayed by asterisks: ** $p < 0.01$, *** $p < 0.001$

will be impacted, thereby triggering community adaptation to sustain ecosystem function. As the warming is accompanied by a change in nutrient composition or an initial increase and subsequent cease in the supply of a particular nutrient (such as iron), microbial community composition will also change, selecting for new dominant members better suited to the shifted environmental conditions.

4.1.3.1 Iron reducers and sulfur-cycling organisms dominate the incubations

The active microorganisms identified in the microbial communities across all treatments (Fig. 3; suppl. Fig. S5-S15) use acetate for anabolic processes and are well known for their distinct ecosystem function. We classified them to sequence level (ASV: amplicon sequence variant) to define the ecology of each organism under environmental change scenarios. The dominant microorganisms included iron reducing bacteria such as (i) Sva1033 (Fig. 3a), previously identified in permanently cold sediments[3,27,28]; (ii) *Desulfuromusa* (Fig. 3b), a well-known metal oxide reducer able to switch between manganese and iron reduction[29]; (iii) unclassified *Geopsychrobacteraceae* (Fig. 3c), very close relatives of *Desulfuromusa*, which harbors many species previously described as iron reducers[30]; (iv) unclassified members of the order Desulfuromonadales (Fig. 4d, l), the overarching order of iron reducers[31]; (v) *Desulfuromonas* (Fig. 3e), a well-studied dissimilatory iron reducing genus often identified in multiple environments from temperate to permanently cold areas[29,32]; and (vi) *Trichloromonas* (formerly *Desulfuromonas*[33]; Fig. 3f) from the *Desulfuromonadaceae* family (according to used silva taxonomy release 138.1[34]) of iron reducers[35].

Other active organisms included those well studied for their role in sulfur cycling such as (i) *Sulfurimonas* (Fig. 3g)[36], (ii) *Sulfurospirillum* (Fig. 3h)[37]; (iii) *Desulfobacter* (Fig. 3i), a well-known sulfate reducer[38] that was only stimulated at 20 °C with sulfate addition; and (iv) unclassified *Arcobacteraceae* (Fig. 3j), detected only at 2 °C and known for its sulfur cycling or metal reduction capabilities[28,39]. Certain identified taxa were stimulated at specific temperatures but not previously connected to sulfur or iron metabolisms *inter alia;* (i) *Colwellia* (Fig. 3k), an extremely psychrophilic heterotrophic bacteria found in cold-polar sediments, sea ice and the deep sea[28,40] and (ii) *Hoeflea* (Fig. 3m), previously isolated from temperate halophilic marine settings[41].

The high relative abundance and capacity to thrive over a wide range of temperature suggest that iron and sulfur cycling organisms dominate and shape the ecosystem functioning of the microbial communities in our incubations (Fig. 3), as similarly found in sub-Antarctic South Georgia sediments[3]. The addition of fresh iron oxide promoted the predominance of seven different organisms (i.e., ASVs) of Sva1033 over a wide temperature range, the most of any

taxon stimulated in this study. This result suggests that Sva1033 will remain the dominant key microorganism for the terminal steps of OM degradation in Antarctic sediments if the current scenario of glacial recession continues to provide fresh iron to the sediments as part of glacial meltwater. Sva1033 was less competitive in the treatments without adding fresh iron oxide, providing the opportunity for other iron reducers such as *Desulfuromonas*, *Trichloromonas,*

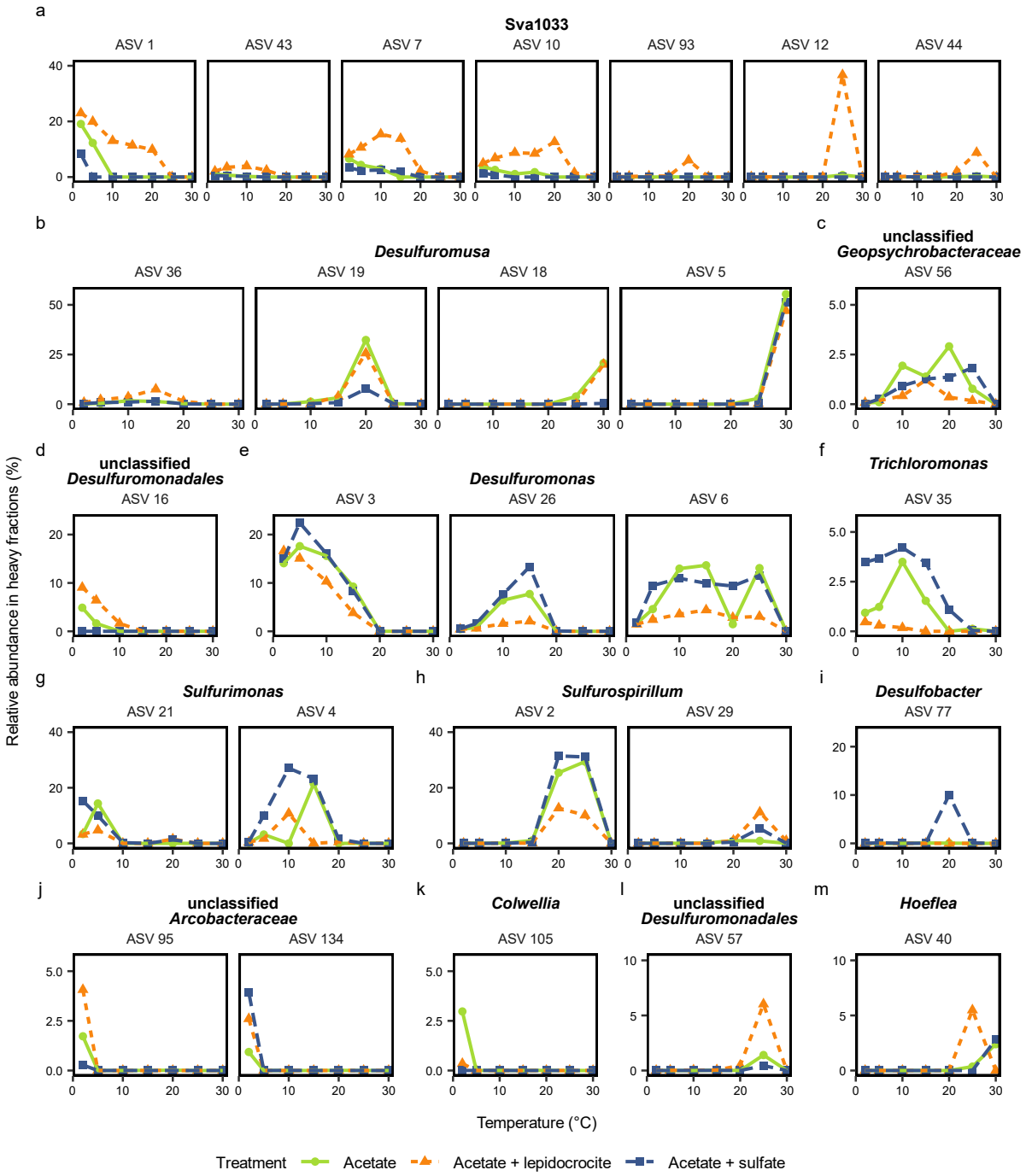

Figure 3: Taxa actively labelled over a wide temperature range in the heavy fractions of the RNA-SIP experiments. The substrate (acetate) provided is a representative intermediate of organic matter degradation. The organisms consistently enriched in the heavy fractions across all temperatures were known iron and sulfur cycling organisms. Dominant microbes were identified on sequence level (= ASV). Plotted is the average of relative abundance in heavy + ultra-heavy fractions from all ^{13}C-labeled incubation experiments. These groups include the main microbes that converted ^{13}C-acetate to form biomass thereby representing the most active members of the microbial community. Note the different y-scales.

and unclassified *Geopsychrobacteraceae* to thrive competitively in those treatments (Fig. 3). The observation that Sva1033 was not competitive when fresh iron oxide supply was limiting and giving rise to the dominance of other recognized iron reducers, especially *Desulfuromonas,* is interesting. It predicts the adaptation pattern of the microbial communities in the sediments to the recently emerging scenario of the Fourcade Glacier receding to land that may eventually result in a decrease of fresh iron supply. Nutrient supply was not the only factor determining the dominance of the activity of one microbe over the other in these experiments as temperature had a similar effect. At 30 °C, we observed that all the previous iron reducers that competed favorably and were active, regardless of the nutrient conditions in the sediments, were absent, except for *Desulfuromusa*, with two distinct organisms that were only stimulated when the conditions became mesophilic (20 °C to 30 °C). At 30 °C, these *Desulfuromusa* organisms were the only iron reducers stimulated to retain iron reducing function in these microbial communities, maintaining 50-55% relative abundance of the entire active populations in all treatments. In another study done at the same study site, *Desulfuromusa* was the main active metal oxide reducer at the *in situ* temperature of 2 °C metabolizing acetate with manganese as the preferred nutrient instead of iron oxides as electron acceptor[42]. Here, we provide further insight into the ecosystem function of *Desulfuromusa* in cold environments, that they are likely outcompeted for growth on acetate by microbes such as Sva1033 and *Desulfuromonas* when the dominant electron acceptor is iron, and the conditions are optimally psychrophilic. However, they can become competitive when manganese is the main nutrient available to support acetate consumption or the sediments are subjected to warmer environmental conditions.

The alternating abundance of *Sulfurimonas* and *Sulfurospirillum* as active populations, mainly in the sulfate amended and the control treatments was interesting (Fig. 3g, h). Both play a similar ecosystem function facilitating sulfur cycling, yet they were well differentiated in proliferation between psychrophilic and mesophilic conditions. *Sulfurimonas* was more adapted to psychrophilic metabolism and was barely detected when the temperature increased to 20 °C (Fig. 3g). *Sulfurospirillum* was detected with a high abundance as *Sulfurimonas* at low temperatures, but only at 20 °C and 25 °C (Fig. 3h). Despite the clear stimulation of microbial activity with sulfate (Fig. 3; suppl. Fig. S1, S3), the only known sulfate reducer identified amongst the active communities was *Desulfobacter* which displayed a 10% relative abundance with sulfate addition at 20 °C (Fig. 3i). Nevertheless, we tested for the prevalence of sulfate reduction activity by quantitative polymerase chain reaction (qPCR) on the messenger RNA (mRNA) transcripts using primers specific for the detection of the dissimilatory sulfite

reductase gene alpha subunit (*dsrA*) which encodes the activity for sulfite reduction to sulfide (suppl. Fig. S16). We found that up to $6x10^{12}$ copies of *dsrA* transcripts were present per ng of complementary DNA (cDNA) across treatments except at 30 °C. A qPCR targeting the bacterial 16S rRNA transcript detected up to $6x10^{15}$ copies of bacterial 16S rRNA per ng of cDNA in the same samples, thereby confirming that the lack of detection of the *dsrA* transcript at that temperature was not due to experimental detection limits. This finding clarifies that sulfate reduction is ongoing in the sediments at *in situ* conditions and up to 25 °C as part of the cryptic sulfur cycle, even as sulfate reducers are not competitive for use of acetate for biomass production. At 30 °C, the absence of sulfate reducers in the heavy fractions, and the non-detection of the *dsrA* mRNA transcript as a signature for sulfate reduction suggests sulfate reduction as a microbial process in the sediments stopped thriving.

4.1.3.2 Distinct keystone species showing metabolic flexibility from psychrophilic to mesophilic temperature

We identified five distinct keystone species – based on physiological capabilities rather than network analysis-based co-occurrence – among the specific organisms (ASVs) that adapted to the effects of increased temperature with great metabolic flexibility, transitioning from psychrophilic to mesophilic metabolism to sustain the key ecosystem function of iron reduction. These include Sva1033, *Desulfuromusa, Desulfuromonas*, an unclassified *Geopsychrobacteraceae*, and *Trichloromonas* (Fig. 3). Amongst the seven observed organisms of Sva1033 (Fig. 3a), two displayed the metabolic flexibility to survive from 2 °C to 20 °C. The first, labeled for identification purposes as ASV 1, was most active at 2 °C (23%) and remained enriched, displaying metabolic flexibility up to 20 °C (10%). ASV 10, although growing optimally at 20 °C (13%), was active down to 2 °C (5%) while ASV 43 and ASV 7, which grew optimally at 10 °C, remained psychrophilic. There were three organisms that grew only at mesophilic temperatures and were not stimulated at psychrophilic ones: ASV 12 (37% only at 25 °C), ASV 44 (9% at 25 °C) and ASV 93 (6%) only at 20 °C. Family Sva1033 was previously identified as an iron reducer only in permanently cold sediments[3,28]. The findings here suggest that there are certain Sva1033 organisms that prefer mesophilic temperatures, and that this iron reducer is metabolically more flexible than previously thought, being able to thrive from 2 °C to 25 °C in our experiments, but not thriving at 30 °C.

While one *Desulfuromusa* organism (ASV 36, Fig. 3b) was stimulated from 2 °C until 20 °C mainly in the iron amended treatment, the other three stimulated *Desulfuromusa* organisms constituted the majority (20–55%) of the active communities from 20 °C to 30 °C (Fig. 3b) but could not compete at psychrophilic conditions. Three *Desulfuromonas* organisms were

identified (Fig. 3e). Particularly ASV 6 was the most metabolically flexible organism identified from all incubations throughout the experiment. This organism was detected with 2% relative abundance at 2 °C and remained detectable up to 25 °C (13%). The other two *Desulfuromonas* organisms, ASV 26 and ASV 3, were only stimulated by psychrophilic conditions reaching up to 13-22% relative abundance. All identified *Desulfuromonas* organisms were better stimulated in the absence of fresh iron oxide supply. One organism (ASV 56) of unclassified *Geopsychrobacteraceae* (Fig. 3c) was detected at 5 °C and was stimulated more abundantly in the absence of fresh iron supply, until 25 °C. One *Trichloromonas* organism (Fig. 3f) was detected in our incubations, its growth stimulated from 2 °C to 20 °C, mainly by sulfate addition and in the control treatments.

By maintaining metabolic flexibility and surviving multiple temperature shifts, these microbes demonstrated that, despite the effect of warming on sediment communities, certain keystone species will adapt over wide temperature ranges to sustain relevant ecosystem functions supported by prevailing environmental conditions. In the case of our site, this function is the release of CO_2 driven by iron reduction as the final sink of OM degradation. The fresh supply of iron oxides from the glacial meltwater supports the activity of iron reducers, ensuring that iron reduction remains a relevant metabolism in the sediments. Therefore, iron reducers, mainly Sva1033, act as keystone species in this specific environment, adapting to increased temperature and sustaining OM degradation. However, in the event of a limited iron supply in the distant future scenario, threatening the activity of Sva1033 in the environment, other iron-reducing microorganisms will replace such ecosystem function acting as keystone species.

4.1.3.3 Implication for the fate of organic matter on an increasingly warming planet

The Antarctic Peninsula experienced an extremely warm event and record-high surface melt in February 2022 [17]. On February 7-8th, 2022, extreme record-high near-surface temperatures (13.6 °C to 13.7 °C) were recorded on King George Island/Isla 25 de Mayo, including the Potter Cove[17] where sediment near the Fourcade Glacier was sampled for our study three years earlier. Similar events occurred in Western Antarctica in February 2020, featuring an unprecedented regional temperature anomaly of + 4.5 °C during a six-day period[43]. In the face of global warming and glacier retreat, warming events will become frequent, causing increased discharge of glacial meltwater into underlying sediments. The discharge of nutrients-containing glacial meltwater from the Fourcade Glacier ice is expected to alter the physical and chemical properties of marine sediments with impact on biological communities[44], and ultimately the fate and rate of degradation of organic matter. One of such impacts is the significant change in the structure and function of microbial communities as comprehensively

demonstrated by our study. We observed that just 10 days of significant warming of 3 °C and above is sufficient to impact the microbial community structure and ecosystem function of active populations in marine sediments from the Antarctic Peninsula (Fig. 2; suppl. Table S1, Fig. S4). The detection of certain microorganisms such as *Colwellia*, *Desulfuromusa*, *Arcobacteraceae* and *Hoeflea* at specific temperature windows is a key finding from our study. It validates the age-old Baas-Becking hypothesis[45] of spatial distribution that "*everything is everywhere, but the environment selects"*. Becking alluded to the remarkable spatial distribution potential of microbes, but that only specifically adapted organisms will thrive and proliferate under specific environmental guides[46,47]. Climate change-driven warming in Antarctica will activate hitherto inactive or low-activity microbial populations as a response to changes in temperature or nutrient flux, helping microbial communities sustain ecosystem functions. For example, *Desulfuromusa* stepped up at 30 °C to ensure iron reduction ecosystem function continues in these sediments when other more successful relatives at lower temperatures could not thrive.

Our study contrasts previous observations in the water column of the Arctic Ocean where ecosystem function under warming scenarios is being performed by new species, introduced to the environment by dispersion from temperate environments[48,49]. The introduction of new better-adapted organisms to sustain ecosystem function in the Arctic Ocean is facilitated by the influence of the Atlantic waters leading to increased warming and saltiness, otherwise called Atlantification[48,50]. Our contrasting observations are in line with the geomorphology of Antarctica, given that Antarctic waters are isolated from the rest of the global oceans by the Antarctic Circumpolar Current (ACC)[51]. Besides, introduction of temperate organisms by dispersion is more likely to occur in pelagic settings than in sediments. Consequently, indigenous distinct microbial populations, instead of newly introduced microbes as reported for the Arctic, respond to warming to conserve ecosystem function in Antarctica as our study reveals. As demonstrated in Figure 3, conservation of ecosystem function is achieved either by keystone species with incredible metabolic flexibility to adapt to changes in temperature and nutrient conditions (such as Sva1033 – ASVs 1 and 10 or *Desulfuromonas* – ASVs 6 and 35) or by previously inactive species better suited to the changing environmental guides (such as *Desulfuromusa* – ASVs 5, 18, and 19).

These findings have implication for the biogeochemical cycle of elements and for the ocean's fluxes and control of CO_2 release to the atmosphere. The types of microbes our study targeted utilize iron and sulfate as electron acceptors to support their ecosystem function of mineralizing a significant portion of the organic matter in marine sediments. A global warming-induced

change in microbial community composition (Fig. 2), which could often be accompanied by the loss of certain specialist microbes or the stimulation of microbes better adapted to the environmental change (Fig. 3), will also affect the rate of CO_2 release from the sediments as simulated by the CO_2 release trajectory in our study (suppl. Fig. S1). Although the temperature ranges that we tested are largely experimental, we argue that the findings are relevant for predicting current and future impacts of climate change on organic matter degradation and associated microbial communities in both permanently cold and temperate environments.

4.1.4 Materials and Methods

4.1.4.1 Sediment sampling

Sediment samples were collected from Potter Cove close to the Fourcade Glacier during the Antarctic summer in 2019. The sediments were collected from the safest spatial distance to the Fourcade Glacier where it was still possible to sample without risk. The geochemical setting of Potter Cove and the site sampled (STA 13; S62°13'31.4"/W58°38'28.2") were previously described[9]. Because of the shallow water depth at the site (15 m), SCUBA divers from the Argentinian Diving Division could retrieve short sediment cores. The cores were immediately processed in the Dallmann laboratory (AWI- DNA/IAA cooperation) of the Argentine Carlini Station. In detail, the 29 cm core (designated as STA13-04) used for this study was sliced into 5 cm sections and stored at 2 °C in 500 mL hermetically closed Schott bottles, under N_2 headspace (99.999% purity, Linde, Germany). After three months in transit back to the laboratory in Germany under constant storage in the dark at near *in situ* conditions, the entire core was pooled to have sufficient material for incubation experiments.

4.1.4.2 Incubation experiments

To study temperature responses of respiring organisms in glacial meltwater-influenced sediments from Potter Cove, short-term incubation experiments were set up. Anoxic sediment slurries were prepared using 5 g sediment to a final volume of 30 mL (1:6 w/v) in 60 mL serum bottle with anoxic, sterile sulfate-free artificial sea water (ASW; composition [L^{-1}]: 26.4 g NaCl, 11.2 g $MgCl_2 \cdot 6\ H_2O$, 1.5 g $CaCl_2 \cdot 2\ H_2O$ and 0.7 g KCl). The ratio 1:6 w/v was used because several bottles (n = 126) were required for the study; however, the sediment available was insufficient for making slurries with larger sediment input. Slurries were made anoxic under N_2 headspace. Thereafter, 18 slurry bottles per temperature were pre-incubated at the various experimental temperatures (2 °C, 5 °C, 10 °C, 15 °C, 20 °C, 25 °C, 30 °C) for 7 days to acclimatize the sediment communities to the incubation temperatures before substrate addition. Afterward, three treatment types were prepared in biological triplicates per

temperature: I. acetate (500 µM) II. acetate and lepidocrocite (5 mM) and III. acetate and sulfate (5 mM) with either natural abundance acetate (^{12}C) or ^{13}C-labelled acetate. After substrate addition, all treatments were subsequently sampled for dissolved iron (Fe^{2+}) and sulfate measurement by collecting 1 mL slurry under anoxic conditions. Thereafter, all treatments were subjected to static incubation in the dark at the respective temperatures. The incubations were run between 10 and 17 days depending on the evolution of ^{13}C-CO_2 in the headspace of incubations at the respective temperatures (see analytical methods section).

4.1.4.3 Analytical methods

As a proxy for iron reduction in these short-term incubations, Fe^{2+} was measured at day 0 and the end time point of the incubations at the various temperatures, i.e., day 10 at both 2 °C and 5° C, day 11 at both 10 °C and 15 °C, day 15 at 30 °C and day 17 at both 20 °C and 25 °C. To arrive at a probable comparative end time point for the incubations at the various temperatures, the evolution of ^{13}C-CO_2 in the headspace of incubations was measured over time (suppl. Fig. S1). Incubations were stopped when $\delta^{13}C$-CO_2 values, expressed in per mille (‰) relative to the Vienna Peedee belemnite (VPDB), were similar at the end time points across the different temperatures. The evolution of $\delta^{13}C$-CO_2 in the headspace was measured by injecting either 100 µL or 500 µL of the gas sample into a Thermo Finnigan Trace GC ultra connected to a Finnigan MAT DELTA Plus IRMS via a Thermo Finnigan GC Combustion III interface using a chromatographic and temperature set-up as previously described[52].

Dissolved ferrous iron accumulation rates were calculated from the slope of the difference in Fe^{2+} concentrations between day 0 and the end point for each temperature. To determine Fe^{2+} concentrations, 1 ml slurry was collected into 1.5 mL reaction tubes under anoxic conditions from the respective time points using N_2 pre-flushed 1 mL syringes. Reaction tubes were centrifuged (15,300 x *g*, 5 min at 4 °C) to obtain supernatants. 100 µL of supernatant were used for dissolved Fe^{2+} measurements as previously described[53] with modifications[54]. Dissolved Fe^{2+} measurement was used as a proxy to calculate iron reduction rates because of the difficulty of detecting total Fe(II) produced in the sediment incubations due to the reaction complex of most of the produced Fe(II) with sediment carbonate system within the sediment matrix[54]. To serve as a proxy for sulfate reduction, sulfate concentrations between the start and end point of the incubations were measured as described elsewhere[3]. The slope of the sulfate concentrations was similarly used as proxy for sulfate reduction rates. Evidence for sulfate reduction via sulfide production was not obtained from all treatments, as characteristic sulfide smell was not detected during the incubations. This could be due to the abiotic reaction of produced sulfide with Fe(II) in the slurries.

4.1.4.4 RNA stable isotope probing

It is highly recommended for successful RNA-SIP density centrifugations to use between 0.5 – 1 µg RNA. This amount of RNA is difficult to obtain from marine sediment due to low biomass. Therefore, to obtain sufficient RNA input for SIP, sediment slurry was pooled from triplicates of the same treatments before nucleic acid extraction. Nucleic acids were extracted following an established protocol[55] with modifications[56]. To obtain DNA-free RNA from nucleic acids, DNA was removed using the RQ1 DNase kit (Promega, Wisconsin, USA). RNA was subjected to a 2% gel electrophoresis to ensure DNA bands were absent followed by a fluorometric quantification of RNA using the Quant-iT RiboGreen kit (Invitrogen, Thermo Fisher Scientific). Given the different RNA concentrations obtained from RNA extraction, isopycnic density centrifugation was performed on an 8-sample rotor using samples with similar RNA concentrations per run. Isopycnic density centrifugation and gradient fractionation were done following a previously described protocol[55] with modifications[56]. After gradient fractionation, RNA gradients were quantified using the Quant-iT RiboGreen kit and immediately stored at -80 °C until further processing. Subsequently, 10 of the 14 obtained fractions per sample (suppl. Fig. S2) were pooled in the following format: fraction 3 and 4 (Ultra-heavy, density: 1.806-1.832 g/ml), fraction 5 and 6 (Heavy, density: 1.797-1.820 g/ml), fraction 7 and 8 (Midpoint, density: 1.786-1.809 g/ml), fraction 9 and 10 (Light, density: 1.774-1.797 g/ml), fraction 11 and 12 (Ultra-light, density: 1.766-1.786 g/ml). To evaluate the enriched microorganisms in the different pooled fractions, reverse transcription of RNA to cDNA was performed using the GoScript reverse transcriptase kit (Promega). The resulting cDNA, derived from 5 pooled fractions per sample, with 6 samples representing the 6 treatments from each temperature, totaling in 210 cDNA samples, served as template for amplicon sequencing. Samples of the treatment with acetate and lepidocrocite at 2 °C were previously published[3] and uploaded to GenBank Short Reads Archive (SRA) under BioSample accessions SAMN16418994 to SAMN16418998 and SAMN16419009 to SAMN16419013, and were re-sequenced for this project. PCR was performed using KAPA HiFi HotStart PCR kit (KAPA Biosystems) with barcoded bacterial 16S rRNA primers (Bac515F (5′-GTGYCAGCMGCCGCGGTAA-3′)[57]; Bac805R (5′-GACTACHVGGGTATCTAATCC-3′)[58]. DNA amplification, PCR product purification and sequencing library preparation were performed as described previously[54]. Amplicon sequencing was performed by Novogene (Cambridge, UK) using a Novaseq6000 platform (2x 250 bp). Raw reads were processed with the DADA2 sequence analysis pipeline[59] as described previously[42,60]. Resulting amplicon sequence variants (ASVs) were taxonomically assigned using the SILVA database (SSU Ref

NR 99 release 138.1[34]) and sequences assigned outside Bacteria or as mitochondria or chloroplasts were removed. Sufficient sequencing depth per sample was checked by rarefaction curves as described previously[42] (suppl. Fig. S17-S19). For identifying the ASVs that were clearly labeled by ^{13}C-acetate, the following calculation was performed: the calculated average of the relative abundance per ASV in heavy and ultra-heavy fractions of ^{13}C-labeled treatments had to be higher than the calculated average in light and ultra-light fractions of ^{13}C-labeled treatments.

The transcripts of sulfate reduction marker gene subunit *dsrA,* encoding dissimilatory sulfite reductase*,* were quantified by quantitative PCR (qPCR) (primer DSR1-F+ (5′-ACSCACTGGAAGCACGGCGG-3′), DSR-R (5′-GTGGMRCCG TGCAKRTTGG-3′)[61]) in cDNA samples also used for amplicon sequencing as described previously[3]. As template, 2 µL cDNA were used and after quantification of cDNA concentration using the Quanti-it PicoGreen kit (Invitrogen, Thermo Fisher Scientific), quantified copies per ng cDNA were calculated. For samples below detection limit an additional qPCR targeting the bacterial 16S rRNA was performed (primer Bac8Fmod (5′-AGAGTTTGATYMTGGCTCAG-3′), Bac338Rmod (5′-GCWGCCWCCCGTAGGWGT3′)[3]) using a similar procedure, as described previously[3].

4.1.4.5 Statistical analysis

A distance-based redundancy analysis (dbRDA) was performed on a Bray-Curtis dissimilarity distance matrix of the bacterial 16S rRNA gene relative abundance data using treatment and incubation temperature as explanatory variables. The significance ($p < 0.05$) of the model was tested with an ANOVA like permutation test[62] (anova.cca function in vegan R package[63], version 2.6.6.1). All analyses and plots were made within the R environment[64] version 4.4.1.

4.1.5 Data availability

The raw sequence data were submitted to European Nucleotide Archive (ENA) under accession number PRJEB82428. All codes used for data analysis were submitted to the Github repository https://github.com/Microbial-Ecophysiology/tempSIP-PotterCove.

4.1.6 Acknowledgments

The authors thank the Instituto Antártico Argentino (IAA) – Dirección Nacional del Antártico (DNA), the crew at Carlini Station, Consejo Nacional de Investigaciones Científicas y Técnicas (CONICET-Res. N◦ 4252/116), and the Alfred Wegener Institute Helmholtz Centre for Polar and Marine Research (AWI) for logistics support during the field campaign to the King George Island/Isla 25 de Mayo in the Antarctic Peninsula. The authors acknowledge Principal Corporal Javier Alvarez from the crew at Carlini Station and Argentinian Navy (Armada Argentina) and the Argentinian Army (Ejército Argentino) divers of CAV 2018-2019 for their support during the sampling at Potter Cove.

4.1.7 Author Contributions

DAA, MWF and GWP designed the study. DAA and GWP conducted the field sampling. DAA, GWP, LCW and CO performed the lab experiments. DAA, LCW, XY, GWP, and TRH analyzed the data. LCW and CN produced the figures. GWP, WMC, SV, SH and MWF facilitated the field trip to the WAP. MWF secured funding for the research. DAA led the study and wrote the manuscript with LCW. All co-authors contributed to the manuscript.

4.1.8 Competing Interests

The authors declare no competing interests.

4.1.9 Funding

This work was supported by the Deutsche Forschungsgemeinschaft (DFG) in the framework of the priority program “Antarctic Research with Comparative Investigation in Arctic Ice Areas” SPP 1158 in the project “Environmental Controls of Iron-Reducing Microorganisms in Antarctic marine sediments (ECIMAS)” (project number 404648014) and the University of Bremen. Graciana Willis-Poratti was funded by individual fellowships supported by the Deutscher Akademischer Austauschdienst [German Academic Exchange Service (DAAD)]: grant numbers 57440915, 57507442 and 57681226.

4.1.10 References

1 Eglinton, T. & Repeta, D. *Organic matter in the contemporary ocean* in *Treatise On Geochemistry* Vol. 6 (eds HD Holland & KK Turekian) 145-180 (Elsevier, 2004).

2 Arndt, S. & LaRowe, D. E. *Organic matter degradation and preservation* in *Encyclopedia Of Geochemistry: A Comprehensive Reference Source On The Chemistry Of The Earth* (ed William M. White) 1-6 (Springer International Publishing, 2017). doi:10.1007/978-3-319-39193-9_184-1.

3 Wunder, L. C. *et al.* Iron and sulfate reduction structure microbial communities in (sub-)Antarctic sediments. *ISME J.* **15**, 3587-3604, doi:10.1038/s41396-021-01014-9 (2021).

4 Banerjee, S., Schlaeppi, K. & van der Heijden, M. G. A. Keystone taxa as drivers of microbiome structure and functioning. *Nat. Rev. Microbiol.* **16**, 567-576, doi:10.1038/s41579-018-0024-1 (2018).

5 Jones, M. E. *et al.* Sixty years of widespread warming in the southern middle and high latitudes (1957–2016). *J. Clim.* **32**, 6875-6898, doi:10.1175/JCLI-D-18-0565.1 (2019).

6 Deregibus, D. *et al.* Potential macroalgal expansion and blue carbon gains with northern Antarctic Peninsula glacial retreat. *Mar. Environ. Res.* **189**, 106056, doi:10.1016/j.marenvres.2023.106056 (2023).

7 Rückamp, M., Braun, M., Suckro, S. & Blindow, N. Observed glacial changes on the King George Island ice cap, Antarctica, in the last decade. *Global Planet. Change* **79**, 99-109, doi:10.1016/j.gloplacha.2011.06.009 (2011).

8 Meredith, M. P. *et al.* Anatomy of a glacial meltwater discharge event in an Antarctic cove. *Philos. Trans. Royal Soc. A* **376**, 20170163, doi:10.1098/rsta.2017.0163 (2018).

9 Henkel, S., Kasten, S., Hartmann, J. F., Silva-Busso, A. & Staubwasser, M. Iron cycling and stable Fe isotope fractionation in Antarctic shelf sediments, King George Island. *Geochim. Cosmochim. Acta* **237**, 320-338, doi:10.1016/j.gca.2018.06.042 (2018).

10 IPCC. *Global Warming of 1.5°C. An IPCC Special Report on the impacts of global warming of 1.5°C above pre-industrial levels and related global greenhouse gas emission pathways, in the context of strengthening the global response to the threat of climate change, sustainable development, and efforts to eradicate poverty*. (eds V. Masson-Delmotte *et al.*), 616 pp. (Cambridge University Press, Cambridge, UK and New York, NY, US, 2018). doi:10.1017/9781009157940.

11 Boyd, P. W. *et al.* Physiological responses of a Southern Ocean diatom to complex future ocean conditions. *Nat. Clim. Chang.* **6**, 207-213, doi:10.1038/nclimate2811 (2016).

12 Kling, J. D. *et al.* Dual thermal ecotypes coexist within a nearly genetically identical population of the unicellular marine cyanobacterium *Synechococcus*. *Proc. Natl. Acad. Sci. USA* **120**, e2315701120, doi:10.1073/pnas.2315701120 (2023).

13 Sun, J., Zhou, H., Cheng, H., Chen, Z. & Wang, Y. Bacterial abundant taxa exhibit stronger environmental adaption than rare taxa in the Arctic Ocean sediments. *Mar. Environ. Res.* **199**, 106624, doi:10.1016/j.marenvres.2024.106624 (2024).

14 Jørgensen, B. B. & Marshall, I. P. G. Slow microbial life in the seabed. *Annu. Rev. Mar. Sci.* **8**, 311-332, doi:10.1146/annurev-marine-010814-015535 (2016).

15 Dumont, M. G. & Murrell, J. C. Stable isotope probing — linking microbial identity to function. *Nat. Rev. Microbiol.* **3**, 499-504, doi:10.1038/nrmicro1162 (2005).

16 Braeckman, U. *et al.* Degradation of macroalgal detritus in shallow coastal Antarctic sediments. *Limnol. Oceanogr.* **64**, 1423-1441, doi:10.1002/lno.11125 (2019).

17 Gorodetskaya, I. V. *et al.* Record-high Antarctic Peninsula temperatures and surface melt in February 2022: A compound event with an intense atmospheric river. *npj Clim. Atmos. Sci.* **6**, 202, doi:10.1038/s41612-023-00529-6 (2023).

18 Monien, D. *et al.* Meltwater as a source of potentially bioavailable iron to Antarctica waters. *Antarct. Sci.* **29**, 277-291, doi:10.1017/S095410201600064X (2017).

19 Neder, C. *et al.* Modelling suspended particulate matter dynamics at an Antarctic fjord impacted by glacier melt. *J. Mar. Syst.* **231**, 103734, doi:10.1016/j.jmarsys.2022.103734 (2022).

20 Michaud, A. B. *et al.* Glacial influence on the iron and sulfur cycles in Arctic fjord sediments (Svalbard). *Geochim. Cosmochim. Acta* **280**, 423-440, doi:10.1016/j.gca.2019.12.033 (2020).

21 Monien, P. *et al.* Redox conditions and trace metal cycling in coastal sediments from the maritime Antarctic. *Geochim. Cosmochim. Acta* **141**, 26-44, doi:10.1016/j.gca.2014.06.003 (2014).

22 Glombitza, C. *et al.* Formate, acetate, and propionate as substrates for sulfate reduction in sub-arctic sediments of Southwest Greenland. *Front. Microbiol.* **6**, doi:10.3389/fmicb.2015.00846 (2015).

23 Samset, B. H. *et al.* Earlier emergence of a temperature response to mitigation by filtering annual variability. *Nat. Commun.* **13**, 1578, doi:10.1038/s41467-022-29247-y (2022).

24 Samset, B. H. *et al.* Steady global surface warming from 1973 to 2022 but increased warming rate after 1990. *Communications Earth & Environment* **4**, 400, doi:10.1038/s43247-023-01061-4 (2023).

25 Bopp, L. *et al.* Multiple stressors of ocean ecosystems in the 21st century: Projections with CMIP5 models. *Biogeosciences* **10**, 6225-6245, doi:10.5194/bg-10-6225-2013 (2013).

26 Moore, J. K., Lindsay, K., Doney, S. C., Long, M. C. & Misumi, K. Marine ecosystem dynamics and biogeochemical cycling in the Community Earth System Model [CESM1(BGC)]: Comparison of the 1990s with the 2090s under the RCP4.5 and RCP8.5 scenarios. *J. Clim.* **26**, 9291-9312, doi:10.1175/JCLI-D-12-00566.1 (2013).

27 Ravenschlag, K., Sahm, K., Pernthaler, J. & Amann, R. High bacterial diversity in permanently cold marine sediments. *Appl. Environ. Microbiol.* **65**, 3982-3989 (1999).

28 Aromokeye, D. A. *et al.* Macroalgae degradation promotes microbial iron reduction via electron shuttling in coastal Antarctic sediments. *Environ. Int.* **156**, 106602, doi:10.1016/j.envint.2021.106602 (2021).

29 Vandieken, V., Mußmann, M., Niemann, H. & Jørgensen, B. B. *Desulfuromonas svalbardensis* sp. nov. and *Desulfuromusa ferrireducens* sp. nov., psychrophilic, Fe(III)-reducing bacteria isolated from Arctic sediments, Svalbard. *Int. J. Syst. Evol. Microbiol.* **56**, 1133-1139, doi:10.1099/ijs.0.63639-0 (2006).

30 Holmes, D. E., Nicoll, J. S., Bond, D. R. & Lovley, D. R. Potential role of a novel psychrotolerant member of the family *Geobacteraceae, Geopsychrobacter electrodiphilus* gen. nov., sp. nov., in electricity production by a marine sediment fuel cell. *Appl. Environ. Microbiol.* **70**, 6023-6030, doi:10.1128/aem.70.10.6023-6030.2004 (2004).

31 Lovley, D. R. *Dissimilatory Fe(III)- and Mn(IV)-reducing prokaryotes* in *The Prokaryotes: Prokaryotic Physiology And Biochemistry* (eds Eugene Rosenberg *et al.*) 287-308 (Springer Berlin Heidelberg, 2013). doi:10.1007/978-3-642-30141-4_69.

32 Reyes, C. *et al.* Potentially active iron, sulfur, and sulfate reducing bacteria in Skagerrak and Bothnian Bay sediments. *Geomicrobiol. J.* **34**, 840-850, doi:10.1080/01490451.2017.1281360 (2017).

33 Waite, D. W. *et al.* Proposal to reclassify the proteobacterial classes *Deltaproteobacteria* and *Oligoflexia*, and the phylum *Thermodesulfobacteria* into four phyla reflecting major functional capabilities. *Int. J. Syst. Evol. Microbiol.* **70**, 5972-6016, doi:10.1099/ijsem.0.004213 (2020).

34 Quast, C. *et al.* The SILVA ribosomal RNA gene database project: improved data processing and web-based tools. *Nucleic Acids Res.* **41**, D590-D596, doi:10.1093/nar/gks1219 (2012).

35 Wang, N. *et al.* Distinguishing anaerobic digestion from electrochemical anaerobic digestion: Metabolic pathways and the role of the microbial community. *Chemosphere* **326**, 138492, doi:10.1016/j.chemosphere.2023.138492 (2023).

36 Han, Y. & Perner, M. The globally widespread genus *Sulfurimonas*: versatile energy metabolisms and adaptations to redox clines. *Front. Microbiol.* **6**, doi:10.3389/fmicb.2015.00989 (2015).

37 Campbell, B. J., Engel, A. S., Porter, M. L. & Takai, K. The versatile ε-proteobacteria: key players in sulphidic habitats. *Nat. Rev. Microbiol.* **4**, 458-468, doi:10.1038/nrmicro1414 (2006).

38 Rabus, R. *et al. Chapter two - a post-genomic view of the ecophysiology, catabolism and biotechnological relevance of sulphate-reducing prokaryotes* in *Adv. Microb. Physiol.* Vol. 66 (ed Robert K. Poole) 55-321 (Academic Press, 2015). doi:10.1016/bs.ampbs.2015.05.002.

39 Vandieken, V. *et al.* Three manganese oxide-rich marine sediments harbor similar communities of acetate-oxidizing manganese-reducing bacteria. *ISME J.* **6**, 2078-2090, doi:10.1038/ismej.2012.41 (2012).

40 Czajka, J. J. *et al.* Model metabolic strategy for heterotrophic bacteria in the cold ocean based on *Colwellia psychrerythraea* 34H. *Proc. Natl. Acad. Sci. USA* **115**, 12507-12512, doi:10.1073/pnas.1807804115 (2018).

41 Jung, M.-Y. *et al. Hoeflea halophila* sp. nov., a novel bacterium isolated from marine sediment of the East Sea, Korea. *Antonie Van Leeuwenhoek* **103**, 971-978, doi:10.1007/s10482-013-9876-6 (2013).

42 Wunder, L. C. *et al.* Manganese reduction and associated microbial communities in Antarctic surface sediments. *Front. Microbiol.* **15**, doi:10.3389/fmicb.2024.1398021 (2024).

43 González-Herrero, S., Barriopedro, D., Trigo, R. M., López-Bustins, J. A. & Oliva, M. Climate warming amplified the 2020 record-breaking heatwave in the Antarctic Peninsula. *Communications Earth & Environment* **3**, 122, doi:10.1038/s43247-022-00450-5 (2022).

44 Falk, U., López, D. A. & Silva-Busso, A. Multi-year analysis of distributed glacier mass balance modelling and equilibrium line altitude on King George Island, Antarctic Peninsula. *Cryosphere* **12**, 1211-1232, doi:10.5194/tc-12-1211-2018 (2018).

45 Baas-Becking, L. G. M. *Geobiologie Of Inleiding Tot De Milieukunde*. (WP Van Stockum & Zoon NV, 1934).

46 Fondi, M. *et al.* "Every gene is everywhere but the environment selects": Global geolocalization of gene sharing in environmental samples through network analysis. *Genome Biology and Evolution* **8**, 1388-1400, doi:10.1093/gbe/evw077 (2016).

47 Fuhrman, J. A. Microbial community structure and its functional implications. *Nature* **459**, 193-199, doi:10.1038/nature08058 (2009).

48 Priest, T. *et al.* Atlantic water influx and sea-ice cover drive taxonomic and functional shifts in Arctic marine bacterial communities. *ISME J.* **17**, 1612-1625, doi:10.1038/s41396-023-01461-6 (2023).

49 Carter-Gates, M. *et al.* Implications of increasing Atlantic influence for Arctic microbial community structure. *Sci. Rep.* **10**, 19262, doi:10.1038/s41598-020-76293-x (2020).

50 Oziel, L. *et al.* Faster Atlantic currents drive poleward expansion of temperate phytoplankton in the Arctic Ocean. *Nat. Commun.* **11**, 1705, doi:10.1038/s41467-020-15485-5 (2020).

51 Chapman, C. C., Lea, M.-A., Meyer, A., Sallée, J.-B. & Hindell, M. Defining Southern Ocean fronts and their influence on biological and physical processes in a changing climate. *Nat. Clim. Chang.* **10**, 209-219, doi:10.1038/s41558-020-0705-4 (2020).

52 Ertefai, T. F. *et al.* The biogeochemistry of sorbed methane in marine sediments. *Geochim. Cosmochim. Acta* **74**, 6033-6048, doi:10.1016/j.gca.2010.08.006 (2010).

53 Viollier, E., Inglett, P., Hunter, K., Roychoudhury, A. & Van Cappellen, P. The ferrozine method revisited: Fe(II)/Fe(III) determination in natural waters. *Appl. Geochem.* **15**, 785-790, doi:10.1016/S0883-2927(99)00097-9 (2000).

54 Aromokeye, D. A. *et al.* Temperature controls crystalline iron oxide utilization by microbial communities in methanic ferruginous marine sediment incubations. *Front. Microbiol.* **9**, 2574, doi:10.3389/fmicb.2018.02574 (2018).

55 Lueders, T., Manefield, M. & Friedrich, M. W. Enhanced sensitivity of DNA- and rRNA-based stable isotope probing by fractionation and quantitative analysis of isopycnic centrifugation gradients. *Environ. Microbiol.* **6**, 73-78, doi:10.1046/j.1462-2920.2003.00536.x (2004).

56 Yin, X. *et al.* CO_2 conversion to methane and biomass in obligate methylotrophic methanogens in marine sediments. *ISME J.* **13**, 2107-2119, doi:10.1038/s41396-019-0425-9 (2019).

57 Parada, A. E., Needham, D. M. & Fuhrman, J. A. Every base matters: assessing small subunit rRNA primers for marine microbiomes with mock communities, time series and global field samples. *Environ. Microbiol.* **18**, 1403-1414, doi:10.1111/1462-2920.13023 (2016).

58 Herlemann, D. P. R. *et al.* Transitions in bacterial communities along the 2000 km salinity gradient of the Baltic Sea. *ISME J.* **5**, 1571-1579, doi:10.1038/ismej.2011.41 (2011).

59 Callahan, B. J. *et al.* DADA2: High-resolution sample inference from Illumina amplicon data. *Nat. Methods* **13**, 581-583, doi:10.1038/nmeth.3869 (2016).

60 Paired-end amplicon sequence processing workflow configurable for mixed-orientation libraries and highly variable insert size v. 1.2.0 (2022). doi:10.12754/misc-2022-0002.

61 Kondo, R., Nedwell, D. B., Purdy, K. J. & Silva, S. Q. Detection and enumeration of sulphate-reducing Bacteria in estuarine sediments by competitive PCR. *Geomicrobiol. J.* **21**, 145-157, doi:10.1080/01490450490275307 (2004).

62 Legendre, P., Oksanen, J. & ter Braak, C. J. F. Testing the significance of canonical axes in redundancy analysis. *Methods Ecol. Evol.* **2**, 269-277, doi:10.1111/j.2041-210X.2010.00078.x (2011).

63 vegan: Community Ecology Package v. 2.6-6.1 (2024).

64 R: A language and environment for statistical computing v. 4.4.1 (R Foundation for Statistical Computing, Vienna, Austria, 2024).

65 DigitalGlobe. WorldView-2 Scene 103001001F612100, 07/03/2013 under a CC BY License, with Permission from Maxar-EU Space Imaging-DigitalGlobe original copyright 2013 (2014).

4.2 Supplementary

4.2.1 Supplementary figures

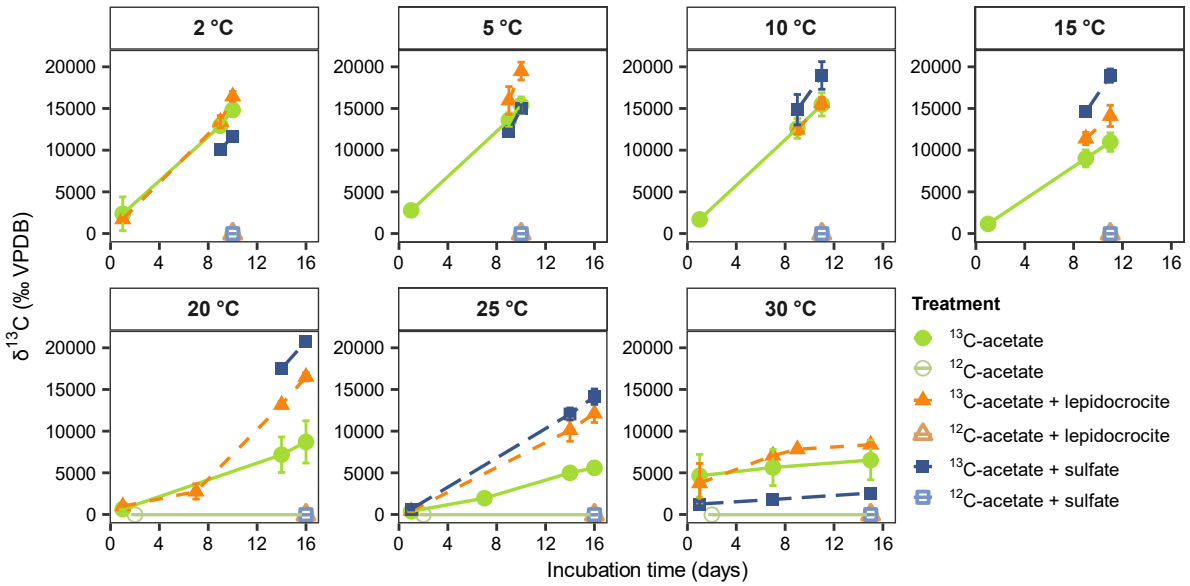

Figure S1: Release of ^{13}C-CO2 (‰) in the headspace of incubations over time confirming the respiration of ^{13}C-acetate to $^{13}C\text{-}CO_2$ across all relevant treatments. Plotted are the calculated average and standard deviation (n = 3) per treatment, distinguished by color, shape and linetype. Samples for SIP analysis were collected after the last incubation time point.

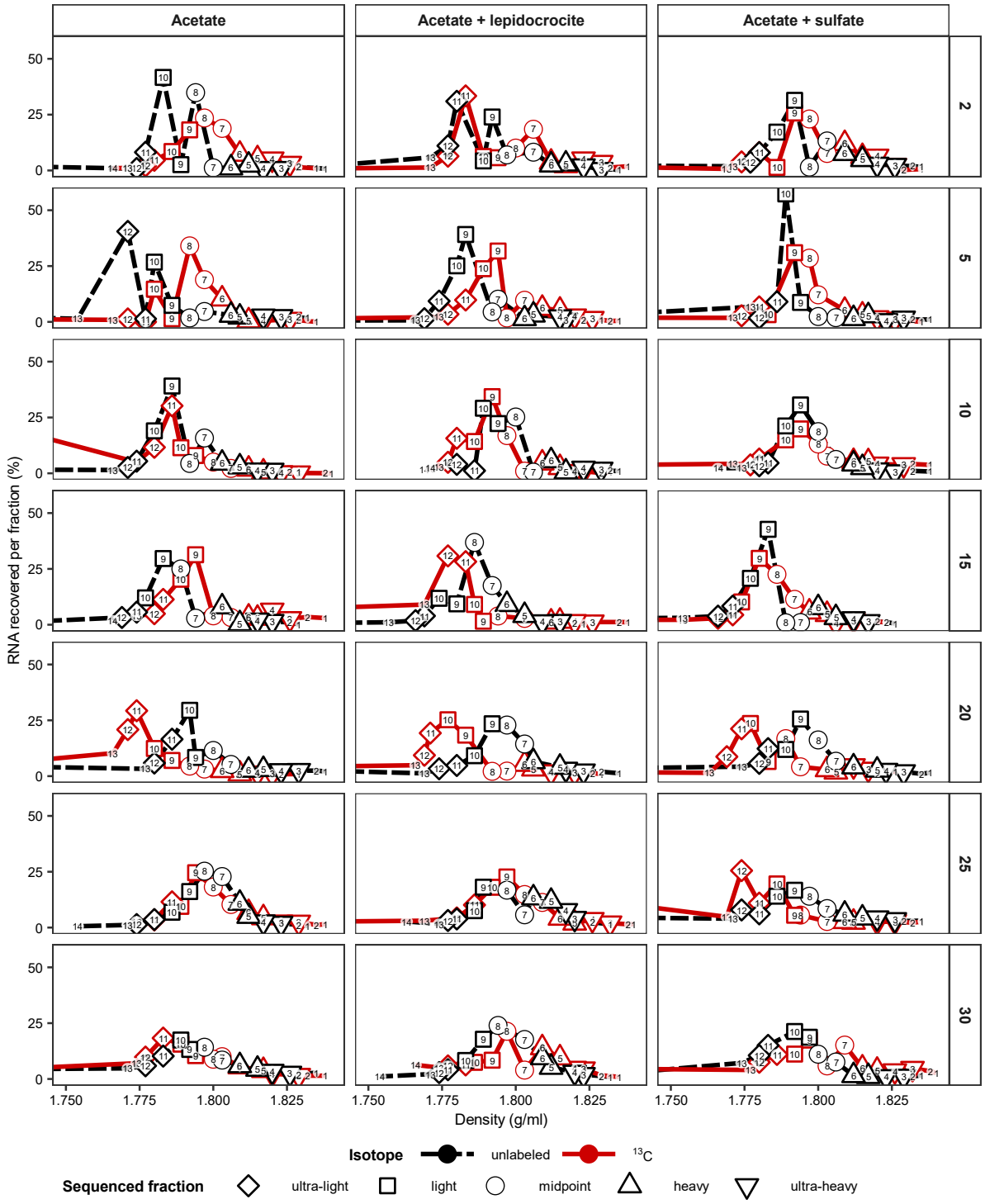

Figure S2: Fractionation profiles of the samples under different treatments (columns) and incubation temperatures (rows). The density of each fraction is plotted against the calculated percentage of RNA recovered from that fraction over the initial total RNA used for the fractionation run. Fractions are numbered from 1 (heavy) to 14 (light). Fractions with density < 1.75 g/ml are not shown and are assumed to consist mainly of water. Labeled (^{13}C) and unlabeled (^{12}C) treatments are distinguished by color and line type. Of each incubation, fractions were pooled for sequencing: 3+4 ultra-heavy, 5+6 heavy, 7+8 midpoint, 9+10 light, 11+12 ultra-light (see main methods). These fractions are marked by different symbols in the plot.

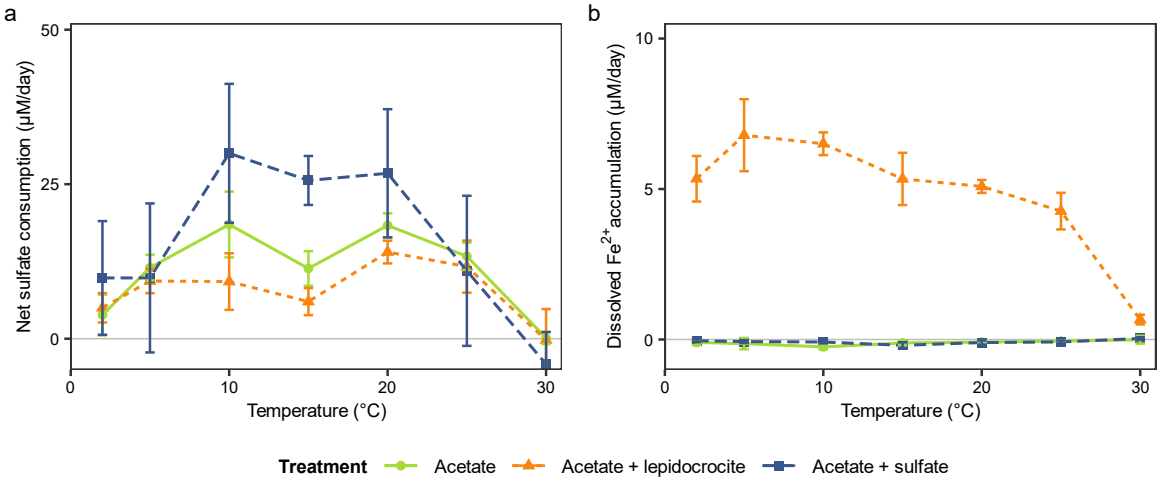

Figure S3: Net consumption of sulfate and accumulation of dissolved ferrous iron in sediment incubations over a short (less than 17 days) period. Plotted are calculated average and standard deviation per treatment and temperature (n = 6) with treatments distinguished by color, shape and linetype.

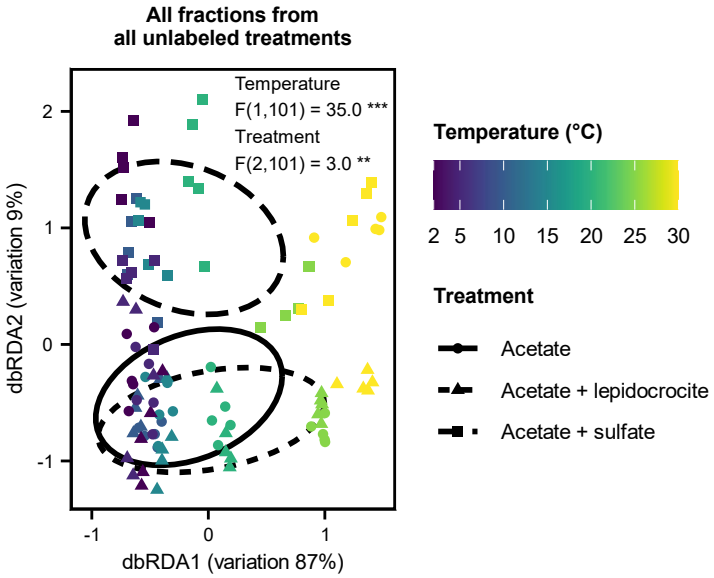

Figure S4: dbRDA ordination plot shows the clustering of all samples for the unlabeled (^{12}C) treatments. The variation contribution of dbRDA1 and dbRDA2 constraining the Bray Curtis distance matrix with the explanatory variables temperature and treatment are displayed. Sample points are distinguished by color for temperature and shape for treatment. The significance for the global model ($F(3,101) = 14.0$, $p < 0.001$) and the individual parameters temperature and treatment (statistics displayed in the plot) were tested. Significance levels are displayed by asterisks: ** $p < 0.01$, *** $p < 0.001$.

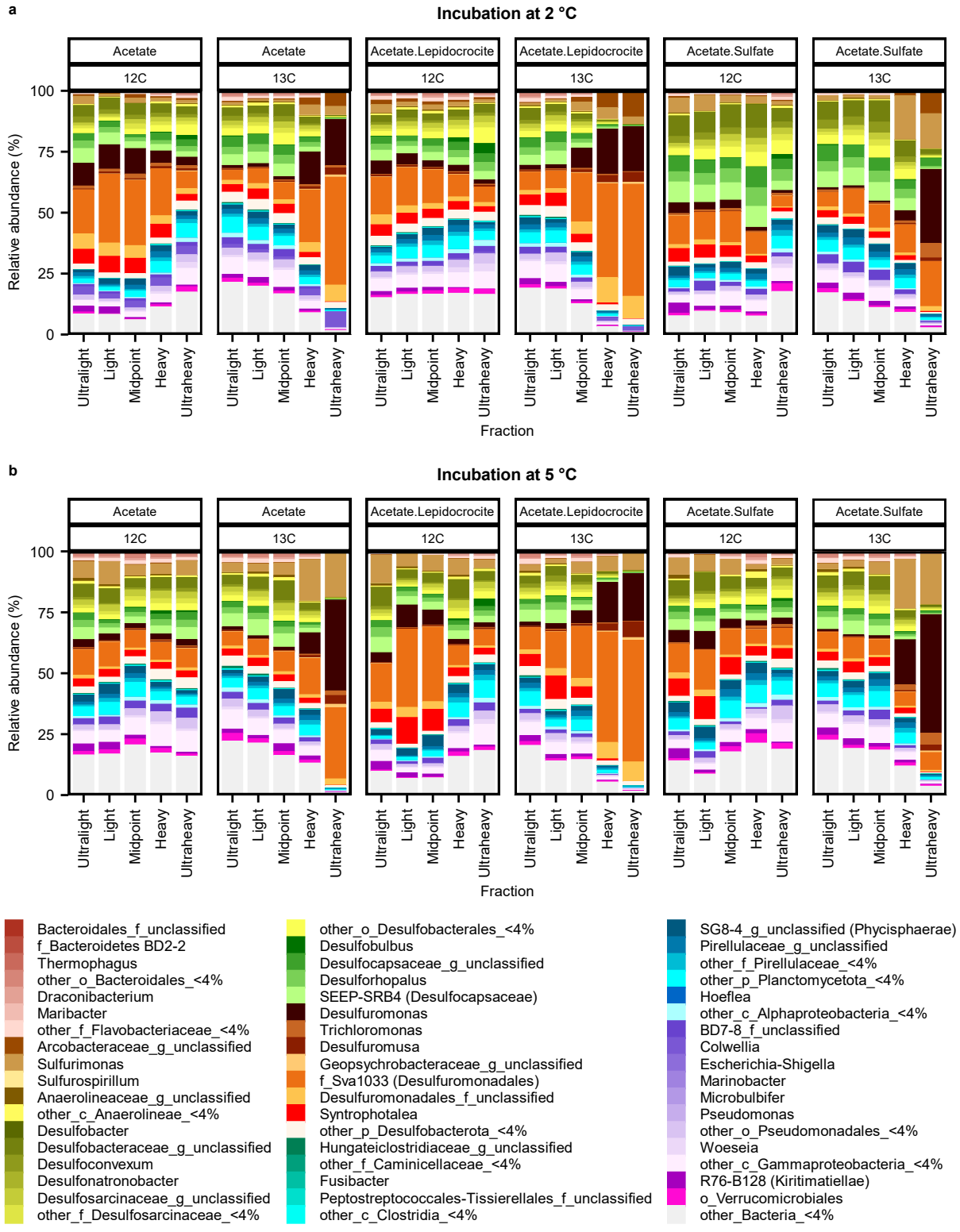

Figure S5: Bacterial 16S rRNA community of 2 °C and 5 °C incubations across labeled (^{13}C) and unlabeled (^{12}C) fractions. Relative abundance of genera above 4% in at least one sample is displayed. Taxa which crossed the 4% threshold on a higher taxonomic rank are indicated by, e.g., f_ for family.

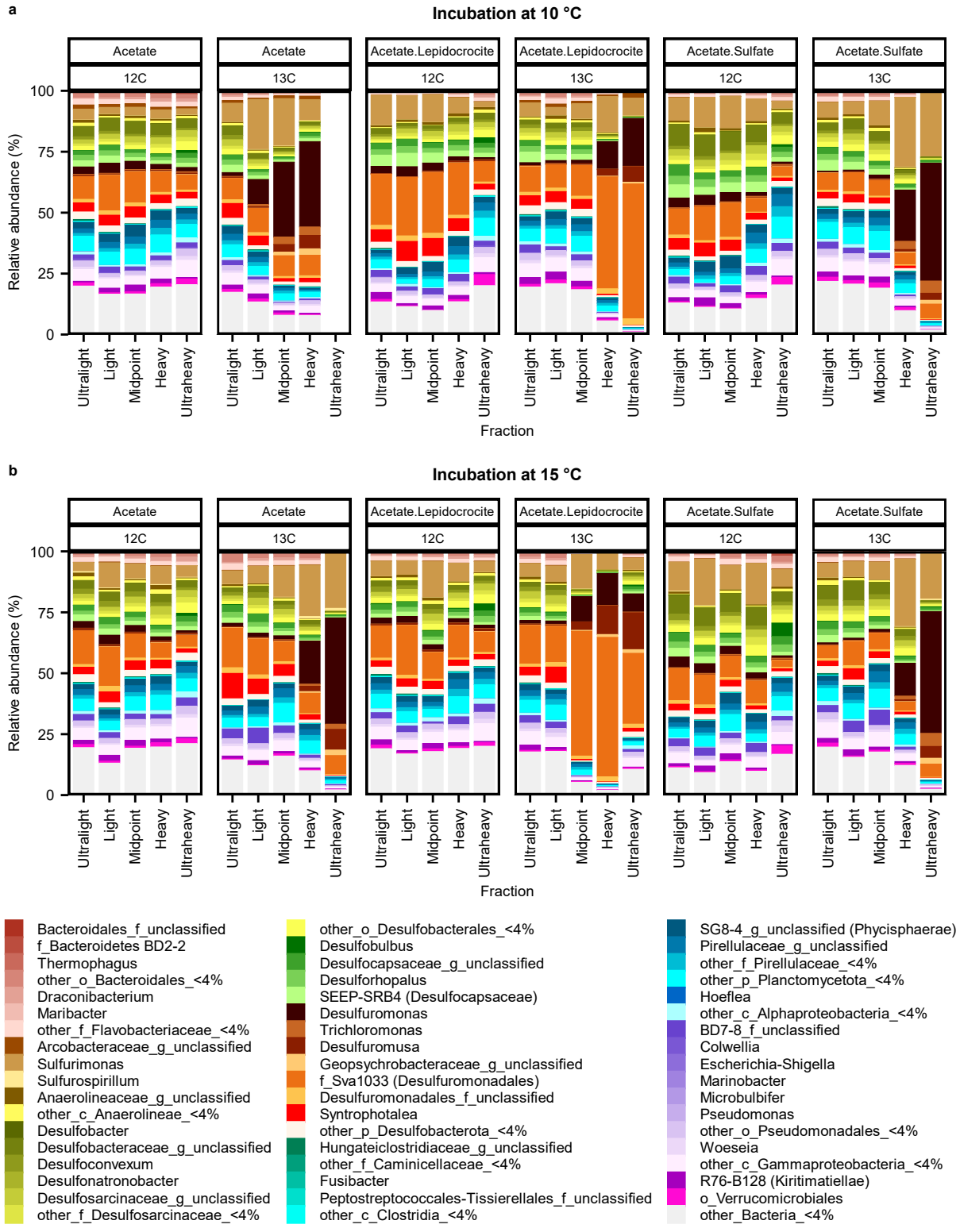

Figure S6: Bacterial 16S rRNA community of 10 °C and 15 °C incubations across labeled (^{13}C) and unlabeled (^{12}C) fractions. Relative abundance of genera above 4% in at least one sample is displayed. Taxa which crossed the 4% threshold on a higher taxonomic rank are indicated by, e.g., f_ for family.

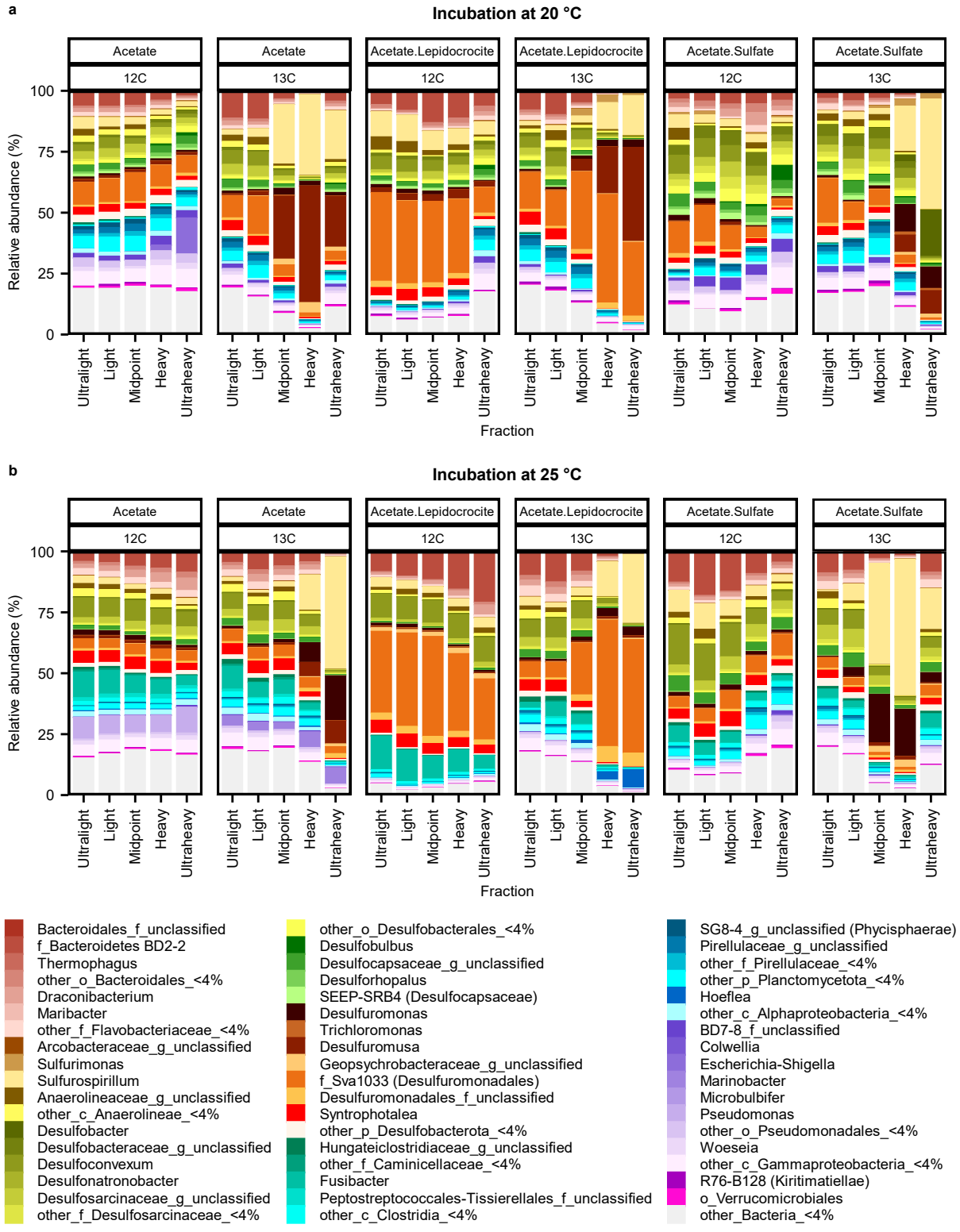

Figure S7: Bacterial 16S rRNA community of 20 °C and 25 °C incubations across labeled (^{13}C) and unlabeled (^{12}C) fractions. Relative abundance of genera above 4% in at least one sample is displayed. Taxa which crossed the 4% threshold on a higher taxonomic rank are indicated by, e.g., f_ for family.

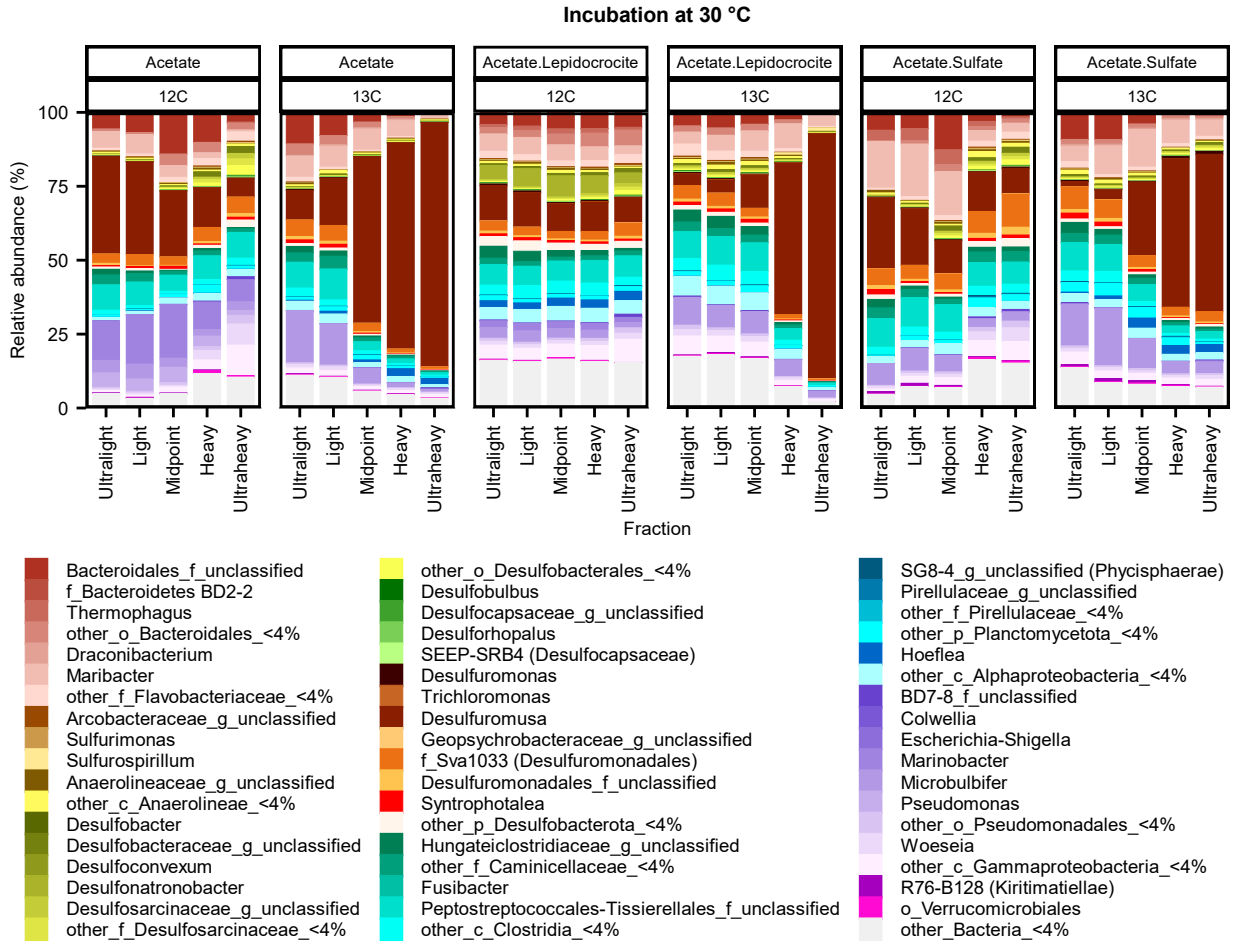

Figure S8: Bacterial 16S rRNA community of 30 °C incubations across labeled (13C) and unlabeled (12C) fractions. Relative abundance of genera above 4% in at least one sample is displayed. Taxa which crossed the 4% threshold on a higher taxonomic rank are indicated by, e.g., f_ for family.

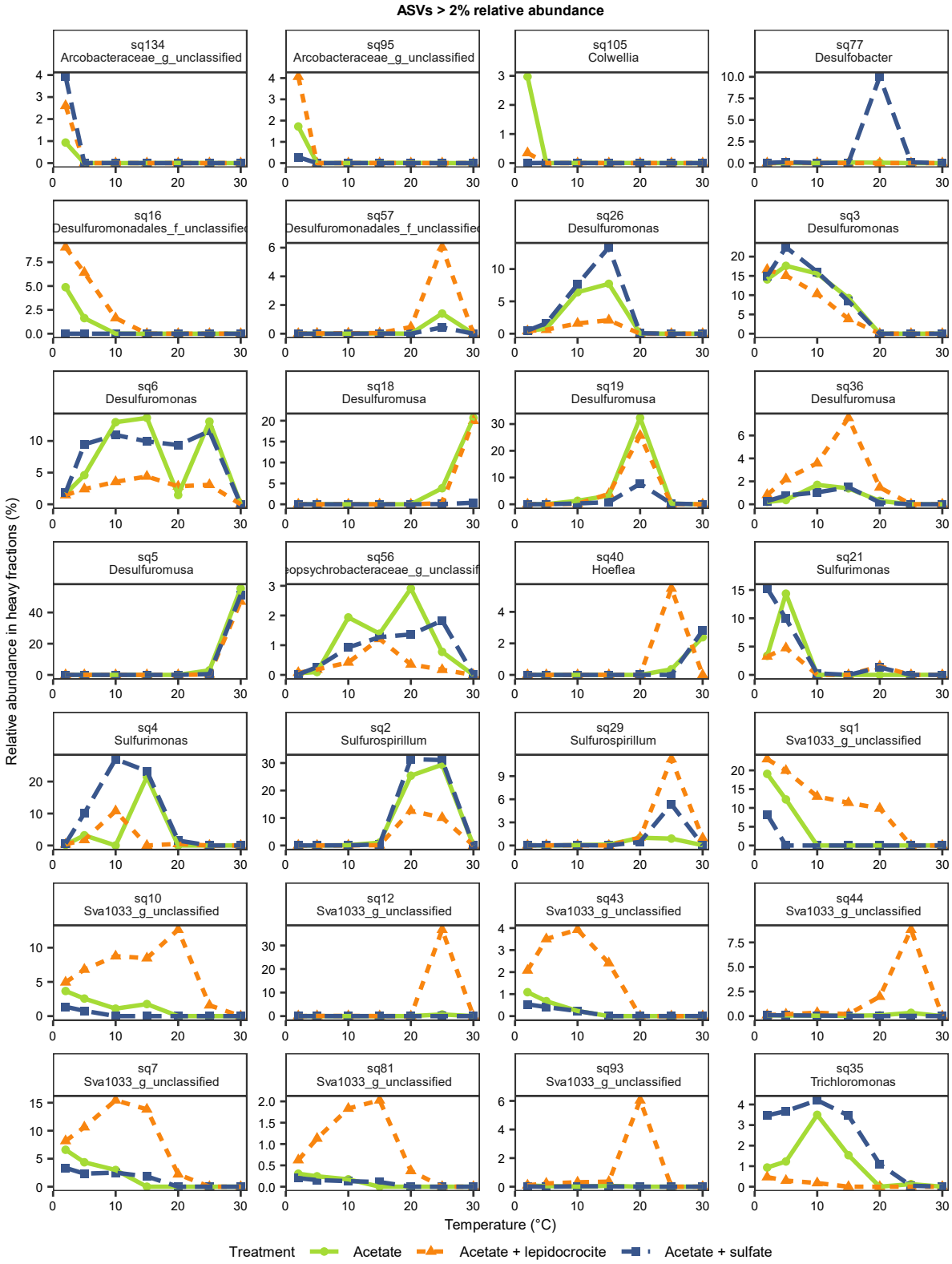

Figure S9: Microorganisms actively incorporating acetate over temperature. Displayed are all clearly labeled ASVs with a relative abundance > 2% in the heavy fractions (i.e., average of relative abundance in ^{13}C heavy + ultra-heavy fractions > ^{13}C light + ultra-light fractions). Treatments are distinguished by color, shape and linetype.

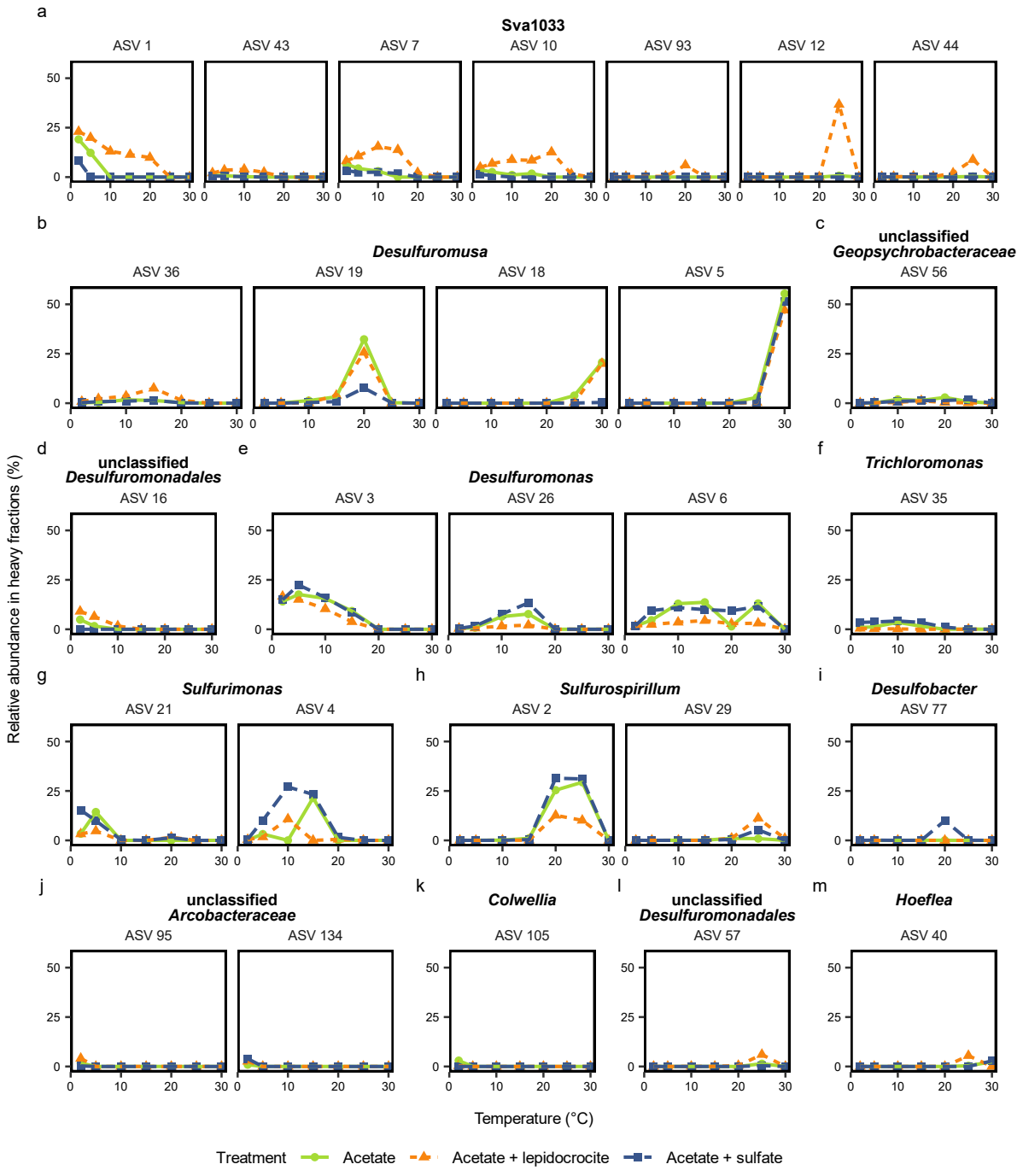

Figure S10: Enriched taxa actively labelled over a wide temperature range in the heavy fractions of the RNA-SIP experiments. The substrate (acetate) provided is a representative intermediate of organic matter degradation. The organisms consistently enriched in the heavy fractions across all temperatures were known as iron and sulfur cycling organisms. Dominant microbes were identified on sequence level (= ASV). Plotted is the average of relative abundance in heavy + ultra-heavy fractions for each ^{13}C-labeled incubation experiment. These groups include the main microbes that used ^{13}C-acetate to form biomass, thereby representing the most active members of the microbial community. Same as main figure 3, but with identical y-scale across all plots.

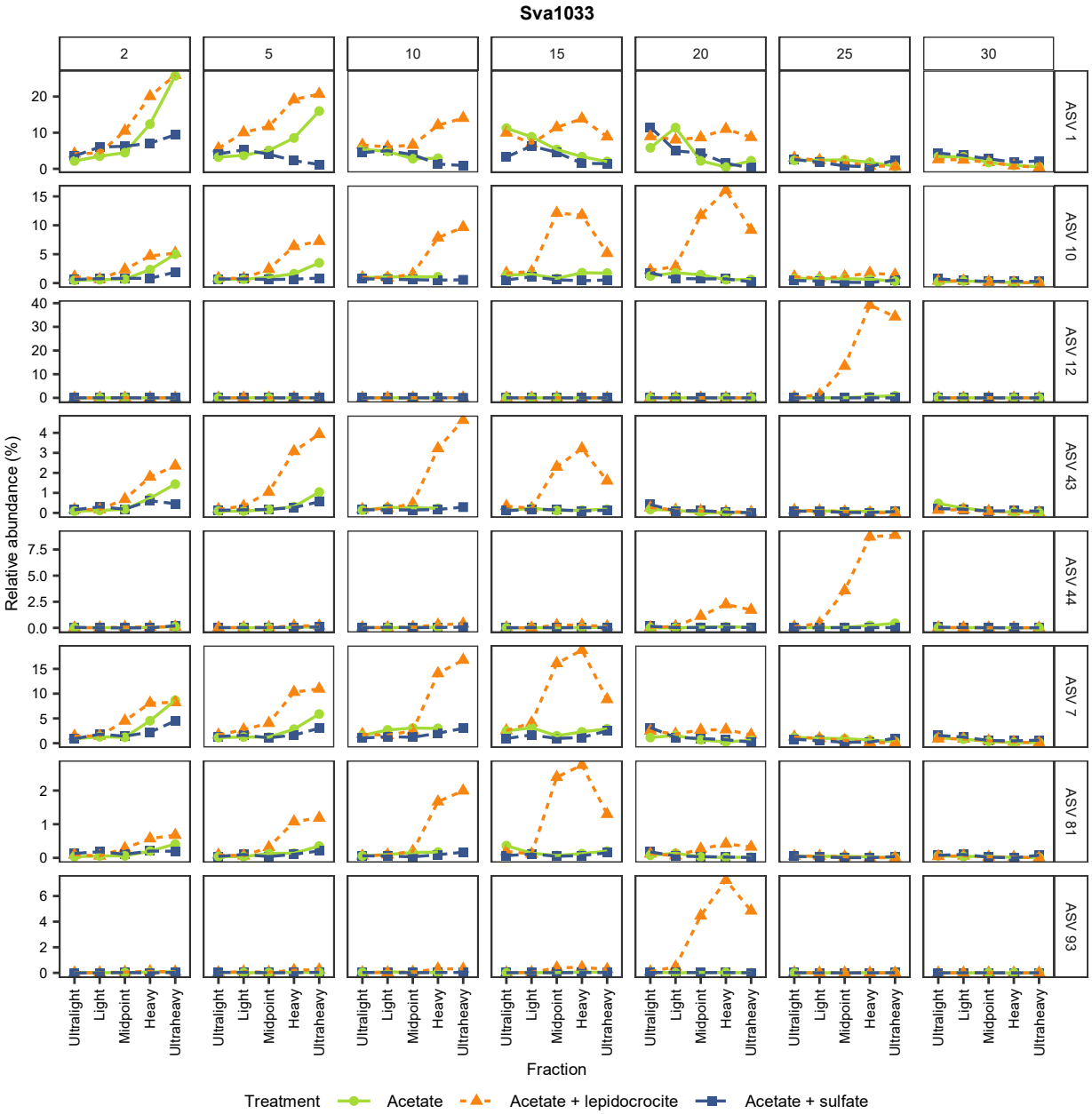

Figure S11: Relative abundance of individual ASVs affiliated with the unclassified family Sva1033 (*Desulfuromonadales*) across ^{13}C fractions at different incubation temperatures. Treatments are distinguished by color, shape and linetype.

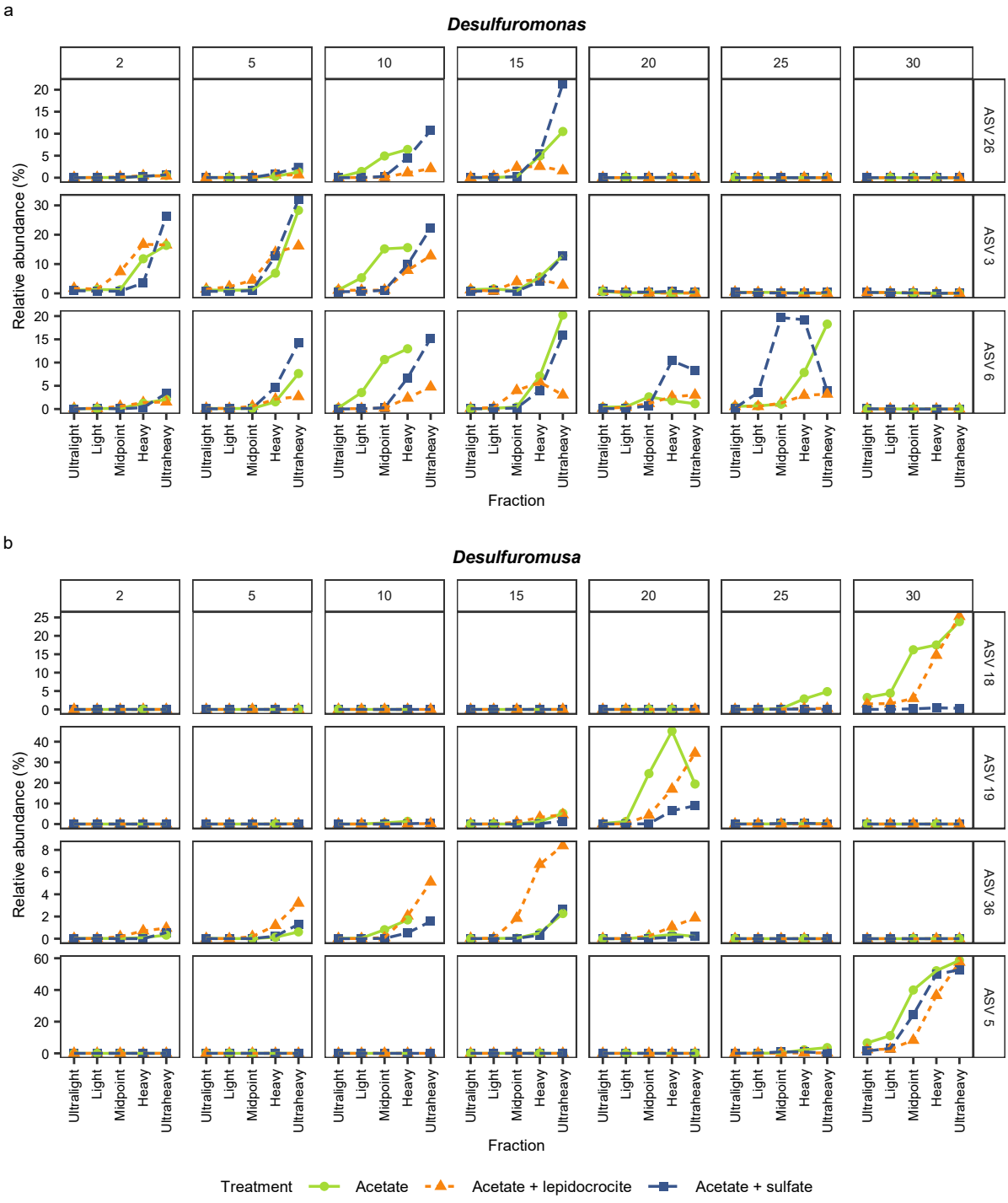

Figure S12: Relative abundance of individual ASVs affiliated with *Desulfuromonas* (a) and *Desulfuromusa* (b) across ^{13}C fractions at different incubation temperatures. Treatments are distinguished by color, shape and linetype.

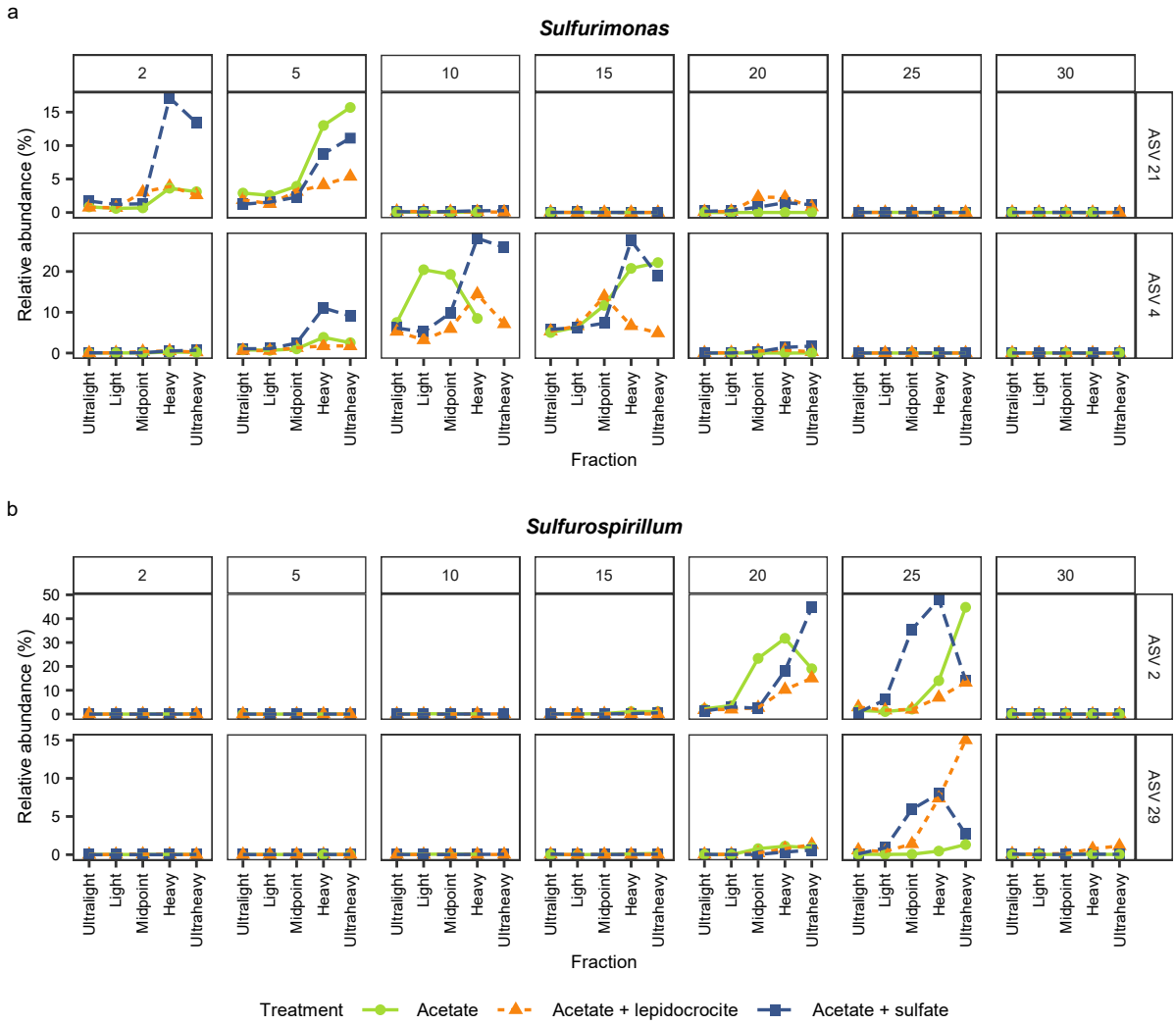

Figure S13: Relative abundance of individual ASVs affiliated with *Sulfurimonas* (a) and *Sulfurospirillum* (b) across ^{13}C fractions at different incubation temperatures. Treatments are distinguished by color, shape and linetype.

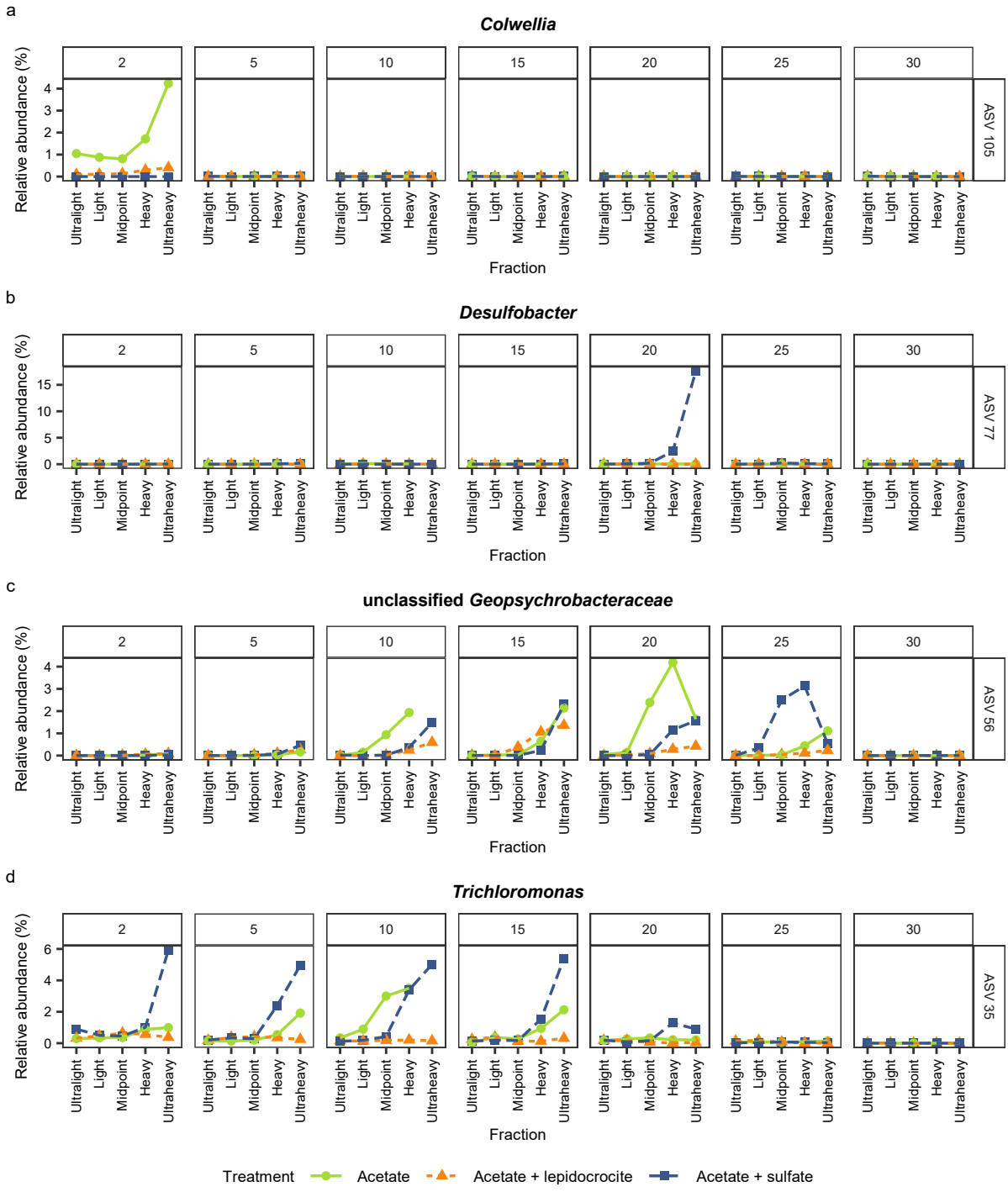

Figure S14: Relative abundance of individual ASVs affiliated with *Colwellia* (a), *Desulfobacter* (b), *Geopsychrobacteraceae* (c) and *Trichloromonas* (d) across ^{13}C fractions at different incubation temperatures. Treatments are distinguished by color, shape and linetype.

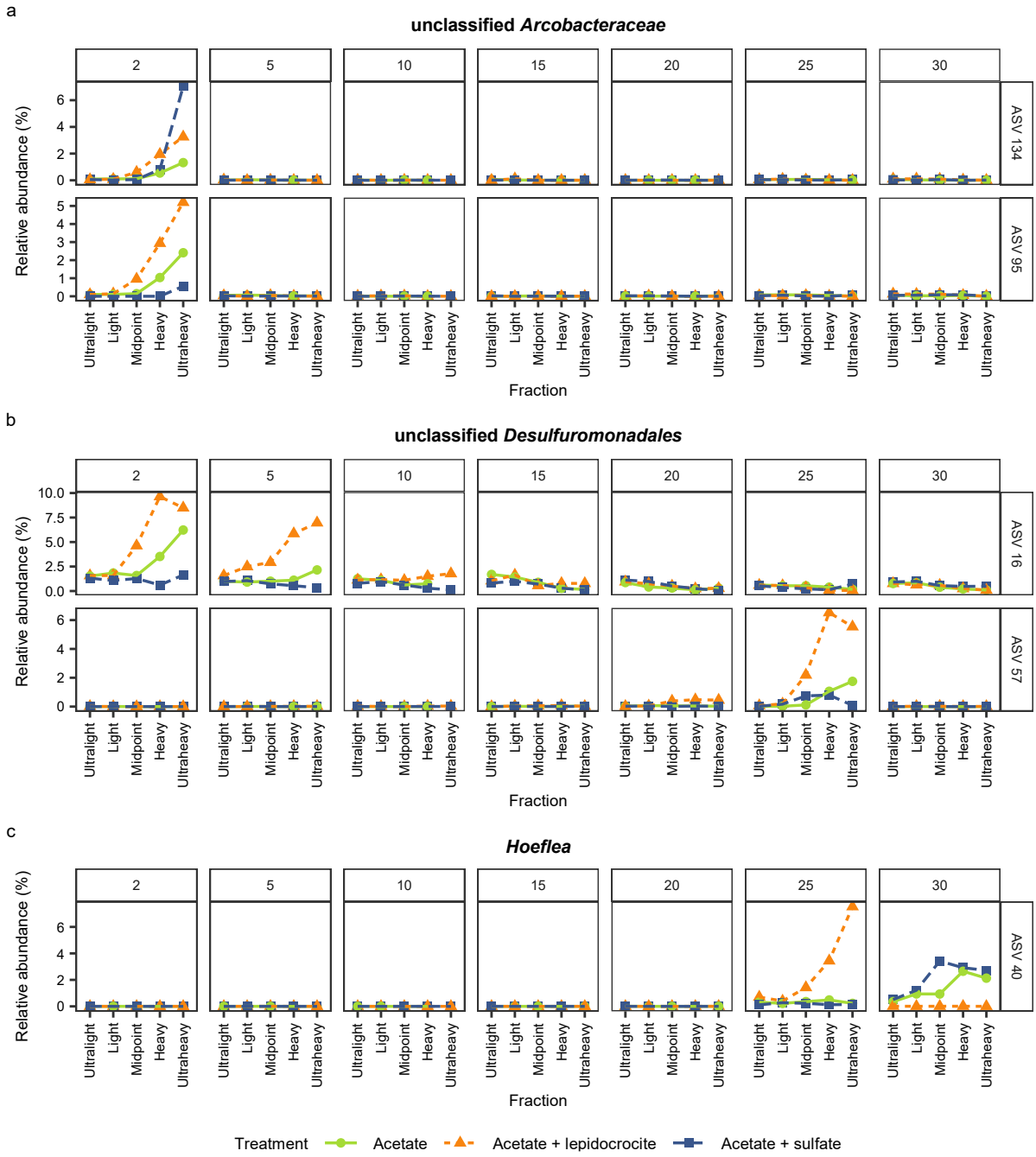

Figure S15: Relative abundance of individual ASVs affiliated with *Arcobacteraceae* (a), *Desulfuromonadales* (b) and *Hoflea* (c) across ^{13}C fractions at different incubation temperatures. Treatments are distinguished by color, shape and linetype.

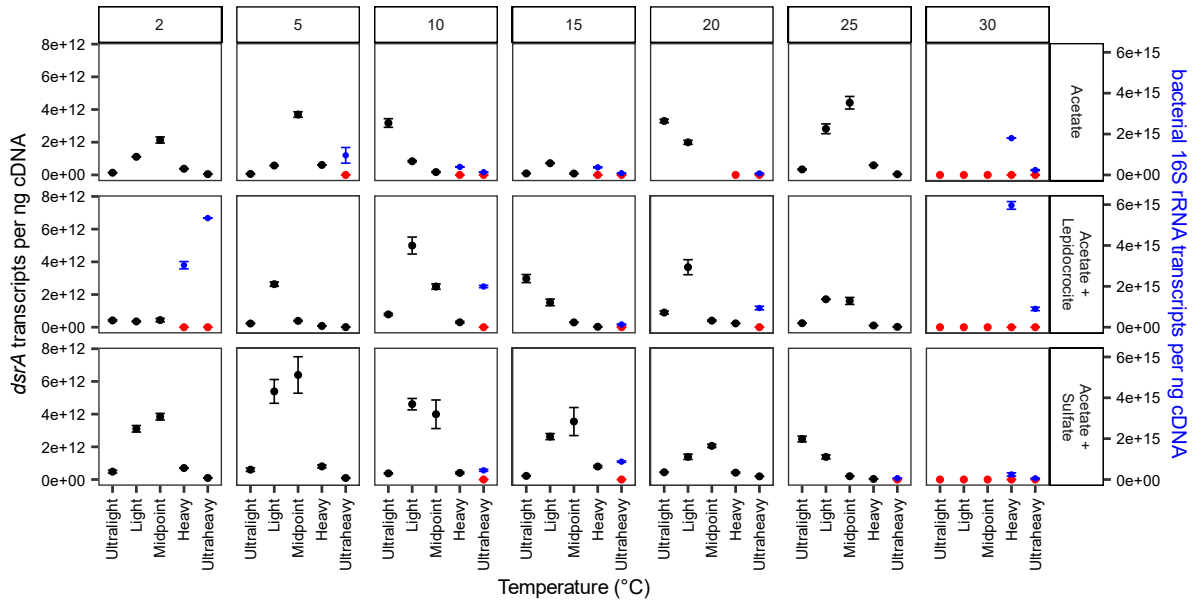

Figure S16: Quantification of the functional gene for sulfate reduction (*dsrA*) and bacterial 16S rRNA at transcript level across ^{13}C-labeled treatments, temperatures and fractions. Transcript numbers were produced by quantitative PCR (qPCR) on cDNA of RNA per stable isotope fraction and calculated per ng supplied cDNA. *dsrA* transcripts are displayed in black and samples below detection limit in red. qPCR of bacterial 16S rRNA was performed only for samples below detection limit and displayed in blue on a different y-scale. Average and standard deviation of technical triplicates were plotted.

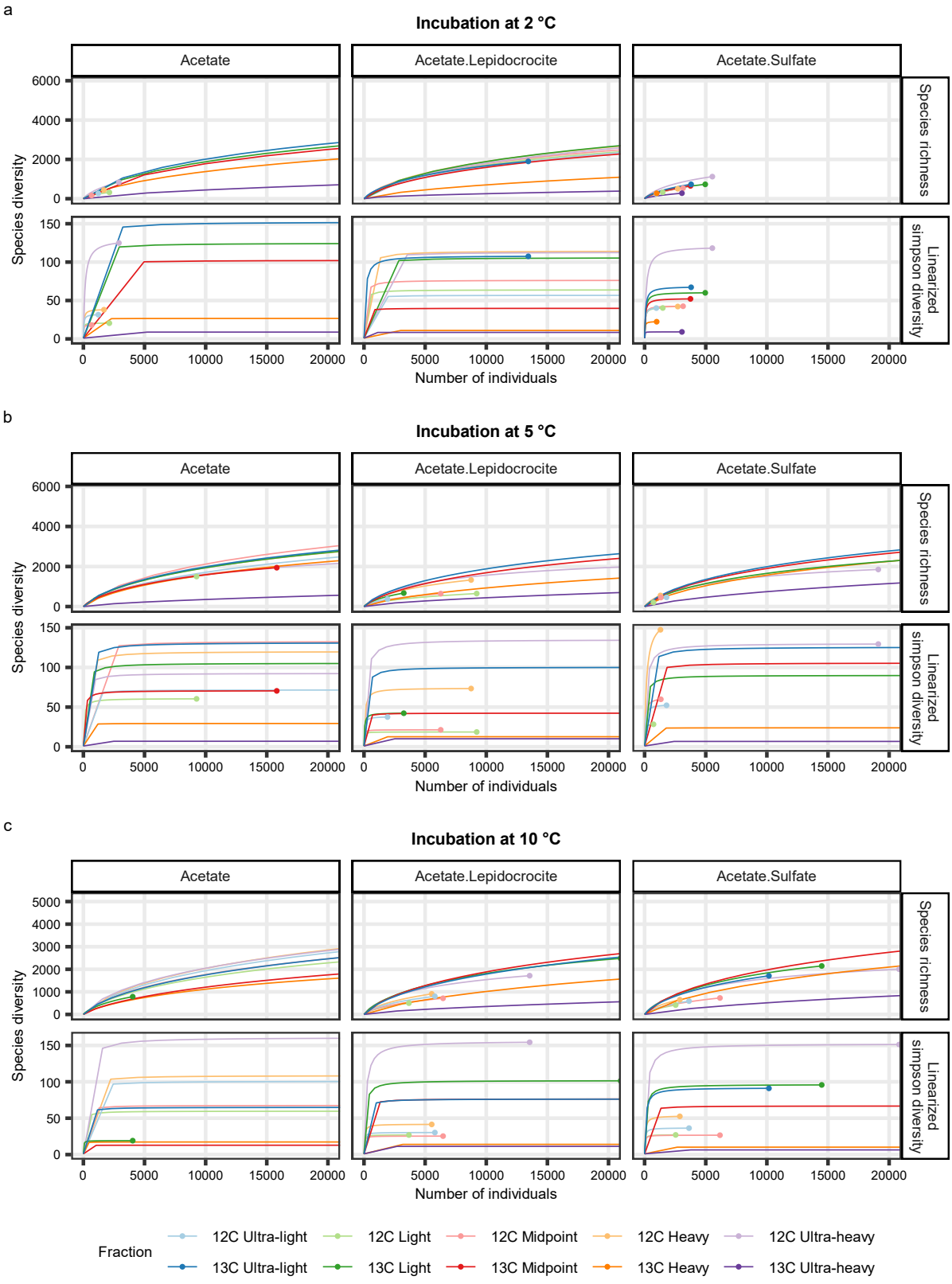

Figure S17: Rarefaction curves of the species diversity observed with the sequences obtained from incubations at 2 °C, 5 °C and 10 °C. The x-axis in the plots is cut at 20000 reads (= Number of individuals).

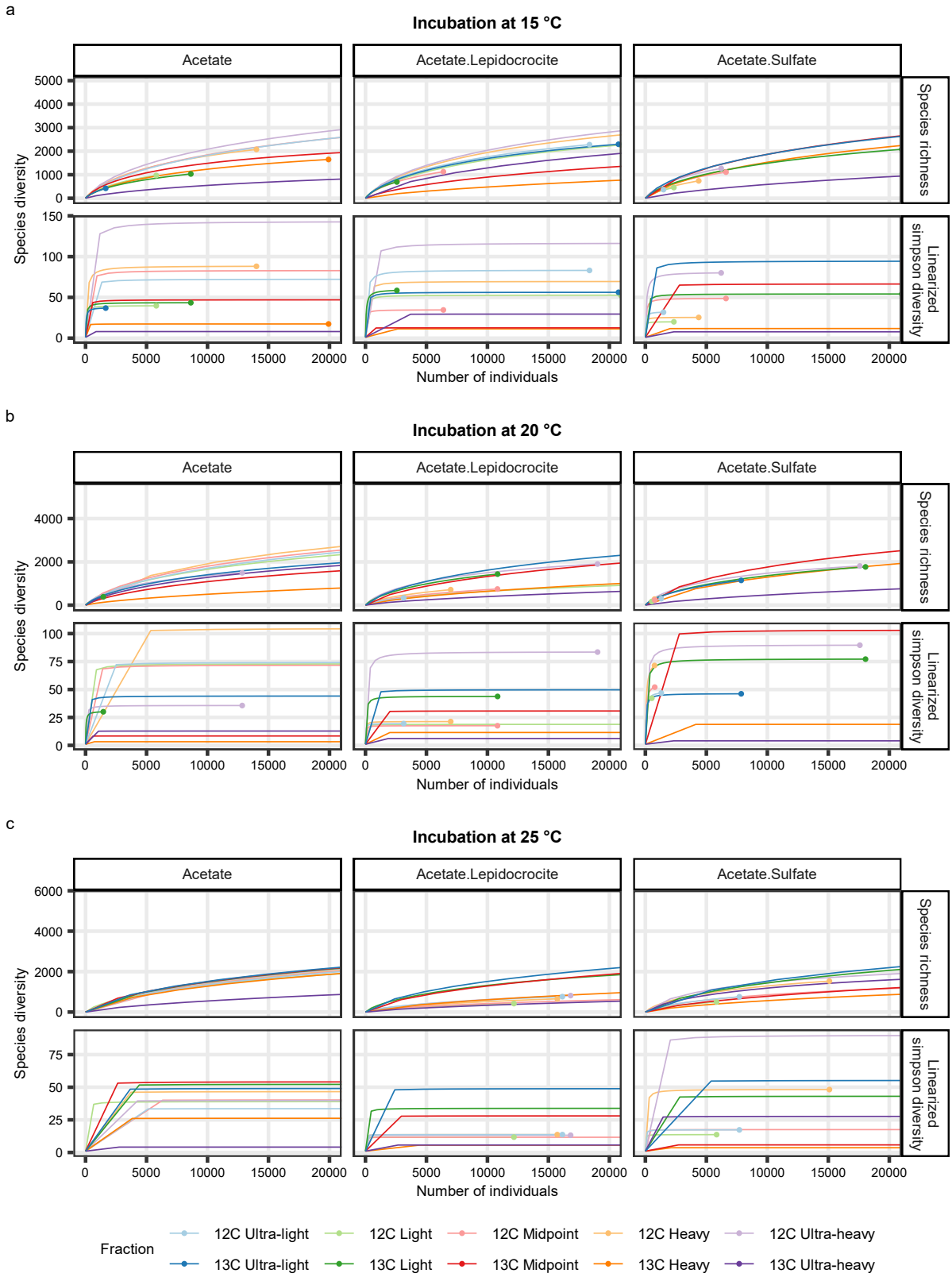

Figure S18: Rarefaction curves of the species diversity observed with the sequences obtained from incubations at 15 °C, 20 °C and 25 °C. The x-axis in the plot is cut at 20000 reads (= Number of individuals).

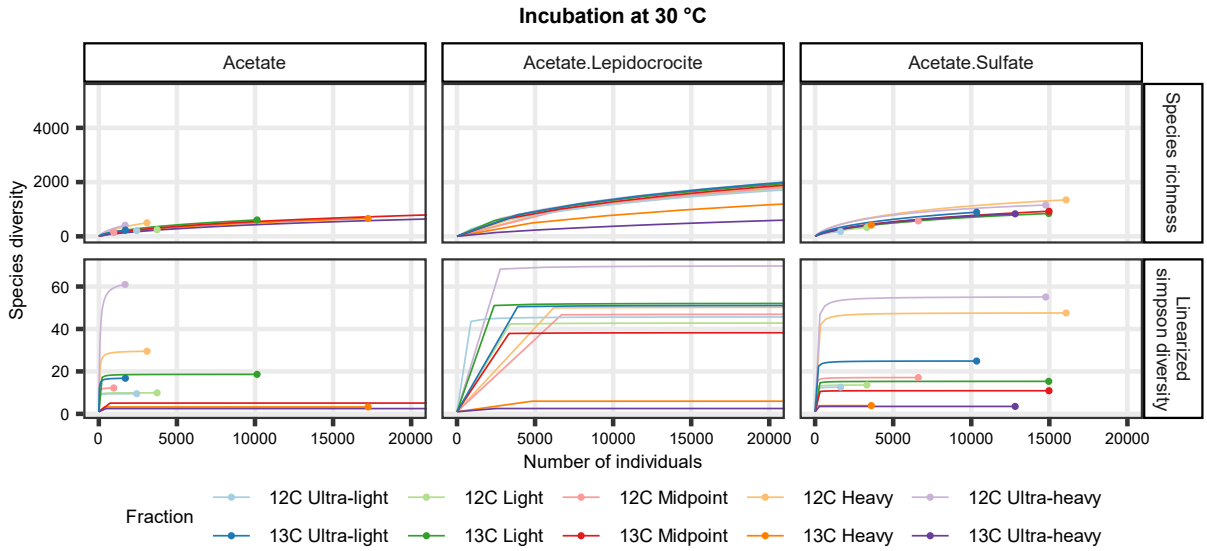

Figure S19: Rarefaction curves of the species diversity observed with the sequences obtained from the incubation at 30 °C. The x-axis in the plot is cut at 20000 reads (= Number of individuals).

4.2.2 Supplementary tables

Table S1: Results (F-statistic and p-value) of the ANOVA-like permutation test of dbRDA models for different data subsets by temperature, isotope and fraction. Test results with not significant p-values (> 0.05) are marked in red, as well as the very low sample numbers per model.

Isotope	Fractions	Temperature range	Complete model		Temperature		Treatment		Residuals
			F	*p*	F	*p*	F	*p*	
all	all	2 - 30 °C	20.41	0.001	53.36	0.001	3.92	0.001	205
^{13}C	all	2 - 30 °C	9.62	0.001	24.10	0.001	2.37	0.001	100
^{13}C	heavy + ultra-heavy	2 - 30 °C	7.24	0.001	16.22	0.001	2.73	0.002	37
^{12}C	all	2 - 30 °C	13.67	0.001	35.03	0.001	2.99	0.003	101
all	all	2 - 5 °C	2.78	0.003	3.38	0.130	2.48	0.007	56
all	all	2 - 10 °C	5.12	0.001	8.33	0.001	3.52	0.001	85
all	all	2 - 15 °C	7.62	0.001	13.60	0.001	4.62	0.001	115
all	all	2 - 20 °C	10.09	0.001	18.74	0.001	5.76	0.001	145
all	all	15 - 30 °C	15.01	0.001	39.82	0.001	2.60	0.004	116
all	all	20 - 30 °C	14.56	0.001	38.50	0.001	2.60	0.007	86
all	all	25 - 30 °C	18.13	0.001	48.26	0.001	3.06	0.005	56
^{13}C	all	2 - 5 °C	1.61	0.139	1.37	0.204	1.73	0.145	26
^{13}C	heavy + ultra-heavy	2 - 5 °C	2.89	0.014	2.11	0.094	3.27	0.012	8
^{13}C	all	2 - 10 °C	2.98	0.002	4.70	0.009	2.14	0.051	40
^{13}C	heavy + ultra-heavy	2 - 10 °C	5.26	0.001	6.15	0.002	4.72	0.001	13
^{13}C	all	2 - 15 °C	4.32	0.001	6.78	0.001	3.10	0.003	55
^{13}C	heavy + ultra-heavy	2 - 15 °C	7.53	0.001	10.62	0.001	5.99	0.001	19
^{13}C	all	20 - 30 °C	7.21	0.001	19.01	0.001	1.32	0.196	41
^{13}C	heavy + ultra-heavy	20 - 30 °C	5.64	0.002	13.78	0.001	1.58	0.183	14
^{13}C	all	25 - 30 °C	7.94	0.001	21.13	0.001	1.35	0.220	26
^{13}C	heavy + ultra-heavy	25 - 30 °C	7.73	0.001	19.24	0.001	1.97	0.136	8

Chapter 5

Microbial ecophysiology of the sulfur cycle in Antarctic sediments

Lea C. Wunder, Janina Barkowsky, Anastasiia Reznik, Katja Laufer-Meiser, Mara D. Maeke, Graciana Willis-Poratti, Susann Henkel, Tim Richter-Heitmann, David A. Aromokeye, Michael W. Friedrich

Manuscript in preparation

Running title:
Sulfur cycling in Potter Cove

Contribution of the candidate to the total work

Experimental concept and design	90%
Experimental work/acquisition of experimental data	60%
Data analysis and interpretation	90%
Preparation of figures and tables	100%
Drafting of the manuscript	100%

Microbial ecophysiology of the sulfur cycle in Antarctic sediments

Lea C. Wunder[a], Janina Barkowsky[a], Anastasiia Reznik[a], Katja Laufer-Meiser[b], Mara D. Maeke[a], Graciana Willis-Poratti[a,c,d], Susann Henkel[e], Tim Richter-Heitmann[a], David A. Aromokeye[a], Michael W. Friedrich[a,f]

a Microbial Ecophysiology Group, Faculty of Biology/Chemistry, University of Bremen, Germany
b GEOMAR - Helmholtz Center for Ocean Research Kiel, Kiel, Germany
c Instituto Antártico Argentino, San Martín, Buenos Aires, Argentina
c Consejo Nacional de Investigaciones Científicas y Técnicas (CONICET), Argentina
e Alfred Wegener Institute Helmholtz Centre for Polar and Marine Research, Bremerhaven, Germany
f MARUM - Center for Marine Environmental Sciences, University of Bremen, Germany

5.1.1 Abstract

Sulfate reduction is important for the terminal step of organic matter degradation in marine sediments, an essential part of marine carbon mineralization and the global carbon cycle. So far, the factors influencing sulfate reduction and the associated sulfur cycle, process rates and active microbial communities involved, were not studied in the Antarctic environment. In this study, we investigated sulfate reduction coupled to hydrogen or acetate oxidation as proxy for lithotrophic and organotrophic processes in the surface sediments of Potter Cove, King George Island/Isla 25 de Mayo, at the West Antarctic Peninsula. In the *in situ* sediments, sulfate reduction likely concurred with iron reduction while typical sulfate-reducing microorganisms were more abundant than iron reducers. Sulfate reduction rates could be stimulated by the addition of hydrogen and acetate in RNA stable isotope probing slurry incubation experiments. *Sulfurimonas*, a known sulfur oxidizer, was the most active microorganism across nearly all treatments and was labeled with ^{13}C-acetate and ^{13}C-dissolved inorganic carbon, identifying it as mixotroph. The taxa Sva0081 (*Desulfosarcinaceae*) and SEEP-SRB4 (*Desulfocapsaceae*) were found in *in situ* sediments and were potentially responsible for observed sulfate reduction, but were only present in the unlabeled fractions of the incubation experiments. Iron-reducing taxa of the order Desulfuromonadales utilized acetate especially when sulfate reduction was inhibited. This study showed that the sulfate-reducing community did not seem to utilize acetate as a major substrate in the same way as shown in different temperate and Arctic environments. Understanding the process of sulfate reduction, sulfur cycling and the different

influencing factors, such as supply of other electron acceptors like iron oxides, is important especially in coastal polar areas, which are currently dominated by iron reduction fueled by glacial meltwater.

5.1.2 Introduction

Organic matter degradation in marine sediments is an important part of the carbon cycle, influencing the sediments function as sink of carbon (LaRowe et al. 2020). In this process, complex organic molecules are broken down through multiple steps and by a network of different organisms until in the last step the oxidation of fermentation products to CO_2 is coupled to the reduction of terminal electron acceptors (LaRowe et al. 2020). Below the oxic zone, these electron acceptors are nitrate, manganese and iron oxide, and sulfate (Froelich et al. 1979). Different redox processes can co-occur in the same zone, e.g., iron and sulfate reduction (Canfield et al. 1993, Jørgensen et al. 2019, Wunder et al. 2021).

Sulfate is one of the most important electron acceptors for organic matter mineralization to CO_2 in marine sediments, especially when other electron acceptors are limited (Vandieken et al. 2006b, Arndt et al. 2013). Sulfate is reduced to sulfide, of which up to 90% gets reoxidized to sulfate again through sulfur intermediates such as elemental sulfur, thiosulfate or tetrathionate, or sulfide can precipitate with other sediment components, e.g., with ferrous iron, or reduce ferric iron to FeS and pyrite (Zopfi et al. 2004, Jørgensen et al. 2019). The geochemistry of the environment influences which further reactions of the produced sulfide and sulfur intermediates take place (Zopfi et al. 2004). Generally, the sulfur cycle is tightly linked to other element cycles such as the iron, manganese, nitrogen and carbon cycle by biotic and abiotic reactions (Wasmund et al. 2017). The reduction of sulfate can be coupled to the oxidation of organic compounds, i.e., fermentation products such as propionate, butyrate, lactate or acetate (Sørensen et al. 1981, Jørgensen et al. 2019). Especially acetate was quantified as one of the major electron donors, e.g., contributing up to 40% to sulfate reduction in marine sediments (Sørensen et al. 1981, Shaw and McIntosh 1990, Finke et al. 2007). Lithotrophic sulfate reduction can be performed with molecular hydrogen (Badziong et al. 1978, Nedwell and Banat 1981). In deeper sediments at the sulfate methane transition zone, sulfate reduction can be coupled to the anaerobic oxidation of methane by a syntrophic consortium of microorganisms (Knittel and Boetius 2009).

Sulfate reduction is performed by a diversity of sulfate-reducing microorganisms, including many uncultured groups, in marine sediments (Jørgensen et al. 2019). These organisms not only play an important role for carbon mineralization, but also for the assembly of the whole microbial sediment community (Liang et al. 2023, Wasmund 2023). In marine surface

sediments, many sulfate reducers belong to the classes Desulfobacteria and Desulfobulbia, especially *Desulfobacteraceae*, *Desulfobulbaceae*, *Desulfovibrionaceae* and *Desulfurivibrionaceae* (Müller et al. 2015, Jørgensen et al. 2019, Langwig et al. 2022). In deeper sediments, also other groups are known for conducting sulfate reduction, such as members of the phyla Firmicutes and Chloroflexi (Wasmund et al. 2017, Jørgensen et al. 2019) and recently also Acidobacteriota (Flieder et al. 2021).

The sulfate-reducing community and reduction rates were investigated in multiple temperate and Arctic environments (Webster et al. 2006, Vandieken and Thamdrup 2013, Na et al. 2015, Beulig et al. 2018, Buongiorno et al. 2019). However, information about microbial community compositions in Antarctic or sub-Antarctic sediments in general is very limited (Bowman et al. 2000, Wunder et al. 2021, Baloza et al. 2023). Especially, active organisms directly linked to sulfate reduction at close-to-*in-situ* conditions were rarely studied at these locations (Purdy et al. 2003, Robador et al. 2015, Yin et al. 2024). As sulfate was identified as an important electron acceptor for final organic matter mineralization in the Arctic environment (Shaw et al. 1984, Vandieken et al. 2006b, Nickel et al. 2008), it raises the question if sulfate reduction is conducted similarly in the Southern Hemisphere. One of the major competing electron acceptors of sulfate in anoxic coastal and shelf sediments in polar environments are iron oxides (Monien et al. 2014, Baloza et al. 2022), as these are supplied by the glaciers and melting sea ice (Death et al. 2014, Raiswell et al. 2016, Monien et al. 2017). Based on thermodynamic theory, iron reduction is regarded as energetically more favorable than sulfate reduction (Froelich et al. 1979, Lovley and Goodwin 1988, Canfield and Thamdrup 2009). However, at multiple, especially temperate locations, it was observed that iron and sulfate reduction occur at the same depths (Canfield et al. 1993, Canfield and Thamdrup 2009, Burdige et al. 2016) and sulfate reducers were detected at high relative abundance in ferruginous zones for a sub-Antarctic location (Wunder et al. 2021).

In order to investigate the process of sulfate reduction and sulfur cycling, its role in organic matter degradation, and the associated microbial community in an Antarctic environment, the sampling site Potter Cove was selected. Potter Cove is located at King George Island/Isla 25 de Mayo at the West Antarctic Peninsula. The cove is heavily influenced by the retreating Fourcade Glacier (Rückamp et al. 2011), supplying glacial meltwater with nutrients such as iron to the environment (Monien et al. 2014, Monien et al. 2017). In the top 30 cm of the sediments, iron reduction, and recently also manganese reduction, were shown as important occurring processes for final organic matter mineralization, identifying Sva1033 (Desulfuromonadales), *Desulfuromusa* and *Desulfuromonas* as the most active bacteria in

these processes (Aromokeye et al. 2021, Wunder et al. 2024). However, sulfate reduction and sulfate reducers were not examined in these experiments.

This study aimed to investigate potential electron donors and the associated microbial community for sulfate reduction in Potter Cove surface sediments. The dominant geochemical processes were predicted from geochemical analyses of the pore water and the microbial community was explored by 16S rRNA and 16S rRNA gene sequencing. Acetate and hydrogen were tested as electron donors in slurry incubations, measuring sulfate reduction rates and identifying active heterotrophic and autotrophic bacteria by RNA stable isotope probing (SIP).

5.1.3 Material and methods

5.1.3.1 Study site

For this study, sampling station 14 (S62°13'54.8"/W58°40'06.6") in Potter Cove (Figure 1) was selected based on previous geochemical measurements of decreasing sulfate and high ferrous iron concentrations (Henkel et al. 2018). In austral summer 2018/2019, sediment samples were retrieved using a hand-held gravity corer (Corer 60, UWITEC, Austria) and processed as described in Wunder et al. (2024). Briefly, two replicate cores were used for pore water extraction and samples were fixed for dissolved Fe^{2+}, sulfate and cations measurements. Further, three replicate cores were sampled for nucleic acid extraction and incubation experiments. The environmental geochemical data was uploaded to the PANGAEA database under https://doi.pangaea.de/10.1594/PANGAEA.941170.

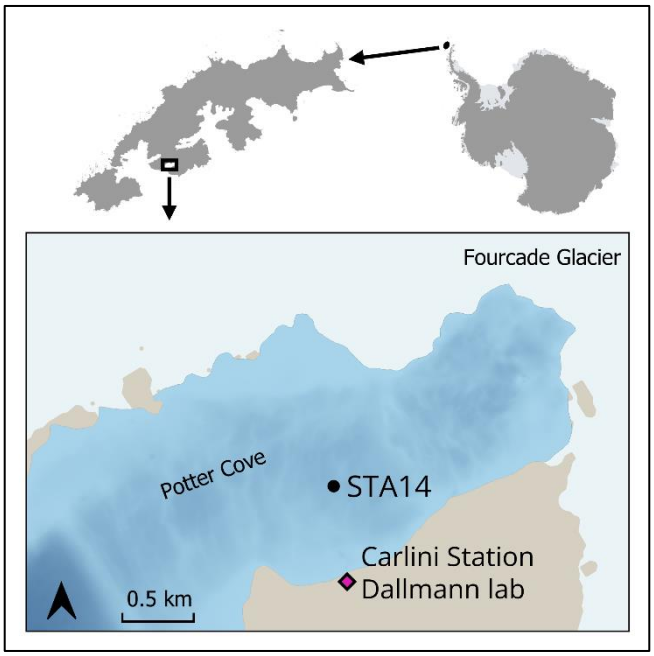

Figure 1: Sediment cores of station 14 taken in Potter Cove, King George Island/Isla 25 de Mayo. Map was created with QGIS 3.34.3 with bathymetry data (Neder et al. 2022) updated from Jerosch et al. (2015), basemap data from SCAR Antarctic Digital Database 2023 and manually smoothed rock outcrop data from Gerrish (2020).

5.1.3.2 Incubation experiment

Slurry incubations were conducted to investigate sulfate reduction with different electron donors and carbon sources. Sediment of the top 10 cm from replicate cores STA14.03 and STA14.04 was mixed in order to cover more microbial diversity of the sampling site and due to material limitation. A slurry in a 1:6 ratio of sediment and anoxic artificial sea water

containing 28 mM sulfate (26.4 g NaCl, 11.2 g $MgCl_2 \cdot 6\ H_2O$, 1.5 g $CaCl_2 \cdot 2\ H_2O$, 0.7 g KCl, 3.98 g $NaSO_4$ per liter; prepared with purified water (Milli-Q)) was prepared under flushing with N_2 (99.999% purity, Linde, Germany). The slurry was distributed with 45 ml per 120-ml serum bottle sealed with butyl rubber stopper and the headspace was exchanged with N_2. Pre-incubation was performed for equilibrating the system at 2°C in the dark for 6 days. As incubations were later amended with ^{13}C-labeled dissolved inorganic carbon (DIC), remaining unlabeled DIC was reduced as much as possible by a cycle of 3 min vacuum – 30 s flushing with N_2 for three times before the addition of substrates.

Seven treatments were set up using different combinations of electron donors and carbon sources (suppl. Table S1). The main treatments contained acetate (Na-acetate, 0.5 mM) and hydrogen (2% in headspace) in combination (I) or either separately (II, III) as electron donors. Control treatments contained molybdate (Na_2MoO_4, 28 mM) in order to inhibit sulfate reduction (Peck 1959) with either hydrogen (IV) or acetate (V). As additional carbon source, all treatments were amended with DIC ($NaHCO_3$, 10 mM). Two additional controls only contained slurry with (VI) or without (VII) DIC. In order to perform stable isotope probing, acetate and DIC substrates were used, all C atoms labeled (99%) with the stable, heavy ^{13}C isotope. For treatment I with acetate and hydrogen, one set of incubations was amended with ^{13}C-labeled acetate and unlabeled DIC and the other with ^{13}C-labeled DIC and unlabeled acetate. For all treatments, additional controls with unlabeled substrates were set up. For each unique treatment, 3-9 replicate bottles were incubated (details suppl. Table S1).

During the incubation period of 19 days, the incubation bottles were sampled anoxically with an N_2-flushed syringe for geochemical measurements every 2-7 days (details suppl. Table S2). Pore water was separated by centrifuging a slurry sample in an N_2-flushed tube for 10 min at 20817 *g*. Subsamples of the supernatant were fixed in 0.75 M HCl for determination of dissolved Fe^{2+}, and in 2.5% Zn-acetate for sulfide (H_2S, HS^-, S^{2-}), or flushed with CO_2 for > 30 s to remove any sulfide for sulfate measurements. For extracting easily dissolvable Fe^{2+}, a slurry sample was incubated in 0.5 M HCl at room temperature for 1 h and subsequently the supernatant was fixed in 1 M HCl. Fe^{2+} was measured with the ferrozine assay (Viollier et al. 2000) using a plate reader (Tecan, Infinite® M Plex). Sulfide was measured with the methylene-blue method (Cline 1969) on a plate reader. Sulfate was measured by ion chromatography equipped with a conductivity detector (Metrohm 930 Compact IC Flex). pH was measured on slurry samples with a pH meter (Sartorius Basic Meter PB-11) immediately after sample retrieval, except for day 0 samples which were measured after storage at 4°C for 6 days. Hydrogen was measured in the headspace by gas chromatography (peak performer PP1,

peak laboratories, USA). Samples of treatments with hydrogen addition were diluted 1:2000 with N_2 prior to measurement. At the end of the incubation, the remaining slurry was frozen at -80°C until nucleic acid extraction.

5.1.3.3 ^{35}S-Sulfate reduction rate measurements

Sulfate reduction rates were measured by incubating a sub-sample of the main incubations for 24 h at every sampling time point following Røy et al. (2014). The control treatments with unlabeled substrates were used (suppl. Table S2). 5 ml of slurry were transferred anoxically into a 10-ml N_2-flushed Hungate tube sealed with a butyl rubber stopper. For treatments containing hydrogen, 2% hydrogen was added to the headspace to ensure same availability of electron donor as in the main incubation. ^{35}S-sulfate radioactive tracer (~ 50 kBq) was added and after 24 h incubation, the sample was stopped with 10 ml of 20% Zn-acetate. Samples were frozen at -20°C until distillation.

The fixed samples were thawed by adding 5% Zn-acetate and the mixture was transferred into a 50-ml tube, rinsing the remaining sediment from the Hungate tube with additional 5% Zn-acetate in order to ensure transfer of all of the sample into the new tube. The tubes were centrifuged at 3398 *g* for 5 min (Allegra X-22 centrifuge, Beckman Coulter) and 0.1 ml of the supernatant was used for the measurement of total sulfate radioactivity. Only the pellet of the incubated sample was used for distillation. It was transferred into the round reaction flask by mixing with dimethylformamide (DMF) and the empty 50-ml tube was additionally rinsed with DMF to ensure complete transfer of the sample. After sealing of the distillation set-up, 0.25 mmol sulfide was added with syringe and needle in order to increase the pool of sulfide in the sample, which did not contain any free sulfide, and therefore ensure all labeled ^{35}S-sulfide was distilled (Røy et al. 2014). The distillation was run for 2 h and sulfide was trapped as Zn-S in 5% Zn-acetate filled glass-reaction tubes. Blank measurements of scintillation cocktail and blank distillation runs were done for each measurement day. The radioactivity was measured using Ultima Gold XR scintillation cocktail on a liquid scintillation counter (TriCarb B2910, Perkin Elmer).

The sulfate reduction rate was calculated in nmol sulfate reduced per cm³ slurry per day following the formula

$$SRR_{slurry} = \frac{A_{TRIS}}{A_{SO_4^{2-}} + A_{TRIS}} \times [SO_4^{2-}] \times 1.06 \times \frac{1}{t} \qquad (1)$$

A_{TRIS} is the total radioactivity of total reduced inorganic sulfur (TRIS) measured in the Zn-acetate traps, $A_{SO_4^{2-}}$ the total radioactivity of $^{35}SO_4^{2-}$ calculated from the activity of measured supernatant, 1.06 the estimated isotope fractionation factor between $^{32}SO_4^{2-}$ and

$^{35}SO_4^{2-}$ (Jørgensen and Fenchel 1974), and *t* the exact incubation time with radioactive tracer in days. The used sulfate concentration [SO_4^{2-}] in nmol/cm³ slurry, considering slurry porosity, was measured in the supernatant of the incubated slurry when the 5 ml sample for incubation with the radioactive tracer was taken (see suppl. for detailed calculation).

The significant differences ($p < 0.05$) in sulfate reduction rates between treatments (excluding molybdate amended treatments IV and V) and time points were tested using the general linear hypothesis test (Herberich et al. 2010). A linear model was created using the "lm" function with default settings and multiple comparisons were performed across all combinations of treatments and time points using the function "glht" with the "Tukey" setting in the R package multcomp (v1.4.26, Hothorn et al. 2008). *P*-values were adjusted for multiple testing by the default method in the multcomp "summary" function. Note, that this procedure does not require any assumption regarding the distribution of data points, sample sizes or variance homogeneity.

5.1.3.4 Nucleic acid extraction

Nucleic acid extraction was performed on *in situ* sediments from station 14 and on slurry samples from the incubation experiment. A phenol-chloroform protocol was used for extracting DNA from 0.5 g *in situ* sediment and combined RNA and DNA from 33-45 ml slurry. Replicates from slurry incubations were pooled for extraction in order to retrieve sufficient RNA amounts for stable isotope probing (SIP, see method section below), except for labeled treatment III (DIC + hydrogen) which was set up with more replicates and kept separate for SIP (see suppl. Table S2, repl. 7, 8, 9). Extraction was performed as described in Wunder et al. (2024) following Lueders et al. (2004) with modifications. The extraction from high amounts of slurry material was performed in five parallel tubes per sample which were eluted in the same final 150 µl DEPC-treated water.

RNA was extracted from 0.5 g *in situ* sediments following a protocol with magnetic beads which achieved higher yields than the phenol-chloroform protocol. Initial steps for cell disruption followed the protocol by Lueders et al. (2004) with beat-beating for 2x 45 s at 6.5 m/s in a liquid volume of ~ 1 ml. After centrifugation at 4°C and 20817 *g* for 20 min, the resulting lysate was further cleaned up with silica magnetic beads (G-Biosciences, Geno Technology Inc., USA). Beads were washed twice with elution buffer (Monarch, New England Biolabs, Germany) prior use. 100 µl lysate was bound to the beads by mixing with 10 µl beads and 1.56 ml binding buffer (Monarch, New England Biolabs, Germany) at 20°C while shaking at 1000 rpm for 15 min. Two washing steps with washing buffer (Monarch, New England Biolabs, Germany) were performed. After brief air drying, the sample was eluted in elution buffer (Monarch, New England Biolabs, Germany) at 4°C while shaking at 1000 rpm for 5 min.

Parallel tubes from the same sample were pooled together again. The detailed protocol steps are described in the supplementary.

The quality of all nucleic acid extracts was evaluated spectrophotometrically with a NanoDrop 1000 (Peqlab Biotechnology Erlangen, Germany). For combined RNA and DNA extracts, DNase treatment was performed on subsamples (DNA-*free*™ Kit, Thermo Fisher Scientific). cDNA was synthesized (GoScript™ Reverse Transcriptase Kit, Promega) from RNA of *in situ* extracts. DNA extracts were quantified with Quanti-iT PicoGreen (Quanti-iT PicoGreen™ dsDNA Assay Kit, Invitrogen™, Thermo Fisher Scientific) measured on a plate reader (Tecan, Infinite® M Plex).

5.1.3.5 Stable isotope probing – density separation

Density separation by ultra-centrifugation was performed on DNA-depleted RNA extracts of incubation samples following the protocol by Yin et al. (2019). Briefly, quantification of RNA was performed with Quanti-iT RiboGreen (Quanti-iT RiboGreen™ RNA-Kit, Invitrogen™, Thermo Fisher Scientific) measured on a plate reader (Tecan, Infinite® M Plex). 1 µg RNA per sample was loaded with formamide, gradient buffer solution and cesium trifluoroacetate solution (CsTFA) for density separation at 124,000 *g* and 20°C for 65 h (Optima L-90 XP ultracentrifuge, Beckman Coulter, Brea, CA). The CsTFA solution was prepared from $CsOH \cdot 2\ H_2O$ (99.5% purity, Sigma-Aldrich, Germany) and trifluoroacetate (TFA, 99.9% purity, Carl Roth, Germany) and sterilized by autoclaving and 0.2 µm filtering. The pH was adjusted to 7.0 and the density to 2.0 g/ml (detailed protocol see suppl.). A mixture of unlabeled and fully ^{13}C-labeled RNA from *Escherichia coli* was run as a control. Samples were separated into 15 fractions and the density was measured by refraction index (refractometer AR200, Reichert Technologies, U.S.) The RNA was precipitated with linear polyacrylamide (LPA, 25 µg), isopropanol, and ammonium acetate. The concentration per fraction was measured by Quanti-iT RiboGreen. Fractions for sequencing were selected by density from heavy, i.e., RNA of labeled microorganisms, to light, i.e., not labeled RNA: ultra-heavy 1.839-1.849 g/ml, heavy 1.830 ± 0.002 g/ml, midpoint 1.810 ± 0.002 g/ml, light 1.799 ± 0.002 g/ml, ultra-light 1.786 ± 0.002 g/ml (suppl. Figure S1). cDNA was synthesized from selected fractions as described above. For ultra-heavy fractions, two fractions were pooled and used as template (suppl. Table S3).

5.1.3.6 Amplicon sequencing

The bacterial community composition was investigated by amplicon sequencing of the 16S rRNA gene V4 region. PCRs were performed using the primer pair Bac515F (5′-GTGYCAGCMGCCGCGGTAA-3′; Parada et al. 2016) and Bac805R

(5′-GACTACHVGGGTATCTAATCC-3′; Herlemann et al. 2011) with 8-bp barcodes attached at the 5`-end for multiplexing several samples per sequencing library. PCR reactions contained 1x KAPA HiFi buffer, 0.3 mM dNTP mix, 0.02 U KAPA HiFi DNA polymerase (KAPA Biosystems), 0.2 mg/ml bovine serum albumin (BSA), 1 mM $MgCl_2$, 1.5 µM each of forward and reverse primer and 2 ng template. The thermal cycling program was the following: initial denaturation at 95°C for 5 min, 30 cycles of denaturation 98°C: 13 s, annealing 60°C: 20 s, elongation 72°C: 20 s; followed by final elongation at 72°C for 1 min. PCR products were checked by agarose gel electrophoresis. For low-concentration samples, multiple PCR products from the same template were pooled in order to achieve enough amplicon. PCR products were purified (Monarch PCR and DNA Cleanup Kit, New England Biolabs, Germany), quantified (Quanti-iT PicoGreen) and pooled in equimolar amounts. Further library preparation and paired-end 2x 250 bp Illumina sequencing (Novaseq6000 platform) was performed by Novogene Co. Ltd. (Cambridge, UK).

5.1.3.7 Sequencing data analysis

The amplicon sequencing data was analyzed following Hassenrueck (2022) based on the dada2 pipeline (Callahan et al. 2016) as described in Wunder et al. (2024). The R software (v4.2.2, R Core Team 2022) was used with R package dada2 (v1.26.0). Sequences were trimmed to a total length of 290 bp (R1 100 or 115 bp, R2 190 or 175 bp, depending on sequencing library and error profile) and after merging, ASVs (amplicon sequence variant) with a length outside 249-254 bp or 300 bp were discarded. ASVs were assigned with the SILVA database (SSU Ref NR 99 release 138.1, Quast et al. 2012) with a bootstrap value of 80.

Further following analyses were performed in R (v4.4.2, R Core Team 2024) with packages tidyverse (v2.0.0, Wickham et al. 2019), taxa (v0.4.3, Foster et al. 2018), metacoder (v0.3.7, Foster et al. 2017) and phyloseq (v1.48.0, McMurdie and Holmes 2013). Overamplification of contamination sequences was observed due to low concentrations for some samples in the incubation data set (Davis et al. 2018). These sequences were identified and removed from the dataset using a combination of sequences identified by the R package decontam (v1.24.0, Davis et al. 2018), read count distribution and comparison of the taxonomic assignment with a list of known, abundantly found contaminating bacteria in laboratories and molecular kits (Knights et al. 2011, Salter et al. 2014) (see suppl. and Table S4 for details, 13 ASVs removed in total). In addition, all sequences outside Bacteria or associated with mitochondria and chloroplasts were removed. Sufficient sequencing depth per sample was checked with rarefaction curves (iNEXT package v3.0.1, Chao et al. 2014; suppl. Figure S2, Figure S3). Read counts were normalized by relative abundance calculations.

In the incubation data set from stable isotope probing, ASVs which were clearly labeled with the provided ^{13}C-substrate were identified by calculating $\overline{Rel.A}_{uh,h} > \overline{Rel.A}_{ul,l}$ with $\overline{Rel.A}_{uh,h}$ as the calculated average of the relative abundance per ASV in heavy and ultra-heavy fractions of ^{13}C-labeled treatments and $\overline{Rel.A}_{ul,l}$ as the calculated average in light and ultra-light fractions. Additionally to the taxonomic assignment during the sequence analysis pipeline, the abundant labeled ASVs were blasted with the blastn algorithm to identify the most similar sequences in the core nucleotide BLAST database, only including sequences from type material (blastn version 2.14.1+, online tool accessed 19.08.24, https://blast.ncbi.nlm.nih.gov/Blast.cgi?PROGRAM=blastn&PAGE_TYPE=BlastSearch&LINK_LOC=blasthome; Altschul et al. 1997; suppl. Table S5). Pairwise sequence dissimilarities were calculated between ASVs of the same taxonomic assignment and abundant ASVs from the same sampling location, Potter Cove (Wunder et al. 2024), using megablast (Zhang et al. 2000) (suppl. Table S5).

Raw sequences were uploaded to the ENA Short Reads Archive under the accession numbers PRJEB72873 (*in situ* DNA data), PRJEB83592 (*in situ* RNA data) and PRJEB83594 (incubation data) and all code used for the data analyses was submitted to the Github repository https://github.com/Microbial-Ecophysiology/sulfate-reducer-SIP-PotterCove.

5.1.4 Results

5.1.4.1 Geochemistry and microbial communities in Potter Cove sediments

In replicate sediment cores of station 14, dissolved ferrous iron (Fe^{2+}) and sulfate were measured in the pore water (Figure 2) to identify ongoing geochemical processes. A ferruginous zone was detected between 2-10 cm core depth with maximum Fe^{2+} concentrations of over 800 µM, which depleted to 0 µM towards the bottom of the core. Fe^{2+} concentrations differed between replicate cores, but followed the same trend. Sulfate concentrations decreased from 27 mM down to 20 mM between 3-15 cm core depth.

The bacterial community in sediments of station 14 was investigated by 16S rRNA sequencing, on DNA level for three replicate cores (STA14.01, STA14.03, STA14.04) and on RNA level for one core (STA14.04, Figure 3). The major represented classes were Bacteroidia, Desulfobacteria, and Gammaproteobacteria. While replicate core STA14.01 and STA14.03 showed very similar distributions of taxa on class level throughout the whole length of the core (Figure 3A, B), in core STA14.04, Bacteroidia and Gammaproteobacteria were four times more abundant in the top 4 cm than below (Figure 3C). Additionally, in core STA14.04 Desulfobulbia was nearly absent while Desulfobacteria was more abundant (20%) than in the

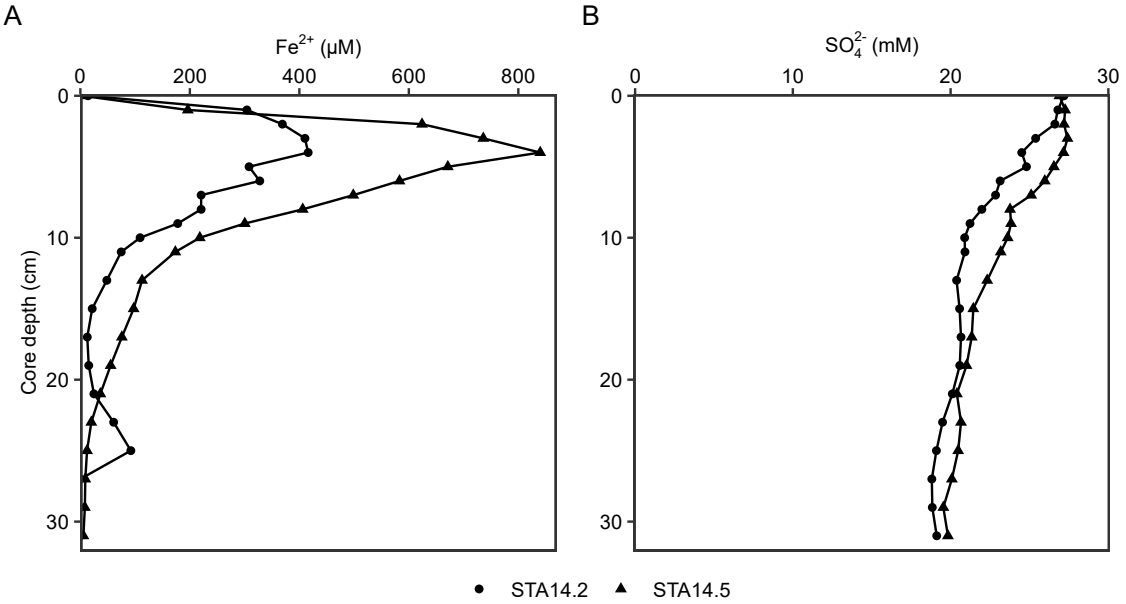

Figure 2: Dissolved Fe^{2+} (**A**) and sulfate (**B**) in pore water of *in situ* sediment cores from station 14. Duplicate cores STA14.02 (●) and STA14.05 (▲) of the same station were distinguished as indicated.

other two cores (14%). This distribution was also visible on RNA level (core STA14.04, Figure 3D). Here, Desulfobacteria was even more abundant with relative abundance values up to 47% in deeper sediment layers.

Investigating the distribution of members of the phylum Desulfobacterota in more detail, cores STA14.01 and STA14.03 showed a higher diversity on genus level, while in core STA14.04 only few taxa dominated. Cores STA14.01 and STA14.03 were dominated by different uncultivated *Desulfosarcinaceae* genera, (SEEP-SRB1, Sva0081, unclassified organism), the cable bacteria *Candidatus* Electrothrix, SEEP-SRB4 (family *Desulfocapsaceae*) and family Sva1033 (Figure 4A, B). Core STA14.04 was dominated only by *Desulfosarcinaceae* genera, especially an unclassified organism on DNA level (Figure 4C), and Sva0081 on RNA level (Figure 4D).

5.1.4.2 Incubation experiment

Incubation experiments were conducted to investigate the relevant active taxa for sulfate reduction, and by extension the sulfur cycle in Antarctic sediments. The influence of different electron donors, i.e., acetate and hydrogen as organic and inorganic fermentation products, was tested. Control treatments were set up without additional electron donors to observe activities thriving on endogenous sediment compounds. Further controls were set up using molybdate to inhibit sulfate reduction.

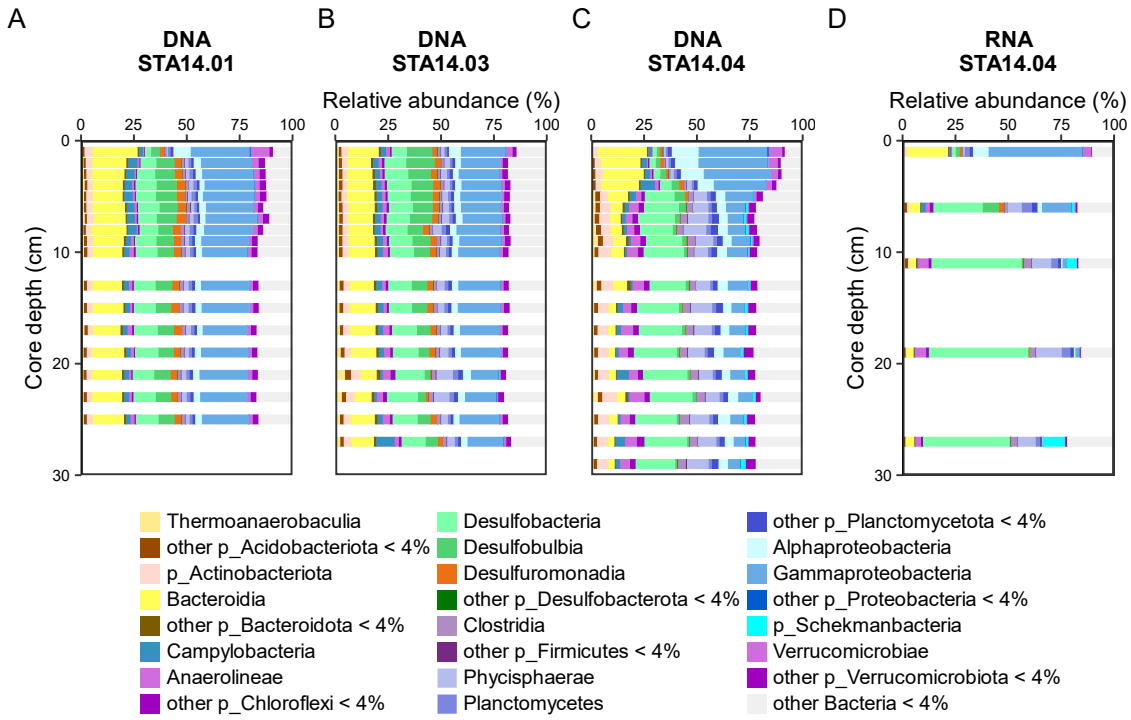

Figure 3: Bacterial community on class level in *in situ* sediments of station 14. Based on 16S rRNA gene (= DNA) sequencing for three replicate cores (A-C) and 16S rRNA (= RNA) sequencing for one core (D). Displayed were all classes with > 4% relative abundance in at least one sample. Some groups which crossed the 4% threshold only on phylum level were indicated by 'p_'.

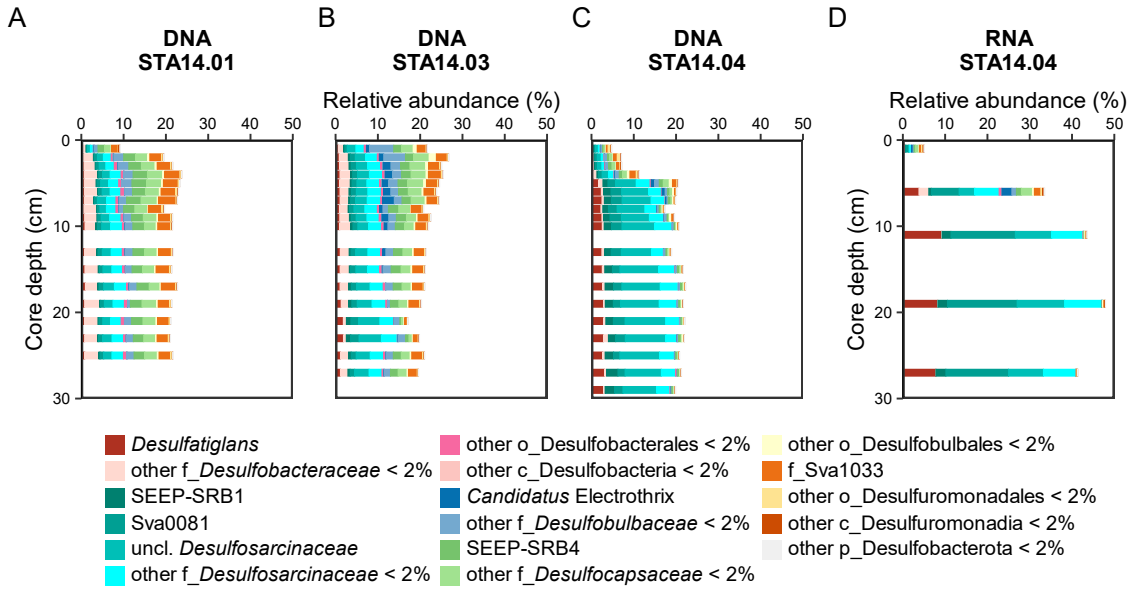

Figure 4: Phylum Desulfobacterota on genus level in *in situ* sediments of station 14. Based on 16S rRNA gene (= DNA) sequencing for three replicate cores (**A-C**) and 16S rRNA (= RNA) sequencing for one core (**D**). Displayed were all genera with > 2% relative abundance in at least one sample. The group Sva1033 has been classified to the family level, indicated by 'f_', as based on SILVA classification.

Geochemical signatures

During the incubation over 19 days, geochemical parameters were measured in the pore water in order to track the dominant biogeochemical processes. The treatment with hydrogen and acetate amendment (I) showed the highest increase of sulfide up to 300 µM, with one replicate even reaching above 3 mM (Figure 5A). All other treatments also increased in sulfide concentrations after 2 days, but only reaching 120-160 µM, if an additional electron donor was added (II, III) and generally staying lower for controls (VI, VII). The sulfide measurements for treatments containing molybdate (IV, V) could not be used because a false positive signal was detected, potentially by an interaction of measurement reagent and molybdate, an effect which was further confirmed by additional experiments (suppl. Figure S4, Figure S5). Ferrous iron concentrations in the slurry pore water stayed below 10 µM for all treatments except the controls with molybdate amendment. For these, ferrous iron increased up to an average of 13 µM with hydrogen amendment (IV) and up to 25 µM with acetate amendment (V) after 19 days (Figure 5B). Concentrations of easily dissolvable ferrous iron (solid phase ferrous iron dissolved with 0.5 M HCl in 1 h: ~ 5 mM) and sulfate (~ 25.5 mM) did not change over incubation time and between treatments (suppl. Figure S4). The hydrogen concentration in the gas phase decreased by ~ 25-50% in treatments amended with hydrogen within 8 days (I, III, IV; suppl. Figure S4).

Sulfate reduction rates were measured in 24 h-incubations of sub-samples of each treatment (Figure 6). At the start of the incubation, the sulfate reduction rate was ~ 1 nmol per cm³ slurry per day. The highest sulfate reduction rates were measured in the treatment with hydrogen and

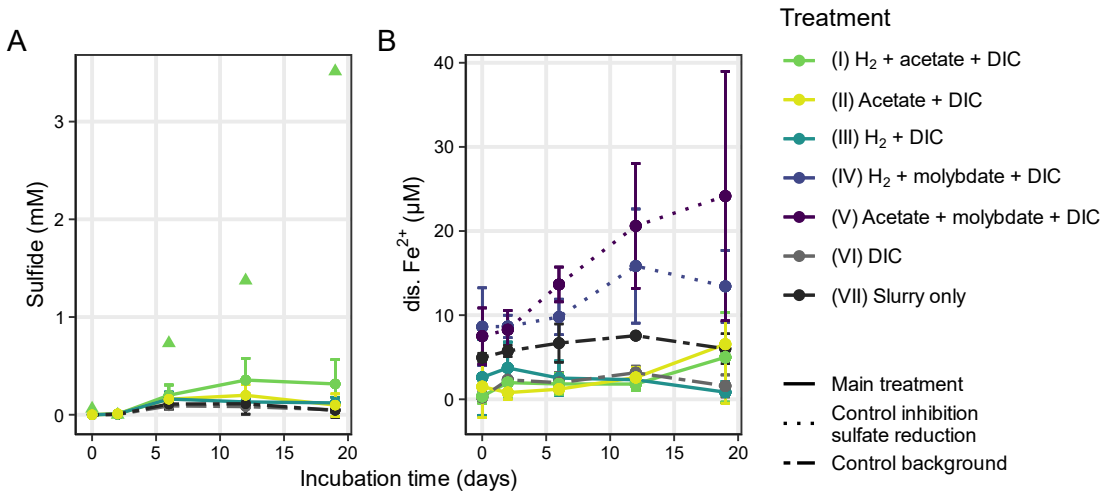

Figure 5: Geochemical measurements in pore water over time. Plotted was the calculated mean per treatment with error bars representing standard deviation for sulfide (**A**) and dissolved ferrous iron (**B**). Replicate 1 of treatment (I) with ^{13}C-labeled acetate (green filled triangle) in plot **A** and was not included in calculating the mean. Treatments were grouped into treatment purpose by line type.

acetate (I) at all time points, with a maximum of 9.2 nmol sulfate reduced per cm³ slurry per day at day 19, which was significantly higher than all other treatments ($p < 0.05$). The other treatments without molybdate addition (II, III, VI, VII) did not differ significantly ($p > 0.05$) from each other. As the slurry preparation included a six-time dilution of the initial sediment, the actual rate of sulfate reduced per cm³ sediment per day can be considered up to six times more, therefore between 6 and 60 nmol sulfate per cm³ sediment per day. Sulfate reduction rates were below the detection limit in molybdate-inhibited controls at all time points.

Active bacteria

RNA-SIP was performed in the incubation experiment, to identify microorganisms actively incorporating the ^{13}C-labeled substrates acetate or DIC (dissolved inorganic carbon) in the different treatments as an indication for coupling of biomass synthesis with the potentially occurring processes such as sulfate reduction or other reactions in the sulfur cycle. After density separation of the RNA, five fractions per sample were selected (suppl. Figure S1, Table S 3) representing the ^{13}C-labeled (= heavy) and unlabeled (= light) community in incubations with ^{13}C-labeled substrates. For each treatment, density separation of controls with unlabeled substrates was conducted to account for density shifts due to high content of guanosine and cytosine in RNA (Dumont and Murrell 2005). Isotope labeling of different taxa was visible in heavy fractions of treatments containing ^{13}C-labeled substrates, while these taxa were not present in heavy fractions of the associated unlabeled controls (suppl. Figure S6).

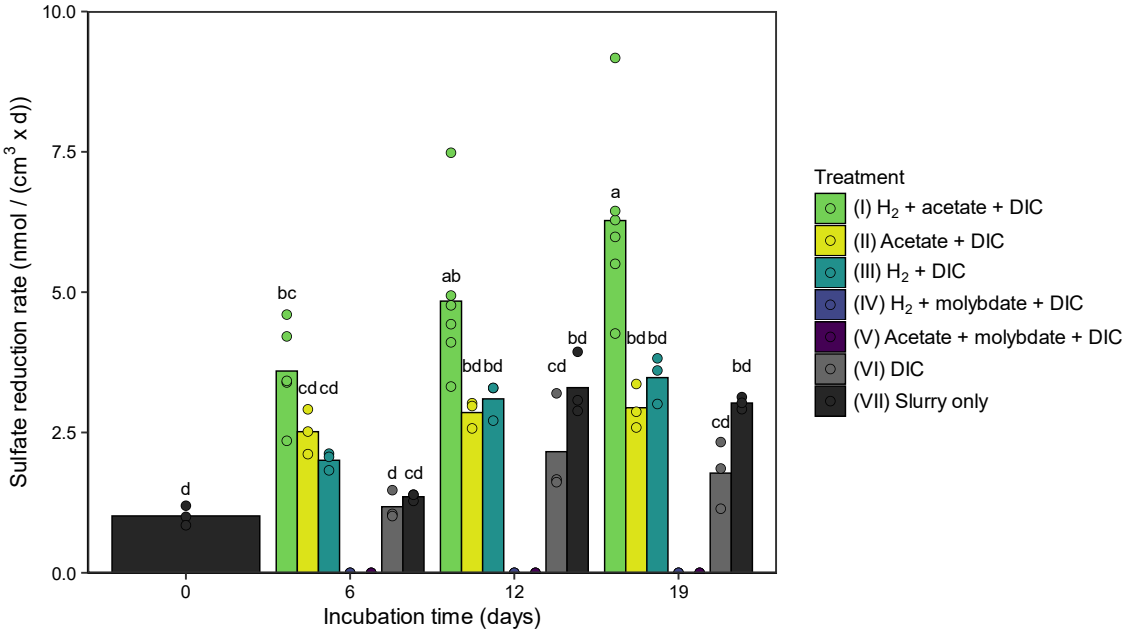

Figure 6: ^{35}S-sulfate reduction rates in nmol sulfate reduced per cm³ slurry per day over treatments and time. Bars represent the calculated mean per treatment and day, with replicates plotted individually as points. Multiple comparison statistics were calculated over all data points, excluding the molybdate amended treatments, which were below detection limit. Significant ($p < 0.05$) differences calculated with the general linear hypothesis test between treatments and time points were represented by letters, i.e., the same letter indicating no significant difference.

Sulfurimonas had the highest relative abundance among ^{13}C-labeled taxa in the treatment with acetate and hydrogen as electron donors (I), set up in two variants with either acetate or DIC containing a ^{13}C-label while the other one was unlabeled (Figure 7A). These were also the treatments with the highest sulfate reduction rate (Figure 6). Regardless of which substrate was ^{13}C-labeled, *Sulfurimonas* was strongly labeled: 88% relative abundance in heavy fractions (average heavy + ultra-heavy fraction) with ^{13}C-DIC or 64% with ^{13}C-acetate. *Sulfurimonas* was labeled when hydrogen was present with either ^{13}C-acetate (II) or ^{13}C-DIC (III) at a relative abundance of 35%. Labeling was much lower (10%) when only ^{13}C-DIC (VI) was present. The sulfate reduction inhibited control treatments with molybdate showed a small labeling of *Sulfurimonas* with ^{13}C-DIC (IV, 19%) but no labeling with ^{13}C-acetate (V, < 1%). While in all other treatments only one *Sulfurimonas* ASV was labeled, four different ASVs were labeled with ^{13}C-DIC, hydrogen and molybdate (IV) (suppl. Figure S7). The main labeled *Sulfurimonas* ASV was 99.2% similar to *Candidatus* Sulfurimonas marisnigri (suppl. Table S5).

Sulfurovum was the most labeled taxon with ^{13}C-DIC, hydrogen and molybdate (IV, 22%) and was not labeled in any other treatment (Figure 7B). It was mainly represented by one ASV, which was 97.6% similar to *Sulfurovum xiamenensis* (suppl. Figure S7, Table S5). Different members of the class Desulfobulbales were labeled with ^{13}C-DIC with (III) or without (VI) hydrogen (Figure 7C): most abundantly labeled in the control treatment containing only ^{13}C-DIC (VI) was the uncultured genus MSBL7 (family *Desulfurivibrionaceae*, 44%). It was also labeled with ^{13}C-DIC and hydrogen (III) in replicate 7 and 9 (~ 18%). Additionally, labeling with ^{13}C-DIC with (III) or without hydrogen (VI) was detected within the taxa *Desulfocapsa* (6%) and *Desulfobulbaceae* (10%). The ASV of *Desulfocapsa* was most similar to *Desulfocapsa sulfexigens* (97%, suppl. Table S5). *Desulfobulbaceae* was represented by two ASVs assigned as *Desulfobulbus* and two additional ASVs unclassified on genus level (suppl. Figure S7). Of the unclassified ASVs, one was most similar to two different *Candidatus* Electrothrix strains (96%, *Ca*. E. aestuarii, *Ca*. E. scaldis). The other ASV was most similar to *Desulfolithobacter dissulfuricans* (97.2%, suppl. Table S5). *Desulforhopalus* was the only member of Desulfobulbales labeled with ^{13}C-acetate, i.e., in the treatment with acetate and hydrogen (I, 3.5%). It was only slightly labeled with ^{13}C-DIC with (III) or without hydrogen (VI) (2%) and was most similar to *Desulforhopalus singaporensis* (98%, suppl. Table S5).

Apart from *Sulfurimonas*, all taxa majorly labeled with ^{13}C-acetate belonged to the order Desulfuromonadales (Figure 7D). The most abundant taxon *Desulfuromonas* was most labeled in the treatment with ^{13}C-acetate and molybdate (V, 46%) and to a lower extend with only ^{13}C-acetate (II, 28%) and with ^{13}C-acetate and hydrogen (I, 9%). It was mainly represented by one

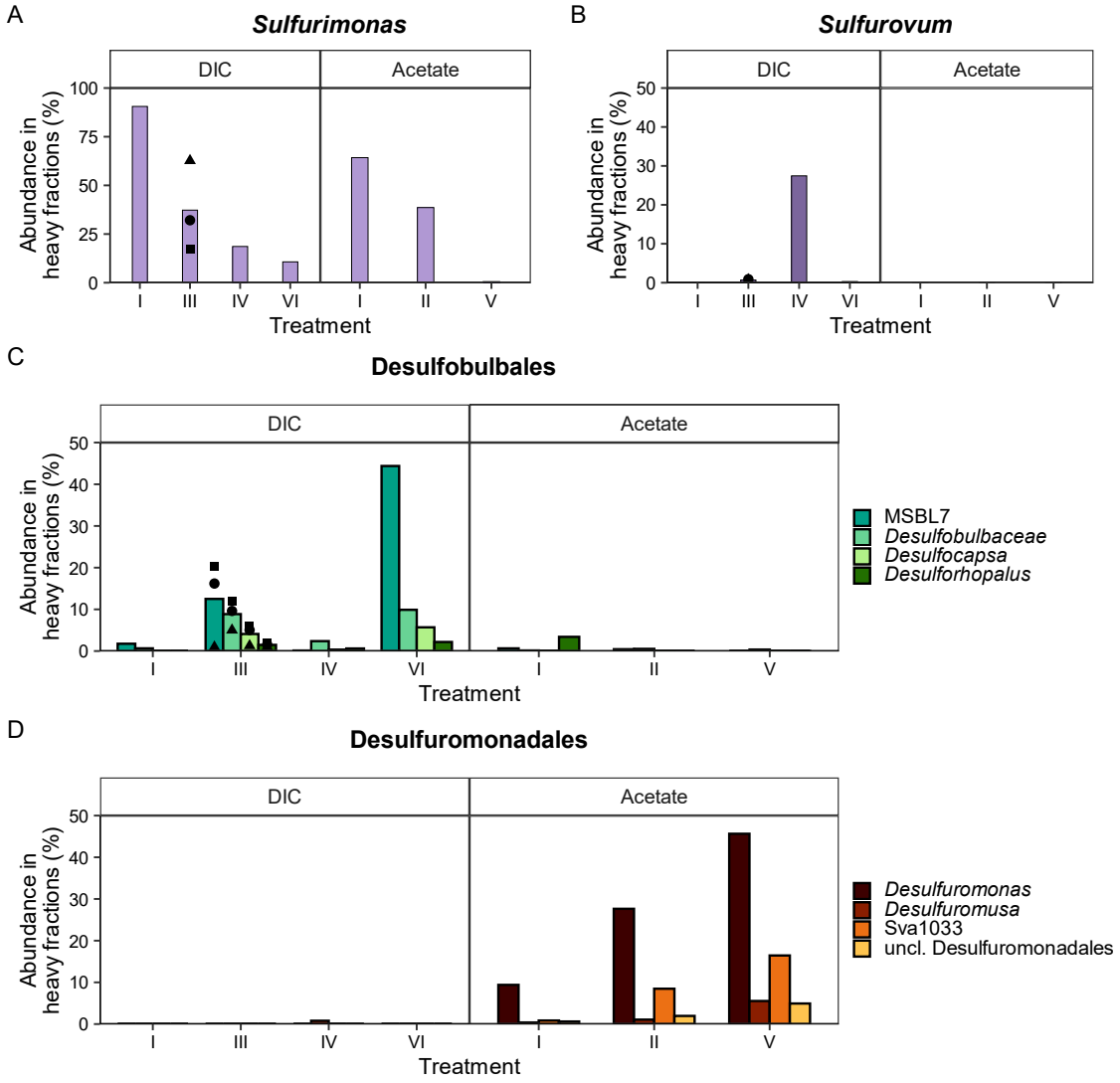

Figure 7: Dominant labeled community in RNA-SIP incubation experiments. Plotted were calculated average relative abundance of 16S rRNA in heavy fractions (heavy and ultra-heavy) for labeled taxa in ^{13}C-DIC and ^{13}C-acetate treatments (see methods for details). Treatments were I: H_2 + acetate + DIC, III: H_2 + DIC, IV: H_2 + DIC + molybdate, VI: DIC, II: Acetate + DIC, V: Acetate + DIC + molybdate. For treatment III, abundances of individual replicate bottles were plotted individually as replicate 7 (■), 8 (▲) and 9 (●) and the bar represents the calculated average. Note the different y-scale for plot **A**.

ASV (suppl. Figure S7), which was most similar to type strain *Desulfuromonas svalbardensis* (99.2%) and identical to the *Desulfuromonas* found in previous Potter Cove experiments (Wunder et al. 2024) (100%, suppl. Table S5). The unclassified family Sva1033 was most labeled with ^{13}C-acetate when sulfate reduction was inhibited by molybdate (V, 16%). It was represented by mostly two ASVs, which were identical to previously identified organisms in Potter Cove experiments (Wunder et al. 2024) (suppl. Table S5). *Desulfuromusa*, *Geothermobacter* and one ASV unclassified on family level (uncl. Desulfuromonadales) were labeled with ^{13}C-acetate in the presence of molybdate (V, each 5-6%, Figure 7D, suppl. Figure S7J).

Different taxa known for sulfate reduction were present in the light fractions of treatments with ^{13}C-substrates and in unlabeled controls. Across all treatments, members of the family *Desulfosarcinaceae* (up to 24% unlabeled fractions) were abundant, especially the uncultivated Sva0081 (up to 15% unlabeled fractions, suppl. Figure S6). In all treatments without molybdate, *Desulfocapsaceae* members, i.e., the uncultivated genus SEEP-SRB4 and one ASV unclassified on genus level, were present (up to 16% unlabeled fractions) but not in treatments where sulfate reduction and sulfur disproportionation was inhibited by molybdate addition (IV, V, < 1%, suppl. Figure S6).

5.1.5 Discussion

In temperate and Arctic marine sediments, sulfate reduction was shown as important electron-accepting process for organic matter degradation (Finke et al. 2007, Vandieken and Thamdrup 2013). Especially in polar environments with melting glaciers, other electron acceptors such as iron and manganese oxides are abundantly supplied by glacial meltwater (Wehrmann et al. 2014, Monien et al. 2017) and were shown to contribute to organic matter degradation in particular in glacial influenced sediments (Jørgensen et al. 2020), also at the study site Potter Cove (Aromokeye et al. 2021, Wunder et al. 2024). An open question remained which role sulfate reduction played for organic matter degradation in this environment and which were the conducting microorganisms.

In this study, concurrent iron and sulfate reduction in sediments of Potter Cove was indicated by geochemical profiles and an abundance of typical sulfate-reducing microorganisms in the sediments. The addition of potential electron donors for sulfate reduction, i.e., acetate and hydrogen, stimulated the process in RNA-SIP incubation experiments. However, the actual electron donor utilized for sulfate reduction remained elusive, as acetate and DIC, as representative substrates for a heterotrophic and autotrophic metabolisms, were both not assimilated by sulfate reducers. Instead, the typical sulfide oxidizer *Sulfurimonas* was highly labeled with both substrates, possibly oxidizing sulfide, produced by sulfate reduction, using an unknown electron acceptor.

5.1.5.1 Unexplained dominance of sulfate-reducing microorganisms in Potter Cove sediments

At the sampling site Potter Cove (STA14, Figure 1), decreasing sulfate concentrations and accumulation of dissolved ferrous iron in the pore water (Figure 2) indicated co-occurrence of sulfate reduction and iron reduction at similar sediment depths, as was found for other marine sediments previously (Canfield and Thamdrup 2009). Ferrous iron reached up to 800 µM in the top 10 cm, similar to surface sediments along the eastern continental shelf of the Antarctic

Peninsula (Baloza et al. 2022). Due to high ferrous iron concentrations, the associated, responsible microorganisms, i.e. iron reducers, were expected in the sediments. 16S rRNA gene sequencing of the *in-situ* microbial community detected the uncultivated family Sva1033 (Desulfuromonadales) (Ravenschlag et al. 1999), known for iron reduction (Wunder et al. 2021), as the most abundant taxon among potential iron reducers and likely involved in iron reduction in the sediment (up to 4%, Figure 4). Sva1033 was previously found in Potter Cove sediments and its capability of microbial iron reduction identified by RNA-SIP incubations in the presence of the low-crystalline iron oxide lepidocrocite (Aromokeye et al. 2021, Aromokeye et al. 2024, Wunder et al. 2024). Other known iron-reducing bacteria such as *Shewanella*, *Geobacter* or other Desulfuromonadales members (Lovley 2013) could not be detected (< 0.5%).

Instead, microorganisms of taxa which were associated with the sulfur cycle, particularly sulfate reduction, were highly abundant. Among these, especially sulfate reducers of the classes Desulfobacteria (up to 21%) and Desulfobulbia (up to 10%) were detected in the microbial community on 16S rRNA gene level (Figure 4) (Robador et al. 2015, Jørgensen et al. 2019). On 16S rRNA level, particularly *Desulfatiglans* (family *Desulfobacteraceae*, up to 9%), uncultured group Sva0081 (family *Desulfosarcinaceae*, up to 16%) and unclassified *Desulfosarcinaceae* members (up to 18%) were abundant (Figure 3D). These taxa were previously observed in surface sediments of Arctic and Antarctic sediments and indirectly associated with sulfate reduction (Robador et al. 2015, Buongiorno et al. 2019, Baloza et al. 2023). While high relative abundance on RNA level cannot directly be translated into activity, it can serve as indicator for protein synthesis potential in the future or as signature of past activity (Blazewicz et al. 2013). The high abundance of the sulfur cycling associated microorganisms on DNA (up to 22%) and RNA (up to 47%) level at the sampling site suggested that they were key microorganisms in these sediments.

Microbial sulfate reduction is one of the dominant terminal electron-accepting processes in marine sediments below the oxic zone (Jørgensen et al. 2019). The availability and quality of organic matter and electron acceptors, e.g., metal oxides and sulfate, influence the occurring processes (Jørgensen 1977). Especially in polar environments such as Antarctica, climate change induced global warming exerts environmental control on these processes, as increased glacial meltwater input supplies more iron oxides into the sediments, where they can be used as electron acceptors (Monien et al. 2017, Henkel et al. 2018). This constant fresh supply is likely responsible for the dominance of iron-reducing activity and utilization of acetate by iron reducers, even when no iron oxides were supplied to incubations (Aromokeye et al. 2024).

Acetate is known as important electron donor for sulfate reduction (Sørensen et al. 1981, Finke et al. 2007), however sulfate reducers could not be labeled with acetate in recent RNA-SIP experiments (Aromokeye et al. 2024, Yin et al. 2024). Therefore, the question arose whether sulfate reducers competed for substrates such as acetate with the iron reducers, or whether they rather performed an autotrophic lifestyle with an inorganic electron donor such as hydrogen (Nedwell and Banat 1981), or used an as of yet unidentified electron donor. In order to explore these questions, RNA-SIP slurry incubations with ^{13}C-labeled acetate, ^{13}C-DIC and hydrogen, alone or in combination, were performed and the sulfate reduction rates were monitored.

5.1.5.2 Stimulation of sulfate reduction by hydrogen and acetate as electron donors

The highest sulfate reduction rates were observed when both hydrogen and acetate were supplied (Figure 6). This agreed with observations from estuarine sediment (Oremland and Polcin 1982) and pure cultures, where sulfate reducers utilized hydrogen as electron donor and acetate solely as carbon source (Badziong et al. 1978). It has to be noted, that the rates measured in this study do not represent actual *in situ* gross sulfate reduction rates. Storage of the sediment and the slurry experiment itself likely influenced the rates; slurry preparation could have a stimulating effect by mixing and supply of fresh substrate (Michaud et al. 2020) but also a negative effect by increasing cell distances in diluted slurry. The actual *in situ* rate was likely between the measured rates ranging from 1-9 nmol reduced sulfate per cm³ slurry per day, and 6-60 nmol sulfate per cm³ sediment per day, the higher number as a result of multiplying by six for the slurry dilution effect. This was a lower rate compared to known sulfate reduction rates from other environments such as the Wadden Sea or the Baltic Sea (20-100 nmol cm^{-3} d^{-1} at *in situ* temperature), which was expected as sulfate reduction thrives at higher rates at mesophilic temperatures, such as in these temperate environments (Robador et al. 2015). Still, Potter Cove rates were comparable with *in situ* rates measured in polar environments such as Arctic fjords of Svalbard, e.g., Kongsfjorden with 10-40 nmol per cm³ and day between 2 and 20 cm core depth (Michaud et al. 2020). However, the measured rate was much smaller compared to 80-120 nmol sulfate per cm³ and day in the shelf-influenced Smeerenburgfjorden, where a clear decrease of sulfate and peak of ferrous iron in the top 10 cm were observed (Michaud et al. 2020), similar to our study (Figure 2). Sulfate-reducing microorganisms already thrived on unidentified residual, potentially organic, compounds in the slurry at the beginning of the incubation experiment, which was indicated by sulfate reduction rates at day 0. However, the increasing rate over time, especially when additional substrate was supplied (Figure 6), suggested that the sediment was starved for electron donors and microorganisms were activated again by their addition. This showed that microorganisms with the ability to utilize acetate and

hydrogen, coupled to sulfate reduction, were present in sediments of Potter Cove and could be stimulated by the addition of these substrates. These active organisms were investigated by RNA-SIP. The comparison of light and heavy fractions of treatments with ^{13}C-labeled substrates allowed to identify microorganisms actively incorporating provided acetate or DIC, i.e., defining them as ^{13}C-labeled organisms (suppl. Figure S7).

5.1.5.3 Surprising lack of labeled sulfate reducers despite sulfate reduction

As the highest sulfate reduction rates were observed in the treatment with acetate and hydrogen (I, Figure 6), we expected the labeling of typical sulfate reducers i.e., abundance in the heavy fractions. Surprisingly, these were not found in the heavy but in the light fractions, especially in treatments with hydrogen addition (Figure 7, suppl., Figure S6A (I), B (III)). The most abundant families were *Desulfosarcinaceae* (Sva0081 and unassigned genera) and *Desulfocapsaceae* (SEEP-SRB4 and unassigned genus closest related to *Desulfomarina profundi*), which both harbor sulfate-reducing microorganisms (Knittel et al. 2003, Dyksma et al. 2017, Wasmund et al. 2017, Watanabe et al. 2017, Jørgensen et al. 2019, Hashimoto et al. 2021, Yin et al. 2024). *Desulforhopalus* was the only known sulfate reducer labeled with ^{13}C-acetate in the presence of hydrogen (I, 3.5%, Figure 7C). The utilization of acetate as carbon source while using hydrogen as electron donor is known for *Desulforhopalus vacuolatus* (Isaksen and Teske 1996), but not for *Desulforhopalus singaporensis* (Lie et al. 1999), the most similar species to the microorganisms found in this incubation (98% identity, suppl. Table S5). We suggest that the detected *Desulforhopalus* species reduced sulfate with hydrogen as electron donor and assimilated carbon from acetate.

The overall very low abundance and labeling of known sulfate reducers with acetate was unexpected, as acetate was identified as major electron donor for sulfate reduction in multiple marine sediments (Sørensen et al. 1981, Winfrey and Ward 1983, Vandieken et al. 2006b) and is the central intermediate of the anaerobic microbial food chain (LaRowe et al. 2020). However, similar observations of a lack of labeled sulfate reducers were made previously in SIP experiments with acetate (Cho et al. 2020, Wunder et al. 2021, Yin et al. 2024). One possible explanation was that sulfate-reducing microorganisms preferred fermentation products of higher molecular mass such as lactate or butyrate. Multiple sulfate reducers are known to perform only incomplete oxidation of small organic molecules producing acetate but cannot thrive on acetate itself (Oremland and Silverman 1979, Lie et al. 1999). In order to test this hypothesis, more experiments would be needed such as SIP incubations with relevant ^{13}C-labeled substrates for which incomplete oxidation is possible, e.g., propionate and butyrate,

or quantification of accumulating fermentation products when sulfate reduction is inhibited (Sørensen et al. 1981).

Another possible explanation was that the present sulfate reducers did not compete for organic compounds with other microorganisms such as iron reducers but fixed CO_2 instead. Some microorganisms phylogenetically associated with sulfate reduction were labeled with ^{13}C-DIC in treatments with occurring sulfate reduction (III, VI, Figure 6), i.e., *Desulfobulbaceae*, *Desulfocapsa* and unclassified genus MSBL7 (Häusler et al. 2014, Jørgensen et al. 2019, Slobodkin and Slobodkina 2019), but not in the treatment containing acetate and hydrogen (I) with the highest sulfate reduction (Figure 7C). This labeling clearly showed their capability of an autotrophic lifestyle, in accordance with previous findings for species of *Desulfobulbaceae* and *Desulfocapsa* (Slobodkin and Slobodkina 2019). The lack of labeling in the treatment with acetate and hydrogen (I) might have been due to the high labeling of *Sulfurimonas* in this treatment, masking the labeling of other organisms due to relative abundance effects. Furthermore, while their absence in molybdate-inhibited treatments suggested a link to sulfate reduction, especially the high relative abundance in the DIC-only control (VI) raised the question of the used electron donor. One possibility was that they did not perform sulfate reduction but instead disproportionation of sulfur compounds, as especially many *Desulfocapsa* species are known for this metabolism (Slobodkin and Slobodkina 2019). A lack of labeling in the molybdate amended control (IV, Figure 7C), where both, sulfate reduction and sulfur disproportionation were inhibited (Peck 1959, Finster et al. 1998), further supported this hypothesis. The unclassified *Desulfobulbaceae* bacteria labeled in this study were most closely related to different cable bacteria *Electrothrix* species and *Desulfolithobacter dissulfuricans*, however only with 96-97% identity (suppl. Table S5). These taxa were previously shown to perform sulfur disproportionation and/or sulfur oxidation (Hashimoto et al. 2022, Wang et al. 2023b). However in this study, they were still labeled to a low amount in the molybdate inhibited treatment (IV, V).

While the stimulation of sulfate reduction by supplying a combination of acetate and hydrogen was a known observation from previous studies (e.g., Smith and Klug 1981, Oremland and Polcin 1982), an open question remained why the activity of sulfate reducers could not be directly linked to both substrates. It was possible, that present sulfate reducers had an underlying activity and were already present and active at the beginning of the incubation, but did not synthesize more fresh RNA over time which could contain the heavier ^{13}C isotope. This was supported by sulfate reduction already at the beginning of the experiment, and would explain their abundance in the light fractions. Vandieken and Thamdrup (2013) suggested that

the labeling in SIP studies might not reflect the importance of the process, if processes with lower and higher energy yield co-occurred. Another possible explanation was that other microorganisms originally competed with sulfate reducers for the same substrates, but were able to use the provided acetate and hydrogen and therefore the addition of these substrates eliminated the competition for the original substrates, allowing sulfate reduction to thrive. We hypothesize that the unlabeled sulfate reducers in the light fractions were responsible for observed sulfate reduction rates.

5.1.5.4 *Sulfurimonas* as most active microorganism likely oxidizing sulfide

With typical sulfate reducers not incorporating the ^{13}C-label, we sought to identify the main active organisms by RNA-SIP. *Sulfurimonas* was the most labeled microorganism in SIP incubations with acetate and hydrogen (I), and incorporated both, ^{13}C-acetate and ^{13}C-DIC (Figure 7A), demonstrating its metabolic flexibility as mixotroph. Its labeling was lower with acetate than with DIC (Figure 7A), likely due to acetate depletion in the sediment prior to the experiment (Aromokeye et al. 2021) so that the organism needed some time to initialize the acetate utilization pathway again, resulting in less incorporation of acetate than the ^{13}C-label of DIC (Perrin et al. 2020). *Sulfurimonas* species are generally known as autotrophs (Inagaki et al. 2003, Takai et al. 2006, Wang et al. 2021b), but the species *Candidatus* Sulfurimonas baltica can also use acetate (97.6% identity to the labeled ASV in this study, suppl. Table S5), while the most closely related species *Candidatus* Sulfurimonas marisnigri (99.2% identity) is not able to use acetate (Henkel et al. 2021).

Sulfurimonas was most labeled in the treatment with the highest sulfate reduction rate (I), but was also labeled with either hydrogen or acetate alone as supplied electron donor (II, III, Figure 6A). In sulfate reduction inhibited controls with molybdate, it was only labeled to a lower extent with hydrogen addition (IV) and completely absent in heavy fractions if only acetate was supplied (V). This indicated that its activity was linked to sulfur cycling which was inhibited by molybdate, so likely sulfate reduction or sulfur compound disproportionation (Peck 1959, Finster et al. 1998).

One hypothesis was that *Sulfurimonas* itself was responsible for the observed sulfate-reducing activity. However, this genus was never linked to sulfate reduction previously; all isolated strains which were tested for sulfate reduction could not perform it (Inagaki et al. 2003, Cai et al. 2014, Wang et al. 2020). Furthermore, the marker gene for sulfate reduction, i.e., dissimilatory sulfite reductase (DSR, Santos et al. 2015), was never detected in any *Sulfurimonas* genomes (Wang et al. 2021a), so sulfate reduction by this taxon would be a very novel finding. Another possibility was an indirect coupling to sulfate reduction by the oxidation

of sulfide produced via sulfate reduction by the microorganisms discussed above. Sulfide is a well-known electron donor for many *Sulfurimonas* species (Inagaki et al. 2003, Han and Perner 2015, Ding et al. 2022), including *Candidatus* Sulfurimonas marisnigri and *Candidatus* S. baltica which couple sulfur oxidation to manganese reduction (Henkel et al. 2021), the closest relatives to the *Sulfurimonas* ASVs identified in our study (99.2%, 97.6% identity, suppl. Table S5).

Acetate could also serve as electron donor for *Sulfurimonas*. However, no labeling of *Sulfurimonas* was observed in the molybdate inhibited treatment with acetate (V, Figure 7A). Following the hypothesis of sulfide oxidation by *Sulfurimonas*, in this treatment any sulfide production by sulfate reduction or sulfur compound disproportionation was inhibited. Additionally, the free ferrous iron would react rapidly with any sulfide potentially produced by sulfur reduction (Figure 5) (Jørgensen 1977). To further confirm the hypothesis that there was no free sulfide present in the molybdate inhibited treatment with acetate (V), a technique for measuring sulfide would be necessary which is not influenced by the present molybdate (suppl. Figure S5, result section). *Sulfurimonas* was labeled in the other molybdate inhibited control with hydrogen and ^{13}C-DIC (IV, Figure 7A), however to a lower extent and the present ASVs were more diverse (suppl. Figure S7A). Here, free sulfide as electron donor could still have been produced by reduction of present endogenous sulfur or thiosulfate coupled to hydrogen oxidation by the labeled taxon *Sulfurovum* (Figure 7B), which is known for this metabolism (Wang et al. 2023a). The very low abundance of *Sulfurovum* in the other treatments with hydrogen addition (I, III) might have been a relative abundance artifact, i.e., it was similarly active, but due to the high activity and therefore abundance of other taxa, its abundance was proportionally less.

The next open question was which electron acceptor *Sulfurimonas* used for sulfide oxidation. Its usual electron acceptors, oxygen and nitrate (Inagaki et al. 2003, Takai et al. 2006, Labrenz et al. 2013, Wang et al. 2021b), were expected to be depleted in the slurry material after long, anoxic storage conditions and because typical organisms associated with these substrates were not detected. Residual metal oxides, i.e., iron or manganese oxides, might have served as electron acceptors, masked by the sediment background. However, then these acceptors were not linked to acetate as electron donor, as otherwise an activity in the treatment with acetate and molybdate (V) should have been visible (Figure 7A). Additionally, in a previous study with Potter Cove sediments, no iron-reducing (Aromokeye et al. 2021, Aromokeye et al. 2024) or manganese-reducing activities were observed by *Sulfurimonas* (Wunder et al. 2024), despite the possibility of manganese reduction by the closely related species *Candidatus* Sulfurimonas

marisnigri (Henkel et al. 2019). Sulfur disproportionation cannot be excluded, as it was recently shown for some *Sulfurimonas* species (Wang et al. 2023b). Though the closest related species *Candidatus* Sulfurimonas marisnigri is not capable of disproportionation (Henkel et al. 2021) and, even though a clearly negative effect of molybdate on *Sulfurimonas* was visible, the microorganism was not completely inhibited by it.

However, *Sulfurimonas* was previously found in a biofilm grown on an anode as electron acceptor (Zhang et al. 2014) and was proposed to use cable bacteria as electron sink if its usual electron acceptors were depleted (Vasquez-Cardenas et al. 2015, Wasmund et al. 2017). Therefore, we propose that *Sulfurimonas* could potentially use another microorganism as electron sink or that it may have used residual metal oxides in the sediment as electron acceptor similarly to its known closest relatives (*Cand*. S. marisnigri 99.2% identity). Its close relationship to a species capable of electron transfer to a solid acceptor (Henkel et al. 2019, Henkel et al. 2021) increased the probability that it had the metabolic capabilities for direct electron transfer (McInerney et al. 2009). To clarify what electron acceptor was being used by *Sulfurimonas* to control the sulfur cycle in these Antarctic sediments, isolation of this strain is essential and a focus of further studies. Further investigation is needed to identify possible partner microorganisms, potentially also in the archaeal community which was not explored in this study, and identify the ultimate terminal electron acceptor used by this partner.

5.1.5.5 Implications for processes in Potter Cove sediments

In the sediments of the central area of Potter Cove (STA14), sulfate and iron reduction likely co-occurred as dominating terminal electron-accepting processes. *In situ*, microorganisms associated with sulfate reduction showed a higher relative abundance over known iron reducers despite high ferrous iron concentrations suggesting a dominance of iron over sulfate reduction. While this study was not designed to investigate direct competition for catabolic electron donors for these terminal electron-accepting processes, the ability to utilize acetate and hydrogen for them could be investigated.

The contribution of iron reduction to organic matter degradation, i.e., here acetate utilization, was shown previously for these sediments (Aromokeye et al. 2021). Also in the current study, members of the class Desulfuromonadales, typically known for iron reduction (Lovley 2013), were labeled with ^{13}C-acetate especially in the molybdate amended treatment (V, Figure 7D) with the highest ferrous iron accumulation (Figure 5B). This indicated that they likely thrived on residual iron oxides in the sediment, rather utilizing the acetate than competing for the hydrogen. All labeled taxa (suppl. Figure S7 I, J, K, L) were previously known to be capable of iron reduction with acetate (Kashefi et al. 2003, Sung et al. 2003, Holmes et al. 2004,

Vandieken et al. 2006a, Wunder et al. 2021). The same or very closely related organisms, i.e. *Desulfuromusa*, *Desulfuromonas* and Sva1033 (100% identity based on 250 bp 16S rRNA sequence, suppl. Table S5), were found in previous incubation experiments conducted with sediment from Potter Cove (Aromokeye et al. 2024, Wunder et al. 2024). This indicated Desulfuromonadales as key acetate utilizers in the sediments of Potter Cove.

Our study suggests that sulfate reduction was not coupled in a similar way to acetate oxidation. In the slurry experiment, most of the sulfate reducers identified did not use acetate but either thrived with a low activity on not labeled compounds or on the oxidation of hydrogen, a metabolism previously shown in salt marsh sediments (Nedwell and Banat 1981). Instead, the sulfide oxidizer *Sulfurimonas* used the provided acetate and could fix CO_2. Utilization of hydrogen or disproportionation of sulfur compounds could not be confirmed or denied. In the *in situ* sediment, this taxon had relative abundances of only < 1-5% (Figure 3, Campylobacteria), but got highly stimulated in the incubations when the sulfate reduction activity was also high. Likely, *Sulfurimonas* outcompeted the iron reducers for acetate as a fresh supply of iron oxides was lacking, but at *in situ* conditions with constant supply of fresh iron by glacial meltwater, the iron reducers would have the advantage (Aromokeye et al. 2024). Furthermore, the incubations were a closed system, while *in situ* part of the ferrous iron was likely reoxidized to easily reducible ferric iron oxides by diffusion to the oxic surface, which could then be reduced again, causing increased iron cycling as suggested for Arctic fjords (Laufer-Meiser et al. 2021). This likely stimulated microbial iron reduction rates *in situ* further. An open question remained which microorganisms detected in the *in situ* sediments were active at the time of sampling and which were dormant awaiting their opportunity to thrive again under environmentally more favorable conditions. For example, during winter the supply of fresh organic matter and glacial meltwater is expected to be lower than in summer, possibly providing an opportunity for the sulfate reducers to thrive when fresh iron oxides are lacking. Another environmental factor connected to global warming is temperature increase, a scenario studied recently in this environment showing the potential of already present microorganisms to keep up the functions of this environment, i.e., organic matter mineralization in form of acetate oxidation (Aromokeye et al. 2024). This previous study and the present study both demonstrated that sulfur cycling and sulfide oxidizing microorganisms, in particular *Sulfurimonas*, utilized acetate, potentially not as electron donor but carbon source. This demonstrated further how the sulfur cycle in theses sediments was tightly linked with organic matter degradation.

5.1.5 References

Altschul, S. F., T. L. Madden, A. A. Schäffer, J. Zhang, Z. Zhang, W. Miller, and D. J. Lipman. (1997). Gapped BLAST and PSI-BLAST: A new generation of protein database search programs. Nucleic Acids Res. **25**:3389-3402. doi:10.1093/nar/25.17.3389.

Arndt, S., B. B. Jørgensen, D. E. LaRowe, J. Middelburg, R. Pancost, and P. Regnier. (2013). Quantifying the degradation of organic matter in marine sediments: A review and synthesis. Earth-Sci. Rev. **123**:53-86. doi:10.1016/j.earscirev.2013.02.008.

Aromokeye, A. D., G. Willis-Poratti, L. C. Wunder, X. Yin, T. Richter-Heitmann, C. Otersen, M. D. Maeke, S. Henkel, C. Neder, S. Vázquez, M. Elvert, W. Mac Cormack, and M. W. Friedrich. (2024). Global warming facilitated environmental change effects on CO_2 releasing microbes in Antarctic sediments. PREPRINT (Version 1) available at Research Square. doi:10.21203/rs.3.rs-5441636/v1.

Aromokeye, D. A., G. Willis-Poratti, L. C. Wunder, X. Yin, J. Wendt, T. Richter-Heitmann, S. Henkel, S. Vázquez, M. Elvert, W. Mac Cormack, and M. W. Friedrich. (2021). Macroalgae degradation promotes microbial iron reduction via electron shuttling in coastal Antarctic sediments. Environ. Int. **156**:106602. doi:10.1016/j.envint.2021.106602.

Badziong, W., R. K. Thauer, and J. G. Zeikus. (1978). Isolation and characterization of *Desulfovibrio* growing on hydrogen plus sulfate as the sole energy source. Arch. Microbiol. **116**:41-49. doi:10.1007/BF00408732.

Baloza, M., S. Henkel, W. Geibert, S. Kasten, and M. Holtappels. (2022). Benthic carbon remineralization and iron cycling in relation to sea ice cover along the Eastern Continental Shelf of the Antarctic Peninsula. J. Geophys. Res. (C Oceans) **127**:e2021JC018401. doi:10.1029/2021JC018401.

Baloza, M., S. Henkel, S. Kasten, M. Holtappels, and M. Molari. (2023). The impact of sea ice cover on microbial communities in Antarctic shelf sediments. Microorganisms **11**:1572. doi:10.3390/microorganisms11061572.

Beulig, F., H. Røy, C. Glombitza, and B. B. Jørgensen. (2018). Control on rate and pathway of anaerobic organic carbon degradation in the seabed. Proc. Natl. Acad. Sci. USA **115**:367-372. doi:10.1073/pnas.1715789115.

Blazewicz, S. J., R. L. Barnard, R. A. Daly, and M. K. Firestone. (2013). Evaluating rRNA as an indicator of microbial activity in environmental communities: Limitations and uses. ISME J. **7**:2061-2068. doi:10.1038/ismej.2013.102.

Bowman, J. P., S. M. Rea, S. A. McCammon, and T. A. McMeekin. (2000). Diversity and community structure within anoxic sediment from marine salinity meromictic lakes and a coastal meromictic marine basin, Vestfold Hills, Eastern Antarctica. Environ. Microbiol. **2**:227-237. doi:10.1046/j.1462-2920.2000.00097.x.

Buongiorno, J., L. Herbert, L. Wehrmann, A. Michaud, K. Laufer, H. Røy, B. Jørgensen, A. Szynkiewicz, A. Faiia, and K. Yeager. (2019). Complex microbial communities drive iron and sulfur cycling in Arctic fjord sediments. Appl. Environ. Microbiol. **85**:e00949-00919. doi:10.1128/AEM.00949-19.

Burdige, D. J., T. Komada, C. Magen, and J. P. Chanton. (2016). Carbon cycling in Santa Barbara Basin sediments: A modeling study. J. Mar. Res. **74**:133-159. doi:10.1357/002224016819594818.

Cai, L., M.-F. Shao, and T. Zhang. (2014). Non-contiguous finished genome sequence and description of *Sulfurimonas hongkongensis* sp. nov., a strictly anaerobic denitrifying, hydrogen- and sulfur-oxidizing chemolithoautotroph isolated from marine sediment. Stand. Genom. Sci. **9**:1302-1310. doi:10.4056/sigs.4948668.

Callahan, B. J., P. J. McMurdie, M. J. Rosen, A. W. Han, A. J. A. Johnson, and S. P. Holmes. (2016). DADA2: High-resolution sample inference from Illumina amplicon data. Nat. Methods **13**:581-583. doi:10.1038/nmeth.3869.

Canfield, D. E., B. B. Jørgensen, H. Fossing, R. Glud, J. Gundersen, N. B. Ramsing, B. Thamdrup, J. W. Hansen, L. P. Nielsen, and P. O. J. Hall. (1993). Pathways of organic carbon oxidation in three continental margin sediments. Mar. Geol. **113**:27-40. doi:10.1016/0025-3227(93)90147-N.

Canfield, D. E. and B. Thamdrup. (2009). Towards a consistent classification scheme for geochemical environments, or, why we wish the term 'suboxic' would go away. Geobiology **7**:385-392. doi:10.1111/j.1472-4669.2009.00214.x.

Chao, A., N. J. Gotelli, T. C. Hsieh, E. L. Sander, K. H. Ma, R. K. Colwell, and A. M. Ellison. (2014). Rarefaction and extrapolation with Hill numbers: A framework for sampling and estimation in species diversity studies. Ecol. Monogr. **84**:45-67. doi:10.1890/13-0133.1.

Cho, H., B. Kim, J. S. Mok, A. Choi, B. Thamdrup, and J. H. Hyun. (2020). Acetate-utilizing microbial communities revealed by stable-isotope probing in sediment underlying the upwelling system of the Ulleung Basin, East Sea. Mar. Ecol. Prog. Ser. **634**:45-61. doi:10.3354/meps13182.

Cline, J. D. (1969). Spectrophotometric determination of hydrogen sulfide in natural waters. Limnol. Oceanogr. **14**:454-458. doi:10.4319/lo.1969.14.3.0454.

Davis, N. M., D. M. Proctor, S. P. Holmes, D. A. Relman, and B. J. Callahan. (2018). Simple statistical identification and removal of contaminant sequences in marker-gene and metagenomics data. Microbiome **6**:226. doi:10.1186/s40168-018-0605-2.

Death, R., J. L. Wadham, F. Monteiro, A. M. Le Brocq, M. Tranter, A. Ridgwell, S. Dutkiewicz, and R. Raiswell. (2014). Antarctic ice sheet fertilises the Southern Ocean. Biogeosciences **11**:2635-2643. doi:10.5194/bg-11-2635-2014.

Ding, S., J. V. Henkel, E. C. Hopmans, N. J. Bale, M. Koenen, L. Villanueva, and J. S. Sinninghe Damsté. (2022). Changes in the membrane lipid composition of a *Sulfurimonas* species depend on the electron acceptor used for sulfur oxidation. ISME commun. **2**:121. doi:10.1038/s43705-022-00207-3.

Dumont, M. G. and J. C. Murrell. (2005). Stable isotope probing – Linking microbial identity to function. Nat. Rev. Microbiol. **3**:499-504. doi:10.1038/nrmicro1162.

Dyksma, S., P. Pjevac, K. Ovanesov, and M. Mussmann. (2017). Evidence for H_2 consumption by uncultured *Desulfobacterales* in coastal sediments. Environ. Microbiol. **20**:450-461. doi:10.1111/1462-2920.13880.

Finke, N., V. Vandieken, and B. B. Jørgensen. (2007). Acetate, lactate, propionate, and isobutyrate as electron donors for iron and sulfate reduction in Arctic marine sediments, Svalbard. FEMS Microbiol. Ecol. **59**:10-22. doi:10.1111/j.1574-6941.2006.00214.x.

Finster, K., W. Liesack, and B. Thamdrup. (1998). Elemental sulfur and thiosulfate disproportionation by *Desulfocapsa sulfoexigens* sp. nov., a new anaerobic bacterium isolated from marine surface sediment. Appl. Environ. Microbiol. **64**:119-125. doi:10.1128/aem.64.1.119-125.1998.

Flieder, M., J. Buongiorno, C. W. Herbold, B. Hausmann, T. Rattei, K. G. Lloyd, A. Loy, and K. Wasmund. (2021). Novel taxa of Acidobacteriota implicated in seafloor sulfur cycling. ISME J. doi:10.1038/s41396-021-00992-0.

Foster, Z. S. L., S. Chamberlain, and N. J. Grünwald. (2018). Taxa: An R package implementing data standards and methods for taxonomic data. F1000research **7**:272. doi:10.12688/f1000research.14013.2.

Foster, Z. S. L., T. J. Sharpton, and N. J. Grünwald. (2017). Metacoder: An R package for visualization and manipulation of community taxonomic diversity data. PLoS Comp. Biol. **13**:e1005404. doi:10.1371/journal.pcbi.1005404.

Froelich, P. N., G. P. Klinkhammer, M. L. Bender, N. A. Luedtke, G. R. Heath, D. Cullen, P. Dauphin, D. Hammond, B. Hartman, and V. Maynard. (1979). Early oxidation of organic matter in pelagic sediments of the eastern equatorial Atlantic: Suboxic diagenesis. Geochim. Cosmochim. Acta **43**:1075-1090. doi:10.1016/0016-7037(79)90095-4.

[Dataset] Gerrish, L. (2020). Automatically extracted rock outcrop dataset for Antarctica (7.3). UK Polar Data Centre, Natural Environment Research Council, UK Research & Innovation. doi:10.5285/178ec50d-1ffb-42a4-a4a3-1145419da2bb.

Han, Y. and M. Perner. (2015). The globally widespread genus *Sulfurimonas*: Versatile energy metabolisms and adaptations to redox clines. Front. Microbiol. **6**. doi:10.3389/fmicb.2015.00989.

Hashimoto, Y., S. Shimamura, A. Tame, S. Sawayama, J. Miyazaki, K. Takai, and S. Nakagawa. (2022). Physiological and comparative proteomic characterization of *Desulfolithobacter dissulfuricans* gen. nov., sp. nov., a novel mesophilic, sulfur-disproportionating chemolithoautotroph from a deep-sea hydrothermal vent. Front. Microbiol. **13**. doi:10.3389/fmicb.2022.1042116.

Hashimoto, Y., A. Tame, S. Sawayama, J. Miyazaki, K. Takai, and S. Nakagawa. (2021). *Desulfomarina profundi* gen. nov., sp. nov., a novel mesophilic, hydrogen-oxidizing, sulphate-reducing chemolithoautotroph isolated from a deep-sea hydrothermal vent chimney. Int. J. Syst. Evol. Microbiol. **71**. doi:10.1099/ijsem.0.005083.

Hassenrueck, C. (2022). Paired-end amplicon sequence processing workflow configurable for mixed-orientation libraries and highly variable insert size. Version 1.2.0. doi:10.12754/misc-2022-0002. Available from: https://git.io-warnemuende.de/bio_inf/workflow_templates/src/branch/master/Amplicon_dada2_MiSeq.

Häusler, S., M. Weber, C. Siebert, M. Holtappels, B. E. Noriega-Ortega, D. De Beer, and D. Ionescu. (2014). Sulfate reduction and sulfide oxidation in extremely steep salinity gradients formed by freshwater springs emerging into the Dead Sea. FEMS Microbiol. Ecol. **90**:956-969. doi:10.1111/1574-6941.12449.

Henkel, J. V., O. Dellwig, F. Pollehne, D. P. R. Herlemann, T. Leipe, and H. N. Schulz-Vogt. (2019). A bacterial isolate from the Black Sea oxidizes sulfide with manganese(IV) oxide. Proc. Natl. Acad. Sci. USA **116**:12153-12155. doi:10.1073/pnas.1906000116.

Henkel, J. V., A. Vogts, J. Werner, T. R. Neu, C. Spröer, B. Bunk, and H. N. Schulz-Vogt. (2021). *Candidatus* Sulfurimonas marisnigri sp. nov. and *Candidatus* Sulfurimonas baltica sp. nov., thiotrophic manganese oxide reducing chemolithoautotrophs of the class *Campylobacteria* isolated from the pelagic redoxclines of the Black Sea and the Baltic Sea. Syst. Appl. Microbiol. **44**:126155. doi:10.1016/j.syapm.2020.126155.

Henkel, S., S. Kasten, J. F. Hartmann, A. Silva-Busso, and M. Staubwasser. (2018). Iron cycling and stable Fe isotope fractionation in Antarctic shelf sediments, King George Island. Geochim. Cosmochim. Acta **237**:320-338. doi:10.1016/j.gca.2018.06.042.

Herberich, E., J. Sikorski, and T. Hothorn. (2010). A robust procedure for comparing multiple means under heteroscedasticity in unbalanced designs. PLoS One **5**:e9788. doi:10.1371/journal.pone.0009788.

Herlemann, D. P. R., M. Labrenz, K. Jürgens, S. Bertilsson, J. J. Waniek, and A. F. Andersson. (2011). Transitions in bacterial communities along the 2000 km salinity gradient of the Baltic Sea. ISME J. **5**:1571-1579. doi:10.1038/ismej.2011.41.

Holmes, D. E., J. S. Nicoll, D. R. Bond, and D. R. Lovley. (2004). Potential role of a novel psychrotolerant member of the family *Geobacteraceae, Geopsychrobacter electrodiphilus* gen. nov., sp. nov., in electricity production by a marine sediment fuel cell. Appl. Environ. Microbiol. **70**:6023-6030. doi:10.1128/aem.70.10.6023-6030.2004.

Hothorn, T., F. Bretz, and P. Westfall. (2008). Simultaneous inference in general parametric models. Biom. J. **50**:346-363. doi:10.1002/bimj.200810425.

Inagaki, F., K. Takai, H. Kobayashi, K. H. Nealson, and K. Horikoshi. (2003). *Sulfurimonas autotrophica* gen. nov., sp. nov., a novel sulfur-oxidizing ε-proteobacterium isolated from hydrothermal sediments in the Mid-Okinawa Trough. Int. J. Syst. Evol. Microbiol. **53**:1801-1805. doi:10.1099/ijs.0.02682-0.

Isaksen, M. F. and A. Teske. (1996). *Desulforhopalus vacuolatus* gen. nov., sp. nov., a new moderately psychrophilic sulfate-reducing bacterium with gas vacuoles isolated from a temperate estuary. Arch. Microbiol. **166**:160-168. doi:10.1007/s002030050371.

[Dataset] Jerosch, K., F. K. Scharf, D. Deregibus, G. L. Campana, K. Zacher-Aued, H. Pehlke, D. Abele, and M. L. Quartino. (2015). High resolution bathymetric compilation for Potter Cove, WAP, Antarctica, with links to data in ArcGIS format. PANGAEA. doi:10.1594/PANGAEA.853593.

Jørgensen, B. B. (1977). The sulfur cycle of a coastal marine sediment (Limfjorden, Denmark). Limnol. Oceanogr. **22**:814-832. doi:10.4319/lo.1977.22.5.0814.

Jørgensen, B. B. and T. Fenchel. (1974). The sulfur cycle of a marine sediment model system. Mar. Biol. **24**:189-201. doi:10.1007/BF00391893.

Jørgensen, B. B., A. J. Findlay, and A. Pellerin. (2019). The biogeochemical sulfur cycle of marine sediments. Front. Microbiol. **10**:849. doi:10.3389/fmicb.2019.00849.

Jørgensen, B. B., K. Laufer, A. B. Michaud, and L. M. Wehrmann. (2020). Biogeochemistry and microbiology of high Arctic marine sediment ecosystems – Case study of Svalbard fjords. Limnol. Oceanogr. **66**:S273-S292. doi:10.1002/lno.11551.

Kashefi, K., D. E. Holmes, J. A. Baross, and D. R. Lovley. (2003). Thermophily in the *Geobacteraceae: Geothermobacter ehrlichii* gen. nov., sp. nov., a novel thermophilic member of the *Geobacteraceae* from the "Bag City" hydrothermal vent. Appl. Environ. Microbiol. **69**:2985-2993. doi:10.1128/aem.69.5.2985-2993.2003.

Knights, D., J. Kuczynski, E. S. Charlson, J. Zaneveld, M. C. Mozer, R. G. Collman, F. D. Bushman, R. Knight, and S. T. Kelley. (2011). Bayesian community-wide culture-independent microbial source tracking. Nat. Methods **8**:761-763. doi:10.1038/nmeth.1650.

Knittel, K. and A. Boetius. (2009). Anaerobic oxidation of methane: Progress with an unknown process. Annu. Rev. Microbiol. **63**:311-334. doi:10.1146/annurev.micro.61.080706.093130.

Knittel, K., A. Boetius, A. Lemke, H. Eilers, K. Lochte, O. Pfannkuche, P. Linke, and R. Amann. (2003). Activity, distribution, and diversity of sulfate reducers and other bacteria in sediments above gas hydrate (Cascadia Margin, Oregon). Geomicrobiol. J. **20**:269-294. doi:10.1080/01490450303896.

Labrenz, M., J. Grote, K. Mammitzsch, H. T. S. Boschker, M. Laue, G. Jost, S. Glaubitz, and K. Jürgens. (2013). *Sulfurimonas gotlandica* sp. nov., a chemoautotrophic and psychrotolerant epsilonproteobacterium isolated from a pelagic redoxcline, and an emended description of the genus *Sulfurimonas*. Int. J. Syst. Evol. Microbiol. **63**:4141-4148. doi:10.1099/ijs.0.048827-0.

Langwig, M. V., V. De Anda, N. Dombrowski, K. W. Seitz, I. M. Rambo, C. Greening, A. P. Teske, and B. J. Baker. (2022). Large-scale protein level comparison of *Deltaproteobacteria* reveals cohesive metabolic groups. ISME J. **16**:307-320. doi:10.1038/s41396-021-01057-y.

LaRowe, D. E., S. Arndt, J. A. Bradley, E. R. Estes, A. Hoarfrost, S. Q. Lang, K. G. Lloyd, N. Mahmoudi, W. D. Orsi, S. R. Shah Walter, A. D. Steen, and R. Zhao. (2020). The fate of organic carbon in marine sediments – New insights from recent data and analysis. Earth-Sci. Rev. **204**:103146. doi:10.1016/j.earscirev.2020.103146.

Laufer-Meiser, K., A. B. Michaud, M. Maisch, J. M. Byrne, A. Kappler, M. O. Patterson, H. Røy, and B. B. Jørgensen. (2021). Potentially bioavailable iron produced through benthic cycling in glaciated Arctic fjords of Svalbard. Nat. Commun. **12**:1349. doi:10.1038/s41467-021-21558-w.

Liang, Q.-Y., J.-Y. Zhang, D. Ning, W.-X. Yu, G.-J. Chen, X. Tao, J. Zhou, Z.-J. Du, and D.-S. Mu. (2023). Niche modification by sulfate-reducing bacteria drives microbial community assembly in anoxic marine sediments. Mbio **14**:e03535-03522. doi:10.1128/mbio.03535-22.

Lie, T. J., M. L. Clawson, W. Godchaux, and E. R. Leadbetter. (1999). Sulfidogenesis from 2-Aminoethanesulfonate (Taurine) fermentation by a morphologically unusual sulfate-reducing bacterium, *Desulforhopalus singaporensis* sp. nov. Appl. Environ. Microbiol. **65**:3328-3334. doi:10.1128/AEM.65.8.3328-3334.1999.

Lovley, D. R. (2013). Dissimilatory Fe(III)- and Mn(IV)-Reducing Prokaryotes. *in* E. Rosenberg, E. F. DeLong, S. Lory, E. Stackebrandt, and F. Thompson, editors. The Prokaryotes: Prokaryotic Physiology and Biochemistry. Springer Berlin Heidelberg, Berlin, Heidelberg. p. 287-308. doi:10.1007/978-3-642-30141-4_69.

Lovley, D. R. and S. Goodwin. (1988). Hydrogen concentrations as an indicator of the predominant terminal electron-accepting reactions in aquatic sediments. Geochim. Cosmochim. Acta **52**:2993-3003. doi:10.1016/0016-7037(88)90163-9.

Lueders, T., M. Manefield, and M. W. Friedrich. (2004). Enhanced sensitivity of DNA- and rRNA-based stable isotope probing by fractionation and quantitative analysis of isopycnic centrifugation gradients. Environ. Microbiol. **6**:73-78. doi:10.1046/j.1462-2920.2003.00536.x.

McInerney, M. J., J. R. Sieber, and R. P. Gunsalus. (2009). Syntrophy in anaerobic global carbon cycles. Curr. Opin. Biotechnol. **20**:623-632. doi:10.1016/j.copbio.2009.10.001.

McMurdie, P. J. and S. Holmes. (2013). phyloseq: An R package for reproducible interactive analysis and graphics of microbiome census data. PLoS One **8**:e61217. doi:10.1371/journal.pone.0061217.

Michaud, A. B., K. Laufer, A. Findlay, A. Pellerin, G. Antler, A. V. Turchyn, H. Røy, L. M. Wehrmann, and B. B. Jørgensen. (2020). Glacial influence on the iron and sulfur cycles in Arctic fjord sediments (Svalbard). Geochim. Cosmochim. Acta **280**:423-440. doi:10.1016/j.gca.2019.12.033.

Monien, D., P. Monien, R. Brünjes, T. Widmer, A. Kappenberg, A. A. Silva Busso, B. Schnetger, and H.-J. Brumsack. (2017). Meltwater as a source of potentially bioavailable iron to Antarctica waters. Antarct. Sci. **29**:277-291. doi:10.1017/S095410201600064X.

Monien, P., K. A. Lettmann, D. Monien, S. Asendorf, A.-C. Wölfl, C. H. Lim, J. Thal, B. Schnetger, and H.-J. Brumsack. (2014). Redox conditions and trace metal cycling in coastal sediments from the maritime Antarctic. Geochim. Cosmochim. Acta **141**:26-44. doi:10.1016/j.gca.2014.06.003.

Müller, A. L., K. U. Kjeldsen, T. Rattei, M. Pester, and A. Loy. (2015). Phylogenetic and environmental diversity of DsrAB-type dissimilatory (bi)sulfite reductases. ISME J. **9**:1152-1165. doi:10.1038/ismej.2014.208.

Na, H., M. A. Lever, K. U. Kjeldsen, F. Schulz, and B. B. Jørgensen. (2015). Uncultured *Desulfobacteraceae* and Crenarchaeotal group C3 incorporate ^{13}C-acetate in coastal marine sediment. Environ. Microbiol. Rep. **7**:614-622. doi:10.1111/1758-2229.12296.

Neder, C., V. Fofonova, A. Androsov, I. Kuznetsov, D. Abele, U. Falk, I. R. Schloss, R. Sahade, and K. Jerosch. (2022). Modelling suspended particulate matter dynamics at an Antarctic fjord impacted by glacier melt. J. Mar. Syst. **231**:103734. doi:10.1016/j.jmarsys.2022.103734.

Nedwell, D. B. and I. M. Banat. (1981). Hydrogen as an electron donor for sulfate-reducing bacteria in slurries of salt marsh sediment. Microb. Ecol. **7**:305-313. doi:10.1007/BF02341425.

Nickel, M., V. Vandieken, V. Brüchert, and B. B. Jørgensen. (2008). Microbial Mn(IV) and Fe(III) reduction in northern Barents Sea sediments under different conditions of ice cover and organic carbon deposition. Deep Sea Res. (II Top. Stud. Oceanogr.) **55**:2390-2398. doi:10.1016/j.dsr2.2008.05.003.

Oremland, R. S. and S. Polcin. (1982). Methanogenesis and sulfate reduction: Competitive and noncompetitive substrates in estuarine sediments. Appl. Environ. Microbiol. **44**:1270-1276. doi:10.1128/aem.44.6.1270-1276.1982.

Oremland, R. S. and M. P. Silverman. (1979). Microbial sulfate reduction measured by an automated electrical impedance technique. Geomicrobiol. J. **1**:355-372. doi:10.1080/01490457909377741.

Parada, A. E., D. M. Needham, and J. A. Fuhrman. (2016). Every base matters: Assessing small subunit rRNA primers for marine microbiomes with mock communities, time series and global field samples. Environ. Microbiol. **18**:1403-1414. doi:10.1111/1462-2920.13023.

Peck, H. D. (1959). The ATP-dependent reduction of sulfate with hydrogen in extracts of *Desulfovibrio desulfuricans*. Proc. Natl. Acad. Sci. USA **45**:701-708. doi:10.1073/pnas.45.5.701.

Perrin, E., V. Ghini, M. Giovannini, F. Di Patti, B. Cardazzo, L. Carraro, C. Fagorzi, P. Turano, R. Fani, and M. Fondi. (2020). Diauxie and co-utilization of carbon sources can coexist during bacterial growth in nutritionally complex environments. Nat. Commun. **11**:3135. doi:10.1038/s41467-020-16872-8.

Purdy, K. J., D. B. Nedwell, and T. M. Embley. (2003). Analysis of the sulfate-reducing bacterial and methanogenic archaeal populations in contrasting Antarctic sediments. Appl. Environ. Microbiol. **69**:3181-3191. doi:10.1128/AEM.69.6.3181-3191.2003.

Quast, C., E. Pruesse, P. Yilmaz, J. Gerken, T. Schweer, P. Yarza, J. Peplies, and F. O. Glöckner. (2012). The SILVA ribosomal RNA gene database project: Improved data processing and web-based tools. Nucleic Acids Res. **41**:D590-D596. doi:10.1093/nar/gks1219.

R Core Team. (2022). R: A language and environment for statistical computing. Version 4.2.2. Available from: https://www.R-project.org.

R Core Team. (2024). R: A language and environment for statistical computing. Version 4.4.1. Available from: https://www.R-project.org.

Raiswell, R., J. R. Hawkings, L. G. Benning, A. R. Baker, R. Death, S. Albani, N. Mahowald, M. D. Krom, S. W. Poulton, J. Wadham, and M. Tranter. (2016). Potentially bioavailable iron delivery by iceberg-hosted sediments and atmospheric dust to the polar oceans. Biogeosciences **13**:3887-3900. doi:10.5194/bg-13-3887-2016.

Ravenschlag, K., K. Sahm, J. Pernthaler, and R. Amann. (1999). High bacterial diversity in permanently cold marine sediments. Appl. Environ. Microbiol. **65**:3982-3989. doi:10.1128/aem.65.9.3982-3989.1999.

Robador, A., A. L. Müller, J. E. Sawicka, D. Berry, C. R. J. Hubert, A. Loy, B. B. Jørgensen, and V. Brüchert. (2015). Activity and community structures of sulfate-reducing microorganisms in polar, temperate and tropical marine sediments. ISME J. **10**:796-809. doi:10.1038/ismej.2015.157.

Røy, H., H. S. Weber, I. H. Tarpgaard, T. G. Ferdelman, and B. B. Jørgensen. (2014). Determination of dissimilatory sulfate reduction rates in marine sediment via radioactive ^{35}S tracer. Limnol. Oceanogr. Methods **12**:196-211. doi:10.4319/lom.2014.12.196.

Rückamp, M., M. Braun, S. Suckro, and N. Blindow. (2011). Observed glacial changes on the King George Island ice cap, Antarctica, in the last decade. Global Planet. Change **79**:99-109. doi:10.1016/j.gloplacha.2011.06.009.

Salter, S. J., M. J. Cox, E. M. Turek, S. T. Calus, W. O. Cookson, M. F. Moffatt, P. Turner, J. Parkhill, N. J. Loman, and A. W. Walker. (2014). Reagent and laboratory contamination can critically impact sequence-based microbiome analyses. BMC Biol. **12**:87. doi:10.1186/s12915-014-0087-z.

Santos, A. A., S. S. Venceslau, F. Grein, W. D. Leavitt, C. Dahl, D. T. Johnston, and I. A. C. Pereira. (2015). A protein trisulfide couples dissimilatory sulfate reduction to energy conservation. Science **350**:1541-1545. doi:10.1126/science.aad3558.

Shaw, D. G., M. J. Alperin, W. S. Reeburgh, and D. J. McIntosh. (1984). Biogeochemistry of acetate in anoxic sediments of Skan Bay, Alaska. Geochim. Cosmochim. Acta **48**:1819-1825. doi:10.1016/0016-7037(84)90035-8.

Shaw, D. G. and D. J. McIntosh. (1990). Acetate in recent anoxic sediments: Direct and indirect measurements of concentration and turnover rates. Estuar. Coast. Shelf Sci. **31**:775-788. doi:10.1016/0272-7714(90)90082-3.

Slobodkin, A. I. and G. B. Slobodkina. (2019). Diversity of sulfur-disproportionating microorganisms. Microbiology **88**:509-522. doi:10.1134/S0026261719050138.

Smith, R. L. and M. J. Klug. (1981). Electron donors utilized by sulfate-reducing bacteria in eutrophic lake sediments. Appl. Environ. Microbiol. **42**:116-121. doi:10.1128/aem.42.1.116-121.1981.

Sørensen, J., D. Christensen, and B. B. Jørgensen. (1981). Volatile fatty acids and hydrogen as substrates for sulfate-reducing bacteria in anaerobic marine sediment. Appl. Environ. Microbiol. **42**:5-11. doi:10.1128/aem.42.1.5-11.1981.

Sung, Y., K. M. Ritalahti, R. A. Sanford, J. W. Urbance, S. J. Flynn, J. M. Tiedje, and F. E. Löffler. (2003). Characterization of two tetrachloroethene-reducing, acetate-oxidizing anaerobic bacteria and their description as *Desulfuromonas michiganensis* sp. nov. Appl. Environ. Microbiol. **69**:2964-2974. doi:10.1128/aem.69.5.2964-2974.2003.

Takai, K., M. Suzuki, S. Nakagawa, M. Miyazaki, Y. Suzuki, F. Inagaki, and K. Horikoshi. (2006). *Sulfurimonas paralvinellae* sp. nov., a novel mesophilic, hydrogen- and sulfur-oxidizing chemolithoautotroph within the *Epsilonproteobacteria* isolated from a deep-sea hydrothermal vent polychaete nest, reclassification of *Thiomicrospira denitrificans* as *Sulfurimonas denitrificans* comb. nov. and emended description of the genus *Sulfurimonas*. Int. J. Syst. Evol. Microbiol. **56**:1725-1733. doi:10.1099/ijs.0.64255-0.

Vandieken, V., M. Mußmann, H. Niemann, and B. B. Jørgensen. (2006a). *Desulfuromonas svalbardensis* sp. nov. and *Desulfuromusa ferrireducens* sp. nov., psychrophilic, Fe(III)-reducing bacteria isolated from Arctic sediments, Svalbard. Int. J. Syst. Evol. Microbiol. **56**:1133-1139. doi:10.1099/ijs.0.63639-0.

Vandieken, V., M. Nickel, and B. B. Jørgensen. (2006b). Carbon mineralization in Arctic sediments northeast of Svalbard: Mn(IV) and Fe(III) reduction as principal anaerobic respiratory pathways. Mar. Ecol. Prog. Ser. **322**:15-27. doi:10.3354/meps322015.

Vandieken, V. and B. Thamdrup. (2013). Identification of acetate-oxidizing bacteria in a coastal marine surface sediment by RNA-stable isotope probing in anoxic slurries and intact cores. FEMS Microbiol. Ecol. **84**:373-386. doi:10.1111/1574-6941.12069.

Vasquez-Cardenas, D., J. van de Vossenberg, L. Polerecky, S. Y. Malkin, R. Schauer, S. Hidalgo-Martinez, V. Confurius, J. J. Middelburg, F. J. R. Meysman, and H. T. S. Boschker. (2015). Microbial carbon metabolism associated with electrogenic sulphur oxidation in coastal sediments. ISME J. **9**:1966-1978. doi:10.1038/ismej.2015.10.

Viollier, E., P. Inglett, K. Hunter, A. Roychoudhury, and P. Van Cappellen. (2000). The ferrozine method revisited: Fe(II)/Fe(III) determination in natural waters. Appl. Geochem. **15**:785-790. doi:10.1016/S0883-2927(99)00097-9.

Wang, J., Q. Zheng, S. Wang, J. Zeng, Q. Yuan, Y. Zhong, L. Jiang, and Z. Shao. (2023a). Characterization of two novel chemolithoautotrophic bacteria of *Sulfurovum* from marine coastal environments and further comparative genomic analyses revealed species differentiation among deep-sea hydrothermal vent and non-vent origins. Front. Mar. Sci. **10**. doi:10.3389/fmars.2023.1222526.

Wang, S., L. Jiang, Q. Hu, L. Cui, B. Zhu, X. Fu, Q. Lai, Z. Shao, and S. Yang. (2021a). Characterization of *Sulfurimonas hydrogeniphila* sp. nov., a novel bacterium predominant in deep-sea hydrothermal vents and comparative genomic analyses of the genus *Sulfurimonas*. Front. Microbiol. **12**. doi:10.3389/fmicb.2021.626705.

Wang, S., L. Jiang, X. Liu, S. Yang, and Z. Shao. (2020). *Sulfurimonas xiamenensis* sp. nov. and *Sulfurimonas lithotrophica* sp. nov., hydrogen- and sulfur-oxidizing chemolithoautotrophs within the *Epsilonproteobacteria* isolated from coastal sediments, and an emended description of the genus Sulfurimonas. Int. J. Syst. Evol. Microbiol. **70**:2657-2663. doi:10.1099/ijsem.0.004087.

Wang, S., L. Jiang, S. Xie, K. Alain, Z. Wang, J. Wang, D. Liu, and Z. Shao. (2023b). Disproportionation of inorganic sulfur compounds by mesophilic chemolithoautotrophic *Campylobacterota*. mSystems **8**:e00954-00922. doi:10.1128/msystems.00954-22.

Wang, S., Z. Shao, Q. Lai, X. Liu, S. Xie, L. Jiang, and S. Yang. (2021b). *Sulfurimonas sediminis* sp. nov., a novel hydrogen- and sulfur-oxidizing chemolithoautotroph isolated from a hydrothermal vent at the Longqi system, southwestern Indian ocean. Antonie Van Leeuwenhoek **114**:813-822. doi:10.1007/s10482-021-01560-4.

Wasmund, K. (2023). Deciphering community interactions of sulfate-reducing microorganisms in complex microbial communities of marine sediments. Mbio **14**:e00513-00523. doi:10.1128/mbio.00513-23.

Wasmund, K., M. Mußmann, and A. Loy. (2017). The life sulfuric: Microbial ecology of sulfur cycling in marine sediments. Environ. Microbiol. Rep. **9**:323-344. doi:10.1111/1758-2229.12538.

Watanabe, M., Y. Higashioka, H. Kojima, and M. Fukui. (2017). *Desulfosarcina widdelii* sp. nov. and *Desulfosarcina alkanivorans* sp. nov., hydrocarbon-degrading sulfate-reducing bacteria isolated from marine sediment and emended description of the genus *Desulfosarcina*. Int. J. Syst. Evol. Microbiol. **67**:2994-2997. doi:10.1099/ijsem.0.002062.

Webster, G., L. C. Watt, J. Rinna, J. C. Fry, R. P. Evershed, R. J. Parkes, and A. J. Weightman. (2006). A comparison of stable-isotope probing of DNA and phospholipid fatty acids to study prokaryotic functional diversity in sulfate-reducing marine sediment enrichment slurries. Environ. Microbiol. **8**:1575-1589. doi:10.1111/j.1462-2920.2006.01048.x.

Wehrmann, L. M., M. J. Formolo, J. D. Owens, R. Raiswell, T. G. Ferdelman, N. Riedinger, and T. W. Lyons. (2014). Iron and manganese speciation and cycling in glacially influenced high-latitude fjord sediments (West Spitsbergen, Svalbard): Evidence for a benthic recycling-transport mechanism. Geochim. Cosmochim. Acta **141**:628-655. doi:10.1016/j.gca.2014.06.007.

Wickham, H., M. Averick, J. Bryan, W. Chang, L. D. A. McGowan, R. François, G. Grolemund, A. Hayes, L. Henry, J. Hester, M. Kuhn, T. L. Pedersen, E. Miller, S. M. Bache, K. Müller, J. Ooms, D. Robinson, D. P. Seidel, V. Spinu, K. Takahashi, D. Vaughan, C. Wilke, K. Woo, and H. Yutani. (2019). Welcome to the Tidyverse. J. Open Source Softw. **4**:1686. doi:10.21105/joss.01686.

Winfrey, M. R. and D. M. Ward. (1983). Substrates for sulfate reduction and methane production in intertidal sediments. Appl. Environ. Microbiol. **45**:193-199. doi:10.1128/aem.45.1.193-199.1983.

Wunder, L. C., D. A. Aromokeye, X. Yin, T. Richter-Heitmann, G. Willis-Poratti, A. Schnakenberg, C. Otersen, I. Dohrmann, M. Römer, G. Bohrmann, S. Kasten, and M. W. Friedrich. (2021). Iron and sulfate reduction structure microbial communities in (sub-)Antarctic sediments. ISME J. **15**:3587-3604. doi:10.1038/s41396-021-01014-9.

Wunder, L. C., I. Breuer, G. Willis-Poratti, D. A. Aromokeye, S. Henkel, T. Richter-Heitmann, X. Yin, and M. W. Friedrich. (2024). Manganese reduction and associated microbial communities in Antarctic surface sediments. Front. Microbiol. **15**. doi:10.3389/fmicb.2024.1398021.

Yin, X., A. C. Kulkarni, and M. W. Friedrich. (2019). DNA and RNA Stable Isotope Probing of Methylotrophic Methanogenic Archaea. *in* M. G. Dumont and M. Hernández García, editors. Stable Isotope Probing: Methods and Protocols. Springer New York, New York, NY. p. 189-206. doi:10.1007/978-1-4939-9721-3_15.

Yin, X., G. Zhou, H. Wang, D. Han, M. Maeke, T. Richter-Heitmann, L. C. Wunder, D. A. Aromokeye, Q.-Z. Zhu, R. Nimzyk, M. Elvert, and M. W. Friedrich. (2024). Unexpected carbon utilization activity of sulfate-reducing microorganisms in temperate and permanently cold marine sediments. ISME J. **18**. doi:10.1093/ismejo/wrad014.

Zhang, T., T. S. Bain, M. A. Barlett, S. A. Dar, O. L. Snoeyenbos-West, K. P. Nevin, and D. R. Lovley. (2014). Sulfur oxidation to sulfate coupled with electron transfer to electrodes by *Desulfuromonas* strain TZ1. Microbiology **160**:123-129. doi:10.1099/mic.0.069930-0.

Zhang, Z., S. Schartz, L. Wagner, and W. Miller. (2000). A greedy algorithm for aligning DNA sequences. J. Comput. Biol. **7**:203-214. doi:10.1089/10665270050081478.

Zopfi, J., T. G. Ferdelman, and H. Fossing. (2004). Distribution and Fate of Sulfur Intermediates – Sulfite, Thiosulfate, and Elemental Sulfur – In Marine Sediments. *in* J. P. Amend, K. J. Edwards, and T. W. Lyons, editors. Sulfur Biogeochemistry – Past and Present. Geological Society of America. p. 97-116. doi:10.1130/0-8137-2379-5.97.

5.2 Supplementary

5.2.1 Supplementary figures

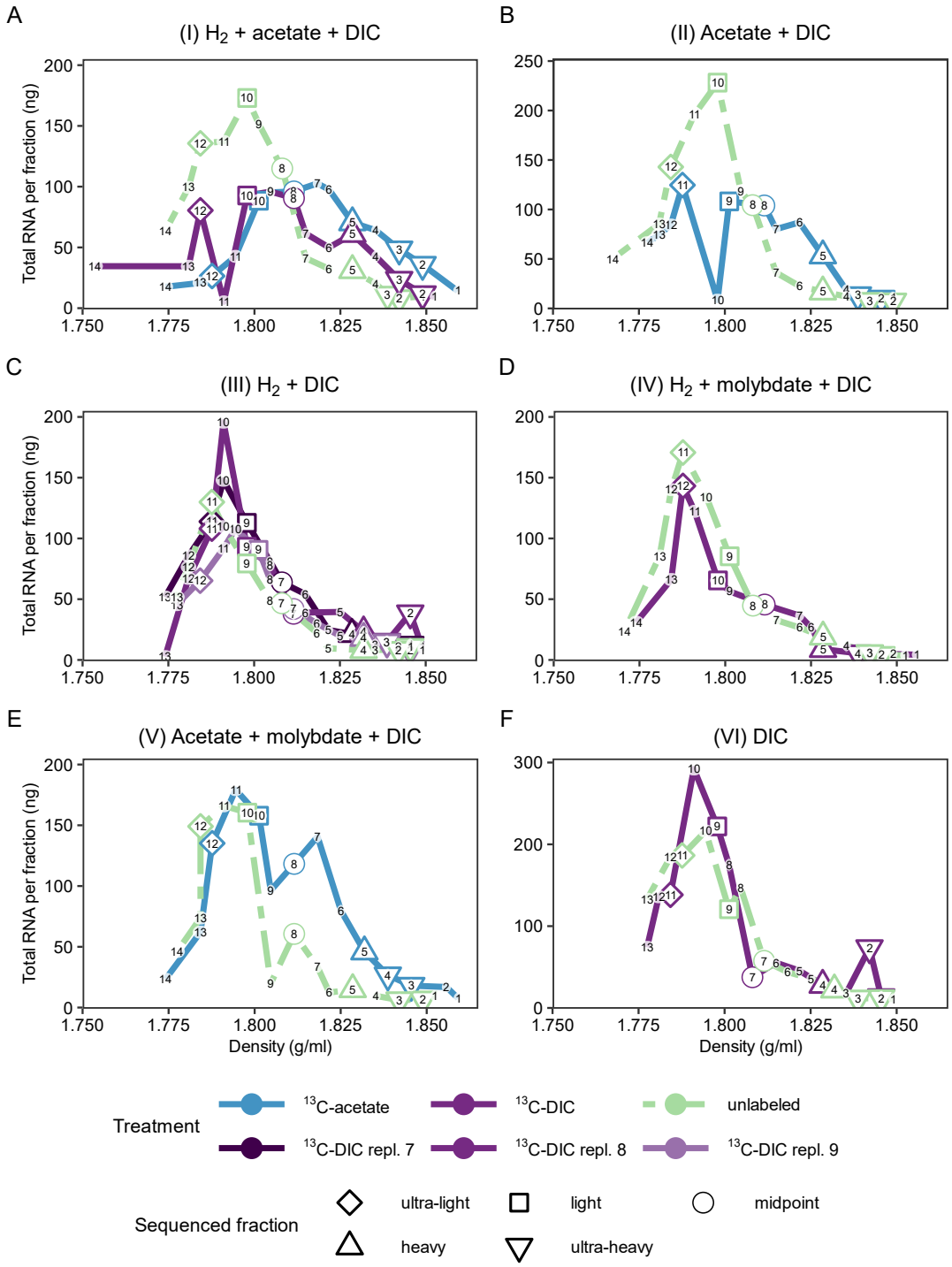

Figure S1: Density separated rRNA from RNA-SIP incubations. Plotted were densities of fractions against calculated total RNA recovered per fraction. Fractions were numbered from 1 to 14 from heavy to light fractions. Fractions with density < 1.75 g/ml were not shown. Labeled and unlabeled treatments were distinguished by color and line type. Fractions chosen for sequencing were marked by different symbols for the named fractions, see Table S3. For treatment III (plot **C**) replicates 7-9 were additionally distinguished by color.

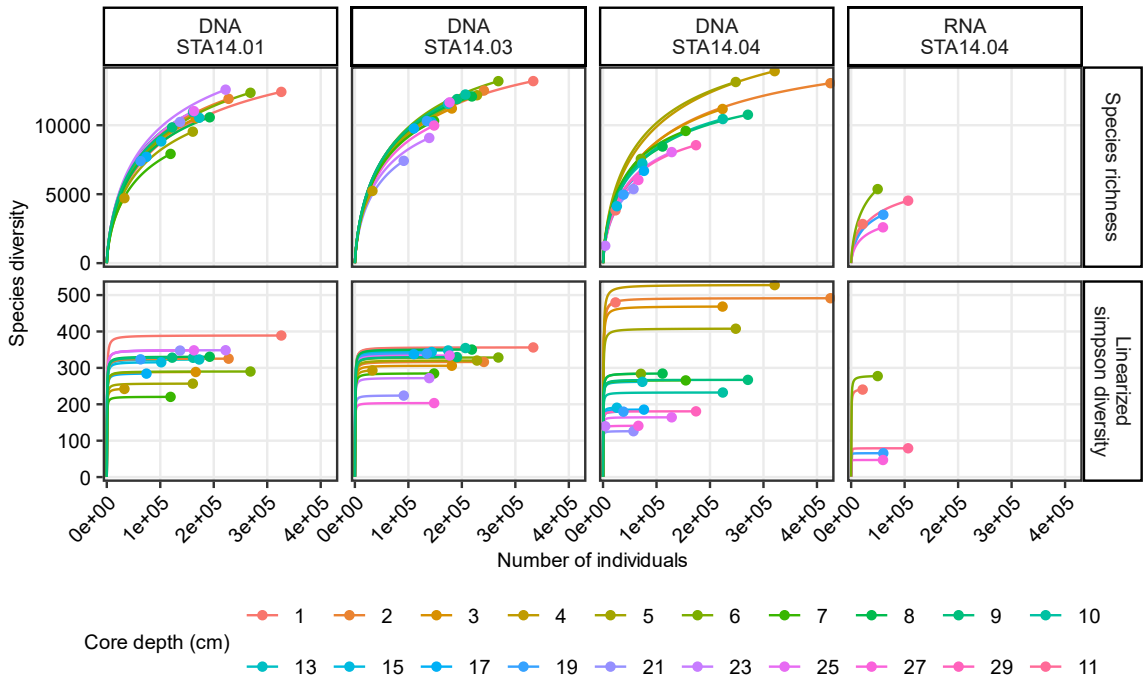

Figure S2: Rarefaction curves of *in situ* sequencing. The end point of each curve was marked by the data point. Sequenced core depths were distinguished by color.

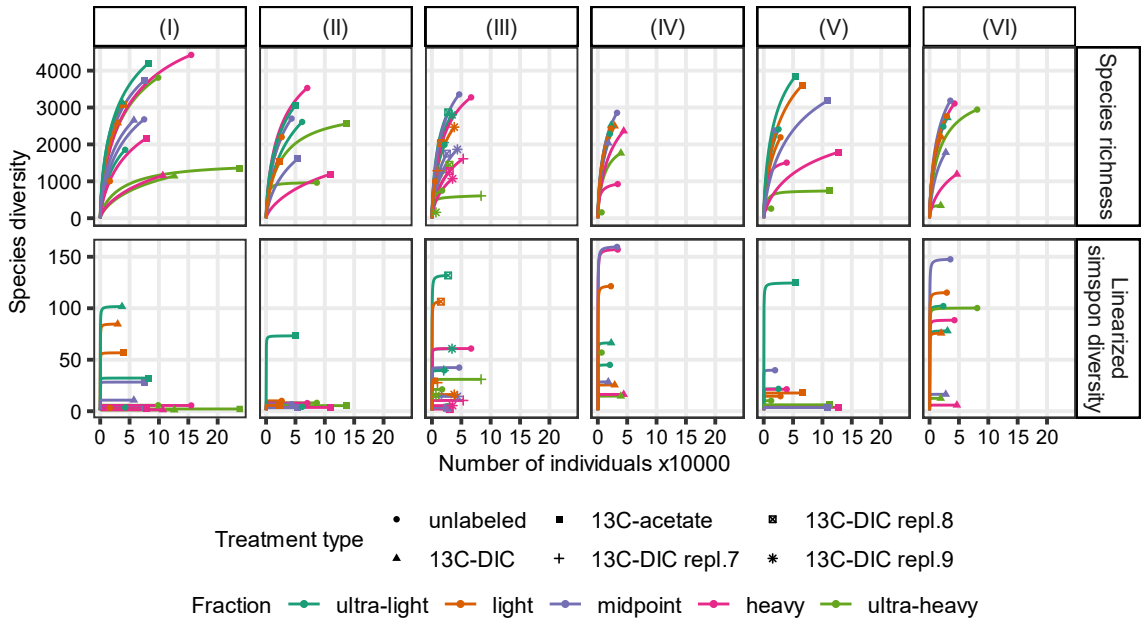

Figure S3: Rarefaction curves of sequenced incubation samples. Treatments in columns were (I) H_2 + acetate + DIC; (II) Acetate + DIC; (III) H_2 + DIC; (IV) H_2 + molybdate + DIC; (V) Acetate + molybdate + DIC; (VI) DIC. Treatment types were distinguished by shape for unlabeled, which different substrate was labeled, and for treatment (III) individual replicates. The end point of each curve was marked by the data point. Sequenced fractions were distinguished by color.

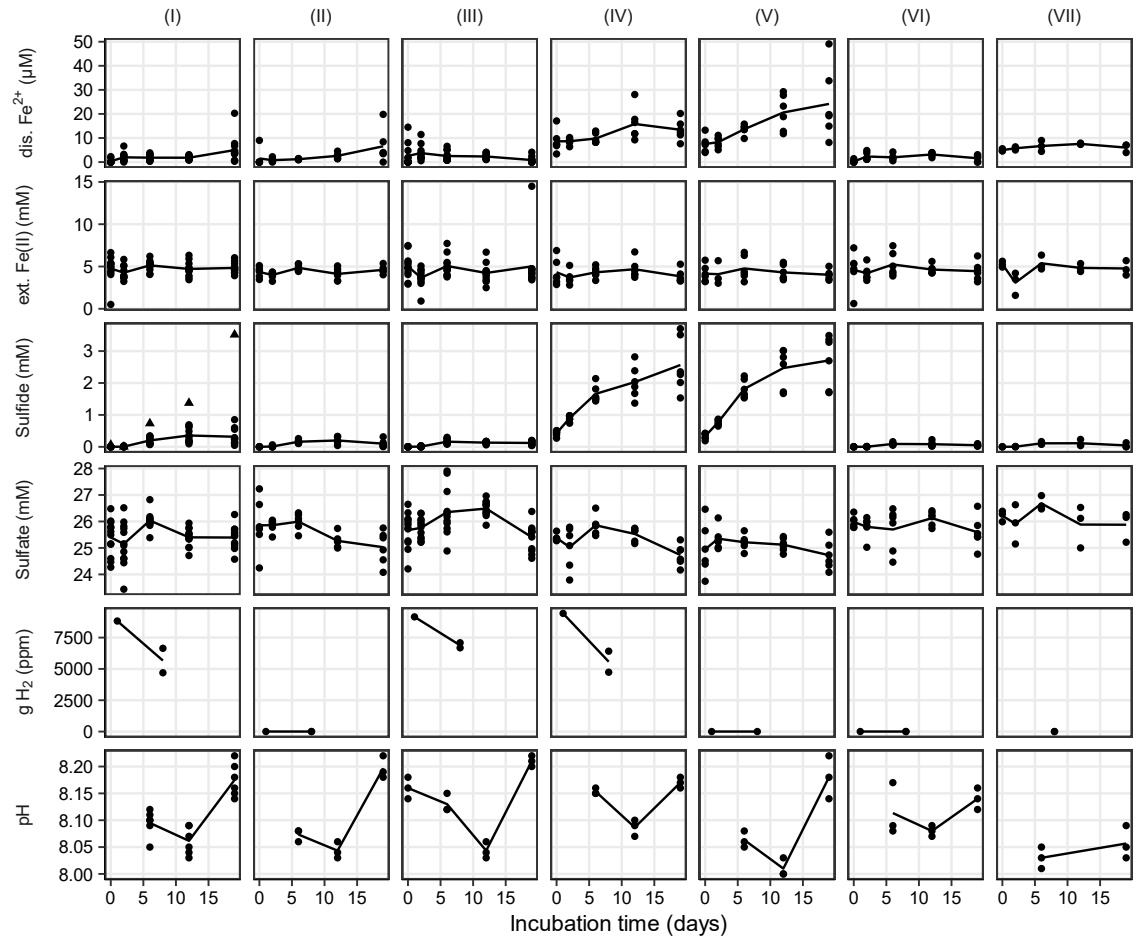

Figure S4: Geochemical measurements over incubation time. Plotted was the calculated mean per treatment and all individual data points. Treatments in columns were (I) H_2 + acetate + DIC; (II) Acetate + DIC; (III) H_2 + DIC; (IV) H_2 + molybdate + DIC; (V) Acetate + molybdate + DIC; (VI) DIC; (VII) Slurry only. Replicate 1 of treatment (I) with ^{13}C-labeled acetate was distinguished by shape in panel of sulfide concentration and was not included in the mean calculation. Note that the sulfide measurement in treatments containing molybdate (IV, V) was highly increased by an artifact caused by interaction of molybdate, sulfide and compounds of the Cline reagent (Figure S5).

Figure S5: Sulfide measurement plate showing standard curve from 18 µM (A1,B1,C1) to 0 µM sulfide (A12,B12,C12), different measured samples (row D) and standard curve with 10 mM molybdate addition (G1-G12) containing the same sulfide concentrations as the standard curve (rows A-C): G1 - 18 µM to G12 - 0 µM sulfide. With molybdate addition, the color changed from blue to more grey and absorption at 670 nm was higher than for the normal standard curve.

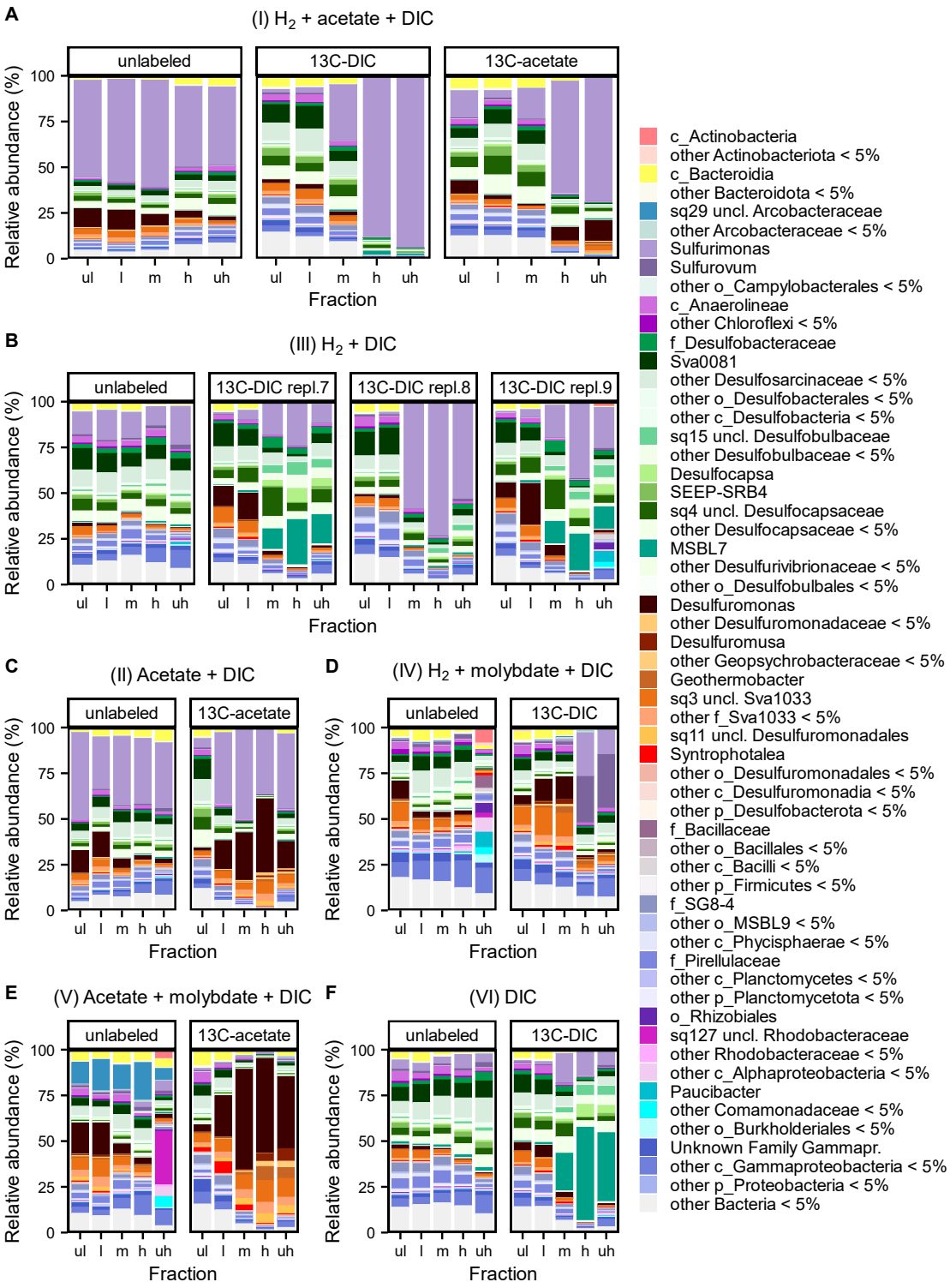

Figure S6: Bacterial 16S rRNA community of SIP incubation experiment. Displayed were all treatments indicating which substrate was labeled and the unlabeled control. Fractions after density separation were ultra-light (ul), light (l), midpoint (m), heavy (h) and ultra-heavy (uh). Genera with a relative abundance above 5% in at least one sample were displayed. Taxa which crossed the 5% threshold on a higher taxonomic rank were indicated by, e.g., f_ for family. If a single, on genus unclassified ASV crossed the threshold, its ASV ID was displayed.

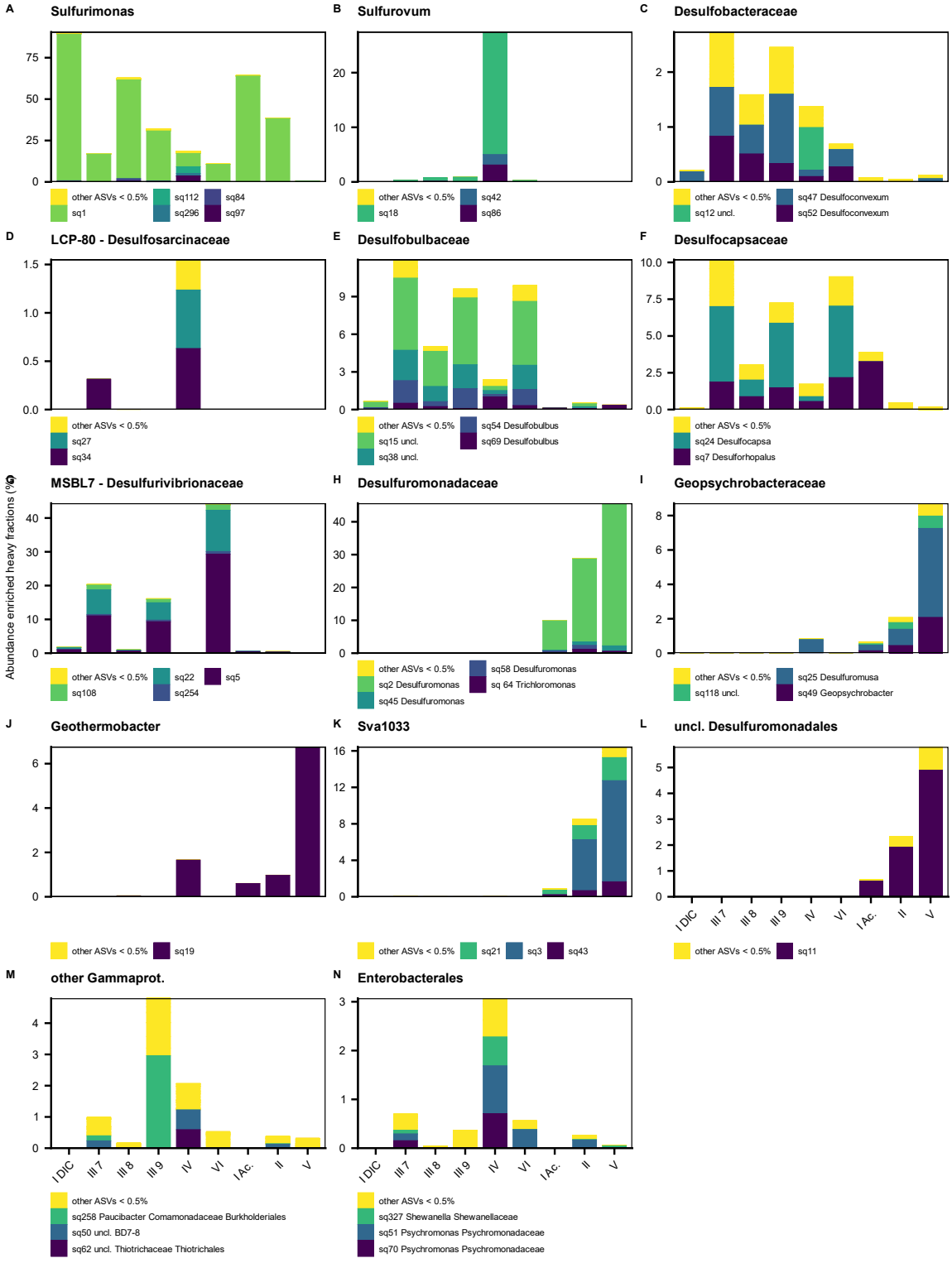

Figure S7: Abundance of ASVs which were labeled > 0.5% in the heavy labeled fractions. Plotted was the calculated average relative abundance of the heavy and ultra-heavy fractions in treatments with ^{13}C-labeled substrates for ASVs which were identified as labeled by comparing heavy to light fractions (see methods for details). ASVs were grouped by taxa indicated in the plot title. For higher taxonomic ranks, ASV taxonomy was noted in the plot legends. Treatments were I DIC: H_2 + acetate + ^{13}C-DIC, III 7-9: H_2 + ^{13}C-DIC replicate 7-9, IV: H_2 + ^{13}C-DIC + molybdate, VI: ^{13}C-DIC, I Acetate: H_2 + ^{13}C-acetate + DIC, II: ^{13}C-acetate + DIC, V: ^{13}C-acetate + DIC + molybdate.

5.2.2 Supplementary tables

Table S1: Detailed slurry incubation set-up.
Supplied substrates as indicated. 13C: substrate was labeled with ^{13}C-carbon. 12C: substrate with natural isotope ratio. All treatments contained 28 mM sulfate as part of the artificial sea water used for slurry preparation.

Treatment No.	DIC (10 mM)	Acetate (0.5 mM)	Hydrogen (2%)	Molybdate (28 mM)	Replicates
I	13C	12C	x		3
	12C	13C	x		3
	12C	12C	x		6
II	12C	13C			3
	12C	12C			3
III	13C		x		9
	12C		x		3
IV	13C		x	x	3
	12C		x	x	3
V	12C	13C		x	3
	12C	12C		x	3
VI	13C				3
	12C				3
VII					3

Table S2: Sampling incubation bottles for geochemistry and extraction

At identical time points, the same samples were taken for geochemical measurements in the slurry (Fe^{2+}, easily dissolvable Fe(II), sulfide, sulfate). The supernatant of 1.2 ml slurry was fixed according to the measurement. Fe^{2+}: 175 µl pore water (pw) + 25 µl 6 M HCl; sulfide: 500 µl pw + 500 µl 5% Zn-acetate; sulfate: 200 µl pw gased for > 30 s with CO_2 gas. For easily dissolvable Fe(II) 100 µl slurry were mixed with 100 µl 1 M HCl, incubated for 1 h at room temperature, centrifuged for 5 min and resulting 160 µl supernatant were fixed with 16 µl 6 M HCl. For day 0, the supernatant of samples which were subsequently frozen for nucleic acid extraction was transferred and used for pH measurement. For nucleic acid extraction for all samples, 5 ml slurry of the indicated replicates were pooled together, except indicated otherwise with *, which were kept separate for extraction. Only day 19 samples were actually extracted, the rest of the samples were stored.

Sample		Parameter								Nucleic acid extraction			
Treat. no	Labeled	Fe^{2+}	Easily dis. Fe(II)	Sulfide	Sulfate	pH		^{35}S-SRR	H_2 headspace				
I	DIC	day 0, 2, 6, 12, 19 repl. 1-9				day 0 repl. 1-3	day 6, 12, 19 repl. 4-6			day 0 repl. 1-3	day 6 repl. 1-3*	day 12 repl. 4-6*	day 19 repl. 7-9*
	none	day 0, 2, 6, 12, 19 repl. 1-3						day 6, 12, 19 repl. 1-3	day 1, 8 repl. 1 / day 8 repl. 3	day 6, 12, 19 repl. 1-3			
II	Acetate	day 0, 2, 6, 12, 19 repl. 1-3				day 6, 12, 19 repl. 1-3				day 6, 12, 19 repl. 1-3			
	none	day 0, 2, 6, 12, 19 repl. 1-3						day 6, 12, 19 repl. 1-3	day 1, 8 repl. 1 / day 8 repl. 3	day 6, 12, 19 repl. 1-3			
III	DIC	day 0, 2, 6, 12, 19 repl. 1-3				day 6, 12, 19 repl. 1-3				day 6, 12, 19 repl. 1-3			
	Acetate	day 0, 2, 6, 12, 19 repl. 1-3				day 6, 12, 19 repl. 1-3				day 6, 12, 19 repl. 1-3			
	none	day 0, 2, 6, 12, 19 repl. 1-6						day 6, 12, 19 repl. 1-6	day 1, 8 repl. 4 / day 8 repl. 6	day 6, 12, 19 repl. 1-3, 4-6			
IV	DIC	day 0, 2, 6, 12, 19 repl. 1-3				day 6, 12, 19 repl. 1-3				day 6, 12, 19 repl. 1-3			
	none	day 0, 2, 6, 12, 19 repl. 1-3						day 6, 12, 19 repl. 1-3	day 1, 8 repl. 1 / day 8 repl. 3	day 6, 12, 19 repl. 1-3			
V	Acetate	day 0, 2, 6, 12, 19 repl. 1-3				day 6, 12, 19 repl. 1-3				day 6, 12, 19 repl. 1-3			
	none	day 0, 2, 6, 12, 19 repl. 1-3						day 6, 12, 19 repl. 1-3	day 1, 8 repl. 1	day 6, 12, 19 repl. 1-3			
VI	DIC	day 0, 2, 6, 12, 19 repl. 1-3				day 6, 12, 19 repl. 1-3				day 6, 12, 19 repl. 1-3			
	none	day 0, 2, 6, 12, 19 repl. 1-3						day 6, 12, 19 repl. 1-3	day 1, 8 repl. 1 / day 8 repl. 3	day 6, 12, 19 repl. 1-3			
VII	none	day 0, 2, 6, 12, 19 repl. 1-3				day 6, 19 repl. 1-3		day 0, 6, 12, 19 repl. 1-3	day 8 repl. 1, 3	day 6, 12, 19 repl. 1-3			

Table S3: Fractionation of incubation samples. Overview which fraction exactly was sequenced, including density and total RNA content in the fraction. See Figure S1 for complete fractionation profile.

Treatment		Fraction			
		No.	Density (g/ml)	RNA found in sample (ng)	Sequenced as
I: H_2 + acetate + DIC	^{13}C-DIC	2	1.849	11.55	ultra-heavy
		3	1.842	23.44	ultra-heavy
		5	1.829	60.96	heavy
		8	1.811	90.53	midpoint
		10	1.798	92.71	light
		12	1.784	80.48	ultra-light
	^{13}C-acetate	2	1.849	35.79	ultra-heavy
		3	1.842	48.42	ultra-heavy
		5	1.829	70.49	heavy
		8	1.811	96.07	midpoint
		10	1.801	88.41	light
		12	1.788	26.45	ultra-light
	unlabeled	2	1.842	8.23	ultra-heavy
		3	1.839	11.16	ultra-heavy
		5	1.829	31.15	heavy
		8	1.808	114.93	midpoint
		10	1.798	172.99	light
		12	1.784	135.63	ultra-light
II: Acetate + DIC	^{13}C-acetate	2	1.846	9.93	ultra-heavy
		3	1.839	13.44	ultra-heavy
		5	1.829	53.35	heavy
		8	1.811	104.01	midpoint
		9	1.801	108.14	light
		11	1.788	124.63	ultra-light
	unlabeled	2	1.849	7.07	ultra-heavy
		3	1.842	7.63	ultra-heavy
		5	1.829	16.87	heavy
		8	1.808	104.34	midpoint
		10	1.798	228.19	light
		12	1.784	142.93	ultra-light
III: H_2 + DIC	^{13}C-DIC repl. 7	1	1.846	12.64	ultra-heavy
		2	1.842	10.89	ultra-heavy
		4	1.829	21.22	heavy
		7	1.808	63.80	midpoint
		9	1.798	112.82	light
		11	1.788	113.85	ultra-light

Treatment		Fraction			
		No.	Density (g/ml)	RNA found in sample (ng)	Sequenced as
III: H_2 + DIC	^{13}C-DIC repl. 8	2	1.846	38.44	ultra-heavy
		3	1.839	15.06	ultra-heavy
		4	1.832	23.24	heavy
		7	1.811	38.01	midpoint
		9	1.798	93.12	light
		11	1.788	108.07	ultra-light
	^{13}C-DIC repl. 9	2	1.846	8.57	ultra-heavy
		3	1.839	14.55	ultra-heavy
		4	1.832	17.96	heavy
		7	1.811	41.93	midpoint
		9	1.801	90.59	light
		12	1.784	65.24	ultra-light
	unlabeled	1	1.846	10.79	ultra-heavy
		2	1.842	8.32	ultra-heavy
		4	1.832	7.99	heavy
		7	1.808	46.63	midpoint
		9	1.798	79.38	light
		11	1.788	129.91	ultra-light
IV: H_2 + DIC + molybdate	^{13}C-DIC	3	1.842	5.31	ultra-heavy
		4	1.839	5.49	ultra-heavy
		5	1.829	8.83	heavy
		8	1.811	45.58	midpoint
		10	1.798	65.44	light
		12	1.788	143.22	ultra-light
	unlabeled	2	1.846	4.18	ultra-heavy
		3	1.842	5.71	ultra-heavy
		5	1.829	19.05	heavy
		8	1.808	44.69	midpoint
		9	1.801	85.30	light
		11	1.788	170.71	ultra-light
V: Acetate + DIC + molybdate	^{13}C-acetate	3	1.846	18.02	ultra-heavy
		4	1.839	26.56	ultra-heavy
		5	1.832	46.00	heavy
		8	1.811	118.24	midpoint
		10	1.801	157.86	light
		12	1.788	135.20	ultra-light
	unlabeled	2	1.849	6.70	ultra-heavy
		3	1.842	6.08	ultra-heavy
		5	1.829	14.94	heavy
		8	1.811	60.59	midpoint
		10	1.798	160.40	light
		12	1.784	149.07	ultra-light

Treatment		Fraction			
		No.	Density (g/ml)	RNA found in sample (ng)	Sequenced as
VI: DIC	^{13}C-DIC	1	1.846	13.29	ultra-heavy
		2	1.842	73.22	ultra-heavy
		4	1.829	27.99	heavy
		7	1.808	37.52	midpoint
		9	1.798	221.92	light
		11	1.784	138.33	ultra-light
	unlabeled	2	1.846	12.06	ultra-heavy
		3	1.839	11.62	ultra-heavy
		4	1.832	22.25	heavy
		7	1.811	57.55	midpoint
		9	1.801	120.69	light
		11	1.788	186.45	ultra-light

Table S4: List of ASVs which were identified as contamination and removed from incubation sequencing data set. Reasons for ASVs considered as contamination were indicated as approach (1) from decontam R package with threshold which identified this ASV, count distribution from approach (2), and if the taxonomy was associated with known contaminants or human pathogens. The taxonomic assignment above Bacteria level was listed. Also see supplementary text for details.

ASV	Reason removal			Taxonomy
	Decontam package	Count distribution	Known contaminant or human associated	
sq13		x	x	Proteobacteria;Gammaproteobacteria;Pseudomonadales;Moraxellaceae;Enhydrobacter
sq26	0.1	x	x	Proteobacteria;Gammaproteobacteria;Burkholderiales;Burkholderiaceae;Ralstonia
sq55	0.15	x	x	Proteobacteria;Gammaproteobacteria;Enterobacterales;Enterobacteriaceae;NA
sq56	0.1	x	x	Proteobacteria;Gammaproteobacteria;Pseudomonadales;Pseudomonadaceae;Pseudomonas
sq60	0.1	x	x	Proteobacteria;Gammaproteobacteria;Burkholderiales;Comamonadaceae;Curvibacter
sq66	0.1	x	x	Proteobacteria;Alphaproteobacteria;Sphingomonadales;Sphingomonadaceae;Novosphingobium
sq71	0.1		x	Proteobacteria;Alphaproteobacteria;Rhizobiales;Xanthobacteraceae;Afipia
sq87	0.1	x	x	Proteobacteria;Gammaproteobacteria;Burkholderiales;Oxalobacteraceae;Duganella
sq175	0.1	x	x	Proteobacteria;Gammaproteobacteria;Enterobacterales;Enterobacteriaceae;Escherichia-Shigella
sq182	0.1	x	x	Proteobacteria;Gammaproteobacteria;Burkholderiales;Oxalobacteraceae;Herbaspirillum
sq399	0.15	x	x	Proteobacteria;Gammaproteobacteria;Burkholderiales;Comamonadaceae;Delftia
sq506	0.1	x	x	Proteobacteria;Gammaproteobacteria;Pseudomonadales;Halomonadaceae;Halomonas
sq515		x	x	Actinobacteriota;Actinobacteria;Micrococcales;Dermacoccaceae;Dermacoccus

Table S5: BLAST results of most abundant ASVs. Indicated was the highest taxonomic assignment from the sequencing pipeline, the best cultured BLAST hit with 100% query coverage and highest percent sequence identity, the NCBI accession number and the associated reference, if present. If there were multiple equally good hits, all hits were listed. sq2, sq3, sq21 and sq25 were specifically compared to ASV sequences from Wunder et al. (2024) from the Potter Cove environment, where they were published in the supplementary. sq1 was specifically compared to *Sulfurimonas* type strains. *: this ASV was not labeled and present in light fractions and unlabeled controls.

ASV	Taxonomy	Closest cultured BLAST hit	Accession	Perc. identity	Query coverage	Reference
sq1	*Sulfurimonas*	*Candidatus* Sulfurimonas marisnigri strain SoZ1	CP054493.1	99.2	100	Henkel et al. 2021
		Candidatus Sulfurimonas baltica strain GD2	CP054492.1	97.61	100	Henkel et al. 2021
sq18	*Sulfurovum*	*Sulfurovum xiamenensis* strain XTW-4	OP810811.1	97.61	100	Wang et al. 2023
sq42		*Sulfurovum xiamenensis* strain XTW-4	OP810811.1	96.83	100	Wang et al. 2023
sq86		*Sulfurovum xiamenensis* strain XTW-4	OP810811.1	97.21	100	Wang et al. 2023
sq5	MSBL7	*Thiovibrio frasassiensis*	NR_189258.1	94.44	100	Aronson et al. 2023
sq22		*Thiovibrio frasassiensis*	NR_189258.1	94.84	100	Aronson et al. 2023
sq15	*Desulfobulbaceae*	*Candidatus* Electrothrix aestuarii isolate Rat1	CP159373.1	96.02	100	Plum-Jensen et al. 2024
		Candidatus Electrothrix scaldis isolate GW3-3	CP138355.1	96.02	100	Hiralal et al. 2024
sq38		*Desulfolithobacter dissulfuricans* strain GF1	AP024233.1	97.21	100	Hashimoto et al. 2022
sq54	*Desulfobulbus*	*Desulfolithobacter dissulfuricans* strain GF1	AP024233.1	97.61	100	Hashimoto et al. 2022
sq69		*Desulfogranum mediterraneum* strain 86FS1	NR_025150.1	98.01	100	Sass et al. 2002
sq7	*Desuforhopalus*	*Desulforhopalus singaporensis* strain T1	NR_028742.1	98.01	100	Lie et al. 1999
sq24	*Desulfocapsa*	*Desulfocapsa sulfexigens* DSM 10523	CP003985.1	97.21	100	Finster et al. 1998
sq4*	*Desulfocapsaceae*	*Desulfomarina profundi* KT2	NR_179352.1	98.01	100	Hashimoto et al. 2021
sq2	*Desulfuromonas*	*Desulfuromonas svalbardensis* strain 112	NR_043213.1	99.2	100	Vandieken et al. 2006
		Desulfuromonas sq1		100	100	Wunder et al. 2024
sq25	*Desulfuromusa*	*Desulfuromusa bakii* strain Gyprop	NR_026175.1	99.6	100	Liesack and Finster 1994
		Desulfuromusa sq22		100	100	Wunder et al. 2024
sq3	Sva1033	*Desulfuromonas acetoxidans* strain DSM 684	NR_121678.1	96.02	100	Pfennig and Biebl 1976
		sq21		96.03	100	this study
		Sva1033 sq5		100	100	Wunder et al. 2024
sq21		*Desulfuromonas acetoxidans* strain DSM 684	NR_121678.1	96.41	100	Pfennig and Biebl 1976
		Sva1033 sq33		100	100	Wunder et al. 2024
sq11	Desulfuromonadales	*Desulfuromonas michiganensis*	NR_114607.1	97.21	100	Sung et al. 2003

5.2.3 Supplementary material and methods

5.2.3.1 Calculation of sulfate reduction rates

Table 1: Constant values used for calculation

Variable ID	Parameter	Value	Unit	Source
δ_{H_2O}	density water	1	g/cm³	
$\delta_{dry\ sediment}$	density dry sediment	2.6	g/cm³	personal comm. S. Henkel
w_{sed}	water content sediment	0.436		calculated from dry weight vs. wet weight of sediment STA14 used for slurry preparation
V_{slurry}	volume slurry used for incubation	5	ml	protocol
$V_{20\%\ Zn-ac}$	volume 20% Zn-acetate used to stop SRR-incubation	10	ml	protocol
$V_{5\%\ Zn-ac}$	volume 5% Zn-acetate used to rinse slurry out of Hungate tube	20*	ml	protocol
$V_{SO_4^{2-}}$	volume supernatant sample used for total activity measurement $A_{SO_4^{2-}.raw}$	0.1	ml	protocol
	isotope fractionation factor	1.06		Jørgensen and Fenchel (1974)

*: for samples distilled on 12.06.23 and 13.06.23 this was 21 ml

Table 2: Parameters measured for sulfate reduction rate calculations.

Variable ID	Subject	Parameter	Unit
t	SRR-incubation	time	days
$A_{blank.dis}$	blank distillation set-up	radioactivity	cpm
A_{blank}	blank scintillation fluid	radioactivity	cpm
$A_{TRIS.raw}$	TRIS in Zn-acetate trap	radioactivity	cpm
$A_{SO_4^{2-}.raw}$	sulfate in supernatant Zn-acetate fixed slurry in falcon tube	radioactivity	cpm
$c_{SO_4^{2-}}$	sulfate in supernatant slurry before SRR-incubation	concentration	mmol/l

Sulfate reduction rate calculation:

Used values described in Table 1 and Table 2

(1) Correct measured radioactivity with blank:
(check if value was below blank = below detection limit)
$A_{TRIS.cor} = A_{TRIS.raw} - A_{blank.dis}$
$A_{SO_4^{2-}.cor} = A_{SO_4^{2-}.raw} - A_{blank}$

(2) Total sulfate radioactivity in sample:
$$A_{SO_4^{2-}} = A_{SO_4^{2-}.cor} \times \frac{V_{slurry} + V_{20\%\ Zn-ac} + V_{5\%\ Zn-ac}}{V_{SO_4^{2-}}}$$

(3) Porosity *in situ* sediment:
$$\varphi_{in\ situ} = \frac{\frac{w_{sed}}{\delta_{H_2O}}}{\frac{w_{sed}}{\delta_{H_2O}} + \frac{1 - w_{sed}}{\delta_{dry\ sediment}}} = 0.668$$

(4) Porosity slurry:
$$\varphi_{slurry} = \frac{1 - \varphi_{in\ situ}}{V_{slurry}} = 0.934$$

(5) Concentration SO_4^{2-} in slurry converted from mmol/l supernatant to nmol/cm³ slurry:
$[SO_4^{2-}] = c_{SO_4^{2-}} \times 1000 \times \varphi_{slurry}$

(6) Sulfate reduction rate in nmol sulfate reduced per cm³ slurry and day:
1.06 is the estimated isotope fractionation factor between $^{32}SO_4^{2-}$ and $^{35}SO_4^{2-}$
$$SRR_{slurry} = \frac{A_{TRIS}}{A_{SO_4^{2-}} + A_{TRIS}} \times [SO_4^{2-}] \times 1.06 \times \frac{1}{t}$$

5.2.3.2 RNA extraction magnetic beads protocol

RNA and DNA were extracted from 0.5 g of sediment using an extraction protocol combining cell lysis with beat-beating and further purification with silica magnetic beads. The initial cell lysis steps followed Lueders et al. (2004). The sample was transferred into a 2-ml tube and ~ 0.7 g zirconium beads, 600 µl 120 mM $NaPO_4$ buffer (pH 8) and 200 µl TNS-solution (500 mM Tris-HCl, 100 mM NaCl, 10% SDS) were added. Beat-beating was performed twice at 6.5 m/s for 45 s. Between beat-beating steps, samples were kept on ice. Samples were centrifuged at 4°C and 20817 *g* for 20 min and the supernatant (= lysate, ~ 600 µl) was transferred into a new 2-ml tube and subsequently kept on ice.

Fresh silica magnetic beads (G-Biosciences, Geno Technology Inc., USA) were washed for each extraction: 10 µl of bead suspension per reaction plus extra margin were transferred into a 2-ml tube, placed in a stand on a magnet (magnetic stand) collecting the beads at the site of the tube for 1 min and carefully pipetting off and discarding the supernatant. Then the tube was removed from the stand and 500 µl elution buffer (Monarch, New England Biolabs, Germany) was added and beads were resuspended by vortexing for 8 s. The tube was gently centrifuged

down with a mini table centrifuge for 1 min to collect bead suspension on the bottom and the tube was placed back onto the magnetic stand. After 1 min, supernatant was discarded and the washing step was repeated for a total of two times. The beads were resuspended in a volume of elution buffer equal to the initial volume.

The lysate was split into multiple 2-ml tubes with a maximum of 100 µl per tube in order to ensure sufficient binding of nucleic acids to the beads. Per tube with lysate, 1.56 ml binding buffer (Monarch, New England Biolabs, Germany) and 10 µl silica magnetic beads were added and mixed by inverting for 5 s. The tube was incubated at 20°C while shaking at 1000 rpm on a thermomixer for 15 min. The liquid was removed by gentle centrifugation for collecting the suspension on the bottom of the tube, placing it on a magnet for 1 min and pipetting off the supernatant. The sample was washed by removing the tube from the magnet, adding 250 µl washing buffer (Monarch, New England Biolabs, Germany), mixing it by pipetting with the beads and removing the liquid as described above. The washing step was repeated for a total of two times. After the second washing step, a smaller-volume pipet was used to ensure to pipet off all remaining liquid and the magnetic beads pellet was briefly dried on the magnetic stand with open lid for a maximum of 5 min. The sample was eluted by removing the tubes from the magnet, adding 20 µl elution buffer or water to the tube, resuspending beads by pipetting, spinning tube down gently and incubating at 4°C and 1000 rpm shaking on a thermomixer for 5 min. The tube was placed in the magnetic stand for 2 min and the supernatant was transferred into a fresh 2-ml tube. The elution procedure was repeated a second time with the same tube. In order to reduce the resulting volume, it is possible to transfer the produced elute into a tube with magnetic beads and DNA/RNA suspension, eluting the nucleic acids into the same volume, but performing the second elution step always with fresh elution buffer or water. With either approach chosen, elutes of the same sample were always pooled into the same tube in the end.

5.2.3.3 Preparation cesium trifluoroacetate solution

Cesium trifluoroacetate solution was prepared for density separation of RNA as part of RNA-stable isotope probing. The solution was prepared under a fume hood. For 500 ml CsTFA solution, a 1L-plastic beaker was rinsed with trifluoroacetate (TFA, 99.9% purity, Carl Roth, Germany), 460 g $CsOH \cdot 2\ H_2O$ (99.5% purity, Sigma-Aldrich, Germany) were weighted in and max. 250 ml pure water (Astacus², membraPure, Germany) were added. The beaker was placed in an ice-bath and solution was stirred. 215 ml TFA were added slowly. If the temperature of the solution increased too rapidly, TFA was added more slowly. The solution was stirred for 30 min and pH was checked with pH paper. The pH was adjusted to 4-5 by

addition of CsOH or TFA. Density was checked by weighing 100 µl of the solution and was adjusted to 2.2 ± 0.05 g/ml by addition of CsOH or water. The solution was autoclaved and subsequently the pH was adjusted to 7.0 and the density to 2.0 g/ml. The solution was filter-sterilized through vacuum-filtration with a 0.2 µm filter into a sterile bottle. The autoclave step can be skipped, then pH is adjusted to 7.0 and density to 2.0 g/ml after TFA addition and subsequent sterilization by filtration is performed. Every new batch CsTFA solution has to be checked by running a control sample of a mixture of unlabeled and fully ^{13}C-labeled RNA from *Escherichia coli* with which a new density – refractory index standard curve is prepared.

5.2.3.4 Sequence analysis – removal of contaminant sequences

The ASV abundance table retrieved from the sequence analysis pipeline (see method section) contained sequences which were assumed to be not present in the biological sample and therefore considered to be contamination. This phenomenon is known and contaminants can originate e.g., from chemicals or kits used during library preparation (Knights et al. 2011, Salter et al. 2014) and are often more abundant in samples with low nucleic acid concentration (Davis et al. 2018). Potential contaminant sequences were identified by two approaches; (1) the R package decontam (v1.24.0, Davis et al. 2018), which compares initial nucleic acid concentration in the PCR product and abundance of ASVs. With this approach, we tested thresholds of 0.1, 0.15 and 0.2 with the frequency method. For approach (2), ASVs were identified which had read counts > 0 in less than 50% of all samples and had total read counts across all samples above the average of total read counts across all samples and ASVs. The list of ASVs of both approaches were combined. For the top 30 most abundant ASVs, the frequency of the individual ASVs was plotted against nucleic acid concentration in PCR products and the taxonomy was compared with a list of taxa frequently identified as contaminants in lab environments (Salter et al. 2014). An ASV was considered as contaminant, if (1.) the frequency-distribution correlated with PCR product concentration, (2.) it only occurred in very few samples and (3.) the taxon was a known contaminant (Table S4).

5.2.4 References

Aronson, H. S., C. Thomas, M. K. Bhattacharyya, S. R. Eckstein, S. R. Jensen, R. A. Barco, J. L. Macalady, and J. P. Amend. (2023). *Thiovibrio frasassiensis* gen. nov., sp. nov., an autotrophic, elemental sulphur disproportionating bacterium isolated from sulphidic karst sediment, and proposal of *Thiovibrionaceae* fam. nov. Int. J. Syst. Evol. Microbiol. **73**. doi:10.1099/ijsem.0.006003.

Davis, N. M., D. M. Proctor, S. P. Holmes, D. A. Relman, and B. J. Callahan. (2018). Simple statistical identification and removal of contaminant sequences in marker-gene and metagenomics data. Microbiome **6**:226. doi:10.1186/s40168-018-0605-2.

Finster, K., W. Liesack, and B. Thamdrup. (1998). Elemental sulfur and thiosulfate disproportionation by *Desulfocapsa sulfoexigens* sp. nov., a new anaerobic bacterium isolated from marine surface sediment. Appl. Environ. Microbiol. **64**:119-125. doi:10.1128/aem.64.1.119-125.1998.

Hashimoto, Y., S. Shimamura, A. Tame, S. Sawayama, J. Miyazaki, K. Takai, and S. Nakagawa. (2022). Physiological and comparative proteomic characterization of *Desulfolithobacter dissulfuricans* gen. nov., sp. nov., a novel mesophilic, sulfur-disproportionating chemolithoautotroph from a deep-sea hydrothermal vent. Front. Microbiol. **13**. doi:10.3389/fmicb.2022.1042116.

Hashimoto, Y., A. Tame, S. Sawayama, J. Miyazaki, K. Takai, and S. Nakagawa. (2021). *Desulfomarina profundi* gen. nov., sp. nov., a novel mesophilic, hydrogen-oxidizing, sulphate-reducing chemolithoautotroph isolated from a deep-sea hydrothermal vent chimney. Int. J. Syst. Evol. Microbiol. **71**. doi:10.1099/ijsem.0.005083.

Henkel, J. V., A. Vogts, J. Werner, T. R. Neu, C. Spröer, B. Bunk, and H. N. Schulz-Vogt. (2021). *Candidatus* Sulfurimonas marisnigri sp. nov. and *Candidatus* Sulfurimonas baltica sp. nov., thiotrophic manganese oxide reducing chemolithoautotrophs of the class *Campylobacteria* isolated from the pelagic redoxclines of the Black Sea and the Baltic Sea. Syst. Appl. Microbiol. **44**:126155. doi:10.1016/j.syapm.2020.126155.

Hiralal, A., J. S. Geelhoed, S. Hidalgo-Martinez, B. Smets, J. R. van Dijk, and F. J. R. Meysman. (2024). Closing the genome of unculturable cable bacteria using a combined metagenomic assembly of long and short sequencing reads. Microb. Genom. **10**. doi:10.1099/mgen.0.001197.

Jørgensen, B. B. and T. Fenchel. (1974). The sulfur cycle of a marine sediment model system. Mar. Biol. **24**:189-201. doi:10.1007/BF00391893.

Knights, D., J. Kuczynski, E. S. Charlson, J. Zaneveld, M. C. Mozer, R. G. Collman, F. D. Bushman, R. Knight, and S. T. Kelley. (2011). Bayesian community-wide culture-independent microbial source tracking. Nat. Methods **8**:761-763. doi:10.1038/nmeth.1650.

Lie, T. J., M. L. Clawson, W. Godchaux, and E. R. Leadbetter. (1999). Sulfidogenesis from 2-Aminoethanesulfonate (Taurine) fermentation by a morphologically unusual sulfate-reducing bacterium, *Desulforhopalus singaporensis* sp. nov. Appl. Environ. Microbiol. **65**:3328-3334. doi:10.1128/AEM.65.8.3328-3334.1999.

Liesack, W. and K. Finster. (1994). Phylogenetic analysis of five strains of gram-negative, obligately anaerobic, sulfur-reducing bacteria and description of *Desulfuromusa* gen. nov., including *Desulfuromusa kysingii* sp. nov., *Desulfuromusa bakii* sp. nov., and *Desulfuromusa succinoxidans* sp. nov. Int. J. Syst. Evol. Microbiol. **44**:753-758. doi:10.1099/00207713-44-4-753.

Lueders, T., M. Manefield, and M. W. Friedrich. (2004). Enhanced sensitivity of DNA- and rRNA-based stable isotope probing by fractionation and quantitative analysis of isopycnic centrifugation gradients. Environ. Microbiol. **6**:73-78. doi:10.1046/j.1462-2920.2003.00536.x.

Pfennig, N. and H. Biebl. (1976). *Desulfuromonas acetoxidans* gen. nov. and sp. nov., a new anaerobic, sulfur-reducing, acetate-oxidizing bacterium. Arch. Microbiol. **110**:3-12. doi:10.1007/BF00416962.

Plum-Jensen, L. E., A. Schramm, and I. P. G. Marshall. (2024). First single-strain enrichments of *Electrothrix* cable bacteria, description of *E. aestuarii* sp. nov. and *E. rattekaaiensis* sp. nov., and proposal of a cable bacteria taxonomy following the rules of the SeqCode. Syst. Appl. Microbiol. **47**:126487. doi:10.1016/j.syapm.2024.126487.

Salter, S. J., M. J. Cox, E. M. Turek, S. T. Calus, W. O. Cookson, M. F. Moffatt, P. Turner, J. Parkhill, N. J. Loman, and A. W. Walker. (2014). Reagent and laboratory contamination can critically impact sequence-based microbiome analyses. BMC Biol. **12**:87. doi:10.1186/s12915-014-0087-z.

Sass, A., H. Rütters, H. Cypionka, and H. Sass. (2002). *Desulfobulbus mediterraneus* sp. nov., a sulfate-reducing bacterium growing on mono- and disaccharides. Arch. Microbiol. **177**:468-474. doi:10.1007/s00203-002-0415-5.

Sung, Y., K. M. Ritalahti, R. A. Sanford, J. W. Urbance, S. J. Flynn, J. M. Tiedje, and F. E. Löffler. (2003). Characterization of two tetrachloroethene-reducing, acetate-oxidizing anaerobic bacteria and their description as *Desulfuromonas michiganensis* sp. nov. Appl. Environ. Microbiol. **69**:2964-2974. doi:10.1128/aem.69.5.2964-2974.2003.

Vandieken, V., M. Mußmann, H. Niemann, and B. B. Jørgensen. (2006). *Desulfuromonas svalbardensis* sp. nov. and *Desulfuromusa ferrireducens* sp. nov., psychrophilic, Fe(III)-reducing bacteria isolated from Arctic sediments, Svalbard. Int. J. Syst. Evol. Microbiol. **56**:1133-1139. doi:10.1099/ijs.0.63639-0.

Wang, J., Q. Zheng, S. Wang, J. Zeng, Q. Yuan, Y. Zhong, L. Jiang, and Z. Shao. (2023). Characterization of two novel chemolithoautotrophic bacteria of *Sulfurovum* from marine coastal environments and further comparative genomic analyses revealed species differentiation among deep-sea hydrothermal vent and non-vent origins. Front. Mar. Sci. **10**. doi:10.3389/fmars.2023.1222526.

Wunder, L. C., I. Breuer, G. Willis-Poratti, D. A. Aromokeye, S. Henkel, T. Richter-Heitmann, X. Yin, and M. W. Friedrich. (2024). Manganese reduction and associated microbial communities in Antarctic surface sediments. Front. Microbiol. **15**. doi:10.3389/fmicb.2024.1398021.

Chapter 6

General discussion

Organic matter mineralization in marine sediments is an important part of the carbon cycle and the understanding of the occurring processes is crucial to predict future changes due to climate change (LaRowe et al. 2020). Organic matter degradation rates coupled to different electron accepting processes were investigated in multiple Arctic and Antarctic environments (Vandieken et al. 2006c, Finke and Jørgensen 2008, Glombitza et al. 2015, Bourgeois et al. 2017, Baloza et al. 2022, Zwerschke et al. 2022), regions which are especially affected by climate change (Moore et al. 2013). Especially the contribution of metal oxides as electron acceptors for organic matter mineralization is of interest, as these are supplied by glacial meltwater (Wehrmann et al. 2014, Monien et al. 2017) and accelerated glacial melting is one of the most prominent changes due to global warming in polar environments (e.g., Rückamp et al. 2011). In previous studies, the microbial community associated with degradation processes was often not identified, or only indirectly linked to an activity by sequencing the microbial communities of *in situ* sediments (Vandieken et al. 2006a, Algora et al. 2013, Buongiorno et al. 2019, Baloza et al. 2023). However, the identity of the associated microorganisms completes our understanding of these systems and potentially enables the identification of keystone species and marker species for different processes, which can be used to identify the processes easily also in other environments.

In this thesis, I aimed to identify the microbial community involved in final organic matter mineralization in permanently cold, glacial influenced surface sediments of Antarctica. I focused on identifying terminal electron acceptors, especially glacial supplied metal oxides, coupled to acetate oxidation and the conducting microbial community. I combined data about *in situ* geochemical processes and microbial community composition with slurry incubation experiments under different conditions in order to link metabolic activities to specific microorganisms (chap. 2-5).

As key findings from the different chapters of this manuscript, I could identify iron reducing microorganisms as the most stimulated acetate oxidizers in experiments with marine sediments of Potter Cove and South Georgia (chap. 2, 4). The uncultured group Sva1033 (Desulfuromonadales) was identified as prominent iron reducer in all studied sediments, its abundance in iron reducing incubations and *in situ* sediments suggesting it as a keystone

species in these environments (chap. 2-5). It even showed acetate oxidizing and iron reducing activities up to 25°C (chap. 4), suggesting its persistent role even under global warming induced increasing temperatures. Next to iron reduction, manganese reduction could also be coupled to acetate oxidation if both substrates were provided, likely contributing to this final step of organic matter mineralization in sediments close to the glacier (chap. 3). Lastly, sulfate reducers did not seem to contribute to acetate oxidation, while they were found abundantly in the *in situ* sediments and sulfate reduction could be stimulated by the addition of acetate and hydrogen (chap. 5). Instead, the typical sulfide oxidizer *Sulfurimonas* was stimulated to high abundances in multiple incubation experiments, but especially in sulfate reducing incubations (chap. 2-5). These glacial influenced sediments likely harbor a complex sulfur cycle, which is discussed in detail below.

In the following discussion, I combine the results of the different chapters to paint a more complete picture (I) which processes likely contributed to acetate oxidation in the investigated environments, (II) which microorganisms were responsible and were potential keystone species in their environments and (III) how future global change might affect the processes in the studied environments. Potter Cove was used as a model site for an Antarctic bay/fjord system, which is influenced by a melting glacier, and results from previous studies were complemented with new insights from the projects of this thesis.

6.1 Acetate degrading processes and microbial players in Antarctic sediments

6.1.1 Geochemical processes

Study sites and in situ measurements of geochemical processes

The investigated sampling sites were fjords around South Georgia, especially Cumberland Bay, and Potter Cove at King George Island/Isla 25 de Mayo at the West Antarctic Peninsula. These environments are highly influenced by iron-laden glacial meltwater input from melting glaciers terminating into the bays around the islands (Hodgson et al. 2014, Henkel et al. 2018). High accumulation of dissolved Fe^{2+} in pore water indicated iron reduction as main terminal electron accepting process in these sediments (chap. 2, Fig. 2; chap. 3, Fig. 2; chap. 5, Fig. 2) (Monien et al. 2014, Henkel et al. 2018, Aromokeye et al. 2021). In the fjord system of Cumberland Bay at South Georgia, geochemistry of the sediments and meltwater supply seemed to be similar to many Arctic fjord systems, e.g., Kongsfjorden or Van Keulenfjorden at Svalbard, which are also influenced by large tidewater glaciers (Jørgensen et al. 2020, Michaud et al. 2020).

The other study site, Potter Cove, is a shallow bay influenced by the Fourcade Glacier. In chapter 3, 4 and 5 of this thesis, sediments from stations close to the glacier (STA01, STA13)

and in the center of the cove (STA14) were investigated, while Aromokeye et al. (2021) directly compared a station close to the glacier (STA10) with a station in the center of the cove (STA14) (Figure 1). At the glacial stations, the geochemical pore water profiles were more similar to the typical fjord systems of Cumberland Bay and Svalbard; the ferrous iron profiles reached deep into the sediment and sulfate profiles stayed more stable, indicating only minor occurring sulfate reduction (chap. 3, Fig. 2) (Monien et al. 2014). In contrast, at the central cove station, ferrous iron showed a prominent large peak in the top 10 cm and depleted below, while the sulfate profile also clearly declined with depth, indicating concurrent iron and sulfate reduction (chap. 5, Fig. 2) (Monien et al. 2014). However, no free sulfide as a clear indicator for sulfate reduction was present at any station. This center station was more similar to shelf sediments, such as along the Antarctic Peninsula (Baloza et al. 2022) or to Smeerenburgfjorden of Svalbard, which is influenced by shelf water as well (Jørgensen et al. 2020, Michaud et al. 2020).

Metabolic processes identified by incubation experiments

In the different projects of this thesis, slurry incubations with the addition of acetate were performed to observe which provided electron acceptor influenced metabolic activities and to investigate the stimulated microbial community.

For sediments from Cumberland Bay, South Georgia, iron reduction could be clearly identified as major process, as the incubation of the slurry alone was sufficient to stimulate accumulation of ferrous iron independent of additionally added electron acceptors (chap. 2, suppl. Fig. S6). Different results were obtained in slurry experiments with Potter Cove sediments; regardless of the station, accumulation of ferrous iron was only visible if acetate and fresh iron oxides, or macroalgae were supplied to the sediment (chap. 3, 4, 5, Aromokeye et al. 2021). This suggested that sediments of Potter

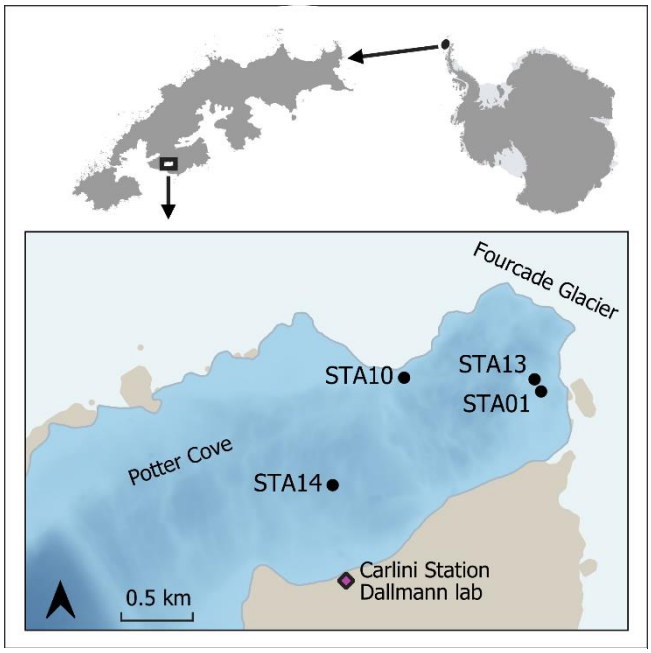

Figure 1: Sediment sampling stations in Potter Cove for different projects. STA13: chap. 2, 4; STA01: chap. 3; STA10: Aromokeye et al. (2021); STA14: chap. 5, Aromokeye et al. (2021).
Map created with QGIS 3.34.3, bathymetry data Neder et al. (2022) updated from Jerosch et al. (2015), basemap data SCAR Antarctic Digital Database 2023, rock outcrop from Gerrish (2020) manually smoothed.

Cove seemed to rely on fresh supply of iron oxides, while sediments of South Georgia contained enough endogenous iron oxides for iron reduction to thrive.

The exact differences between South Georgia and Potter Cove sediments were not clear. Potentially, the iron oxides in the sediments differed in quantity or quality, i.e., accessibility for microbial iron reduction (Bonneville et al. 2004, Laufer et al. 2020). This was supported by up to 0.7 wt.% "easily reducible" iron oxides (leachable iron oxides with hydroxylamine-HCl, mostly ferrihydrite and lepidocrocite) in sediments of Cumberland Bay (Köster 2014) compared to only 0.25-0.4 wt.% in sediments of Potter Cove (Henkel et al. 2018). However, the used iron extraction protocol (Poulton and Canfield 2005) gave no information about actual bioavailability of the iron oxides and no measurements of different solid iron phases were conducted on the exact sediments used for the slurry experiments. Furthermore, the availability of other endogenous substrates, which were needed for iron reduction, could have differed. It was unlikely, however, that the different storage periods of the sediment samples caused differences in iron oxides depletion. The sediments from South Georgia were stored for two years prior to incubation experiments and in these iron reduction could still be stimulated just by slurry preparation (chap. 2). In contrast, Potter Cove sediments were stored for less than one year prior to incubations described in Aromokeye et al. (2021) and chapter 4, where slurry preparation and acetate addition alone were not sufficient for a similar stimulation. While it was not clear which process exactly might have been responsible for the different activities in each of the studied sites, my overall conclusion is that Potter Cove sediments were likely more dependent on constant supply of fresh iron oxides by the glacial meltwater to maintain acetate degradation coupled to iron reduction than South Georgia sediments. Detailed analyses of quantity and quality of present iron oxides are needed for further validation.

6.1.2 Key acetate degrading bacteria in (sub-) Antarctic sediments

Linking metabolic processes with microbial communities

16S rRNA gene sequencing of the microbial communities in *in situ* sediments identified potentially responsible microorganisms for observed geochemical processes. In projects of this thesis, strikingly, typical iron reducing taxa were only detected at extremely low abundances at all ferruginous sampling locations, except for the uncultivated family Sva1033 within the order Desulfuromonadales, which harbors many iron reducing taxa (Lovley 2013). Instead, an abundance of known sulfur cycling or sulfate reducing bacteria was detected, such as *Desulfobacteraceae*, *Desulfobulbaceae*, *Desulfosarcinaceae* and *Desulfocapsaceae* (chap. 2, Fig. 3; chap. 3, suppl. Fig. S8; chap. 5, Fig. 4) (Jørgensen et al. 2019, Diao et al. 2023).

However, proposing metabolic activities by taxonomic affiliation alone is difficult; phylotypes even within the same species can be diverse (Lidstrom and Konopka 2010) and many uncultivated taxa with unknown metabolic capabilities are abundant in marine sediments (Petro et al. 2017, Wang et al. 2021a). Correlation analyses between abundant taxa and measured variables, such as nutrients in pore water, provide first indications of potential metabolisms (Jorgensen et al. 2012) but are alone not sufficient to confidently determine which metabolism a certain microorganism might perform *in situ*. Modern techniques such as metagenomic and metatranscriptomic sequencing or even single-cell sequencing help to close this gap, especially for uncultivated organisms (Rinke et al. 2013, Hedlund et al. 2014, Solden et al. 2016). Another approach is to incubate the sediment with certain substrates to stimulate processes of interest and investigate the responding microbial community. The use of RNA-SIP with selected ^{13}C-labeled substrates is even more specific, allowing labeling and taxonomic identification of active microorganisms which incorporate the provided substrate into the RNA molecule (Dumont and Murrell 2005). Monitoring the incubation experiment carefully by measuring changing geochemical variables such as ferrous iron, sulfate or sulfide further allows linking the active microbes to the most likely metabolism.

Keystone species Sva1033

In experiments of this thesis, irrespective of the condition of the incubation experiment or sediment origin, always the same bacterial groups were stimulated by adding acetate (chap. 2-5). The major stimulated group was the uncultivated family Sva1033 (Desulfuromonadales). This group was first discovered in sediments of Svalbard over 25 years ago (Ravenschlag et al. 1999), but prior to the studies in this thesis, only suggestions about its potential metabolisms were made based on correlations with *in situ* data (Tu et al. 2017, Buongiorno et al. 2019). Sva1033 was clearly stimulated and labeled if acetate was amended in all experiments. Additional iron oxides lead to a higher stimulation, but were not mandatory at *in situ* temperatures of 2°C (chap. 2-5, Aromokeye et al. 2021). At higher temperatures, Sva1033 heavily relied on fresh iron oxide supply to compete for acetate with other present microorganisms (chap. 4). Iron was identified as the main, most favorable electron acceptor for Sva1033 (chap. 2, 4) and there were first indications for manganese oxides as possible electron acceptors as well (chap. 3). Furthermore, Sva1033 was able to thrive on endogenous electron acceptors in the sediments at close-to *in situ* conditions (chap. 2-5), which could be residual iron and manganese oxides or also sulfur compounds as electron acceptors. Sulfate was identified as an unlikely electron acceptor for Sva1033, as it was clearly labeled in SIP incubations, if sulfate reduction was inhibited by molybdate addition (chap. 2, 5). This was in

contrast to sulfate reduction as proposed metabolism for Sva1033 in Arctic sediments of Svalbard (Buongiorno et al. 2019). Sva1033 even kept its key function as acetate degrader over a wide temperature range up to 25°C, indicating that in future scenarios of increasing temperatures it might still able to play its key role in the sediments (chap. 4).

More investigations are necessary to identify these other proposed electron acceptors for this organism, for which the isolation of a Sva1033 species would be very advantageous. Additionally, it would allow officially describing this new taxonomic group with standardized taxonomy. We tried enrichment and isolation of Sva1033. However, it proofed to be very difficult, as other taxa, particularly *Desulfuromonas*, always dominated the enrichments already after the first transfer into fresh medium (unpublished data). Therefore, we hypothesized that Sva1033 was highly dependent on fresh iron oxides, while *Desulfuromonas* could also use "aged" iron oxides, which might be more encrusted by, e.g., organic matter (O'Loughlin et al. 2010). This hypothesis was supported by a higher abundance of *Desulfuromonas* in incubation experiments which were conducted after a longer sediment storage time (> 3 years, chap. 3, 5) compared to experiments set up more quickly after sediment retrieval (< 1 year, Aromokeye et al. 2021). This was further supported by directly comparing acetate utilization when iron or sulfate were supplied; Sva1033 was more labeled when iron oxides were supplied, while *Desulfuromonas* was more labeled with sulfate or no additional electron acceptor, likely thriving on the residual iron oxides from the slurry (chap. 4).

Sva1033 can be proposed as keystone species for organic matter degradation in Antarctic sediments. It was abundant in the investigated *in situ* sediment samples of Potter Cove (chap. 3, 5) and South Georgia (chap. 2) and was also found in other Antarctic (Baloza et al. 2023) and many Arctic (e.g., Ravenschlag et al. 1999, Buongiorno et al. 2019, Begmatov et al. 2021, Walker et al. 2023) sediments. It is potentially important also on a global scale, as indicated by occurrences in not-polar environments, such as shallow and deeper temperate sediments (Rubin-Blum et al. 2022, Stuij et al. 2024, Zhu et al. 2024), deep-sea cold seep sediment (Xin et al. 2022) or terrestrial environments, such as mud volcanos (Tu et al. 2017, Slobodkin et al. 2024). Besides the polar sites, Sva1033 was especially often found in estuaries across the globe, from the Mediterranean Sea to China and Australia, and many of these sediments were characterized by heavy metal contaminations (e.g., Sun et al. 2013, Zoppini et al. 2020, Aldeguer-Riquelme et al. 2022, Wang et al. 2022b, Bracewell et al. 2023). As Sva1033 is classified as family by the SILVA taxonomy (Quast et al. 2012, release 138.1), it would be interesting to compare the sequences found in different environments and experimental conditions. One issue was the inconsistent taxonomy for uncultured taxa between prominent

databases; e.g., there is no clear representative for Sva1033 in the Genome Taxonomy Database (GTDB, Parks et al. 2018), which is often used to classify metagenome assembled genomes. Providing a consistent taxonomy would be necessary to further describe this group and make it easier for future research to identify and reference Sva1033.

Desulfuromonas and Desulfuromusa

Besides Sva1033, there were a few other taxonomic groups, which could be identified as important microorganisms associated with acetate degradation, as they occurred in multiple experiments under varying conditions. The known iron reducer *Desulfuromonas* (Vandieken et al. 2006b) was already mentioned above. It was labeled with acetate in all iron reducing SIP incubations with Potter Cove or South Georgia sediments (chap. 2, 4, 5, Aromokeye et al. 2021), but also occurred without acetate addition when only manganese oxides were added (chap. 3). *Desulfuromonas* was shown to thrive on sulfur reduction (Pfennig and Biebl 1976), which could have fuel its observed activity in incubations without additional electron acceptors. Partially, this result is similar to another stimulated taxon, *Desulfuromusa*, which was shown to occupy a niche of organotrophic manganese reduction under favorable conditions in Potter Cove sediments (chap. 3). In slurry experiments with sediments from South Georgia and Potter Cove, *Desulfuromusa* was also found labeled with acetate under iron reducing conditions (chap. 2, 4, 5, Aromokeye et al. 2021), potentially thriving on residual manganese oxides left in the slurry. One possible explanation why Sva1033 apparently outcompeted these other organisms such as *Desulfuromonas* or *Desulfuromusa* was that Sva1033 might be more successful in thriving on freshly provided iron oxides, such as those constantly supplied in these polar environments due to glacier retreat.

Arcobacteraceae

All of the taxa discussed so far belong to the order Desulfuromonadales. The other taxa that were stimulated by acetate addition in the different incubations were *Sulfurimonas* and *Arcobacteraceae* and both belong to the order Campylobacterales (formerly Epsilonproteobacteria). This order contains many organisms capable of oxidizing reduced sulfur compounds (Yamamoto and Takai 2011). *Arcobacteraceae* was stimulated and labeled with acetate, likely reducing iron, in multiple incubation experiments with South Georgia and Potter Cove sediment (chap. 2-5, Aromokeye et al. 2021). Iron and manganese reducing capabilities were shown for this taxon previously (Vandieken et al. 2012, Roalkvam et al. 2015). Interestingly, *Arcobacteraceae* was especially stimulated if acetate and molybdate were present (chap. 2, 5), potentially due to less competition by directly or indirectly inhibited microorganisms. Another possibility would be that this taxon could use molybdate as electron

acceptor, as has been shown for other bacteria (Ahmad et al. 2013). This theory might be interesting to investigate further, as this taxon could be involved in heavy metal decontamination (Ahmad et al. 2013). In general, these results showed that *Arcobacteraceae* contributed to organic matter mineralization, i.e., acetate oxidation, in the permanently cold sediment of Antarctica. *Sulfurimonas* showed very interesting abundance patterns especially in treatments with sulfate. These results are discussed in more detail in the section below.

6.2 The carbon cycle in Potter Cove under the influence of climate change

Impact of global warming on the Fourcade Glacier and meltwater supply

The sampling site Potter Cove, used here as a model system of an Antarctic bay influenced by a retreating glacier, is located at King George Island/ Isla 25 de Mayo, at the tip of the West Antarctic Peninsula (Figure 1). It is already heavily affected by global warming, visible by temperature increase and accelerated glacial melting (Rückamp et al. 2011, Latorre et al. 2023). It is influenced by the Fourcade Glacier that terminates into the bay and retreated with a rate of 40 m per year in the past decade, revealing 0.18 km² of newly ice-free area (2008-2018, Meredith et al. 2018, Deregibus et al. 2023). The glacier transformed from grounded to floating tidewater glacier to land-terminating glacier, supplying the bay with subglacial meltwater, groundwater discharge and surficial meltwater streams (Meredith et al. 2018, Falk and Silva-Busso 2021). The glacial meltwater releases high amounts of suspended particulate matter (SPM) into the bay, which is further distributed by a cyclonic circulation (Neder et al. 2022).

The studies that investigated the distribution of SPM and their effect on the benthic communities and sediments were all conducted with data acquired between 1991 and 2017, with the majority from before 2014 (Klöser et al. 1996, Schloss et al. 2012, Marina et al. 2017, Monien et al. 2017, Henkel et al. 2018, Jerosch et al. 2018, Meredith et al. 2018, Jerosch et al. 2019, Neder et al. 2020, Braeckman et al. 2021, Deregibus et al. 2023). The samples used in the studies of this thesis were retrieved in austral summer 2018/19, thereby representing one of the newest datasets. The glacier retreated to land in 2016, and it is unknown how the supply and distribution of SPM developed since then. While the transition from grounded to floating tidewater glacier increased the supply of SPM to the bay (Monien et al. 2017, Neder et al. 2022), the complete retreat to land likely reduces the supply of SPM on the long term, as the catchment area of the glacier, i.e., the area of underlying rock it grinds on, is reduced (Milner et al. 2017), as visible in fjords around Svalbard (Herbert et al. 2020, Herbert et al. 2021). Neder et al. (2022) proposed that with the retreat of the glacier to land, glacial meltwater streams will first supply more SPM from the moraines in front of the glacial front and will then eventually dry out and SPM supply will cease.

Influence of suspended particulate matter and glacial retreat on primary productivity

The retreat of the glacier and associated supply of SPM into the cove influences the environment in near and far proximity in many different ways. In Potter Cove, the main primary producers are macroalgae, while phytoplankton and terrestrial organic matter are not as important (Fabiano et al. 1996, Schloss and Ferreyra 2002, Quartino and Boraso de Zaixso 2008). The primary productivity of present macroalgae is negatively affected by a higher load of SPM in the water column, leading to lower light penetration due to increased turbidity (Schloss et al. 2012, Campana et al. 2018). On the other hand, the retreating glacier also has a stimulating effect on macroalgae growth by exposing more solid substrate, which macroalgae can colonize (Campana et al. 2018, Neder et al. 2022). Together, the macroalgae were proposed to produce a positive carbon fixation rate, so called "blue carbon", balancing reduced primary productivity due to more turbid water with increased biomass due to macroalgae colonization at more locations (Deregibus et al. 2023).

Macroalgae as base of the food-web in Potter Cove

As prime organic matter source, the macroalgae are an essential key component in the food-web of Potter Cove (Marina et al. 2017). They are consumed by macrobenthos, microphytobenthos and microorganisms in the sediment, while meiobenthos, in turn, feeds on these utilizers instead of on the algae detritus directly (Braeckman et al. 2019, Aromokeye et al. 2021). Furthermore, macrobenthos is responsible for burying algae detritus deeper into the sediments into anoxic zones, where it can be further degraded by microorganisms (Braeckman et al. 2019). For complete mineralization by the microbial community, the first steps of degradation were conducted through hydrolysis and fermentation by bacteria such as *Psychromonas* (Pelikan et al. 2020, Aromokeye et al. 2021) (Figure 2). The resulting compounds, e.g., long-chain fatty acids lactate, butyrate or propionate, could be further fermented to acetate, which was then oxidized further, or directly oxidized to CO_2 by bacteria such as *Moritella*, *Marinifilum* and *Colwellia* (Aromokeye et al. 2021). The oxidation processes were coupled to final electron acceptors. Close to the sediment surface, oxygen was depleted within the first few millimeters, which was visible from the geochemical profiles of nitrate and ferrous iron (e.g., chap. 3). Nitrate was depleted rapidly within the first millimeters in sediments further out in the cove and within the first 1-2 cm in sediments closer to the glacier (Aromokeye et al. 2024). Deeper in the sediment, geochemical signatures of manganese and iron reduction became visible (chap. 3, 5, Monien et al. 2014, Henkel et al. 2018), which were quantified as major final electron accepting processes in Arctic sediments, contributing up to 43% to > 90% to organic carbon mineralization (Vandieken et al. 2006a, Vandieken et al. 2006c). Similar rate

measurements are needed for an exact quantification of these processes, but incubation experiments conducted during this thesis already gave clear indications of the importance of these processes in Potter Cove sediments.

Glacial-supplied iron oxides

The iron oxides, used as electron acceptors, were supplied from glacial meltwater through subglacial discharge, groundwater discharge or, now majorly surficial, glacial meltwater streams and SPM (Monien et al. 2017, Henkel et al. 2018, Falk and Silva-Busso 2021). As the amount, distribution and transportation of SPM changes with the retreating glacier, this also influences the supply of iron oxides to the sediments at different locations. Furthermore, the characteristics of iron oxides were highly dependent on the type of glacier and potential transport over land through an oxic environment (Henkel et al. 2018, Laufer et al. 2020, Michaud et al. 2020, Laufer-Meiser et al. 2021). The iron reducing microbial community and associated degradation rates were influenced by iron oxide crystallinity and microbial availability (Jensen et al. 2003, Bonneville et al. 2004, Laufer et al. 2020).

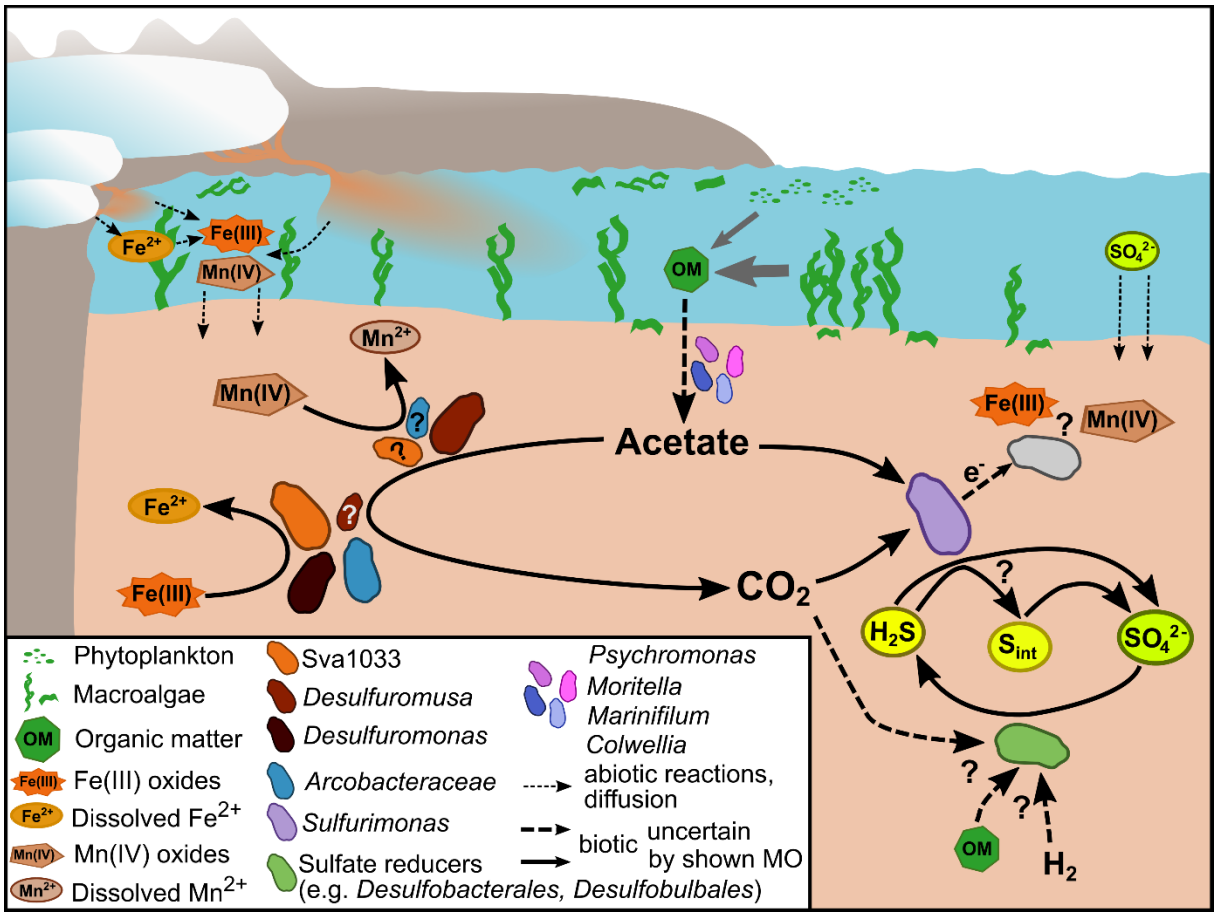

Figure 2: Organic matter degradation in anoxic sediments of Potter Cove. Microbial processes likely occurring in the sediments were displayed. Further abiotic interactions were not shown. Unresolved processes and unknown contributions of microbial players were marked by ? and different arrows, see legend. Compounds from the sea water were transported by physical processes, such as diffusion, and bioturbation into the sediments. H_2S represents all sulfide species, i.e. H_2S, HS^-, S^{2-}. S_{int} are sulfur intermediates such as elemental sulfur, thiosulfate, tetrathionate and polysulfides. MO: microorganisms

Close to the glacier, a high supply of inorganic material by surficial or subglacial meltwater fueled the sediments with a high content of iron oxides, e.g., 6 wt.% total Fe at STA10 (Henkel et al. 2018). However, not all of this iron was available for microbial iron reduction, but it contained many crystalline phases, which were more difficult to access for microorganisms (Bonneville et al. 2004, Laufer et al. 2020). Subglacial discharge was proposed to contain more "easily reducible" iron oxides (leachable by hydroxylamine-HCl, mainly lepidocrocite and ferrihydrite following Poulton and Canfield (2005)), compared to surficial meltwater streams, due to redox processes occurring beneath the glacier (Henkel et al. 2018). In Potter Cove, sequential solid phase iron extractions of these "easily reducible" iron oxides showed this for sediments in close glacial proximity (0.3 wt.% at STA10) compared to sediments close to a surficial glacial meltwater stream entering the bay (0.2 wt.% at STA04), but no measurements for a site in the central cove were available (Henkel et al. 2018).

At the same time, close to the glacier, there is usually not much organic material available to serve as electron donor, as visible in Arctic fjords (Wehrmann et al. 2014). Total organic carbon (TOC) data for deeper reaching sediments in Potter Cove was limited, however increasing TOC content with increasing distance to the glacier were observed in the top 1 cm of the sediments (Monien et al. 2014). Limited organic matter availability could result in reduction of only a part of the iron oxides, while much of them were buried by high sedimentation rates and still got microbially reduced at deeper sediment depths (Michaud et al. 2020), as was also proposed for Potter Cove sediments close to the glacier based on isotopic iron signatures (STA10, Henkel et al. 2018). Also the very deep reaching ferruginous profiles (> 30 cm, end of core) at stations close to the glacial front, very likely produced by iron reducing bacteria belonging to Sva1033 (Desulfuromonadales), *Desulfuromonas* and *Arcobacteraceae* (STA10 in Aromokeye et al. 2021, STA01 in chap. 3, STA13 in chap. 4) indicated a limitation of electron donors and not iron oxides. Close to the glacier, as additional electron accepting process contributing to organic matter mineralization, dissimilatory manganese reduction by *Desulfuromusa* (chap. 3) was fueled by manganese oxides, which were likely supplied by SPM in glacial meltwater as well (Wadham et al. 2013, Wehrmann et al. 2014) (Figure 2).

Iron recycling in sediments of the central cove

In typical fjord systems such as those found at Svalbard, the constant supply of iron oxides decreased with further distance from the glacier while the organic matter content increased, leading to higher organic matter mineralization rates and associated sulfate and iron reduction (Wehrmann et al. 2014). Sulfate reduction dominated over iron reduction with further distance to the glacier, leading to a more compressed redox profile with iron reduction limited to the top

centimeters (Herbert et al. 2021). However, the rates of iron reduction in this narrow depth interval were much higher compared to close to the glacier, and produced ferrous iron could be reoxidized back to ferric iron which could then be easily reduced again, leading to iron recycling (Wehrmann et al. 2014, Laufer-Meiser et al. 2021). Iron oxidation could occur abiotically with oxygen, but also biotically by iron oxidizing microorganism (Laufer et al. 2016).

The compressed redox profile and much higher ferrous iron concentrations at the sampling station in the center of the cove (STA14, chap. 5) compared to the glacial front (e.g., STA01, chap. 3) gave first indication that increased recycling of iron oxides also occurred in sediments of Potter Cove. Further indications for this process, resulting in fewer but microbially more easily available iron oxides in sediments in the central cove than at the glacial front, were found in incubations with iron reducing activity of different sediments: in the central cove slurries, iron reduction was stimulated more rapidly, but in glacial front slurries iron reduction occurred for a longer time period and resulted in higher maximal ferrous iron concentrations (Aromokeye et al. 2021).

Iron recycling is enhanced by mixing the sediment through bioturbation or ice scouring, i.e. scraping of icebergs on the bottom of the seafloor, bringing the ferrous iron into contact with oxygen or other reducing agents (Hines and Jones 1985, Beam et al. 2018). In the center of the cove, bioturbation was likely the more important factor as the water depth was quite deep (40 m) for ice scouring. Bioturbation might even increase more in the future, as the benthic fauna responsible for this process likely also increases in abundance together with their substrate, the macroalgae (Campana et al. 2018, Braeckman et al. 2019). One has to keep in mind, that in a batch slurry incubation, the recycling of iron did not occur as it would *in situ*, as the access to oxygen and a mixing of the sediments were lacking.

Increased amounts of ferrous iron in the sediment could also lead to increased release of dissolved iron to the overlying water column, where it could fuel, as limiting nutrient, primary productivity (Boyd et al. 2004, Herbert et al. 2021), resulting in a positive feed-back loop when increased supply of organic matter stimulates more iron reduction in the underlying sediments again. Addition of macroalgae was even shown to stimulate iron reduction in the sediments directly by its own, without the need for additional fresh iron (Aromokeye et al. 2021). The sampled station 14 in the central cove (chap. 5) might present a possible future scenario also for locations closer to the glacier, when the supply of glacial meltwater and associated, high amounts of easily available iron oxides cease, as predicted for Arctic fjords (Jørgensen et al. 2020).

Contribution of sulfate reduction

Next to metal oxides, sulfate is usually a prominent electron acceptor for final organic matter mineralization in marine sediments (Jørgensen et al. 2019). In the sediments of Potter Cove, the geochemical profiles suggested concurrent sulfate and metal reduction by decreasing sulfate concentrations with depth and an abundance of microorganisms typically involved in sulfate reduction (chap. 5). This signature was more prominent in stations with further distance to the glacier, where the redox zonation was more condensed (STA14, chap. 5), which agrees with observations in Arctic fjords (e.g., Michaud et al. 2020). However, in our incubation experiments, we were not able to link sulfate reduction directly to acetate degradation by typical sulfate reducing bacteria (chap. 2, 4, 5), as discussed in more detail below. There were multiple possible explanations arising from these observations: (I) sulfate reducers were not involved in organic matter mineralization directly but fix CO_2 instead or (II) sulfate reducers utilized fermentation products of higher molecular weight, e.g., lactate or butyrate, than the tested acetate. Hypothesis I would mean that sulfate reduction did not contribute to CO_2 release from the sediment by mineralization but might even fix and bury more carbon. Sulfate reduction would not be completely uncoupled from organic matter degradation, as it still required an electron donor, e.g., hydrogen produced by fermentation (Oremland and Polcin 1982). Hypothesis II would mean that sulfate reduction did directly contribute to organic matter degradation, but potentially producing smaller organic compounds such as acetate, which were then further oxidized, instead of releasing only CO_2. This last oxidizing step might then be performed by other microorganisms such as iron or manganese reducers. In a future scenario of cease of glacial meltwater and supply of iron, where acetate degrading iron and manganese reducers disappear, likely other microorganisms such as different acetate utilizing sulfate reducers would fill in the niche and degrade the acetate.

Effects of temperature increase

Temperature increase was another effect of global warming clearly observed in the last years at the northern tip of the West Antarctic Peninsula, where the sampling site Potter Cove is located (Jones et al. 2019). Just in the last four years, the temperature record was broken multiple times with extremely high temperatures in 2020 and 2022 (Francelino et al. 2021, Gorodetskaya et al. 2023). These heatwaves could have negative effects on primary productivity, as already shown recently for phytoplankton in Potter Cove (Latorre et al. 2023). Further, this thesis showed that increasing temperature led to a shift in parts of the sediment microbial community, stimulating different, already present microorganisms, while there were

a few keystone species, such as Sva1033 and *Desulfuromonas*, resilient to the temperature effect (chap. 4).

Further investigation is needed to quantify if temperature increase affects the rates of organic matter degradation in these sediments. In sediments from Svalbard, temperature did not influence organic matter degradation rates directly, but the rates were instead controlled by organic matter flux to the sediments (Jørgensen et al. 2020). However, the results reported in this thesis told that qualitative iron and sulfate reduction rates were affected by temperature in incubation experiments, leading to decreasing iron reduction above 10°C and an optimum for sulfate reduction between 10°C and 20°C, which was > 10°C above the current *in situ* temperature of 2°C (chap. 4). This agreed with previous experiments, showing that the temperature leading to highest sulfate reduction rates was 10 to 15°C higher than the *in situ* temperature, but still specific for different locations such as temperate or permanently cold sediments (Finke and Jørgensen 2008). However, *in situ* water/sediment temperatures of 10°C at the Antarctic Peninsula are still very far in the future. Different models predicted a temperature increase by up to 3°C until 2100, so reaching up to 5°C *in situ* temperature (Bopp et al. 2013, Moore et al. 2013), while more recent studies suggested that these models underestimate the change due to polar amplification effects (Casado et al. 2023). Still, 10°C sea surface temperature in the Antarctic is a far future scenario.

In conclusion, global warming probably will affect and already affects Potter Cove in two major ways. Firstly, temperature increase has likely a direct negative impact on primary productivity in the water column and shifts the microbial community, while presumably still remaining their function, in the sediments. Secondly, accelerated glacial melting could influence primary productivity positively by revealing more area for macroalgae colonization, but also negatively by more SPM in the water column. Further, it probably changes the nutrient supply into the sediments, which is likely the much more important factor for the microbially influenced carbon cycle in these coastal Antarctic sediments.

6.3 Cryptic sulfur cycling in glacial influenced Antarctic sediments

6.3.1 Sulfur cycling in marine sediments

Iron and, to a lower extend, manganese reduction were clearly identified as important processes for final organic matter mineralization in sediments of South Georgia and Potter Cove by geochemical profiles of the pore water and the incubation experiments with acetate (discussion above, chap. 2-5, Monien et al. 2014, Henkel et al. 2018). However, also sulfate reduction was a main contributing process to organic matter mineralization in many marine sediments

(Jørgensen 1982, Vandieken et al. 2006c, Arndt et al. 2013, Liang et al. 2023). The depletion of sulfate in the pore water of Potter Cove and South Georgia sediments suggested some occurring sulfate reduction, likely concurrent with iron reduction (chap. 2, 3, 5, Monien et al. 2014). While the depletion of sulfate was higher in the center of the cove than close to the glacier (STA14 chap. 5 vs. STA01 chap. 3; Monien et al. 2014), no free sulfide was detected in the pore water of any station. The abundance of sulfate reducing and sulfur cycling bacteria in all investigated *in situ* sediments, i.e., *Desulfobacteraceae*, *Desulfobulbaceae*, *Desulfosarcinaceae* and *Desulfocapsaceae* (Jørgensen et al. 2019, Diao et al. 2023), further indicated occurring sulfate reduction (Table 1; chap. 2, Fig. 3; chap. 3, suppl. Fig. S8; chap. 5, Fig. 4). However, in none of the conducted experiments an enrichment or labeling of typical sulfate reducers by sulfate and acetate, a typical electron donor for this process (Sørensen et al. 1981, Winfrey and Ward 1983, Vandieken et al. 2006c), was observed (chap. 2, 4, 5).
This raised two major questions: (1) what happened with the sulfide produced by sulfate reduction? and (2) on which electron donors did the sulfate reducers thrive?

Cryptic sulfur cycling by sulfide reoxidation masking sulfate reduction

For answering question one, we need to have a look at the sulfur cycle in marine sediments, which was described in more detail in the introduction of this thesis. The sulfur cycle in marine sediments is tightly linked with other element cycles, e.g., the iron and manganese cycle, by biotic and abiotic reactions (Wasmund et al. 2017). Up to 90% of sulfide produced by sulfate reduction is rapidly recycled and can be reoxidized through different intermediates back to sulfate (Jørgensen et al. 2019). The gross sulfate reduction rate can be masked by replenishing of the sulfate pool from reoxidation or diffusion from overlying seawater, leading to a "cryptic sulfur cycle" (Canfield et al. 2010, Findlay et al. 2020). The reoxidation of sulfide can be abiotic or microbially mediated and is ultimately linked to the reduction of oxygen, directly or by reoxidation of upwards diffusing reduced compounds, contributing to substantial oxygen consumption of marine sediments (Jørgensen 1982, Luther et al. 2011). Biotic sulfide oxidation rates were calculated to exceed abiotic rates due to thermodynamic and kinetic constraints in most environments (Luther et al. 2011), but biotic and abiotic reactions cannot be viewed as isolated systems and are therefore both very important.

Abiotic sulfide reoxidation

For abiotic oxidation, sulfide can get into direct contact with oxygen by upward diffusion or by the transportation of oxygen into deeper sediment layers by bioturbation (Pischedda et al. 2008, van de Velde and Meysman 2016) or, specifically in glacial influenced environments such as Potter Cove and South Georgia, iceberg scouring (Betzler et al. 2016). Additionally,

sulfide can be abiotically oxidized by iron and manganese oxides incompletely to sulfur intermediates such as elemental sulfur or thiosulfate, or completely to sulfate (Jørgensen and Nelson 2004, Poulton et al. 2004, Luther et al. 2011). Both metal oxides were present in the sediments of Potter Cove and South Georgia (chap. 3, Monien et al. 2014, Henkel et al. 2018, Schlosser et al. 2018), indicating the possibility of this process. Ferrous iron, produced by microbial or abiotic iron reduction, could precipitate with sulfide to FeS and finally form pyrite (Jørgensen 1977). Pyrite was especially detected in higher amounts close to the glacial front, where it was proposed to originate mainly from eroded bedrock, but also from the sulfidization of iron (Henkel et al. 2018). Pyrite represents the main sulfur pool in marine sediments, while other products of sulfide reoxidation such as elemental sulfur and FeS are more rapidly further oxidized to sulfate, replenishing the sulfate pool and masking sulfate reduction (Jørgensen and Nelson 2004). In the investigated sediments, all described abiotic processes likely contributed to the reoxidation of sulfide.

Biotic sulfide reoxidation

There are different biotic processes that can further contribute to sulfide oxidation; sulfide can be oxidized by microorganisms coupled to the reduction of electron acceptors such as oxygen, and nitrate (Jørgensen and Nelson 2004) or, as recently demonstrated, manganese oxides (Henkel et al. 2019). Microorganisms developed different strategies such as long distance electron transfer or internal storage compounds to access their electron acceptors and donors, as these are usually spatially separated (Wasmund et al. 2017). Well known typical sulfide or sulfur oxidizers such as *Thiobacillus*, *Thiomicrospira* or large sulfur bacteria within the family *Beggiatoaceae* (Jørgensen and Nelson 2004, Wasmund et al. 2017) were not found in the investigated sediments or incubation experiments (chap. 2-5). However, there is also a diversity of microorganisms capable of oxidizing reduced sulfur compounds across Alphaproteobacteria, Gammaproteobacteria and Campylobacterales such as uncultured *Rhodobacteraceae*, *Sedimenticola*, *Thiotrichaceae* (*Cocleimonas*, *Leucothrix*, *Thiothrix*), *Arcobacter*, *Sulfurovum* or *Sulfurimonas* (Grabovich et al. 2002, Tanaka et al. 2011, Lenk et al. 2012, Wasmund et al. 2017). Some of these taxa were detected especially in sediments close to the surface and in the slurry incubation background (Table 1).

Cable bacteria in Potter Cove sediments

Interestingly, in sediments of the central Potter Cove (STA14), sequences associated with cable bacteria (*Candidatus* Electrothrix) were detected down to 12 cm core depth (chap. 5). These bacteria can couple the oxidation of sulfide to the reduction of oxygen or nitrate via long-distance electron transport over multiple centimeters (Nielsen et al. 2010, Pfeffer et al. 2012,

Dong et al. 2024), but were not detected in Antarctic sediments previously and were usually found in shallower sediment layers (Dong et al. 2024). This raised the question how they could survive at such unusual depths, since they typically can bridge only 1-2 cm from sulfide source to oxygen at the sediment surface (Pfeffer et al. 2012, Dong et al. 2024). They were typically detected in undisturbed, stable sediments or stable patches in more disturbed sediment (Dong et al. 2024). This agreed with their abundance only further out in the cove rather than near the glacier, as the water depth was much deeper and the sediment was likely less disturbed by icebergs at the central site in the cove.

Sulfur disproportionation

Another likely contributing biotic process was disproportionation of elemental sulfur or thiosulfate to sulfide and sulfate (Finster 2008, Michaud et al. 2020). Microorganisms known for sulfur disproportionation can be found in many taxonomic groups such as within Desulfobulbales (*Desulfocapsa*, *Desulfobulbus*) or Campylobacterales (*Sulfurovum*, *Sulfurimonas*) (Slobodkin and Slobodkina 2019). These taxa were also detected in the investigated sediments and incubation experiments of Potter Cove and South Georgia, indicating that this process could also contribute to cryptic sulfur cycling in the studied environments (Table 1).

Despite the many arising questions, the occurrence of different sulfur cycling microbes suggested active sulfide oxidation, sulfate reduction and disproportionation in these sediments. Potentially, there were even more present microbes involved in this process, which were not previously associated with sulfur compound oxidation. It was suggested that there is likely a vast diversity of so far undiscovered sulfur oxidizing microorganisms, as some of the best known sulfur oxidizers were actually not abundant in the environment and did not account for estimated sulfur compound oxidation rates (Wasmund et al. 2017).

Electron donors for sulfate reduction

Geochemical profiles and *in situ* microbial communities alone were not sufficient to answer the second question, which electron donor was utilized by observed sulfate reducing microorganisms. As already mentioned, typical sulfate reducers were not enriched or labeled with acetate as electron donor in the variety of experiments performed in the framework of this thesis. Other recent literature showed a similar lack of labeling of sulfate reducers by acetate, or also lactate, butyrate, propionate and ethanol (Cho et al. 2020, Yin et al. 2024).

Table 1: Microorganisms involved in sulfur cycling detected in different *in situ* sediments and incubation experiments. Proposed metabolism according to literature: SR – sulfate reduction, SD – sulfur or thiosulfate disproportionation, SO – reduced sulfur compound oxidation; superscript indicates which reference for which metabolism. Projects of this thesis are indicated in which the taxon occurred with > 1% relative abundance. If no treatment or group of treatments is specified, sequences were detected across all treatments. Used abbreviations: PC – Potter Cove, SG – South Georgia, CB – Cumberland Bay at South Georgia, inc. – incubation, unlabeled – sequences only detected in light fractions or unlabeled controls, labeled – sequences detected in heavy labeled fractions. Ch. – chapter of PhD thesis. * : Aromokeye et al. (2021).

Taxon	Proposed metabolism	Literature	Projects with taxa occurring > 1% relative abundance	Ch.
Desulfatiglans (*Desulfobacteraceae*)	SR	Robador et al. (2015)[SR]	PC *in situ* station 14	5
			PC Mn inc. slurry background	3
			PC temp SIP inc. with sulfate, unlabeled	4
			CB *in situ*	2
Desulfobulbus (*Desulfobulbaceae*)	SD, SR	Slobodkin and Slobodkina (2019)[SD, SR]	PC SR-SIP inc. with SR activity, labeled in background	5
			PC macroalgae SIP inc. unlabeled	*
			PC temp SIP inc. unlabeled	4
			CB SIP inc. unlabeled	2
			SG *in situ*	2
Uncl. *Desulfobulbaceae*	SD, SR	Slobodkin and Slobodkina (2019)[SD, SR]	PC *in situ* station 01	3
			PC Mn inc. slurry background	3
			PC SR-SIP inc. with SR activity, labeled in background	5
			PC temp SIP inc. unlabeled	4
			CB SIP inc. unlabeled	2
Desulfocapsa (*Desulfobulbaceae*)	SD, SR	Slobodkin and Slobodkina (2019)[SD, SR]	PC SR-SIP inc. with SR activity, labeled in background, not in molybdate inhibited treatment	5
			CB SIP inc. unlabeled	2
Desulforhopalus (*Desulfobulbaceae*)	SR	Lie et al. (1999)[SR]	PC Mn inc.	3
			PC SR-SIP inc. with SR activity, labeled in background	5
			PC macroalgae SIP inc. unlabeled	*
			PC macroalgae inc.	*
			PC temp SIP inc. with sulfate < 20°C, unlabeled	4
			CB *in situ*	2

Table 1 cont.

Taxon	Proposed metabolism	Literature	Projects with taxa occurring > 1% relative abundance	Ch.
SEEP-SRB4 (*Desulfocapsaceae*)	SR	Knittel et al. (2003)[SR]	PC *in situ* station 14	5
			PC *in situ* station 01	3
			PC Mn inc.	3
			PC SR-SIP inc. with SR activity, unlabeled	5
			PC macroalgae SIP inc. unlabeled	*
			PC macroalgae inc.	*
			PC temp SIP inc. with sulfate < 20°C , unlabeled	4
			SG *in situ*	2
Uncl. *Desulfocapsaceae*	SD, SR	Slobodkin and Slobodkina (2019)[SD, SR]	PC *in situ* station 01	3
			PC Mn inc.	3
			PC SR-SIP inc. with SR activity, unlabeled	5
			PC temp SIP inc. unlabeled	4
MSBL7 (*Desulfurivibrionaceae*)	SR?	Häusler et al. (2014)[SR]	PC SR-SIP inc. with SR activity, labeled in background, not in molybdate inhibited treatment	5
Sva0081 (*Desulfosarcinaceae*)	SR?	Wasmund et al. (2017)[SR]	PC *in situ* station 14	5
			PC SR-SIP inc. with SR activity, unlabeled	5
			PC macroalgae SIP inc. unlabeled	*
			SG *in situ*	2
			CB SIP inc. unlabeled	2
SEEP-SRB1 (*Desulfosarcinaceae*)	SR	Knittel and Boetius (2009)[SR]	PC *in situ* station 14	5
			PC macroalgae inc.	*
			SG *in situ*	2
			CB SIP inc. unlabeled	2
Uncl. *Desulfosarcinaceae*	SR	Jørgensen et al. (2019)[SR]	PC *in situ* station 14	5
			PC *in situ* station 01	3
			PC Mn inc.	3
			PC temp SIP inc. unlabeled	4
Sva0485 (phylum)	SR	Vuillemin et al. (2018)[SR]	CB SIP inc. unlabeled	2
			SG *in situ*	2

Table 1 cont.

Taxon	Proposed metabolism	Literature	Projects with taxa occurring > 1% relative abundance	Ch.
Sulfurimonas (*Sulfurimonadaceae*)	SO, SD	Wasmund et al. (2017)[SO], Wang et al. (2023b) [SD]	PC *in situ* station 14	5
			PC *in situ* station 01	3
			PC Mn inc. end of incubation	3
			PC SR-SIP inc. with SR activity, labeled	5
			PC macroalgae SIP inc. labeled	*
			PC macroalgae inc.	*
			PC temp SIP inc. 2-15°C, labeled	4
			SG *in situ*	2
			CB SIP inc. labeled, not in molybdate inhibited treatment	2
Sulfurovum (*Sulfurovaceae*)	SO, SD	Wasmund et al. (2017)[SO], Wang et al. (2023b)[SD]	PC *in situ* station 14	5
			PC *in situ* station 01	3
			PC SR-SIP inc. in molybdate inhibited treatment, labeled	5
			PC macroalgae inc.	*
			SG *in situ*	2
Cocleimonas (*Thiotrichaceae*)	SO	Tanaka et al. (2011)[SO]	PC *in situ* station 01	3
			PC *in situ* station 14	5
			PC temp SIP inc. 30°C, unlabeled	4
Leucothrix (*Thiotrichaceae*)	SO	Grabovich et al. (2002)[SO]	PC *in situ* station 01, surface	3
			PC *in situ* station 14, surface	5
Uncl. *Rhodobacteraceae*	SO	Lenk et al. (2012)[SO]	PC *in situ* station 01	3
			PC *in situ* station 14	5
			PC temp SIP inc. 30°C, unlabeled	4
			SG *in situ*	2
Candidatus Electrothrix (*Desulfobulbaceae*)	SO	Pfeffer et al. (2012)[SO]	PC *in situ* station 14	5

However, in initial SIP experiments (chap. 2, Aromokeye et al. 2021), typical sulfate reducers were detected in the light fractions, indicating that they apparently did not feed on the provided acetate but showed some activity nonetheless. Multiple sulfate reducers are known to prefer fermentation products with higher molecular weight such as lactate, propionate or butyrate that they can oxidize incompletely (Sørensen et al. 1981), producing acetate but not utilizing it (Oremland and Silverman 1979, Lie et al. 1999). Others thrive autotrophically by fixing CO_2 and oxidize the fermentation product hydrogen (Oremland and Polcin 1982, Finke and Jørgensen 2008). Thus, chapter 5 of this thesis aimed to investigate this phenomenon in a more targeted approach by also testing an autotrophic lifestyle for sulfate reducers.

Sulfate reducing microorganisms

Sulfate reduction rate measurements with radioactive sulfate clearly showed a stimulation of this process by the addition of acetate and hydrogen, indicating the presence of a microbial community in the slurry, which could be activated and was able to utilize these substrates (chap. 5). In accordance with previous observations, typical sulfate reducers were again not labeled with acetate. The exception was *Desulforhopalus*, a known sulfate reducer (Isaksen and Teske 1996) which was labeled in low abundance (3.5%) in the treatment with the highest sulfate reduction rate amended with hydrogen, acetate and sulfate (chap. 5).

However, the vast majority of sulfate reducers was found in the light fractions especially in treatments with hydrogen addition (Table 1, chap. 5), but no labeling was observed by ^{13}C-labeled dissolved inorganic carbon (DIC), which would have been expected if they performed an autotrophic lifestyle. Instead, *Sulfurimonas* was the most active and labeled microorganism, whose activity and potential metabolism is being discussed below in detail. In addition, some taxa, e.g., *Desulfobulbaceae* and *Desulfocapsa*, were labeled with ^{13}C-DIC. Isolated strains of these taxa are capable of sulfate reduction but also sulfur compound disproportionation (Slobodkin and Slobodkina 2019). Disproportionation or reduction of more reduced sulfur compounds, such as elemental sulfur or thiosulfate, was the more likely performed metabolism in this experiment, as discussed in further detail in chapter 5 (Table 1, chap. 5). I propose that the observed sulfate reduction was performed by Sva0081, unclassified *Desulfosarcinaceae*, SEEP-SRB4 and unclassified *Desulfocapsaceae* detected in the isotopically light fractions of RNA-SIP experiments (chap. 5), using an unknown electron donor from the sediment. All of these microorganisms were detected in Potter Cove sediments and some were detected in South Georgia sediments (Table 1), suggesting that they might indeed be responsible for sulfate reduction *in situ*.

Importance of sulfur cycling reactions at different sampling locations

Sulfur cycling likely differed between the investigated stations, suggested by differing geochemical profiles and microbial communities. For sediments of South Georgia and close to the glacial front in Potter Cove (STA01), ferrous iron was present in the pore water through the whole length of the core, > 30 cm, without distinct surface peaks, while sulfate decreased only slowly with depth or stayed even stable (Fig. 2 chap. 2, Fig. 2 chap. 3).

In general, the rates of iron and sulfate reduction and other associated microbial sulfur cycling were likely much lower in close proximity to the glacier due to lower availability of organic matter compared with more distant sites, as also visible from increasing TOC values, for the top 1 cm of the sediment, with further distance to the glacier (Monien et al. 2014), as discussed in more detail above. Independent of the actual used electron donor, sulfate reduction was still dependent on supply of organic matter; even if they did not use it directly, then they used hydrogen produced by fermentation of organic matter. Gross sulfate reduction rates, estimated by depletion of sulfate, were likely largely underestimated due to replenishing of the sulfate pool by diffusion from the water column and reoxidation of produced sulfide, leading to the described cryptic sulfur cycle (Canfield et al. 2010, Findlay et al. 2020). Lower sulfate reduction rates can promote this effect even further as less sulfate is removed in the first place.

Sulfur cycling at glacial stations

Stations in closer proximity to the glacier showed higher sedimentation rates (Monien et al. 2017) and subsequent burial of reactive iron and manganese oxides at a higher rate. Therefore, abiotic reoxidation of sulfide by iron and manganese oxides was likely the dominant oxidation process in deeper sediment layers close to the glacier, as for iron oxides indicated by isotope signatures and increasing iron-sulfur compounds found with sediment depth (Henkel et al. 2018). Different mixing processes that can supply oxygen to the sediment can accelerate sulfide oxidation; iceberg scouring was likely more important close to the glacier, mixing the sediment and simultaneously reducing the importance of bioturbation, as benthic organisms were removed (Deregibus et al. 2017). With further distance to the glacier, the importance of iceberg scouring vs. bioturbation were likely reversed (Pasotti et al. 2015).

One major product of sulfide oxidation by iron oxides is pyrite, which is more stable than other products and the major sulfur pool buried in the sediments, therefore not contributing to complete reoxidation to sulfate (Jørgensen and Nelson 2004). The other main products of sulfide reoxidation are sulfur intermediates such as elemental sulfur; these can then be disproportionated by microorganisms, further replenishing the sulfate pool and feeding produced sulfide back into the reoxidation loop (Finster 2008). At these glacial stations, in

sediments at the surface, sulfide oxidation coupled to oxygen or nitrate reduction by microorganisms might still have contributed to sulfide reoxidation. In general, it was expected to detect iron reducing (Sva1033), sulfate reducing (SEEP-SRB4) and sulfur disproportionating (*Desulfocapsa*) microorganisms through the whole core depth, starting 2-3 cm below sediment surface, while more typical sulfide oxidizers were expected close to the surface (Table 1).

Sulfur cycle in distance to the glacier

At sites with further distance to the glacier, the pore water sulfate decreased much more rapidly with depth and very high ferrous iron concentrations within the top 10 cm were observed (chap. 5), suggesting higher rates of sulfate and iron reduction in general compared to glacial stations. The redox zonation was more condensed compared to glacial sites and there was likely a high recycling of iron occurring, producing fresh Fe(III) oxides, which were easily accessible for microbial reduction again (see discussion above). Sulfur cycling at this station might have occurred a bit differently than close to the glacier; the produced sulfide likely precipitated rapidly to FeS due to the high amounts of ferrous iron (Jørgensen 1977). FeS can be further oxidized to elemental sulfur or sulfate by manganese oxides (Jørgensen and Nelson 2004), replenishing the sulfate pool and producing dissolved manganese, which was observed in the pore water of these sediments (Monien et al. 2014). Easily bioavailable iron oxides, which are freshly produced by iron recycling, could be rapidly used by iron reducing microorganisms again instead of participating in reoxidizing sulfide, while more "aged" metal oxides were likely much less reactive towards sulfide as they were altered through diagenesis and encrustation with sediment compounds (Roden 2003, Raiswell 2011). This might have led to more pronounced biotic reoxidation of sulfide and different competition for available electron acceptors with further distance to the glacier compared to glacial front sites, as reflected in a slightly different microbial community (chap. 3 vs. 5). Furthermore, sulfide oxidizing microbes might have competed differently with each other for available electron acceptors. Detailed investigation of the abundance, activity and metabolic capabilities of the microbial community over depth by e.g., metagenomic and metatranscriptomic analyses can be used to explore these hypotheses further.

6.3.2 The role of *Sulfurimonas*

Known distribution and metabolic abilities of Sulfurimonas

The genus *Sulfurimonas* harbors typical sulfur oxidizing microorganisms, abundantly found in deep-sea hydrothermal vent environments (Han and Perner 2015, Molari et al. 2023, Wang et al. 2023a), but also in other anoxic environments like marine pelagic water column (Henkel et

al. 2021), freshwater (Biderre-Petit et al. 2024) and sediments (Timmer-ten Hoor 1975, Cai et al. 2014, Wang et al. 2020, Wang et al. 2022a). They can use a wide range of electron donors such as sulfite, elemental sulfur, thiosulfate, sulfide and hydrogen (Han and Perner 2015). Oxygen and nitrate are the mainly used electron acceptors, but some species are also capable of using nitrite and manganese oxides (Han and Perner 2015, Henkel et al. 2019). So far, no species was found to utilize iron oxides or sulfate (Inagaki et al. 2003, Cai et al. 2014, Wang et al. 2020, Henkel et al. 2021). The tolerance towards potentially toxic compounds such as oxygen or sulfide differs between species, ranging from strict anaerobes (Cai et al. 2014) to atmospheric oxygen concentrations (Ratnikova et al. 2020, Molari et al. 2023) and from sulfide concentrations of a maximum of 20 µM (Henkel et al. 2021) to over 2 mM (Ratnikova et al. 2020). Recently, disproportionation of elemental sulfur and thiosulfate was demonstrated for a few species (Wang et al. 2023b). Most *Sulfurimonas* species are autotrophs, fixing CO_2 through the reverse TCA cycle, but a few also utilize organic compounds such as acetate (Han and Perner 2015, Henkel et al. 2021, Wang et al. 2021b).

Occurrences of Sulfurimonas in projects of this thesis

Sulfurimonas was found across all projects of this PhD thesis, but its extremely high abundance in the sulfate reduction SIP experiment (chap. 5, Fig. 7) mainly caught my attention. The experiments from chapter 5 were designed to identify the active sulfate reducers through stable isotope probing. Acetate and dissolved organic carbon were chosen as ^{13}C-labeled substrate, so autotrophic and heterotrophic microorganisms could be targeted. Surprisingly, no typical sulfate reducers were labeled, but instead *Sulfurimonas* was labeled very heavily with both carbon sources (chap. 5).

In addition to this SIP experiment, *Sulfurimonas* was also found with low abundance, but still very clearly labeled with acetate, in multiple SIP experiments with Potter Cove and South Georgia sediment, when molybdate was not present (chap. 2, 4, 5, Aromokeye et al. 2021). However, the presence of acetate seemed not to be crucial, as enrichment of *Sulfurimonas* was also visible in simple slurry experiments after a longer incubation time (20 days) in the background (chap. 3, suppl. Fig. S6). Indication for potential labeling was also visible with DIC in the incubation experiment with iron oxides and macroalgae with Potter Cove sediment from a site close to the glacier (Aromokeye et al. 2021). Furthermore, we could enrich *Sulfurimonas* up to 90% with acetate and sulfate in anoxic Widdel medium, reduced with 2 mM sulfide, transferred from slurry incubations prepared with Potter Cove sediment (unpublished data).

Phylogenetic relation between Sulfurimonas ASVs from Potter Cove

The sequences of *Sulfurimonas* detected in the different experiments with Potter Cove sediment were compared (Figure 3), revealing two main ASVs (amplicon sequence variant) in slurry incubations (chap. 3-5) and one ASV from the enrichment (see above). The ASVs detected in slurry incubations were 98% identical with each other, even though the sediment originated from different sampling sites in the bay (chap. 3-5). *Candidatus* Sulfurimonas marisnigri was the closest related, cultivated species to both *Sulfurimonas* ASVs detected in the slurry experiments (99.2% identity). This species is very sensitive to sulfide (max. 20 µM), even though it requires it as electron donor (Henkel et al. 2019). This sulfide sensitivity was very different to the strain found in this thesis, which tolerated up to 3 mM sulfide (chap. 5, Fig. 5). The ASV in the sediment-free enrichment was only 90% identical to the slurry ASVs, likely representing a different genus. Thus, experimental results from the sediment-free enrichment must be taken with caution when implying a similar metabolism for strains detected in slurry incubations. Still, the enriched *Sulfurimonas* originated from the same sediment of Potter Cove, therefore it was present and able to survive in the same environment.

Sulfide oxidation by Sulfurimonas

As a general observation, enrichment and labeling of *Sulfurimonas* was always very prominent if also sulfate was supplied and was mostly inhibited if molybdate was used as sulfate reduction inhibitor. This implied that *Sulfurimonas* was more or less dependent on sulfate, and sulfate reduction would be the most obvious metabolism. However, as mentioned above, this microorganism is not known to be capable of doing sulfate reduction. On the contrary, different *Sulfurimonas* pure cultures were tested for this metabolism and were not able to perform it (Inagaki et al. 2003, Cai et al. 2014, Wang et al. 2020). Also the dissimilatory sulfite reductase (DSR), the marker gene for sulfate reduction (Santos et al. 2015), was never found in genomes of *Sulfurimonas* (Wang et al. 2021b, Biderre-Petit et al. 2024). We proposed that the observed activity of *Sulfurimonas* was fueled by sulfide oxidation and a syntrophic relationship to other microorganisms producing this sulfide, i.e. sulfate or sulfur reducers or sulfur disproportionaters (chap. 5).

Utilized electron acceptor by Sulfurimonas

The open question that remained was, which was the electron acceptor used by *Sulfurimonas* under these conditions? The typical electron acceptors utilized by this genus, i.e. nitrate and oxygen, should neither have been available in sediment-free enrichment nor in the slurry incubations. Even though I deem it very unlikely, I cannot completely exclude the possibility of oxygen penetration into the experiments. However, any penetrating oxygen should have

reacted very rapidly with the free sulfide and free ferrous iron, which were measured during the incubations.

Other possible present electron acceptors, at least in the slurry environments, were metal oxides. The use of manganese oxides was tested in Potter Cove sediments, resulting in no indications for this metabolism for *Sulfurimonas* (chap. 3). Iron reduction coupled to acetate oxidation was tested on the *Sulfurimonas* enrichment, and there were no indications for this metabolism either (unpublished data). Metagenomic and metatranscriptomic sequencing was performed on the *Sulfurimonas* enrichment and revealed a high expression of multiheme

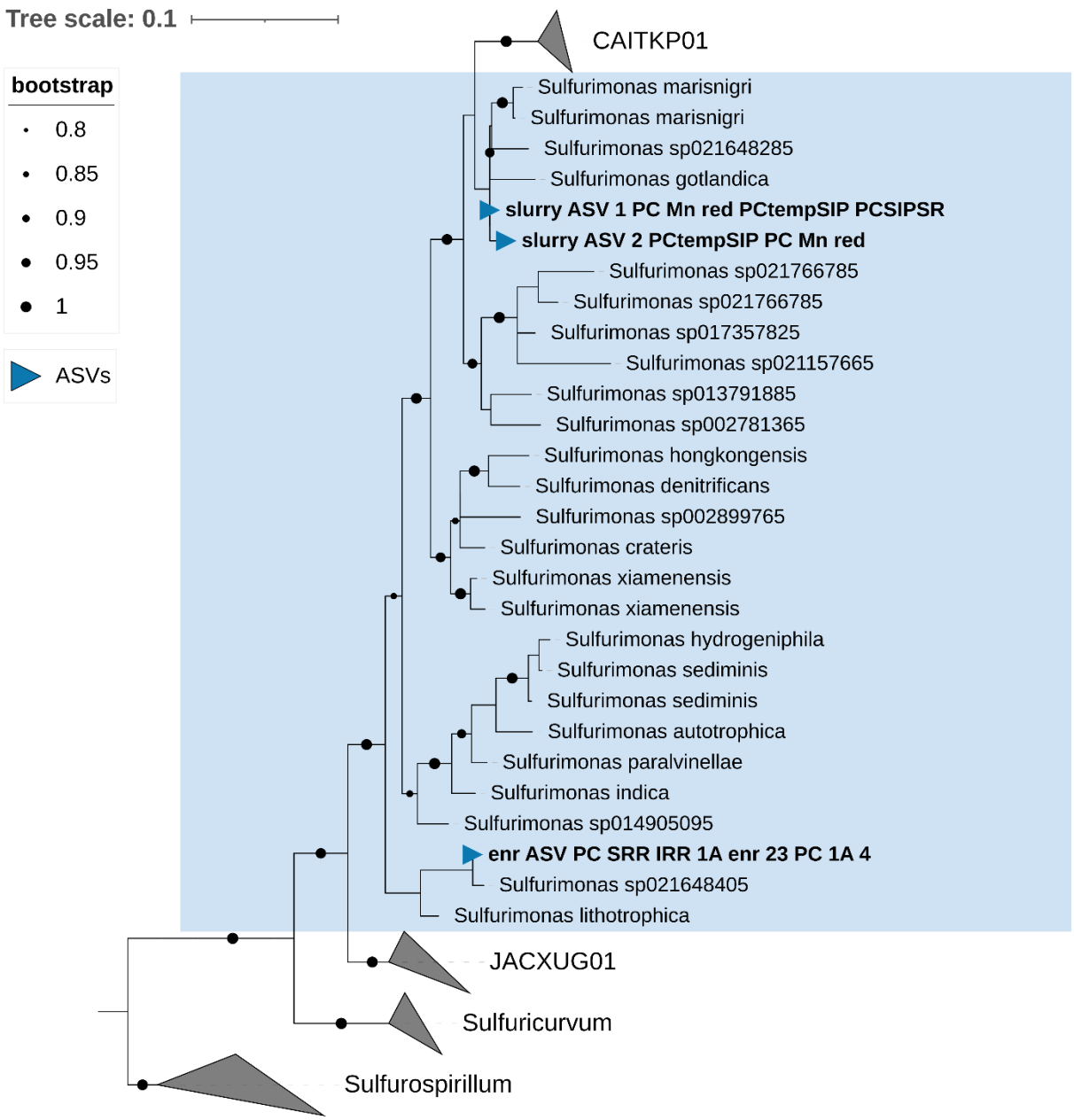

Figure 3: Phylogenetic tree of 16S rRNA gene sequences of the family *Sulfurimonadaceae*. ASVs retrieved in this thesis were marked with blue triangle: "slurry ASV" 1 and 2 of slurry incubations (chap. 3-5), "enr ASV" of sediment-free enrichment (see text). 16S rRNA gene sequences for tree construction were retrieved from good quality genomes (completeness, contamination) of GTDB using barrnap. The tree was calculated from 51 non-redundant sequences with a length > 1000 bp using fast tree with 1500 bootstraps. Shorter and ASV sequences were added after tree computing with epa-ng and gappa. Bootstrap values > 0.8 were displayed.

cytochromes (unpublished data), which can be involved in extracellular electron transfer (Shi et al. 2016).

I suggest that *Sulfurimonas* used another microorganism as electron sink (chap. 5). This was proposed previously for *Sulfurimonas*, with cable bacteria as the electron accepting partner (Vasquez-Cardenas et al. 2015). However, the question remained which electron acceptor was used by this partner organism. Sulfate was of course the electron acceptor available in all these incubations, but this would create a perpetuum mobile, circling electrons from sulfate to sulfide and back to sulfate again without another energy source. Syntrophic interactions involving the cycling of sulfur compounds between different microorganisms were shown for multiple mixed cultures, e.g., sulfate reducer *Desulfovibrio desulfuricans* with sulfide oxidizer *Thiobacillus thioparus* (van den Ende et al. 1997) or sulfate reducer *Desulfovibrio vulgaris* and phototroph *Chromatium vinosum* together with a third syntrophic partner, either *Escherichia coli* fermenting glucose (Loka Bharati et al. 1980) or a bacterium anaerobically degrading cellulose (Loka Bharati et al. 1982). However, these reactions were energetically possible because they were driven either by light energy or by a powerful electron acceptor, i.e., oxygen. For the proposed syntrophic consortium of sulfate reducers, *Sulfurimonas* and another microorganism, this extra energy source needs to be identified.

Possibility of disproportionation by Sulfurimonas

Disproportionation would circumvent the need for an electron acceptor and was demonstrated recently for some strains of *Sulfurimonas* (Wang et al. 2023b). For example, thiosulfate or elemental sulfur, produced by partial reoxidation of sulfide originating from sulfate reduction, could be used by *Sulfurimonas*. However, molybdate addition, which inhibits sulfate reduction but also thiosulfate and elemental sulfur disproportionation (Finster et al. 1998), affected the abundance and labeling of *Sulfurimonas* negatively (chap. 2, 5). Still, *Sulfurimonas* was labeled to a low amount even with molybdate addition in the presence of hydrogen, sulfate and potentially sulfur reducing microorganisms (chap 5), indicating that there was at least one other metabolism it could thrive on, even if it did perform disproportionation in some treatments.

The combined results of this thesis showed a potential novel strain of *Sulfurimonas* capable of performing an anaerobic, mixotrophic lifestyle under psychrophilic conditions. Additionally to the presence of *Sulfurimonas* in Antarctic sediments of Potter Cove (chap. 5), it was also detected up to 5% relative abundance in Arctic sediments of Svalbard (Vishnupriya et al. 2021). Open questions regarding the exact metabolism remained and further experiments are needed

to investigate this. It will enable us to draw further conclusions regarding its global importance not only in hydrothermal vent environments, but also in anoxic sediments.

6.4 Conclusion and outlook

In this thesis the question was tackled which final terminal electron acceptors and associated microorganisms were responsible for the final steps of organic matter mineralization by studying acetate degradation in Antarctic marine sediments. I could show that this process was mainly coupled to iron reduction in glacial sediments from two (sub-) Antarctic locations: in the Cumberland Bay fjord system at South Georgia and in Potter Cove at King George Island/Isla 25 de Mayo at the northern tip of the West Antarctic Peninsula. Both locations are already heavily affected by global warming with rapidly retreating glaciers. These glaciers supply nutrients through glacial meltwater into the surrounding sediments and especially iron oxides enter the sediments by this process. This thesis showed how crucial this iron oxide supply was for organic matter degradation in the form of acetate oxidation. Under the right circumstances, also manganese oxides were shown to contribute to acetate oxidation. But first and foremost, the microbial community in sediments of Potter Cove seemed to depend on the constant fresh supply of iron oxides to keep up the iron reducing activity. Therefore, a change in meltwater supply in that system would likely highly influence the processes in the sediments. In both, sediments of South Georgia and Potter Cove, a core bacterial community was identified, which was responsible for the acetate degradation. The major taxon was the uncultured family Sva1033 (Desulfuromonadales) which was detected in many recent studies also in other, iron influenced, cold sediments. This further underlined its importance as key acetate degrader and iron reducer in a variety of mainly cold environments. A few other bacterial taxa contributed majorly to acetate degradation under the right conditions, but were not as abundant *in situ*, i.e. *Desulfuromonas*, *Desulfuromusa* and *Arcobacteraceae*, and were likely to occupy more specific niches. In a future changing environment where their environmental conditions were met, they would likely increase in abundance and activity.

Surprisingly, no sulfate reducers seemed to contribute to acetate degradation; besides similar observations made in recent RNA-SIP experiments (e.g., Yin et al. 2024), these results were in contrast with many other experiments with pure cultures of sulfate reducers or sediments from Arctic or temperate environments. This might imply that they did not take part in organic matter mineralization in these environments and thus they avoided the competition for organic compounds with iron or manganese reducers. However, it was not possible to label sulfate reducers with DIC, which would have identified them as autotrophs. It would be necessary to test more different substrates, also fermentation products with higher molecular weight such as

lactate or butyrate, to see if sulfate reducers used these substrates instead. Sulfate reducers were very abundant *in situ*, so the next step would be to identify the exact processes they were involved in. I proposed their sulfate reducing activities by taxonomic affiliation, but further analyses such as metagenomics, metatranscriptomics and quantitative analyses such as qPCR of marker gene transcripts are needed to investigate these hypotheses.

With the observation of apparent different activities and communities in Antarctic compared to Arctic environments, another question arose about the used methodology. Stable isotope probing experiments, or also in general incubation experiments, priming for different metabolic processes are quite rare with Arctic sediments. It would be interesting to apply the same methodology we used in this thesis systematically to sediments from other locations, such as Arctic fjord systems or also shelf sediments from the Arctic and Antarctic.

In general, the microbial sediment community of the Antarctic is severely understudied. This thesis contributed with results about microbial physiology and a brief description of the microbial community for some sites of Potter Cove. As a next step, a thorough description of the microbial sediment community in the cove would be interesting, especially regarding spatial location in the bay and distance to the glacier and observed geochemical signatures. Furthermore, the possibility of a cryptic sulfur cycle, masking the production of sulfide and depletion of sulfate, would be interesting to study in more detail in the sediments of Potter Cove. This could be achieved by geochemical analysis of the solid phase iron, sulfur and manganese compounds and their isotopic composition, comparing sampling sites at different locations in the bay.

In the context of climate change and retreating glaciers, especially the quality of iron oxides supplied by the glacial meltwater will change or has already changed, as the glaciers retreat on land and the metal oxides are altered during the transport through the oxic environment. Up-to-date data from recent years about the quantity and distribution of suspended particulate material in Potter Cove would help to confirm or deny these predicted changes. These will likely influence the microbial community and the processes they conduct, hence also CO_2 emissions caused by organic matter degradation. Comparing a time series of samples from the same location over the years would shed first light on the question of what is expected to happen in the future with the sediment microbial communities. This knowledge could then be projected to other locations in Antarctica allowing to predict changes in the element cycles in the future due to global warming.

6.5 References

Ahmad, S. A., M. Y. Shukor, N. A. Shamaan, W. P. Mac Cormack, and M. A. Syed. (2013). Molybdate reduction to molybdenum blue by an Antarctic bacterium. BioMed Res. Int. **2013**:871941. doi:10.1155/2013/871941.

Aldeguer-Riquelme, B., E. Rubio-Portillo, J. Álvarez-Rogel, F. Giménez-Casalduero, X. L. Otero, M.-D. Belando, J. Bernardeau-Esteller, R. García-Muñoz, A. Forcada, J. M. Ruiz, F. Santos, and J. Antón. (2022). Factors structuring microbial communities in highly impacted coastal marine sediments (Mar Menor lagoon, SE Spain). Front. Microbiol. **13**. doi:10.3389/fmicb.2022.937683.

Algora, C., F. Gründger, L. Adrian, V. Damm, H.-H. Richnow, and M. Krüger. (2013). Geochemistry and microbial populations in sediments of the Northern Baffin Bay, Arctic. Geomicrobiol. J. **30**:690-705. doi:10.1080/01490451.2012.758195.

Arndt, S., B. B. Jørgensen, D. E. LaRowe, J. Middelburg, R. Pancost, and P. Regnier. (2013). Quantifying the degradation of organic matter in marine sediments: A review and synthesis. Earth-Sci. Rev. **123**:53-86. doi:10.1016/j.earscirev.2013.02.008.

[Dataset] Aromokeye, D. A., G. Willis-Poratti, L. C. Wunder, S. Henkel, and M. W. Friedrich. (2024). Pore water geochemistry at sampling site Potter Cove STA01. PANGAEA. doi:10.1594/PANGAEA.941109.

Aromokeye, D. A., G. Willis-Poratti, L. C. Wunder, X. Yin, J. Wendt, T. Richter-Heitmann, S. Henkel, S. Vázquez, M. Elvert, W. Mac Cormack, and M. W. Friedrich. (2021). Macroalgae degradation promotes microbial iron reduction via electron shuttling in coastal Antarctic sediments. Environ. Int. **156**:106602. doi:10.1016/j.envint.2021.106602.

Baloza, M., S. Henkel, W. Geibert, S. Kasten, and M. Holtappels. (2022). Benthic carbon remineralization and iron cycling in relation to sea ice cover along the Eastern Continental Shelf of the Antarctic Peninsula. J. Geophys. Res. (C Oceans) **127**:e2021JC018401. doi:10.1029/2021JC018401.

Baloza, M., S. Henkel, S. Kasten, M. Holtappels, and M. Molari. (2023). The impact of sea ice cover on microbial communities in Antarctic shelf sediments. Microorganisms **11**:1572. doi:10.3390/microorganisms11061572.

Beam, J. P., J. J. Scott, S. M. McAllister, C. S. Chan, J. McManus, F. J. R. Meysman, and D. Emerson. (2018). Biological rejuvenation of iron oxides in bioturbated marine sediments. ISME J. **12**:1389-1394. doi:10.1038/s41396-017-0032-6.

Begmatov, S., A. S. Savvichev, V. V. Kadnikov, A. V. Beletsky, I. I. Rusanov, A. A. Klyuvitkin, E. A. Novichkova, A. V. Mardanov, N. V. Pimenov, and N. V. Ravin. (2021). Microbial communities involved in methane, sulfur, and nitrogen cycling in the sediments of the Barents Sea. Microorganisms **9**:2362. doi:10.3390/microorganisms9112362.

Betzler, C., P. Feldens, H. C. Hass, G. Kuhn, N. Wittenberg, and A.-C. Wölfl. (2016). Submarine landforms related to glacier retreat in a shallow Antarctic fjord. Antarct. Sci. **28**:475-486. doi:10.1017/S0954102016000262.

Biderre-Petit, C., D. Courtine, C. Hennequin, P. E. Galand, S. Bertilsson, D. Debroas, A. Monjot, C. Lepère, A.-M. Divne, and C. Hochart. (2024). A pan-genomic approach reveals novel *Sulfurimonas* clade in the ferruginous meromictic Lake Pavin. Mol. Ecol. Resour. **24**:e13923. doi:10.1111/1755-0998.13923.

Bonneville, S., P. Van Cappellen, and T. Behrends. (2004). Microbial reduction of iron(III) oxyhydroxides: Effects of mineral solubility and availability. Chem. Geol. **212**:255-268. doi:10.1016/j.chemgeo.2004.08.015.

Bopp, L., L. Resplandy, J. C. Orr, S. C. Doney, J. P. Dunne, M. Gehlen, P. Halloran, C. Heinze, T. Ilyina, R. Séférian, J. Tjiputra, and M. Vichi. (2013). Multiple stressors of ocean ecosystems in the 21st century: Projections with CMIP5 models. Biogeosciences **10**:6225-6245. doi:10.5194/bg-10-6225-2013.

Bourgeois, S., P. Archambault, and U. Witte. (2017). Organic matter remineralization in marine sediments: A Pan-Arctic synthesis. Global Biogeochem. Cycles **31**:190-213. doi:10.1002/2016GB005378.

Boyd, P. W., C. S. Law, C. S. Wong, Y. Nojiri, A. Tsuda, M. Levasseur, S. Takeda, R. Rivkin, P. J. Harrison, R. Strzepek, J. Gower, R. M. McKay, E. Abraham, M. Arychuk, J. Barwell-Clarke, W. Crawford, D. Crawford, M. Hale, K. Harada, K. Johnson, H. Kiyosawa, I. Kudo, A. Marchetti, W. Miller, J. Needoba, J. Nishioka, H. Ogawa, J. Page, M. Robert, H. Saito, A. Sastri, N. Sherry, T. Soutar, N. Sutherland, Y. Taira, F. Whitney, S.-K. E. Wong, and T. Yoshimura. (2004). The decline and fate of an iron-induced subarctic phytoplankton bloom. Nature **428**:549-553. doi:10.1038/nature02437.

Bracewell, S. A., T. L. Barros, M. Mayer-Pinto, K. A. Dafforn, S. L. Simpson, and E. L. Johnston. (2023). Contaminant pulse following wildfire is associated with shifts in estuarine benthic communities. Environ. Pollut. **316**:120533. doi:10.1016/j.envpol.2022.120533.

Braeckman, U., F. Pasotti, R. Hoffmann, S. Vázquez, A. Wulff, I. R. Schloss, U. Falk, D. Deregibus, N. Lefaible, A. Torstensson, A. Al-Handal, F. Wenzhöfer, and A. Vanreusel. (2021). Glacial melt disturbance shifts community metabolism of an Antarctic seafloor ecosystem from net autotrophy to heterotrophy. Commun. Biol. **4**:148. doi:10.1038/s42003-021-01673-6.

Braeckman, U., F. Pasotti, S. Vázquez, K. Zacher, R. Hoffmann, M. Elvert, H. Marchant, C. Buckner, M. L. Quartino, W. Mác Cormack, K. Soetaert, F. Wenzhöfer, and A. Vanreusel. (2019). Degradation of macroalgal detritus in shallow coastal Antarctic sediments. Limnol. Oceanogr. **64**:1423-1441. doi:10.1002/lno.11125.

Buongiorno, J., L. Herbert, L. Wehrmann, A. Michaud, K. Laufer, H. Røy, B. Jørgensen, A. Szynkiewicz, A. Faiia, and K. Yeager. (2019). Complex microbial communities drive iron and sulfur cycling in Arctic fjord sediments. Appl. Environ. Microbiol. **85**:e00949-00919. doi:10.1128/AEM.00949-19.

Cai, L., M.-F. Shao, and T. Zhang. (2014). Non-contiguous finished genome sequence and description of *Sulfurimonas hongkongensis* sp. nov., a strictly anaerobic denitrifying, hydrogen- and sulfur-oxidizing chemolithoautotroph isolated from marine sediment. Stand. Genom. Sci. **9**:1302-1310. doi:10.4056/sigs.4948668.

Campana, G. L., K. Zacher, D. Deregibus, F. R. Momo, C. Wiencke, and M. L. Quartino. (2018). Succession of Antarctic benthic algae (Potter Cove, South Shetland Islands): Structural patterns and glacial impact over a four-year period. Polar Biol. **41**:377-396. doi:10.1007/s00300-017-2197-x.

Canfield, D. E., F. J. Stewart, B. Thamdrup, L. De Brabandere, T. Dalsgaard, E. F. Delong, N. P. Revsbech, and O. Ulloa. (2010). A cryptic sulfur cycle in oxygen-minimum-zone waters off the Chilean coast. Science **330**:1375-1378. doi:10.1126/science.1196889.

Casado, M., R. Hébert, D. Faranda, and A. Landais. (2023). The quandary of detecting the signature of climate change in Antarctica. Nat. Clim. Chang. **13**:1082-1088. doi:10.1038/s41558-023-01791-5.

Cho, H., B. Kim, J. S. Mok, A. Choi, B. Thamdrup, and J. H. Hyun. (2020). Acetate-utilizing microbial communities revealed by stable-isotope probing in sediment underlying the upwelling system of the Ulleung Basin, East Sea. Mar. Ecol. Prog. Ser. **634**:45-61. doi:10.3354/meps13182.

Deregibus, D., G. L. Campana, C. Neder, D. K. A. Barnes, K. Zacher, J. M. Piscicelli, K. Jerosch, and M. L. Quartino. (2023). Potential macroalgal expansion and blue carbon gains with northern Antarctic Peninsula glacial retreat. Mar. Environ. Res. **189**:106056. doi:10.1016/j.marenvres.2023.106056.

Deregibus, D., M. L. Quartino, K. Zacher, G. L. Campana, and D. K. A. Barnes. (2017). Understanding the link between sea ice, ice scour and Antarctic benthic biodiversity – The need for cross-station and international collaboration. Polar Rec. **53**:143-152. doi:10.1017/S0032247416000875.

Diao, M., S. Dyksma, E. Koeksoy, D. K. Ngugi, K. Anantharaman, A. Loy, and M. Pester. (2023). Global diversity and inferred ecophysiology of microorganisms with the potential for dissimilatory sulfate/sulfite reduction. FEMS Microbiol. Rev. **47**. doi:10.1093/femsre/fuad058.

Dong, M., L. P. Nielsen, S. Yang, L. H. Klausen, and M. Xu. (2024). Cable bacteria: Widespread filamentous electroactive microorganisms protecting environments. Trends Microbiol. **32**:697-706. doi:10.1016/j.tim.2023.12.001.

Dumont, M. G. and J. C. Murrell. (2005). Stable isotope probing – Linking microbial identity to function. Nat. Rev. Microbiol. **3**:499-504. doi:10.1038/nrmicro1162.

Fabiano, M., P. Povero, and R. Danovaro. (1996). Particulate organic matter composition in Terra Nova Bay (Ross Sea, Antarctica) during summer 1990. Antarct. Sci. **8**:7-13. doi:10.1017/S095410209600003X.

Falk, U. and A. Silva-Busso. (2021). Discharge of groundwater flow to Potter Cove on King George Island, Antarctic Peninsula. Hydrol. Earth Syst. Sci. **25**:3227-3244. doi:10.5194/hess-25-3227-2021.

Findlay, A. J., A. Pellerin, K. Laufer, and B. B. Jørgensen. (2020). Quantification of sulphide oxidation rates in marine sediment. Geochim. Cosmochim. Acta **280**:441-452. doi:10.1016/j.gca.2020.04.007.

Finke, N. and B. B. Jørgensen. (2008). Response of fermentation and sulfate reduction to experimental temperature changes in temperate and Arctic marine sediments. ISME J. **2**:815-829. doi:10.1038/ismej.2008.20.

Finster, K. (2008). Microbiological disproportionation of inorganic sulfur compounds. J. Sulphur Chem **29**:281-292. doi:10.1080/17415990802105770.

Finster, K., W. Liesack, and B. Thamdrup. (1998). Elemental sulfur and thiosulfate disproportionation by *Desulfocapsa sulfoexigens* sp. nov., a new anaerobic bacterium isolated from marine surface sediment. Appl. Environ. Microbiol. **64**:119-125. doi:10.1128/aem.64.1.119-125.1998.

Francelino, M. R., C. Schaefer, M. d. L. M. Skansi, S. Colwell, D. H. Bromwich, P. Jones, J. C. King, M. A. Lazzara, J. Renwick, S. Solomon, M. Brunet, and R. S. Cerveny. (2021). WMO evaluation of two extreme high temperatures occurring in February 2020 for the Antarctic Peninsula Region. BAMS **102**:E2053-E2061. doi:10.1175/BAMS-D-21-0040.1.

[Dataset] Gerrish, L. (2020). Automatically extracted rock outcrop dataset for Antarctica (7.3). UK Polar Data Centre, Natural Environment Research Council, UK Research & Innovation. doi:10.5285/178ec50d-1ffb-42a4-a4a3-1145419da2bb.

Glombitza, C., M. Jaussi, H. Røy, M.-S. Seidenkrantz, B. Lomstein, and B. Jørgensen. (2015). Formate, acetate, and propionate as substrates for sulfate reduction in sub-Arctic sediments of Southwest Greenland. Front. Microbiol. **6**. doi:10.3389/fmicb.2015.00846.

Gorodetskaya, I. V., C. Durán-Alarcón, S. González-Herrero, K. R. Clem, X. Zou, P. Rowe, P. Rodriguez Imazio, D. Campos, C. Leroy-Dos Santos, N. Dutrievoz, J. D. Wille, A. Chyhareva, V. Favier, J. Blanchet, B. Pohl, R. R. Cordero, S.-J. Park, S. Colwell, M. A. Lazzara, J. Carrasco, A. M. Gulisano, S. Krakovska, F. M. Ralph, T. Dethinne, and G. Picard. (2023). Record-high Antarctic Peninsula temperatures and surface melt in February 2022: A compound event with an intense atmospheric river. npj Clim. Atmos. Sci. **6**:202. doi:10.1038/s41612-023-00529-6.

Grabovich, M. Y., N. M. Dul'tseva, and G. A. Dubinina. (2002). Carbon and sulfur metabolism in representatives of two clusters of bacteria of the genus *Leucothrix*: A comparative study. Microbiology **71**:255-261. doi:10.1023/A:1015838207918.

Han, Y. and M. Perner. (2015). The globally widespread genus *Sulfurimonas*: Versatile energy metabolisms and adaptations to redox clines. Front. Microbiol. **6**. doi:10.3389/fmicb.2015.00989.

Häusler, S., M. Weber, C. Siebert, M. Holtappels, B. E. Noriega-Ortega, D. De Beer, and D. Ionescu. (2014). Sulfate reduction and sulfide oxidation in extremely steep salinity gradients formed by freshwater springs emerging into the Dead Sea. FEMS Microbiol. Ecol. **90**:956-969. doi:10.1111/1574-6941.12449.

Hedlund, B. P., J. A. Dodsworth, S. K. Murugapiran, C. Rinke, and T. Woyke. (2014). Impact of single-cell genomics and metagenomics on the emerging view of extremophile "microbial dark matter". Extremophiles **18**:865-875. doi:10.1007/s00792-014-0664-7.

Henkel, J. V., O. Dellwig, F. Pollehne, D. P. R. Herlemann, T. Leipe, and H. N. Schulz-Vogt. (2019). A bacterial isolate from the Black Sea oxidizes sulfide with manganese(IV) oxide. Proc. Natl. Acad. Sci. USA **116**:12153-12155. doi:10.1073/pnas.1906000116.

Henkel, J. V., A. Vogts, J. Werner, T. R. Neu, C. Spröer, B. Bunk, and H. N. Schulz-Vogt. (2021). *Candidatus* Sulfurimonas marisnigri sp. nov. and *Candidatus* Sulfurimonas baltica sp. nov., thiotrophic manganese oxide reducing chemolithoautotrophs of the class *Campylobacteria* isolated from the pelagic redoxclines of the Black Sea and the Baltic Sea. Syst. Appl. Microbiol. **44**:126155. doi:10.1016/j.syapm.2020.126155.

Henkel, S., S. Kasten, J. F. Hartmann, A. Silva-Busso, and M. Staubwasser. (2018). Iron cycling and stable Fe isotope fractionation in Antarctic shelf sediments, King George Island. Geochim. Cosmochim. Acta **237**:320-338. doi:10.1016/j.gca.2018.06.042.

Herbert, L. C., N. Riedinger, A. B. Michaud, K. Laufer, H. Røy, B. B. Jørgensen, C. Heilbrun, R. C. Aller, J. K. Cochran, and L. M. Wehrmann. (2020). Glacial controls on redox-sensitive trace element cycling in Arctic fjord sediments (Spitsbergen, Svalbard). Geochim. Cosmochim. Acta **271**:33-60. doi:10.1016/j.gca.2019.12.005.

Herbert, L. C., Q. Zhu, A. B. Michaud, K. Laufer-Meiser, C. K. Jones, N. Riedinger, Z. S. Stooksbury, R. C. Aller, B. B. Jørgensen, and L. M. Wehrmann. (2021). Benthic iron flux influenced by climate-sensitive interplay between organic carbon availability and sedimentation rate in Arctic fjords. Limnol. Oceanogr. **66**:3374-3392. doi:10.1002/lno.11885.

Hines, M. E. and G. E. Jones. (1985). Microbial biogeochemistry and bioturbation in the sediments of Great Bay, New Hampshire. Estuar. Coast. Shelf Sci. **20**:729-742. doi:10.1016/0272-7714(85)90029-0.

Hodgson, D. A., A. G. C. Graham, H. J. Griffiths, S. J. Roberts, C. Ó. Cofaigh, M. J. Bentley, and D. J. A. Evans. (2014). Glacial history of sub-Antarctic South Georgia based on the submarine geomorphology of its fjords. Quat. Sci. Rev. **89**:129-147. doi:10.1016/j.quascirev.2013.12.005.

Inagaki, F., K. Takai, H. Kobayashi, K. H. Nealson, and K. Horikoshi. (2003). *Sulfurimonas autotrophica* gen. nov., sp. nov., a novel sulfur-oxidizing ε-proteobacterium isolated from hydrothermal sediments in the Mid-Okinawa Trough. Int. J. Syst. Evol. Microbiol. **53**:1801-1805. doi:10.1099/ijs.0.02682-0.

Isaksen, M. F. and A. Teske. (1996). *Desulforhopalus vacuolatus* gen. nov., sp. nov., a new moderately psychrophilic sulfate-reducing bacterium with gas vacuoles isolated from a temperate estuary. Arch. Microbiol. **166**:160-168. doi:10.1007/s002030050371.

Jensen, M. M., B. Thamdrup, S. Rysgaard, M. Holmer, and H. Fossing. (2003). Rates and regulation of microbial iron reduction in sediments of the Baltic-North Sea transition. Biogeochemistry **65**:295-317. doi:10.1023/A:1026261303494.

Jerosch, K., H. Pehlke, P. Monien, F. Scharf, L. Weber, G. Kuhn, M. H. Braun, and D. Abele. (2018). Benthic meltwater fjord habitats formed by rapid glacier recession on King George Island, Antarctica. Philos. Trans. Royal Soc. A **376**:20170178. doi:10.1098/rsta.2017.0178.

[Dataset] Jerosch, K., F. K. Scharf, D. Deregibus, G. L. Campana, K. Zacher-Aued, H. Pehlke, D. Abele, and M. L. Quartino. (2015). High resolution bathymetric compilation for Potter Cove, WAP, Antarctica, with links to data in ArcGIS format. PANGAEA. doi:10.1594/PANGAEA.853593.

Jerosch, K., F. K. Scharf, D. Deregibus, G. L. Campana, K. Zacher, H. Pehlke, U. Falk, H. C. Hass, M. L. Quartino, and D. Abele. (2019). Ensemble modeling of Antarctic macroalgal habitats exposed to glacial melt in a polar fjord. Front. Ecol. Evol. **7**. doi:10.3389/fevo.2019.00207.

Jones, M. E., D. H. Bromwich, J. P. Nicolas, J. Carrasco, E. Plavcová, X. Zou, and S.-H. Wang. (2019). Sixty years of widespread warming in the southern middle and high latitudes (1957–2016). J. Clim. **32**:6875-6898. doi:10.1175/JCLI-D-18-0565.1.

Jørgensen, B. B. (1977). The sulfur cycle of a coastal marine sediment (Limfjorden, Denmark). Limnol. Oceanogr. **22**:814-832. doi:10.4319/lo.1977.22.5.0814.

Jørgensen, B. B. (1982). Mineralization of organic matter in the sea bed – The role of sulphate reduction. Nature **296**:643-645. doi:10.1038/296643a0.

Jørgensen, B. B., A. J. Findlay, and A. Pellerin. (2019). The biogeochemical sulfur cycle of marine sediments. Front. Microbiol. **10**:849. doi:10.3389/fmicb.2019.00849.

Jørgensen, B. B., K. Laufer, A. B. Michaud, and L. M. Wehrmann. (2020). Biogeochemistry and microbiology of high Arctic marine sediment ecosystems – Case study of Svalbard fjords. Limnol. Oceanogr. **66**:S273-S292. doi:10.1002/lno.11551.

Jørgensen, B. B. and D. C. Nelson. (2004). Sulfide Oxidation in Marine Sediments: Geochemistry Meets Microbiology. *in* J. P. Amend, K. J. Edwards, and T. W. Lyons, editors. Sulfur Biogeochemistry - Past and Present. Geological Society of America. p. 63-81. doi:10.1130/0-8137-2379-5.63.

Jorgensen, S. L., B. Hannisdal, A. Lanzén, T. Baumberger, K. Flesland, R. Fonseca, L. Øvreås, I. H. Steen, I. H. Thorseth, R. B. Pedersen, and C. Schleper. (2012). Correlating microbial community profiles with geochemical data in highly stratified sediments from the Arctic Mid-Ocean Ridge. Proc. Natl. Acad. Sci. USA **109**:E2846-E2855. doi:10.1073/pnas.1207574109.

Klöser, H., M. L. Quartino, and C. Wiencke. (1996). Distribution of macroalgae and macroalgal communities in gradients of physical conditions in Potter Cove, King George Island, Antarctica. Hydrobiologia **333**:1-17. doi:10.1007/BF00020959.

Knittel, K. and A. Boetius. (2009). Anaerobic oxidation of methane: Progress with an unknown process. Annu. Rev. Microbiol. **63**:311-334. doi:10.1146/annurev.micro.61.080706.093130.

Knittel, K., A. Boetius, A. Lemke, H. Eilers, K. Lochte, O. Pfannkuche, P. Linke, and R. Amann. (2003). Activity, distribution, and diversity of sulfate reducers and other bacteria in sediments above gas hydrate (Cascadia Margin, Oregon). Geomicrobiol. J. **20**:269-294. doi:10.1080/01490450303896.

Köster, M. (2014). (Bio-)geochemische Prozesse in den eisenreichen Seep-Sedimenten der Cumberland-Bucht Südgeorgiens, Subantarktis. Bachelor Thesis. University of Bremen, Bremen, Germany.

LaRowe, D. E., S. Arndt, J. A. Bradley, E. R. Estes, A. Hoarfrost, S. Q. Lang, K. G. Lloyd, N. Mahmoudi, W. D. Orsi, S. R. Shah Walter, A. D. Steen, and R. Zhao. (2020). The fate of organic carbon in marine sediments – New insights from recent data and analysis. Earth-Sci. Rev. **204**:103146. doi:10.1016/j.earscirev.2020.103146.

Latorre, M. P., C. M. Iachetti, I. R. Schloss, J. Antoni, A. Malits, F. de la Rosa, M. De Troch, M. D. Garcia, X. Flores-Melo, S. I. Romero, M. N. Gil, and M. Hernando. (2023). Summer heatwaves affect coastal Antarctic plankton metabolism and community structure. J. Exp. Mar. Biol. Ecol. **567**:151926. doi:10.1016/j.jembe.2023.151926.

Laufer-Meiser, K., A. B. Michaud, M. Maisch, J. M. Byrne, A. Kappler, M. O. Patterson, H. Røy, and B. B. Jørgensen. (2021). Potentially bioavailable iron produced through benthic cycling in glaciated Arctic fjords of Svalbard. Nat. Commun. **12**:1349. doi:10.1038/s41467-021-21558-w.

Laufer, K., J. M. Byrne, C. Glombitza, C. Schmidt, B. B. Jørgensen, and A. Kappler. (2016). Anaerobic microbial Fe(II) oxidation and Fe(III) reduction in coastal marine sediments controlled by organic carbon content. Environ. Microbiol. **18**:3159-3174. doi:10.1111/1462-2920.13387.

Laufer, K., A. B. Michaud, H. Røy, and B. B. Jørgensen. (2020). Reactivity of iron minerals in the seabed toward microbial reduction – A comparison of different extraction techniques. Geomicrobiol. J. **37**:170-189. doi:10.1080/01490451.2019.1679291.

Lenk, S., C. Moraru, S. Hahnke, J. Arnds, M. Richter, M. Kube, R. Reinhardt, T. Brinkhoff, J. Harder, R. Amann, and M. Mußmann. (2012). *Roseobacter* clade bacteria are abundant in coastal sediments and encode a novel combination of sulfur oxidation genes. ISME J. **6**:2178-2187. doi:10.1038/ismej.2012.66.

Liang, Q.-Y., J.-Y. Zhang, D. Ning, W.-X. Yu, G.-J. Chen, X. Tao, J. Zhou, Z.-J. Du, and D.-S. Mu. (2023). Niche modification by sulfate-reducing bacteria drives microbial community assembly in anoxic marine sediments. Mbio **14**:e03535-03522. doi:10.1128/mbio.03535-22.

Lidstrom, M. E. and M. C. Konopka. (2010). The role of physiological heterogeneity in microbial population behavior. Nat. Chem. Biol. **6**:705-712. doi:10.1038/nchembio.436.

Lie, T. J., M. L. Clawson, W. Godchaux, and E. R. Leadbetter. (1999). Sulfidogenesis from 2-Aminoethanesulfonate (Taurine) fermentation by a morphologically unusual sulfate-reducing bacterium, *Desulforhopalus singaporensis* sp. nov. Appl. Environ. Microbiol. **65**:3328-3334. doi:10.1128/AEM.65.8.3328-3334.1999.

Loka Bharati, P. A., R. Baulaigue, and R. Matheron. (1980). Breakdown of d-glucose by mixed cultures of *Escherichia coli*, *Desulfovibrio vulgaris*, and *Chromatium vinosum*. Curr. Microbiol. **4**:371-376. doi:10.1007/BF02605380.

Loka Bharati, P. A., R. Baulaigue, and R. Matheron. (1982). Degradation of cellulose by mixed cultures of fermentative bacteria and anaerobic sulfur bacteria. Zentralblatt für Bakteriologie Mikrobiologie und Hygiene: I. Abt. Originale C: Allgemeine, angewandte und ökologische Mikrobiologie **3**:466-474. doi:10.1016/S0721-9571(82)80003-3.

Lovley, D. R. (2013). Dissimilatory Fe(III)- and Mn(IV)-Reducing Prokaryotes. *in* E. Rosenberg, E. F. DeLong, S. Lory, E. Stackebrandt, and F. Thompson, editors. The Prokaryotes: Prokaryotic Physiology and Biochemistry. Springer Berlin Heidelberg, Berlin, Heidelberg. p. 287-308. doi:10.1007/978-3-642-30141-4_69.

Luther, G. W., A. J. Findlay, D. J. MacDonald, S. M. Owings, T. E. Hanson, R. A. Beinart, and P. R. Girguis. (2011). Thermodynamics and kinetics of sulfide oxidation by oxygen: A look at inorganically controlled reactions and biologically mediated processes in the environment. Front. Microbiol. **2**. doi:10.3389/fmicb.2011.00062.

Marina, T. I., V. Salinas, G. Cordone, G. Campana, E. Moreira, D. Deregibus, L. Torre, R. Sahade, M. Tatián, E. Barrera Oro, M. De Troch, S. Doyle, M. L. Quartino, L. A. Saravia, and F. R. Momo. (2017). The food web of Potter Cove (Antarctica): Complexity, structure and function. Estuar. Coast. Shelf Sci. **200**:141-151. doi:10.1016/j.ecss.2017.10.015.

Meredith, M. P., U. Falk, A. V. Bers, A. Mackensen, I. R. Schloss, E. Ruiz Barlett, K. Jerosch, A. Silva Busso, and D. Abele. (2018). Anatomy of a glacial meltwater discharge event in an Antarctic cove. Philos. Trans. Royal Soc. A **376**:20170163. doi:10.1098/rsta.2017.0163.

Michaud, A. B., K. Laufer, A. Findlay, A. Pellerin, G. Antler, A. V. Turchyn, H. Røy, L. M. Wehrmann, and B. B. Jørgensen. (2020). Glacial influence on the iron and sulfur cycles in Arctic fjord sediments (Svalbard). Geochim. Cosmochim. Acta **280**:423-440. doi:10.1016/j.gca.2019.12.033.

Milner, A. M., K. Khamis, T. J. Battin, J. E. Brittain, N. E. Barrand, L. Füreder, S. Cauvy-Fraunié, G. M. Gíslason, D. Jacobsen, D. M. Hannah, A. J. Hodson, E. Hood, V. Lencioni, J. S. Ólafsson, C. T. Robinson, M. Tranter, and L. E. Brown. (2017). Glacier shrinkage driving global changes in downstream systems. Proc. Natl. Acad. Sci. USA **114**:9770-9778. doi:10.1073/pnas.1619807114.

Molari, M., C. Hassenrueck, R. Laso-Pérez, G. Wegener, P. Offre, S. Scilipoti, and A. Boetius. (2023). A hydrogenotrophic *Sulfurimonas* is globally abundant in deep-sea oxygen-saturated hydrothermal plumes. Nat. Microbiol. **8**:651-665. doi:10.1038/s41564-023-01342-w.

Monien, D., P. Monien, R. Brünjes, T. Widmer, A. Kappenberg, A. A. Silva Busso, B. Schnetger, and H.-J. Brumsack. (2017). Meltwater as a source of potentially bioavailable iron to Antarctica waters. Antarct. Sci. **29**:277-291. doi:10.1017/S095410201600064X.

Monien, P., K. A. Lettmann, D. Monien, S. Asendorf, A.-C. Wölfl, C. H. Lim, J. Thal, B. Schnetger, and H.-J. Brumsack. (2014). Redox conditions and trace metal cycling in coastal sediments from the maritime Antarctic. Geochim. Cosmochim. Acta **141**:26-44. doi:10.1016/j.gca.2014.06.003.

Moore, J. K., K. Lindsay, S. C. Doney, M. C. Long, and K. Misumi. (2013). Marine ecosystem dynamics and biogeochemical cycling in the Community Earth System Model [CESM1(BGC)]: Comparison of the 1990s with the 2090s under the RCP4.5 and RCP8.5 scenarios. J. Clim. **26**:9291-9312. doi:10.1175/JCLI-D-12-00566.1.

Neder, C., V. Fofonova, A. Androsov, I. Kuznetsov, D. Abele, U. Falk, I. R. Schloss, R. Sahade, and K. Jerosch. (2022). Modelling suspended particulate matter dynamics at an Antarctic fjord impacted by glacier melt. J. Mar. Syst. **231**:103734. doi:10.1016/j.jmarsys.2022.103734.

Neder, C., R. Sahade, D. Abele, R. Pesch, and K. Jerosch. (2020). Default versus configured-geostatistical modeling of suspended particulate matter in Potter Cove, West Antarctic Peninsula. Fluids **5**:235. doi:10.3390/fluids5040235.

Nielsen, L. P., N. Risgaard-Petersen, H. Fossing, P. B. Christensen, and M. Sayama. (2010). Electric currents couple spatially separated biogeochemical processes in marine sediment. Nature **463**:1071. doi:10.1038/nature08790.

O'Loughlin, E. J., C. A. Gorski, M. M. Scherer, M. I. Boyanov, and K. M. Kemner. (2010). Effects of oxyanions, natural organic matter, and bacterial cell numbers on the bioreduction of lepidocrocite (γ-FeOOH) and the formation of secondary mineralization products. Environ. Sci. Technol. **44**:4570-4576. doi:10.1021/es100294w.

Oremland, R. S. and S. Polcin. (1982). Methanogenesis and sulfate reduction: Competitive and noncompetitive substrates in estuarine sediments. Appl. Environ. Microbiol. **44**:1270-1276. doi:10.1128/aem.44.6.1270-1276.1982.

Oremland, R. S. and M. P. Silverman. (1979). Microbial sulfate reduction measured by an automated electrical impedance technique. Geomicrobiol. J. **1**:355-372. doi:10.1080/01490457909377741.

Parks, D. H., M. Chuvochina, D. W. Waite, C. Rinke, A. Skarshewski, P.-A. Chaumeil, and P. Hugenholtz. (2018). A standardized bacterial taxonomy based on genome phylogeny substantially revises the tree of life. Nat. Biotechnol. **36**:996-1004. doi:10.1038/nbt.4229.

Pasotti, F., E. Manini, D. Giovannelli, A.-C. Wölfl, D. Monien, E. Verleyen, U. Braeckman, D. Abele, and A. Vanreusel. (2015). Antarctic shallow water benthos in an area of recent rapid glacier retreat. Mar. Ecol. **36**:716-733. doi:10.1111/maec.12179.

Pelikan, C., K. Wasmund, C. Glombitza, B. Hausmann, C. W. Herbold, M. Flieder, and A. Loy. (2020). Anaerobic bacterial degradation of protein and lipid macromolecules in subarctic marine sediment. ISME J. doi:10.1038/s41396-020-00817-6.

Petro, C., P. Starnawski, A. Schramm, and K. U. Kjeldsen. (2017). Microbial community assembly in marine sediments. Aquat. Microb. Ecol. **79**:177-195. doi:10.3354/ame01826.

Pfeffer, C., S. Larsen, J. Song, M. Dong, F. Besenbacher, R. L. Meyer, K. U. Kjeldsen, L. Schreiber, Y. A. Gorby, M. Y. El-Naggar, K. M. Leung, A. Schramm, N. Risgaard-Petersen, and L. P. Nielsen. (2012). Filamentous bacteria transport electrons over centimetre distances. Nature **491**:218-221. doi:10.1038/nature11586.

Pfennig, N. and H. Biebl. (1976). *Desulfuromonas acetoxidans* gen. nov. and sp. nov., a new anaerobic, sulfur-reducing, acetate-oxidizing bacterium. Arch. Microbiol. **110**:3-12. doi:10.1007/BF00416962.

Pischedda, L., J. C. Poggiale, P. Cuny, and F. Gilbert. (2008). Imaging oxygen distribution in marine sediments. The importance of bioturbation and sediment heterogeneity. Acta Biotheor. **56**:123-135. doi:10.1007/s10441-008-9033-1.

Poulton, S. W. and D. E. Canfield. (2005). Development of a sequential extraction procedure for iron: Implications for iron partitioning in continentally derived particulates. Chem. Geol. **214**:209-221. doi:10.1016/j.chemgeo.2004.09.003.

Poulton, S. W., M. D. Krom, and R. Raiswell. (2004). A revised scheme for the reactivity of iron (oxyhydr)oxide minerals towards dissolved sulfide. Geochim. Cosmochim. Acta **68**:3703-3715. doi:10.1016/j.gca.2004.03.012.

Quartino, M. L. and A. L. Boraso de Zaixso. (2008). Summer macroalgal biomass in Potter Cove, South Shetland Islands, Antarctica: Its production and flux to the ecosystem. Polar Biol. **31**:281-294. doi:10.1007/s00300-007-0356-1.

Quast, C., E. Pruesse, P. Yilmaz, J. Gerken, T. Schweer, P. Yarza, J. Peplies, and F. O. Glöckner. (2012). The SILVA ribosomal RNA gene database project: Improved data processing and web-based tools. Nucleic Acids Res. **41**:D590-D596. doi:10.1093/nar/gks1219.

Raiswell, R. (2011). Iron transport from the continents to the open ocean: The aging-rejuvenation cycle. Elements **7**:101-106. doi:10.2113/gselements.7.2.101.

Ratnikova, N. M., A. I. Slobodkin, A. Y. Merkel, D. S. Kopitsyn, V. V. Kevbrin, E. A. Bonch-Osmolovskaya, and G. B. Slobodkina. (2020). *Sulfurimonas crateris* sp. nov., a facultative anaerobic sulfur-oxidizing chemolithoautotrophic bacterium isolated from a terrestrial mud volcano. Int. J. Syst. Evol. Microbiol. **70**:487-492. doi:10.1099/ijsem.0.003779.

Ravenschlag, K., K. Sahm, J. Pernthaler, and R. Amann. (1999). High bacterial diversity in permanently cold marine sediments. Appl. Environ. Microbiol. **65**:3982-3989. doi:10.1128/aem.65.9.3982-3989.1999.

Rinke, C., P. Schwientek, A. Sczyrba, N. N. Ivanova, I. J. Anderson, J.-F. Cheng, A. Darling, S. Malfatti, B. K. Swan, E. A. Gies, J. A. Dodsworth, B. P. Hedlund, G. Tsiamis, S. M. Sievert, W.-T. Liu, J. A. Eisen, S. J. Hallam, N. C. Kyrpides, R. Stepanauskas, E. M. Rubin, P. Hugenholtz, and T. Woyke. (2013). Insights into the phylogeny and coding potential of microbial dark matter. Nature **499**:431-437. doi:10.1038/nature12352.

Roalkvam, I., K. Drønen, R. Stokke, F. L. Daae, H. Dahle, and I. H. Steen. (2015). Physiological and genomic characterization of *Arcobacter anaerophilus* IR-1 reveals new metabolic features in *Epsilonproteobacteria*. Front. Microbiol. **6**:987. doi:10.3389/fmicb.2015.00987.

Robador, A., A. L. Müller, J. E. Sawicka, D. Berry, C. R. J. Hubert, A. Loy, B. B. Jørgensen, and V. Brüchert. (2015). Activity and community structures of sulfate-reducing microorganisms in polar, temperate and tropical marine sediments. ISME J. **10**:796-809. doi:10.1038/ismej.2015.157.

Roden, E. E. (2003). Fe(III) oxide reactivity toward biological versus chemical reduction. Environ. Sci. Technol. **37**:1319-1324. doi:10.1021/es026038o.

Rubin-Blum, M., G. Sisma-Ventura, Y. Yudkovski, N. Belkin, M. Kanari, B. Herut, and E. Rahav. (2022). Diversity, activity, and abundance of benthic microbes in the Southeastern Mediterranean Sea. FEMS Microbiol. Ecol. **98**. doi:10.1093/femsec/fiac009.

Rückamp, M., M. Braun, S. Suckro, and N. Blindow. (2011). Observed glacial changes on the King George Island ice cap, Antarctica, in the last decade. Global Planet. Change **79**:99-109. doi:10.1016/j.gloplacha.2011.06.009.

Santos, A. A., S. S. Venceslau, F. Grein, W. D. Leavitt, C. Dahl, D. T. Johnston, and I. A. C. Pereira. (2015). A protein trisulfide couples dissimilatory sulfate reduction to energy conservation. Science **350**:1541-1545. doi:10.1126/science.aad3558.

Schloss, I. R., D. Abele, S. Moreau, S. Demers, A. V. Bers, O. González, and G. A. Ferreyra. (2012). Response of phytoplankton dynamics to 19-year (1991–2009) climate trends in Potter Cove (Antarctica). J. Mar. Syst. **92**:53-66. doi:10.1016/j.jmarsys.2011.10.006.

Schloss, I. R. and G. A. Ferreyra. (2002). Primary production, light and vertical mixing in Potter Cove, a shallow bay in the maritime Antarctic. Polar Biol. **25**:41-48. doi:10.1007/s003000100309.

Schlosser, C., K. Schmidt, A. Aquilina, W. B. Homoky, M. Castrillejo, R. A. Mills, M. D. Patey, S. Fielding, A. Atkinson, and E. P. Achterberg. (2018). Mechanisms of dissolved and labile particulate iron supply to shelf waters and phytoplankton blooms off South Georgia, Southern Ocean. Biogeosciences **15**:4973-4993. doi:10.5194/bg-15-4973-2018.

Shi, L., H. Dong, G. Reguera, H. Beyenal, A. Lu, J. Liu, H.-Q. Yu, and J. K. Fredrickson. (2016). Extracellular electron transfer mechanisms between microorganisms and minerals. Nat. Rev. Microbiol. **14**:651-662. doi:10.1038/nrmicro.2016.93.

Slobodkin, A. I., I. I. Rusanov, G. B. Slobodkina, A. R. Stroeva, N. A. Chernyh, N. V. Pimenov, and A. Y. Merkel. (2024). Diversity, methane oxidation activity, and metabolic potential of microbial communities in terrestrial mud volcanos of the Taman Peninsula. Microorganisms **12**:1349. doi:10.3390/microorganisms12071349.

Slobodkin, A. I. and G. B. Slobodkina. (2019). Diversity of sulfur-disproportionating microorganisms. Microbiology **88**:509-522. doi:10.1134/S0026261719050138.

Solden, L., K. Lloyd, and K. Wrighton. (2016). The bright side of microbial dark matter: Lessons learned from the uncultivated majority. Curr. Opin. Microbiol. **31**:217-226. doi:10.1016/j.mib.2016.04.020.

Sørensen, J., D. Christensen, and B. B. Jørgensen. (1981). Volatile fatty acids and hydrogen as substrates for sulfate-reducing bacteria in anaerobic marine sediment. Appl. Environ. Microbiol. **42**:5-11. doi:10.1128/aem.42.1.5-11.1981.

Stuij, T. M., D. F. R. Cleary, R. J. M. Rocha, A. R. M. Polonia, D. A. Machado e Silva, J. C. Frommlet, A. Louvado, Y. M. Huang, N. J. De Voogd, and N. C. M. Gomes. (2024). Development and validation of an experimental life support system to study coral reef microbial communities. Sci. Rep. **14**:21260. doi:10.1038/s41598-024-69514-0.

Sun, M. Y., K. A. Dafforn, E. L. Johnston, and M. V. Brown. (2013). Core sediment bacteria drive community response to anthropogenic contamination over multiple environmental gradients. Environ. Microbiol. **15**:2517-2531. doi:https://doi.org/10.1111/1462-2920.12133.

Tanaka, N., L. A. Romanenko, T. Iino, G. M. Frolova, and V. V. Mikhailov. (2011). *Cocleimonas flava* gen. nov., sp. nov., a gammaproteobacterium isolated from sand snail (*Umbonium costatum*). Int. J. Syst. Evol. Microbiol. **61**:412-416. doi:10.1099/ijs.0.020263-0.

Timmer-ten Hoor, A. (1975). A new type of thiosulphate oxidizing, nitrate reducing microorganism: *Thiomicrospira denitrificans* sp. nov. Neth. J. Sea Res. **9**:344-350. doi:10.1016/0077-7579(75)90008-3.

Tu, T.-H., L.-W. Wu, Y.-S. Lin, H. Imachi, L.-H. Lin, and P.-L. Wang. (2017). Microbial community composition and functional capacity in a terrestrial ferruginous, sulfate-depleted mud volcano. Front. Microbiol. **8**:2137. doi:10.3389/fmicb.2017.02137.

van de Velde, S. and F. J. R. Meysman. (2016). The influence of bioturbation on iron and sulphur cycling in marine sediments: A model analysis. Aquat. Geochem. **22**:469-504. doi:10.1007/s10498-016-9301-7.

van den Ende, F. P., J. Meier, and H. van Gemerden. (1997). Syntrophic growth of sulfate-reducing bacteria and colorless sulfur bacteria during oxygen limitation. FEMS Microbiol. Ecol. **23**:65-80. doi:10.1111/j.1574-6941.1997.tb00392.x.

Vandieken, V., N. Finke, and B. B. Jørgensen. (2006a). Pathways of carbon oxidation in an Arctic fjord sediment (Svalbard) and isolation of psychrophilic and psychrotolerant Fe(III)-reducing bacteria. Mar. Ecol. Prog. Ser. **322**:29-41. doi:10.3354/meps322029.

Vandieken, V., M. Mußmann, H. Niemann, and B. B. Jørgensen. (2006b). *Desulfuromonas svalbardensis* sp. nov. and *Desulfuromusa ferrireducens* sp. nov., psychrophilic, Fe(III)-reducing bacteria isolated from Arctic sediments, Svalbard. Int. J. Syst. Evol. Microbiol. **56**:1133-1139. doi:10.1099/ijs.0.63639-0.

Vandieken, V., M. Nickel, and B. B. Jørgensen. (2006c). Carbon mineralization in Arctic sediments northeast of Svalbard: Mn(IV) and Fe(III) reduction as principal anaerobic respiratory pathways. Mar. Ecol. Prog. Ser. **322**:15-27. doi:10.3354/meps322015.

Vandieken, V., M. Pester, N. Finke, J.-H. Hyun, M. W. Friedrich, A. Loy, and B. Thamdrup. (2012). Three manganese oxide-rich marine sediments harbor similar communities of acetate-oxidizing manganese-reducing bacteria. ISME J. **6**:2078-2090. doi:10.1038/ismej.2012.41.

Vasquez-Cardenas, D., J. van de Vossenberg, L. Polerecky, S. Y. Malkin, R. Schauer, S. Hidalgo-Martinez, V. Confurius, J. J. Middelburg, F. J. R. Meysman, and H. T. S. Boschker. (2015). Microbial carbon metabolism associated with electrogenic sulphur oxidation in coastal sediments. ISME J. **9**:1966-1978. doi:10.1038/ismej.2015.10.

Vishnupriya, S., T. Jabir, K. P. Krishnan, and A. A. Mohamed Hatha. (2021). Bacterial community structure and functional profiling of high Arctic fjord sediments. World J. Microbiol. Biotechnol. **37**:133. doi:10.1007/s11274-021-03098-z.

Vuillemin, A., F. Horn, A. Friese, M. Winkel, M. Alawi, D. Wagner, C. Henny, W. D. Orsi, S. A. Crowe, and J. Kallmeyer. (2018). Metabolic potential of microbial communities from ferruginous sediments. Environ. Microbiol. **20**:4297-4313. doi:10.1111/1462-2920.14343.

Wadham, J. L., R. De'ath, F. M. Monteiro, M. Tranter, A. Ridgwell, R. Raiswell, and S. Tulaczyk. (2013). The potential role of the Antarctic Ice Sheet in global biogeochemical cycles. Earth Environ. Sci. Trans. **104**:55-67. doi:10.1017/S1755691013000108.

Walker, A. M., M. B. Leigh, and S. L. Mincks. (2023). Benthic bacteria and archaea in the North American Arctic reflect food supply regimes and impacts of coastal and riverine inputs. Deep Sea Res. (II Top. Stud. Oceanogr.) **207**:105224. doi:10.1016/j.dsr2.2022.105224.

Wang, F., M. Li, L. Huang, and X.-H. Zhang. (2021a). Cultivation of uncultured marine microorganisms. Mar. Life Sci. Technol. **3**:117-120. doi:10.1007/s42995-021-00093-z.

Wang, J., Q. Zheng, S. Wang, J. Zeng, Q. Yuan, Y. Zhong, L. Jiang, and Z. Shao. (2023a). Characterization of two novel chemolithoautotrophic bacteria of *Sulfurovum* from marine coastal environments and further comparative genomic analyses revealed species differentiation among deep-sea hydrothermal vent and non-vent origins. Front. Mar. Sci. **10**. doi:10.3389/fmars.2023.1222526.

Wang, S., L. Jiang, Q. Hu, L. Cui, B. Zhu, X. Fu, Q. Lai, Z. Shao, and S. Yang. (2021b). Characterization of *Sulfurimonas hydrogeniphila* sp. nov., a novel bacterium predominant in deep-sea hydrothermal vents and comparative genomic analyses of the genus *Sulfurimonas*. Front. Microbiol. **12**. doi:10.3389/fmicb.2021.626705.

Wang, S., L. Jiang, X. Liu, S. Yang, and Z. Shao. (2020). *Sulfurimonas xiamenensis* sp. nov. and *Sulfurimonas lithotrophica* sp. nov., hydrogen- and sulfur-oxidizing chemolithoautotrophs within the *Epsilonproteobacteria* isolated from coastal sediments, and an emended description of the genus Sulfurimonas. Int. J. Syst. Evol. Microbiol. **70**:2657-2663. doi:10.1099/ijsem.0.004087.

Wang, S., L. Jiang, S. Xie, K. Alain, Z. Wang, J. Wang, D. Liu, and Z. Shao. (2023b). Disproportionation of inorganic sulfur compounds by mesophilic chemolithoautotrophic *Campylobacterota*. mSystems **8**:e00954-00922. doi:10.1128/msystems.00954-22.

Wang, Z., S. Wang, Q. Lai, S. Wei, L. Jiang, and Z. Shao. (2022a). *Sulfurimonas marina* sp. nov., an obligately chemolithoautotrophic, sulphur-oxidizing bacterium isolated from a deep-sea sediment sample from the South China Sea. Int. J. Syst. Evol. Microbiol. **72**. doi:10.1099/ijsem.0.005582.

Wang, Z., K. Yang, J. Yu, D. Zhou, Y. Li, B. Guan, Y. Yu, X. Wang, Z. Ren, W. Wang, X. Chen, and J. Yang. (2022b). Soil bacterial community structure in different micro-habitats on the tidal creek section in the Yellow River estuary. Front. Ecol. Evol. **10**. doi:10.3389/fevo.2022.950605.

Wasmund, K., M. Mußmann, and A. Loy. (2017). The life sulfuric: Microbial ecology of sulfur cycling in marine sediments. Environ. Microbiol. Rep. **9**:323-344. doi:10.1111/1758-2229.12538.

Wehrmann, L. M., M. J. Formolo, J. D. Owens, R. Raiswell, T. G. Ferdelman, N. Riedinger, and T. W. Lyons. (2014). Iron and manganese speciation and cycling in glacially influenced high-latitude fjord sediments (West Spitsbergen, Svalbard): Evidence for a benthic recycling-transport mechanism. Geochim. Cosmochim. Acta **141**:628-655. doi:10.1016/j.gca.2014.06.007.

Winfrey, M. R. and D. M. Ward. (1983). Substrates for sulfate reduction and methane production in intertidal sediments. Appl. Environ. Microbiol. **45**:193-199. doi:10.1128/aem.45.1.193-199.1983.

Xin, Y., N. Wu, Z. Sun, H. Wang, Y. Chen, C. Xu, W. Geng, H. Cao, X. Zhang, B. Zhai, and D. Yan. (2022). Methane seepage intensity distinguish microbial communities in sediments at the Mid-Okinawa Trough. Sci. Total Environ. **851**:158213. doi:10.1016/j.scitotenv.2022.158213.

Yamamoto, M. and K. Takai. (2011). Sulfur metabolisms in epsilon-and gamma-*Proteobacteria* in deep-sea hydrothermal fields. Front. Microbiol. **2**:192. doi:10.3389/fmicb.2011.00192.

Yin, X., G. Zhou, H. Wang, D. Han, M. Maeke, T. Richter-Heitmann, L. C. Wunder, D. A. Aromokeye, Q.-Z. Zhu, R. Nimzyk, M. Elvert, and M. W. Friedrich. (2024). Unexpected carbon utilization activity of sulfate-reducing microorganisms in temperate and permanently cold marine sediments. ISME J. **18**. doi:10.1093/ismejo/wrad014.

Zhu, Q.-Z., X. Yin, H. Taubner, J. Wendt, M. W. Friedrich, M. Elvert, K.-U. Hinrichs, and J. J. Middelburg. (2024). Secondary production and priming reshape the organic matter composition in marine sediments. Sci. Adv. **10**:eadm8096. doi:10.1126/sciadv.adm8096.

Zoppini, A., L. Bongiorni, N. Ademollo, L. Patrolecco, T. Cibic, A. Franzo, M. Melita, M. Bazzaro, and S. Amalfitano. (2020). Bacterial diversity and microbial functional responses to organic matter composition and persistent organic pollutants in deltaic lagoon sediments. Estuar. Coast. Shelf Sci. **233**:106508. doi:10.1016/j.ecss.2019.106508.

Zwerschke, N., C. J. Sands, A. Roman-Gonzalez, D. K. A. Barnes, A. Guzzi, S. Jenkins, C. Muñoz-Ramírez, and J. Scourse. (2022). Quantification of blue carbon pathways contributing to negative feedback on climate change following glacier retreat in West Antarctic fjords. Global Change Biol. **28**:8-20. doi:10.1111/gcb.15898.

Acknowledgements

There were many people who supported me in one way or the other during my PhD to whom I would like to extend my thanks and gratitude.

Firstly, I would like to thank Michael Friedrich for the possibility to conduct this work in his lab, after he already gave me first insides into the exciting possibility of own research and supported me greatly during my Bachelor and Master studies. Thank you for your advice, support and supervision, making time for me also on short notice when an urgent problem comes up again.

I want to thank Prof. Ian Marshal for reviewing my thesis and being part of my thesis defense committee. I thank Prof. Kai Bischof for leading my thesis defense committee.

I want to thank Dr. Tim Ferdelman for being part of my thesis defense committee, but also giving advice as part of my thesis committee during the whole period of my PhD, taking the time to introduce me into the world of sulfur cycling and radioactive rate measurements.

My deepest gratitude and appreciation I want to extend to David, who always believed in me and motivated me since I came into the microbial ecophysiology group in the beginning of my Bachelors. David, you introduced me into the world of microbial ecology and how science in this field works and took your time to include me in real research when I was just a little Hiwi. Your enthusiasm is very contagious and motivated me many times when I was frustrated from, so I thought, inconclusive results. Even when you left to begin your new job, you still supported me from the far. Thank you so much!

I also want to thank Graciana who supported me so much since she joined our group and in whom I found a dear friend, even over the long distance to Argentina. Especially the cruise to South Georgia was a great experience with you together! I hope we will go together to Antarctica one day as well.

During my PhD, I worked together with and met many different scientists who helped me to expand my horizon in many different aspects. I want to thank Gunter Wegener for introducing me into radioactive isotope work. I want to thank Katja Laufer-Meiser for doing this further in regards of sulfate reduction rate measurements, making the fifth chapter of this thesis so much more complete and also that I could find such a friend in you. I want to thank Susann Henkel for all her support during my PhD, with again another sulfate measurement, reading manuscripts and other things at short notice and answering all my endless questions about sediment geochemistry and Potter Cove. I want to thank all the nice people from the Island Impact Cruise to South Georgia, making the great time with a really nice work-atmosphere

possible. Even though this cruise did not contribute to my thesis directly, it greatly expanded my understanding about ecology, the polar environment and how field work actually works! So thank you again, David, Michael and Sabine Kasten for giving me the possibility to participate in this cruise! I will always remember this life time experience!

I thank dearly the great group of people at the microbial ecophysiology group, former and current ones! I really enjoy the atmosphere in our group where people help each other and also just sit together for a coffee, chatting about lab but also life problems. I couldn't have done this without you! So thank you, Tim, Yunru, Wenxuan, Karen, Darjan, Charlotte, Nazila, Maja and Angela for your help with all kind of things around the office and labs. Thank you Sabine, Verena and (long ago, but still) Tina, for your support with all kind of bureaucracy or also just another pen. I want to thank the many Azubis, which helped me during the many hours in the lab, especially Constantin to whom I could just give a problem and he would solve it.

Thank you, Tobi, Karl-Heinz, Annika, Ajinkya, Celina and Shreya, who are now gone for quite a while already, but all taught me a lot in different ways. It is always nice to see you again!

I want to thank my Bachelor students, Carolin, Inga, Janina and Anastasiia for their great work during their time. I hope I could also teach you some things which will help you in your future.

I want to thank the MPI for Marine Microbiology and MarMic, especially Christiane Glöckner, for their support during my PhD enabling me to go to conferences or also just have a mental support coffee.

I also want to thank my old Marmic master class for the great time! I have the feeling we will never lose touch completely, even though we start to spread all around the globe now.

And then of course, I want to thank the people who kept me mentally saint during sometimes very stressful times. My friends, especially Mara, who always has an open ear, also when she is stressed out herself, and Bene, Jannika and my flat mates, Daniel, Witho and Caro who sometimes save me from starvation, or also just very unhealthy food, during long work days and nights and or just give me some greatly needed distraction now and then.

I want to thank my family, my parents, my grandma and my siblings, where I know that they always have my back, irrespective of distance or time of day. I always had the feeling that I can completely rely on you and that gives an invaluable degree of mental security to me.

And lastly I want to thank my partners who went with me through good and bad times during my PhD. I could not have done it without you.

Universität Bremen

Versicherung an Eides Statt

Ich, Lea Charlotte Wunder,

versichere an Eides Statt durch meine Unterschrift, dass ich die vorstehende Arbeit selbständig und ohne fremde Hilfe angefertigt und alle Stellen, die ich wörtlich dem Sinne nach aus Veröffentlichungen entnommen habe, als solche kenntlich gemacht habe, mich auch keiner anderen als der angegebenen Literatur oder sonstiger Hilfsmittel bedient habe.
Ich versichere an Eides Statt, dass ich die vorgenannten Angaben nach bestem Wissen und Gewissen gemacht habe und dass die Angaben der Wahrheit entsprechen und ich nichts verschwiegen habe.
Die Strafbarkeit einer falschen eidesstattlichen Versicherung ist mir bekannt, namentlich die Strafandrohung gemäß § 156 StGB bis zu drei Jahren Freiheitsstrafe oder Geldstrafe bei vorsätzlicher Begehung der Tat bzw. gemäß § 161 Abs. 1 StGB bis zu einem Jahr Freiheitsstrafe oder Geldstrafe bei fahrlässiger Begehung.

_____ _____

Ort, Datum Unterschrift

Universität Bremen

Ort, Datum: _____

.

Erklärungen zur elektronischen Version und zur Überprüfung einer Dissertation

Hiermit betätige ich gemäß §7, Abs. 7, Punkt 4, dass die zu Prüfungszwecken beigelegte elektronische Version meiner Dissertation identisch ist mit der abgegebenen gedruckten Version.

Ich bin mit der Überprüfung meiner Dissertation gemäß §6 Abs. 2, Punkt 5 mit qualifizierter Software im Rahmen der Untersuchung von Plagiatsvorwürfen einverstanden.

_____
Unterschrift